Waveform Modelling for the Laser Interferometer Space Antenna

LISA Consortium Waveform Working Group

Abstract. LISA, the Laser Interferometer Space Antenna, will usher in a new era in gravitational-wave astronomy. As the first anticipated space-based gravitational-wave detector, it will expand our view to the millihertz gravitational-wave sky, where a spectacular variety of interesting new sources abound: from millions of ultra-compact binaries in our Galaxy, to mergers of massive black holes at cosmological distances; from the beginnings of inspirals that will venture into the ground-based detectors' view to the death spiral of compact objects into massive black holes, and many sources in between. Central to realising LISA's discovery potential are waveform models, the theoretical and phenomenological predictions of the pattern of gravitational waves that these sources emit. This white paper is presented on behalf of the Waveform Working Group for the LISA Consortium. It provides a review of the current state of waveform models for LISA sources, and describes the significant challenges that must yet be overcome.

Corresponding email: wav-wg-chairs@lisamission.org

Niaesh Afshordi,[1] Sarp Akçay [iD],[2] Pau Amaro Seoane [iD],[3,4,5,6] Andrea Antonelli,[7] Josu C. Aurrekoetxea [iD],[8] Leor Barack [iD],[9] Enrico Barausse [iD],[10] Robert Benkel,[11] Laura Bernard [iD],[12] Sebastiano Bernuzzi,[13] Emanuele Berti [iD],[7] Matteo Bonetti,[14,15] Béatrice Bonga [iD],[16] Gabriele Bozzola,[17] Richard Brito [iD],[18] Alessandra Buonanno [iD],[11] Alejandro Cárdenas-Avendaño [iD],[19] Marc Casals [iD],[20,21,2] David F. Chernoff [iD],[22] Alvin J. K. Chua [iD],[23,24] Katy Clough,[25] Marta Colleoni [iD],[26] Mekhi Dhesi,[9] Adrien Druart,[27] Leanne Durkan [iD],[28] Guillaume Faye,[29] Deborah Ferguson,[28,30] Scott E. Field [iD],[31] William E. Gabella [iD],[32] Juan García-Bellido [iD],[33] Miguel Gracia-Linares,[28] Davide Gerosa [iD],[14,15,34] Stephen R. Green [iD],[35] Maria Haney [iD],[36] Mark Hannam,[37] Anna Heffernan [iD],[38,1,39] Tanja Hinderer [iD],[40] Thomas Helfer [iD],[41] Scott A. Hughes,[42] Sascha Husa [iD],[43,38] Soichiro Isoyama [iD],[23] Michael L. Katz [iD],[44,11] Chris Kavanagh [iD],[2] Gaurav Khanna,[45] Larry E. Kidder [iD],[46] Valeriya Korol [iD],[47] Lorenzo Küchler [iD],[9,27,48] Pablo Laguna [iD],[28] François Larrouturou,[49] Alexandre Le Tiec,[12] Benjamin Leather [iD],[11,2] Eugene A. Lim [iD],[50] Hyun Lim [iD],[51] Tyson B. Littenberg,[44] Oliver Long [iD],[11,9] Carlos O. Lousto [iD],[52] Geoffrey Lovelace [iD],[53] Georgios Lukes-Gerakopoulos [iD],[54] Philip Lynch [iD],[11,2] Rodrigo P. Macedo [iD],[55] Charalampos Markakis,[25] Elisa Maggio [iD],[11] Ilya Mandel,[56,57] Andrea Maselli,[58,59] Josh Mathews [iD],[23] Pierre Mourier [iD],[38] David Neilsen,[60] Alessandro Nagar,[61,62] David A. Nichols [iD],[63] Jan Novák,[64] Maria Okounkova,[65] Richard O'Shaughnessy,[52] Naritaka Oshita [iD],[66,67,68] Conor O'Toole,[2] Zhen Pan,[1] Paolo Pani [iD],[69] George Pappas,[70] Vasileios Paschalidis [iD],[71] Harald P. Pfeiffer [iD],[11] Lorenzo Pompili [iD],[11] Adam Pound [iD],[9] Geraint Pratten [iD],[34] Hannes R. Rüter [iD],[11] Milton Ruiz [iD],[72,30] Zeyd Sam,[9] Laura Sberna [iD],[11] Stuart L. Shapiro,[30] Deirdre M. Shoemaker [iD],[28] Carlos F. Sopuerta [iD],[43,73] Andrew Spiers [iD],[9] Hari Sundar [iD],[74] Nicola Tamanini,[75] Jonathan E. Thompson [iD],[76,37] Alexandre Toubiana,[11] Antonios Tsokaros [iD],[30,77] Samuel D. Upton [iD],[54,9] Maarten van de Meent [iD],[55,11] Daniele Vernieri [iD],[78] Jeremy M. Wachter [iD],[79] Niels Warburton [iD],[2] Barry Wardell [iD],[2] Helvi Witek [iD],[30] Vojtěch Witzany [iD],[80] Huan Yang [iD],[1,39] and Miguel Zilhão [iD][81]

(Coordinators and contributors)

K. G. Arun,[82] Miguel Bezares,[83,84] Alexander Bonilla [iD],[85] Christian Chapman-Bird [iD],[86] Geoffrey Compère,[87] Bradley Cowden [iD],[2] Kevin Cunningham [iD],[2] Chris Devitt [iD],[2] Sam Dolan [iD],[88] Francisco Duque,[11] Conor Dyson,[55] Chris L. Fryer,[51] Jonathan R. Gair [iD],[11] Bruno Giacomazzo,[14,15,89] Priti Gupta,[90] Wen-Biao Han [iD],[91] Roland Haas [iD],[92] Eric W. Hirschmann [iD],[60] E. A. Huerta [iD],[93,94,95] Philippe Jetzer,[96] Bernard Kelly,[97,98,99] Mohammed Khalil,[1] Nicole Lloyd-Ronning,[100] Sylvain Marsat,[75] Germano Nardini [iD],[101] Jakob Neef [iD],[2] Adrian Ottewill [iD],[2] Christiana Pantelidou [iD],[2] Gabriel Andres Piovano [iD],[2] Jaime Redondo-Yuste,[55] Laura Sagunski [iD],[102] Leo C. Stein [iD],[103] Viktor Skoupý,[80,54] Ulrich Sperhake [iD],[104] Lorenzo Speri [iD],[11] Thomas F.M. Spieksma,[55] Chris Stevens,[105] David Trestini [iD],[106] and Alex Vañó-Viñuales [iD][18]

(Endorsers)

[1] *Perimeter Institute for Theoretical Physics, Waterloo, Ontario N2L 2Y5, Canada*

[2] *School of Mathematics and Statistics, University College Dublin, Belfield, Dublin 4, Ireland*

[3] *Universitat Politècnica de València, València, Spain*

[4] *Max Planck Institute for Extraterrestrial Physics, Garching, Germany*

[5] *Higgs Centre for Theoretical Physics, Edinburgh, United Kingdom*

[6] *Kavli Institute for Astronomy and Astrophysics, Beijing 100871, China*

[7] *William H. Miller III Department of Physics and Astronomy, Johns Hopkins University, Baltimore, Maryland 21218, USA*

[8] *Astrophysics, University of Oxford, Denys Wilkinson Building, Keble Road, Oxford OX1 3RH, United Kingdom*

[9] *School of Mathematical Sciences and STAG Research Centre, University of Southampton, Southampton, SO17 1BJ, United Kingdom*

[10] *SISSA, Via Bonomea 265, 34136 Trieste, Italy and INFN Sezione di Trieste IFPU - Institute for Fundamental Physics of the Universe, Via Beirut 2, 34014 Trieste, Italy*

[11] *Max Planck Institute for Gravitational Physics (Albert Einstein Institute), D-14476 Potsdam, Germany*

[12] *Laboratoire Univers et Théories, CNRS, Observatoire de Paris, Université PSL, Université Paris Cité, 92190 Meudon, France*

[13] *Theoretisch-Physikalisches Institut, Friedrich-Schiller-Universität Jena, 07743, Jena, Germany*

[14] *Dipartimento di Fisica "G. Occhialini", Universitá degli Studi di Milano-Bicocca, Piazza della Scienza 3, 20126 Milano, Italy*

[15] *INFN, Sezione di Milano-Bicocca, Piazza della Scienza 3, 20126 Milano, Italy*

[16] *Institute for Mathematics, Astrophysics and Particle Physics, Radboud University, 6525 AJ Nijmegen, The Netherlands*

[17] *The University of Arizona, Department of Astronomy, Tucson, AZ 85721, USA*

[18] *CENTRA, Departamento de Física, Instituto Superior Técnico – IST, Universidade de Lisboa – UL, Avenida Rovisco Pais 1, 1049-001 Lisboa, Portugal*

[19] *Princeton Gravity Initiative, Princeton University, Princeton, New Jersey 08544, USA*

[20] *Institut für Theoretische Physik, Universität Leipzig, Brüderstraße 16, 04103 Leipzig, Germany.*

[21] *Centro Brasileiro de Pesquisas Físicas (CBPF), Rio de Janeiro, CEP 22290-180, Brazil.*

[22] *Department of Astronomy, Cornell University, Ithaca, New York 14853, USA*

[23] *Department of Physics, National University of Singapore, Singapore 117551*

[24] *Department of Mathematics, National University of Singapore, Singapore 119076*

[25] *School of Mathematical Sciences, Queen Mary University of London, Mile End Rd, London E1 4NS, United Kingdom*

[26] *Departament de Física, Universitat de les Illes Balears, IAC3 – IEEC, Crta. Valldemossa km 7.5, E-07122 Palma, Spain*

[27] *Université Libre de Bruxelles, Gravitational Wave Centre, International Solvay Institutes, CP 231, B-1050 Brussels, Belgium*

[28] *Center of Gravitational Physics, Weinberg Institute, University of Texas at Austin, TX, 78712, USA*

[29] *GReCO, Institut d'Astrophysique de Paris, UMR 7095, CNRS, Sorbonne Universit´e, 98bis boulevard Arago, 75014 Paris, France*

[30] Department of Physics and Illinois Center for Advanced Studies of the
Universe, University of Illinois at Urbana-Champaign, Urbana, Illinois 61801, USA

[31] Department of Mathematics and Center for Scientific Computing &
Data Science Research, University of Massachusetts, Dartmouth, MA 02747

[32] Department of Physics and Astronomy, Vanderbilt University, Nashville TN 37235

[33] Instituto de Física Teórica IFT-UAM/CSIC,
Universidad Autónoma de Madrid, 28049 Madrid, Spain

[34] School of Physics and Astronomy & Institute for Gravitational Wave
Astronomy, University of Birmingham, Birmingham, B15 2TT, United Kingdom

[35] School of Mathematical Sciences, University of Nottingham
University Park, Nottingham NG7 2RD, United Kingdom

[36] Nikhef, Science Park 105, 1098 XG Amsterdam, The Netherlands

[37] School of Physics and Astronomy, Cardiff University,
Queens Buildings, Cardiff, CF24 3AA, United Kingdom

[38] Departament de Física, Universitat de les Illes Balears, IAC3
– IEEC, Crta. Valldemossa km 7.5, E-07122 Palma, Spain

[39] University of Guelph, Guelph, Ontario N1G 2W1, Canada

[40] Institute for Theoretical Physics, Utrecht University,
Princetonplein 5, 3584CC Utrecht, The Netherlands

[41] Institute for Advanced Computational Science, Stony
Brook University, Stony Brook, NY 11794 USA

[42] Department of Physics and MIT Kavli Institute, Massachusetts
Institute of Technology, Cambridge, MA 02139, USA

[43] Institut de Ciències de l'Espai (ICE, CSIC), Campus UAB,
Carrer de Can Magrans s/n, 08193 Cerdanyola del Vallès, Spain

[44] NASA Marshall Space Flight Center, Huntsville, Alabama 35811, USA

[45] Department of Physics and Center for Computational
Research, University of Rhode Island, Kingston, RI 02881

[46] Cornell Center for Astrophysics and Planetary Science, Cornell University, Ithaca NY 14853

[47] Max-Planck-Institut für Astrophysik, Karl-
Schwarzschild-Straße 1, 85741 Garching, Germany

[48] Institute for Theoretical Physics, KU Leuven,
Celestijnenlaan 200D, B-3001 Leuven, Belgium

[49] Deutsches Elektronen-Synchrotron DESY, Notkestr. 85, 22607 Hamburg, Germany

[50] Theoretical Particle Physics and Cosmology Group, Physics Department,
Kings College London, Strand, London WC2R 2LS, United Kingdom

[51] Center for Theoretical Astrophysics, Los Alamos
National Laboratory, Los Alamos, NM 87545, USA

[52] Center for Computational Relativity and Gravitation, School
of Mathematical Sciences, Rochester Institute of Technology,
85 Lomb Memorial Drive, Rochester, New York 14623, USA

[53] Nicholas and Lee Begovich Center for Gravitational-Wave Physics and Astronomy,
California State University, Fullerton, Fullerton, California, 92831, USA

[54] Astronomical Institute of the Czech Academy of Sciences,
Boční II 1401/1a, CZ-141 00 Prague, Czech Republic

[55] Niels Bohr International Academy, Niels Bohr
Institute, Blegdamsvej 17, 2100 Copenhagen, Denmark

[56] School of Physics and Astronomy, Monash University, Clayton, Victoria 3800, Australia

[57]*OzGrav: The ARC Centre of Excellence for Gravitational Wave Discovery, Australia*
[58]*Gran Sasso Science Institute (GSSI), I-67100 L'Aquila, Italy*
[59]*INFN, Laboratori Nazionali del Gran Sasso, I-67100 Assergi, Italy*
[60]*Department of Physics and Astronomy, Brigham Young University, Provo, UT 84602, USA*
[61]*INFN Sezione di Torino, Via P. Giuria 1, 10125 Torino, Italy*
[62]*Institut des Hautes Etudes Scientifiques, 91440 Bures-sur-Yvette, France*
[63]*Department of Physics, University of Virginia,*
P.O. Box 400714, Charlottesville, VA 22904-4714, USA
[64]*Department of Physics, Faculty of Mechanical Engineering, Czech Technical*
University in Prague, Technická 1902/4, Prague 6, 16607, Czech republic
[65]*Department of Physics, Pasadena City College, Pasadena, California 91106, USA*
[66]*Center for Gravitational Physics and Quantum Information (CGPQI), Yukawa*
Institute for Theoretical Physics (YITP), Kyoto University, 606-8502, Kyoto, Japan
[67]*The Hakubi Center for Advanced Research, Kyoto University,*
Yoshida Ushinomiyacho, Sakyo-ku, Kyoto 606-8501, Japan
[68]*RIKEN iTHEMS, Wako, Saitama, 351-0198, Japan*
[69]*Dipartimento di Fisica, Sapienza Università di Roma & INFN*
Sezione di Roma, Piazzale Aldo Moro 5, 00185, Roma, Italy
[70]*Department of Physics, Aristotle University of Thessaloniki, Thessaloniki 54124, Greece*
[71]*The University of Arizona, Departments of Astronomy and Physics, Tucson, AZ 85721, USA*
[72]*Departamento de Astronomía y Astrofísica, Universitat de*
Valéncia, Dr. Moliner 50, 46100, Burjassot (València), Spain
[73]*Institut d'Estudis Espacials de Catalunya (IEEC), Edifici Nexus,*
Carrer del Gran Capità 2-4, despatx 201, 08034 Barcelona, Spain
[74]*University of Utah, Salt Lake City, UT 84112, USA*
[75]*Laboratoire des 2 Infinis - Toulouse (L2IT-IN2P3), Université*
de Toulouse, CNRS, UPS, F-31062 Toulouse Cedex 9, France
[76]*Theoretical Astrophysics Group, California Institute*
of Technology, Pasadena, CA 91125, U.S.A.
[77]*Research Center for Astronomy and Applied*
Mathematics, Academy of Athens, Athens 11527, Greece
[78]*Dipartimento di Fisica "E. Pancini", Università di Napoli "Federico II" and INFN, Sezione*
di Napoli, Compl. Univ. di Monte S. Angelo, Edificio G, Via Cinthia, I-80126, Napoli, Italy.
[79]*School of Sciences & Humanities, Wentworth*
Institute of Technology, Boston, MA 02155, USA
[80]*Institute of Theoretical Physics, Faculty of Mathematics and*
Physics, Charles University, CZ-180 00 Prague, Czech Republic
[81]*Centre for Research and Development in Mathematics and Applications,*
Department of Mathematics, University of Aveiro, 3810-193 Aveiro, Portugal
[82]*Chennai Mathematical Institute, Siruseri, 603103, India*
[83]*Nottingham Centre of Gravity, University of Nottingham,*
University Park, Nottingham, NG7 2RD, United Kingdom
[84]*School of Mathematical Sciences, University of Nottingham,*
University Park, Nottingham, NG7 2RD, United Kingdom
[85]*Observatório Nacional, Rua General José Cristino 77,*
São Cristóvço, 20921-400 Rio de Janeiro, RJ, Brazil
[86]*SUPA, University of Glasgow, Glasgow G128QQ, United Kingdom*

[87] *Université Libre de Bruxelles, International Solvay Institutes, CP 231, B-1050 Brussels, Belgium*

[88] *Consortium for Fundamental Physics, School of Mathematics and Statistics, University of Sheffield, Hicks Building, Hounsfield Road, Sheffield S3 7RH, United Kingdom*

[89] *INAF, Osservatorio Astronomico di Brera, Via E. Bianchi 46, I-23807 Merate, Italy*

[90] *Department of Physics, Indian Institute of Science, Bangalore 560012, India*

[91] *Shanghai Astronomical Observatory, CAS, 200030, Shanghai, China*

[92] *University of Illinois*

[93] *Data Science and Learning Division, Argonne National Laboratory, Lemont, Illinois 60439, USA*

[94] *Department of Computer Science, The University of Chicago, Chicago, Illinois 60637, USA*

[95] *Department of Physics, University of Illinois at Urbana-Champaign, Urbana, Illinois 61801, USA*

[96] *Department of Physics, University of Zürich, Winterthurerstrasse 190, 8057 Zürich, Switzerland*

[97] *Center for Space Sciences and Technology, University of Maryland Baltimore County, 1000 Hilltop Circle Baltimore, MD 21250, USA*

[98] *Gravitational Astrophysics Lab, NASA Goddard Space Flight Center, Greenbelt, MD 20771, USA*

[99] *Center for Research and Exploration in Space Science and Technology, NASA Goddard Space Flight Center, Greenbelt, MD 20771, USA*

[100] *Computational Physics and Methods Group, Los Alamos National Lab, Los Alamos, NM 87544, USA*

[101] *Faculty of Science and Technology, University of Stavanger, 4036 Stavanger, Norway*

[102] *Institute for Theoretical Physics, Goethe University, 60438 Frankfurt am Main, Germany*

[103] *Department of Physics and Astronomy, University of Mississippi, University, MS 38677, USA*

[104] *Department of Applied Mathematics and Theoretical Physics, University of Cambridge, Wilberforce Road, Cambridge CB3 0WA, United Kingdom*

[105] *School of Mathematics and Statistics, University of Canterbury, Christchurch 8041, New Zealand*

[106] *CEICO, Institute of Physics of the Czech Academy of Sciences, Na Slovance 2, 182 21 Praha 8, Czechia*

(Dated: 3 November 2023)

6

Contents

Notation

G	gravitational constant	
c	speed of light	
m_1	mass of the primary	$m_1 > m_2$
m_2	mass of secondary	$m_2 < m_1$
M	total mass	$m_1 + m_2$
μ	reduced mass	$m_1 m_2 / M$
q	large mass ratio	m_1 / m_2
ϵ	small mass ratio	m_2 / m_1
ν	symmetric mass ratio	$m_1 m_2 / M^2$
S_i	spin angular momentum of body i	
a_i	Kerr spin parameter of body i	$S_i / (m_i c)$
χ_i	dimensionless spin of body i	$a_i c^2 / (G m_i) \equiv S_i c / (G m_i^2)$
e	orbital eccentricity	
Ω	orbital frequency	
μ_S	string tension	

Table 1. Frequently used symbols throughout this whitepaper, G and c are set to 1 throughout.

List of acronyms

AAK	Augmented Analytic Kludge
AGN	active galactic nuclei
BBH	binary black hole
BH	black hole
BHNS	binary black hole-neutron star
BHPT	black hole perturbation theory
BNS	binary neutron star
BWD	binary white dwarf
CHE	close hyperbolic encounters
CO	compact object
CPU	central processing unit
CS	cosmic string
EFT	effective field theory
EMRI	extreme mass-ratio inspiral
EOB	effective one-body
FD	frequency domain
FEW	Fast EMRI Waveforms
GB	Galactic binary
GPU	graphical processing unit
GR	general relativity
GSF	gravitational self-force
GW	gravitational wave
IMBH	intermediate mass black hole
IMRI	intermediate mass-ratio inspiral
ISCO	innermost stable circular orbit
LISA	Laser Interferometer Space Antenna
LVK	LIGO-Virgo-KAGRA Collaboration
MBH	massive black hole
MBHB	massive black hole binary
NR	numerical relativity
NS	neutron star

ODE	ordinary differential equation
PBH	primordial black holes
PDE	partial differential equation
PM	post-Minkowskian
PN	post-Newtonian
QCD	quantum chromodynamics
QNM	quasi-normal mode
ROM	reduced-order model
SDSS	Sloan Digital Sky Survey
SNR	signal-to-noise ratio
SOBH	stellar-origin black hole
SOBHB	stellar-origin black hole binary
SPA	stationary phase approximation
TD	time domain
UCXB	ultra-compact X-ray binary
WDBH	white dwarf-black hole
WDNS	white dwarf-neutron star
XMRI	extremely-large mass-ratio inspiral

1. Introduction

Waveforms, theoretical predictions for gravitational wave (GW) signals, play a vital role in GW astronomy. Most GW signals are buried deep in instrumental noise. By using waveforms as matched filters, such signals can be detected. Once a GW is found the properties of its source can be inferred by further comparing the system to theoretical waveforms. The Laser Interferometer Space Antenna (LISA) will open a window on a new frequency band of GWs in the mHz regime. In this band we will encounter a slew of new sources of GWs ranging from local Galactic white-dwarf binaries to distant mergers of massive black holes (MBHs), and many sources in between. Realizing the science potential of LISA detection and measurement of GW signals will require new waveform models, which will need to cover a much wider range of sources while being significantly more accurate than the models used currently in ground based GW observations by LIGO, Virgo, and KAGRA [1, 2].

A large class of GW sources expected for LISA feature the inspiral of a binary of compact objects decaying under the emission of GWs, often leading to a merger at the end. Producing theoretical waveforms for such events requires solving the relativistic two body problem. This is a notoriously difficult problem with no known closed form solution for radiating binaries. There are three main approaches to obtain approximate solutions to the relativistic two-body problem from first principles. First, numerical relativity (NR) takes the non-linear partial differential equations (PDEs) of general relativity (GR), puts them on a grid, and evolves them on a supercomputer. Second, one can make a weak field approximation and obtaining a perturbative analytical solution leading to post-Newtonian (PN) or post-Minkowskian (PM) theory (depending on whether a simultaneous slow motion approximation is introduced). Finally, gravitational self-force (GSF) theory expands the two-body dynamics in powers of the (small) ratio of the masses of the two bodies. Studies of homogeneous perturbations of isolated black holes (BHs) and associated quasi-normal mode (QNM) calculations are used to model the post-merger behaviour.

Each of these four approaches has its own natural domain of applicability. Due to its computational cost NR is limited to a relatively low number of orbits before merger and to systems with comparable masses. The weak-field approximation of PN theory limits its application to the early inspiral, while GSF theory is at its best when dealing with binaries with relatively disparate mass-ratios. The post-merger phase of binaries containing a BH can be modelled with black hole perturbation theory (BHPT). As illustrated in Fig. 1, the natural domains of applicability of the four first-principle approaches to the relativistic two-body problem are largely complementary, and building waveforms for LISA will require input from all four — sometimes for modelling a single source. Effective waveform models like effective one-body (EOB) and the Phenom-family combine inputs from the different approaches to provide waveforms that can straddle these domains.
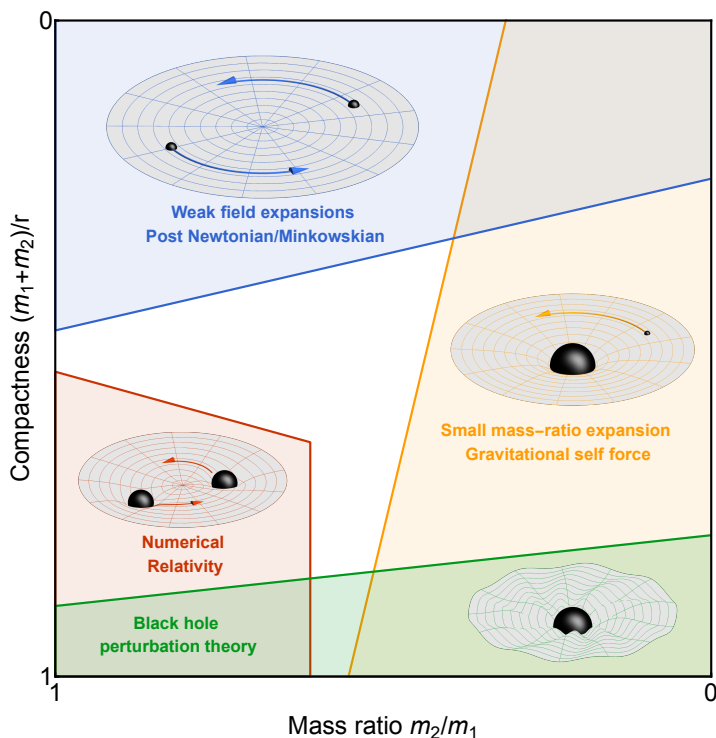
Figure 1. A sketch of the natural domains of applicability of the four main approaches to solving the relativistic two-body problem. The approaches are largely complementary and building waveforms for LISA will require input from all four. The solid lines shown are illustrative of the reach of each approach. The precise reach of each region depends on the source type and the accuracy requirements of the model. In addition, the Effective-One-Body and Phenomenological models absorb information from the four main approaches to produce more global models that can compute waveforms sourced by binaries across large portions of the parameter space.

The LISA Waveform Working Group (WavWG) serves as an interface between the LISA Science Group — tasked with realizing LISA's scientific mission — and the wider scientific community developing waveform models and studying the relativistic two-body problem. It serves to prioritize waveform development, inform the wider community of LISA's waveform modelling needs, and as a recruiting pool for waveform related tasks and projects in the LISA Science Group.

In this white paper, the WavWG discusses the current status of waveform modelling and what further development is needed in realize LISA's science. It is organized in five main sections. In §2 we take a brief inventory of the sources LISA is expected to observe along with their expected parameters. This sets the primary goals for waveform model accuracy and parameter space coverage. §3 discusses what requirements LISA data analysis puts on waveform models in terms of accuracy, efficiency, and format. The main approaches to modelling waveforms from compact binaries are described in §4, discussing both their status to date, and challenges to be overcome to meet LISA's waveform requirements. §5 discusses methods for accelerating the production of waveform models.

Finally, §6 covers the modeling for beyond GR, beyond Standard Model, and cosmic strings sources. We note that while stochastic signals are of considerable interest, this paper does not address them as the focus here is on individual detectable sources. For the reader's convenience, we have provided a table of notation used throughout the paper in Table 1 and a list of commonly used acronyms on the page proceeding this introduction.

---

2. LISA Sources

LISA will be sensitive to a wide range of GW sources in the mHz regime. In this section, we take an inventory of anticipated sources that need to be modelled to extract useful scientific results *and* are well-enough understood at this stage to be modelled in some detail. A more extensive survey of LISA's expected sources and the science that can be done with them can be found in the whitepaper produced by the LISA Astrophysics Working Group [3]. The short summaries here mainly focus on the expected parameter ranges to provide a context for the modelling approaches discussed in the rest of the white paper. Conventional long-lived astronomical sources include massive black hole binaries (MBHBs), extreme mass-ratio inspirals (EMRIs), intermediate mass-ratio inspirals (IMRIs), Galactic binaries (GBs) and stellar-origin black hole binaries (SOBHBs). These sections (2.1– 2.5) present LISA sources in GR and the Standard Model. Theoretically interesting but empirically speculative sources include cosmic strings (CSs) and sources based on physics beyond GR and beyond the Standard Model are discussed in Secs. 2.6 and 2.7.

A key metric for the detectability of sources is their signal-to-noise ratio (SNR). This is defined via the standard formula

$$\text{SNR}^2 = 4 \int \frac{|h(f)|^2}{S_n(f)} df, \tag{1}$$

where $h(f)$ is the GW strain and $S_n(f)$ the noise power spectral density of the detector [4, 5]. Unless otherwise stated this is computed for an observation period of up to 4 years.

2.1. Massive black hole binaries (MBHBs)

Coordinator: Enrico Barausse
Contributors: M. Bonetti, J. Garcia-Bellido

2.1.1. Description In the local Universe, MBHs are observed in the centers of virtually all massive galaxies [6, 7], as well as in many low mass dwarf galaxies [8–10]. Their cosmic evolution is inextricably intertwined with that of their host galaxies. The latter provide MBHs with gas out of which they grow by accretion (thereby shining as quasars or active galactic nucleis (AGNs)), and MBHs influence the evolution of their hosts by injecting energy into their surroundings (AGN feedback) [11–13]. This co-evolution of MBHs and galaxies is reflected in the scaling relations between MBH mass and galactic properties [14–19], although the detailed physical processes leading to their emergence are still not fully understood.

Present day galaxies/dark matter haloes are believed to have formed hierarchically from the merger of smaller systems. Likewise, "seed" MBHs are expected to inhabit at least

a fraction of the high redshift progenitors of today's galaxies (see [20] for a review). These seed BHs are expected to grow by a combination of gas accretion and mergers [21–27]. Their coalescences, as well as those of the later generations of MBHs that they give rise to, are indeed a prime target for LISA [28–32].

By detecting MBH mergers, LISA could confirm or disprove this hierarchical scenario for the evolution of MBHs. Indeed, considerable uncertainties exist about the timescale on which MBHs form a bound binary and eventually coalesce, after two galaxies have merged. The main uncertainty is whether MBH pairs can efficiently make their way from separations of hundreds of pc down to the sub-pc scales on which gravitational waves dominate the dynamics [31, 33–45]. First dynamical friction and then stellar and/or gaseous hardening are the main drivers of the evolution of MBHs on their path to coalescence. Triple or quadruple MBH interactions, which naturally arise in models where the evolution of MBH pairs/binaries is slow or even stalls [46–48], should in any case ensure LISA detection rates of at least a few per year [31, 46]. Conversely, the observed detection rate will inform us about the efficiency with which MBH binaries come together and merge in nature [31], even though that information may be partly degenerate with the number of MBH seeds formed at high redshift. In that respect, it is worth pointing out the possibility that there may be massive primordial black holes (PBH) formed during the radiation era that may act as seeds for the MBH population [49, 50]. In that case, MBH mergers could occur at much higher redshift.

2.1.2. Expected source parameters Further information on the underlying astrophysics can be gained by measuring the parameters of MBH binaries. Measurements of the component masses will allow for constraining the initial mass function of the seed black holes at high redshift [28–31, 51]. Indeed, the latter may form as relatively low-mass black holes ($\sim 100 - 1000 M_\odot$), e.g. from the collapse of the first generation of stars [52], or they may be born already as higher mass seeds of $\sim 10^4 - 10^5 M_\odot$ (e.g. from the collapse of massive quasi-stars [53], runaway instabilities in stellar clusters [54, 55], instabilities of protogalactic disks [21], etc.). Spin measurements, together with mass measurements, will clarify the properties of the accretion process and its importance in the evolution of MBHs relative to mergers [56–58]. Measurements of distance will allow for placing the detected system at the right epoch in the history of the universe. Further help in this respect will naturally be provided by sufficiently accurate/precise sky localization, which might allow for the identification of an electromagnetic counterpart; and, therefore, a direct measurement of photometric or spectroscopic redshift [59, 60]. In the presence of independent redshift and distance measurements, one may even attempt to construct a GW-based cosmography, potentially measuring the Hubble constant or the density of matter/dark energy in our universe [59]. Finally, measurements of the eccentricity and mass ratio will provide insight on the mechanism driving MBH pairs to separations at which GW emission is enough to lead to a merger within a Hubble time [31, 46].

In more detail, current expectations on the parameters of MBHBs and their seeds from astrophysical models are generally as follows:

- Source frame total masses range from a few 10^2 to a few $10^8 M_\odot$, with possible peaks around 10^3 and $10^5 M_\odot$ for respectively light and heavy seed formation in some models. See, e.g., Fig. 2 of Ref. [31].

- Comparable mass binaries with mass ratio $\epsilon \equiv m_2/m_1$ between 0.1 and 1 are expected to make up the bulk of LISA detections, although tails extending down to $\epsilon \sim$ a few $\times 10^{-3}$ may be present (cf. Fig. 3 of [31]).

- Large uncertainties generally affect the prediction for spin magnitudes and orientations. Moderate to large spins $\gtrsim 0.7$ are expected in models calibrated to electromagnetic measurements (i.e. iron Kα) of MBH spins in local AGNs [58], but the spins of the first generations of MBH mergers are relatively unknown. Similarly, spins may be approximately parallel at the peak of the star formation $z \sim 2 - 3$, where gas torques may align them with the orbital angular momentum to within $10 - 30$ degrees [61], but the situation may be different at higher and lower redshift.

- Eccentricity may be very significant and evolving in the LISA window ($e > 0.9$ upon entrance into the LISA band and up to 0.1 at plunge) if triple/quadruple MBH interactions are more efficient than gas and stellar interactions to drive the binary's evolution at $\sim$pc scales [46].

- Event rates and SNRs can vary significantly according to the underpinning astrophysical model [30, 31, 51]: in light seed scenarios rates may be as low as a few per year, especially if feedback from supernova explosions is included [31], which results in most events having small total masses and thus low SNRs (below 100). More generally, the number of light seed detections may be threshold limited [31, 46]. This is again especially true if supernova feedback is included, as most events have SNRs of a few tens in that case. In heavy seed scenarios, instead, irrespective of whether supernova feedback is included or not, rates and SNRs tend to be larger, i.e. roughly a few tens of detections in 4 yr and SNRs up to several thousands.

- Environmental effects from gas and stars have negligible impact in the LISA observation window [62], although they might leave a recognizable imprint in the eccentricity distribution of detected events [63]. The same applies to MBH triple/quadruple interactions, which are expected to cause the aforementioned very high "relic" eccentricity when the binaries enter the LISA band [46].

- When delays between galaxy and MBH mergers are accounted for, the highest number of detections is expected around $z \sim 2 - 4$ [31].

In addition to the large parameter space described above, waveform templates for MBHBs will also need to accurately represent the waveform for many hundreds or thousands of cycles before merger — see, e.g., Fig. 16 of Ref. [60].

Parameter	Notation	Astrophysically relevant range
Total mass in the detector frame	M	$10^5 - 10^7 M_\odot$
Mass ratio (> 1)	q	$1 - 10$
Dimensionless spin	$\max|\chi_i|$	$0 - 0.998$
Eccentricity entering LISA band	e_{init}	$0 - 0.99$
Eccentricity at last stable orbit	e_{merge}	< 0.1
Signal to noise ratio	SNR	$10 - 10^4$

Table 3. Summary of the anticipated parameters for LISA MBHB sources. The total mass of a massive binary in the source frame ranges from $10^2 - 10^8 M_\odot$ while moving to the detector frame picks up a factor of ~ 10 giving the range $10^3 - 10^9 M_\odot$. This is squeezed on both ends by another factor of 10 (SNR and LISA band constrain the low and high limits respectively) giving a possible range of $10^4 - 10^8 M_\odot$ with the majority of sources expected between $10^5 - 10^7 M_\odot$ [31]. The mass ratio, q is expected to range from $1-1000$, again with the majority of sources expected to be in the $1-10$ range [31].

2.2. Extreme mass-ratio inspirals (EMRIs)

Coordinator: Huan Yang
Contributors: S. Akcay, P. Amaro Seoane, S. Bernuzzi, J. Gair, A. Heffernan, T. Hinderer, S. A. Hughes, S. Isoyama, G. Lukes-Gerakopoulos, A. Nagar, Z. Pan, Z. Sam, C. F. Sopuerta, V. Witzany

2.2.1. Description

EMRIs are binaries in which one member is substantially more massive than the other. The canonical EMRI is expected to be a stellar mass compact body (typically a black hole of 10–$100\,M_\odot$) captured by a BH of 10^5–$10^7\,M_\odot$ by multibody scattering processes in the core of a galaxy [64]. EMRIs can also form via the capture of other compact objects such as neutron stars or white dwarfs, though the small mass of these objects reduces their detectability with LISA [65]. A consequence of the large mass-ratio of EMRIs is the quite slow inspiral of the smaller body, executing 10^4–10^5 of orbits as it moves through the black hole's strong field [66, 67]. Binaries involving a MBH orbited by a substellar object, such as a brown dwarf, are called extremely-large mass-ratio inspirals (XMRIs) and these are potential LISA sources if they form around the MBH in the centre of the Milky Way [68]. Measuring the gravitational waves generated by the strong-field orbits of E/XMRIs will make it possible to map the properties of massive black holes with great precision [69, 70].

2.2.2. Expected source parameters

The expected LISA detection rate of EMRIs depends on several astrophysical ingredients [69], including the mass/spin function of MBHs at different redshifts, the fraction of MBHs living in stellar cusps, stellar-mass compact objects (COs) capture rate per MBH, the characteristic mass of stellar-mass COs and their orbit eccentricities. The mass function of MBHs is usually modelled as a power law $dn/d\log M = n_0 \, (M/3 \times 10^6 M_\odot)^{\pm 0.3}$ [57, 71], with n being the MBH number density and $n_0 \in (0.002, 0.005)\,\mathrm{Mpc}^{-3}$. MBHs can be extremely spinning with

$a \approx 0.998$, slowly spinning with $\chi_1 \approx 0$ or of an extending spin distribution in the range $0 \leq \chi_1 \leq 1$, depending on their growth channels (accretion and/or mergers) [58, 72, 73]. The fraction of MBHs living in stellar cusps is determined by how frequently MBHs merge, when the stellar cusps are destroyed, and their regrowth time after mergers. COs in stellar cusps captured by MBHs generically reside in low angular momentum orbits with large eccentricities, which subsequently decay to the range of $0 < e < 0.2$ at the final plunge [69]. The capture rate depends on the cusp relaxation time and the density profile of the cusp [74]. Taking into account of all these uncertainties with semi-analytic models, Babak *et al.* [69] forecasted that there will be several to thousands of EMRIs detected by LISA per year, assuming the contributing COs are BHs with mass 10 or 30 $M_\odot$, and a detection threshold of SNR = 20. On the other hand, recent rate studies predicted that accretion disk-assisted EMRI formation may be more common for LISA detection [75, 76], thanks to the high efficiency of disks in transporting stellar-mass black holes towards galaxy centers. These disk-assisted EMRIs tend to have negligible eccentricity comparing to the EMRIs formed by gravitational capture.

For XMRIs their extremely slow evolution means they will spend millions of years in the LISA band. Although the event rate of an XMRI forming is quite low, their long duration in band means in the Galactic centre there could be a few dozen sources, some of which may be highly eccentric. Due to the short distance between the centre of the Galaxy and the solar system, the SNRs can range from 10 to 10^4 [68].

2.2.3. Science with EMRIs Constraining model parameters of EMRIs from their GW signals benefits from the large number of cycles completed in the LISA band [69, 73, 77–79]: all intrinsic parameters of an EMRI (the redshifted masses, the MBH spin magnitude, and the CO orbit eccentricity at plunge) can be measured with fractional uncertainty $\sim 10^{-6} - 10^{-4}$; external parameters are mainly determined by the GW amplitude and its modulation with time, where the luminosity distance $D_{\rm L}$, the source sky location $\Omega_{\rm s}$ and the MBH spin direction Ω_a can be measured with fractional uncertainty $\sigma(\ln D_{\rm L}) \approx {\rm SNR}^{-1}$, median solid angle uncertainties $\sigma(\Omega_{\rm s}) \approx 0.05({\rm SNR}/100)^{-5/2}{\rm deg}^2$ and $\sigma(\Omega_{\rm a}) \approx 30\sigma(\Omega_{\rm s})$, respectively. In light of the source location constraints in both radial and transverse directions, a fraction of low-redshift EMRIs are expected to be traced back to their host galaxies without the aid of any electromagnetic counterparts [73].

To identify the nature of the secondary in an EMRI, in the case of a light black hole or a neutron star, the only potentially detectable parameter beyond its mass will be a component of its spin [80, 81]. For less compact objects, such as white dwarfs or brown dwarfs, there is a possibility of gaining some information about their tidal quadrupoles [82]. However, all of the parameters of the secondary beyond its mass may be poorly constrained and partially or wholly degenerate with parameters controlling other sub-leading effects.

Detection of EMRIs will provide critical information with which to understand the growth history of MBHs and their environment. Different growth mechanisms, i.e., via mergers and/or via gas accretion, predict significantly different mass and spin distribution for MBHs [56–58, 83]. With a population of EMRI events, the co-evolution of MBH masses and spins over cosmic time can be measured to further reveal how they are formed and how they grew [56–58, 73]. N-body calculations have shown that EMRI rates sensitively depend on stellar distribution at galactic centers, so that the rate inferred from observation will also be able to constrain various distribution models [69]. Environmental effects, including the interaction with possible accretion disk around the MBH and close stellar objects near the EMRI system, may induce sizeable phase shifts to the EMRI waveform [62, 84]. The accretion channel has illustrated that MBHs with AGNs will account for a significant number of EMRIs [76]. Estimates of the resulting GW phase correction vary over many orders of magnitude ($0.1 - 10^4$ rad / year), depending on the assumed disk model [85, 86]. Tidal resonances induced by the tidal field of nearby stars and stellar-mass black holes can generate a phase correction of $\mathcal{O}(1)$ in a significant fraction of the phase space [87]. The main uncertainty comes from the population of nearby stellar-mass objects, which may come from the (disk)-migrating stellar-mass objects in the AGN or leftovers from the previous AGN life cycle (Fig. 6 of [88]), or simply from the mass segregation effect ([89, 90]).

By precisely mapping the background spacetime geometry of a MBH [91], EMRIs can be used to check whether the Kerr metric description is accurate and GR holds in the strong-field regime [92]. At the innermost stable circular orbit (ISCO) of a typical MBH, the curvature scale is higher than Solar-system curvatures but lower than curvatures of some well-observed compact-binaries [93]. Consequently, modified gravities satisfying existing observational constraints generically predict very small deviations from GR in the standard EMRI scenario. However, since EMRIs are expected to be highly sensitive to small departures from the standard Kerr black hole background paradigm [94, 95], EMRIs will allow us to further tightly constrain any deviations caused by an additional scalar or vector channel for radiation in the long-term dissipation of energy and angular momentum [96]. In fact, even in the case where the field of the primary is just a generic stationary axisymmetric GR vacuum field, we should be able to determine the matter multipoles of the primary [97, 98] and check possible violations of the no-hair theorem [99], e.g., a deviation from the Kerr solution in the quadrupole moment [100].

In addition, as is true for all extragalactic LISA sources, various cosmological dispersion and propagation effects can be tightly constrained from EMRI signals, especially if the EMRI host galaxy is identified [96].

Parameter	Notation	Astrophysically relevant range
Total mass in the detector frame	M	$10^5 - 10^7 M_\odot$
Mass ratio (> 1)	q	$10^4 - 10^6$
Dimensionless spin	$\max|\chi_i|$	$0 - 0.998$
Eccentricity entering LISA band	e_{init}	$0 - 0.8$
Eccentricity at last stable orbit	e_{merge}	$0 - 0.2$
Signal to noise ratio	SNR	$20 - 100$

Table 4. Summary of the anticipated parameters for LISA EMRI sources. Total masses of $10^5 - 10^7 M_\odot$ will be seen by LISA [71] with those greater than $10^7 M_\odot$ starting outside the LISA band [64]. Regardless of formation channel, the smaller compact body is expected to be a stellar mass black hole giving an expected mass ratio of $10^4 - 10^6$ [69, 75], or even $10^4 - 10^7$ if neutron star EMRIs are included. Using MBH of $3 \times 10^6 M_\odot$ as a basis, the "loss-cone" EMRIs are expected to have high eccentricities, capped at ~ 0.8 entering the LISA band [101], while the accretion channel tends to have smaller eccentricities [76]. Evolving a large sample of compact bodies from capture results in a flat eccentricity distribution for the last stable orbit in the range $0 < e < 0.2$ [69]. A small tail of outlying higher eccentricities is possible. There is also the possibility of GW bursts from unbound / hyperbolic systems [102, 103]. Ref. [69] predicts the loudest EMRIs to have SNR ~ 100 per year.

2.3. Intermediate mass-ratio inspirals (IMRIs)

Coordinator: Carlos F. Sopuerta
Contributors: M. Dhesi, M. Hannam, T. Hinderer, D. Neilsen, H. Pfeiffer, H. Sundar, N. Warburton

2.3.1. Description An IMRI is a binary system with mass ratio in the range $10 \lesssim q \lesssim 10^4$ placing it between comparable mass binaries and EMRIs. IMRIs can come in two flavors, both of which contain an intermediate mass black hole (IMBH) with mass in the range 10^2-$10^4 M_\odot$. There is little observational evidence for BHs in the IMBH mass range, mainly because their main formation channel is inside globular clusters, the interiors of which are very difficult to observe [104]. However, recent GW observations with ground-based detectors have found a population of BHs formed from binary black hole (BBH) mergers with a total mass greater than $10^2 M_\odot$ [105, 106]. The largest observed remnant (of GW190521) has a mass of $\sim 150 M_\odot$ [107, 108]. At the other end of the mass range, we have evidence of BHs with masses in the range 10^4-$10^5 M_\odot$ from observations of dwarf galaxies out to redshift ~ 2.4 [109, 110]. These may correspond to an interpolation of the mass function observed for low MBH mass [9].

The two flavors in which IMRIs are expected to appear are: (i) Light IMRIs. A stellar-origin black hole (SOBH), or another sufficiently massive and compact object, inspiraling into an IMBH. For instance, dwarf galaxies or globular clusters may contain an IMBH which could capture an SOBH [111]. In this case, it is quite likely that the merger occurs outside the LISA frequency band, at higher frequencies. It is thus possible that an IMRI can be observed during its inspiral with LISA and have its merger seen by

ground-based GW observatories (only for light IMBHs, with mass $\lesssim 10^3\,M_\odot$ [112]). (ii) Heavy IMRIs. Dynamical friction can produce the orbital decay of globular clusters into a galactic nucleus allowing the formation of an IMBH–MBH binary system, with the MBH in the LISA mass range (10^5-$10^7 M_\odot$) [113, 114]. Another possible channel to form heavy IMRIs is the merger of a dwarf galaxy satellite with its main galaxy [115]. A third possibility is the formation of an IMBH in a galactic nuclei via hierarchical mergers [116] via migration traps in AGN [117]. Interestingly, GW190521 may have occurred in such an environment [118].

For more information on possible formation channels, and the uncertain event rates for these binaries, see the LISA Astrophysics Working Group White Paper [3] and [119–121], or the IMRI reviews [64, 119, 122]. The nature of the different formation channels for IMRIs (both light and heavy) may lead to distinct IMRI dynamics so that LISA detections may shed some light on what are the most viable formation scenarios.

2.3.2. Science with IMRIs As we only have evidence for IMBHs at the two ends of the mass range that defines these objects, the search for IMRIs with LISA is especially relevant with huge discovery potential. Event rates and parameter estimates for IMRIs can provide valuable information about the formation and growth of IMBHs in globular clusters, as well as details of stellar dynamics in those systems. This information is often difficult to glean from electromagnetic observations [104].

For heavy IMRIs the masses and spin of the MBH can be measured to within an relative error of a fraction of a percent [123]. Unlike EMRIs, where the spin on the secondary can be difficult to constrain [124, 125], the spin of the IMBH can be constrained to within $\sim 10\%$ [123]. IMRIs spend a long time orbiting in the strong field and due to their high SNR (relative to EMRIs) this makes then uniquely precise probes of GR and the Kerr hypothesis [126]. They can also be sensitive to modifications to Einstein's equations of GR, such as modified gravity, extra fields, and extra dimensions [127, 128].

Finally, *multiband* GW astronomy observations of light IMRIs consisting of observing the inspiral in the LISA detector and the merger in ground-based detectors [129–132] offers a range of increased science potential [121, 133, 134]. In particular, observing the inspiral with LISA can place tight constraints on the sky location and the merger time which can allow for targeted alerts for electromagnetic counterparts to the merger. Conversely, knowledge of the source parameters from ground-based observations of the merger can allow researchers to perform targeted searches for IMRIs in the archived LISA data [135]. Multiband observations can also enhance the potential for performing tests of GR by breaking degeneracies between some parameters in the waveform models [136].

Parameter	Notation	Heavy IMRIs	Light IMRIs
Binary mass	M	$10^4 - 10^7 M_\odot$	$10^2 - 10^4 M_\odot$
Mass ratio (> 1)	q	$10 - 10^4$	$10 - 10^4$
Dimensionless spin	$\max|\chi_i|$	$0 - 0.998$	$0 - 0.998$
Eccentricity entering LISA band	e_{init}	$0 - 0.9995$	$0 - 0.9995$
Eccentricity at last stable orbit or leaving LISA band	e_{merge}	$0 - 0.9$	$0 - 0.9$
Signal to noise ratio	SNR	$10 - 10^2$	$10 - 10^3$

Table 5. Summary of the anticipated parameters for LISA IMRI sources. By defintion, light IMRIs' primary BH is from $10^2 M_\odot$ to $10^4 M_\odot$, i.e., an IMBH, while heavy IMRIs' primary BH is a MBH [3]. Again the definition of an IMRI has a mass ratio from comparable (10^2) up to 10^5, above which the binary is defined as an EMRI. Eccentricity can be quite high for both light and heavy IMRIs entering the LISA band [119]. SNRs are taken from Table 9 of the Astrophysics Working Group White Paper [3]. Although this table represents the best knowledge for each individual parameter, further restrictions of the IMRI parameter space may be possible by combining SNR information with astrophysical knowledge.

2.4. Galactic Binaries (GBs)

Coordinator: Milton Ruiz
Contributors: V. Korol, H. Lim, V. Paschalidis, S. L. Shapiro, A. Tsokaros

2.4.1. Description   Our Galaxy is home to a variety of stellar binaries formed by white dwarfs, neutron stars, and black holes. Approximately a million years before their anticipated merger, these compact binaries transition into the millihertz GW frequency band accessible with LISA. Given such long evolution timescales, these systems will manifest as nearly-monochromatic sources of gravitational waves. Furthermore, these compact binaries will be detectable in large numbers by LISA, potentially emerging as the most numerous GW source within the millihertz band [137].

Galactic compact binaries represent a key source class for the LISA mission. Firstly, their existence as GW sources is confirmed, as several have already been identified and characterised with electromagnetic telescopes (see [138] for overview). Gravitational radiation from some of these known sources has already been measured indirectly by monitoring binary orbital contraction over extended periods [139–141]. Secondly, as we can anticipate their GW signatures before the mission, these binaries have been suggested as "verification sources" for LISA (e.g. [142]). Most notably, Galactic compact object binaries accessible to LISA promise a wealth of insights into stellar and binary evolution. This encompasses understanding the nature of compact objects, unravelling the physical processes that govern binary interactions, and exploring their role in the formation and evolution of the Milky Way – see the LISA Astrophysics white paper [3] for a review. Finally, it is noteworthy that a substantial portion of these binaries will not be individually resolvable by LISA, contributing to an unresolved stochastic foreground that will act as an additional source of noise for the instrument. Therefore, accurate

characterization of this foreground is crucial to ensuring the precise characterization of other LISA sources.

Here we consider Galactic double compact objects, which we refer to as GBs, specifically those where at least one component is a compact object other than a black hole (binaries with two stellar origin black holes are treated in the next section). These can be categorised into various subtypes: binary white dwarfs (BWDs), with the subset of accreting BWDs, known as AM Canum Venaticorum or AM CVns in literature; binary neutron stars (BNSs); and mixed systems. The mixed systems encompass white dwarf-neutron stars (WDNSs), which can emerge as ultra-compact X-ray binarys (UCXBs) in electromagnetic radiation, white dwarf-black holes (WDBHs), and binary black hole-neutron stars (BHNSs).

2.4.2. Masses, mass-ratios, eccentricities, and known LISA verification sources   Observing GB using electromagnetic observatories poses a significant challenge due to their inherently small size and dimness (in some cases the entire absence of electromagnetic emissions). These features, when combined with selection effects and incompleteness of dedicated electromagnetic surveys, has limited our ability to know the true distributions of their parameters such as orbital separations, component masses, mass ratios, and eccentricities. Thus, much of our understanding of these binaries primarily hinges upon population synthesis studies. However, electromagnetic observations using Sloan Digital Sky Survey (SDSS) and Gaia have recently improved our understanding [137, 143, 144]

Binary population synthesis studies (e.g., Table 6 in [3]) show that for frequencies less than approximately 2 mHz, the BWDs form an unresolved foreground for LISA (see also [145–148]). Binaries with frequencies greater than approximately 2 mHz and/or closer than a few kpc do not overlap with this background [3, 145, 149] and are called "resolvable". However, not all resolvable GBs are detectable, and unresolved GBs can also be detectable. Only binary systems with a significant SNR may be detected by LISA within a 4-year mission. Theoretical estimates suggest that among the hundreds of millions of binaries in the Galaxy, the number of resolvable binaries are about 6,000-10,000 BWDs, 100-300 WDNSs, 2-100 BNSs, 0-3 WDBHs and 0-20 BHNSs [3]. However, the number of detectable binaries above the noise are about 6000 BWDs, 100 WDNSs, 30 BNSs, 3 WDBHs and 3 BHNSs [150].

The chirp mass, a key distinctive parameter among compact binary classes, varies significantly across different binary systems. For instance, BWDs typically peak at a chirp mass of around $0.25M_\odot$ (e.g. [151]), while BNS tend to have a chirp mass around $1.2M_\odot$ [152]. Systems comprising BHs and neutron stars (NSs) exhibit even higher chirp masses. However, it is important to note that LISA's limited ability to measure frequency derivatives for $f < 2$ mHz, and thus the chirp mass may introduce potential classification ambiguities. For example, a nearby BWD system may be misidentified as a more distant BNS. Another discriminative feature could be

the eccentricity measurements [152, 153]. BWDs, typically formed via isolated binary evolution, are expected to be circularised due to recurrent mass transfer episodes. Contrastingly, BNS systems detectable in the LISA band might present measurable eccentricities due to natal kicks imparted by the supernova explosions that birth the NSs. Nevertheless, some rare eccentric BWD can form in globular clusters or via triple interactions (e.g. [154]).

There are approximately 30 GBs, identified through electromagnetic detection, that have been confirmed as resolvable verification targets for the LISA mission. Notably, 16 of these are expected to be detectable within merely three months of scientific operations, proving invaluable in the early stages of the mission by assisting in the validation of LISA's performance relative to pre-launch expectations. These GBs are characterised by orbital periods ranging from ~ 300 to ~ 6000 seconds, equivalent to GW frequencies approximately between 0.5 and 6 mHz. Their total mass typically lies between 0.5 to $1.0 M_\odot$, with mass ratios roughly between 0.1 and 0.7. Their estimated SNRs can exceed 100 after four years of integration [155].

Certain types of binaries can be sources of low and high frequencies, and hence can straddle both the LISA and ground-based detector bands. This is true for mixed binaries when unstable mass transfer leads to merger. Gravitational waves from the inspiral and merger of WDNSs may go from LISA to ground-based from potential oscillations of the NS after merger and/or its eventual collapse to a BH [156–158]. The same straddling of LISA/ground-based frequency bands holds for stellar-mass black hole binaries [134].

2.4.3. Modeling requirements & methods to improve/remove the Galactic background
GBs can be classified as detached or interacting (mass-transferring), depending on whether significant mass transfer occurs between the components. This classification is crucial for modelling their GW signals accurately. Although these systems are practically monochromatic to first order, the frequency does evolve with time. In particular, there is a difference in how the frequency evolves for detached binaries and interacting binaries. The orbital evolution of detached binaries is driven by the emission of gravitational waves, causing a gradual inward spiral of the binary (manifested as a negative frequency derivative in the GW signal). On the other hand, in accreting binaries, the redistribution of mass between the components results in an increase in their separation (leading to a positive frequency derivative in the GW signal) [156, 159]. This leads to different requirements for waveform modelling. Note also that the shortest period binaries can be tidally-locked and corotating [160]. For binaries near the Roche separation, tidal effects may have a non-negligible contribution to the phase evolution of the wave [161, 162]. Understanding the frequency evolution will help determine if mass transfer is taking place [163] and/or tidal interactions are at play. A large number of mass-transferring systems may constrain the physics of mass transfer and the efficiency of angular momentum removal from the disk/companion system and its reinjection back into the orbit [156].

Some of the GW sources that LISA will observe may be part of triple or higher-order multiple systems (e.g. [164, 165]). This includes sources in the Galactic disc that form through isolated triple evolution, as well as those in dense environments. When a BWD system — as the most common Galactic LISA source — is part of a larger system with an additional stellar or even a substellar object, the gravitational interaction with the substellar object introduces a modulation in the observed GW frequency due to the Doppler effect. This is a consequence of the motion of the BWD around the centre of mass of the three-body system. As the orbit of the tertiary must be larger than that of the inner binary for the system to remain stable, the modulation timescale will be longer than the GW frequency produced by the inner BWD. However, to detect this modulation with LISA, it should also be shorter than the mission's lifetime [166–168].

Signals from many GBs will be below the BWD confusion background, which is generated both by detached and interaction/mass-transferring BWDs. Efforts have been made to remove this background in order to resolve more binaries (see e.g. [169–172]). Notice that the modeling of this confusion background may provide insight about the BWD population in the Milky Way (and nearby satellite galaxies).

Parameter	Notation	BWD	WDNS	BNS
Total Chirp Mass	M	$0.1 - 1 M_\odot$	$0.4 - 1.2 M_\odot$	$1.1 - 1.6 M_\odot$
Mass Ratio (> 1)	q	$1 - 10$	$1 - 5$	$1 - 1.6$
Eccentricity in LISA band	e_{init}	0	$0 - 1$	$0 - 1$
Signal to Noise Ratio	SNR	< 1000	< 1000	< 1000

Table 6. Summary of the anticipated parameters for LISA GB sources. BWDs can have a chirp mass between $0.1 - 1 M_\odot$ [173], mass ratios of $1 - 10$ (which can reach 100 for AM CVns systems) and spins ranging from seconds to hours [174, 175]. WDNSs and BNSs will have chrip masses in the range $0.4 - 1.2 M_\odot$ [176] and $1.1 - 1.6 M_\odot$ [177, 178] respectively. These binaries involving a pulsar have spins from seconds down to milliseconds [179] and near any eccentricity [152, 177]. As these sources are considered nearly monochomatic in the LISA band, their eccentricity is expected to evolve only a negligable amount inband.

2.5. Stellar origin black hole binaries (SOBHBs)

Coordinators: Antoine Klein and Ilya Mandel
Contributor: D. Gerosa

2.5.1. Description Stellar origin BH binaries are BBHs with component masses ranging from a few solar masses up to about $\sim$ 50-100$M_\odot$, where models of pair-instability supernovae predict a mass gap to appear [180–182]. Those systems are in a mass range such that they can be observed by both LISA and by ground-based detectors, as they sweep through a few decades in frequency during the last stage of their inspiral. This broad coverage of the GW frequency spectrum makes it possible to probe the evolutionary history of such binaries [134, 183].

A circular BBH with two 45 M$_\odot$ components will merge in about 10 years from a GW frequency of $\sim$ 10 mHz [134, 184]. It is thus possible to track its evolution from the LISA band to the ground-based detector band, taking advantage of LISA's ability to better measure some of the system properties at low frequency and the improved measurements of parameters such as the remnant spin (estimated from the post-merger ringdown) from high-frequency data. Of particular interest for LISA is the sky localisation capability, which is generally quite limited for BBHs in current ground-based detector data [185]. The long duration of observations in the LISA band means that the detector will complete multiple orbits around the Sun, and thus effectively act as an instrument with a baseline of order the size of the orbit. The accuracy of sky localisation can be estimated as [183]

$$\sigma_\theta \sim 0.025 \frac{0.01 \text{Hz}}{f} \frac{8}{\text{SNR}} \frac{\text{AU}}{\text{baseline}}, \tag{2}$$

where the GW frequency f should be replaced by the detector bandwidth for a source that evolves out of the band during the observation, and SNR is the signal-to-noise ratio. For a 2 AU baseline, this would yield sub-degree localization, though the exact localization accuracy would depend on the source location in the orbital plane. Another example could involve the measurements of BH spins and spin-orbit misalignments, which store information about formation scenarios [116, 186–189]. While we may expect that high-frequency ground-based observations are best suited to measure mass ratios and spin-orbit couplings, which enter the waveform at higher orders in the orbital frequency, LIGO-Virgo-KAGRA Collaboration (LVK) observations to date have demonstrated the challenge of making such measurements precisely [106]. LISA could observe $\gtrsim 10^5$ orbital cycles and therefore possibly place more precise constraints.

Beyond individual sources, LISA could track changes in the source population as binaries evolve in frequency. For example, LVK observations indicate that the majority of black holes in merging BBHs have masses $\lesssim 40M_\odot$ [190], low to moderate spins [191–193], and most have circularized by the time of merger [194]. On the other hand, LISA could observe BBHs while they are still eccentric, which would likely indicate dynamical

formation [195, 196]. The appearance of sources at higher frequencies would on its own indicate high birth eccentricity [197].

Another possibility worth mentioning is the detectability of a third body, particularly a massive black hole (MBH), through its impact on the binary's GW signature. Nuclear clusters around an MBH have been proposed as a possible BBH merger site, with possible assistance from gas in an active galactic nucleus [117, 198, 199]. Ref. [183] argued that even when the orbital period of a binary of mass $M_{\rm bin}$ around an MBH of mass $M_{\rm MBH} \gg M_{\rm bin}$ is much longer than the observation duration $T_{\rm obs}$, the orbital acceleration of the binary due to the MBH could still be detectable provided the GW frequency $f_{\rm GW}$ exceeds

$$f_{\rm GW} \gtrsim 0.02\,{\rm Hz} \left(\frac{M_{\rm MBH}}{10^6\,M_\odot} \right)^{-1} \left(\frac{a}{\rm pc} \right)^2 \left(\frac{T_{\rm obs}}{5{\rm yr}} \right)^{-2} \left(\frac{\rm SNR}{8} \right)^{-1}, \qquad (3)$$

where a is the distance from the binary to the MBH. A BBH merger in a massive globular cluster of a similar mass could carry a comparable signature.

2.5.2. Expected source parameters Judging by evidence from ground-based observations, the majority of BBHs observed so far have chirp masses between 5 and $\sim 40 M_\odot$ [190], though BH masses could extend down to the maximum neutron star mass and up to the IMBH mass range, especially if hierarchical mergers in dense dynamical environments fill the mass gap from pair-instability supernovae [116, 200, 201]. LISA will be particularly sensitive to more massive BBHs.

Most observed BBHs have mass ratios $q \lesssim 3.3$, which is consistent with the bulk of model predictions, but systems with more extreme mass ratios are possible, such as GW190814, which involved a 23 $M_\odot$ BH and a $\sim 2.6 M_\odot$ companion [202]. As mentioned above, most observed BBHs have low to moderate companion spins, though it remains unclear whether this is a generic feature of stellar-mass BHs [203, 204]. Lastly, high eccentricities and generic spin-orbit misalignments could be a telltale sign of dynamical formation in dense stellar environments or in hierarchical triples (see Refs. [205, 206] for reviews of formation channels).

BBHs emit the bulk of their orbital energy above the LISA frequency band; therefore, moderate SNRs are expected except for fortuitously nearby sources [134]. The minimal SNR for detection of BBHs will be influenced by the technical challenges associated with searching for signals with a complicated morphology and many in-band cycles [207]. Furthermore, beyond an SNR threshold for detection, signals must also show evidence of frequency evolution in order for masses to be measurable, so that BBHs can be identified among the much larger population of signals from double white dwarfs [152].

Parameter	Notation	range for majority of sources
Chirp Mass	M	5–40
Mass Ratio (> 1)	q	1–3.3
Dimensionless Spin	$\max|\chi_i|$	0–0.3
Eccentricity entering LISA band	e_{init}	0–1
Eccentricity at last stable orbit	e_{merge}	out of band
Signal to Noise Ratio	SNR	< 50

Table 7. Summary of the anticipated parameters for LISA SOBHB sources. The most recent data release from LVK indicates a mass distribution of BBHs centred around $5 - 40 M_\odot$ [190], however their masses could theoretically extend down to neutron star mass ($2 M_\odot$) and up towards IMBH ($100 M_\odot$) [116, 182, 200, 201]. LVK observations also show a mass ratio and effective spin distribution between $1 - 1.33$ and $0 - 0.3$ respectively [190], with more extreme mass ratio binaries observed [202] and the possibility of higher spins theoretically possible [203, 204]. Sources that appear in the LISA band will fully circularise by the time they reach the LVK band, so LVK observations cannot constrain LISA band eccentricities, which depend on the still uncertain formation channels. If we consider a SNR threshold for detection of 12, then 98.7% of sources in an isotropic homogeneous Universe would have SNR < 50.

2.6. Cosmic strings

Coordinators: Barry Wardell
Contributors: D. Chernoff, J. Wachter

2.6.1. Description Strings are effectively one-dimensional stress energy sources. If a network of strings is generated at early times then it can have many cosmological consequences including the production of gravitational waves (see [208] for a general review) that are potentially observable by LISA. String sources postulated by Grand Unified Theories (GUTs) have been ruled out by observations of the CMB [209, 210]. However, String Theory suggests new sources —fundamental strings and D-branes wrapped on small dimensions— in the context of certain inflationary string theory scenarios [211–224]. Macroscopic cosmic strings (CSs) are created and stretched to superhorizon scales by inflation (see [225, 226] for a review). Extensions to the Standard Model that introduce new symmetry breakings in-between the GUT and electro-weak scale can also produce viable strings [227, 228].

Irrespective of the detailed microscopic origin, these CSs may evolve to generate a network with some common features: after the Universe enters its radiation dominated phase the long, horizon-crossing strings begin to collide, break, reconnect and form small, sub-horizon scale loops. All string elements are dynamical, radiating gravitational waves and possibly other quanta [229–237]. Isolated loops, for example, radiate their entire rest mass energy and eventually disappear. Together the string elements generate a stochastic GW background [238–260] and GW bursts [244, 246, 250, 251, 256, 257, 260–266]. Detection and measurement of the string-generated gravitational waves by LISA will be informative for cosmology and high energy physics (see the whitepaper from the

28

LISA Cosmology Working Group for a summary [267]).

The physics of CSs is sensitive to (1) the set of fields to which the string couples, (2) whether the strings are global or local, (3) the ratio of the characteristic string width to curvature scale. Here, we assume that the strings are minimally coupled (they interact with each other but only radiate gravitational waves), local and well-described in the classical limit by the Nambu-Goto action. We refer to this as the "minimally coupled-string network". There are additional possibilities but this defines a wide, interesting arena for this whitepaper.

Average properties of the minimally coupled string network are encapsulated in the Velocity One Scale (VOS) model [252, 268–270]. It turns out that all quantitative features depend primarily on the string tension μ_S, or $G\mu_S/c^2$ in dimensionless terms. In particular, the total density in string components is parametrically small when the tension is small.

The VOS model is a valuable guide for forecasting the observations LISA may make. For specific numerical estimates below we assume minimally coupled local strings and adopt the following secondary parameters: intercommutation probability ~ 1 (intersecting field theory strings break and reconnect with probability of order unity [271] whereas string theory strings do so with smaller probability [272]), number of string species 1 (multiple species exist in realistic string constructions, for a review see [225]), fraction ~ 0.2 of long length strings chopped into loops of size ~ 0.1 of the horizon (for review of the small and large components inferred from simulation see [267, 273]) and rate of gravitational energy loss $dE/dt = \Gamma G\mu_S^2 c$ implied by dimensionless parameter $\Gamma = 50$ [239, 255, 274, 275]. Broadly speaking, changes to these adopted secondary values do not qualitatively change the network properties predicted by the VOS model. Many network properties are *not* included in VOS and have not yet been addressed in simulations. For example, isolated loops should evolve under the force of radiative backreaction (see [276–279]) but that process is not included in current numerical simulations and so it is difficult to accurately incorporate into statistical descriptions. These model-dependent, as opposed to parameter-dependent, uncertainties are important systematic deficiencies in our understanding and hard to quantify.

2.6.2. Tension limits The most well-studied modern scenario involves Type IIB string theory and low tension strings produced at the end of brane inflation. Strings — not monopoles nor domain walls — are produced when a brane and anti-brane pair annihilate and initiate the Big Bang cosmology. The primary parameter, string tension, cannot currently be calculated a priori from theory. Instead we must turn to observations.

Empirical upper bounds on $G\mu_S/c^2$ have been derived from null results for experiments involving lensing [280–287], GW background and bursts [239, 244, 261, 262, 265, 288–297], pulsar timing [243, 245, 255, 258, 298–300], cosmic microwave background radiation

[209, 210, 301–311]. It has long been recognized [225] that all such bounds are model-dependent and typically involve observational and astrophysical uncertainties. Constraints from the CMB power spectrum rely on well-established gross properties of large-scale string networks and are relatively secure. Limits from optical lensing in fields of background galaxies rely on the theoretically well-understood deficit angle geometry of a string in spacetime but require a precise understanding of optical selection effects. Bounds from big bang nucleosynthesis rely on changes to the expansion rate from extra gravitational energy density but only constrain the strings formed prior to that epoch. Roughly speaking, these limits imply $G\mu_S/c^2 \lesssim 3 \times 10^{-8} - 3 \times 10^{-7}$ (see [244] for comparisons of limits). More stringent bounds on tension generally invoke additional assumptions [312]. Gravitational wave experiments [244, 266, 295, 313] can monitor the occurrence of bursts. In particular, the LVK set a bound $G\mu_S/c^2 \lesssim 4 \times 10^{-15}$ based on non-detection of assumed cusp-like bursts [314]. Long-term pulsar timing searches for a stochastic background have set the bound of $G\mu_S/c^2 \lesssim 1.5 \times 10^{-11}$ [255, 257, 258, 300]. In the future LISA may achieve limits as low as $G\mu_S \sim 10^{-17}$ for Nambu-Goto strings [267, 315].

2.6.3. Loop sources for LISA The VOS model for the minimally coupled string network generates a loop size distribution weighted towards small sizes [256]. For string tensions $G\mu_S/c^2 \ll 10^{-7}$ the string loops are the most important elements of the network for GW science [267]. Small tensions imply weak GW damping. The undamped string is a non-linear oscillator with a fundamental period $T = \ell/(2c)$ and frequency $f = 1/T$. The Fourier transform of its motion yields power in all harmonics nf for $n \geq 1$. A survey of the loop dynamics reveals large scale motions and distinctive small scale feature: cusps (infinitesimal bits of the string that move at the speed of light twice per fundamental period) and kinks (discontinuous changes of slope that perpetually circumnavigate the loop). Gravitational wave emission is sourced not only by the large scale oscillations but also by cusps and kinks. All long-lived loops are expected to possess cusps or kinks else they intercommute and produce kinks. Cusp-generated power decays with harmonic n asymptotically $\propto n^{-4/3}$, kink-generated power $\propto n^{-5/3}$ and kink-kink collisions $\propto n^{-2}$ [239, 261–263]. At high frequencies, cusps dominate if they are present. Conversely, the period-averaged area of the sky illuminated by gravitational radiation increases from cusps to kinks to large scale modes.

There are three scenarios for LISA detections. (1) Loop decay creates a stochastic GW background from a large number of unresolved sources [267]. (2) Specific cusp or kink containing sources produce bursts of emission that stand above the general background [316]. (3) A few nearby loops, possibly associated with the Galaxy, produce emission that is strong, smooth and always on [273, 317–319].

2.6.4. Science with Cosmic Strings (1) Interesting fundamental results are destined to emerge whether or not LISA detects evidence of gravitational radiation from strings. A

positive result for the stochastic background will allow the inference of the string tension; a negative result will provide upper limits on the tension of any string component that might be present [267]. If the network has a String Theory origin then either determination helps guide progress towards a realistic model scenario for String Theory that incorporates the Standard Model.

(2) A positive detection (either background, burst or nearby loop) is also fundamentally significant for cosmology because loops of macroscopic size are created during an epoch of inflation, supporting the inflationary paradigm [320–322]. The universe's precise inflationary scenario remains a profound problem for cosmology and for fundamental physics. The almost scale-invariant density perturbation spectrum predicted by inflation is strongly supported by cosmological observations, in particular the cosmic microwave background radiation [210].

A negative detection is also very informative. The production of string-like structures is a rather generic theoretical prediction whenever inflation does occur [228, 323]. A negative result might be explained if the strings are unstable and/or couple to additional fields that promote their decay. This sort of result will guide the search for models that allow such interactions.

2.7. Beyond GR and beyond Standard Model sources

Coordinator: Helvi Witek, Paolo Pani
Contributors: N. Afshordi, R. Benkel, G. Bozzola, R. Brito, A. Cárdenas-Avendaño, E. Maggio, M. Okounkova, V. Paschalidis, C. Sopuerta

2.7.1. Introduction

BHs and compact binaries, and their GW emission have tremendous potential to probe for new physics beyond the Standard Model in the strong-field, nonlinear regime of gravity. LISA is likely to detect loud sources, such as MBHBs and EMRIs, which will allow us to test the nature of BHs, the validity of GR in the strong-field, highly-dynamical regime of gravity, or the presence of additional fundamental fields with unprecedented precision. These observations can help us address fundamental questions such as [77, 92, 95, 324–326]: (i) What is the nature of dark matter, and how can BH detections with LISA aid the search for new particles? (ii) What is the nature of gravity? Are there new fundamental fields and GW polarizations, as predicted by some extensions of GR and of the Standard Model? (iii) How do gravitational waves propagate over cosmological distances? (iv) Are the massive objects observed at galactic centers consistent with the rotating BHs predicted by GR? (v) Do exotic compact objects other than BHs and neutron stars exist in the universe? This complex topic in the context of LISA science is discussed in depth in the White paper of LISA's Fundamental Physics Working Group [315]. Here we briefly summarize the most relevant sources for probing fundamental physics with LISA as a guide for the modelling of gravitational waveforms in GR and beyond.

2.7.2. Black holes and ultralight fields

2.7.2.1. Description Ultralight bosonic fields such as axions, axion-like particles or dark photons are predicted in several particle and theoretical physics models. A remarkable example is the string axiverse scenario, which predicts a multitude of axion-like particles emerging naturally from string theory compactifications [327]. These ultralight particles play a crucial role in diverse areas of physics and have been proposed (i) as a solution to the strong CP problem in quantum chromodynamics (QCD) [328], (ii) as compelling dark matter candidates [329, 330] and (iii) in cosmology [331]. Excitingly, we can employ BHs to search for (or constrain) ultralight bosons in a mass range that is complementary to traditional particle colliders or direct detection experiments [324, 332–336]. This surprising connection between BHs and particle physics is provided by the superradiant instability of BHs [332, 337–342]: low-frequency bosonic fields scatter off a rotating BH superradiantly, thereby extracting mass and angular momentum from the BH. Fields of mass-energy μ_B are efficiently confined in the vicinity of a BH with mass M if the gravitational coupling $M\mu_\mathrm{B} \lesssim 0.4$ [343–347], corresponding to $\mu_\mathrm{B} \lesssim 10^{-16}(M/10^6 M_\odot)\,\mathrm{eV}$. In this case they efficiently form a

bosonic condensate ("cloud") around the BH. An alternative formation scenario involves accretion of such ultra-light fields onto BHs [348, 349] in the same mass range. If the bosonic field is complex, this process gives rise to hairy BHs [350–353].

The details of the cloud's formation depends on the initial parameters such as the BH spin and the gravitational coupling between BH and bosonic field [354–356]. Once formed, the condensate dissipates by emitting a quasi-monochromatic GW signal [334–336, 354, 356–363]. The presence of boson clouds can also significantly affect the dynamics of binaries: for example, it increases the eccentricity of comparable mass BH binaries and yields a GW phase shift [364]; In EMRIs the GW signal is modified relative to the vacuum case [365–368], and the presence of a secondary BH yields resonances [369–372]. The detection of EMRIs can be used to infer the bosons' mass [373, 374]. "dragging" of the cloud [375], dynamical friction [376] or tidal effects [377].

2.7.2.2. Expected source parameters All "traditional" GW sources in the LISA band, including compact, comparable-mass BH binaries, EMRIs, and isolated spinning massive BHs, are potentially affected by bosonic clouds. Therefore, they are also good sources to act as cosmic laboratories for ultralight fields. Because the underlying mechanism only relies on the gravitational coupling, but is independent from the coupling of the bosons to the Standard Model of particle physics, they probe for all types of bosons, i.e., (pseudo-) scalars such as axion-like particles [327, 328], ultralight dark matter [329, 330], ultralight vector [378, 379] and tensor [363, 380] fields. LISA sources are particularly well suited for detecting or constraining ultra-light bosons in the mass range $\mu_{\rm B} \in [10^{-19}, 10^{-15}]$ eV [335, 336, 363, 381, 382] (and even wider for massive spin-2 fields [380]), and they are suited for multi-wavelength searches in combination with ground-based instruments [383].

2.7.3. Binary black holes as probes of the nature of gravity

2.7.3.1. Description Does GR, our Standard Model of gravity, truly describe gravitational phenomena at all scales? It is expected to break down at high-energy scales as signaled by the presence of singularities inside BHs or at the Big Bang. At these scales a more complete theory of quantum gravity is needed that consistently combines gravity and quantum mechanics. However, GR cannot be quantized with standard approaches and it is not renormalizable. Therefore, GR (or a quantized version thereof) is not a viable candidate for quantum gravity. While a complete theory of quantum gravity remains elusive, most candidates predict similar extensions to GR such as higher curvature corrections or (non-minimial) coupling to new fields. BHs provide an ideal probe to search for such beyond-GR theories because, e.g., the presence of additional fields may endow BHs with scalar hair (or "charges"), thus violating the no-hair theorems of GR [384, 385]. More specifically, new fundamental fields arise in

several low-energy effective field theories of gravity [326], e.g., in the low-energy limit of quantum gravity, in the Horndeski class of scalar-tensor theories, tensor-vector-scalar theories [386], and in theories with quadratic curvature corrections. Such fields also arise in extensions of the Standard Model of particle physics, e.g., electric fields in mini-charged dark matter [387], primordial magnetic monopoles [388], darkly charged dark-matter [389], and the aforementioned bosonic clouds formed around BHs due to the superradiant instability.

In comparable-mass compact binaries, the coalesence of such "hairy" BHs generates additional scalar radiation that accelerates the inspiral and yields a GW phase shift. Furthermore, new polarization channels can exist in modified gravity theories. The detection or absence of such extra polarizations will be an important probe for new physics. In addition to modifications to the background solutions and the GW emission, modified theories of gravity may also change the physical properties of the gravitational waves once they are emitted, e.g., by changing the dispersion relation, the polarization and the way they interact with matter and with the detector [86, 325]. As modifications to the propagation of gravitational waves accumulate with the distance traveled, and the capability to put constraints on the mass of the graviton (Compton GW wavelength) scales with the chirp mass, comparable-mass binaries are the mose effective systems for measuring these effects [92].

EMRIs will provide an excellent probe of the multipolar stucture of its primary object and, thus, test if the primary is consistent with the Kerr BH metric predicted by GR. GW measurements will reveal details of both the conservative (time-symmetric) and the dissipative (time-asymmetric) sectors of the gravitational theory. Additional degrees of freedom, such as dynamical scalar or vector fields, will introduce modifications to the motion of bodies, and additional sources of GW energy and angular momentum emission. Given that in most modified theories the gravitational field is described by a spin-2 metric tensor field and by additional fields [326], the interaction between matter and the new fields may give rise generally to an effective "fifth force", leading to deviations from the universality of free fall [390], or in other words, to violations of the "strong" equivalence principle. How well a beyond-GR theory may be constrained depends on the relative PN order at which the correction enters and on the dimensions of the extra couplings [96, 391, 392]. In particular, theories with higher-order curvature invariants, such as the Gauss–Bonnet invariant [393–395] or the Pontryagin density [396] can be better tested with IMRIs and EMRIs [119, 127, 397].

2.7.3.2. Expected source parameters Both MBHBs and EMRIs can be employed to test gravity and the nature of compact objects with LISA [315]. For example, with nearly equal-mass BHs, one can perform null tests with inspiral-merger-ringdown consistency and BH spectroscopy, as well as searching for specific deviations with parametrized inspiral and ringdown waveforms. The beyond-GR modifications in the modelling of these signals (including PN theory, BH perturbation theory, effective-one-body

approaches, and numerical relativity) are discussed in Sec. 6.

With EMRIs one can constrain the multipolar structure of the primary object's spacetime with exquisite precision, thus testing whether the primary object is consistent with the Kerr BH metric predicted in GR. The parametrization of the waveforms will depend on the type of test carried out. For instance, when testing the geometry of the dark objects inhabiting galactic centers assuming GR, the parameters would describe the deviations from Kerr, e.g., multipole moments, tidal parameters or post-Kerr parameters. On the other hand, when testing GR, the parameters would describe the modifications of GR, e.g., additional coupling constants, extra dimensions length scale or higher-order corrections.

With both types of sources one can search for novel radiation channels due to extra polarizations or additional charges present in beyond-GR theories.

2.7.4. Testing the Kerr-hypothesis: BH mimickers and echoes

2.7.4.1.   Description   Exotic compact objects (ECOs) are horizonless objects which are predicted in some quantum gravity extensions of GR [398–402] and in the presence of exotic matter fields in the context of GR [95, 403–405]. The theoretical motivations for ECOs are the regularity of their inner structure and the overcoming of semi-classical puzzles such as that of the information loss [406–408]. These ideas have inspired a plethora of models including gravastars [409, 410], boson stars [411–414], wormholes [415–417], fuzzballs [408, 418] and others [419–424].

ECOs are classified in terms of their compactness, reflectivity and possible extra degrees of freedom related to additional fields [95, 425]. Two important categories are [426]: *ultracompact objects*, whose exterior spacetime has a photon sphere, and *clean-photon-sphere objects* (ClePhOs), so compact that the round-trip time of the light between the photon sphere and the object's surface is longer than the instability timescale of photon orbits. If the remnant of a merger is an ultracompact object, the ringdown signal differs from the BH ringdown at early stages and is dominated by the modified QNMs of the object [427, 428]. Conversely if the remnant of the merger is a ClePhO, the prompt ringdown is nearly indistinguishable from that of a BH because it is excited at the light ring [429]. The details of the object's interior appear at late times in the form of a modulated train of GW echoes [429–434]. The time delay between echoes depends on the compactness of the object and/or the energy scale of new physics [435], whereas the amplitude is related to the reflectivity of the object [95].

Many of these ECOs could be ruled out based on theoretical grounds. Horizonless compact objects are affected by an ergoregion instability when spinning sufficiently fast [436–439]. The endpoint of the instability could be a slowly spinning ECO [332, 440] or dissipation within the object could lead to a stable remnant [441, 442]. Furthermore, ultracompact horizonless objects might be generically affected by a light-ring instability

at the nonlinear level [440, 443, 444]. Current and future GW detectors will constrain models of ECOs in almost all the regions of their parameter space [428, 445–447]. In particular, searching for echoes in the post-merger signal of MBHBs with LISA [448] will provide a clean smoking gun of deviations from the standard, "vacuum", BH prediction. Furthermore, EMRIs could constrain the reflectivity of the primary object to unprecedented levels [449].

2.7.5. Expected source parameters   The source parameters depend on the specific signal used to search for and constrain ECOs. The echo signal depends on the parameters of the remnant (in particular mass and spin), on its compactness, and especially on its effective reflectivity, which is zero for a classical BH [95, 450]. The reflectiviy can be generically a complex function of the frequency and of other remnant parameters. In an inspiral, besides the standard binary parameters, ECOs are characterized by anomalous multipole moments and nonvanishing tidal deformability, sharing in this case properties similar to those of BHs in modified gravity theories. In an EMRI, besides the different multipolar structure [451–462] and tidal deformability [463, 464] of the central object, a key parameter is again the (frequency-dependent) reflectivity [449].

3. Modelling requirements from data analysis

Ideally, waveform models should be infinitely accurate, evaluate instantly and be available in any format desired. In practice, none of these are achievable. The practical accuracy, efficiency and format requirements are set by the way LISA data is analyzed. This section starts with a brief overview of how LISA data analysis is expected to work. (For a more detailed description, see the LISA Data analysis whitepaper [465].) The remaining sections discuss how data analysis sets requirements on the accuracy, efficiency and formats of waveform models, providing the necessary framing for the discussion of waveform models in the rest of this whitepaper.

3.1. Data analysis for LISA

Contributor: Tyson Littenberg

The foundation of gravitational wave data analysis is rooted in the conceptual simplicity of the measurement: observing relative changes in the separation between a collection of "proof masses" in free fall due to leading-order perturbations in the underlying spacetime metric, which propagate (effectively) uninhibited through the Universe. This is in stark contrast to, for example, electromagnetic observations, where the photons' propagation from source to detector is influenced by intervening material (e.g., dispersion, scattering, absorption, reprocessing), and then undergoes complicated interactions with the instruments themselves (e.g., focusing optics, filters, diffraction, absorption by the detector) before registering as a signal. This is not to take away from the heroic effort and ingenuity required to develop the measurement system that is sensitive to the unfathomably small space-time perturbations themselves. However, given a detector that can achieve the necessary sensitivities, it is a tractable task to derive its response to incident gravitational waves from first principles.

As a result, GW data analysis methods have primarily developed around a *forward* problem, where the detector response is predicted from a hypothetical source and that predication is then tested against the data [466]. There are notable exceptions, particularly in some searches for unmodelled GW transients in ground-based interferometer data [467], which approach the analysis as an *inverse* problem, starting with the observed data and working backward to solve for the input signal.

Any analysis is only as good as the models that go into it. The phenomenal sensitivity, accuracy and precision of GW observations is not achievable without highly accurate, coherent models for the gravitational waveforms themselves (the focus of this whitepaper), as well as the detector response and noise characteristics.

Under the assumption that the noise is Gaussian, the likelihood that the hypothetical

model, parameterized by θ, would produce the observed data $\mathbf{d}$ is

$$p(\mathbf{d}|\theta) = \frac{1}{\sqrt{\det(2\pi\mathbf{C})}}e^{-\frac{1}{2}\mathbf{r}^\dagger\mathbf{C}^{-1}\mathbf{r}},\tag{4}$$

where $\mathbf{r} = \mathbf{d} - \sum_i \mathbf{h}_i$ is a vector of all residual data samples after the discrete GW signals $\mathbf{h}_i$ have been subtracted, $\mathbf{C}$ is the noise covariance matrix $C_{ij} \propto \langle n_i|n_j\rangle$, and $\mathbf{n}$ is noise such that, in the absence of any GW signals, $\mathbf{d} = \mathbf{n}$. The likelihood is testing whether the residual is consistent with the ansatz that, in the absence of discrete gravitational waves, the data is Gaussian characterized by $\mathbf{C}$. Note the emphasis on *discrete* gravitational waves – a stochastic background of GW signals appears in the data model as a "noise" term, which modifies $\mathbf{C}$ with particular covariances that set it apart from instrument noise. See [468] for a detailed look at how the likelihood is derived, simplifications that produce slightly different forms of the equation in the literature, and a unified treatment of discrete and stochastic signals.

Also note that Eq. (4) does not prescribe a representation of the data. The game, as it were, is to represent the data in a way that minimizes the number of non-zero components of $\mathbf{C}^{-1}$ and thereby minimize the computational cost of evaluating the likelihood. It is the case under the assumption of stationary noise (i.e. $\mathbf{C}$ is constant over the observation time) that the discrete Fourier transform diagonalizes $\mathbf{C}$, which is why much of the GW analysis literature is based in the Fourier domain. For LISA, due to the long duration signals expected, the assumption of stationary noise will be dubious at best, and so analysis methods may trend towards other representations for the data (e.g., time-frequency methods with short Fourier transforms, discrete wavelet transforms, etc.), but the fundamental likelihood function remains the same.

The closest analog to the LISA analysis of individual sources is found in the analysis of ground-based interferometer data from the LVK collaboration, which are heavily reliant on waveform models. There are two major differences between LVK and LISA that limits the applicability of the analogy. First: At current detector sensitivities, the rate of detectable sources is such that they are still sparsely distributed through the data, with typical signals present in the most sensitive frequency band of the detectors for $O(10 \text{ s})$ at a rate of $O(\text{a few/week})$. LISA, on the other hand, will be signal-dominated, with tens of thousands of continuous Galactic sources overpowering the instrument noise below $O(3 \text{ mHz})$ and, depending on the rate and mass distribution of massive black hole mergers, several extremely high SNR mergers in band for $O(\text{weeks})$ to $O(\text{months})$, overwhelming any other contributions to the data stream. Thus, whereas the LVK searches are primarily "data mining" endeavors, sifting through a large volume of noisy data for rare and comparatively weak signals, LISA's primary challenges are twofold: Source confusion due to the large number of sources simultaneously detectable; and model accuracy due to both the large number of waveform cycles over which models must stay phase coherent, and to contend with such high SNRs so as to not contaminate lower-amplitude sources with residual power.

The second key difference between the LVK collaboration and LISA experiences is the volume of the parameter space itself. Ground-based searches for compact mergers span a mass range for the components of O(1-100) $M_\odot$. While challenging, this mass range is small enough that precomputed grids of template waveforms covering the parameter space can be used when searching for candidates (see, e.g., [469]). The LISA parameter space for comparable-mass black hole mergers, for example, is several orders of magnitude larger, spanning $O(10^3 - 10^8 \text{ M}_\odot)$, both eliminating the possibility of using grid-based methods and expanding the range of possible mass ratios encountered by the analysis. To date, the most successful prototype LISA analyses have used stochastic sampling algorithms [470–472], still relying on template waveforms but using data-driven methods to concentrate waveform calculations in the high-probability regions of parameter space. While LVK analysis of compact mergers is hierarchical, with clear distinction between the "search" and "parameter estimation" steps, those two functions blur together for many prototype LISA pipelines. Stochastic sampling algorithms put more pressure on the computational efficiency of waveform calculations, since template generation is part of the analysis pipeline itself, as opposed to pre-computing and then reusing a (large) table of waveforms generated on a fixed grid.

Note that while 3rd generation ground-based GW detectors will trend towards higher event rates, signal durations and signal strengths, the LISA forecasted maximum signal strengths are uniquely in excess of signal-to-noise ratios $\sim 10^4$ [473]. As a result, while the continued improvement of ground-based detectors and analysis methods naturally leads to evolution of the waveform models that directly benefit analysis of LISA data, the waveform development for 3rd generation detectors is necessary but not sufficient to fully achieve LISA's potential. LISA puts unique pressure on the accuracy, breadth of parameter space and computational efficiency of waveform models.

It is also worth considering that the signal-processing part of the LISA science ground segment is divided between two paradigms: the so called "low latency" and "global" analyses. The global analysis is the joint fit to all GW signals in the data, and it is here where waveform accuracy is most important, in order to prevent mismatches with loud signals from contaminating weaker signals that are simultaneously present in the data stream. The global analysis is computationally intensive, and having efficient waveform generation tools is necessary for it to be tractable. However, the global-fit processing speed is more forgiving than that of the low-latency analyses, since the goal is to produce thorough source catalogs with a relatively relaxed release schedule on a $O(\text{monthly})$ to $O(\text{yearly})$ cadence.

For the low-latency analysis the trade-off is inverted, as computational speed and localization information are prioritized over all else. The low-latency pipelines will run $\sim$daily, and will likely use a subset of the data (e.g. by bootstrapping based on the most recently completed analysis). The primary goal is to provide actionable information for joint multimessenger observations of transients. There are other functions of the low-latency pipelines, for example providing source-subtracted residuals to the instrument

team for assessment of detector performance etc., but under the purview of waveform generation time is of the essence. One thing to therefore consider at the architectural level of the waveform generation software is the need for tools that can be responsive to different demands on the speed/accuracy spectrum for processing sources, depending on the primary goal of the analysis.

3.2. Accuracy requirements

Coordinator: Deborah Ferguson and Maarten van de Meent
Contributors: M. Haney, R. O'Shaughnessy

Inaccuracies in waveform models affect the analysis of LISA data in three main ways. First, if the modelled waveforms do not sufficiently resemble the signals produced by Nature, this can hamper our ability to detect and identify sources in the data. Second, errors in the model will introduce some level of bias in the estimation of the source parameters, and could potentially masquerade as beyond-GR effects. Finally, if particularly loud sources are not perfectly subtracted from the data stream, their residuals can contaminate the searches for other sources. Below, we discuss the impact of these effects and how they lead to accuracy requirements for LISA waveform models.

3.2.1. Detection and identification

The impact of modeling errors on detection rates are fairly well understood in the case of a matched filter search for a single source in the data [474–476]. Suppose we have some waveform model, $h_{\mathrm{model}}(\vec{\lambda})$, depending on some set of parameters $\vec{\lambda}$, and we are looking for some true waveform h_{true} in the data, then the *fitting factor* is defined by

$$\mathcal{F} = \max_{\vec{\lambda}} \frac{\langle h_{\mathrm{true}} | h_{\mathrm{model}}(\vec{\lambda}) \rangle}{\langle h_{\mathrm{true}} | h_{\mathrm{true}} \rangle \langle h_{\mathrm{model}}(\vec{\lambda}) | h_{\mathrm{model}}(\vec{\lambda}) \rangle}, \tag{5}$$

where $\langle \cdot | \cdot \rangle$ is the usual noise weighted inner product,

$$\langle h_1 | h_2 \rangle = 4 \Re \int \frac{\bar{h}_1(f) h_2(f)}{S_n(f)} \mathrm{d}f, \tag{6}$$

with $S_n(f)$ the noise power spectral density of the detector [4, 5]. The fitting factor measures the effective loss in SNR due to using an imperfect model. Consequently, if the used models have a fitting factor $\mathcal{F}$ for a particular source, the maximum range at which such a source can be detected is reduced by a factor $\mathcal{F}$. Whether this has any impact on the detection rate depends on the type of source. Some LISA MBHBs sources are so loud that even the earliest (and therefore furthest) such events would be easily detectable [31], in which case the fitting factor of the used model has little to no effect on the detection rate. For other, quieter sources (such as EMRIs, SOBHBs, or GBs) the detection rate is more range limited, and a poor fitting factor $\mathcal{F}$ could lead to a reduction of the number of detections by a factor $\mathcal{F}^3$ (assuming a uniform

distribution of the source through a spatially flat universe). An appropriate norm for what degree of loss of sources is deemed admissible for achieving LISA's science goals needs to be established. An additional consideration here is that increasing the number of unresolved sources could adversely affect the searches for others sources such as any cosmological GW backgrounds [477, 478].

The above is valid for an idealized case, where the search is conducted using a continuous bank of templates. In practice, a search would use a discretized template bank, meaning that the effective fitting factor is increased due to the template spacing. Moreover, as noted in Section 3.1, a fully coherent search of the LISA data seems infeasible. Instead, LISA pipelines will most likely employ semi-coherent [479, 480] or stochastic [481, 482] search strategies. In a semi-coherent search, template and data are both partitioned into short segments, and the template–data overlap for each segment is maximized over several extrinsic parameters. Waveforms used in such a search need only to stay phase-coherent over the shorter segments. For example, it was shown in [480] that templates with $> 97\%$ overlap accuracy over $\gtrsim 10^6$ s will still be sufficient to detect $> 50\%$ of EMRIs detectable with fully coherent, precise templates.

3.2.2. Parameter estimation LISA parameter inference nominally involves a joint multi-source fit for all available sources in the data [483–486]. For the purposes of the discussion below, we approximate this process as independent parameter inference for individual sources, resolving the source from detector noise and the confusion noise of all other signals in the data. Within that context, the impact of waveform sytematics on parameter inference has been historically estimated using well-understood analytic techniques; see, e.g., [487, 488]. The most frequently used ingredients in analytic waveform standards are the match or *faithfulness* $\mathcal{M}$, which is the overlap between a signal h_{true} and template $h_{template}$ maximized over the coalescence time and phase of the template; the *Fisher matrix* $\langle \partial_a h(\lambda) | \partial_b h(\lambda) \rangle$; and the inner product $\langle \partial_a h | \delta h \rangle$ between derivatives of the waveform and residuals δh between two signal approximations. The simplest and most conservative waveform accuracy standards for parameter inference are expressed in terms of limits on the mismatch $1 - \mathcal{M}$, which nominally must be $\lesssim 1/SNR^2$ to avoid introducing systematic bias comparable to the statistical error *for a single source* [474, 475, 489]. For a population of sources, in principle systematic biases could stack in hierarchical population inference, and the most conservative threshold would be $1/(N_s SNR^2)$ where N_s is the typical number of sources [490, 491]. However, this threshold is likely to be much too conservative for many applications, as the impact of systematic errors may be much smaller than features in the source population; see, e.g., [1].

Because the impact of systematic biases depends strongly on the nature and scale of the bias relative to astrophysical features, general conclusions about systematic bias cannot be drawn, and (barring negligible systematic error) must be assessed for each science goal individually by performing hierarchical population inference. For example,

most SOBHBs in quasicircular orbits are in wide, relatively slowly-evolving orbits in the LISA band. For 90% of LISA-relevant SOBHBs (in population models consistent with current LVK observations), 2PN-accurate waveforms are sufficiently faithful for parameter estimation without biases [60]. At the other extreme, MBHBs will have extremely high amplitudes, with minute statistical error [484–486, 492]. Nominally, the very conservative accuracy thresholds described above would suggest a mismatch error target of order $1/(N_s SNR^2) \simeq O(1/(10 * (1000)^2)) \simeq 10^{-7}$, for statistical errors to be small compared to statistical errors for the recovered population of MBHBs [488]. This threshold may be needed for applications that require joint inference on all massive MBHBs (e.g., tests of general relativity), but can be dramatically relaxed for any astrophysical interpretation of the MBHB population. Further studies will be necessary to establish specific requirements on waveform accuracy for each context in which parameter estimation is critical.

3.2.3. Contamination Contamination effects occur when the residual from one source cannot be fully removed and impedes the interpretation of other, subdominant sources in the data. For such strong sources, systematic errors may be larger than statistical errors [488]. Though measurement error may have little impact on the astrophysical interpretation of the strong sources, the potentially substantial residuals produced by inaccurate models of their gravitational waves will introduce artifacts which contaminate downstream data analysis [483–486, 493]. For instance, for numerical relativity waveforms, insufficiently resolved grids can cause significant residuals even for simulations with precisely the same parameters as the observed signal [2]. The impact of errors arising from such imperfect modeling of strong sources can only be properly assessed with full joint hierarchical inference, using realistic models and contamination targets. Because of the diversity of sources that could be contaminated by residuals left by imperfect models for MBHB sources, much remains to be done to comprehensively assess key questions: How do modelling residuals from loud sources impact the detection and identification of other sources? Which sources are most affected? And what are the implications for the required modelling accuracy?

3.3. Efficiency considerations

Coordinator: Mark Hannam and Jonathan Thompson
Contributors: A. Chua and M. Katz

We shall discuss here the efficiency requirements imposed by search and inference for the two main classes of strong-field source that will be observable by LISA: MBHs and EMRIs. Relatively weaker-field sources such as GBs and SOBHs are a lesser concern; modeling of their signals (to the accuracy required for data analysis) is significantly easier, and computational cost is dominated by the need to attain a sampling resolution that is adequate for the typical duration, bandwidth and abundance of each source type.

Thus the efficiency requirements for these sources may be addressed on the analysis end with suitable approximations, or at the modeling–analysis interface where techniques such as those in Section 5 may be applied.

3.3.1. *Extreme-mass-ratio inspirals*

EMRIs are the only LISA sources that combine the issue of strong-field complexity with that of long-lived signals, and thus they pose great challenges for both waveform modeling and data analysis. The main problem in EMRI search is *information volume*: the space of LISA-observable EMRIs is gargantuan, requiring 10^{30}–10^{40} templates to cover in a naive grid-based search [479].‡ This is unfeasible regardless of waveform efficiency. One possible solution relies on semi-coherent filtering, which essentially returns less informative templates that cover larger regions in parameter space, allowing extensive searches to be performed in a viable amount of time. Assuming that computing performance in the 2030s lies around the 10^2-teraflop regime (achievable at present with $\sim 10^3$-node clusters), semi-coherent segments of $\lesssim 10^6$ s would enable the analysis to be completed over the mission lifetime [479].

In practice, EMRI search will probably use semi-coherent filtering within stochastic algorithms, rather than template banks. Thus the estimates in [479] are very conservative, as stochastic searches are generally far more efficient than grid-based searches at the same number of template evaluations, even with a large multiplier (e.g., repeated runs) to ensure proper coverage of the parameter space. Note, however, that a potentially large number of additional templates will be required in the assessment of detection significance for each candidate source, although it remains unclear whether such an assessment will eventually be performed in the search or inference stage.

The efficiency requirements for inference are more straightforward, in that the analysis algorithms will not differ too much from those used in LVK parameter estimation. An estimated 10^6–10^9 templates will be required per source posterior distribution. If we want to produce a posterior in less than 10 days we need waveforms that can be produced in $\lesssim$ 1ms. The estimated number of template evaluations per posterior also assumes that the prior regions for posterior sampling can be sufficiently localized to begin with; this is certainly possible in principle, but may require multiple search stages beforehand in a hierarchical approach.

3.3.2. *Massive black hole sources*

Generally, MBH sources are expected to be detectable for ∼week to hours prior to the merger. Due to this detection time frame and large signal-to-noise ratio of MBH binaries, coherent analysis over the full waveform template will most likely be employed for both search and parameter estimation. Therefore, from a waveform production perspective, these two analyses are roughly the same even if search and parameter estimation employ different schemes for achieving their various goals [494]. One way a search algorithm may differ from a parameter

‡ As a point of reference, banks of 10^5–10^8 templates are used to detect LVK BBH mergers [207].

estimation algorithm for MBHs, in terms of the waveform generation, is in the use of higher-order harmonics. Recent work [495, 496] has shown the importance of higher-order modes in parameter estimation for LISA. However, as detailed in [494], searching over the dominant harmonic may be acceptable for initially and roughly locating sources throughout the high-dimensional parameter space. With this said, this is a matter of adding or removing modes (that we assume are available in a model), not altering the fundamental waveform generation method.

Given this idea that the waveform generation is similar for both search and parameter estimation for MBHs, the following discusses how efficiency requirements relate to the stages of waveform creation. As discussed in Sec. 5.1, there are generally two main parts to waveform creation in the context of LISA: sparse, accurate waveform calculations and a scaling method to achieve a full waveform from the sparse information. MBH waveforms can be generated beginning with sparse calculations of the amplitude and phase for each harmonic mode with an accurate waveform model. Depending on the specific analysis type, these sparse calculations are then upsampled to the desired search or parameter estimation settings. Producing accurate and upsampled waveforms *directly* from the accurate waveform generator is unnecessary and time-consuming: various methods allow for the upsampling of sparse, smooth functions in an accurate and much more efficient manner. This construction leads to two different waveform generation efficiency requirements. The first is the overall waveform (including upsampling). With similar requirements to EMRIs given in the section above, we expect to collect at least $\sim 10^6$ MCMC samples for a given source posterior distribution. To accomplish this in ~ 10 days, we need to generate waveforms at a rate of $\sim /1$s on a single central processing unit (CPU) core.

The other efficiency requirement deals with the separation of the accurate waveform generation from the scaling operation. Generally, the scaling operation is the bottleneck for LISA where waveforms can have up to $\sim 10^6$–10^8 data points. Therefore, the requirement on the scaling part is that a waveform on a single CPU core be scaled in ~ 1 second or less. This condition, therefore, also sets the requirement for the accurate waveform portion assuming its sparsity prevents it from becoming the bottleneck. This requirement is that the sparsely sampled, accurate waveform must be of a similar or lower order of magnitude in timing when compared with the scaling operation.

3.4. Interface and data format requirements

Contributors: Tyson Littenberg

An additional key consideration for optimally supporting LISA analyses is the need for a flexible interface between waveform generation software and analysis pipelines. It is important for verification and validation of pipelines, and as a means for cross-checking results, to have independently developed algorithms targeting the same sources. (There

is also the added benefit of a constructive competition between development teams.) As per the previous discussion around Eq. (4), different analysis pipelines will likely be built around different representations of the data. Template generation is generally the computational bottleneck, and so it needs to be optimized for the application. At the same time, the benefits of having independent pipelines become liabilities if the analyses are not interfacing to the same waveform generation tools. As a result, it is of paramount importance that the waveform and pipeline development teams are collaborating early and often to avoid unnecessary or redundant transformations of the waveforms by the analysis pipelines (consider, e.g., a waveform that is initially computed in the time domain but then output in the Fourier domain, being called by an analysis pipeline that uses a discrete wavelet domain representation of the data).

The demand for flexibility of the waveform-analysis interface affects more than just the choice of a basis set used to represent the template. There have been promising developments in low-cost likelihood evaluations that use the instantaneous amplitude and phase of the template waveform, sampled on an adaptive grid, to concentrate computations to regions where the signal is changing most rapidly [494, 496]. Such considerations are difficult to retroactively incorporate in established template generation algorithms, but present opportunities for increased efficiency if they are part of the original waveform algorithm designs.

4. Modelling approaches for compact binaries

Detecting and inferring the parameters of compact binaries systems requires waveform template which, in turn, necessitates solving the relativistic two-body problem. Unlike in the Newtonian counterpart, it is not possible to only solve for the motion of the two bodies; one must solve for the dynamical evolution of the full spacetime. In general there are no known closed-form solutions to the nonlinear Einstein field equations for radiating binaries and so a variety of techniques have been developed to compute solutions either numerically or via perturbative expansions. The three main approaches that directly solve the Einstein field equations are numerical relativity (NR), post-Newtonian/Minkowskian (PN/PM) theory, and gravitational self-force (GSF).

Each of these approaches has strengths and weaknesses that leads them to being best employed in different regions of the binary configuration parameter space. Numerical Relativity directly solves the Einstein field equations to produce exact solutions up to numerical error. Post-Newtonian theory analytically computes relativistic corrections to the binary's motion and GW emission as a series expansion in powers of the orbital velocity as a fraction of the speed of light. The closely related post-Minkowskian approach expands field equations around flat Minkowski spacetime in powers of the gravitational constant without any restriction of the velocity of the binary. Gravitational self-force expands the Einstein field equations in powers of the (small) mass ratio. Fig. 2 gives a quantitive description of the strengths and weakness of each approach in the orbital separation – mass-ratio parameter space for non-spinning quasi-circular binaries.

In addition to the above approaches there are also effective frameworks that attempt to cover large portions of the parameter space. The physically motivated Effective-One-Body model takes inspiration from the solution to the Newtonian problem and describes the binary as the motion of a test body in spacetime of a deformed single black hole. Much progress can be made analytically with this approach by absorbing post-Newtonian and post-Minkowskian corrections, and further calibration can be applied using numerical results from the NR and GSF methods. The Phenomenological (Phenom) waveform models do not attempt to solve the relativistic two-body problem. Instead they aim to directly model the waveforms by building upon fast post-Newtonian models with further calibration from NR and GSF. The EOB and Phenom models are heavily used in analysis of GW data from current ground-based detectors.

In this section we outline the status of the above approaches and discuss the required development needed to reach the accuracy requirements outlined in Sec. 3.2. Concerns about the speed of waveform generation are addressed in Sec. 5. The status and requires for LISA of these approaches can be found in Sec. 4.1 for numerical relativity, Sec. 4.2 for weak-field post-Newtonian and post-Minkowskian expansions, Sec. 4.3 GSF, Sec. 4.5 for EOB, and Sec. 4.6 for Phenomenological models. These sections focus on modelling within GR; see Sec. 6 for a discussion on modelling in alternate theories of gravity.
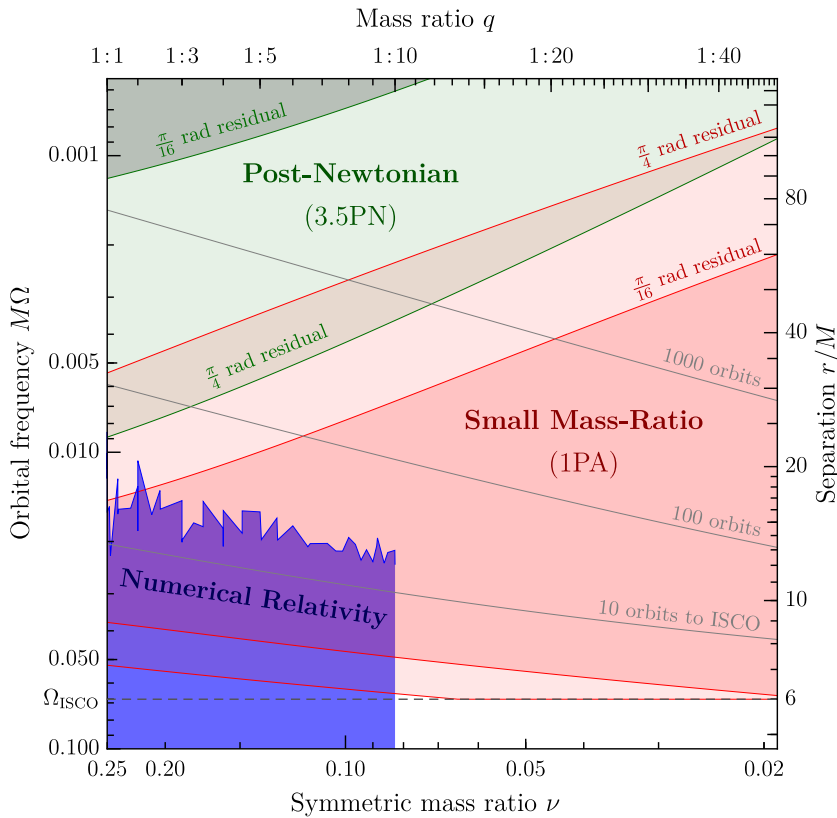
Figure 2. Region of applicability of different approximation techniques for non-spinning quasi-circular binary BH inspiral. The 1PA region is a prediction derived from fitting NR data to an expansion of the form (14). The shaded regions indicate ranges within which the cumulative orbital phase-error is less than $\pi/4$ and $\pi/16$ radians, respectively. Recent direct calculations of post-adiabatic (1PA) waveforms suggest the 1PA region shown is over-optimistic for $\nu > 0.1$, but they have borne out the prediction for $\nu < 0.1$ [497]. The gray lines show the location of binaries with 10 (resp. 100 and 1000) orbits left before they reach the ISCO. This figure is reproduced from Ref. [498].

4.1. Numerical relativity

Coordinators: Mekhi Dhesi, Deborah Ferguson, and Deirdre Shoemaker
Contributors: S. Bernuzzi, G. Bozzola, K. Clough, D. Ferguson, W. Gabella, M. Gracia, R. Haas, M. Hannam, E. Huerta, S. Husa, L. Kidder, P. Laguna, C. Lousto, G. Lovelace, D. Neilsen, V. Paschalidis, H. Pfeiffer, G. Pratten, H. Rüter, M. Ruiz, S. Shapiro, J. Thompson, A. Tsokaros, H. Witek, M. Zilhao

4.1.1. Description Numerical relativity solves Einstein's field equations through direct numerical integration on supercomputers (see e.g. the books [499–503]), providing the spacetime geometry and dynamics of the system in addition to the gravitational radiation emitted. Such solutions of the full nonlinear field equations without

approximations are critical to our understanding of highly dynamic regimes without symmetries, such as the late inspiral and merger of compact binaries.

The first steps at numerical solutions of Einstein's equations date back several decades [504, 505] and tremendous progress since then enabled the first simulations of inspiraling and merging binary black holes [506–508]. These breakthroughs initiated an explosive growth of the field, as illustrated, e.g. in the reviews [509–512]. By now, NR has become a critical part of the modeling the gravitational waves of the late inspiral and merger phase of coalescing binaries (e.g. [513–516]), which in turn underpins the analyses of all observed gravitational waves from coalescing binaries.

In order to solve Einstein's field equations, modern NR codes generally use the 3+1 approach [517, 518] in which the four-dimensional spacetime is sliced into three-dimensional hypersurfaces, and Einstein's equations are reformulated as a Cauchy problem with constraints. The first stage in numerically solving a compact binary inspiral is the construction of initial data, for which Einstein's constraint equations are reformulated as elliptic equations either in the context of the conformal-thin-sandwich formulation [519, 520] or the puncture approach [521]. The resulting coupled nonlinear partial differential equations are solved with custom-purpose elliptic solvers [522–524]. Numerous improvements over the years increased the generality of the physical conditions that can be achieved and the numerical quality of the solution, e.g. [525–529]. Moreover, entirely new codes were developed [530–534]. The time evolution is encoded in a set of coupled, hyperbolic partial differential equations with suitable gauge conditions and boundary conditions, where three main approaches have emerged: the generalized-harmonic formulation [535–537], the Baumgarte-Shapiro-Shibata-Nakamura formulation [538, 539] and different versions of the Z4 formulation of Einstein's equations [540–546] (see Table 8). Gravitational radiation must be propagated to future null infinity (see review [547]), which is often accomplished by extrapolation of GW modes extracted at finite radius [548, 549]. Alternatively, Cauchy-Characteristic Extraction [550–552] directly yields the waveforms at infinity, with improved recovery of non-oscillatory GW modes and GW memory effects [553]. Gauge conditions and transformations at future null infinity must be treated with care [554] to yield well-behaved numerical waveforms with well-defined waveform modes [555]. Cauchy codes have difficulty resolving the memory effect [515, 553]. Instead, most approaches to computing the memory effect use Cauchy NR waveforms (or NR calibrated waveform models) and the asymptotic Einstein equations to determine the unresolved memory effect in the Cauchy simulations that is required to satisfy Einstein's equations [556–561]. This approximate approach agrees with the Cauchy-Characteristic extracted waveforms, though comparisons over a wider range of the BBH parameter space would be useful.

Once BBH simulations became possible, the NR community quickly achieved many firsts, including the first simulations of unequal-mass BBH coalescences [562, 563], the first with spinning binaries [564], the first eccentric mergers [565] and first comparisons with PN calculations [566–569]. NR calculations of the merger revealed features of the

non-linear regime, among them that BHs with spins aligned with the orbital angular momentum merge at higher frequency [564], as well as the calculation of the recoil velocity imparted on the remnant BH [562, 563, 570]; in particular it was found that BH spins oriented approximately parallel to the orbital plane can lead to recoil velocities of several 1000's km/s [571–573].

Analysis of GW observations requires waveforms that cover the entire frequency band of the relevant detector at high accuracy. This has motivated large efforts to improve the accuracy of NR simulations [537, 569, 574, 575], length of the inspiral [513, 576], and coverage of increasingly large portions of parameter space in increasing detail. Parameter space exploration was initially performed through community-wide Numerical INJection Analysis (NINJA) [577, 578] and Numerical-Relativity-Analytical-Relativity (NRAR) [579] collaborations, which also yielded important cross-checks between different codes [579, 580]. Newer and more extensive parameter space surveys are listed in Table 8. Waveform models developed with NR information are described in Sec. 4.5 and 4.6. NR surrogate models [581, 582] are directly built on NR simulations, and are particularly important for the analysis of high-mass BBH systems like GW150921 [107, 108]. NR simulations can also be directly used for GW data-analysis, where they serve as synthetic signals [583] for quantifying the response of GW search and parameter-estimation pipelines [584, 585], and to conduct indirect analyses of observations [586–588].

NR also offers important information for the ringdown phase, characterized by an exponential decay as the remnant BH settles into a Kerr black hole. NR results determined the remnant parameters (mass, spin, recoil velocity) [582, 589–594]. Detailed NR calculations of the emitted gravitational waves during merger and ringdown yield the initial amplitudes and phases of quasi-normal ringdown modes and underpin theoretical studies of what information about nonlinear processes are accessible through the emitted gravitational waves [595], and how the ringdown phase can be used to test GR and to probe the no-hair and area theorems [596–603].

Due to our focus on the role of NR in the LISA mission, this section primarily covers vacuum spacetimes with a short discussion on environmental effects that include matter; the important work of NR with neutron stars is not included.

4.1.2. Suitable for what sources? The coalescence of BBHs is a primary source for LISA for a vast range of BH mass. Those BBH systems that merge in the LISA band require NR to produce the waveforms during the late inspiral and merger. In order to quantify the mass ranges that merge in the LISA band, we compute the masses for which the frequency of ringdown and inspiral are both in the LISA band. The dominant quasi-normal mode for a non-spinning black hole has a frequency of $f = 12.07 \text{mHz} \, (M/10^6 M_\odot)^{-1}$ [604], which will be within the LISA band for BH masses of roughly $10^4 - 10^8 M_\odot$. Turning to the inspiral, NR simulations of BBH typically cover a

few tens of orbits before merger, starting at GW frequencies of $f \sim 1\text{mHz} \, (M/10^6 M_\odot)^{-1}$, placing this part of the inspiral into LISA band for $10^3 - 10^7 M_\odot$. This estimate implies that BBHs of mass $10^4 - 10^8 M_\odot$ will have at least part of its waveform within coverage of NR. NR is capable of modeling these binaries for comparable mass ratios of less than 1:100.

NR simulations become increasingly costly with increasing mass-ratio and with very large spins, whereas there is only minor dependence of computational cost on other BBH parameters like spin-direction and orbital eccentricity. Parameter space coverage is improving over time. The next section describes what parameters NR currently covers and in Sec. 4.1.5 we discuss where efforts are needed to achieve complete coverage of the potential range of source parameters.

4.1.3. Status of the Field Since the breakthrough in NR in 2005/2006 [506–508] and the subsequent "gold-rush" to explore nonlinear phenomena in black hole and neutron star mergers, NR has now matured into a reliable tool for accurately computing gravitational waveforms needed to characterize GW data. In this section we briefly describe the landscape of current and future numerical relativity codes, their cross-validation and the parameter space coverage of currently available numerical waveforms.

The community has developed a number of successful NR codes that target a variety of goals for BBH spacetimes including covering increasing fractions of the parameter space (so far mostly comparable mass ratios and moderate spins), increasing number of GW cycles, accuracy of waveforms and interactions with matter. Table 8 provides a comprehensive list of currently available NR codes, some of which are briefly described in A. Their capabilities have been sufficient for the detection and characterization of GW signals with current ground-based GW detectors. However, data collected with future space- or next generation ground-based instruments will have a higher SNR and its interpretation requires much improved NR waveforms.

In particular, LISA sources present a formidable challenge to NR (see Sec. 4.1.5), both with regard to the characteristic features of the target BBH systems (e.g., high spins, large mass ratios, eccentric orbits, etc.) and the quality of the GW data due to, e.g., high signal-to-noise ratios and sources remaining in band for very long times. Computational simulations that meet the accuracy requirements for these demanding BBH configurations, for sufficiently long times, will require exascale computational resources. It will also require continued research in NR to develop new algorithms, computational techniques and software to tackle these challenges faced by existing code bases. Some new codes are under development, and they are included in Table 8.

Given the complexity of NR codes, cross-validation is an important component of code verification and it is by no means trivial that results obtained with different code bases agree. They employ, for example, different theoretical formulations of Einstein's equations for the evolution and initial data and different methods for the

Code	Open Source	Public catalog	Formulation	Hydro	Beyond GR
AMSS-NCKU [544, 605–607]	Y	–	BSSN/Z4c	–	Y
BAM [574, 608–610]	–	[516, 611, 612]	BSSN/Z4c	Y	–
BAMPS [613–615]	–	–	GHG	Y	–
COFFEE[616, 617]	Y	–	GCFE	–	Y
Dendro-GR [618, 619]	Y	–	BSSN/CCZ4	–	Y
Einstein Toolkit [620, 621]	Y	–	BSSN/Z4c	Y	Y
*Canuda [358, 359, 622]	Y	–	BSSN	–	Y
*IllinoisGRMHD [623]	Y	–	BSSN	Y	–
*LazEv [507, 624]	–	[625–628]	BSSN/CCZ4	–	–
*Lean [629, 630]	Partially	–	BSSN	–	Y
*MAYA [631]	–	[631]	BSSN	–	Y
*NRPy+ [632]	Y	–	BSSN	Y	–
*SphericalNR [633, 634]	–	–	spherical BSSN	Y	–
*Spritz [635, 636]	Y	–	BSSN	Y	–
*THC [637–639]	Y	[611]	BSSN/Z4c	Y	–
*WhiskyMHD [640]	–	[641]	BSSN	Y	–
ExaHyPE [642]	Y	–	CCZ4	Y	–
FIL[643]	–	–	BSSN/Z4c/CCZ4	Y	–
GR-Athena++ [644]	Y	–	Z4c	Y	–
GRChombo [645–647]	Y	–	BSSN/CCZ4	–	Y
HAD [648–650]	–	–	CCZ4	Y	Y
Illinois GRMHD [651, 652]	–	–	BSSN	Y	–
MANGA/NRPy+ [653]	Partially	–	BSSN	Y	–
BH@H/NRPy+ [632, 654]	–	–	BSSN	–	–
MHDuet [655, 656]	–	–	CCZ4	Y	Y
SACRA [657–661]	–	[662]	BSSN/Z4c	Y	Y
SACRA-SFS2D [663, 664]	–	–	BSSN/Z4c	Y	–
SpEC [515, 665]	–	[513, 515, 666]	GHG	Y	Y
SpECTRE [667, 668]	Y	–	GHG	Y	–
SPHINCS_BSSN [669]		–	BSSN	SPH	–

Table 8. List of numerical relativity codes. We indicate if a code is open-source, if it has been used to produce public gravitational waveform catalogs, the formulation of Einstein's equation used (GHG: generalized harmonic, BSSN: Baumgarte-Shapiro-Shibata-Nakamura, CCZ4 / Z4c variants of the Z4 formulation, GCFE: generalised conformal field equations), if a code implements general relativistic hydrodynamics, and if it is capable of simulating compact binaries beyond general relativity. An asterisk indicates codes that are either (partially) based on the open-source Einstein Toolkit or are co-funded by its grant. Note this table was created jointly for this paper and Ref. [512].

GW extraction. They also employ different numerical techniques (e.g, pseudo-spectral or high-order finite differences discretization) and numerical implementations, e.g., for the grid structure. First systematic code comparisons and studies on the integration of NR with data analysis and analytical approximations have been conducted in Refs. [577, 579, 580, 584, 670, 671]. For example, the NINJA project [577, 584] focused on building a NR data analysis framework and to develop first injection studies. The initial study presented a sample of 23 NR waveforms of BBHs with moderate mass ratios $q \lesssim 4$, considering only the dominant the $\ell = |m| = 2$ GW mode. The follow-up study increased to statistics to 60 NR waveforms. While no cross-validation between the NR waveforms were performed, NINJA was crucial to identify technical and conceptual issues, that a hybridization with PN or EOB may be needed and that more than only the dominant GW mode may be necessary. The Samurai project [580] conducted a detailed cross-validation of gravitational waveforms obtained with five different NR codes. It focused on one BBH system, namely an equal-mass, non-spinning, quasi-circular (eccentricity $\lesssim 0.0016$) binary completing about six orbits before their merger. Focusing on the dominant $\ell = |m| = 2$ multipole, it was found that the waveforms' amplitude and phase agree within numerical error. It was also found that these NR waveforms were indistinguishable for SNR ≤ 14 and would yield mismatches of $\lesssim 10^{-3}$ for binaries with $M \sim 60 M_{\odot}$ (using the anticipated detector noise curves at the time). The Numerical-Relativity–Analytical-Relativity (NRAR) collaboration [579] made important strides towards constructing more accurate inspiral-merger-ringdown waveforms by combining analytical and NR computations, and by defining new accuracy standards that would be needed for GW parameter estimation. The collaboration pushed cross-validation of NR codes to new frontiers by considering quasi-circular BBHs (with initial eccentricity $\leq 2 \cdot 10^{-3}$) with both unequal mass (up to $q \leq 3$) and moderately spinning BHs (up to $\chi_i \sim \pm 0.6$) completing about 20 GW cycles before merger. The study also included a binary of non-spinning BHs with $q = 10$, the highest mass ratio for quasi-circular binaries at the time. For the first time, the seven involved NR codes performed 22 targeted simulations to meet the required accuracy standards. They employed the same analysis code to estimate the uncertainties due to the numerical resolution and waveform extractions. The simulations exhibited a relative amplitude error in the $\ell = |m| = 2$ multipole of $\lesssim 1\%$ and a cumulative phase error of $\lesssim 0.25$rad. Finally, Ref. [671] presented a comparison of targeted simulations for the first GW event, GW150914, concluding that the waveforms were sufficiently accurate to effectively analyse LIGO data for comparable events. A comparison between different time evolution formulations of Einstein's equations, namely BSSN and Z4c, was performed in Refs. [544, 672].

The cross-validation studies between different NR codes have been crucial for building confidence in their results. As summarized above, they have been conducted in limited regions of parameter space (e.g., low mass ratios, some moderate spins, low eccentricity). As the demand on NR waveforms increases, such as covering a larger region of parameter space, including eccentric or spin-precessing BBHs, including higher

multipoles (typically up to $\ell = 8$) that are excited by asymmetric systems and further improving their accuracy, extended validation studies become important. With the technical and computational developments, the numerical data becomes more and more sensitive to mismatches, e.g., in the initial data, evolution or wave extraction. Therefore, a careful study of the initial data and initial parameters, of wave extraction techniques (e.g., extrapolation of waveforms extracted at finite radii vs. Cauchy characteristic extraction vs. Cauchy characteristic matching) or the choice of asymptotic Bondi-van der Burg-Metzner-Sachs frame will be needed [673].

The starting point for any simulation is the construction of constraint satisfying initial data. After decades of work (see, e.g., Refs. [521, 523, 525, 528, 674–678] and references therein), multiple codes are now capable of generating BBH initial data where the BHs are on a quasi-circular orbit or where the orbit has non-zero eccentricity.

Several groups worldwide have created public catalogs of BBH merger simulations with approximately $5,700$ waveforms available at the time of this writing [513, 515, 516, 625–628, 631]; see also Table 8. Nowadays, NR waveforms survey several configurations in the extensive BBH parameter space spanned by their mass ratios, spin magnitudes and directions, and eccentricity. Fig. 3 illustrates the portion of the parameter space covered by the publicly available waveforms at the time of this paper's publication. Focussing on quasi-circular binaries, it shows that the parameter space is best sampled for moderate mass ratios and spins.

Consequently, there are three dimensions in the BBH parameter space — spin, mass ratio and eccentricity — that require further waveform development. For example, most runs with spinning BHs concentrate on spins $\chi \lesssim 0.9$, because simulating BHs with spin closer to the extremal Kerr limit is technically challenging. It requires a much higher numerical resolution and, more importantly, the initial data is more difficult to construct. There are some codes capable of constructing initial data for BHs with spins above $\chi = 0.95$; see, e.g., Refs. [525, 679, 680]. Another challenging regime in BBH simulations is that of unequal mass binaries. Most simulations in the public catalogs cover the regime $q \lesssim 8$ for spinning BHs, and up to $q \lesssim 18$ for nonspinning binaries, as can be seen in Fig. 3. However, simulations above $q = 20$ are scarce: the first high-mass ratio simulations up to $q = 100$ [681] (see also [618]) and, more recently, up to $q = 1024$ [682] were achieved for head-on collisions. The frontier for quasi-circular inspirals are mass ratios of $q = 128$ [683, 684]. New techniques such as worldtube excision to model intermediate mass ratios of $q = 100\text{-}10^4$ are under development [685, 686].

Most NR simulations to-date have focused on quasi-circular inspirals because it is expected that any eccentricity present during a binary's formation will have been emitted through GW radiation when it close to merger [184]. However, there are several astrophysical scenarios that predict eccentric binaries [687–694]. The NR community is beginning to explore the eccentric parameter space [588, 628, 695–708] as well as hyperbolic encounters [709–712].
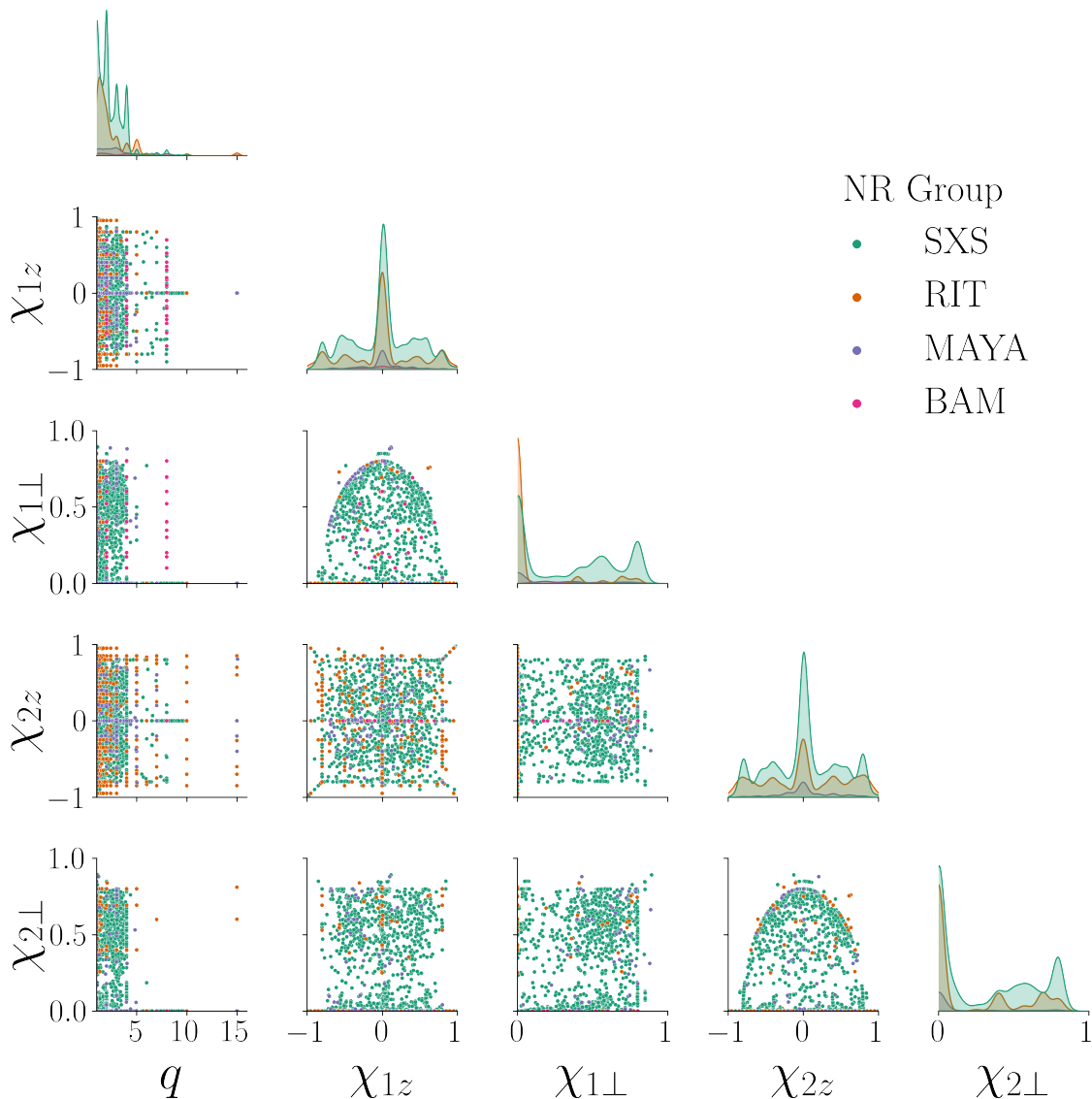
Figure 3. Parameter space coverage of public waveform catalogs in the quasi-circular limit. Shown are mass-ratio q, projections of the BH spins onto the orbital angular momentum ($\chi_{1/2\,z}$), and magnitude of spin-components orthogonal to the orbital angular momentum ($\chi_{1/2\,\perp}$) for waveform catalogs of different NR groups. Data as of June 2023.

Simulating eccentric binaries is challenging for a few reasons: (i) unlike in Newtonian gravity, there is no unique definition of eccentricity, and NR groups have explored different definitions [702, 713–716]; (ii) increasing the eccentricity to for a fixed separation requires that the BBH would have to start further and further apart to undergo several GW cycles before merger which yields higher numerical cost. Despite these challenges, eccentric NR runs are becoming increasingly available, although the parameter space in mass ratio and spin is not (yet) well sampled, particularly for precessing systems.

In summary, the BBH parameter space is currently covered as follows:

- Non-spinning BBH mergers with mass ratio $q \leq 18$ [513, 515, 578, 579, 625, 626, 631, 717] — see [683, 718] for binaries with mass ratios $q = 64, 100$, and 128.

- BBHs with moderate random spins and $q \leq 8$ [513, 516, 579, 625, 626, 631], aligned-spin binaries of $\chi \leq 0.85$ with $q \leq 18$ [514, 719], and a few with very high spins ($\chi \sim 0.99$) [575, 680, 720].

- Eccentric BBHs with $q \leq 10$ [588, 695, 699, 701].

Note that BBH simulations in GR are scale-invariant with respect to the total mass of the system; therefore, a BBH waveform can be re-scaled for both ground-based and space-based gravitational wave detectors without having to repeat the NR computation. However, the mass scaling will determine the physical starting frequency of the signal, and therefore whether the NR waveform covers the entire sensitivity band of the detector.

4.1.4. Environmental Effects The NR community has made great strides in simulating binaries in a matter-rich environment. This Whitepaper focuses on ways the environment directly impacts the predicted gravitational waves; for EM signatures of BBH mergers, we refer to the Astrophysics Working Group White Paper [3] and references therein.

The gravitational waves emitted during the merger of a BBH in an accretion disk are likely unaffected by the accreting matter [721], although Ref. [722] indicates that accretion disk densities greater than $10^6 - 10^7$ g cm^{-3} would alter the coalescence dynamics enough to be relevant for ground-based GW detectors.

In addition to EM counterparts, there are other possible sources for LISA modeled by NR. One such class of signals arises from the magnetorotational collapse of a supermassive stars; see, e.g., [723] for a recent review and [724] for early NR work. Recently the GW signatures from such collapsing supermassive stars were calculated in [725, 726], where it was shown that LISA could observe such events out to redshift $z \simeq 3$. Ref [726] also computed possible EM counterparts and predicted that these systems could be sources of very long gamma-ray bursts.

Another potential source of gravitational waves detectable by LISA that is currently unmodeled comes from instabilities in accretion disks around BHs. The particular case of the Papaloizou-Pringle instability [727] of self-gravitating disks has been studied in [728] without BH spin, and in [729] including spin. In [729] it was shown that BH spin could potentially increase the duration of the near monochromatic signal from the instability, and that LISA could detect gravitational waves generated by the Papaloizou-Pringle instability around $10^5 M_\odot$ BHs out to redshift $z \simeq 1$.

Finally, for a detailed discussion of environmental effects and the challenges they could present for precision tests of GR, such as dark matter environments, we refer the interested reader to the Fundamental Physics Whitepaper [315] and references therein.

4.1.5. Challenges in NR Improvements in hardware and numerical techniques continue to speed up simulations, yet some corners of the binary parameter space continue to demand challenging simulations that are costly in terms of runtime and computational resources. Three of the most pressing challenges facing NR are i) producing waveforms that cover the anticipated parameter space of unequal mass, highly spinning, and eccentric binaries, ii) producing long-lived waveforms with sufficient numbers of GW cycles, and iii) producing these waveforms at standards of accuracy set by LISA's sensitivity.

Parameter coverage: The BBH parameter space for the LISA mission, as summarized in Table (3) has mass ratios that span from 1:1 to 1:1000, BH spins from 0 to 0.998, and a wide range of eccentricities. As discussed in § 4.1.3, almost all NR simulations to date are for $q \leq 8$, $\chi \leq 0.8$ and $e \approx 0$; and, therefore, there is significant work to be done to supply waveforms that cover the full potential parameter space for LISA. We also discuss LISA waveform catalogs.

Producing waveforms for systems with large mass ratios is a challenge for the broader waveform community with various approaches existing to bridge the gap between NR solutions and small mass ratio approximations. This is especially relevant for IMRIs. High-mass ratios are demanding due to the need to resolve the smaller mass black hole and provide appropriate gauge conditions [684]. As discussed in § 4.1.3, several new codes are being developed by the NR community with the goal of having simulations with large mass ratios ($q > 50$) be routinely possible. In addition to pushing the NR capacity to larger mass ratios, new methods for modeling IMRIs are currently being explored [685, 730], which combine black-hole perturbation theory and NR techniques to significantly increase the numerical efficiency of simulations. Coordination between the GSF and NR communities as well as the construction of open source platforms to share NR [515, 625, 631] and GSF waveforms, such as the `Einstein Toolkit` [620] and the `Black Hole Perturbation Toolkit` [731], will streamline and accelerate such endeavors.

A second challenge is producing many generic simulations with BH spins that are very large in magnitude, i.e., approaching 1. The simplest approach to solving the initial data problem is to use the Bowen and York method [521, 732]; however, this method cannot construct BHs with high spins, $\chi \gtrsim 0.93$ [733–735]. In addition, resolving the region of spacetime near the horizons requires computationally expensive, very high resolution. This is exacerbated in evolution methods using excision to handle the singularities [575]. As mentioned previously, NR codes have successfully achieved some high spins, including several aligned-spin binaries with spins ($\chi \sim 0.99$) [575, 680, 720] by using new formulations that move beyond the conformally flat ansatz for puncture methods [528] and new techniques for handling the excision region [575].

Finally, several astrophysical scenarios produce non-zero eccentricity in the LISA

frequency band [736]. NR is capable of and has been producing eccentric runs [588, 695, 699, 701, 708, 737]; the challenge is simulations must start with the BHs more widely separated than in quasi-circular configurations. This is again a computational cost.

The source modeling community has continued to improve the modeling of these sources, developing more accurate inspiral-only models [738–742], and inspiral-merger-ringdown models that combine analytical approximations [743] with eccentric NR waveforms [588, 695, 700–706].

Gravitational wave cycles: Even after new NR codes attain the ability to simulate accurate, generic high mass ratios, advances in approximate methods will still be needed. LISA will observe BBH mergers for months or even years, and it is unrealistic (and unnecessary given the accuracy of approximate waveform models calibrated with NR [514, 581, 719, 744, 745]) to use NR to describe the entire evolution of binary systems, from inspiral to ringdown. Semi-analytic models of the inspiral-merger-ringdown have been very effective in ground-based GW astronomy, notably Effective-One-Body [746–751], Phenomenological [719, 744, 752–754] and surrogate models [582, 755–757]. Additionally, combining GSF methods to model the inspiral evolution with NR for the late-inspiral, merger and ringdown stages as described in [685] is a promising avenue of study.

Accuracy Massive BBH mergers in LISA could have high (on the order of 1000) signal-to-noise (SNR) ratios and NR must model these loud signals accurately enough not only to infer the correct source properties, but also to subtract the signal from LISA data, revealing quieter, high-interest signals that may lay underneath. The full implications of these requirements for NR waveform accuracy have yet to be assessed, but an initial study [2] suggests that NR waveforms will require a substantial increase in accuracy, compared to today's most accurate waveforms, to be indistinguishable from a high-SNR observation with the same source properties. A similar assessment for next-generation ground-based detectors concluded that NR waveforms will need an order of magnitude more accuracy to avoid bias in the inferred source properties for the high signal-to-noise sources that these detectors will observe [1]. The impact of using insufficiently accurate templates is highlighted in Figure 4.

These accuracy requirements are even more challenging for NR if the BHs are precessing, if one or both BHs are spinning nearly as rapidly as possible, or if one BH is much more massive than the other. Let us illustrate how quickly computational cost rises, by quantifying computational cost increases relative to a fiducial baseline simulation with mass-ratio q_0 and initial frequency $M\Omega_0$. Cost increases arise for multiple reasons.

First, the explicit evolution schemes used in NR codes are subject to the Courant-Friedrichs-Levy (CFL) condition, which limits the possible time step to the dynamic
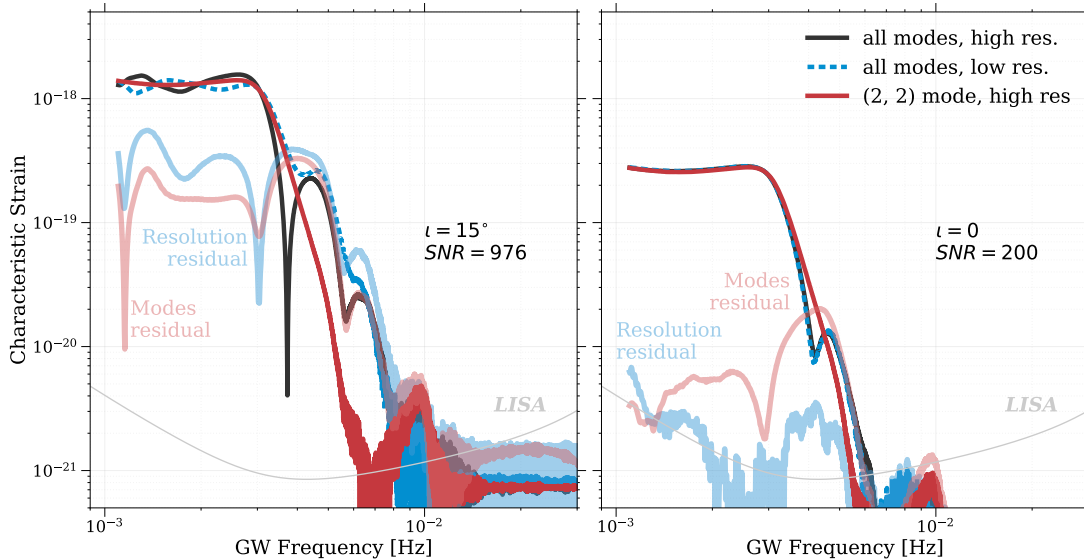
Figure 4. Illustration of how numerical errors in a template may leave a residual in high-SNR signals. The left panel represents a BBH at high SNR (detector mass $M_{\mathrm{det}} = 5 \times 10^6 M_\odot$, aligned spin of $\chi = 0.2$ on the larger BH at distance $D_L = 30\,\mathrm{Gpc}$ and at inclination $\iota = 15°$). The black line is the characteristic strain $(2f\tilde{h}(f))$ obtained at high numerical resolution from all spherical harmonic modes. The blue dashed line is the corresponding quantity obtained from a low resolution simulation, with the light blue line denoting the difference to the high-resolution waveform. The solid red line is a high resolution template containing only the $(l, m) = (2, 2)$ mode, with the light red line showing the difference to the black line. If this system were searched for with the low-resolution (or (2,2)-mode only) waveforms, then the shaded lines would remain as residuals after subtraction. The SNR of the residual due to resolution in the left panel is 342, clearly indicating the need for higher accuracy NR simulations. The right panel represents a more frequently expected system, where the SNR is 200 and $\iota = 0°$. Here, the residual due to resolution has an SNR of 2.4. Figure adapted from [2].

time of the smaller BH, $\Delta t \propto m_2$. As the mass ratio increases, the number of time-steps per unit $M = m_1 + m_2$ of evolution time will therefore increase as

$$f_{\mathrm{CFL}} \sim \frac{q}{q_0}. \tag{7}$$

Second, the total inspiral time of a BBH can be estimated by PN expansions [758] as $T \propto 1/\nu(M\Omega)^{-8/3}$, where $M\Omega$ is the initial dimensionless frequency of a binary. A change in mass ratio and initial frequency will modify the computational cost in proportion to T, i.e. by a factor

$$f_{\Omega_{\mathrm{low}}} = \left(\frac{\nu}{\nu_0}\right)^{-1} \left(\frac{\Omega}{\Omega_0}\right)^{-8/3}. \tag{8}$$

Thirdly, LISA has higher accuracy requirements than current NR simulations. We denote by $f_\tau(A)$ the increase in computational cost that is needed to reduce the truncation error τ by a factor $A > 1$, i.e. $\tau \to \tau/A$.

A fourth cause for increased computational cost arises from the desire of achieving a certain overall phase error, which is important for GW waveform modeling. For longer simulations, phase accuracy must be preserved over more cycles. From PN theory, the orbital phase to merger scales as $\Phi \propto \nu^{-1}(M\Omega_i)^{-5/3}$. To achieve a fixed overall phase-error (say, 1 radian), the relative phase error must decrease $\propto 1/\Phi$, yielding an increase in computational cost by a factor

$$f_\Phi \sim f_\tau \left(\left(\frac{\nu}{\nu_0} \right)^{-1} \left(\frac{\Omega}{\Omega_0} \right)^{-5/3} \right). \tag{9}$$

The challenge now is that in order to achieve higher mass ratio simulations starting at similar (or lower) initial frequency, and possibly also achieving higher accuracy, each of the factors just outlined increases very rapidly and that these factors multiply for an overall cost increase by a factor

$$C = f_{\mathrm{CFL}}\, f_{\Omega_{\mathrm{low}}}\, f_\tau\, f_\Phi. \tag{10}$$

To obtain concrete numerical estimates, we assume that f_τ is a power law, $f_\tau(A) = A^\alpha$. This assumption is satisfied for finite difference codes, where a convergence order of k in $(3+1)$ dimension yields $\alpha = 4/k$. In terms of α, the overall cost increase is given by

$$C \sim \left(\frac{q}{q_0} \right)^{2+\alpha} \left(\frac{\Omega_0}{\Omega} \right)^{8/3+5\alpha/3} A^\alpha, \tag{11}$$

where we have also used $\nu \approx 1/q$, which is valid at large q.

We can now make concrete estimates: Increasing the mass-ratio by a factor of 2, lowering the initial frequency by a factor of $1/2$, and increasing accuracy by a factor of 2, and assuming the NR code under consideration maintains perfect 8-th order convergence into the regime of longer, more accurate simulations at higher mass-ratio (i.e. $\alpha = 1/2$), increases the computational cost two orders of magnitude. More ambitiously, increasing the mass-ratio by a factor of 10, reducing initial frequency by a factor $1/4$ and increasing accuracy by a factor 10 increases the computational cost by five orders of magnitude. Codes based on spectral methods, e.g. SpEC, will likely result in a smaller f_τ; even so, increases in computational cost are very challenging as one goes to longer simulations at higher mass-ratio.

The NR codes that have been instrumental in providing public BBH waveforms use either a spectral method or box-in-box mesh refinement. These methods scale well to the order of 1000 cores, but they cannot scale to hundreds of thousands or millions of cores. For example, codes using high-order finite-difference stencils incur ever-increasing inter-core communication costs as the number of cores increases and this cost eventually becomes prohibitive. These codes are parallelization bound and do not parallelize beyond current usage. Since individual computer cores are no longer dramatically increasing in speed (Moore's law has moved from single core performance

into increasing the number of cores), it therefore seems unlikely that these codes will be able to simulate long BBH inspirals at mass-ratios significantly larger than 10. In the section on next-generation codes, we explore how this is being improved.

For a more general discussion on waveform accuracy, see § 3.2.

NR Catalogs The LISA data analysis groups could have access to NR waveforms via a bespoke LISA catalog or as a public catalog. A bespoke catalog would have NR waveforms created specifically to meet those aforementioned requirements, potentially interfacing and merging existing catalogs and extending with its own dedicated entries (similar to the LVK catalog [583]). If a bespoke LISA catalog is not created or deemed unnecessary due to a possible future abundance of NR public waveforms (current catalogs are indicated in Table 8) we will need a software interface with existing NR waveform catalogs that is curated and cultivated with time. A full catalog of NR waveforms achieving all requirements will take time, possibly until the launch of LISA. We put forth the following priorities for the NR waveforms: 1) an accuracy assessment of current and near-term achievable NR waveforms, 2) the assessment of current and near-term accessible parameter space, 3) the development of NR waveforms for the most likely LISA events at the required accuracy, 4) assessment of systematic bias in simulated LISA signals with currently available waveforms, and 5) the development of NR waveform for all potential parameters at the necessary accuracy.

4.2. Weak field approximations (post-Newtonian/post-Minkowskian)

Coordinator: Laura Bernard and Chris Kavanagh
Contributors: A. Antonelli, G. Faye, J. Garcia-Bellido, M. Haney, F. Larrouturou, A. Le
Tiec, O. Long

4.2.1. Description The PN formalism is an approximation method in GR that is
well suited to describe the orbital motion of—and the GW emission from—binary
systems of compact objects, in a regime where the typical orbital velocities are small
compared to the vacuum speed of light c and the gravitational fields are weak. It has
played and continues to play a central role in the construction of template banks for
the detection and analysis of GW signals generated by binary systems of black hole
and/or neutron star, which are now routinely observed by the LVK collaboration's
detectors [107, 185, 202, 759–762]. More precisely, PN results are at the core of several
classes of template banks, including phenomenological waveforms and effective one-body
waveforms (see Secs. 4.5 and 4.6).

In PN theory, the general relativistic corrections to the Newtonian motion and to the
leading GW emission (i.e. Einstein's quadrupole formulas) are computed in a systematic
manner in powers of the small PN parameter $v^2/c^2 \sim GM/(c^2 r)$, where v and r are the
typical binary relative velocity and separation, M is the sum of the component masses,
and $v^2 \sim GM/r$ for bound orbits. Indeed, the most promising sources of gravitational
waves for existing and planned interferometric detectors are bound systems of compact
objects. By convention, a contribution of "nPN" order refers to equation-of-motion
terms that are $O(1/c^{2n})$ smaller than the Newtonian acceleration, or, in the radiation
field, smaller by that factor relative to the standard quadrupolar field.

The PN approximation dates back to the pioneering works of Lorentz and Droste [763],
as well as Einstein, Infeld and Hoffman [764], who computed the leading 1PN corrections
to the Newtonian equations of motion in a system of N point masses. During the 1980s,
those results were extended to 2.5PN to provide a rigorous basis for interpreting binary
pulsar observations [765, 766]. For binary systems of compact objects, the state of the
art corresponds to gravitational waveforms that include all of the relativistic corrections
up to 4PN order, in the simplest case of nonspinning bodies moving along a sequence
of quasi-circular orbits.

Another complementary weak field approximation can be found by relaxing the small
velocity assumption of the PN approximation and demanding only that $GM/(c^2 r) \ll 1$.
This scheme, known as the PM approximation, has a long and venerable history, in the
context of both unbound scattering where velocities can be arbitrarily large [767, 768]
and far-zone–near-zone matching for bound orbits within certain PN schemes (see e.g.,
Ref. [758]).

As discussed below, much work has recently been dedicated to (i) push this accuracy to

PN order	Dynamics				Dissipative flux			
	non-spinning	spinning			non-spinning	spinning		
		SO	SS	higher spins		SO	SS	higher spins
0	$\checkmark$	-	-	-	-	-	-	-
1	$\checkmark$	-	-	-	-	-	-	-
1.5	-	$\checkmark$	-	-	-	-	-	-
2	$\checkmark$	-	$\checkmark$	-	-	-	-	-
2.5	$\checkmark$	$\checkmark$	-	-	$\checkmark$	-	-	-
3	$\checkmark$	-	$\checkmark$	-	-	-	-	-
3.5	$\checkmark$	$\checkmark$	-	$\checkmark\,(S^3)$	$\checkmark$	-	-	-
4	$\checkmark$	-	$\checkmark$	$\checkmark\,(S^4)$	$\checkmark$	$\checkmark$	-	-
4.5	$*$	$\checkmark$	-	$\checkmark\,(S^3)$	$\checkmark$	-	$\checkmark$	-
5	$*$	-	$\checkmark$	$\checkmark\,(S^4)$	$\checkmark$	$\checkmark$	-	-
5.5	$*$			$\checkmark\,(S^5)$	$\checkmark$	$\checkmark$	$\checkmark$	-
6				$\checkmark\,(S^6)$	$\checkmark$	$\checkmark$	$\checkmark$	$\checkmark\,(S^3)$
6.5				$\star$	$\checkmark$	$\checkmark$	$\checkmark$	
7				$\star$	$\checkmark$			

Table 9. State-of-the-art of known PN results for both the conservative and dissipative dynamics as well as for the gravitational flux. Contrary to the text, everything is stated as absolute order. For example, the 6PN absolute order for the non-spinning flux in the table corresponds to the 3.5PN relative order results as stated in the text. Hereditary effects are only known as non-local contributions. An instantaneous expression can be obtained by performing a low-eccentricity expansion. SO and SS refer to spin-orbit and spin-spin interactions respectively.

$*$ means that only a partial result is known at those orders. At 5 and 5.5PN order, the results were obtained by the combination of PN traditional techniques with scattering amplitudes and self-force.

$\star$ means that the dynamics is known at all leading order in the spin.

4.5PN order, (ii) include the effects of the spins of the compact objects (see also Table 9), (iii) generalize the results from circular to eccentric orbits, and (iv) explore the overlap and synergies with other approximation methods (PM approximation, small-mass-ratio approximation, effective one-body model). The reader is referred to the review articles [758, 769–776] and to the textbooks [777, 778] for more information.

4.2.2. Suitable for what sources? The PN approximation is well suited to describe the dynamics and gravitational emission of compact binary systems in the early inspiral stage. While it can in principle be applied to model BH binaries of any mass ratio, it is expected to be more accurate for comparable to intermediate mass BHBs, as the gravitational field should remain small until the final cycles. For mass ratio above $q \gtrsim 100$, when the small body remains for long timescales close to the supermassive BH, the gravitational field is strong and the weak-field approximation will lose accuracy (see Fig. 2).

The PM approximation is best suited to close hyperbolic encounters (CHE), which

could be detected with LISA for a population of massive PBH in dense clusters forming part of the halos of galaxies, as studied in Refs. [779, 780]. It also provides valuable resummations of terms in the PN approximation and is used to improve bound compact binary coalescence models when combined with PN results.

PN waveforms are ideally suited to model binaries that are in an early stage of their inspiral while in the LISA band such as SOBHBs and GBs.

4.2.3. Status

4.2.3.1. Equations of motion and waveforms without spin. For an isolated, non-spinning compact binary system, the phase evolution and GW modes during the inspiral stage are currently respectively known up to 4.5PN and 4PN [781–789]. As for the LISA requirements, it was established in [790] that the 2PN waveform will be enough for the parameter estimation of roughly 90% of the detectable SOBHBs, while the 3PN waveform phasing is needed for the systems that will merge within the mission lifetime. Nevertheless it will be quite valuable to push the current accuracy up to 4.5PN order for at least two main reasons. The first one is that it may be necessary for the parameter estimation of black hole binaries with large masses. The second one is that this accuracy will be very beneficial for the calibration of numerical waveforms, and for testing the second-order self-force computations.

For quasi-circular orbits, the gravitational phase $\phi(t)$ is computed via the so-called energy *flux-balance equation*, $\frac{\mathrm{d}E}{\mathrm{d}t} = -\mathcal{F}_{\mathrm{GW}}$, where E is the conserved energy and $\mathcal{F}_{\mathrm{GW}}$ is the flux of radiation emitted. Both quantities are functions of the gravitational phase, which is thus obtained by a simple integration. The amplitude and polarizations are obtained by the same radiative multipole moments that are used when computing the flux, as explained later. For recent reviews, see [758, 772, 774, 791, 792].

At 4PN precision, three different techniques are used to compute the binding energy: the canonical Hamiltonian formulation of General Relativity [793–797], the Fokker Lagrangian approach [798–802] and effective field theory (EFT) [774, 803–808]. All of these methods derive the energy as a conserved quantity associated with the equations of motion for two point-like particles, and naturally give physically equivalent results. The Hamiltonian approach has been pushed up to 6PN, yielding incomplete results [809], see Sec. 4.2.3.4. Exploiting synergies between traditional PN methods and EFT, the logarithmic contributions in the energy have also been computed up to 7PN [810].

The flux of gravitational radiation can be expressed as a generalisation of the famous

Einstein quadrupole formula [811, 812], as [813]

$$\mathcal{F}_{\mathrm{GW}} = \sum_{\ell \geq 2} \frac{G}{c^{2\ell+1}} \left[\alpha_\ell \, U_L^{(1)} U_L^{(1)} + \frac{\beta_\ell}{c^2} \, V_L^{(1)} V_L^{(1)} \right]$$

$$= \sum_{\ell \geq 2} \frac{G}{c^{2\ell+1}} \left[\alpha_\ell \, I_L^{(\ell+1)} I_L^{(\ell+1)} + \frac{\beta_\ell}{c^2} \, J_L^{(\ell+1)} J_L^{(\ell+1)} \right] + \mathcal{F}_{\mathrm{tails}} \,, \qquad (12)$$

where the U_L (resp. V_L) are the mass (current) radiative multipole moments and the I_L (resp. J_L) are the mass (current) source multipole moments, the $\{\alpha_\ell, \beta_\ell\}$ are collections of numbers and the superscript (n) denotes n time derivatives. To connect radiative moments to sources moments, their non-linear interactions (occurring during the propagation from the source to the detector) have been singled out in $\mathcal{F}_{\mathrm{tails}}$. The radiative moments are also directly involved in the computation of polarisations [813], and thus their determination is crucial.

The contribution $\mathcal{F}_{\mathrm{tails}}$ is known up to 4.5PN order, using traditional PN methods [814], and was confirmed by an independent PN re-expansion of resumed waveforms [815]. The computation of the required moments is currently done using the Multipolar-post-Minkowskian-post-Newtonian (MPM-PN) algorithm [758]. The major piece of this work is the derivation of the mass quadrupole ($\ell = 2$) up to 4PN order: the main result has been obtained [781, 783–786], including the tail-of-memory contribution [816]. The other moments involved are the mass octupole and the current quadrupole, already known at the required order (3PN) [782, 817], and higher moments that are either known or trivial (i.e. needed at the Newtonian order only), see notably [818]. Collecting all these results, the complete flux of gravitational radiation is fully known at 4PN [789]. Using the flux-balance equation and taking into account the effects of absorption of the gravitational wave by the black holes' [819–823], this result yields the gravitational phase at 4.5PN [788]. Note that two other methods are able to deal with high PN multipole moments, both currently developed up to 2PN: the direct integration of the relaxed equations (DIRE) [824] and EFT [825]. As half-PN orders are often easier to compute than integer ones, one can probably push the results up to 4.5PN order, including the amplitudes of the gravitational modes. A first step in this program is to control the dissipative, radiation reaction effects in the equations of motion. Table 9 summarizes the current knowledge regarding PN dynamics and flux without spin.

Finally, there have been some works trying to map the BMS (Bondi-Metzner-Sachs) flux-balance laws to equivalent PN results in the harmonic gauge [826]. By transforming the metric from harmonic coordinates to radiative Newman-Unti (NU) coordinates, they were able to obtain the mass and angular momentum aspects and the Bondi shear as a function of the quadrupole moment [827]. In particular, they rederive the displacement memory effect (see also [556]) and provide expressions for all Bondi aspects relevant to the study of leading and subleading memory effects [828].

4.2.3.2. Equations of motion and waveforms with spin. In the last decade, the effect of the proper rotation of the components of binary systems have been included in the orbital equations of motion to 4PN order, extending previous works dating back to the 70's [829]. In the post-Newtonian terminology, the physical spin is rescaled as S/c. The leading spin interactions, the so-called spin-orbit interaction (SO), couple the mass m_1 of a particle with the spin of the other, hence those contributions scale as $\frac{Gm_1}{c^2} \times \frac{S_2}{c} \sim \mathcal{O}(\frac{1}{c^3})$ and are regarded as being of 1.5PN order. Meanwhile the first effect due to spin-spin interaction, scaling as $\frac{G}{c^2} \times \frac{S_1}{c} \times \frac{S_2}{c} \sim \mathcal{O}(\frac{1}{c^4})$, is quadratic in spin (SS) and arises at 2PN order. We refer to the successive subleading PN contributions to a given spin interaction (e.g. SO or SS) as the next-to-leading (NL), next-to-next-to-leading (NNL) and so on. Moving beyond the 2PN two-body dynamics including SO interactions [830], it becomes increasingly difficult to resort to an explicit model, where the bodies are described as small balls of fluid [831]. The most efficient strategy consists in adopting an effective point of view and considering that the two objects are point particles endowed with a classical spin.

The definition of spin in GR was first introduced by Mathisson [832], and rephrased later by Tulczyjew [833]. The covariant equations of evolution obeyed by a spinning test particle were obtained in their usual form by Papapetrou [834] and later generalized by Dixon to bodies endowed with higher-order multipole moments [835]. The equations of motion and precession served as a starting point to investigate the dynamics of binary systems at next-to-leading (NL: 2.5PN) [836, 837] and NNL (3.5PN) order linear in spin (SO interactions) [838], assuming that all Dixon moments other than the masses and the spins vanish. The metric is obtained by solving iteratively Einstein's equations in harmonic coordinates [839] for the pole-dipole stress-energy tensor. Later, to compute the SS corrections at NL (3PN) order [840], the contribution of the Dixon quadrupoles was added, so as to account for the self deformation of the bodies produced by their own spins.

The direct computation of a generalized Lagrangian (i.e. depending on the accelerations) for two spinning particles, using EFT in harmonic coordinates, was performed in stages from the mid-2000's on by integrating out the gravitational field entering the full 'field plus matter' Lagrangian with the help of standard Feymann diagram expansions [841–843]. The NL S_1–S_2 (3PN) interactions [844, 845] were computed first, before the NL S_1–S_1 (3PN) contributions [846] and NL SO (2.5PN) interactions [847, 848] were considered. Equivalent results were obtained in parallel by means of Hamiltonian methods based of the Arnowitt-Deser-Misner (ADM) formulation of GR [849–851].

After the canonical treatment of the spin was better understood [851, 852], the computations of the Hamiltonian were pushed up to NNL (3.5PN) order for the SO [853, 854], to NNL (4PN) order for the S_1–S_2 interactions [849, 855] and to NL (3PN) order for the S^2 interaction [856]. A fully equivalent Lagrangian for the latter effects was found using EFT [857]. Once the EFT degrees of freedom and the gauge choice corresponding to the spin-supplementary condition were clearly identified, the

PN leading terms to all orders in spins were computed [858–861] and the spin part of the harmonic Lagrangian was completed up to the NNNL (5PN) order [862, 863].

Note that reaction forces, dissipative in essence, are absent from the previous treatments, which exclusively describe the conservative dynamics. Nonetheless, they can be computed from balance equations [864], or more directly from the Papapetrou evolution equations, or from the conservation of an appropriate stress-energy tensor [865]. One may even construct a Schwinger-Keldysh Lagrangian where each degree of freedom is formally doubled. This was done for the NL SO and SS effects at 4PN and 4.5PN respectively in Refs. [866, 867], and to all orders in spin in Ref. [868] (see also the approach developed for ADM Hamiltonians [869] at leading SO and SS orders).

Knowing the near-zone dynamics of two spinning particles [839], one can insert the corresponding PN metric into the right-hand side of Einstein's equations in harmonic coordinates, which yields the expression of the effective non-linear source entering the integrand of the multipole moments, as defined in the multipolar post-Minkowskian (MPM) formalism [870], or, equivalently, in EFT [871]; hence one gets the relevant mass, current and gauge moments in the spinning case [872]. The expression for the radiative moments in terms of the former quantities has been derived for general isolated systems [817], but the hereditary terms therein are more delicate to evaluate than for mere point-mass particles on circular orbits, since the orbital plane is now generically precessing. They have however been handled for the leading [873] and NL [874] SO interactions, which required the full integration of the (approximately) conservative dynamics up to the considered order.

Finally concerning the gravitational radiation, the GW flux has been obtained to NNL (4PN) order both for the SO and SS contributions [840, 875]. The GW phase, built from the radiative moments and the Noetherian energy, has been obtained within the MPM formalism at the NNL (4PN) order for the SO contributions [874, 876] (in continuation of previous works at leading order (2PN) [877, 878] and NL (3PN) orders [879]), at the NNL (4PN) order for the SS terms [840], and at leading order for the spin cube contributions [880]. Similar results were obtained with the EFT formalism [881] for which state-of-the-art results are also the NNL (4PN) order [875]. The waveform modes have been obtained to NNL (3.5PN) order [882] in the quasi-circular orbit approximations. By contrast, the radiation amplitude has been computed up to the NL (2PN) order only [883], although it is currently provided in a ready-to-use form for precessing quasi-circular orbits to the even lower 1.5PN order [884].

See Table 9 for a summary of on the current knowledge about the PN spinning dynamics and flux.

4.2.3.3. Eccentric-orbit waveforms. The modeling of inspiral waveforms from compact binaries in eccentric orbits commonly relies on quasi-Keplerian parametrization (QKP) as a semi-analytic representation of the perturbative, slowly precessing post-

Newtonian motion. The conservative motion as well as instantaneous and hereditary contributions to the secular ("orbital averaged") evolution of the orbital elements are known to 3PN order, in both modified harmonic and ADM-type coordinates [885–889] and to 4PN order in the ADM-type coordinates only [890].

The complete 3PN-accurate GW amplitudes from non-spinning eccentric binaries have been derived using the multipolar post-Minkowskian formalism, including all instantaneous, tail and non-linear contributions to the spherical harmonic modes [742, 891, 892]. Going beyond the usual approximation of radiation reaction as an adiabatic process (and the associated "orbital averaging" in QKP), [885, 892–894] provide post-adiabatic, oscillatory corrections to the secular evolution of GW phase and amplitude.

For spinning eccentric binaries that have component spins aligned with the orbital angular momentum, the effects of spin-orbit and spin-spin couplings on the binary evolution and gravitational radiation have been worked out to leading order in QKP (i.e., up to 1.5PN and 2PN in the equations of motion) [895]. Subsequent work has aimed to extend the treatment of spins in QKP to higher PN orders [896, 897]. The waveforms modes to NL (3PN) order for aligned spins and eccentric orbits have been derived in [748, 898], including tail and memory contributions. While the instantaneous contributions were derived for generic motion, the hereditary contributions were computed first in a small-eccentricity expansion, then extended to larger eccentricities using a resummation. Regarding precessing eccentric systems, gravitational waveforms have been obtained to leading order in the precessing equation [899]. A fully analytical treatment has also been proposed up to 2PN order in the spin, including higher harmonics [900].

In practice, the semi-analytic approach of QKP requires a numerical evolution of the orbit described by a coupled system of ordinary differential equations (ODEs) and a root-finding method to solve the Kepler problem, and therefore lacks the computational efficiency required for most data analysis applications. The post-circular (PC) formalism [901] provides a method to recast the time-domain response function $h(t)$ into a form that permits an approximate fully analytic Fourier transform in stationary phase approximation (SPA), under the assumption that the eccentricity is small, leading to non-spinning, eccentric Fourier-domain inspiral waveforms as a simple extension to the quasi-circular PN approximant TaylorF2. More recent work has extended the PC formalism to 3PN, with a bivariate expansion in eccentricity and the PN parameter [894, 902], and has included previously unmodeled effects of periastron advance [903].

The parameter space coverage of Fourier-domain waveforms in the PC formalism is limited by the necessary expansion in small eccentricity. Newer models aim for validity in the range of moderate to high eccentricities, by utilizing numerical inversions in SPA and resummations of hypergeometric functions to solve orbital dynamics [741, 904] or by applying Padé approximation on analytic PC schemes expanded into high orders in

eccentricity. A semi-analytic frequency-domain model for eccentric inspiral waveforms in the presence of spin-induced precession has been developed with the help of a shifted uniform asymptotics (SUA) technique to approximate the Fourier transform, a numerical treatment of the secular evolution coupled to the orbital-averaged spin-precession, and relying on small eccentricity expansion only for the amplitude [905].

4.2.3.4. Insight from scattering   One can gain surprising insight in the relativistic two-body problem by investigating *unbound* orbits. Studying such systems implies analyzing the scattering of compact objects and the approximation to the two-body problem most naturally applicable to it, the PM expansion. Recently, there has been renewed interest in the subject, as it has been realized that PM information from unbound systems can be transferred to bound ones, as done for instance via Hamiltonians [906–908] or between gauge-invariant quantities [909–913]. Moreover, PM expansions can be independently obtained from scattering-amplitude calculations [914], as done at 3PM order [915–918] for the nonspinning sector (see also earlier results at 2PM order [919–923] and at 4PM [924–929]). Another method that has been successfully used is the worldline quantum field theory approach [930–932].

The 3PM radiative contribution, which cancels a divergence in the 3PM conservative part, has been obtained in Refs. [933–939]. The radiative effects in PM expansions have been further explored in [940–943] and the radiative contributions to the scattering problem were obtained in a PN expansion [944–950].

A Hamiltonian including spin-orbit coupling at the 2PM approximation has been obtained [951] by extracting the dynamical information from a scattering situation with the help of "scattering holonomy" [910, 952]. Likewise effects at 'spin-squared' have been determined at the 2PM level using both amplitude [953] and the EFT formalism [954–959]. To 3PM order, SO and SS contributions have been determined [960]. Effects of arbitrary orders in spin in the scattering angle have also been studied by means of purely classical methods [868, 961, 962]. Those results have been recovered at 1PM order through the computation of quantum scattering amplitudes for minimally coupled massive spin-n particles and gravitons in the classical limit, as n goes to infinity [963]. Notably, the tree-level amplitude has been found to generate the full series of black-hole spin-induced multipole moments [964]. Tidal effects in PM expansions have also been investigated [965–972].

The aforementioned results have naturally prompted discussions and comparisons between the GW astrophysics and scattering-amplitude communities, which is made possible by the use of pivotal gauge-invariant quantities for comparisons. The scattering angle of unbound compact-object interactions is one such pivotal quantity that, at least in a perturbative sense through the orders so-far considered, is thought to encapsulate the complete conservative dynamics. Not only does it provide a common ground to exchange information between independent PM calculations [973] or between PM and

EOB schemes [906, 907, 961, 974–978], but it has also proven extremely useful to PN theory.

The PM expansion of the scattering angle allows one to extract previously unknown PN information through a synergistic combination of constraints from its simple mass-ratio dependence and gravitational self-force (GSF) results, as first realized at 5PN [979, 980]. Such construct has been exploited to partially calculate the 6PN dynamics [809, 981], allowing a nontrivial check at 3PM-6PN order of the 3PM result [916, 982] (see also [918, 983]), as well as to the generic spin-orbit and aligned bilinear-in-spin sectors at NNNL [984, 985] (see also [986] for more on the interface between PM and GSF theory). GSF scattering observables can also provide a powerful handle on PM dynamics across all mass ratios. Calculations of the scattering angle to first-order (second-order) in the mass ratio fully determine the complete two-body Hamiltonian through 4PM (6PM) order [987].

4.2.3.5. First laws and gauge invariant comparisons. The orbital dynamics of a binary system of compact objects exhibits a fundamental property, known as the first law of binary mechanics, that takes the form of a simple variational relation. This formula relates local properties of the individual bodies (e.g. their masses, spins, redshifts, spin precession frequencies), to global properties of the binary system, (e.g. gravitational binding energy, total angular momentum, radial action variable, fundamental frequencies). The first law was first established for binary systems of nonspinning compact objects moving along circular orbits [988], as a particular case of a more general variational relation, valid for systems of black holes and extended matter sources [989]. This first law was later extended to generic bound eccentric orbits [990], including the effect of the GW tails that appear at the leading 4PN order [991], as well as to spinning compact binaries, for spin aligned or anti-aligned with the orbital angular momentum [992]. In the context of the small mass-ratio approximation (see Sec. 4.3), analogous relations were established for a test particle or a small self-gravitating body orbiting a Kerr black hole, by accounting for the conservative part of the first-order gravitational self-force (GSF) [993, 994]. These various first laws of binary mechanics have proven useful for a broad variety of applications, including to:

- Determine the numerical values of the "ambiguity parameters" that appeared in the derivations of the 4PN two-body equations of motion [793–795, 797–800, 995];
- Compute the exact first-order conservative GSF contributions to the gravitational binding energy and angular momentum for circular-orbit nonspinning black hole binaries, allowing for a coordinate-invariant comparison to NR results [996];
- Calculate the GSF-induced correction to the frequency of the Schwarzschild [996, 997] and Kerr ISCO [998, 999];
- Calibrate the potentials that enter the EOB model for circular orbits [997, 1000] and mildly eccentric orbits [1001–1003], and spin-orbit couplings for spinning

binaries [1004];

- Test the cosmic censorship conjecture in a scenario where a massive particle subject to first-order GSF falls into a nonspinning black hole along unbound orbits [1005];

- Define the analogue of the redshift variable of a particle for black holes in NR simulations, this allowing further comparisons to the predictions of the PN and GSF approximations [1006, 1007];

- Provide a benchmark for the calculations of the first-order GSF-induced frequency shift of the Schwarzschild innermost bound stable orbit [1008] and the second-order GSF contribution to the gravitational binding energy [1009].

The first law of binary mechanics for circular orbits has been extended to account for finite-size effects such as the rotationally-induced and tidally-induced quadrupole moments of the compact objects [1010, 1011]. Other interesting directions would be to extend the first law to generic precessing spinning compact binaries, and to establish it in the context of the PM approximation and for unbound orbits.

4.2.4. Environmental effects The evolution of relativistic magneto-hydrodynamics, circumbinary disks around supermassive binary black holes have been studied in the weak-field approximation. This relies on the techniques of matched asymptotics to analytically describe a non-spinning binary system up to 2.5PN order [1012], on which the magnetic field is then numerically evolved [1013, 1014]. These results have later been extended to spinning, non-precessing binary black-holes [1015, 1016] and to spinning, precessing black-hole spacetimes [1017].

Another astrophysical environmental effect concerns the presence of a third body around a massive binary back hole. Hierarchical triplets may undergo several type of resonances [1018], that can result for example in Kozai-Lidov oscillations [1019, 1020]. This is an interchange between the eccentricity of the two-body inner orbit and its inclination relative to the plane of the third body studied. Such an effect is particularly interesting for LISA as it involves high eccentricity systems and can result in an enhancement of gravitational radiation. A general-relativistic treatment of triple hierarchical systems has been performed in a weak-field approximation up to 2.5PN order in the dynamics [1021]. The quadrupolar and octupolar waveforms have also been obtained by numerically integrating the three-body system trajectories from the PN expansion [1022]. Other studies on the Kozai-Lidov oscillations in GR have employed an expansion in powers of the ratio between the two semi-major axis up the the hexadecapole order [1022] and later to second-order in the quadrupolar perturbation [1023]. Finally, an effective two-body approach to the hierarchical three-body problem has been proposed [1024] and the mass quadrupole to 1PN order was derived under this formalism [1025].

4.2.5. Challenges Post-Newtonian information in data analysis enters primarily through the use of semi-analytical models (see Secs. 4.5,4.6). To avoid parameter estimation biases due to waveform uncertainties, developments in PN theory will be needed to increase the accuracies of these models for the next generation of GW detectors (see 3 and [1] for a discussion in the context of third-generation ground-based detectors).

One of the most significant challenges in the PN formalism will be the completion of the 5PN order. First, due to the so-called "effacement principle" [1026], the point-particle approximation breaks at this order. Finite-size and tidal effects have to be taken into account, the latter being known up to 7PN [1027–1030]. In addition, due to the complexity of the computations involved, it seems highly unlikely to achieve the derivation of the complete gravitational phase at 5PN during the next decade, even if partial results are already obtained. In this regard, the interplay with GSF and scattering amplitudes will be crucial to make significant progress in this direction.

Exploiting the links between asymptotic symmetries and hereditary effects in the PN formalism should improve the matching to NR as memory effects are starting to be included in NR waveforms [673] (see also Sec. 4.1).

Regarding spinning binary systems, although the orbital dynamics are known up to the 4PN order, it might not be sufficient for LISA data analysis. In the near future one should primarily focus, at lower orders, on the exterior gravitational field, outside the matter source, extending to infinity. Indeed, new multipole moments will have to be computed to reach the same level of accuracy for the GW amplitude as for the flux, notably the 3PN SS contributions to the current quadrupole. The next step will consist in moving on to 4PN order, to do as well as the current equations of evolution. For this purpose, the NNL SS piece of the 4PN mass quadrupole will be required.

Another important topic, in order to combine information coming from the PN framework and numerical relativity, will be to connect the magnitude of the spin used in PN expressions to the rigorous definitions employed in numerical simulations [1031, 1032]. The problem of comparing the spin axis is even more intricate since, for now, its direction has not been given a satisfactory unambiguous meaning in any of these schemes [1033].

Regarding eccentric waveforms, most current models have focused on a low eccentricity expansion and non-spinning or aligned spin systems. It is crucial to make progress in both directions. First one has to go beyond the small eccentricity approximation, as some have started investigating [741, 904]. Second, it will be important to have reliable fully precessing and eccentric waveforms in order to span all the parameter space expected for LISA sources.

Notwithstanding the amount of work and progress already made, studies of the scattering of compact objects still explore a relatively uncharted territory. Obvious extensions of the work reported above will involve pushing scattering calculations of both spinning and nonspinning systems to higher PM orders in the conservative sector,

both from a fully classical and amplitude approach. Such new information would help in obtaining new nontrivial PN information via the continued exploitation of the scattering angle's mass-ratio dependence, as well as continuing the fruitful exchange between the communities. The interconnectedness of the PM, PN and GSF approximations should also be explored in the context of tidal effects (information from PM is available, e.g., [965]). Scattering studies should also explore dissipative radiation-reaction effects. It is important to push these calculations, so that the accuracy gained in the dissipative dynamics goes on par with that of the conservative sector.

4.3. Small-mass-ratio approximation (gravitational self-force)

Coordinators: Marta Colleoni and Adam Pound
Contributors: S. Akcay, E. Barausse, B. Bonga, R. Brito, M. Casals, A. Druart, L. Durkan, A. Heffernan, T. Hinderer, S. A. Hughes, S. Isoyama, C. Kavanagh, L. Kuchler, A. Le Tiec, B. Leather, G. Lukes-Gerakopoulos, O. Long, P. Lynch, C. Markakis, A. Maselli, J. Mathews, C. O'Toole, Z. Sam, A. Spiers, S. D. Upton, M. van de Meent, N. Warburton, V. Witzany

4.3.1. Description When the secondary object in a binary is significantly smaller than the primary, we can treat the mass ratio $\epsilon = m_2/m_1 = 1/q$ as a small parameter and seek a perturbative solution for the spacetime metric, $g_{\alpha\beta} = g_{\alpha\beta}^{(0)} + \epsilon h_{\alpha\beta}^{(1)} + \epsilon^2 h_{\alpha\beta}^{(2)} + \ldots$ The background metric $g_{\alpha\beta}^{(0)}$ then describes the spacetime of the primary in isolation, typically taken to be a Kerr BH. At zeroth order, the secondary behaves as a test mass in the background, moving on a geodesic of $g_{\alpha\beta}^{(0)}$. At subleading orders, it generates the perturbations $h_{\alpha\beta}^{(n)}$, which then exert a *self-force* back on it, accelerating it away from geodesic motion and driving the inspiral. These perturbations $h_{\alpha\beta}^{(n)}$ also encode the emitted waveforms.

The perturbative field equations and trajectory of the secondary are determined using *GSF theory*, a collection of techniques for incorporating a small gravitating object into an external field [91, 1034–1037]. Using matched asymptotic expansions (or EFT [1038]), the small object is reduced to a point particle, or more generally to a puncture in the spacetime geometry, equipped with the object's multipole moments. For a compact object, higher moments scale with higher powers of the small mass m_2, such that one additional multipole moment appears at each order in ϵ. This multipolar particle (or puncture) is found to obey a generalized equivalence principle, behaving as a test body in a certain effective, smooth, vacuum metric $g_{\alpha\beta}^{(0)} + \epsilon h_{\alpha\beta}^{\mathrm{R}(1)} + \epsilon^2 h_{\alpha\beta}^{\mathrm{R}(2)} + \ldots$ [1035, 1039–1051].

The *regular fields* $h_{\alpha\beta}^{\mathrm{R}(n)}$ that influence the secondary's motion can be calculated directly, using a puncture scheme in which they are the numerical variables [1052, 1053]. Alternatively, they can be extracted from the full fields $h_{\alpha\beta}^{(n)}$ using a mode-by-mode subtraction [1054–1057] or other methods [1058, 1059], as reviewed in [1037, 1060, 1061]. In either approach, the perturbative field equations can be solved using the methods of BHPT [731, 1037, 1062–1071].

A key feature of this model is its clean separation of time scales: because the self-force is small, inspirals occur slowly, over $\sim 1/\epsilon$ orbits. On the time scale of a few orbits, the secondary's trajectory is approximately a bound geodesic of $g_{\alpha\beta}^{(0)}$ (illustrated in Fig. 5), which in Kerr spacetime is generically triperiodic, undergoing radial, polar, and azimuthal motion with frequencies Ω_r, Ω_θ, and Ω_ϕ [1037, 1072–1075]. Over the long inspiral, the frequencies slowly evolve due to dissipation. The
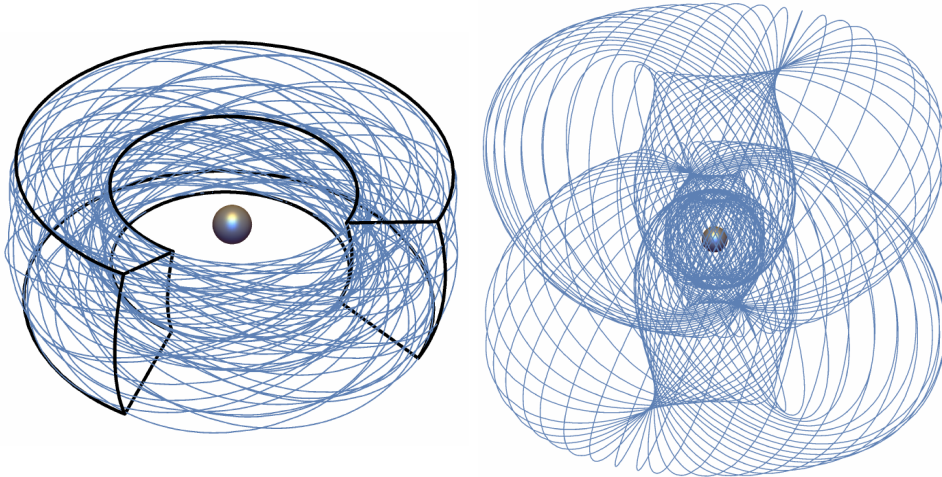
Figure 5. Geodesics of Kerr spacetime. Left: a non-resonant geodesic, which fills a toroidal shape. Right: a resonant geodesic. Images taken from [91].

field equations can therefore be solved using a two-timescale expansion [1037, 1076–1081], $h_{\alpha\beta}^{(n)} = \sum_{k^A \in \mathbb{Z}} h_{\alpha\beta}^{(n,k^A)}(J^B, x^a) e^{ik^A \psi_A}$. Here x^a are spatial coordinates, and all time dependence is encoded in the set of system parameters J^A (the secondary's orbital energy, angular momentum, and Carter constant, the primary's mass and spin, etc.), and the set of orbital phases ψ_A. The parameters J^A evolve slowly, on the inspiral time scale $t \sim 2\pi/(\epsilon\Omega)$, while the phases ψ_A evolve on the orbital time scale $t \sim 2\pi/\Omega$, with evolution equations of the form [738, 1037, 1077, 1080, 1081]

$$\frac{dJ^A}{dt} = \epsilon G_{(1)}^A(J^B) + \epsilon^2 G_{(2)}^A(J^B) + O(\epsilon^3), \quad \frac{d\psi_A}{dt} = \Omega_A^{(0)}(J^B) + \epsilon\Omega_A^{(1)}(J^B) + O(\epsilon^2). \quad (13)$$

Formulating the problem in this way enables practical methods of solving the Einstein equations [1037, 1080] as well as facilitating rapid waveform generation [738, 1037, 1082].

The two-timescale description will frame much of the discussion below. However, there are some special cases of interest that it does not apply to, such as scattering orbits [1083–1087]. Even in an inspiral, there are regions of parameter space in which the approximation breaks down: at the end of the inspiral, when the secondary transitions into a final plunge into the primary [1088–1093], and during resonances, which occur when at least two of the frequencies Ω_A have a rational ratio, causing a linear combination of phases, $k^A \psi_A$, to become approximately stationary [1094–1096]. Such resonances can arise from a variety of physical causes, outlined below, with significant observational consequences.

Many of the core tools in GSF modelling, as well as advanced codes described in the sections below, have been consolidated in the open-source Black Hole Perturbation Toolkit [731], which provides a hub for GSF code development, as well as in the Black Hole Perturbation Club [1097]. In particular, the Fast EMRI Waveforms (FEW) package [1098], which exploits GSF models' multiscale structure, has provided a flexible framework for rapid waveform generation.

4.3.2. Suitable for what sources? Historically, the GSF approximation has been motivated by EMRIs, with mass ratios in the interval $10^{-7} \lesssim \epsilon \lesssim 10^{-3}$ as far as LISA sources are concerned (see Table 4). The GSF model's accuracy for a typical EMRI can be estimated from the evolution equations (13). On the inspiral time scale, the solutions for the orbital phases, and therefore the GW phase, take the form

$$\psi_A = \frac{1}{\epsilon} \left[\psi_A^{(0)} + \epsilon \psi_A^{(1)} + O(\epsilon^2) \right]. \tag{14}$$

Following Ref. [1077], the leading term in this expansion is referred to as *adiabatic* order (0PA), and the nth subleading term as nth *post-adiabatic* order (nPA). An adiabatic approximation, which has large phase errors $\sim \epsilon^0$ over an inspiral, is expected to suffice for detection of EMRIs using the semi-coherent searches discussed in Sec. 3.3.1. A 1PA approximation, which will have phase errors $\sim \epsilon \ll 1$ rad over the final year of inspiral, should suffice for parameter extraction even for loud EMRIs with SNR > 50.

A large and growing body of evidence [497, 498, 681, 708, 996, 999, 1006, 1007, 1099–1107] suggests that the GSF approximation can also accurately model IMRIs (see Table 5). It can even provide a useful model of CO binaries with *comparable* masses when it is re-expressed as an expansion in powers of the symmetric mass ratio $\nu \equiv m_1 m_2/(m_1 + m_2)^2 = \epsilon + O(\epsilon^2)$. We refer to Ref. [1108] for an early review and Refs. [497, 708] for recent analyses of the accuracy of 1PA models in the $1 \lesssim q \lesssim 100$ regime. Further study is required to assess whether 1PA models meet expected accuracy requirements for specific classes of astrophysical sources in this range of mass ratios.

Besides compact binary inspirals, the GSF approximation can be used for other classes of sources. A leading-order GSF model, comprising a point source on a geodesic trajectory, should be suitable for XMRIs [68, 1109] and fly-by burst signals [1083–1087]. GSF theory may also be relevant for modelling gravitational waves from cosmic strings [277–279]. Inspirals of less compact bodies into MBHs (e.g., white or brown dwarfs or main-sequence stars prior to tidal disruption), and three-body "binary EMRIs", can be modelled by including sufficiently high multipole moments in the particle or puncture [82, 1110].

4.3.3. Status The current status of GSF models is summarized in Fig. 6, which also summarizes the necessary inputs for a waveform model at 0PA and 1PA order.

4.3.3.1. Adiabatic approximation At leading order in the two-timescale expansion, only the geodesic frequencies $\Omega_A^{(0)}$ and time-averaged dissipative piece $G_{(1)}^A$ of the first-order self-force are required to drive the evolution [1073, 1111]. The secondary's motion in this approximation can be regarded as an adiabatic inspiral through a sequence of geodesic orbits [1077, 1112]. The waveform can then be built from a corresponding sequence of "snapshot" Fourier mode amplitudes together with the leading phases in

Background Spacetime	Orbital Configuration	Adiabatic	Post-1-adiabatic			
		1SF (Dissipative)	1SF (Conservative)	2SF (Dissipative)	Spin Effects (Conservative)	Spin Effects (Dissipative)
Schwarzschild	Circular	✓✓✓	✓✓✓	✓✓✓	✓✓✓	✓✓✓
	Eccentric	✓✓✓	✓✓✓	✗	✓✓ , ✓✓✓*	✓, ✓✓*
Kerr	Circular	✓✓✓	✓✓	✗	✓,✓✓*	✓✓✓*
	Eccentric Equatorial	✓✓✓	✓✓	✗	✓,✓✓*	✓✓*
	Generic	✓✓✓	✓	✗	✓	✓*
	Resonances	✓✓✓	✓	✗	✗	✗
✓✓✓ Evolving Waveform ✓✓ Driven Inspiral ✓ Snapshot Calculation *(Anti-)Aligned Spin Only						

Figure 6. Progress in modelling EMRIs using GSF methods. '1SF' and '2SF' indicate calculations involving the first or second-order self-force, respectively, and 'spin effects' indicates calculations that take into account the secondary's spin (the spin of the primary is accounted for in all 'Kerr' calculations. 'Snapshot calculations' (single tick) are ones in which self-force effects are calculated on fixed geodesic orbits.

Eq. (14). Alternatively, outside the two-timescale scheme, a time-domain field equation can be solved with an adiabatically inspiraling source particle [1105, 1113–1116].

$G^A_{(1)}$ is most conveniently computed using "flux-balance" formulas [1117–1121], in which the "work" done by the dissipative self-force balances the fluxes of gravitational waves to infinity and down the horizon (or flux-like quantities in the case of the Carter constant). Methods of computing fluxes in GSF theory are well developed [340, 1113, 1116, 1122–1127], and have been numerically implemented for generic (inclined and eccentric) geodesics about a Kerr BH [1128–1131]. The fluxes have also been calculated analytically (by expanding $h^{(1)}_{\alpha\beta}$ in a PN series [1069, 1132, 1133]) to high PN order for circular [1134–1136], eccentric [1137–1139], and generic orbital configurations [1140–1142].

After decades of progress [66, 1091, 1143–1149], adiabatic inspirals and waveforms are now being computed for generic orbits in Kerr, both numerically [1150] and within the analytical BHPT-PN framework mentioned above [1151].

Once fluxes and waveform mode amplitudes have been computed across the parameter space, adiabatic waveforms can be efficiently generated using a combination of neural network and reduced-order techniques [1098, 1148], a method that lends itself to graphical processing unit (GPU) acceleration techniques; see Sec. 5.2. This approach should ultimately meet the efficiency requirements described in Sec. 3.3.1. However, due to the high-dimensional parameter space, significant work remains to populate the parameter space. As a consequence, data analysis development has so far relied on semi-relativistic "kludge" models that approximate the adiabatic evolution and waveform generation [480, 1152–1155].

4.3.3.2. Post-1-adiabatic self-force effects: 1SF The 1PA terms in the two-timescale expansion ($\Omega_A^{(1)}$ and $G_{(2)}^A$) take as input the conservative piece of the first-order self-force (1SF, $\propto h_{\alpha\beta}^{(1)}$) and the dissipative piece of the second-order self-force (2SF, $\propto h_{\alpha\beta}^{(2)}$). Once these ingredients have been computed, a 1PA waveform-generation scheme takes the same form as a 0PA one [1037, 1080].

Numerical computations of the full first-order self-force have made tremendous progress, evolving from Lorenz-gauge calculations [998, 1061, 1071, 1156–1160] to more efficient methods relying on radiation gauges [1161–1168]. These developments culminated in 1SF calculations along generic bound geodesics in Kerr spacetime [1169], and work is still ongoing to further improve 1SF methods [1170–1172].

High-precision numerics and BHPT-PN methods have also made possible high-order PN expansions of numerous conservative invariants, such as the Detweiler redshift [1165, 1173–1179], the periastron advance [999, 1180], and other invariants [1181–1186], which have played a key role in the synergies with PN theory and EOB described in Secs. 4.2 and 4.5.

Modern 1SF calculations mostly rely on frequency-domain methods and mode-by-mode subtraction or puncture schemes to calculate $h_{\alpha\beta}^{\mathrm{R}(1)}$. However, there have also been advances in time domain (TD) calculations based on either finite-difference schemes [1085, 1112, 1187, 1188] or spectral methods [1189–1196], along with improved time-stepping methods [1197–1199]. There is also ongoing work to directly obtain the retarded Green function [1059, 1200–1203], which would then allow direct evaluation of the self-force [1039, 1040].

As at 0PA, calculations of the self-force and of GW amplitudes across the parameter space have been used to simulate self-forced inspirals [738, 1082, 1204–1206] and generate waveforms [1205, 1207]. To date, this has only been done for equatorial orbits and quasi-spherical orbits [1206], due to the computational expense of current 1SF calculations for generic orbits.

4.3.3.3. Post-1-adiabatic self-force effects: 2SF The dissipative piece of the second-order self-force ($G_{(2)}^A$) contributes to the GW phasing at the same 1PA order as the first-order conservative self-force, but calculations of it are less mature. After years of development of the governing formalism [1047–1051, 1208–1210] and of practical implementation methods [1037, 1061, 1079, 1211–1216], Refs. [1009, 1106, 1107] recently carried out the first concrete calculations of physical second-order quantities in the restricted case of quasicircular orbits around a Schwarzschild BH. These calculations culminated in the first complete 1PA waveforms in Ref. [1107]. Figure 7 shows a comparison between one of these 1PA waveforms and an NR waveform for $q = 10$. As alluded to in Sec. 4.3.2, the 1PA approximation agrees well with NR even at this moderate mass ratio.
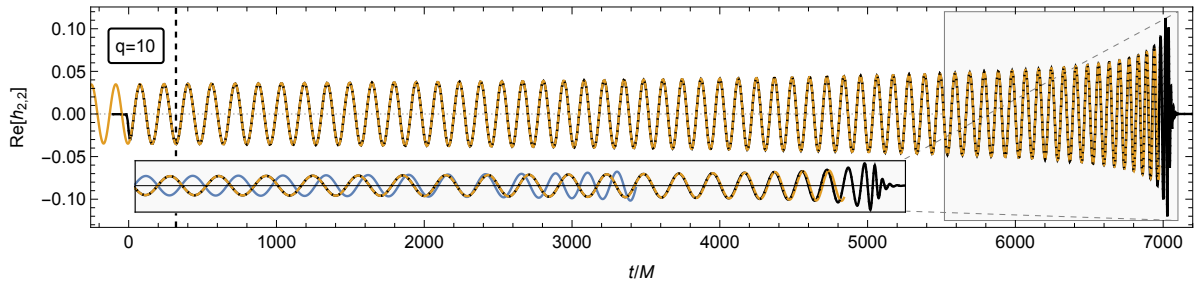
Figure 7. 1PA GSF waveform for a quasicircular, nonspinning binary with mass ratio $q = 10$ (orange). The inset shows a zoomed portion of the waveform near the merger. Also included for comparison are the 0PA GSF waveform (blue, inset only) and the waveform for the same binary produced using an NR simulation in the SXS catalog (SXS:BBH:1107, in black). The three waveforms are aligned in time and phase at $t = 320M$, when the orbital separation is $\approx 13.83M$. Image reproduced from Ref. [1107].

These 1PA waveforms have also more recently been extended to include a slowly spinning primary [1217]. Sec. 4.3.5 discusses the next major barrier in GSF calculations: 2SF calculations with a rapidly spinning primary, eccentricity, and inclination.

4.3.3.4. Transient resonances Resonances are a ubiquitous feature of the strong-field dynamics around BHs in GR [1218, 1219], and their observational imprints on waveforms can be significant. Transient self-force resonances, between the orbital frequencies Ω_r and Ω_θ, will have strong observational consequences for EMRIs [1094, 1095, 1111, 1220, 1221]. Essentially *all* LISA-type EMRIs pass through at least one dynamically significant resonance, leading to a large, $O(1/\sqrt{\epsilon})$ (i.e., 0.5PA) contribution to the waveform phase [67, 1222, 1223]. The magnitude of this effect depends sensitively on the orbital phase at the resonance. As a result, modelling it requires 1PA accuracy prior to resonance. There are ongoing efforts to understand the impact of these resonances and include them in evolutions [87, 1096, 1120, 1121, 1151, 1224–1229].

There also occur resonances between the r and φ frequencies and between the θ and φ frequencies. These do not change the intrinsic inspiral dynamics, but they can lead to a strong net emission of linear momentum that results in a 'kick' to the system's center of mass [1230, 1231]. The maximum kick velocity can reach $\sim 30,000 \times \epsilon^{3/2}$ km/s (depending on the primary spin and on the orbital eccentricity), which, for IMRI systems, could be comparable to the escape velocity from a typical globular cluster.

4.3.3.5. Merger and ringdown The two-timescale expansion breaks down as the secondary object approaches the separatrix between bound and plunging orbits. There, the secondary enters a gradual transition across the separatrix [1088, 1089, 1091, 1092] followed by an approximately geodesic plunge. The transition motion has been mostly studied within the EOB framework using resummed PN expansions [1088, 1232–1239]

78

or within the GSF approach using simplifying approximations [1089–1092, 1115, 1240, 1241]. Merger-ringdown waveforms have been generated from the final plunge at first order [1242, 1243], and complete inspiral-merger-ringdown waveforms have been generated by solving time-domain equations for first-order perturbations sourced by the combined inspiral-transition-plunge motion [757, 1105, 1114–1116]. Only recently, Refs. [1093, 1244, 1245] took a first step toward 1PA/2SF inspiral-merger-ringdown waveforms by developing a systematic expansion of the transition motion and metric perturbation that matches to the two-timescale expansion for quasicircular, equatorial inspirals into a Kerr BH.

4.3.3.6. Spin and finite-size effects When its multipole structure is accounted for, the secondary obeys the Mathisson-Papapetrou-Dixon equations of a test body [832, 834, 835, 1246, 1247] in the effective metric; such a result is expected to hold to all perturbative orders for both BHs and material bodies [1035, 1046, 1248].

The spin contributes first-order conservative and second-order dissipative forces in the equations of motion, leading to 1PA, $\mathcal{O}(\epsilon^0)$ contributions to the final inspiral phase [1249]. Spin also generally breaks the integrability of Kerr geodesic motion [1250]; the resulting potential phenomena, like prolonged resonances, can leave a significant imprint on the gravitational waves [80, 1251–1254] and may contribute $\mathcal{O}(1)$ to the GW phase. Away from these resonances, the spinning-particle motion is perturbatively separable to linear order in spin [80] and easily incorporated into a two-timescale approximation [1249, 1255].

For dissipative effects, a spin-flux balance law has been established [1256], and GW fluxes were computed for a variety of binary configurations [1254, 1256–1265]. Waveforms from generic inspirals into a Schwarzschild BH have also been computed including 1SF and first-order conservative spin effects [1266] but excluding dissipative spin effects. Waveforms including *all* 1PA spin effects from circular equatorial inspirals into Schwarzschild [1249] and Kerr BHs [124] have been produced, and the spin's complete 1PA contribution to the GW phase has been calculated for eccentric equatorial inspirals into a Kerr BH [1267]. A formulation of the first-order conservative spin-forced motion for generic orbits about a Kerr BH [1268, 1269] paved the way for calculations of the spin's complete impact on fully generic 1PA waveforms, beginning with recent snapshot computations of energy and angular momentum fluxes [81].

The secondary's higher moments are unlikely to contribute at 1PA order. The tidal quadrupole's contribution to the acceleration scales with ϵ^4 [1270] and can only become relevant for non-compact objects [1255]. The spin also induces a quadrupole deformation of the secondary, which creates an acceleration $\sim \epsilon^2$ [82, 1110] that is unlikely important for EMRIs (up to resonances) but might be relevant for IMRIs [82].

4.3.4. Environmental effects   In the preceding sections, we have focused on the simplest GSF model: an isolated vacuum BH orbited by a single body. This will not fully describe astrophysical small-mass-ratio binaries. Accreting matter will be present at some level, and there are likely to be additional bodies nearby. Accounting for these effects will be necessary to achieve the stringent accuracy requirements that EMRIs, in particular, place on GSF models.

There are three ways we can modify GSF models to include such effects: (i) perturbatively, by adding "small" matter fields or metric perturbations to the spacetime, which then exert small forces on the secondary; (ii) non-perturbatively, by modifying the background spacetime and introducing "large" matter fields; (iii) by changing boundary conditions, imagining (for example) modifications very near the BH horizon or non-asymptotically flat perturbations due to external matter. Sec. 6 discusses how these classes of modifications can also be used to incorporate beyond-GR effects.

Although important aspects of the astrophysical environment of EMRIs are uncertain, it is expected that there will be other stellar-mass bodies nearby. These bodies create an additional metric perturbation, which should be sufficiently small to be treated as a linear perturbation. The influence of the perturbation is generally negligible, except at moments when two or more of the orbital frequencies characterising the perturbed EMRI system become commensurate. At those times, an EMRI experiences a tidal resonance [1271], an orbital resonance akin to the mean motion resonance known from planetary dynamics [1272]. Calculations across the parameter space showed that a single resonance can dephase the waveform by several radians over the inspiral [84, 87, 1273, 1274], and that most EMRIs will cross multiple tidal resonances before plunge. If LISA can reliably measure these resonances, they can be used to learn about the tidal environment of EMRI systems.

Accretion and gas interactions will also be present at some level in any astrophysical EMRI system. Order-of-magnitude estimates suggest they will be negligible unless the primary BH powers an AGN (in which case it would be surrounded by an accretion disk with which the secondary is likely to interact) [62, 86, 1275, 1276]. Since AGNs are believed to make up 1–10% of local galaxies, only a comparable fraction of EMRIs are expected to be significantly affected by accretion and gas interactions. For those systems, accretion onto the primary and secondary, as well as dynamical friction from the disk and planetary-like migration within it, are expected to cause secular effects comparable to those of GW fluxes [62, 86, 1275]. Recently work has begun to incorporate the disk and other potential nonvacuum effects into GSF models by adding torques to 0PA Kerr models [1277] or by working perturbatively on an exact nonvacuum background [1278, 1279].

The direct gravitational pull from AGN disks is likely to be negligible [62], but if more dense disks/rings exist in nature, the effect may be significant [1280]. Exact spacetime solutions describing thin disks or rings around BHs [1278, 1281–1283] show that orbits

80

in such situations are non-integrable, exhibiting characteristic phenomena like chaos and prolonged resonances [1284]. If these effects are significant in realistic scenarios, GSF models should be able to account for them through perturbative corrections on top of a Kerr background [87, 1285–1287].

4.3.5. Challenges The principal goal of GSF waveform modelling is to develop complete 1PA models for generic orbital configurations around a spinning, Kerr BH. To be complete, these models must include the spin of the companion, transitions across resonances, and the final plunge. They must also be sufficiently modular to incorporate beyond-GR and environmental effects, and there are strong motivations to explore other regions of the parameter space, such as scatter orbits and comparable masses. We summarize here the main challenges in developing and implementing such models.

4.3.5.1. Post-1-adiabatic calculations 1PA models are currently missing two ingredients: the effects of the companion's spin for generic binary configurations, and dissipative 2SF effects; see Fig. 6. Both must be incorporated into a unified two-timescale expansion of the field equations, the orbital motion, and the spin evolution.

While substantial work remains to calculate 1PA spin effects for generic binary configurations, these calculations can leverage existing methods for point-particle sources. Therefore, 2SF calculations represent the overriding obstacle to 1PA accuracy. Practical 2SF calculations have, thus far, been restricted to quasicircular orbits in a Schwarzschild background [1009, 1106, 1107]. As discussed in Sec. 2.2, the majority of EMRIs are expected to have significant eccentricity and may have highly precessing orbital planes when they enter the LISA band, meaning 2SF techniques need to be extended to cover generic orbital configurations. They must also be extended to the realistic case of a Kerr background.

Eccentricity and inclination bring multiple challenges. Most recent self-force calculations have utilized decompositions into Fourier modes (the natural setting of the two-timescale expansion) and angular harmonics. Eccentric, inclined orbits can require $\sim 10^5$ modes, all of which will couple to one another in the second-order source. The sum of Fourier modes can also suffer from poor convergence: in the existing 2SF puncture scheme, the source for $h_{\alpha\beta}^{\mathrm{R}(2)}$ has finite differentiability on the puncture's worldline, leading to slow power-law convergence (the Gibbs phenomenon). At first order, similar problems were overcome using methods of extended solutions [1159, 1160, 1165, 1169, 1288–1290] that restore exponential convergence. These have inspired a new scheme, applicable at second order, known as the method of extended effective sources [1291], which has been demonstrated in the case of a scalar-field toy model for eccentric orbits about a Schwarzschild BH. Work now remains to apply it to gravitational perturbations, both at first and second order, and to orbits in Kerr spacetime.

The extension to Kerr spacetime brings more challenges. Second-order calculations in Schwarzschild have so far relied on directly solving the perturbative Einstein equations, which are not separable in Kerr spacetime. At first order, this problem was overcome using radiation-gauge methods, in which the metric perturbation is reconstructed from a solution to the (fully separable) Teukolsky equation [1064, 1066, 1068]. One path to 2SF calculations is to extend that method to second order [1170, 1292–1294]. The standard method of metric reconstruction [1066, 1068] fails beyond linear order, but recent work found an extension to all orders [1170, 1293]. Recent work on second-order flux-balance laws [1295] also suggests that 1PA rates of change of energy and angular momentum (though perhaps not the Carter constant) can be computed directly from a solution to the second-order Teukolsky equation, without the need for metric reconstruction.

An additional obstacle is that in radiation-gauge implementations, the first-order metric perturbation has gauge singularities that extend away from the particle. There is a rigorous procedure to extract physical 1SF quantities despite these singularities [1163, 1167, 1168], but the singularities become ill defined in the second-order field equations [1170]. Several avenues are being explored to resolve this problem [1170, 1171, 1296, 1297].

There are also challenges common to all these 2SF calculations: at second order, the field equations have a noncompact source that falls off slowly at large distances [1079] and is burdensome to compute due to the strong nonlinear singularity at the particle [1213]. Recent work [1051, 1294] has shown that both problems might be mitigated by using gauges adapted to the lightcone structure of the perturbed spacetime. However, additional work will be required to implement these gauge choices in a practical numerical scheme.

4.3.5.2. Covering the parameter space Even once numerical implementations of all necessary ingredients are available, spanning the full EMRI parameter space remains a considerable challenge at both 0PA and 1PA orders. This is due to the high dimensionality of the parameter space and the high computational burden of self-force calculations, particularly at second order. Covering the EMRI parameter space will likely involve a combination of (i) using analytic results to reduce the region of the parameter space where high-precision interpolation of numerical data is required, (ii) better interpolation methods, and (iii) improvements in computational efficiency of current numerical calculations. We address each of these three below in the context of 0PA inspirals, 1PA inspirals, and waveform calculations.

Computing adiabatic inspirals requires interpolating the rates of change $(G_{(1)}^A)$ of the orbital energy, angular momentum, and Carter constant across the four-dimensional parameter space of the primary spin and three orbital elements. For an adiabatic model sufficiently accurate to build 1PA corrections upon, we need to interpolate $G_{(1)}^A$ to better than a relative accuracy of ϵ^{-1}. The central challenge is then constructing such a high-

accuracy interpolant over the 4D parameter space. Recent work has demonstrated advantages of Chebyshev interpolation for this purpose [1082]. The region of the parameter space, and the accuracy of the interpolation of the numerical data, can also be reduced by constructing global fits informed by analytic results.

At 1PA order we must also compute the change in the mass of the primary during the inspiral [1080], and so the parameter space grows to five dimensions. There are also corrections due the spin of the secondary, but fortunately, these can be added on separately. At 1PA order the accuracy requirements of the contributions are much lower, at $\sim 10^{-2} - 10^{-3}$ relative [1205]. This should allow analytic results to assist in reducing the parameter space that numerical results need to cover. Such analytical results could be obtained by extending BHPT-PN calculations. Alternatively, they could be obtained from EOB dynamics, following the programme in Refs. [1298–1304]. Regions of high eccentricity may also be more easily covered using advanced time-domain codes [1085, 1187, 1192–1194, 1196, 1197, 1305].

4.3.5.3. Extending the parameter space The challenges above are centered on "vanilla" regions of the parameter space: the inspiral phase away from resonances, which is amenable to a two-timescale expansion. However, it is also critical to include accurate transitions across resonances, particularly in the EMRI regime. In addition to the dominant r-θ resonances that occur in a self-forced inspiral, prolonged resonances may occur due to spin, external matter, or a non-Kerr central object [1096, 1221, 1306]. Similarly, the transition from inspiral to plunge can also be important, particularly for more comparable masses [497, 498, 1105]. Both resonances and the plunge will require matching the two-timescale expansion to specialized approximations in those parameter regions [67, 87, 1037, 1093, 1096, 1226, 1244].

There are also reasons to compute self-force effects on scattering orbits, whether to model hyperbolic, burst sources or to inform PM and PN dynamics, as described in 4.2.3.4 (and possibly to infer properties of bound, self-forced orbits [910, 1307]). Explorations of scatter orbits have only recently begun [1086, 1087, 1308, 1309]. While bound-orbit self-force calculations can utilise the orbit's discrete Fourier spectrum, scatter orbits have a continuous spectrum [1083, 1084], suggesting some clear advantages to simulations in the time domain [1008, 1086, 1087].

In addition to including more of the two-body GR parameter space, considerable work must be done to include possible beyond-GR and environmental effects in GSF models. Fortunately, the GSF model is relatively modular. This means most additional effects can be added separately, as described in Sec. 6.4, and are readily incorporated into frameworks such as FEW [1098]. However, modelling these additional effects will be particularly challenging if they are not amenable to a two-timescale treatment, or if they are too large to be treated perturbatively.
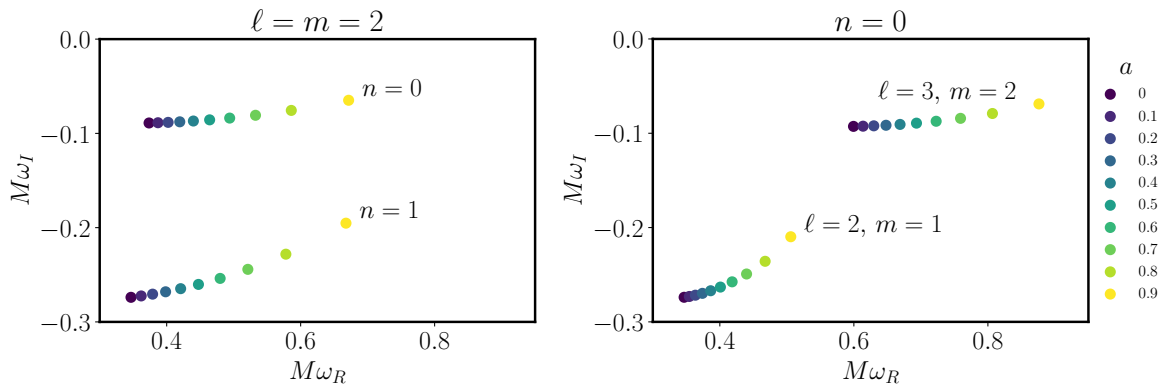
Figure 8. Real and imaginary parts of the Kerr quasinormal mode frequencies, coloured by the BH spin (from $a = 0$ in dark blue to $a = 0.9$ in yellow). Left: $\ell = m = 2$ fundamental and first overtone modes. Right: modes with different angular numbers (ℓ, m).

4.4. Perturbation theory for post-merger waveforms (quasi-normal modes)

Coordinators: Stephen R. Green and Laura Sberna
Contributors: E. Berti, R. P. Macedo, P. Mourier, N. Oshita, M. van de Meent

4.4.1. Description Following a compact binary merger, the remnant object settles into a stationary state through a process known as the "ringdown". The ringdown signal is interesting because it involves a collection of discrete modes that encode information about the final object. For a BH merger, the no-hair theorems of general relativity predict that the final state is itself a Kerr BH (see, e.g., [1310]), yielding precise predictions for the ringdown frequencies. We consider this case here.

At late times, the ringdown is best described using BHPT. This involves expanding the spacetime metric $g_{\alpha\beta} = g_{\alpha\beta}^{(0)} + \epsilon g_{\alpha\beta}^{(1)} + \epsilon^2 g_{\alpha\beta}^{(2)} + ...$ [1062, 1063, 1311] and solving order-by-order in the Einstein equation. At zeroth order, the background metric $g_{\alpha\beta}^{(0)}$ describes the remnant Kerr BH. At first order, $g_{ab}^{(1)}$ satisfies the Einstein equation linearized about Kerr. Rather than work directly with the metric perturbation, it is convenient to use instead the Newman-Penrose formalism, expressing the perturbation in terms of the (complex) Weyl curvature scalars. Equations for the $s = \pm 2$ linearized Weyl scalars ψ_0 and ψ_4 famously decouple yielding a separable wave-like equation discovered by Teukolsky [340, 1064, 1122, 1312]. Both ψ_0 and ψ_4 uniquely describe $g_{ab}^{(1)}$ up to gauge and perturbations to other Kerr spacetimes [1065], and in particular describe the GW degrees of freedom, with ψ_4 most relevant for gravitational radiation at infinity. Similarly, spin-weight $s = \pm 1$ and $s = 0$ Teukolsky equations describe electromagnetic and scalar-field perturbations, respectively.

Homogeneous solutions to the Teukolsky equation can be obtained by imposing

boundary conditions corresponding to the physical requirement that radiation is infalling at the BH horizon and outgoing at infinity. For each spin weight, this eigenvalue problem admits a countably infinite, discrete spectrum of complex-frequency *quasinormal modes (QNMs)* [1313, 1314], see Fig. 8. Each QNM is labelled by three integers: two spin-weighted spheroidal-harmonic quantum numbers used to separate the angular dependence ($\ell \geq 2$, $-\ell \leq m \leq \ell$) and an "overtone number" $n \geq 0$, which sorts the frequencies in ascending order of the absolute value of their imaginary part. Negative (real) frequency modes are related to modes with negative m by the symmetry $-\omega_{n\ell m}^* = \omega_{n\ell-m}$. Kerr quasinormal frequencies (QNFs) have a strictly negative imaginary part, hence the modes decay with time, due to absorption by the BH horizon and radiation to infinity. These frequencies are moreover uniquely determined by the Kerr mass and spin in agreement with no-hair theorems. For detailed reviews on QNMs, see, e.g., [1315–1318].

In contrast to normal modes, QNMs of Kerr do not form a complete basis, and therefore cannot fully describe the ringdown for all times, even at linear order. At *early* times, the linear response to a perturbation is dominated by a "direct" emission of radiation (also known as the prompt response) [1316, 1319, 1320]. At *late* times, the perturbation is dominated by a power-law "tail" (associated with a branch cut in the frequency plane of the Green's function of the Teukolsky equation), which arises due to the asymptotic properties of the wave-equation potential at large distances from the horizon [1320, 1321]. QNMs are most important at *intermediate* times, and for realistic inspirals they tend to dominate the majority of the post-merger signal. They have therefore proven extremely relevant for waveform modeling, either to analyze the ringdown in isolation or for combined inspiral-merger-ringdown waveforms. Indeed, a single QNM can be used to infer the mass and spin of the remnant, whereas additional modes or inspiral information enable consistency checks on GR [106, 597, 604, 1322–1324].

4.4.2. Suitable for what sources? LISA is expected to detect the ringdown of MBHB and IMRI sources for which the merger occurs during the LISA observational time, and for which remnant QNFs fall within the LISA frequency band [604, 1325, 1326]. For EMRIs, the ringdown is likely to be too weak to resolve, a potential exception being those with near-extremal primaries [1327, 1328].

One can easily estimate the mass range of remnants with ringdowns within the LISA band. Indeed, the longest lived (fundamental, $\ell = m = 2, n = 0$) QNM has frequency $f_0 \simeq 0.4/(2\pi M_{\text{final}})$, with the exact value depending on the remnant's spin. For this to lie within the LISA band, $[10^{-4}, 10^{-1}]$ Hz, the mass of the remnant must therefore fall within the range $[10^8, 10^5]$ M$_\odot$. Ringdown modelling will be particularly important for MBHBs at the higher end of the mass spectrum, since their inspiral will take place outside the LISA band and contribute little to the SNR [1329].

4.4.3. Status At linear order in BHPT and for most of the duration of the signal, the ringdown is well described by a superposition of QNMs. For a given BH mass and spin, the Kerr QNFs were first computed numerically in [1322]. The most accurate and reliable numerical method is Leaver's continued fraction approach [1330–1332] (see Mathematica notebook and data at [1333]) and in particular its spectral refinement [1144, 1334] (implemented in the Python package `qnm` [1335]). Kerr QNFs can also be estimated analytically using WKB (Wentzel–Kramers–Brillouin) or WKB-inspired approximations [1336–1341]. QNM modeling should be performed in a certain preferred BMS frame [555, 1342]. Afterwards it can be transformed to a different desired reference frame, e.g., a frame co-precessing with the binary [754, 1343], a frame set prior to a merger kick [1344], or the post-Newtonian preferred frame appropriate to modeling the early inspiral [555].

In addition to the frequencies, the QNM component of the ringdown signal also comprises the amplitude and phase of each mode. Unlike the frequencies, these quantities are not uniquely determined by the remnant, but rather depend on the particular initial conditions that led to its formation. In principle, the amplitudes and phases can be computed from the spacetime right after the formation of a common BH horizon [1320, 1345], and hence from the binary parameters [1346, 1347]. However, this data is hard to predict analytically, and moreover challenging to extract from NR simulations. Common practice is therefore to calibrate the desired mode amplitudes and phases by fitting against NR simulations [1342, 1346, 1348–1353]. Alternatively, initial data can be estimated at the level of the Teukolsky equation using an Ori-Thorne procedure [1090, 1115, 1354–1356].

For binary BH mergers of comparable masses, the linear ringdown model—a superposition of a finite number of QNMs with arbitrary amplitudes and phases—has been extensively compared against NR simulations. At late times ($\gtrsim 10M$ after the peak of the waveform), the general consensus is that the linear model provides a good, stable, and consistent fit to the numerical waveform. At these times, the waveform is well described by a small number of overtones (dominated by the $\ell = m = 2$ multipole and overtones with $n \lesssim 2$), and fitting for the frequencies and decay rates allows for accurate inference of the remnant mass and spin [567, 1342, 1350, 1353, 1357–1361]. More surprisingly, several studies indicate that the linear model applies even at much earlier times, provided higher (ℓ, m, n) modes are included in the model [1342, 1357–1359]. However, the relevance of the linear model at these times ($\lesssim 10M$ after the peak of the waveform) and, in particular, the role of spherical-spheroidal mode mixing, nonlinear modes and higher overtones ($n > 2$), is still actively debated [1342, 1353, 1362–1369].

A complete linear-order model of the post-merger signal should also include back-scattering of radiation against the background potential. This is well approximated by a power-law tail $h \sim t^{-n_{\text{tail}}}$ at late times, where $n_{\text{tail}} = 7$ for generic gravitational perturbations of Kerr [1321, 1370, 1371]. So far the tail contribution has not been

confidently identified in NR simulations of binary BH mergers, so it is usually neglected in waveform modeling.

At very early times (around the peak amplitude) we expect higher order BHPT to become relevant. Beyond-linear-order perturbations satisfy the same equations as at linear order, but now with source terms made up of lower-order perturbations [1292, 1294, 1372–1376]. It is therefore natural to expect the signal to deviate from a simple superposition of linear QNMs. Such deviations could include new driven frequencies that are combinations of the first-order QNFs [1377, 1378], or corrections to the first order modes, in terms of the mode amplitudes, phases, and frequency spectrum [1379, 1380]. Indeed, a driven second-order mode (which in quasicircular mergers appears in the $\ell = m = 4$ multipole, sourced by the square of the $\ell = m = 2$ fundamental mode) was recently identified in binary BH simulations [1349, 1364, 1365, 1381, 1382]. Notably, the amplitude of the second-order mode was comparable to the amplitude from linear order, raising questions about perturbative convergence.

Detailed second-order calculations remain challenging, and are complicated by aspects of metric reconstruction and regularization of singularities. Nevertheless, second-order Kerr perturbations in the ringdown context were recently calculated numerically [1380]. Additional analytic progress in the higher-order ringdown has included the development of a bilinear form under which Kerr QNMs are orthogonal [1383, 1384] (see also [1385]), new methods to reconstruct the metric in the presence of a first-order source [1293], and the use of analytic approximations [1378]. These calculations have considerable overlap with the self-force problem, where significant progress has recently been made at second order, see Sec. 4.3.3.

4.4.4. Challenges The main challenges in post-merger signal modeling using BHPT concern the inclusion of higher modes, the instability and quick damping of overtones, non-QNM ringdown components (e.g., from tails or the prompt response), and nonlinear effects.

Higher (ℓ, m, n) modes are predicted by BHPT to arise in generic binary mergers. However, there is no consensus on whether it is consistent to include more than a few overtones ($n \geq 1$) in a purely linear model [1353, 1357, 1368]. The challenge lies in the fact that higher overtones decay rapidly, and therefore are relevant at early times, when nonlinearities are also expected to become more significant. Despite providing good fits to the signal, higher overtones might simply play the role of fitting noise, nonlinearities, or non-QNM components (such as tails or the prompt response) in the signal. For asymmetric binaries (with precession, eccentricity, or unequal mass ratios) angular modes beyond $\ell = m = 2$ may also have significant amplitudes (see e.g. [600, 1342, 1361, 1386]), and their fundamental ($n = 0$) modes have lifetimes similar to the fundamental $\ell = m = 2$ mode.

Recent theoretical studies also indicate that the QNM spectrum itself could be

unstable [1387–1393], with overtones particularly sensitive to nonlinear perturbations, small environmental effects, and deviations from vacuum general relativity. However the experimental implications of this instability are not fully understood.

The size of power-law tail contributions due to back-scattering has yet to be estimated for binary BHs in full GR. Reference [1353] cautioned that, at the linear level, the tail contribution can be comparable to that of high-overtone QNMs with $n \simeq 5$. This should motivate a more careful study of the contribution of back-scattering effects in the post-merger signal.

No study has yet quantified which (if any) LISA-band ringdown sources will require higher-order perturbation theory. Ideally, starting from a first-order perturbation, a nonlinear model would predict detailed corrections including the amplitude of driven modes, shifts in amplitudes and phases for first-order modes, and any frequency drifts. Some initial progress towards such a model includes agnostic fits of numerical relativity waveform catalogues [1353], numerical studies [1380], and developments in BH perturbation theory [1294, 1383].

Some studies have speculated that nonlinearities could be stronger for near-extreme remnants, whose spectrum contains long-lived modes with commensurate frequencies. In this limit, nonlinear effects could lead to gravitational turbulence [1394] and connect with the Aretakis instability of extremal BHs [1395]. To assess these possibilities, it will be necessary to extend calculations beyond scalar-field toy models [1394] to full general relativity, see for example Ref. [1396].

4.5. Effective-one-body waveform models

Coordinators: Tanja Hinderer, Geraint Pratten
Contributors: S. Akcay, A. Antonelli, S. Bernuzzi, A. Buonanno, J. Garcia-Bellido, A. Nagar, L. Pompili

4.5.1. General description The effective-one-body (EOB) approach was originally introduced in Refs. [746, 1088, 1232, 1397, 1398] with the aim of providing GW detectors with semianalytic waveform models for the entire coalescence of compact-object binaries (i.e., the inspiral, plunge, merger and ringdown), resumming PN information around the strong-field test-body limit. Since the breakthrough in NR in 2005 [506–508], the EOB framework has incorporated information from the NR simulations, thus producing highly-accurate waveform models for GW observations (e.g., see the review articles [791, 1399] and discussion below). Over the years, the EOB framework has been extended to the scattering problem, and has incorporated analytical information from other methods, such as the PM approach and GSF theory, as illustrated in Fig. 9.

The EOB waveform models consist of three main building blocks: 1) the Hamiltonian, which describes the conservative dynamics, 2) the radiation-reaction (RR) force, which accounts for the energy and angular momentum losses due to GW emission, and 3) the inspiral-merger-ringdown waveform modes, built upon improved PN resummations for the inspiral part, and functional forms calibrated to NR waveforms for the merger-ringdown signal. We now briefly review these three key ingredients.

A fundamental pillar of the EOB approach is the map of the real two-body dynamics into that of an effective test mass or test spin in a deformed Schwarzschild or Kerr background, with the deformation parameter being the symmetric mass ratio $\nu = \mu/M$, where $\mu = m_1 m_2/M$ is the reduced mass and $M = m_1 + m_2$ is the total mass. More specifically, the real or EOB Hamiltonian, H_{EOB}, is related to the effective Hamiltonian, H_{eff}, by [746]

$$H_{\text{EOB}} = M\sqrt{1 + 2\nu\left(\frac{H_{\text{eff}}}{\mu} - 1\right)}. \tag{15}$$

Interestingly, such a relation agrees with calculations in quantum electrodynamics [1400] aimed at deriving an approximate binding energy for charged particles with comparable masses in the eikonal approximation; it has been shown to hold exactly at 1PM order [906], and it has been extensively used in scattering-theory computations [906, 907, 961, 974]. The above energy-map (15) achieves a concise resummation of PN information into the Hamiltonian via a small number of terms. In the center-of-mass frame, the EOB equations of motion read:

$$\frac{d\boldsymbol{r}}{dt} = \frac{\partial H_{\text{EOB}}}{\partial \boldsymbol{p}}, \qquad \frac{d\boldsymbol{p}}{dt} = -\frac{\partial H_{\text{EOB}}}{\partial \boldsymbol{r}} + \boldsymbol{\mathcal{F}}, \qquad \frac{d\boldsymbol{S}_{1,2}}{dt} = \frac{\partial H_{\text{EOB}}}{\partial \boldsymbol{S}_{1,2}} \times \boldsymbol{S}_{1,2}, \tag{16}$$

where $\boldsymbol{r}$ and $\boldsymbol{p}$ are the canonical variables, notably the relative position and momentum,
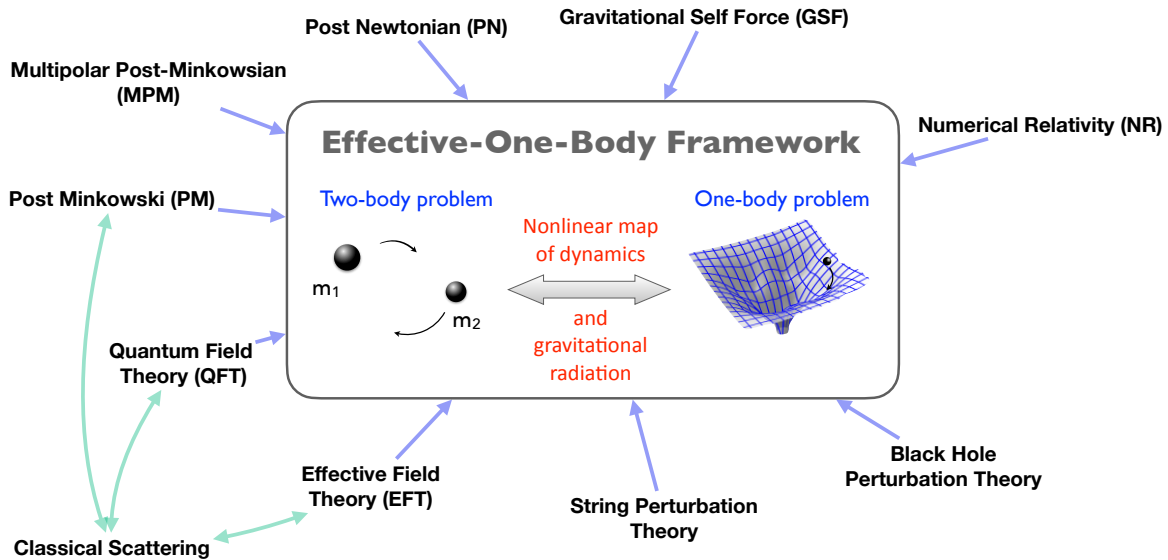
Figure 9. Theoretical inputs to the EOB framework. The EOB theory draws on a variety of perturbative results from numerous approaches in different regimes, as well as from NR simulations, as illustrated here.

respectively, $\boldsymbol{\mathcal{F}}$ is the RR force, and $\boldsymbol{S}_i$ with $i = 1, 2$ are the spins of the compact objects. For example, in the nonspinning limit, where the dynamical variables reduce to (r, ϕ, p_r, p_ϕ), the effective Hamiltonian in the gauge of Refs. [746, 1397] reads

$$H_{\mathrm{eff}} = \mu \sqrt{A_\nu(r) \left[\mu^2 + A_\nu(r) \bar{D}_\nu(r) \, p_r^2 + \frac{p_\phi^2}{r^2} + Q_\nu(r, p_r) \right]}, \qquad (17)$$

where the potentials $A_\nu(r)$ and $D_\nu(r)$ differ from the Schwarzschild ones due to PN corrections depending on ν. The higher-order (yet) unknown PN corrections in $A_\nu(r)$ might be informed to NR simulations. The potential $Q_\nu(r)$ is a non-geodesic term that needs to be introduced at 3PN order [1397] to preserve the mapping (15), and reduces to zero in the test-mass limit.

Precessing-spin EOB waveforms for the inspiral-merger-ringdown were first built in Ref. [1232] using the nonspinning EOB Hamiltonian [746, 1088, 1397] augmented with a spinning PN Hamiltonian [758]. The EOB Hamiltonian for spinning objects was first developed in Ref. [1398], and then in Refs [1401–1404]. These papers follow the structure of the Hamiltonian advocated in Ref. [1398] that in the large mass-ratio limit reduces to the one of a (nonspinning) test mass on a Kerr background. Furthermore, another line of research, which started in Refs. [1405, 1406], built EOB Hamiltonians for spinning objects such that, in the large mass-ratio limit, they reduce to the one of a test spin on a Kerr background [1405, 1407]. The two different spinning Hamiltonians were comprehensively compared in Refs. [1408, 1409].

In the original EOB model [1088], the radiation-reaction force of Eq. (16) was given by a suitable Padé resummation of the PN-expanded energy flux at 2.5PN order, following the

seminal work of Ref. [1410]. Subsequently, the (quasi-circular) radiation-reaction force, that is the flux of angular momentum, has been expressed as the sum of factorized and resummed multipoles according to the procedure introduced in Refs. [1234, 1411]. This approach was then first extended to spinning bodies in Ref. [1146] and then improved in Refs. [1263, 1412–1416] by means of additional factorizations and resummation of the orbital and spin parts, and the inclusion of higher-order PN terms.

The factorization of each waveform multipole proposed in Ref. [1411] reads

$$h_{\ell m}^{\text{insp-plunge}}(t) = h_{\ell m}^{(N,\epsilon)} \, S_{\text{eff}}^{(\epsilon)} \, T_{\ell m} \, e^{i\delta_{\ell m}} \, (\rho_{\ell m})^{\ell} \, h_{\ell m}^{\text{NQC}} \,, \tag{18}$$

where $h_{\ell m}^{(N,\epsilon)}$ is the Newtonian contribution and ϵ denotes the parity of the mode. The factor $T_{\ell m}$ resums an infinite number of leading-order logarithms arising from tail effects [1234] (see also Ref. [817]), the term $e^{i\delta_{\ell m}}$ is a residual phase correction due to sub-leading order logarithms in hereditary contributions, and the functions $\rho_{\ell m}$ are the residual amplitude corrections. These functions were originally obtained as PN-expansions [1411], but in some versions of the EOB models, it was found useful to further resum them using Padé approximants for improved strong-field robustness [1263, 1414, 1415]. Another approach consists of calibrating effective high-order PN parameters entering the $\rho_{\ell m}$'s to improve their accuracy, doing so either using NR data [1412, 1413, 1416, 1417] or second-order GSF results [1418].

The factor $h_{\ell m}^{\text{NQC}}$ is the phenomenological next-to-quasi-circular (NQC) correction [1419] to the waveform that is informed by NR simulations, and it is designed to correctly shape the waveform during the late plunge up to merger, where the motion is not quasi-circular and the resummed quasi-circular waveform lacks information. The complete EOB waveform is constructed by attaching the merger-ringdown mode, $h_{\ell m}^{\text{merger}-\text{RD}}(t)$, to the inspiral-plunge one, $h_{\ell m}^{\text{insp}-\text{plunge}}(t)$, at a suitable matching time $t = t_{\text{match}}$, around the peak of the EOB orbital frequency (which approximately corresponds to merger time), that is [1088]:

$$h_{\ell m}(t) = h_{\ell m}^{\text{insp}-\text{plunge}-\text{merger}}(t) \, \Theta \left(t_{\text{match}}^{\ell m} - t \right) + h_{\ell m}^{\text{ringdown}}(t) \, \Theta \left(t - t_{\text{match}}^{\ell m} \right) \,, \tag{19}$$

where $\Theta(t)$ is the Heaviside step function. Inspired by results for the infall of a test mass into a BH [1420] and the close-limit approximation [1421], several EOB waveform models used a superposition of QNMs for the dominant mode [567, 1088, 1114, 1235, 1239, 1398, 1412, 1413, 1422–1425]. More recently, an NR-informed fit of the amplitude and phase has become standard [1426]. This framework is similar in spirit to the rotating source approximation developed in Ref. [1427], but with significant technical differences. An important input into the merger-ringdown part of the EOB model is the mapping between progenitor binary parameters and the mass and spin of the final remnant. This is needed to determine the frequency of QNMs of the remnant, and it is obtained from NR results [591, 1428].

There is considerable freedom in modeling and resumming the EOB Hamiltonian, radiation-reaction force and GW modes, and spin effects. Those different choices,

together with variations in the gauge adopted and deformations of the potentials in the Kerr spacetime, have led to two main EOB families: `SEOBNR` (e.g., see Refs. [745, 747, 1416, 1429]) and `TEOBResumS` (e.g., see Refs. [751, 1403, 1430, 1431]), which we discuss in detail in Secs. 4.5.3 and 4.5.4 below. The EOB waveform program advances along two interrelated directions. The first comprises theoretical advances on the underlying structure and mapping of analytical results from PN, PM and GSF approaches. The second involves testing and refining the models using NR information and rendering them available for use in data analysis. The EOB waveform models are intrinsically in the time domain (TD), which provides a more direct relation between source physics and asymptotic radiation than frequency-domain models. Modeling both the dynamics and radiation is useful for gaining deeper insights into strong-field nonlinearities and it enables more thorough tests of the robustness of different aspects of the waveform based on examining the behavior of various characteristic quantities under changes in the binary's parameters, and on comparing different gauge-invariant quantities between EOB, NR, or perturbative results — for example the binding energy and fluxes [908, 996, 1432–1435], periastron advance [1102, 1103, 1436], scattering angles [711, 977, 978, 1437] or spin-precession invariant [1436] and redshift. At the same time, this also makes EOB models computationally more expensive than IMR waveform models, which describe only the asymptotic GW signals in the frequency domain (FD), as discussed in Sec. 4.6. However, the computational cost is not an insurmountable problem. Much recent work has significantly improved the computational efficiency of EOB models through the development of optimized codes [1408, 1438–1441], by building reduced-order models (ROMs) [1417, 1442–1451], implementing the quasi-adiabatic approximation [751, 1408, 1440, 1452], and making use of machine-learning methods [1449, 1451, 1453, 1454]. Close Hyperbolic Encounters could also be searched for with both ground- and space-based interferometers using machine learning [1455].

EOB waveform models have been constructed for quasi-circular non-spinning [567, 796, 1088, 1397, 1411, 1422–1424, 1456–1458] and spinning [745, 747, 751, 1232, 1239, 1398, 1401–1404, 1406, 1407, 1409, 1412, 1413, 1416, 1417, 1425, 1429, 1430, 1459–1464] binaries. Furthermore, orbital eccentricity [705, 743, 748–750, 1465, 1466] and matter effects [1434, 1467–1472] (see Sec. 6.5) , as well as information from PM [906–908, 976–978] and conservative GSF information [497, 975, 997, 1000, 1418, 1473–1477] have been also incorporated in EOB models. The required effort to advance the EOB modeling involves: 1) obtaining new analytical information and mapping it into the EOB framework; 2) resumming the results into full waveform models with additional flexibility for calibrations to NR; and 3) testing and comparing models to assess their performance and accuracy. We now describe each of on the two main EOB families in some more detail.

4.5.2. *Suitable for what sources?* Inspiral-merger-ringdown signals from massive black-hole binaries (MBHBs) will be within the LISA band (see Sec. 2.1), making EOB

family	waveform model	spins	ecc./hyper.	NR & Teukolsky calib. region	CP-frame modes
1st	*EOBNRv1 [1422]			$q \leq 4$	
	EOBNRv2 [1457]			$q \leq 3$	$(2,2)$
2nd	SEOBNRv0 [1460]			$q = 1, \chi_{1,2} = \pm 0.4$	
	*EOBNRv2HM [1423]			$q \leq 6$	$(2,2),(2,1),(3,3),(4,4),(5,5)$
	*EOBNRv2HM_ROM [496]				
3rd	*SEOBNRv1 [1412]	✓		$q \leq 6, \chi_{1,2} = \pm 0.4$	$(2,2)$
	*SEOBNRv1_ROM [1443]				
	*SEOBNRv2 [1413]			NR: $q \leq 8, |\chi_{1,2}| \leq 0.98$ Teuk.: $q = 1000, |\chi_{1,2}| \leq 0.99$	
	*SEOBNRv2_ROM [1444]				
	SEOBNRv2P [1239]	✓✓			$(2,2),(2,1)$
	*SEOBNRv3P [1413, 1425]				
4th	*SEOBNRv4 [745]	✓		NR: $q \leq 8, |\chi_{1,2}| \leq 0.995$ Teuk.: $q = 1000, |\chi_{1,2}| \leq 0.99$	$(2,2)$
	*SEOBNRv4_ROM [745]				
	*SEOBNRv4P [747]	✓✓			$(2,2),(2,1)$
	*SEOBNRv4HM [1416]	✓			
	*SEOBNRv4HM_ROM [1447]				$(2,2),(2,1),(3,3),(4,4),(5,5)$
	*SEOBNRv4PHM [747]	✓✓			
	*SEOBNRv4PHM_surr [1448]				
	*SEOBNRv4EHM [749]	✓	✓		
	*SEOBNRv4PHM_4dq2 [1451]	✓✓			$(2,2),(2,1),(3,3),(4,4)$
5th	*SEOBNRv5 [1417]	✓		NR: $q \leq 20, |\chi_{1,2}| \leq 0.998$ Teuk.: $q = 1000, |\chi_{1,2}| \leq 0.99$	$(2,2)$
	*SEOBNRv5_ROM [1417]				
	*SEOBNRv5HM [1417]				$(2,2),(2,1),(3,2),(3,3),$ $(4,3),(4,4),(5,5)$
	*SEOBNRv5PHM [1429]	✓✓			

✓ aligned spin, ✓✓ arbitrary spin orientations.
* implemented in `LALsuite`, and for the latest version (v5) in the open-source Python package `pySEOBNR` [1478].

Table 10. Progress in the development of `SEOBNR` models. The NR-calibration region refers only to calibration against aligned-spin NR waveforms. We indicate the coprecessing modes as CP modes. The surrogate models `SEOBNRv4PHM_surr` and `SEOBNRv4PHM_4dq2`, and the eccentric/hyperbolic model `SEOBNRv4EHM` are implemented in LALSuite, but they have not been reviewed, yet, and they are not publicly available at the moment. The surrogate models are limited in length and binary's parameter space (see Refs. [1448, 1451] for details).

models naturally applicable for these sources. The bulk of MBHB events observable by LISA are expected to have mass ratios $q \lesssim 10$, but some systems may have mass ratios of up to several hundreds. Most tests and calibrations of EOB models have been for $q \lesssim 20$, but the fact that EOB models interpolate between this regime and the test-body limit with information from BH perturbation theory makes them structurally well-suited for larger-q systems. Spin precession and eccentricity effects, both simultaneously relevant for MBHBs and IMRIs, have to date been separately included in EOB models. These considerations apply not only for MBHBs but also for describing intermediate mass-ratio binaries (IMRIs) discussed in Sec. 2.3. Importantly, EOB models have been either validated [497, 1477] or improved using perturbation-theory and GSF information [975, 1000, 1418, 1474–1476], which is relevant for IMRIs and also EMRIs. EOB models are also suitable to stellar-origin binaries Sec. 2.5, whose early-inspiral signals will be within the LISA band. For inspirals, EOB models provide a more accurate though less efficient description than pure PN-based models, where, e.g.,

Ref. [1441] shows that using EOBSPA+PA is rather efficient while searches using PN waveforms would miss a significant portion of events. Using EOB waveforms will further be important for connecting the LISA portion of SOBHB signals with the corresponding merger signals measurable in future ground-based detectors. The EOB approach also allows for the inclusion of additional physical effects, for instance, from gravity theories beyond GR and environmental effects as explained in Sec. 6.5.

As discussed in Sec. 4.5.6, while EOB models are naturally suited to the above sources, significant further advances in the modeling accuracy, complexity of physical effects, robustness over a wide range of parameter space, and efficiency will be required for their use in LISA data analysis.

4.5.3. The SEOBNR waveform models

The EOBNR family of waveform models § has been developed with two main goals: i) make use of the most accurate analytical information for the two-body dynamics and gravitational radiation (PN, PM, GSF) and results from NR and Teukolsky-code simulations to build physical, highly-accurate waveform models of compact-object binaries, and ii) make them available to GW detectors for searches and inference studies. The history, since 2007, and the current status of EOBNR models are illustrated in Table 10. These models have been implemented into the LIGO Algorithms Library (LALsuite) [1479], and more recently in the open-source Python package pySEOBNR [1478]. These codes were then reviewed by the LVK Collaboration. Here we summarize the main milestones, focusing on the binary BHs, while leaving details of the modeling improvements (two-body inspiraling dynamics, transition merger to ringdown, RR effects, GW modes, resummation of EOB potentials, etc.) to the corresponding publications.

Building on the original work on the EOB framework [746, 1088, 1232, 1397], the first EOBNR model calibrated to nonspinning NR waveforms was developed in Ref. [1422], following initial comparisons to NR equal-mass nonspinning binaries in Ref. [567], in which the importance of including overtones in the EOB description of the merger-ringdown signal was pointed out. EOBNRv1 was employed by Initial and Enhanced LIGO, and Virgo for the first searches of coalescing binary BHs [1480–1483]. The calibration to spinning binaries with equal masses was considered in Ref. [1460], employing an EOB Hamiltonian for a test mass in a deformed Kerr spacetime [1401]. The nonspinning waveforms with higher modes were first modeled in Ref. [1423] with the improved factorized waveforms [1146, 1234, 1411], thus marking the second generation of EOBNR models.

The third-generation of EOBNR models encompassed significant advances in including spin effects in the two-body dynamics and radiation, resumming perturbative information, and calibration to NR simulations. An EOB Hamiltonian for a test spin in a deformed Kerr spacetime was derived in Refs. [1405–1407]. It included all PN

§ The generic name SEOBNRvnEPHM indicates that the version vn of the EOB model is calibrated to NR simulations (NR), includes spin (S) and precessional (P) effects, eccentricity (E) and higher modes (HM).

corrections in the test-body limit, at linear order in the test-body's spin. To enforce the presence of a photon orbit (and peak of the orbital frequency) for aligned-spin binary BHs, it used a logarithmic (instead of Padé) resummation of the EOB potentials. Those improvements led to the aligned-spin model `SEOBNRv1` [1412], and the first spin-precessing model, `SEOBNRv2P` [1239], which adopted the co-precessing frame description of Refs. [1484, 1485] to efficiently handle precessional effects. Those models also included information for the merger-ringdown waveforms from the test-body limit, notably from time-domain Teukolsky waveforms obtained in Refs. [1114]. With the availability of a larger set of accurate SXS NR waveforms, and further analytical results from PN theory, the model was upgraded to `SEOBNRv2` [1413], with its precessing version known as `SEOBNRv3P` [1425]. These third-generation `SEOBNR` models were used in the template bank of the modeled searches (`gstLAL` and `pyCBC`), and for parameter-estimation of GW signals detected during the first observing run (O1) of Advanced LIGO [185, 761].

The fourth generation of models included substantial and more efficient (via Markov-chain–Monte-Carlo methods) re-calibrations of the aligned-spin baseline models, such as `SEOBNRv4` [745], and phenomenological ansatzes for the merger-ringdown based on Ref. [1426]. The `SEOBNRv4` model was completed by including higher modes [1416], arbitrary spin orientations [747], and extended to eccentric and hyperbolic orbits for aligned spins in Ref. [749], using GW modes recast in factorized form in Ref. [748] (see also Refs. [704, 706, 743, 1486] for other eccentric `EOBNR` models). These updated models for quasi-circular orbits were used for the template banks of modeled searches, and extensively for inference studies during the second (O2) and third (O3) runs of Advanced LIGO and Virgo [106, 108, 202, 1487, 1488].

Among the highlights of the fifth generation of models, they were calibrated to NR waveforms with larger mass-ratios and spins using a catalog of 442 SXS simulations [1417], and they incorporate for the first-time information from second-order GSF in the nonspinning modes and radiation-reaction force [1418]. The models include several higher modes, notably the $|m| = \ell$ modes for $\ell = 2$–5, the $(2, |1|)$, $(3, |2|)$ and $(4, |3|)$ modes. Differently from the `SEOBNRv3` and `SEOBNRv4` Hamiltonians, the `SEOBNRv5` reduces in the test-body limit to the one of a test mass in the Kerr spacetime. The accurate precessing-spin dynamics of `SEOBNRv5PHM` [1429] was obtained including partial precessing-spin information in the EOB Hamiltonian in the co-precessing frame by orbit averaging the in-plane spin components of the full precessing Hamiltonian at 4PN order [1489]. Furthermore, the evolution equations for the spin and angular momentum vectors were computed in a PN-expanded, orbit-averaged form for quasi-circular orbits, similarly to what was done in Refs. [751, 1490, 1491], but with important differences due to the distinct gauge and spin supplementary conditions [1489], and the inclusion of orbit-average in-plane spin effects. Thanks to a simpler (but more approximated) precessing-spin inspiraling dynamics, which allows for the use of the post-adiabatic approximation [1408, 1452], and the new high-performance Python infrastructure `pySEOBNR` [1478], the computational efficiency of the `SEOBNRv5PHM` models

has improved significantly, generally $\sim$ 8–20 times faster than the previous generation `SEOBNRv4PHM`. This is particular important in view of the use of these waveform models with next-generation detectors on the ground and with LISA, which have a much broader bandwidth.

Furthermore, `SEOBNR` waveform models have also been used to extend the NR surrogate models (see Sec. 5.1) to lower frequencies, by hybridizing them [756, 1492, 1493], and to build IMR phenomenological waveform models (see Sec. 4.6). For the latter, `SEOBNR` models have been employed to construct time-domain hybrid NR waveforms, and also to calibrate the phenomenological models in regions of the parameter space where NR waveforms are not available [719, 753, 1494].

Quite importantly for LISA and next-generation detectors on the ground, the computational efficiency of the time-domain `SEOBNR` models can also be improved by building surrogate and ROM versions [745, 1417, 1443, 1444, 1448]. Lastly, the efficient and flexible `pySEOBNR` infrastructure [1478], which uses Bayesian algorithms to calibrate waveforms against NR simulations, will allow to swiftly include and test new analytical information (PN,PM,GSF) (and their possible resummations) as soon as they become available. This is crucial to improve waveform models by at least two orders of magnitude to match the expected waveform accuracy requirements.

Extensions of the `SEOBNR` models to extreme mass-ratio inspirals were obtained in Refs. [1000, 1115, 1413, 1474, 1475], and to non-vacuum binary systems and gravity theories beyond GR are discussed in Sec. 6.5.

4.5.4. The `TEOBResumS` waveform models The `TEOBResumS` model builds upon early EOB developments at the Institut des Hautes Etudes Scientifiques (IHES) that define the basics structure of the model. The name suggests the key features: arbitrary compact binaries with tidal (T) and generic spins (S) interactions are modeled by making systematic use of analytical resummations. This name has first appeared in the tidal model of Ref. [1434] and in the tidal and spinning model of Ref. [1430]. The latter include the factorized waveform described above [1235, 1411], the systematic resummation of EOB potentials via Padé approximants [1235, 1401, 1402, 1424, 1495], NQC corrections [1233, 1234, 1424, 1459, 1461], attachment of the ringdown around the peak of the orbital frequency (i.e., light-ring crossing) [1234, 1424], the concept of centrifugal radius for incorporating spin-spin interactions [1403], resummed gyro-gravitomagnetic functions [1401–1403] and the factorized NR-informed ringdown waveform [1426]. These developments made heavy use of results in the test-mass limit obtained by means of a new approach to black hole perturbation theory [1116, 1233, 1234, 1237, 1238] to understand each physical element entering the structure of the waveform and striving for physical completeness, simplicity, accuracy and efficiency. Currently, `TEOBResumS-GIOTTO` is a unified framework to generate complete inspiral-merger-postmerger waveforms for any type of quasi-circular compact binary (BBH, BNS,

Physical content		GIOTTO	DALI
Analytic information	$A(r)$	Pseudo 5PN, resummed	Pseudo 5PN, resummed
	$D(r)$	3PN, resummed	5PN, resummed
	$Q(r, p_{r_*})$	3PN	5PN (local)
	G_S, G_{S_*}	3.5PN	3.5PN
	r_c	NLO	NLO
NR information	a_c^6	Effective parameter in $A(r)$	
	c_{N3LO}	Effective parameter in G_S, G_{S_*}	
	NQCs	Ensure correct transition between plunge and merger	
	Ringdown	Phenomenological model, quasi-circular	
	BBH NR Validation region	$q \geq 10$ and test-mass with $|\chi_{1,2}| \geq 0.99$; $10 < q < 128$ no-spins	
Spins	Aligned	✓	✓
	Precessing	✓	-
Orbital dynamics		Circular	Generic (bound & open)
Subdominant CP modes	Inspiral to merger	$(\ell, |m|) \leq 8$	
	Merger/ringdown	$(\ell, |m|) = (2,1), (2,2), (3,2), (3,3), (4,2), (4,4), (5,5)$	

Table 11. Current/default physics incorporated in `TEOBResumS`. `TEOBResumS` is developed open source and publicly available at https://bitbucket.org/eob_ihes/teobresums/. Symbols are defined in the text. Historical milestones in the model developments and the associated references can be found in the Wiki page of the repository. Robustness tests and the detailed parameter space coverage can be found in the Wiki page and are continuously updated. `TEOBResumS` can also be installed via `pip install teobresums`. The code is interfaced to state-of-art GW data-analysis pipelines, including bilby and pycbc. The code uses semantic versioning since the deployment of the GIOTTO version. Earlier versions of `TEOBResumS` are implemented in LAL Simulation and reviewed by LVK.

BHNS)[1472, 1496, 1497]. `TEOBResumS-Dalí` is the model's extension to generic orbits and describes bound orbits with arbitrary eccentricity [705, 750, 1498, 1499], hyperbolic orbits and scattering [711, 1500, 1501]. The key features of the models are summarized in Table 11 and described in the following. An extension of the model that relies on GSF-informed potentials [1001, 1476] so as to generate extreme-mass-ratio-inspirals (EMRIs) is available [497, 1477], and work on scalar-tensor gravity (building upon Refs. [1502, 1503]) is also currently in progress [1504–1506].

The structure of the spin-aligned effective `TEOBResumS` Hamiltonian is

$$H_{\text{eff}} = H_{\text{eff}}^{\text{orbital}} + H_{\text{eff}}^{\text{SO}}, \tag{20}$$

where $H_{\text{eff}}^{\text{orbital}}$ incorporates even-in-spin contributions (spin-spin couplings), while $H_{\text{eff}}^{\text{SO}}$ incorporates odd-in-spin ones (spin-orbit couplings). The spin-orbit contribution reads

$$H_{\text{eff}}^{\text{SO}} = G_S S + G_{S_*} S_*, \tag{21}$$

where (G_S, G_{S_*}) are the gyro-gravitomagnetic functions and $S \equiv S_1 + S_2$, while $S_* = m_2/m_1 S_1 + m_1/m_2 S_2$ are useful combinations of the spins [1401, 1402, 1507]. In the large-mass-ratio limit, S becomes the spin of the largest black hole, while S_* is the spin of the small body. The orbital contribution $H_{\text{eff}}^{\text{orbital}}$ incorporates the three EOB potentials (A, D, Q). The A function employs the full 4PN information [796] augmented by an effective 5PN term, parametrized by the coefficient a_6^c, which is informed by NR

simulations. In `GIOTTO`, both (D, Q) are kept at 3PN accuracy. In the latest versions of `Dalí`, the full 5PN information is being currently explored [1497]. The spin-orbit sector includes next-to-next-to-leading-order (NNLO) analytical information [1402] in the (resummed) gyro-gravitomagnetic functions [1403] augmented by an effective N^3LO coefficient c_3 that is informed by NR simulations. Spin-spin couplings are incorporated using the concept of centrifugal radius [1403], r_c, and starting from NLO accuracy. `TEOBResumS` can deal with generically oriented spins, thus incorporating the precession of the orbital plane and the related modulation of the waveform. Spin-precession in the quasicircular case is incorporated with an efficient yet accurate hybrid EOB-post-Newtonian scheme based on the common "twist approach" [751, 1464, 1472].

In `GIOTTO`, the radiation reaction and multipolar waveform (up to $\ell = m = 8$) are implemented as an upgraded version of the factorized and resummed procedure introduced in Ref. [1411]; see Refs. [1415, 1431]. In addition, NR information is used to determine NQC waveform corrections (multipole by multipole) so as to correctly shape the waveform around merger. The latter is then attached to a NR-informed, phenomenological description of the ringdown based on Ref. [1431]. Importantly, NR information is included in such a way to maintain consistency between waveform and fluxes [1496]. The leading-order horizon absorption terms are implemented in the model since its early version [1403]. In `Dalí`, the radiation reaction on generic orbits is obtained by incorporating generic Newtonian prefactors in the factorized quasicircular EOB waveform [705, 750]. This approach, which is extended to include resummed 2PN terms, has been verified against exact Teukolsky fluxes for highly eccentric and hyperbolic geodesics and currently provides the best available representation of the radiation reaction [1508–1510]. A new paradigm to incorporate PN results into EOB, which promises a further boost in performance, has been recently proposed in Ref. [1466]. The inclusion of matter effects and application to probing the nature of compact objects is discussed in Sec. 6.5.

On the algorithmic side, the development of `TEOBResumS` has introduced two key analytical acceleration techniques, namely the post-adiabatic (PA) approximation of the EOB dynamics [1440] and the EOBSPA [1441]. The PA approximation is an iterative procedure to solve the circularized EOB dynamics at given radii (or frequency) thus bypassing the need to numerically solve the system of ODEs. Performances are reported in e.g. Refs [1440, 1449, 1463, 1496] and show that `TEOBResumS`'s waveform generation times are competitive with some of the fastest waveforms and machine learning approximants for long signals (i.e. BNS inspirals), while retaining the original EOB accuracy. The EOBSPA is a technique to generate multipolar FD EOB waveforms using the stationary phase approximation. Ref. [1441] illustrates that the EOBSPA is computationally competitive with current phenomenological and surrogate models, and can generate (virtually) arbitrarily long and faithful waveforms up to merger for any BNS. Currently, the EOBSPA is also the only alternative to PN methods for efficiently generating intermediate-mass binary black hole inspiral waveforms for LISA [1441].

4.5.5. Environmental effects The EOB approach provides considerable freedom for incorporating yet unknown effects, such as beyond-GR gravity (see Sec. 6.6), exotic BH-like objects, or environmental effects. Analyzing the presence of such effects critically relies on accurate GR waveforms for comparison and benefits from the techniques developed for GR. While the modeling of astrophysical environments has not yet been explored directly within the EOB waveforms program, there is in principle no obstruction to incorporating them. For example, perturbative and numerical studies of environmental effects are already available (as discussed in Secs. 4.2, 4.3 and 4.1) and have identified key distinctive features, which could be mapped into EOB models similarly to what has already been accomplished for other physical effects. Likewise, existing capabilities of using EOB-baseline models for parameterized tests of GR could be extended to include environmental effects in a parameterized, phenomenological way at the level of waveforms. These two approaches could be useful for different purposes.

4.5.6. Challenges Employing EOB waveforms for GW signals of LISA sources requires a significant continued effort to improve the accuracy and include all physical effects. Importantly, the waveform models must incorporate the simultaneous effects of high spins at generic orientations, eccentricity, and large mass ratios q, all of which also require many more higher modes. Furthermore, we require additional flexibility to discover new physics from beyond GR and the Standard Model of particle physics, as discussed in Sec. 6. In terms of accuracy, the models must describe high signal-to-noise-ratio events of MBHBs, at more than an order of magnitude higher than the calibration standards achieved to date, and they have to be tested for the expected LISA detector response.

The effort to meet these requirements involves substantial further model developments on the theoretical and computational fronts. On the theoretical side, advances on the structure of the EOB models to incorporate more information from perturbative schemes are essential. This effort relies on inputs from higher-order calculations with more realistic physics from PN, PM, and GSF to develop robust EOB models for a wide range of the parameter space. While several proof-of-principle studies have been carried out on including PM and GSF information, more work is needed to incorporate them in full state-of-the-art models in a way that can readily be updated as more information becomes available. Methods for including precessing-spins and moderate eccentricity effects (where the systems circularize before merger) are in place but only separately. In principle, the EOB Hamiltonian is fully generic but other components of the model are not, and require further structural developments to incorporate larger eccentricities, as well as the simultaneous effect of precessing spins. Further considerations will also be required on the sets of dynamical variables used to evolve the inspirals, for example, action-angle variables versus the canonical Cartesian coordinates, or a mixture of them. The higher complexity when including both precession and eccentricity effects is challenging, and requires due care to ensure gauge-invariant comparisons. As for

existing models, insights from the small-mass-ratio limit will likely prove useful to address this challenge.

On the practical side, significant further work on testing, calibrating, and optimizing the EOB models against NR results is crucial to attain the accuracy required for LISA sources discussed in Sec. 3.2. This in turn relies on the availability of accurate NR waveforms over a wider parameter space, as detailed in Sec. 4.1. Current EOB models are only calibrated in the aligned-spin sector. However, this would need to be changed, and the calibration be extended to precessing spins to achieve the much higher accuracy requirements of LISA sources.

Furthermore, accurate waveforms for LISA that include eccentricity, precessing spins, large mass ratio, higher modes, and means to test for new physics have a highly complex structure characterized by a large number of different frequencies. Accurately capturing these features significantly slows down the computations of waveforms and enlarges the dimensionality of the parameter space. While EOB waveforms are a priori less efficient than closed-form models, there exist a number of approaches to overcome these shortcomings, as discussed above in Secs. 4.5.1, 4.5.3 and 4.5.4.

4.6. Phenomenological waveform models

Coordinators: Sascha Husa, Maria Haney
Contributors: M. Colleoni, M. Hannam, A. Heffernan, J. Thompson

4.6.1. Description After the binary black hole breakthrough of 2005, a pragmatic approach to developing waveform models for compact binary coalescence was required. Such models needed to describe the waveform from inspiral to ringdown, be tuned to NR, and suit a wide range of GW data analysis applications. Key requirements for broad applicability were (and still are) computational efficiency and broad coverage of the parameter space. This has led to several generations of frequency-domain and more recently also time-domain models, which have been implemented in the open source `LALSuite` framework [1479] under the name of IMRPhenom, and which are constructed in terms of piecewise closed form expressions for the amplitude and phase of spherical harmonic modes. A careful choice of the closed-form expressions allows the maximal compression of information about the waveform into a small number of coefficients that vary across the parameter space. More recently, fast ODE integration techniques have also been developed to model the evolution of the component spins in precessing binaries [1511]. The principal objective of the phenomenological waveform program has been to deliver waveform models that keep up with requirements of data analysis applications and are updated to become increasingly accurate as detectors become more sensitive.

To construct the models, one proceeds in three stages: First, an appropriate piecewise ansatz is developed for simple functions, e.g. the amplitude and phase of spherical or spheroidal harmonics. This ansatz is split into regions, for example corresponding to the inspiral, merger, and ringdown, where physical insight about the different regions can be exploited. Fig. 10 shows the three regions used in current models, where in each such region closed-form expressions are developed to approximate a discrete data set of calibration waveforms. Future upgrades may increase the number of regions to increase accuracy. The analytical ansatz attempts to incorporate physical insight, e.g. regarding perturbative information concerning the inspiral and ringdown. For the inspiral, an ansatz is typically constructed as a deformation of a post-Newtonian description. In the ringdown, black hole perturbation theory can be used to link features in the waveform to the quasinormal frequencies determined by the final mass and spin of a black hole. The ansatz is then fitted to each waveform in a calibration data set, resulting in a set of generalized coefficients for each waveform. This stage is usually referred to as the "direct fit". The input data consist of NR data and perturbative descriptions at low frequency, such as post-Newtonian expansions or EOB models. Most typically, these types of input data are used in the form of hybrid waveforms, which are constructed by gluing inspiral approximants to shorter NR data. Finally, the coefficients are interpolated across the parameter space, which we will refer to as the "parameter space fit". In both stages of fits it is essential to avoid both overfitting and underfitting.
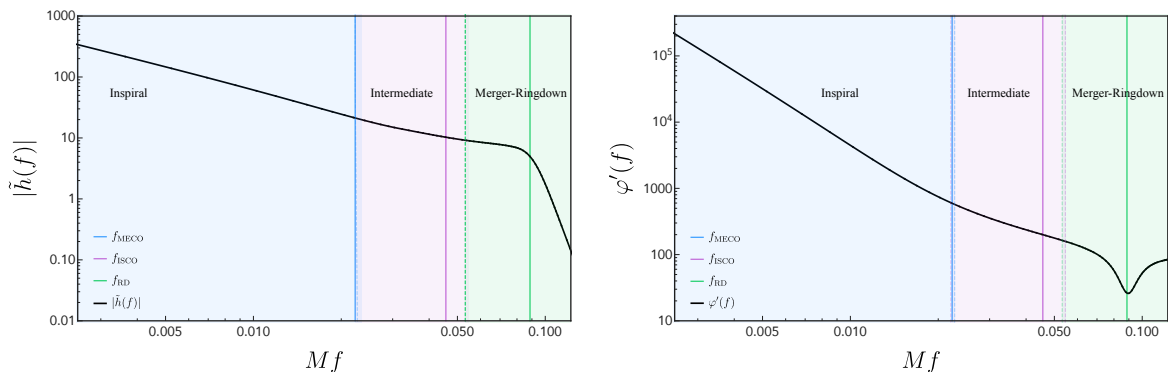
Figure 10. Illustration of the regions used in Phenom models exemplified by the IMRPhenomX model. The plots show the Fourier domain amplitude (left) and phase derivative (right) of the $\ell = 2, m = -2$ spherical harmonic mode. Vertical lines mark the frequencies of the ISCO for the remnant black hole, the MECO (minimum energy circular orbit as defined in [1512]) and the ringdown frequency of the fundamental mode. Figure adapted from [753].

Waveform model development has been increasingly "data driven", adapting phenomenological descriptions to the available data sets, while also using physical insight and perturbative information. The inspiral descriptions, for example, extend post-Newtonian expansions, and the black hole ringdown is formulated in terms of exponentially damped oscillations with complex frequencies that depend on the dimensionless spin of the remnant. In addition, approximate maps have been used, e.g. to map the non-precessing waveforms to precessing ones. Such maps:

- Allow to increase the region of the parameter space where the models can be employed before sufficiently extensive catalogues of NR waveforms are available.

- Give guidance for future more sophisticated models that are calibrated to NR.

The "phenom" approach sketched above facilitates the development of simple and robust codes and very rapid evaluation of the waveforms, and is also well suited to benefit from parallelisation, e.g., through GPUs [495] or similar hardware. Phenom models have already been used in computationally efficient parameter estimation studies of MBHB sources for LISA [495]. Initially, only frequency domain models were developed [514, 719, 744, 752, 753, 1513–1525], since they are naturally adapted to matched filter techniques carried out in the frequency domain. More recently, time domain models have also been developed [1490, 1494, 1511], which can simplify modelling complex phenomena such as precession or eccentricity.

Four generations of such models have been constructed to date in the frequency domain, progressing from the $\ell = |m| = 2$ mode for quasi-circular non-spinning binaries to multi-mode precessing waveforms, as will be described in Sec. 4.6.3. The flexibility of the phenomenological approach is also well suited to parameterize unknown information, e.g., beyond-GR effects (see Sec. 6.6).

102

4.6.2. Suitable for what sources? Massive black hole binaries have already been modelled with the phenom approach, i.e., comparable-mass black-hole binaries, described in Sec. 2.1. The bulk of such binaries detected by LISA is expected to have mass ratios $q = m_1/m_2$ up to ~ 10 (see Sec. 2.1.2), where phenom models have already been calibrated to NR. The main challenge to model such binaries for LISA is to significantly increase the accuracy, corresponding to the much higher expected values for the signal-to-noise-ratio (SNR) with LISA. However, a tail down to mass ratios of a few times 10^{-3} also has to be expected (Sec. 2.1.2). The latest generation of phenom models has indeed already been calibrated to perturbative numerical waveforms that correspond to solutions of the Teukolsky equation [753, 1524] at mass ratios of $\approx 10^{-3}$. Significant progress will still be required regarding both the input calibration waveforms and the models to increase the accuracy, in particular for larger spins and the inspiral. Developments and challenges toward computing large mass ratio NR waveforms are discussed in Sec. 4.1, including synergies between traditional numerical methods, analytical and self-force methods. In principle, the phenom approach may be well suited to some EMRI systems as well. Extension to EMRIs seems most feasible for non-precessing quasi-circular systems, but may not be practical for precessing or eccentric systems, where the signal can be extremely complex.

Stellar-origin binaries (Sec. 2.5) and Galactic binaries (Sec. 2.4) are types of sources for which the phenomenological approach is likely to provide a well suited framework. It can be adapted to produce computationally efficient models that can be tuned to data analysis requirements. However, to our knowledge, no work has yet been carried out in this direction. Finally, one of the strengths of the phenom approach is precisely that it allows for the easy inclusion of approximate phenomenological models of physical effects. In this sense, parameterised modifications to GR or models of environmental effects would in principle be straightforward to include.

4.6.3. Status To date four generations of FD models have been developed, as well as a first generation of time domain models, which correspond to the most recent FD models in terms of parameter space coverage and accuracy. These models have been implemented in the LIGO Algorithms library (LALsuite) [1479] and reviewed by the LIGO-Virgo-KAGRA collaboration. To date, the models have only been calibrated to non-precessing quasi-circular numerical waveforms. Precession has been implemented via the "twisting" approximation [744, 752, 1490, 1517–1520], which is based on the fact that in the inspiral the precession timescale is much smaller than the orbital timescale. Consequently, the precessing motion contributes little to the GW luminosity, and the inspiral rate is dominated by the non-precessing dynamics. One can thus approximately map non-precessing to precessing waveforms, and in a further step one can use fast PN approximants to describe the Euler angles that rotate the orbital plane and waveform. An effective analytical single-spin description for the Euler angles including next-to-next-to-leading order (NNLO) orbit-averaged PN effects has been developed in [1526],

and a double spin approximation based on a multiple-scale analysis (MSA) has been developed in [489]. For the third generation of these models, an approximate map has also been used to construct subdominant harmonics from the $l = |m| = 2$ mode, but this approximation has been dropped in the fourth generation, calibrating instead to NR. A key shortcoming of implementations of the twisting-up approach in the frequency domain [744, 752, 1517–1520] has been the use of the SPA, which is not appropriate for the late inspiral, merger and ringdown. Possible strategies for going beyond the SPA have been discussed in [1527], but will require further study and testing. Further shortcomings of the twisting-up approach have recently been discussed in [1528].

Before discussing the current generation of models we briefly summarize the historical development of the first three generations:

(i) The first generation consists of the non-spinning PhenomA model for the $l = |m| = 2$ modes of non-precessing binaries [1513, 1514].

(ii) Second generation models PhenomB [1515] and PhenomC [1516] included non-precessing spins, where the two spin degrees of freedom are described by a single effective spin. Also, the precessing PhenomP [744] model was constructed from PhenomC using an approximate "twisting-up" map between precessing and non-precessing waveforms.

(iii) The PhenomD [514, 719] model for the $l = |m| = 2$-mode significantly improved the fidelity of the phenomenological ansatz and the quality of the NR calibration. Several models have been derived from IMRPhenomD:

- PhenomPv2 [1517] updates the PhenomP model for precession.
- PhenomHM [1518] adds subdominant harmonics based on an approximate map from the $l = |m| = 2$ mode to subdominant harmonics.
- PhenomPv3 [1519] upgrades the NNLO effective single-spin description of precession that had been used for the first two versions of PhenomP to a double-spin description based on the MSA approximation [489].
- PhenomPv3HM [1520] includes subdominant harmonics in the twisting-up construction. Furthermore, matter effects have been included in terms of tidal phase corrections [1521, 1522] and amplitude corrections of NS-BH systems [1523].

The PhenomD model has been implemented for use in the LISA data challenge infrastructure [1529], and has been used in the "Radler" edition of the LISA data challenge. The PhenomD and PhenomPv2 models have been used for parameter estimation for observed GW events since the first detection of gravitational waves, the GW150914 event [1530]. Its derivatives including subdominant harmonics have also been used to analyse events during the third observing run. A detailed study of waveform systematics [585] found these models to be accurate enough for the GW150914 event, but also highlighted the need for further improvements. This is consistent with a more recent study concerning the need for further improvements

for upcoming upgrades to ground-based GW detectors [1].

The PhenomX [752, 753, 1524, 1525] family provides a thorough upgrade of third generation phenom models. PhenomXAS [753] replaces PhenomD for the dominant mode, increasing the accuracy by roughly two orders of magnitude in terms of mismatch:

- The number of NR waveforms used for calibration is increased from 20 to ~ 400.
- Teukolsky waveforms are included in the data set in order to extend the model to EMRI waveforms.
- Final spin and mass include EMRI information derived from circular geodesics.
- Both spin degrees of freedom are calibrated to numerical data.
- Heuristic parameter space fits have been replaced by the systematic hierarchical fitting approach described in [1428]. An ansatz is selected among classes of polynomial and rational functions by minimizing not only the RMS errors, but also information criteria that approximate a full Bayesian approach, which avoids overfitting and underfitting. This method has, however, not yet been applied to dimensions larger than 3 (i.e. precession or spinning eccentric binaries).

PhenomXHM [1524] extends PhenomXAS to the sub-dominant modes, and PhenomXPHM [752] adds precession via the twisting-up procedure, and allows to switch between the NNLO and MSA descriptions for the Euler angles. A first calibration of Phenom models to precessing NR simulations has recently been presented [754, 1343], paving the way for further increasing the accuracy of precessing and eventually generic models in the future. Extensions to BNS and BH-NS systems following the approaches of third generation models are in progress.

The fourth generation PhenomX family demonstrates that a significant increase in the accuracy of phenom models can be paired with a significant decrease in computational cost. Consequently, PhenomX provides the fastest Inspiral-Merger-Ringdown (IMR) waveforms currently available for data analysis without GPU acceleration [752, 1525]. Parameter estimation application with GPU acceleration for PhenomHM has been presented in [495]. Part of the improvement in efficiency is due to the "multibanding method", which is based on [1531]: analytical error estimates determine the grid spacing for interpolation from a coarse grid, and a standard iterative scheme is used to rapidly evaluate the complex exponentials required to compute the waveform from the amplitude, phase, and the Euler angles used in "twisting up".

Most recently, the time-domain PhenomT model family [1490, 1494, 1511] has been constructed to mirror the features of PhenomX in the time domain. A key motivation for the development of time domain models is that they do not require an analytical approximation to the Fourier transform in order to obtain explicit expressions for a "twisted-up" precessing waveform. This also simplifies the incorporation of analytical results, e.g., concerning the precessing ringdown frequencies; similar simplifications are

Waveform Family	Domain	Waveform Model	Spins		Mode Content	Eccentricity	Calibration Region
1st generation	FD	IMRPhenomA	✗			no	$q \leq 4$
2nd generation		IMRPhenomB	✓				NR calibration: $q \leq 4$, $|\chi_{1/2}| \leq 0.75$ $|\chi_{1/2}| \leq 0.85$ (for q = 1)
		IMRPhenomC	✓				
		IMRPhenomP	✓✓	CP	$(2,\pm2)$		
3rd generation		IMRPhenomD	✓				NR calibration: $q \leq 18$, $|\chi_{1/2}| \leq 0.85$ $-0.95 \leq \chi_{1/2} \leq 0.98$ (for q = 1)
		IMRPhenomPv2	✓✓	CP			
		IMRPhenomPv3	✓✓				
		IMRPhenomHM	✓		$(2,\pm2),(2,\pm1),(3,\pm3),$ $(4,\pm3),(4,\pm4)$		
		IMRPhenomPv3HM	✓✓	CP			
4th generation		IMRPhenomXAS	✓		$(2,\pm2)$	in development	NR calibration: $q \leq 18$, $|\chi_{1/2}| \leq 0.99$ Teukolsky calibration: $q \leq 1000$
		IMRPhenomXP	✓✓	CP			
		IMRPhenomXHM	✓		$(2,\pm2),(2,\pm1),(3,\pm2),$ $(3,\pm3),(4,\pm4)$		
		IMRPhenomXPHM	✓✓	CP			
	TD	IMRPhenomT	✓		$(2,\pm2)$	in development	NR calibration: $q \leq 18$, $|\chi_{1/2}| \leq 0.99$ Teukolsky calibration: $q \leq 1000$
		IMRPhenomTP	✓✓	CP			
		IMRPhenomTHM	✓		$(2,\pm2),(2,\pm1),(3,\pm3),$ $(4,\pm4),(5,\pm5)$		
		IMRPhenomTPHM	✓✓	CP			
✗ no spins		✓ spins aligned with orbital angular momentum			✓✓ precessing spins		CP mode content in co-precessing frame

Table 12. Progress in the development of phenomenological waveform models in frequency domain (FD) and time domain (TD).

hoped for when modelling eccentricity. For future developments, it is foreseen that both frequency and time domain models will be upgraded in parallel, and that each of the two "branches" will benefit from progress with the other.

The historical development and current status of phenom models is sketched in Fig. 12.

4.6.4. Environmental effects The phenom approach provides significant freedom to incorporate additional features, such as poorly known subdominant GR effects, beyond-GR effects (see Sec. 6.6), and environmental effects. We note that analysing the presence of such effects also requires accurate GR waveforms for comparison and will benefit from the techniques developed for GR. Work toward tests of GR or the presence of environmental effects may call for improving the accuracy or other features of GR models. While the modelling of environmental effects has not yet been explored in the phenomenological waveform program, the phenomenological models are primed for their addition in two ways:

(i) The modular structure of phenomenological waveforms should facilitate the incorporation of known environmental effects, e.g. by augmenting PN information about the inspiral with information about environmental effects.

(ii) Environmental effects for which a quantitative model is not yet available could be incorporated into the phenom ansatz in a parameterised way, similar to existing GW tests for theory-agnostic deviations from GR.

In both cases it will be useful to have both frequency and time domain phenomenological waveform models available, allowing one to choose the natural domain for a given effect.

4.6.5. Challenges Waveform modelling for comparable mass binaries in general faces four main challenges:

 (i) The availability of a sufficient number of high-accuracy numerical relativity waveforms throughout the parameter space, including precession and eccentricity. (This is not specific for phenom models.)

 (ii) The lack of accurate analytical descriptions, in particular for precession and eccentricity. Here, specific challenges arise for the phenom approach, which uses "deformed" PN expressions as the basis for constructing a computationally efficient inspiral ansatz. This will benefit in particular from further analytical developments in precession and eccentricity.

(iii) The development of modelling techniques that can produce efficient models from high-dimensional data sets. For the phenom approach, it may turn out to be difficult to develop closed form expressions that accurately represent the full morphology of precessing and eccentric binaries, and to accurately interpolate the full parameter space without compromising computational speed.

(iv) Development of an overall data analysis strategy and concrete code framework. The flexibility and modularity of the phenom approach could be exploited to develop variants of models with different tradeoffs between accuracy and speed, or accuracy and broad coverage of parameter space, which can then be utilised to optimise computational efficiency.

Significant coupling between these challenges is foreseen, e.g. the number and quality of NR waveforms required will also depend on the progress with analytical results. In addition, there will be more sophisticated data analysis approaches, which could exploit the advantages and disadvantages of different models, or tunable parameters, which could allow one to trade accuracy for speed. These could eventually give guidance for the development of waveform models that are designed as an integral part of the data analysis strategy. These challenges are not specific to LISA, but apply in general to further model improvements. LISA, however, poses particular challenges due to the extreme accuracies required for the loudest events.

The detector response itself is significantly more complicated than for ground-based detectors (see e.g. [1527]), and the problem of developing fast and accurate waveform models, as well as strategies of how to best employ them in data analysis applications, resolving tradeoffs of accuracy versus computational cost, can not be completely decoupled from considerations regarding the detector response. In the context of GW data analysis for the current generation of ground based detectors, a software framework for waveforms has been established [1479], along with best practices for waveform review. These practices will need to be extended to the context of LISA waveforms, the

more complicated detector response, and the integration into the LISA data analysis infrastructure. In order to understand these questions, in particular the systematic errors and their consequences for both searches and (especially) parameter estimation, it will be necessary that efficient and well documented implementations of the LISA response functions are publicly available, integrated into software packages for matched filter calculations and Bayesian inference.

The non-precessing quasi-circular sector will provide important initial guidance on how to connect with EMRI descriptions (or to which degree this is possible). This will provide an arena for toy-model explorations of highly accurate models in limited regions of parameter space, determining the limits of accuracy and computational efficiency that can be achieved, as well as studying issues of accuracy and efficiency related to the LISA detector response. It is therefore important to continue pushing to higher accuracies with these models.

The development of accurate phenomenological models of precessing systems is expected in both the time and frequency domains. Time-domain models will build on [1490], which is foreseen to serve as a testing ground to calibrate to NR and describe effects such as the mode asymmetry associated with large recoils [1528, 1532, 1533]. Further progress in the precessing inspiral will crucially depend on progress with approximations, such as those based on the MSA [489] or dynamical renormalisation group (DRG) [1534, 1535]. In order to accurately describe the late inspiral, merger and ringdown of precessing systems in the frequency domain, further tests and implementations of the strategies discussed in [1527] will be required, such as analytical treatments that go beyond the SPA.

Eccentric waveform modes are again likely to require cross-pollination between frequency and time domain models (motivating in part the development of PhenomT in parallel to PhenomX), and significant advances in the development of analytical descriptions for the inspiral phase of spinning and eccentric binaries. This is particularly true where binary systems show both precession and eccentricity. It will be important to understand whether simple approaches twisting up eccentric waveforms will be sufficient for moderate SNR. Further investigations will determine if these prescriptions are adequate to determine binary parameters with sufficient accuracy, such that only a moderate number of NR waveforms is required to develop an accurate local model for high SNR events.

A key challenge is to develop models that are accurate across a large region of parameter space, describing well the changes of waveform morphology, e.g., as the mass ratio increases, or as spin alignment migrates between aligned and anti-aligned with the orbital angular momentum. For current ground-based detectors, parameter estimation posteriors are typically rather broad, so refined models in a smaller region of the parameter space would have very limited use. For LISA, however, it is foreseen that a hierarchy of models will be developed: those that are sufficiently accurate to identify

signals across large portions of parameter space, and others that further increase the accuracy for smaller regions of parameter space, which would be used for the most accurate parameter estimation of the loudest signals. Models with parameters allowing one to trade accuracy for computational efficiency would be appropriate for hierarchical approaches to data analysis. This approach could also be extended further by mixing descriptions in terms of closed-form expressions with equation-solving, e.g. to improve the accuracy of describing eccentricity or precession. An important open question is how to incorporate results from the self-force program (see Sec. 4.3) into phenomenological models, and how to use ideas developed for the phenomenological waveforms program to accelerate self-force waveforms.

5. Waveform generation acceleration

Coordinator: Alvin Chua, Michael Katz
Contributors: S. Field

The stringent efficiency requirements described in Sec. 3.3 naturally necessitate the acceleration of waveform models, in order to enable the LISA science analysis. The two main strategies to achieve this are the development of improved computational techniques, and hardware acceleration.

5.1. Computational techniques

To maximize the science returns from highly relativistic LISA sources with exacting modeling requirements, we require waveform-acceleration techniques that do not compromise waveform accuracy. The general solution to this problem is to construct interpolants or fits for high-fidelity waveform data, where the data comes from an accurate underlying model that is too slow to use directly in data analysis studies (e.g., as it involves solving PDEs). This data can describe either the full time-/frequency-series representation of the waveform, or specific waveform components that are more computationally expensive. While many waveform acceleration techniques have appeared in the literature, most rely on the three steps summarized below.

5.1.1. Step 1: Data representation

A gravitational waveform's parametric dependence is generally too complicated to model directly with an acceptable degree of accuracy. Instead, the waveform is typically decomposed into waveform data pieces that are simpler, more slowly varying functions of parameters and time. If we were to take a machine-learning viewpoint of the problem, data pieces are features of the data, and discovering what problem-specific features to extract is a feature engineering task. How should we define our features?

For non-precessing BBHs in quasi-circular orbits, an amplitude and phase decomposition for each (ℓ, m) angular-harmonic mode is an obvious choice for our data pieces. For precessing systems, the problem becomes significantly more complicated as the modes have a rich signal morphology. Here, the general approach has been to transform the modes to a co-rotating frame where the system has significantly reduced dynamical features [581, 582, 1536]. It is often advantageous to further decompose the data into symmetric and asymmetric mode combinations [581, 582, 1536]. The price of this simplification is that the frame dynamics must also be modeled, so that the co-rotating modes can be transformed back into the inertial frame of the detector. For eccentric BBH systems, which will be important for LISA science, the optimal data representation is currently unknown.
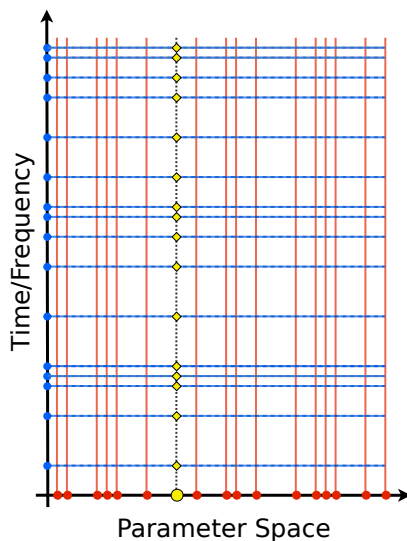
Figure 11. Waveform acceleration can be achieved by building a surrogate model through a sequence of three steps. (Step 1) The red solid lines show the waveform training data evaluated at specific parameter values. (Step 2) Reduced-order modeling is used to compress the waveform data through a dimensional-reduction step, and the blue dots represent the data that needs to be modeled after compression. (Step 3) The blue lines indicate fits for the compressed waveform data across the parameter space. The yellow dot shows a generic parameter value, say $\boldsymbol{\lambda}_0$, that is not in the training set. To compute the waveform for this value, each fit is evaluated at $\boldsymbol{\lambda}_0$ (the yellow diamonds), and then the reduced-order representation is used to reconstruct the decompressed waveform (the dotted black line).

The highly disparate masses and large separation of timescales in EMRI systems allow their inspirals to be modeled within the two-timescale framework [1080]. This allows the trajectory of the inspiral through the orbital configuration phase space to be computed in milliseconds [1098, 1107]. The waveform is then computed by sampling the metric amplitudes along this inspiral typically by evaluating a precomputed interpolant of the amplitudes. Most often these amplitudes are computed in the frequency domain so the waveform is decomposed into harmonics of not just angular dependence, but also the fundamental frequencies in the system [1130, 1144]. Generically precessing and eccentric EMRI waveforms are extremely complex, but the above description effectively breaks the waveform down into slowly evolving sinusoids. The only drawback is that there are far more modes to compute and sum for a typical waveform ($\gtrsim 10^5$), though in practice many of these do not carry much power [1098].

5.1.2. Step 2: Reduced-order modeling   The waveform quantities of interest often reside in a representation space of extremely high dimensionality D, and must generally be interpolated or fitted over a parameter space of modest dimensionality d as well. For example, the full waveform itself for strong-field LISA sources typically has $D \gtrsim 10^4$ and $d \sim 10$. These computational difficulties can often be mitigated through the use of

111

dimensional-reduction tools [1537–1548], the collection of which is broadly referred to as ROMs.

ROMs aim to remove redundancies in large data sets, making them more amenable to analysis, and identifying relevant features for further approximation. It typically begins with a greedy algorithm or singular value decomposition that identifies the set of n "most important" values in parameter space, whose associated waveform quantities span a *reduced-basis* space within which the model is well approximated [1442, 1443, 1547, 1548]. This serves as both a dimensional-reduction step as well as a parametric-sampling step.

While invaluable for reducing computational cost on the representation end ($n \ll D$), the compression provided by ROMs does not actually lessen the intrinsic complexity of the model. Indeed, the successful application of ROMs relies on sufficient coverage of the parameter space with training data in the first place—or, more realistically, on truncation of the parameter domain to compensate. ROM themselves also do not address the issue of interpolating or fitting the reduced representation at high accuracy, which can be challenging even in parameter-spaces with $d \gtrsim 3$.

5.1.3. Step 3: Interpolation and fitting The last step is to interpolate or fit each compressed data piece (viewed as scalar- or vector-field data) over $d > 3$ dimensions, and to do so both accurately ($\lesssim 10^{-6}$ error) and efficiently ($\lesssim 1$ seconds). In the context of sources and models for ground-based observing, a variety of choices have appeared, including polynomials [1442], splines [1443], Gaussian process regression [1549], deep neural networks [1450, 1451, 1550, 1551], and forward stepwise greedy regression using a custom basis [581]. A recent review article provides informative comparisons between some methods [1552]. The accuracy and efficiency goals of models for ground-based observing are more modest, however, and it is unclear if these methods will continue to work for LISA MBHs [1, 2], or for EMRIs in full generality [1148]. As such, other interpolation and regression methods should continue to be explored.

5.1.4. Status of techniques In the GW literature, the term surrogate modeling is sometimes used as a generalization of ROMs (for the full waveform) to include additional steps beyond dimensional reduction. ROM surrogates have been built for many different waveform families, regions of parameter space, and signal durations. Early models focused on closed-form waveform families largely as a proof-of-principle exercise [1544–1548, 1553]. Since then, ROM techniques have been further developed and refined for various LVK (hence comparable-mass) applications: EOB [1442–1444, 1447, 1448], NR [581, 582, 755, 1492, 1536], multiple subdominant modes [581, 582, 755, 1442, 1447, 1492, 1536], frequency-domain waveforms [1443, 1444, 1447], time-domain waveforms [581, 582, 755, 1442, 1492, 1536], generically precessing systems [581, 582, 755, 1536], neutron star inspirals with tidal effects [1445, 1446, 1554], and

waveforms with $\sim 10^4$ cycles [1443, 1444, 1447, 1492].

When applied to computationally expensive models such as EOB or NR, ROM surrogates can accelerate the generation of a single waveform by factors of 10^2 (EOB models; described by ODEs) to 10^8 (NR models; described by partial differential equations), while being nearly indistinguishable to the underlying model. EOB surrogates are extensively used as part of LVK parameter-estimation efforts as well as template-bank detection [761, 1530]. NR surrogates have been used in numerous targeted follow-up studies on specific BBH events [107, 1488, 1555–1557]. As such, ROM techniques have been essential to the widespread use of both EOB and NR waveforms for realistic data analysis efforts with LVK data.

The present surrogate framework is ill-suited to EMRI waveform modeling, where the increased duration and mode complexity combine to increase the information content of the model by at least 20 orders of magnitude [207, 479, 480]. Surrogates might be useful in special cases of the IMRI regime, where these difficulties are lessened. There has been recent work on the first models [757, 1105] for quasi-circular, non-spinning IMRI systems, based on solutions to the time-domain Teukolsky equation rescaled to fit NR results. The latest surrogate waveform model in this series covers the last $30,000M$ of the inspiral-merger-ringdown signal, with mass ratios ranging from 2.5 to 10^4. To put this in context, for a million-Solar-mass system, this is equivalent to approximately 2 days of signal, which is inadequate for the expected observable duration of months to years for an EMRI of that mass.

In the angular- and frequency-based decomposition of an EMRI model, the problem separates naturally into two main parts: that of generating the inspiral trajectory (from which the waveform phasing is straightforwardly derived), and that of generating the waveform amplitude for each of the $\sim 10^5$ constituent modes. Fast frameworks for EMRI trajectory generation already exit [738, 1080]. They present no computational difficulties at adiabatic order (for search); however, their extension to post-adiabatic order (for inference) will require interpolating the first-order fluxes to a relative precision of the mass ratio ($\sim \epsilon$) [1205]. Trajectory-level interpolation with ROM is unlikely to be of practical use, due to issues of accuracy and parameter-space extensiveness. The accuracy requirements on the waveform amplitudes are far less stringent, though, and it is here that ROM compression and neural-network interpolation has been applied to good effect (in the mode direction, rather than the time/frequency direction) [1148].

5.1.5. Future challenges LISA data analysis has three distinctive features that will require new ideas in waveform acceleration. First, the waveforms are significantly longer in duration, which will stress both computational resources and current ROM techniques. Second, as compared to LVK waveform modeling, LISA accuracy requirements are significantly more demanding. The fitting schemes will thus need to deliver higher accuracies while also contending with increased dimensionality. Finally,

the orbital motion of LISA introduces a time-dependency in the response of the detector, which also needs to be modeled efficiently for data analysis applications; see, e.g., [1527].

In terms of source-specific challenges, eccentricity is expected to play a more important role in the modeling and interpretation of LISA MBHs. This will necessarily increase the problem from 7 to 9 parametric dimensions. While this should not pose significant difficulty for the dimensional-reduction step [1548, 1558], the parameter-fitting step will be vastly more difficult, and it is unlikely that any of the existing techniques will continue to perform well. For EMRIs, the main difficulty is ensuring that the waveform-amplitude fit retains its accuracy when extended from eccentric Schwarzschild orbits at present [1148] to generic Kerr orbits with a much larger parameter and representation space.

5.2. Hardware accelerators / configurations

In addition to computational techniques, generating waveforms with a variety of hardware accelerators can vastly improve analysis time. Hardware acceleration, in a general sense, means hardware designed for a specific type of optimization when compared to general-purpose CPUs. Some examples of commonly used hardware accelerators include GPUs, Field-Programmable Gate Arrays (FPGAs), Tensor Processing Units (TPUs), and Artificial Intelligence (AI)-accelerators.

GPUs are designed specifically for parallel computations. These devices leverage a large number of compute cores ($\sim 1000s$) and specialized memory structure to make a large number of independent calculations simultaneously. From an algorithmic standpoint, many of the methods discussed in Sec. 5.1 can be implemented on GPUs to achieve considerable gains in efficiency. These include, but are not limited to, artificial neural networks (matrix multiplication), interpolation, parallel sorting, and basis transformation. Additionally, some accurate waveform calculations can be implemented in parallel, allowing for all or parts of waveforms to be implemented entirely for GPUs. Programming for GPUs is generally performed in `C/C++` or, as of more recently, `Python`.

While GPUs take advantage of their parallel architecture, they are still programmed using specific software for a fixed hardware unit. FPGAs, on the other hand, represent "programmable hardware." These devices are programmed at the device level to implement customized hardware flow designed for specific tasks. Their most common usage is in neural networks and signal processing. Programming on FPGAs is done in `Verilog` or `VHDL`, although some wrappers in `C/C++` are starting to become available.

5.2.1. Status In recent years, GPUs have seen increased interest from the community for use in waveform creation, as well as GW-related analysis in general. Unfortunately, FPGAs are yet to be utilized in the GW community. GPUs have been used for precessing waveforms, as well as population analysis related to ground-based observations from the

114

LVK observing network [1559]. In this work, the waveform and the detector response were calculated directly on the GPU hardware. To limit the cost of Bayesian inference in ground-based observing, GPUs were recently used to greatly accelerate the creation of surrogate waveform models using techniques such as artificial neural networks [1450]. The creation of MBHB waveforms has also been implemented for LISA, including both the source-frame waveforms and the LISA response function for use in LISA parameter estimation studies [495] ($\sim$500x acceleration). The generation scheme for this work calculated, in parallel, accurate waveforms and LISA response information on sparse grids. Then, to scale to the full data stream, cubic spline interpolation was leveraged. This technique is generally well-suited for parallelization.

For EMRIs, GPUs have been used to improve the efficiency of black hole perturbation theory calculations within the GSF community [1560–1562]. In this work, the many harmonics of EMRI metric perturbation are computed in parallel as the orbit evolves. In terms of data-analysis related waveform creation for EMRIs, the Augmented Analytic Kludge (AAK) [480] waveform from the `EMRI Kludge Suite` was accelerated with GPUs (`gpuAAK`) for use in the LISA Data Challenges ($\sim$1000x). Additionally, the first fully relativistic fast and accurate EMRI waveform that goes beyond the kludge approximations was implemented on GPUs resulting in a considerable increase in efficiency ($\sim$2000x) [1098, 1148]. Both the `gpuAAK` and the fast and accurate EMRI waveforms generate sparse orbital and phase trajectories in serial on a CPU. These sparse trajectories are then scaled with spline interpolation to the full waveform sampling rate. This scaling is performed for each separate harmonic mode so that they can be properly and accurately combined into the final waveform. It is actually this summation over $\sim 10^6 - 10^7$ time points, each with a combination of $\sim$1000s of harmonic modes, that most requires the GPU architecture for optimal results.

5.2.2. Challenges A central challenge when working with GPUs, FPGAs, or any other specialized hardware is the trade-off between efficiency and streamlined code creation and maintenance. For optimal efficiency, it is generally necessary to implement code specific to each type of hardware. This could mean implementation in an entirely different language with, for example, an FPGA, or an adjustment for different hardware or software requirements for each application. An example of this is the use of shared memory in GPUs. Shared memory is a small amount of memory available on the GPU chip, which is much faster to access in comparison to the larger global memory located off of the chip. Leveraging shared memory is essential to achieving optimal efficiency for many applications. There is no use of this form of shared memory on CPUs. Therefore, it may be desirable to implement a fast GPU version and a mirror CPU version that effectively uses the same exact code as the GPU version with slight adjustments. On the other hand, a CPU version optimized for a CPU may be needed, creating two separate codes. In general, it is helpful to minimize the amount of code duplication as much as possible, but that may be governed by efficiency requirements.

Many applications require some parallelization over CPUs in addition to specific hardware considerations. Understanding how to best leverage all resources is key to achieving maximal efficiency. With that said, maximal efficiency should be achieved while maintaining a constant user interface. This allows for the application of a waveform within a desired program while using a variety of hardware.

Another general concern about the use of specialized hardware is just that: it is specialized. Purchasing specialized hardware in place of CPUs will penalize the breadth at which the hardware can be used. This has generally hurt the availability of accelerators at large. Similarly, accelerators come at a variety of prices. Academic-grade GPUs (indicating they have strong performance in double precision) are generally expensive. However, the newest generations of accelerators combined with modern algorithms within the GW field have proven that efficiency is not only highly desirable, but cost efficient when compared to the equivalent number of CPUs (up to ~ 1000s). Fortunately, researchers now often have access to clusters of CPUs, GPUs, TPUs, and AI-accelerators through local, national, and international scale computing centres. Ultimately, the combination of a variety of hardware will be necessary to accomplish the scientific goals of the LISA mission.

6. Modelling for beyond GR, beyond Standard Model, and cosmic string sources

Coordinators: Richard Brito and Daniele Vernieri
Contributors: J. Aurrekoetxea, L. Bernard, G. Bozzola, A. Cárdenas-Avendaño, D. Chernoff, K. Clough, T. Helfer, T. Hinderer, E. Lim, G. Lukes-Gerakopoulos, E. Maggio, A. Maselli, D. Nichols, J. Novák, M. Okounkova, P. Pani, G. Pappas, V. Paschalidis, M. Ruiz, A. Toubiana, A. Tsokaros, J. Wachter, B. Wardell, H. Witek

As explained in Sec. 2.7, the observation of gravitational waves with LISA has an enormous potential to probe physics beyond GR and the Standard Model of particle physics, in regimes that have so far not been explored [92, 315]. In order to fulfill this potential, we need to construct accurate waveforms that take into account signatures of new physics. As we will discuss in this Section, this is in fact a very challenging task that for most cases is still at its early stages of development.

In this section we provide a brief summary of how beyond GR theories and the effect of beyond Standard Model physics can be modelled using the techniques presented in Sec. 4. The discussion will be mostly concerned with modelling the *generation* of gravitational waves by LISA sources in the presence of new physics. Beyond-GR effects can also affect the way gravitational waves *propagate* on cosmological scales, see e.g. [267, 1563–1570]. In general, separation of scales allows to add modifications to the GW propagation on top of any waveform model for which the generation problem is understood and therefore we do not discuss this possibility here. More details on this problem can be found in Refs. [267, 1566]. We will also not discuss in detail the potential implications that LISA observations will have for fundamental physics, since a more detailed review on this issue can be found in LISA's Fundamental Physics Working Group white paper [315].

This section follows a similar structure to Sec. 4 where various modelling approaches for compact binaries are discussed. However, the modelling of gravitational waves emitted by cosmic strings is discussed in a separate subsection 6.7, mainly because these sources require modelling approaches that are specific to cosmic strings.

6.1. Numerical relativity

6.1.1. Beyond GR NR simulations of BBH mergers in beyond-GR theories are only at their infancy and have only been performed in a handful of theories, e.g. [606, 622, 630, 1571–1581]. Even though most studies have so far focused on proof-of-principle simulations, in recent years there has been significant improvements in this topic.

The earliest NR simulations of BBH mergers in beyond GR theories focused on a particular class of scalar-tensor theories that are known to possess a well-posed initial value problem [606, 630, 1571, 1582]. In these scalar-tensor theories, BHs satisfy no-

hair theorems [384, 1583], and BBH mergers are indistinguishable from GR. However, in more complex extensions of GR, or for scalar matter with nontrivial boundary conditions (e.g., cosmological boundary conditions or large scalar-field gradients), BHs can carry a scalar charge, and these solutions need not be unique. One of the main difficulties when trying to do NR simulations in more complex theories is the fact that the well-posedness of the initial value problem (see e.g. [501, 1584, 1585]) in alternative theories is for most cases particularly challenging to establish [1579, 1580, 1586–1602].

To circumvent these problems, two treatments have been proposed in which alternative theories are considered as effective field theories of gravity. One approach uses an *order-by-order expansion* [622, 1572, 1574, 1575, 1603–1605], in which the spacetime metric and extra fields are expanded around GR, order-by-order in the coupling constant ‖, to guarantee well-posedness. The second approach, the so-called *equation-fixing* method, proposes to use a scheme inspired by the Israel-Stewart treatment of viscous relativistic hydrodynamics, in which an effective damping controls higher frequency modes while preserving the physics of the low frequency modes (nearly) untouched [1581, 1589, 1606–1608]. In this second approach the alternative theory equations of motion are viewed as a low-energy effective deviation from the Einstein equations, such that the theory can be captured by the low-energy degrees of freedom. Although these methods are quite generic, they have so far been mainly employed in theories with higher derivative terms in the metric [622, 1572, 1574, 1575, 1581, 1600, 1603–1605, 1607, 1609, 1610], such as quadratic theories of gravity with an extra scalar field (for which the order-by-order expansion was used), namely dynamical Chern-Simons gravity (dCS) [396, 1611–1613], Einstein dilaton Gauss-Bonnet gravity (EdGB) [326, 395, 1614, 1615] or more generic Einstein scalar Gauss-Bonnet theories (ESGB) [1616–1618]. Unlike the simplest scalar-tensor theories, in dCS and EdGB BHs naturally possess scalar "hair", and therefore deviations from GR naturally occur. Some ESGB theories are prone to BH scalarization, i.e., a process in which GR BHs become unstable against the spontaneous development of scalar hair for large enough spacetime curvatures [1616–1619] (see also [1610, 1620–1625] for a similar process but where scalarization is controlled by the magnitude of the BH spin).

In particular, using the order-by-order expansion mentioned above, BBH simulations were done in dCS [1574, 1575] and EdGB [622, 1609]. Importantly, this scheme also simplifies the problem of covering the parameter space needed to build IMR waveforms for parameter estimation purposes. Since NR is *scale-invariant* and the dCS and EdGB coupling parameters are scaled out of the order-by-order expansion scheme [1574], a simulation for one set of BBH parameters (masses and spins) can be applied to any total mass, and any valid value of the coupling constants. With enough NR simulations, one can thus hope to cover the the full BBH parameter space, build a surrogate model for parameter estimation [582], and perform model-dependent tests of GR with gravitational

‖ Sometimes this is also called "order-reduction scheme." This is not to be confused with order-reduction schemes in which the field equations themselves are used to replace higher-order curvature terms that are then kept only to a given (reduced) order in the coupling constant.

waves. Work towards model-dependent tests using full IMR signals obtained through this method has been done in Ref. [1626], where parameter estimation was performed on full BBH waveforms in dCS.

Despite their promises and advantages, the schemes mentioned above also suffer from some important problems. The main problem with the order-by-order expansion scheme is the fact that solutions may be plagued by secularly growing solutions signaling the breakdown of perturbation theory on long timescales. As proposed in Ref. [1627], such problem could potentially be solved using renormalization-group techniques that can be used to build solutions valid over the secular timescale. For the equation-fixing method on the other hand, there are first studies in spherical symmetry [1607, 1608, 1628, 1629] and for BBH mergers in some beyond-GR theories [1581]. A more detailed quantitative analysis is needed to identify how much a given "equation-fixing" choice affects low-energy modes in scenarios of interest, and to fully characterize the accuracy of these approximate schemes [1630].

These problems can be avoided for cases where a given theory in its full form can be shown to have a well posed initial value problem. Important work in this direction has recently been done. For example, nonlinear evolutions of BBHs in quadratic gravity were presented in Ref. [1631]. Furthermore, BBHs simulations have been performed in cubic Horndeski theories [1577] which are known to be well-posed in the standard gauges used in numerical GR [1593]. For more generic theories, it has been recently shown that, at sufficiently weak coupling, the equations of motion for Horndeski gravity theories possess a well posed initial value problem in a modified version of the generalized harmonic gauge formulation [1594, 1595]. Quite remarkably, using this formulation it could in principle be possible to perform simulations in all Horndeski theories of gravity without having to resort to the two schemes mentioned above [1580]. In particular, Ref. [1576] used this modified generalized harmonic (MGH) formulation to perform the first numerical simulations of BBH mergers in shift-symmetric ESGB gravity, without approximations, which were also recently compared against PN results in Ref. [1632]. Simulations of head-on BH collisions in ESGB theories that exhibit spontaneous BH scalarization [1578] and simulations of binary neutron stars in shift-symmetric Einstein-scalar-Gauss-Bonnet [1633] have also been done. Based on the MGH formulation, a modified version of the CCZ4 formulation of Einstein's equations has also been proposed, which has been used to prove the well-posedness of the most general scalar-tensor theory of gravity with up to four derivatives, in singularity avoiding coordinates [1579]. This was then used to perform (circular and equal-mass) BBH merger simulations in such theories [1579, 1634].

Finally, NR simulations have also been done in theories in which BHs possess an electric or magnetic charge [1573, 1635–1639], possibly coming from mini-charged dark matter [387]), primordial magnetic monopoles [388]), or in specific classes of scalar-tensor-vector modified theories of gravity [386]. In all these cases the field equations can be cast in a form that is mathematically equivalent to Einstein-Maxwell theory (or

to Einstein-Maxwell with an extra scalar field for some theories [1573, 1640]), which is known to possess a well-posed initial boundary value problem [1641].

6.1.2. Boson clouds Simulations of BHs surrounded by massive bosonic fields have been widely studied, focusing mostly on the evolution of bosonic fields around isolated BHs (see e.g. [344, 347–349, 356, 358–360, 376, 1642–1648]). This has led to the first successful nonlinear evolution of the superradiant instability of minimally-coupled Proca fields around a spinning BH in [356, 360]. These works have laid down the possibility to study the impact of minimally-coupled bosonic fields in BBH systems within NR [364, 367, 368, 377, 1649–1651] but such studies are still in their infancy.

6.1.3. Exotic compact objects ECOs come in many different flavors, and the state of numerical simulations of ECO mergers vary widely, depending on the source. For example, simulations of string-theoretical models including fuzzballs, wormholes, firewalls or gravastars have not yet been performed because the theoretical foundations — the field content, equations of motion, equations of state (where applicable), solution space — are under active investigation. Formulations suitable for numerical relativity are not yet available.

In contrast, binary boson stars that are compact objects composed of real or complex bosonic (scalar or vector) fields, with and without self interaction potentials, have received a lot of attention [403, 430, 1652–1672]. These boson stars may be treated as potential dark matter components (see Sec. 2.7), or simply as toy model proxies for unknown exotic objects. Several works have also considered mixed collisions of BHs or neutron stars with these types of bosonic ECOs [1673–1675]. Besides these simulations, mergers of extremely compact perfect fluid stars have also been performed in [1676, 1677]. Most binary boson star simulations have explored new phenomena that arise during their merger or the qualitative structure of the gravitational radiation emitted. For model specific tests of gravity more accurate waveforms will be needed which, in turn, requires improved initial data and more accurate numerical evolutions.

In summary, despite the progress in the last few years, most of the studies mentioned above have only provided a proof of principle for the stable evolution of some families of ECOs and of fundamental fields around BHs in NR, and have primarily aimed at identifying significant qualitative differences between their signals and those of traditional binary candidates. Key areas for improvements include the numerical accuracy of such simulations and the quality of the initial data [364, 1651, 1671, 1678, 1679]. For example for boson stars, a formalism is currently lacking to ensure that the superimposed boosted objects are not in an excited state, the risk being that such artifacts in the initial data are wrongly attributed as features of the ECO signal. Less challenging, but equally important refinements are reducing the eccentricity of the initial orbits (most simulations thus far have been head-on mergers, or only achieve a few orbits

before the plunge), and initial errors in the Hamiltonian and momentum constraints (many simulations rely on constraint damping which reduces control over the initial data parameters). Efforts to solve some of these problems are currently underway, in particular see [1679] where a novel method to solve the initial data constraints has been formulated and that could be particularly useful when the sources involve fundamental fields. See also Ref. [1672] where numerical simulations of binary boson stars were performed using constraint satisfying initial data.

Whilst feasible given these improvements, a significant effort would be required to create a template bank of waveforms of a similar quality to those used for BH and neutron star mergers. This is true even if the class of objects were restricted to a simple model, such as minimally coupled, non self-interacting, non spinning complex scalar boson stars. Refining the NR tools with which we study such objects is work that is merited in the run up to the mission. In particular, key goals are (1) unambiguously identifying characteristic deviations in the merger signals of ECOs and of BHs surrounded by fundamental fields (e.g. to be used to motivate parameterised deviations in IMR consistency tests) and (2) expanding the classes of objects for which simulations of mergers have been performed to qualitative examples in all sufficiently predictive ECO cases. A first NR waveform catalog of Proca star mergers is available [1669].

6.2. Weak-field approximations

6.2.1. Beyond GR Applying weak field approximation techniques to theories beyond GR raises several difficulties which have prevented obtaining high-order PN results, with the exception of a small set of alternative theories of gravity. For most cases only the leading non-GR correction is known (see e.g. [392, 1680]). The most advanced results concern scalar-tensor theories, for which the equations of motion are known up to 3PN order [1681–1683], including finite-size effects [1684, 1685]. The gravitational flux and waveform are known up to 2PN order [1686] while the scalar energy flux is known to 1.5PN order beyond the quadrupolar formula [1687, 1688]. We expect the full scalar plus gravitational waveform to be known up to 2PN order beyond the GR leading term in the next few years, which should result in the first full waveform model beyond GR [1689] shortly thereafter. The scalar-tensor equations of motion have been used to obtain similar results in other theories such as Einstein-Maxwell-scalar [1690, 1691] and ESGB theories [1685, 1692–1694]. The main difficulty encountered in more involved theories, such as the Horndeski family [1695], is related to the need for a mechanism to screen the fifth force in the solar system. As an example, the Vainshtein mechanism requires to keep non-linearities in the description of the dynamics even in the weak field limit, rendering the definition of a perturbative method challenging [1696–1703].

Given the many different alternative theories of gravity proposed over the years and the difficulty in constructing accurate waveforms in many of these theories, the most common approach to build beyond GR waveforms for data analysis purposes has been

to use theory-agnostic phenomenological frameworks, such as the parametrised post-Einsteinian (ppE) formalism [1704], the generalized IMR formalism [1705] or the flexible theory-independent approach [1706]. In these frameworks, deviations from GR are assumed to be small and are treated as perturbative corrections to the signal predicted by GR. For example, in the ppE formalism the inspiral phase of the frequency domain waveform is given by:

$$\tilde{h}(f) = \tilde{h}_{GR}(f)[1 + \alpha_i(\pi\mathcal{M}f)^{a_i}]e^{i\beta_j(\pi\mathcal{M}f)^{b_j}} , \tag{22}$$

where $\tilde{h}_{GR}(f)$ is the frequency domain waveform of GR, $\mathcal{M}$ is the chirp mass of the binary, while the deviations from GR are described by the dimensionless parameters α_i, β_j, a_i and b_j. The index i and j indicate the PN order at which the modification enters and are also introduced as a reminder that modifications could enter at different PN orders, in which case we should sum over all of them. Different values for the generic beyond GR parameters can be mapped to distinct physical effects and gravitational theories (see e.g. [1563, 1707–1716]), allowing to use this formalism to place constraints on such theories. Extensions of the ppE formalism to include higher-harmonic GW modes have also been recently formulated [1706, 1717], as well as an extension for precessing binaries [1718]. The latter was based on the recent computation of time- and frequency-domain analytical waveforms emitted for quasicircular precessing BH binaries in dCS gravity [1719] and in binaries composed of deformed compact objects with generic mass quadrupole moments [461].

As a final remark, we should note that while the ppE approach is a very useful and powerful method to perform null tests of GR, a qualitative and quantitative interpretation of a constraint on the ppE parameters (or measurements of a deviation from GR) only makes sense when accessed with respect to specific theories [1720]; see e.g. Refs. [1721, 1722]. Hence theory-agnostic approaches should only be seen as complementary, and not as alternatives, to explicit computations of waveforms in specific alternative theories.

6.2.2. Dark matter and boson clouds Weak field approximations have been widely used to study the impact of dark matter environments on binary systems [62, 1723, 1724]. Such an environment can affect the binary dynamics through dynamical friction [1725], accretion and the gravitational pull of the environment itself [62, 1723, 1724]. These effects typically modify the waveform at negative PN orders and can be captured within the ppE formalism presented above [62, 1724].

In this context, Newtonian approximations have also been used to study binary systems moving inside bosonic structures, mainly motivated by the fact that ultralight bosons are promising candidates to describe dark matter [329]. For example, Refs. [1726, 1727] studied how compact binaries travelling through these structures would be affected by dynamical friction and emission of scalar radiation. In particular, it was found that, for sources in the LISA band, scalar radiation affects the gravitational waveform

at leading -6 PN order with respect to the dominant quadrupolar term [1726, 1727]. In addition, BHs surrounded by boson clouds have been studied within a weak-field approximation [369–372, 375, 377, 1728–1731] showing that a plethora of signatures, including tidally induced resonances [369, 371], floating and kicking orbits [371, 1728, 1732, 1733] and ionization of the cloud [1730, 1734–1736] can occur. Finally, it was recently shown that sufficiently light bosonic fields can also be bound to and engulf a binary BH system as a whole, showing a rich phenomenology [366, 367, 1737], which could potentially lead to additional signatures besides the ones we discussed above. A main problem with those studies is that they have mostly been performed within a weak-field approximation, neglecting high PN corrections and nonlinear effects close to merger. It would be especially important to extend such studies beyond the weak-field regime and further explore the physics of ultralight fields around binary BHs with full NR simulations (see Sec. 6.1.2 for recent attempts).

6.2.3. Exotic compact objects In the inspiral phase, the nature of the coalescing bodies can be studied through (i) their multipolar structure; (ii) (the absence of) tidal heating; and (iii) their tidal deformability. In particular, the multipole moments of an ECO will be different from those of their Kerr counterpart [451–462], which at leading order enters as a 2PN correction to the GW phase due to the object's quadrupole moment [461, 1738]. In addition, tidal interactions during the coalescence also provide unique signatures able to disentangle BHs from ECOs in the form of tidal heating. For BH binaries a small fraction of the emitted radiation is lost through the horizon [821, 1144, 1739–1741]. Absorption at the horizon introduces a 2.5PN (4PN) $\times \log v$ correction to the GW phase of spinning (nonspinning) binaries, relative to the leading term. On the other hand, exotic matter is expected to weakly interact with gravitational waves, leading to a smaller absorption during the inspiral, and therefore to a suppressed contribution to the accumulated GW phase from tidal heating [441, 1742–1745]. Finally, tidal deformations can be strong enough, especially during the late stages of the inspiral, to modify the binary's orbital evolution leaving an imprint on the emitted waveform encoded in the ECO's tidal Love numbers [1746], which at leading order introduces a 5PN correction to the GW phase [1027]. Overall more work is needed to construct fully consistent inspiral waveforms for ECOs that incorporate all these ingredients. For example, for the inspiral of boson stars with quartic interactions, such a waveform was only recently constructed in Refs. [1747, 1748]. It would be important to extend this to other types of ECOs.

6.3. Perturbation theory for post-merger waveforms

6.3.1. Beyond GR The ringdown phase of a GW signal emitted by a BBH merger event can be described using BH perturbation theory and is dominated by the QNMs of the remnant [1315, 1317]. Owing to the very large SNR with which LISA will be able to detect the ringdown phase of supermassive BHs [604, 1346],

we expect to be able to measure several QNMs for a single event up to very large distances [604, 1323, 1326, 1749]. This will allow to perform precise consistency tests of the QNMs and test the hypothesis that the remnant of a BBH merger is well described by the Kerr metric in GR [598, 604, 1323, 1324, 1346, 1352, 1355–1357, 1359, 1362, 1750–1758]. Due to these prospects, significant work has been done in recent years in order to accurately model the ringdown phase of BBH mergers within GR [1342, 1349, 1351, 1356–1358, 1361, 1364, 1381, 1426, 1759–1761].

For beyond GR theories, however, there has been significantly less progress, even though QNM measurements can, in principle, be powerful probes of beyond GR physics. In particular, for beyond GR theories, the ringdown of a BBH merger is typically expected to differ from the ringdown in GR (although not necessarily for all non-GR theories). Computations of QNMs in beyond GR theories are very challenging, especially for rotating BHs for which the separability of the perturbative equations present in GR [1312] is in general absent. Then, one may employ numerical methods to compute QNMs for non-separable equations, see e.g. Refs. [1762–1766]). In addition, most rotating BH solutions in alternative theories, for the cases where they differ from Kerr, are only known either perturbatively, through a small-spin expansion around non-spinning backgrounds [1767–1771], or they are given in the form of numerical solutions of the field equations (e.g. [351, 352, 1772–1776]), complicating the problem even further. Furthermore, BH spacetimes may change their character as compared to GR. For example, it was shown that BHs in ESGB and dCS gravity are of Petrov-type I [1777] (instead of the more symmetric type-D spacetimes like the Kerr metric). Therefore, even though QNMs have been computed for a handful of theories and BH solutions (see e.g. [62, 451, 1770, 1778–1788]), the vast majority of these results either assumed non-rotating or slowly-spinning BH backgrounds or relied on approximations such as the eikonal/geometric optics approximation. Methods to circumvent some of these problems were formulated in Refs. [1765, 1789–1793] where modified Teukolsky equations governing the perturbations of non-Kerr spinning BHs arising in theories beyond GR, were derived in the case where the deviations from the Kerr geometry are small. Another approach would be to rely on fits of time-domain waveforms computed from numerical simulations in selected classes of theories beyond GR. However, this is quite a challenging task, even in GR [1342, 1349–1351, 1357, 1358, 1361, 1363, 1364, 1381, 1759–1761], besides the fact that such simulations are still only possible for a handful of cases, has emphasized in Sec. 6.1.1.

6.3.2. Exotic compact objects The vibration spectra of ECOs have been computed for a wide class of models, although mostly for spherically symmetric configurations, including: boson stars [1794, 1795], gravastars [1796–1799], wormholes [429, 1800, 1801], quantum structures [430, 1802–1807], and in a model-indepedent fashion using the membrane paradigm [428]. Typically, the QNMs of ECOs differ from the BH QNMs due to the presence of a surface instead of an event horizon [95] and the excitation

124

of the internal oscillation modes of the objects [451, 1808, 1809]. In addition, the isospectrality of axial and polar modes of spherically symmetric BHs in GR [1314] is broken in ECOs, which are instead expected to emit a characteristic "mode doublet". The detection of such doublets would be a irrevocable signature of new physics [428, 1317, 1785, 1805]. The formation of an exotic ultracompact object may also lead to the emission of GW echoes in the post-merger signal [426, 429] (see also Sec. 2.7). Several phenomenological GW templates for echoes have been developed based on standard GR ringdown templates with additional parameters [425, 1810, 1811], the superposition of sine-Gaussians [1812], hybrid methods that put together information from perturbation theory and the pre-merger orbital dynamics [1813–1815], using the close-limit approximation [1816], and analytical models that explicitly depend on the physical parameters of the ECO [448, 1817–1819].

6.4. Small mass-ratio approximation

6.4.1. Beyond GR Although there have been substantial advances in GSF models in GR (see Sec. 4.3), self-force calculations for theories beyond GR are in their infancy. The most detailed studies in this vein have so far investigated changes to the emitted GW flux for scalar-tensor and higher-order curvature theories of gravity [127, 1732, 1780, 1820–1823], and for theories of massive gravity when assuming a Schwarzschild BH background [1824]; there are only a few examples of formulations of a full self-force theory beyond GR [1825, 1826]. But recently it has been argued that for a vast class of theories, no-hair theorems or separation of scales lead metric and scalar perturbations to decouple [1827]. In particular, in the large class of higher-derivative gravity models, the modification to GR scales with the curvature, i.e., with the inverse of the mass. Consider, for example, the Kretschmann curvature scalar $\mathcal{K} = R_{\mu\nu\rho\sigma}R^{\mu\nu\rho\sigma}$. On the horizon of a Schwarzschild BH of mass M it scales as $\mathcal{K} \sim M^{-4}$. Consequently, higher-curvature modifications to a supermassive BH are negligible. This allows the background spacetime to be treated as the Kerr solution, and changes in the binary's evolution to be fully controlled by the scalar field charge of the small BH [1827–1831]. In this regard, the study of small-mass-ratio binaries in generalized scalar-tensor theories of gravity can benefit from efforts already devoted to investigating self-forces on scalar charges, and their orbital evolution around BHs [1086, 1228, 1229, 1289, 1832–1841].

6.4.2. Dark matter and boson clouds For EMRI and IMRI systems, the largest effect of dark matter is to produce a significant drag force through dynamical friction [1725], which increases the rate of inspiral of the small compact object [62, 365, 1724, 1842, 1843] (accretion and the usual gravitational pull of the dark matter can be significant, but are in general subleading effects [62, 1723, 1724, 1844]). This typically requires very high densities of dark matter surrounding the intermediate or supermassive BH [62, 1842]. The required densities can be achieved when the IMBH or SMBH adiabatically grows

125

in a dark-matter halo, and the distribution of dark matter near the BH gets compressed into a "spike" with significantly higher densities than the surrounding halo [1845–1848]. Sufficiently large densities may also be achieved for clouds of ultralight bosons formed around MBHs, as discussed in Sec. 2.7. If they exist, these clouds would introduce additional metric perturbations that perturb the companion's orbit, and they would respond to the gravity of the companion. If the cloud contributes a sizable fraction of the BH's mass, its gravity would necessitate a change in the background geometry (see Refs. [1849, 1850] for such an example), dramatically complicating the GSF model. Building accurate IMRI/EMRI waveforms evolving in a dark matter spike or boson cloud is also crucial to distinguish these environments from other astrophysical environments, such as accretion disks. In fact, recent studies strongly suggest that these different types of environments leave distinguishable signatures in IMRI or EMRI waveforms [373, 374, 1277, 1848, 1851–1853]. Therefore the detection of such systems could also be used to identify and learn about the environment surrounding supermassive BHs.

To date, studies of the gravitational effects of dark matter spikes and boson clouds on binary systems, such as EMRIs and IMRIs, have mostly relied on Newtonian or post-Newtonian approximations for the orbit and the matter distribution [369, 372–375, 1723, 1728, 1733–1736, 1842, 1844, 1848, 1854–1856]. Generalizing some of these calculations to the fully relativistic case is in principle feasible. Indeed, first steps in this direction were recently done in Refs. [1278, 1279, 1857] where a generic and fully-relativistic formalism to study EMRI systems in spherically-symmetric, non-vacuum BH spacetimes was developed. For boson clouds, a fully relativistic framework that assumes that the impact of the cloud on the BH geometry can be treated perturbatively, was proposed in Ref. [1858].

However, there are important open problems to be solved. First, generalizing the formulation of Refs. [1278, 1279, 1857, 1858] to non-spherically-symmetric backgrounds is a non-trivial task, and secondly, for dynamic matter distributions [1855], evolving the matter environment coupled to the binary system at first post-adiabatic order will likely be a complex problem.

Finally, it is worth noting that boson clouds themselves can also be strong sources of nearly-monochromatic gravitational waves potentially detectable by LISA [324, 327, 334, 335, 357, 361–363, 379, 381, 1859]. The gravitational waves emitted by these sources can be computed using the same techniques typically used in the small mass-ratio approximation: one can consider the cloud as being a small perturber of a Kerr background geometry and use the Teukolsky formalism to compute GW emission from a boson cloud [335, 357, 361, 363, 1859].

6.4.3. Beyond GR BHs and exotic compact objects A key goal of the LISA mission, is to determine whether the dark central objects in galactic cores are genuine BHs,

and if so, whether they are accurately described by GR BHs. With EMRIs we expect to be able to constrain fractional deviations from the quadrupole moment of the Kerr solution at a level smaller than 10^{-4} [92, 98], which would allow to impose stringent constraints on ECOs and non-GR BHs. Work to include these modifications in GSF models has been done by considering the large central object as a "bumpy" BH. Bumpy BHs are spacetimes that include the Kerr limit, but that differ in a parameterized way, typically by modifying the spacetime's multipole moment structure [97, 460, 1860–1863]. The "bumps" can be introduced directly into the background metric, or (if they are sufficiently small) they can be treated as additional metric perturbations. A benefit of the bumpy BH framework is that it is agnostic about the mechanism which produces the BH's bumps. They could describe non-GR physics (to exactly recover BH solutions in specific alternative theories [1864, 1865], for example), or if the central object is an ECO, they could be tidally induced by the companion, encoding the ECO's tidal Love numbers [463, 464, 1270, 1746, 1866–1872]. Because bumpy BHs break the symmetries of Kerr that yield integrable motion [1873], orbits in these spacetimes are generically chaotic [1874–1877] and subject to prolonged resonances [1306, 1876–1878]. Most of the work considering EMRIs around spacetimes with a multipolar structure different from Kerr, constructed approximate "kludge" waveforms [460, 480, 1863, 1879, 1880] generated considering geodesics in a perturbed Kerr spacetime with parameters evolved using post-Newtonian equations [98, 100, 1221, 1862, 1874]. While these approaches are believed to reproduce the main features of the orbit, they will not be enough to get to the precision required to determine that the inspiral is indeed an inspiral into a Kerr BH or not [1069, 1874], and much more work is needed to build such waveforms. The additional parameters in such models will also typically increase the possibility of degeneracies, making it important to fully understand possible discernible features, such as characteristic variations of the amplitude and the energy emission rate [1252] or the appearance of prolonged resonances [1221, 1306, 1877]. If the central object is an ECO, in addition to nonintegrable motion and geodesic resonances [1881], it will also lack a true event horizon. This causes a change in boundary conditions: in a BH spacetime, fields are purely ingoing on the horizon, while in an ECO spacetime, fields obey a boundary condition of (partial) reflection at the effective surface. The effect of this reflection has been taken into account for the dissipative first-order self-force in [449, 1744, 1882–1885]. In addition, the modes of the ECO could also be excited during the inspiral of the small compact object [449, 1795, 1883, 1884, 1886–1889] (see Ref. [1889] where the conditions for such modes to be effectively excited during the inspiral were studied in more detail). Depending on the object's properties, this could cause the rate of the inspiral to change significantly in the vicinity of each resonance. For the dissipative first-order self-force, the effect on the emitted GW flux has been modelled for gravastars [1886], boson stars [1795] and an exotic ultracompact object with an exterior Schwarzschild or Kerr geometry but with a hard surface close to the would-be horizon [449, 1883, 1884]. An object plunging in the interior of an ECO would also be subject to additional forces that can dominate the dynamics, such as dynamical

friction [1725] and accretion. The impact of these effects on the orbit dynamics and GW waveforms has been modeled for small compact objects plunging onto boson stars using a Newtonian approximation [365] (see also [1890] for earlier work on the same subject were dynamical friction and accretion had been neglected).

6.5. Effective-one-body waveform models

EOB waveforms with generic deviations from GR have been developed based on a parameterized form for performing theory-agnostic tests. These include deformations to the GW phase (see Eq. (22)) which are added as corrections to frequency-domain EOB waveforms in GR [596, 597, 1706, 1891, 1892], or parameterized deformations of the QNMs in time-domain EOB waveforms, which have been used to perform tests of the no-hair theorem in GR and constrain higher-order curvature theories of gravity [596–598, 1752, 1893, 1894].

Recent work has also computed the EOB dynamics for non-spinning binaries in various theories beyond GR as a foundational step towards enabling model-dependent tests. Results are available for scalar-tensor theories of gravity [1502–1504, 1895], Einstein-Maxwell-dilaton theories [1896] and Einstein-scalar-Gauss-Bonnet gravity [1692, 1895]. The EOB approach has also been used to compute the two-body potential energy of point-like particles in theories exhibiting a Vainshtein screening [1897]. Developing these results into full EOB waveform models and including more realistic physics remains an open task.

For non-vacuum binaries involving e.g. ECOs or boson clouds around BHs, a number of generic matter effects during the inspiral change the GW signals away from those of a BH binary (see discussion in previous subsections). Several of the dominant matter effects for neutron star binaries are included in EOB models that could also have broader applicability to ECOs or non-vacuum BHs. These effects are described in a parameterized form, where the nature of the object is encoded in characteristic coefficients such as the bodies' multipole moments, tidal and rotational Love numbers, and QNM frequencies. Specifically, the effects of rotational deformation and adiabatic tides are currently included in the TEOBResum family of models discussed in Sec. 4.5 in the way described in Refs. [1029, 1430, 1434, 1440, 1463, 1469, 1472, 1898–1900], with the state-of-the-art models incorporating the known adiabatic gravitoelectric and -magnetic tidal terms up to $\ell = 8$ in different resummation schemes [1469, 1899–1901], dynamical tides from the fundamental modes [1467, 1468, 1902] as well as nonlinear-in-spin effects dependent on the nature and interior structure of the object [1430, 1463]. The SEOBNR models include tidal effects using the dynamical tidal models for the fundamental modes from [1467, 1468], which have recently been further developed [1470, 1903, 1904]. Matter effects have also been incorporated in the ROMs of SEOBNR waveforms in the frequency domain by augmenting the ROMs developed for BBHs with analytical closed-form expressions correcting the GW phase to include tidal and spin-induced multipole effects

based on PN calculations for the rotational quadrupole effects [1905] and tidal models that are specific to calibrations to NR simulations of neutron star binaries [1521, 1906], though in principle could be replaced by more general frequency-domain tidal models.

However, significant work remains. Besides the improvement of current EOB models already discussed in Sec. 4.5, other improvements that are specific to ECOs or non-vacuum BHs include, for example, incorporating more effects from spins and relativistic phenomena in the matter sector (which are likely to be more important for compact ECOs than for neutron stars); incorporating parameterized absorption coefficients; and the inclusion of effects specific to dark matter spikes and boson clouds already discussed in Secs. 6.2.2 and 6.4.2. In addition, a remaining challenge is to develop full IMR waveforms. Possible avenues for constructing full waveforms for binaries with matter have been explored, e.g., in the context of binary neutron stars [1907], by using NR-informed analytical models that build on quasiuniversal features found in these systems [1907–1909], and for the tidal disruption in BH-neutron-star binaries [1471, 1472, 1910]. To achieve similar complete waveforms for ECOs, it is worth mentioning that a phenomenological model was proposed in Ref. [1911], which used EOB waveforms with tidal effects to describe the inspiral phase and a toy model inspired by Ref. [1912] to model the post-merger dynamics of the system. Whether this model is an accurate enough description for known ECOs, e.g. boson stars, remains to be fully studied.

6.6. Phenomenological waveform models

The phenomenological waveform models of Sec. 4.6 already provide standard tools for tests of GR with the current generation of ground-based detectors [596, 597, 1891, 1913, 1914]. In particular, parameterized tests (in the spirit of ppE formalism, see Sec. 6.2.1) have been employed to probe theory-agnostic deviations from GR in the Phenom ansatz describing the phase evolution of an observed signal [1705, 1706] and to test the BH nature of compact binaries from waveform signatures of spin-induced quadrupole moments [1915]. At a more fundamental level, such tests depend on the parameterization of the waveform model, and face a number of practical and conceptual problems, e.g., varying the phenomenological coefficients in such models by amounts that are too large, pathologies may arise in the waveform. Some improvements can be expected from adding time domain models [1490] to the existing frequency domain models, thus providing very different waveform parameterizations to be varied. Going beyond theory agnostic tests, the flexibility of phenomenological models also provides a natural ground to develop models for beyond GR theories or "exotic" physics, such as boson stars and boson clouds around BHs. A key problem is the very large parameter space for such theories, and significant technical and conceptual progress will be required to develop mature approaches. Natural first steps for the near future would be, for example, to calibrate accurate models to small "toy model" regions of some beyond

GR theories, and to develop simple toy models that do not require any calibration to numerical waveforms.

6.7. Modeling cosmic strings

Waveform models for GW emission are needed for LISA for three types of anticipated searches: for the stochastic background, for individual bursts and for individual, coherent, nonlinear oscillatory waveforms. There are significant uncertainties in the properties of the underlying string elements (the number of objects, the presence of cusps, kinks and small scale structure, the size distribution of the objects, the spatial and velocity distribution of the objects). Here, however, we concentrate on the modeling of the *waveforms* generated by one or more loops while also mentioning some of the incompletely known loop properties that will influence the waveforms.

6.7.1. Nambu–Goto, smooth loops with cusp/kink features
We begin with minimally coupled string networks with loops that are smooth on large scales and include cusps or kinks but no other small scale structure.

The underlying formalism to calculate the gravitational signal to lowest order in the string tension μ_S is well known [1916]. Early research focused on calculating the individual loop waveforms for relatively simple loops [274, 275, 1917–1923]. Both the burst waveforms and the relevant statistical averages for the background implicitly follow. FFT techniques work well to estimate the power at low to moderate harmonics [255, 1919] and additional numerical techniques have been devised specifically to handle higher harmonics [1924].

In the case of LVK, small scale features dominate emission at high frequencies. A similar situation pertains to LISA, which will be sensitive to the high frequencies of the astrophysically relevant low tension strings. The development of an asymptotic approach Refs. [261, 262, 290] was an important quantitative and qualitative advance. High frequency emission sourced by cusps and kinks is approximately independent of the large scale loop structure. The important features of cusp waveforms in this limit are that (1) the cusp power spectrum falls off at high frequencies as $f^{-4/3}$; and (2) the GWs from the cusp are strongly beamed in the direction of cusp motion and exponentially suppressed at frequencies $f \gtrsim 1/(\theta^3 T)$ for angle θ with respect to that direction (with T the periodicity of the string). The waveform's time dependence is $\propto |t - t_c|^{1/3}$, where t_c is the time at which the cusp formation event is noted by an observer situated in the beam of emission ($\theta = 0$), and so the cusp waveform is called *sharp* or *spiky*. This sharpness is softened for $0 < \theta \ll 1$. Similar analyses are applicable to kinks.

The genericity of the high frequency predictions for cusps and kinks, the independence with respect to the large scale loop structure and the simplicity of the templates are all important, and the results have been exploited in astrophysically-motivated searches

[291, 294, 297, 1925].

The outlook and need for waveforms is as follows:

(1) The existing asymptotic treatments of kink and cusp emission are likely to be sufficient for modeling an unresolved stochastic wave background. That is because the energy flux derived from averaging over time, space and angle, which is implicit in such a calculation, depends upon low-order moments of the loop's full beam pattern that can be derived from the asymptotic results.

(2) More refined models of the burst waveform that do not, strictly speaking, lie in the asymptotic regime are needed. Such waveforms can account for geometric effects when the observer does not lie directly in the cusp direction and for anisotropies in the beam shape. These can be found by extending the asymptotic treatment.

(3) Existing calculational methodologies for full loops are accurate and efficient at low to moderate modes. LISA and pulsar timing arrays will probe both low and high order modes. Hybridization methods giving models of the beam that span the full range of modes will be required for any loop sources that stand out above the stochastic background [1924].

6.7.2. Nambu–Goto, small-scale structure Each time a long horizon-crossing string intercommutes it gains two kinks. Small scale structure builds up on the string [1926–1930]. Gravitational backreaction probably smoothens the string at small scales [1931–1934]. The wigglyness that remains has been evaluated [1926, 1927] but never determined directly by simulation. Ref. [1935] found that small-scale structure near the cusp rounded off the sharpness of the cusp waveform but affected only observers very near to the direction of cusp motion. Alternatively, Ref. [1927] found that the small scale structure enhanced intercommutation on a newly formed loop and excised the cusp when it first begins to form. It will be important to investigate the effect of small structure on loop dynamics and the resultant waveforms. This can be done parametrically as the amount and character of the wigglyness increases on otherwise simple loops.

6.7.3. Nambu–Goto for Pseudocusps As a last note, in addition to cusp waveforms, some authors [1936] have studied the bursts due to "pseudocusps", i.e., string trajectories which very closely approach, but do not strictly reach, the cusp configuration. These pseudocusp burst waveforms are of lower amplitude than true cusps, and follow the same power spectrum decay of $f^{-4/3}$ at high frequencies. Accounting for them in a search can lead to an enhancement in the number of expected burst events.

6.7.4. Beyond Nambu–Goto for cusps

Gauge theory strings with energy scale $\mu_S^{1/2}$ have a characteristic core width $\sim \mu_S^{-1/2}$ whereas classical superstrings are always well-represented by the zero thickness Nambu–Goto limit. When a cusp forms the string instantaneously doubles back upon itself. Ref. [1937] predicts that a region of string around the cusp, of the order of the string thickness, will annihilate into particles due to overlap. For strings with large tensions (near that of the GUT scale) this modification to the cusp shape is at a small enough scale that it does not meaningfully affect the cusp waveform. However, as tension decreases the physical scale increases. It may prove useful to compare the waveform of the gauge theory cusp to the superstring cusp. This can be done by parametrically varying the core width in Abelian-Higgs simulations.

A final assumption about the standard cusp waveform model is that it relies only on properties universal to all strings. However, superstrings possess additional features that could modify their cusp waveforms. Ref. [290] suggested modifications to the amplitude based on the dimensionless loop-length parameter α. For example, cusps very near to Y-junctions will have their burst amplitude modified by a correction factor that depends on the nearby string geometry [263], while the extra degrees of freedom on superstrings (extra dimensions) can lead to a strong suppression of both cusp rate and burst amplitude [1938].

6.7.5. Cosmic strings and GW production in numerical relativity

While in most cases, perturbative methods (e.g., Nambu–Goto strings coupled to perturbative gravity [1932]) are sufficient, situations may arise when perturbative methods are insufficient and gravitational backreaction becomes of $\mathcal{O}(1)$, even if the string tension $G\mu_S$ is small. For example, a string with a sharp kink can easily lead to a locally strong field situation [1939]. In such strong field limits, the full machinery of NR must be employed. The construction of full NR solutions for cosmic strings was recently achieved by [1940, 1941], where stable dynamical solutions for an Abelian-Higgs string minimally coupled to gravity was found. This opens the door to not just the detailed exploration of the string dynamics, but also the characterization of the GW signals that can then be searched for.

The Abelian-Higgs model minimally coupled to gravity can be recast into the standard BSSN/CCZ4 formalism, and solved using finite differences (we refer the reader to [1940] for details). Presently, solutions for infinite static strings, planar loops [1940] and single traveling wave solutions [1942] have been constructed. Once a string configuration is constructed and successfully evolved, the work required to extract useful GW signals from them follows very similarly to that of any standard NR simulations, see Sec. 4.1.

As an example, in [1941], the gravitational waveform emitted during the BH formation of a collapsing circular cosmic string was computed, and it was shown that the waveform is dominated by the BH formation and ringdown phase, with the primary contribution being the $\ell = 2$, $m = 0$ mode (as opposed to quasi-circular compact binary merger

signals which are dominated by the $\ell = 2$, $m = 2$ mode). Intriguingly, due to the large asymmetric ejection of material in the formation process, a large GW memory was also seen.

The future prospects for using NR to compute GW signals from such strong gravity events is very promising. For example, a full general relativistic treatment of the GW emission from cosmic string cusps and kinks is long overdue, but is now within reach. Presently, the main obstacle to explore more complicated string configurations is the need for the construction of accurate initial conditions – a usual problem in any NR endeavor, here made more difficult by the presence of fundamental matter fields. Nevertheless, this area is ripe for further exploration.

7. Afterword

LISA will usher in an era of millihertz GW astronomy that will open a window to new classes of sources and offer unprecedented opportunities to probe our understanding of the universe. Integral to this scientific vision are predictions of the source waveforms, which are necessary for the detection and interpretation of GW events.

This white paper has analyzed the question of waveform preparedness in the LISA era. It has reviewed the modelling requirements from astrophysical and data analysis perspectives, and has analyzed the status of the main approaches to modelling waveforms from compact binaries both in vacuum GR and in the presence of environmental influences or effects from new physics beyond GR and the Standard Model. This white paper also provides guidance on new developments that are needed for the different approaches, both in terms of modelling accuracy and the covered parameter space, so that gravitational wave models will be ready for the LISA era.

The experience with ground-based GW detectors has to some extent prepared the community. For example, several approaches that predict the waveforms for comparable mass black hole binaries can be applied directly to massive black hole binaries due to the simple mass scaling of GR. However, these models are not currently sufficient to fully realize LISA's science goals. In particular they insufficiently cover the parameters of eccentricity, highly asymmetric mass-ratios, and high spin magnitudes. In addition, the possibility of very strong massive black hole binary signals places additional demands on the accuracy of these models, well beyond what can currently be achieved.

For extreme-mass-ratio inspirals, leading-order (adiabatic) models that are sufficient to enable some LISA science are becoming available, and these models can be evaluted fast enough for use in LISA data analysis. In order to enable the full spectrum of LISA science with EMRIs post-adiabatic models are needed. These have recently been developed for the simplest orbital configurations (non-spinning, quasi-circular). It also looks likely that these models can cover much of the intermediate mass ratio parameter space. Significant work remains to extend these post-adiabatic models to cover the full parameter space of precessing and eccentric parameter binaries where both components are spinning.

The modelling of sources in theories beyond GR is still in its infancy with significant effort needed. For example, the majority of computations have focused on higher derivative gravity, that are most interesting in the high curvature regime, or on Horndeski models. Moreover, simulations of compact binaries in extensions of GR are, at the time of writing this white paper,proof-of-concept. That is, they have been done for nearly equal-mass binaries, typically of non spinning black holes, and at relatively low resolution. This is comparable to the state of numerical relativity in GR about 15 years ago (i.e., few years after the breakthrough in 2005). Likewise, perturbative or PN calculations have only started to go beyond the leading order in the correction. To

perform theory-specific tests of gravity, more work is needed, both in terms of modelling accuracy and in covering (parts of) the parameter space of black hole masses, spins and additional theory-specific parameters.

The good news is that in all approaches there are clear ideas of what needs to be done in order to reach the modelling requirements for LISA. Doing so will require a concerted effort over the next decade. Given sufficient resources, we are positive that all goals can be achieved.

We particularly recommend that the community conduct more investigations into the waveform standards and waveform interface. While lessons have been learned from ground-based detectors, LISA will offer unique challenges that will need to be addressed by the waveform and data analysis communities working together.

Appendix A: Descriptions of NR codes

Description of some numerical relativity codes that focus, in particular, on modelling LISA sources. A more extensive list is given in Table 8.

BAM BAM is a modular code framework initially developed at the University of Jena and is now maintained and further developed by the CoRe (Computational Relativity) Collaboration [574, 608–610]. BAM employs finite differences for the discretization of spacetime fields, and high-resolution shock-capturing methods for the evolution of general relativistic hydrodynamics variables. It features automated code generation with Mathematica, adaptive mesh refinement (AMR) in space and time, and parallelization with MPI and OpenMP for large scale HPC, recently at 70% on up to 50k cores. BAM is employed for the simulation of compact binary mergers, e.g., [516, 530, 1899, 1943]. A major focus is on binary black hole, binary neutron star, and black hole - neutron star systems [1944], plus more exotic compact objects or merger scenarios [1673]. Recent updates allow the study of radiation hydrodynamics [1945], magnetohydrodynamics, and the usage of an entropy-viscosity limiter for the flux computation [1946]. BAM has contributed numerical data for the development and validation of e.g. Phenom-type and EOB waveform models. Several hundred binary neutron star merger simulations are available as part of the existing CoRe database [611, 612].

BAMPS The Jena-Lisbon collaboration is developing the code bamps, a new and highly scalable NR code for exascale applications using pseudo-spectral and DG methods [613, 614]. A key feature is hp-refinement for spectral element methods [615], which allows highly scalable and accurate simulations, currently with a focus on smooth fields. To date, bamps has already been employed for the study of GW collapse [614, 1947], simulations with scalar fields for collapse and for boson stars are in development. Further applications include simple neutron star spacetimes [613], and studies of new techniques regarding the dual foliation framework [1948].

Dendro-GR Dendro-GR [618, 1949, 1950] uses an unstructured grid with a localized, wavelet-based refinement scheme to evolve the BSSN formulation of the Einstein equations using moving punctures. In test simulations of a BBH with a mass ratio of $10 : 1$, Dendro-GR shows good scaling to over 10^5 cores.

Einstein Toolkit The Einstein Toolkit [620, 621] is an open-source cyberinfrastructure for computational astrophysics, with more than 300 registered users worldwide. It implements Einstein's equations, or extensions thereof, in the BSSN or CCZ4 formulation together with the moving puncture gauge. It employs the method of lines, in which spatial derivatives are implemented as up to 8th order finite differences together with a collection of direct time integration techniques (e.g., fourth order Runge-Kutta integrator). The Einstein Toolkit is based on the Cactus computational toolkit [1951] and the Carpet boxes-in-boxes AMR package [1952,

1953]. It also provides a multipatch infrastructure consisting of Cartesian boxes-in-boxes meshes in the region where the binaries evolve (typical size $\sim 50 \ldots 100M$), and a spherical outer region in the wave zone (typical radius $\sim 1000 \ldots 2000M$) provided by the Llama code. Kreiss-Oliger dissipation is employed to reduce high frequency noise at refinement boundaries. The toolkit uses hybrid MPI/OpenMP parallelization. The Einstein Toolkit has been a broad community project with a multitude of software that is based on its infrastructure or that has been developed within its framework. The additional software is indicated by asterisks in Table 8.

Einstein Toolkit – CarpetX The Einstein Toolkit consortium is developing a new AMR driver, CarpetX [1954], for the Einstein Toolkit. CarpetX leverages the AMReX framework [1955] to provide scalable adaptive mesh refinement for physics modules. CarpetX will provide: efficient support for both CPUs and GPUs; parallelization via MPI and OpenMP; SIMD vectorization; scalable I/O based on the ADIOS2 file format [1956] and the openPMD metadata standard; and more. CarpetX offers block-structured AMR based on local error estimates, exact conservation across mesh interfaces, higher order prolongation operators, and scalable elliptic solvers based on PETSc [1957]. CarpetX is available as open source and was used in production in Ref. [1958].

GR-Athena++ Another example is GR-Athena++[644] based on the astrophysical (radiation) magnetohydrodynamics code Athena++ [1959]. GR-Athena++ leverages on Athena++'s oct-tree AMR and exploits hybrid parallelism at different levels. The standard distributed approach is augmented by a dynamical tasklist for the procedures in each mesh block that overlaps calculation and communication (thus mitigating some of the overhead associated with high order finite differencing). In-core vectorization and other optimization techniques of the basic kernels [1960] are also employed. This approach leads to a high parallel efficiency, with strong scaling efficiencies above 95% for up to 10^4 CPUs and excellent weak scaling is up to 10^5 CPUs measured in a production BBH setup with AMR.

GRChombo GRChombo ([645–647]) is an open-source NR code built using an optimized version of the publicly available library Chombo[1961] developed at LBNL. It is based on established methods of solving the Einstein equations, but the highly flexible AMR capability and templating over physics classes makes it suited to strong gravity problems in beyond-GR scenarios (e.g. Horndeski gravity [1962], cosmic strings [1941]), which have been key targets of the code. GRChombo is written entirely in `C++14`, using hybrid MPI/OpenMP parallelism and vector intrinsics (in particular, the evolution calculations are explicitly vectorised) to achieve improved performance on the latest architectures. It has good strong scaling up to around 4,000 cores for typical binary BH problems, at which point it becomes limited by problem size as with most traditional codes.

The next release of Chombo is designed to be performance portable to different heterogeneous architectures (including GPUs), which GRChombo should be able

to leverage to improve scaling further.

Illinois GRMHD The Illinois GRMHD evolution code [651, 652, 1963] solves the Einstein field equations via the BSSN scheme with puncture gauge conditions, utilizes a conservative high-resolution, shock-capturing (HRSC) scheme for the matter and adapts the Carpet infrastructure to implement AMR. The code solves the magnetic induction equation by introducing a magnetic vector potential, which guarantees that the B-field remains divergence-free for any interpolation scheme used on refinement level boundaries. This formulation reduces to a standard constrained transport (CT) scheme on uniform grids. An improved Lorenz gauge condition for evolving the vector potential in AMR without the appearance of spurious B-fields on refinement level boundaries is implemented. This gauge exhibits no zero-speed modes, enabling spurious magnetic effects to propagate off the grid quickly. The GRMHD code recently added a radiation module built to handle transport (photons or neutrinos) via the M1 moment formalism. A version of the Illinois GRMHD code has been released as an open-source module that has been ported to the Einstein Toolkit, where it has been documented and rewritten to make it more user-friendly, modular and efficient. The code has been used to simulate numerous scenarios related to LISA sources (e.g., BHBH mergers, BHBH mergers in gaseous clouds and magnetized disks, etc.) and their associated gravitational waveforms.

MHDuet The publicly available code MHDUET [655, 656, 1964, 1965] is generated by the open-source platform SIMFLOWNY to run under the SAMRAI infrastructure, which provides the parallelization and the adaptive mesh refinement. There are different versions of the code, either to study alternative gravity theories or to include large-eddy-simulations and neutrino transport.

SACRA The SimulAtor for Compact objects in Relativistic Astrophysics (SACRA) code solves Einstein's equation with the BSSN-puncture formulation together with a Z4c constraint propagation prescription and the relativistic hydrodynamics equation with the HRSC scheme [657, 658]. It implements the box-in-box conservative AMR with parallelization by MPI and OpenMP. The code has been used to simulate compact binary mergers such as NSNS mergers, BHNS mergers, and BHBH mergers. The NSNS waveform catalog SACRA Gravitational Wave Data Bank is available at [662]. The latest version of SACRA has a couple of branches, such as SACRA-TD, to simulate the tidal disruption of an ordinary star by the SMBH [1966], or SACRA-MG to simulate a compact object in scalar-Gauss-Bonnet theory [659] and scalar-tensor theory [660]. SACRA also has a version to solve high-dimensional Einstein's equation [661]. In addition, it features modules for neutrino radiation transport [1967], MHD [1968, 1969] and viscous hydrodynamics [1970].

SACRA-SFS2D is a viscous-radiation hydrodynamics [663] and radiation magnetohydrodynamics code [664] in full general relativity. These codes can be applied to the

collapse of massive stars and supermassive stars to a stellar-mass and supermassive black hole [1971], to the post-merger evolution of the neutron-star binaries [1972], and to collapsar modeling [1973].

SpEC The Spectral Einstein Code (`SpEC`) [665] is a pseudo-spectral GR code developed by the Simulating eXtreme Spacetimes collaboration. `SpEC` is capable of evolving BBH and binaries with neutron stars. It incorporates an elliptic solver to construct initial data [522, 526, 529], eccentricity reduction [1974–1976], constraint-preserving and non-reflective outer boundary conditions [536, 1977, 1978], and implements hp-AMR [735, 1979]. Extracted gravitational waves are extrapolated to future null infinity [515, 548, 1980] and corrected for center-of-mass drift [1981]. `SpEC` is a highly accurate NR code for BBH, and has computed large waveform catalogs of BBH inspirals encompassing several tens of orbits [513, 515]. `SpEC` has evolved BBH with spins as large as 0.994 [1982], inspirals as long as 170 orbits [576] as well as eccentric binaries [708].

SpECTRE The Simulating eXtreme Spacetimes collaboration is developing the next-generation code SpECTRE [667, 668], which uses a discontinuous-Galerkin-finite-difference hybrid method [1983–1985] for accurate and robust neutron star simulations combined with task-based parallelism, showing good scaling to over $600,000$ cores [667]. Using Cauchy-Characteristic extraction, SpECTRE is able to resolve gravitational wave memory [552, 553] and improve hybridization with post-Newtonian waveforms by ensuring numerical relativity waveforms are in the same BMS frame as the post-Newtonian waveforms [555]. Improvements for efficiently simulating binary black holes with mass ratios $q > 10$ aim to reduce the computational cost of such simulations by a factor of q [686]. SpECTRE also incorporates a flexible elliptic solver [533, 1986, 1987].

Spritz `Spritz` is an open-source code that solves the equations of general relativistic magnetohydrodynamics and that can take into account finite temperature nuclear equations of state and neutrino emission [635, 1988, 1989]. The code is based on the Einstein Toolkit framework and implements also high-order methods for the hydrodynamic equations.

WhiskyMHD `WhiskyMHD` is a fully general relativistic magnetohydrodynamic code based on the Einstein Toolkit [640]. The code has been used mainly to perform simulations of binary neutron star mergers, but it has also been used to perform the first simulations of magnetized plasma around merging supermassive black holes in the ideal magnetohydrodynamic approximation [1990].

Acknowledgements

References

[1] M. Pürrer and C.-J. Haster, Gravitational waveform accuracy requirements for future ground-based detectors, Phys. Rev. Res. **2**, 023151 (2020), arXiv:1912.10055 [gr-qc].

[2] D. Ferguson, K. Jani, P. Laguna, and D. Shoemaker, Assessing the readiness of numerical relativity for LISA and 3G detectors, Phys. Rev. D **104**, 044037 (2021), arXiv:2006.04272 [gr-qc].

[3] P. A. Seoane *et al.* (LISA), Astrophysics with the Laser Interferometer Space Antenna, Living Rev. Rel. **26**, 2 (2023), arXiv:2203.06016 [gr-qc].

[4] P. Amaro-Seoane *et al.* (LISA), Laser Interferometer Space Antenna, arXiv:1702.00786 [astro-ph.IM].

[5] T. Robson, N. J. Cornish, and C. Liu, The construction and use of LISA sensitivity curves, Class. Quant. Grav. **36**, 105011 (2019), arXiv:1803.01944 [astro-ph.HE].

[6] T. Gehren, J. Fried, P. A. Wehinger, and S. Wyckoff, Host galaxies of quasars and their association with galaxy clusters., Astrophysical Journal **278**, 11 (1984).

[7] J. Kormendy and D. Richstone, Inward bound: The Search for supermassive black holes in galactic nuclei, Ann. Rev. Astron. Astrophys. **33**, 581 (1995).

[8] A. E. Reines, G. R. Sivakoff, K. E. Johnson, and C. L. Brogan, An actively accreting massive black hole in the dwarf starburst galaxy Henize 2-10, Nature **470**, 66 (2011), arXiv:1101.1309 [astro-ph.CO].

[9] A. E. Reines, J. E. Greene, and M. Geha, Dwarf Galaxies with Optical Signatures of Active Massive Black Holes, Astrophys. J. **775**, 116 (2013), arXiv:1308.0328 [astro-ph.CO].

[10] V. F. Baldassare, M. Geha, and J. Greene, A search for optical AGN variability in 35,000 low-mass galaxies with the Palomar Transient Factory, Astrophys. J. **896**, 10 (2020), arXiv:1910.06342 [astro-ph.HE].

[11] D. J. Croton, V. Springel, S. D. M. White, G. De Lucia, C. S. Frenk, L. Gao, A. Jenkins, G. Kauffmann, J. F. Navarro, and N. Yoshida, The Many lives of AGN: Cooling flows, black holes and the luminosities and colours of galaxies, Mon. Not. Roy. Astron. Soc. **365**, 11 (2006), [Erratum: Mon.Not.Roy.Astron.Soc. 367, 864 (2006)], arXiv:astro-ph/0602065.

[12] C. M. Dickey, M. Geha, A. Wetzel, and K. El-Badry, AGN All the Way Down? AGN-like Line Ratios Are Common in the Lowest-mass Isolated Quiescent Galaxies, Astrophysical Journal **884**, 180 (2019), arXiv:1902.01401 [astro-ph.GA].

[13] R. S. Sharma, A. M. Brooks, R. S. Somerville, M. Tremmel, J. Bellovary, A. C. Wright, and T. R. Quinn, Black Hole Growth and Feedback in Isolated ROMULUS25 Dwarf Galaxies, Astrophysical Journal **897**, 103 (2020), arXiv:1912.06646 [astro-ph.GA].

[14] L. Ferrarese and D. Merritt, A Fundamental relation between supermassive black holes and their host galaxies, Astrophys. J. Lett. **539**, L9 (2000), arXiv:astro-ph/0006053.

[15] K. Gebhardt *et al.*, A Relationship between nuclear black hole mass and galaxy velocity dispersion, Astrophys. J. Lett. **539**, L13 (2000), arXiv:astro-ph/0006289.

[16] A. J. Barger, ed., *Supermassive black holes in the distant universe* (Kluwer Academic, Dordrecht, Netherlands, 2004).

[17] J. Kormendy and L. C. Ho, Coevolution (Or Not) of Supermassive Black Holes and Host Galaxies, Ann. Rev. Astron. Astrophys. **51**, 511 (2013), arXiv:1304.7762 [astro-ph.CO].

[18] N. J. McConnell and C.-P. Ma, Revisiting the Scaling Relations of Black Hole Masses and Host Galaxy Properties, Astrophys. J. **764**, 184 (2013), arXiv:1211.2816 [astro-ph.CO].

[19] M. Schramm and J. D. Silverman, The black hole - bulge mass relation of Active Galactic Nuclei in the Extended Chandra Deep Field - South Survey, Astrophys. J. **767**, 13 (2013), arXiv:1212.2999 [astro-ph.CO].

[20] M. A. Latif and A. Ferrara, Formation of supermassive black hole seeds, Publ. Astron. Soc. Austral. **33**, e051 (2016), arXiv:1605.07391 [astro-ph.GA].

[21] M. Volonteri, G. Lodato, and P. Natarajan, The evolution of massive black hole seeds, Mon. Not. Roy. Astron. Soc. **383**, 1079 (2008), arXiv:0709.0529 [astro-ph].

[22] M. Volonteri, The Formation and Evolution of Massive Black Holes, Science **337**, 544 (2012), arXiv:1208.1106 [astro-ph.CO].

[23] A. Lupi, M. Colpi, B. Devecchi, G. Galanti, and M. Volonteri, Constraining the high redshift formation of black hole seeds in nuclear star clusters with gas inflows, Mon. Not. Roy. Astron. Soc. **442**, 3616 (2014), arXiv:1406.2325 [astro-ph.GA].

[24] L. Mayer, D. Fiacconi, S. Bonoli, T. Quinn, R. Roskar, S. Shen, and J. Wadsley, Direct formation of supermassive black holes in metal-enriched gas at the heart of high-redshift galaxy mergers, Astrophys. J. **810**, 51 (2015), arXiv:1411.5683 [astro-ph.GA].

[25] R. Valiante, R. Schneider, M. Volonteri, and K. Omukai, From the first stars to the first black holes, MNRAS **457**, 3356 (2016), arXiv:1601.07915 [astro-ph.GA].

[26] J. A. Regan, E. Visbal, J. H. Wise, Z. Haiman, P. H. Johansson, and G. L. Bryan, Rapid formation of massive black holes in close proximity to embryonic protogalaxies, Nature Astronomy **1**, 0075 (2017), arXiv:1703.03805 [astro-ph.GA].

[27] J. H. Wise, J. A. Regan, B. W. O'Shea, M. L. Norman, T. P. Downes, and H. Xu, Formation of massive black holes in rapidly growing pre-galactic gas clouds, Nature **566**, 85 (2019), arXiv:1901.07563 [astro-ph.GA].

[28] A. Sesana, F. Haardt, P. Madau, and M. Volonteri, Low - frequency gravitational radiation from coalescing massive black hole binaries in hierarchical cosmologies, Astrophys. J. **611**, 623 (2004), arXiv:astro-ph/0401543.

[29] A. Sesana, F. Haardt, P. Madau, and M. Volonteri, The gravitational wave signal from massive black hole binaries and its contribution to the LISA data stream, Astrophys. J. **623**, 23 (2005), arXiv:astro-ph/0409255.

[30] A. Klein *et al.*, Science with the space-based interferometer eLISA: Supermassive black hole binaries, Phys. Rev. D **93**, 024003 (2016), arXiv:1511.05581 [gr-qc].

[31] E. Barausse, I. Dvorkin, M. Tremmel, M. Volonteri, and M. Bonetti, Massive Black Hole Merger Rates: The Effect of Kiloparsec Separation Wandering and Supernova Feedback, Astrophys. J. **904**, 16 (2020), arXiv:2006.03065 [astro-ph.GA].

[32] E. Barausse, K. Dey, M. Crisostomi, A. Panayada, S. Marsat, and S. Basak, The PTA detections: implications for LISA massive black hole mergers, arXiv:2307.12245 [astro-ph.GA].

[33] M. C. Begelman, R. D. Blandford, and M. J. Rees, Massive black hole binaries in active galactic nuclei, Nature **287**, 307 (1980).

[34] Q. Yu, Evolution of massive binary black holes, Mon. Not. Roy. Astron. Soc. **331**, 935 (2002), arXiv:astro-ph/0109530.

[35] M. Milosavljevic and D. Merritt, Long term evolution of massive black hole binaries, Astrophys. J. **596**, 860 (2003), arXiv:astro-ph/0212459.

[36] A. Sesana, M. Volonteri, and F. Haardt, The imprint of massive black hole formation models on the LISA data stream, Mon. Not. Roy. Astron. Soc. **377**, 1711 (2007), arXiv:astro-ph/0701556.

[37] G. Lodato, S. Nayakshin, A. R. King, and J. E. Pringle, Black hole mergers: can gas discs solve the 'final parsec' problem?, Mon. Not. Roy. Astron. Soc. **398**, 1392 (2009), arXiv:0906.0737 [astro-ph.CO].

[38] F. M. Khan, A. Just, and D. Merritt, Efficient Merger of Binary Supermassive Black Holes in Merging Galaxies, Astrophys. J. **732**, 89 (2011), arXiv:1103.0272 [astro-ph.CO].

[39] M. Preto, I. Berentzen, P. Berczik, and R. Spurzem, Fast coalescence of massive black hole binaries from mergers of galactic nuclei: implications for low-frequency gravitational-wave astrophysics, Astrophys. J. Lett. **732**, L26 (2011), arXiv:1102.4855 [astro-ph.GA].

[40] M. Colpi, Massive binary black holes in galactic nuclei and their path to coalescence, Space Sci. Rev. **183**, 189 (2014), arXiv:1407.3102 [astro-ph.GA].

[41] E. Vasiliev, F. Antonini, and D. Merritt, The Final-parsec Problem in the Collisionless Limit, Astrophysical Journal **810**, 49 (2015), arXiv:1505.05480 [astro-ph.GA].

[42] A. Sesana and F. M. Khan, Scattering experiments meet N-body – I. A practical recipe for the evolution of massive black hole binaries in stellar environments, Mon. Not. Roy. Astron. Soc. **454**, L66 (2015), arXiv:1505.02062 [astro-ph.GA].

[43] F. Dosopoulou and F. Antonini, Dynamical friction and the evolution of Supermassive Black hole Binaries: the final hundred-parsec problem, Astrophys. J. **840**, 31 (2017), arXiv:1611.06573 [astro-ph.GA].

[44] M. Tremmel, F. Governato, M. Volonteri, T. R. Quinn, and A. Pontzen, Dancing to CHANGA: a self-consistent prediction for close SMBH pair formation time-scales following galaxy mergers, MNRAS **475**, 4967 (2018), arXiv:1708.07126 [astro-ph.GA].

[45] E. Bortolas, P. R. Capelo, T. Zana, L. Mayer, M. Bonetti, M. Dotti, M. B. Davies, and P. Madau, Global torques and stochasticity as the drivers of massive black hole pairing in the young Universe, Mon. Not. Roy. Astron. Soc. **498**, 3601 (2020), arXiv:2005.02409 [astro-ph.GA].

[46] M. Bonetti, A. Sesana, F. Haardt, E. Barausse, and M. Colpi, Post-Newtonian evolution of massive black hole triplets in galactic nuclei – IV. Implications for LISA, Mon. Not. Roy. Astron. Soc. **486**, 4044 (2019), arXiv:1812.01011 [astro-ph.GA].

[47] T. Ryu, R. Perna, Z. Haiman, J. P. Ostriker, and N. C. Stone, Interactions between multiple supermassive black holes in galactic nuclei: a solution to the final parsec problem, Mon. Not. Roy. Astron. Soc. **473**, 3410 (2018), arXiv:1709.06501.

[48] M. Mannerkoski, P. H. Johansson, A. Rantala, T. Naab, and S. Liao, Resolving the Complex Evolution of a Supermassive Black Hole Triplet in a Cosmological Simulation, Astrophys. J. Lett. **912**, L20 (2021), arXiv:2103.16254 [astro-ph.GA].

[49] S. Clesse and J. García-Bellido, Massive Primordial Black Holes from Hybrid Inflation as Dark Matter and the seeds of Galaxies, Phys. Rev. D **92**, 023524 (2015), arXiv:1501.07565 [astro-ph.CO].

[50] J. García-Bellido, Primordial black holes and the origin of the matter–antimatter asymmetry, Phil. Trans. Roy. Soc. Lond. A **377**, 20190091 (2019).

[51] A. Sesana, J. Gair, E. Berti, and M. Volonteri, Reconstructing the massive black hole cosmic history through gravitational waves, Phys. Rev. D **83**, 044036 (2011), arXiv:1011.5893 [astro-ph.CO].

[52] P. Madau and M. J. Rees, Massive black holes as Population III remnants, Astrophys. J. Lett. **551**, L27 (2001), arXiv:astro-ph/0101223.

[53] M. C. Begelman, Evolution of supermassive stars as a pathway to black hole formation, Mon. Not. Roy. Astron. Soc. **402**, 673 (2010), arXiv:0910.4398 [astro-ph.CO].

[54] S. F. Portegies Zwart and S. McMillan, Black hole mergers in the universe, Astrophys. J. Lett. **528**, L17 (2000), arXiv:astro-ph/9910061.

[55] N. C. Stone, A. H. W. Küpper, and J. P. Ostriker, Formation of Massive Black Holes in Galactic Nuclei: Runaway Tidal Encounters, Mon. Not. Roy. Astron. Soc. **467**, 4180 (2017), arXiv:1606.01909 [astro-ph.GA].

[56] E. Berti and M. Volonteri, Cosmological black hole spin evolution by mergers and accretion, Astrophys. J. **684**, 822 (2008), arXiv:0802.0025 [astro-ph].

[57] E. Barausse, The evolution of massive black holes and their spins in their galactic hosts, Mon. Not. Roy. Astron. Soc. **423**, 2533 (2012), arXiv:1201.5888 [astro-ph.CO].

[58] A. Sesana, E. Barausse, M. Dotti, and E. M. Rossi, Linking the spin evolution of massive black holes to galaxy kinematics, Astrophys. J. **794**, 104 (2014), arXiv:1402.7088 [astro-ph.CO].

144

[59] N. Tamanini, C. Caprini, E. Barausse, A. Sesana, A. Klein, and A. Petiteau, Science with the space-based interferometer eLISA. III: Probing the expansion of the Universe using gravitational wave standard sirens, JCAP **04**, 002, arXiv:1601.07112 [astro-ph.CO].

[60] A. Mangiagli, A. Klein, M. Bonetti, M. L. Katz, A. Sesana, M. Volonteri, M. Colpi, S. Marsat, and S. Babak, Observing the inspiral of coalescing massive black hole binaries with LISA in the era of Multi-Messenger Astrophysics, Phys. Rev. D **102**, 084056 (2020), arXiv:2006.12513 [astro-ph.HE].

[61] M. Dotti, M. Volonteri, A. Perego, M. Colpi, M. Ruszkowski, and F. Haardt, Dual black holes in merger remnants. II: spin evolution and gravitational recoil, Mon. Not. Roy. Astron. Soc. **402**, 682 (2010), arXiv:0910.5729 [astro-ph.HE].

[62] E. Barausse, V. Cardoso, and P. Pani, Can environmental effects spoil precision gravitational-wave astrophysics?, Phys. Rev. D **89**, 104059 (2014), arXiv:1404.7149 [gr-qc].

[63] C. Roedig and A. Sesana, Origin and Implications of high eccentricities in massive black hole binaries at sub-pc scales, J. Phys. Conf. Ser. **363**, 012035 (2012), arXiv:1111.3742 [astro-ph.CO].

[64] P. Amaro-Seoane, Relativistic dynamics and extreme mass ratio inspirals, Living Rev. Rel. **21**, 4 (2018), arXiv:1205.5240 [astro-ph.CO].

[65] C. Hopman and T. Alexander, The effect of mass-segregation on gravitational wave sources near massive black holes, Astrophys. J. Lett. **645**, L133 (2006), arXiv:astro-ph/0603324.

[66] L. S. Finn and K. S. Thorne, Gravitational waves from a compact star in a circular, inspiral orbit, in the equatorial plane of a massive, spinning black hole, as observed by LISA, Phys. Rev. D **62**, 124021 (2000), arXiv:gr-qc/0007074.

[67] C. P. L. Berry, R. H. Cole, P. Cañizares, and J. R. Gair, Importance of transient resonances in extreme-mass-ratio inspirals, Phys. Rev. D **94**, 124042 (2016), arXiv:1608.08951 [gr-qc].

[68] P. Amaro-Seoane, Extremely large mass-ratio inspirals, Phys. Rev. D **99**, 123025 (2019), arXiv:1903.10871 [astro-ph.GA].

[69] S. Babak, J. Gair, A. Sesana, E. Barausse, C. F. Sopuerta, C. P. L. Berry, E. Berti, P. Amaro-Seoane, A. Petiteau, and A. Klein, Science with the space-based interferometer LISA. V: Extreme mass-ratio inspirals, Phys. Rev. D **95**, 103012 (2017), arXiv:1703.09722 [gr-qc].

[70] V. Vazquez-Aceves, Y. Lin, and A. Torres-Orjuela, Sgr A* Spin and Mass Estimates through the Detection of an Extremely Large Mass-ratio Inspiral, Astrophys. J. **952**, 139 (2023), arXiv:2206.14399 [astro-ph.HE].

[71] J. R. Gair, C. Tang, and M. Volonteri, LISA extreme-mass-ratio inspiral events as probes of the black hole mass function, Phys. Rev. D **81**, 104014 (2010), arXiv:1004.1921 [astro-ph.GA].

[72] M. Dotti, M. Colpi, S. Pallini, A. Perego, and M. Volonteri, On the orientation and magnitude of the black hole spin in galactic nuclei, Astrophys. J. **762**, 68 (2013), arXiv:1211.4871 [astro-ph.CO].

[73] Z. Pan and H. Yang, Probing the Growth of Massive Black Holes with Black Hole-Host Galaxy Spin Correlations, Astrophys. J. **901**, 163 (2020), arXiv:2007.03783 [astro-ph.CO].

[74] P. Amaro-Seoane and M. Preto, The impact of realistic models of mass segregation on the event rate of extreme-mass ratio inspirals and cusp re-growth, Class. Quant. Grav. **28**, 094017 (2011), arXiv:1010.5781 [astro-ph.CO].

[75] Z. Pan and H. Yang, Formation Rate of Extreme Mass Ratio Inspirals in Active Galactic Nuclei, Phys. Rev. D **103**, 103018 (2021), arXiv:2101.09146 [astro-ph.HE].

[76] Z. Pan, Z. Lyu, and H. Yang, Wet extreme mass ratio inspirals may be more common for spaceborne gravitational wave detection, Phys. Rev. D **104**, 063007 (2021), arXiv:2104.01208 [astro-ph.HE].

[77] L. Barack *et al.*, Black holes, gravitational waves and fundamental physics: a roadmap, Class. Quant. Grav. **36**, 143001 (2019), arXiv:1806.05195 [gr-qc].

[78] E. A. Huerta and J. R. Gair, Influence of conservative corrections on parameter estimation for extreme-mass-ratio inspirals, Phys. Rev. D **79**, 084021 (2009), [Erratum: Phys.Rev.D 84,

145

049903 (2011)], arXiv:0812.4208 [gr-qc].

[79] S. McGee, A. Sesana, and A. Vecchio, Linking gravitational waves and X-ray phenomena with joint LISA and Athena observations, Nature Astron. **4**, 26 (2020), arXiv:1811.00050 [astro-ph.HE].

[80] V. Witzany, Hamilton-Jacobi equation for spinning particles near black holes, Phys. Rev. D **100**, 104030 (2019), arXiv:1903.03651 [gr-qc].

[81] V. Skoupy, G. Lukes-Gerakopoulos, L. V. Drummond, and S. A. Hughes, Asymptotic gravitational-wave fluxes from a spinning test body on generic orbits around a Kerr black hole, Phys. Rev. D **108**, 044041 (2023), arXiv:2303.16798 [gr-qc].

[82] M. Rahman and A. Bhattacharyya, Prospects for determining the nature of the secondaries of extreme mass-ratio inspirals using the spin-induced quadrupole deformation, Phys. Rev. D **107**, 024006 (2023), arXiv:2112.13869 [gr-qc].

[83] A. R. King, J. E. Pringle, and J. A. Hofmann, The Evolution of Black Hole Mass and Spin in Active Galactic Nuclei, Mon. Not. Roy. Astron. Soc. **385**, 1621 (2008), arXiv:0801.1564 [astro-ph].

[84] B. Bonga, H. Yang, and S. A. Hughes, Tidal resonance in extreme mass-ratio inspirals, Phys. Rev. Lett. **123**, 101103 (2019), arXiv:1905.00030 [gr-qc].

[85] N. Yunes, B. Kocsis, A. Loeb, and Z. Haiman, Imprint of Accretion Disk-Induced Migration on Gravitational Waves from Extreme Mass Ratio Inspirals, Phys. Rev. Lett. **107**, 171103 (2011), arXiv:1103.4609 [astro-ph.CO].

[86] E. Barausse, V. Cardoso, and P. Pani, Environmental Effects for Gravitational-wave Astrophysics, J. Phys. Conf. Ser. **610**, 012044 (2015), arXiv:1404.7140 [astro-ph.CO].

[87] P. Gupta, L. Speri, B. Bonga, A. J. K. Chua, and T. Tanaka, Modeling transient resonances in extreme-mass-ratio inspirals, Phys. Rev. D **106**, 104001 (2022), arXiv:2205.04808 [gr-qc].

[88] Z. Pan and H. Yang, Supercritical Accretion of Stellar-mass Compact Objects in Active Galactic Nuclei, Astrophys. J. **923**, 173 (2021), arXiv:2108.00267 [astro-ph.HE].

[89] R. Emami and A. Loeb, Observational signatures of the black hole mass distribution in the galactic center, JCAP **02**, 021, arXiv:1903.02578 [astro-ph.HE].

[90] R. Emami and A. Loeb, Detectability of gravitational waves from a population of inspiralling black holes in Milky Way-mass galaxies, Mon. Not. Roy. Astron. Soc. **502**, 3932 (2021), arXiv:1903.02579 [astro-ph.HE].

[91] L. Barack and A. Pound, Self-force and radiation reaction in general relativity, Rept. Prog. Phys. **82**, 016904 (2019), arXiv:1805.10385 [gr-qc].

[92] E. Barausse *et al.*, Prospects for Fundamental Physics with LISA, Gen. Rel. Grav. **52**, 81 (2020), arXiv:2001.09793 [gr-qc].

[93] C. M. Will, *Theory and Experiment in Gravitational Physics* (Cambridge University Press, 2018).

[94] C. Bambi, Testing the Kerr black hole hypothesis, Mod. Phys. Lett. A **26**, 2453 (2011), arXiv:1109.4256 [gr-qc].

[95] V. Cardoso and P. Pani, Testing the nature of dark compact objects: a status report, Living Rev. Rel. **22**, 4 (2019), arXiv:1904.05363 [gr-qc].

[96] K. Chamberlain and N. Yunes, Theoretical Physics Implications of Gravitational Wave Observation with Future Detectors, Phys. Rev. D **96**, 084039 (2017), arXiv:1704.08268 [gr-qc].

[97] F. D. Ryan, Gravitational waves from the inspiral of a compact object into a massive, axisymmetric body with arbitrary multipole moments, Phys. Rev. D **52**, 5707 (1995).

[98] L. Barack and C. Cutler, Using LISA EMRI sources to test off-Kerr deviations in the geometry of massive black holes, Phys. Rev. D **75**, 042003 (2007), arXiv:gr-qc/0612029.

[99] B. Carter, Axisymmetric Black Hole Has Only Two Degrees of Freedom, Phys. Rev. Lett. **26**, 331 (1971).

[100] K. Glampedakis and S. Babak, Mapping spacetimes with LISA: Inspiral of a test-body in a 'quasi-Kerr' field, Class. Quant. Grav. **23**, 4167 (2006), arXiv:gr-qc/0510057.

[101] C. Hopman and T. Alexander, The Orbital statistics of stellar inspiral and relaxation near a massive black hole: Characterizing gravitational wave sources, Astrophys. J. **629**, 362 (2005), arXiv:astro-ph/0503672.

[102] C. P. L. Berry and J. R. Gair, Extreme-mass-ratio-bursts from extragalactic sources, Mon. Not. Roy. Astron. Soc. **433**, 3572 (2013), arXiv:1306.0774 [astro-ph.HE].

[103] C. P. L. Berry and J. R. Gair, Expectations for extreme-mass-ratio bursts from the Galactic Centre, Mon. Not. Roy. Astron. Soc. **435**, 3521 (2013), arXiv:1307.7276 [astro-ph.HE].

[104] J. E. Greene, J. Strader, and L. C. Ho, Intermediate-Mass Black Holes, Ann. Rev. Astron. Astrophys. **58**, 257 (2020), arXiv:1911.09678 [astro-ph.GA].

[105] R. Abbott *et al.* (LIGO Scientific, VIRGO), GWTC-2.1: Deep Extended Catalog of Compact Binary Coalescences Observed by LIGO and Virgo During the First Half of the Third Observing Run, arXiv:2108.01045 [gr-qc].

[106] R. Abbott *et al.* (LIGO Scientific, VIRGO, KAGRA), GWTC-3: Compact Binary Coalescences Observed by LIGO and Virgo During the Second Part of the Third Observing Run, arXiv:2111.03606 [gr-qc].

[107] R. Abbott *et al.* (LIGO Scientific, Virgo), GW190521: A Binary Black Hole Merger with a Total Mass of $150 M_\odot$, Phys. Rev. Lett. **125**, 101102 (2020), arXiv:2009.01075 [gr-qc].

[108] R. Abbott *et al.* (LIGO Scientific, Virgo), Properties and Astrophysical Implications of the 150 $M_\odot$ Binary Black Hole Merger GW190521, Astrophys. J. Lett. **900**, L13 (2020), arXiv:2009.01190 [astro-ph.HE].

[109] M. Mezcua, F. Civano, S. Marchesi, H. Suh, G. Fabbiano, and M. Volonteri, Intermediate-mass black holes in dwarf galaxies out to redshift ∼2.4 in the Chandra COSMOS-Legacy Survey, MNRAS **478**, 2576 (2018), arXiv:1802.01567 [astro-ph.GA].

[110] J. E. Greene, J. Strader, and L. C. Ho, Intermediate-Mass Black Holes, Annual Reviews of Astronomy & Astrophysics **58**, 257 (2020), arXiv:1911.09678 [astro-ph.GA].

[111] M. Arca-Sedda, P. Amaro-Seoane, and X. Chen, Merging stellar and intermediate-mass black holes in dense clusters: implications for LIGO, LISA, and the next generation of gravitational wave detectors, Astron. Astrophys. **652**, A54 (2021), arXiv:2007.13746 [astro-ph.GA].

[112] J. R. Gair, I. Mandel, M. C. Miller, and M. Volonteri, Exploring intermediate and massive black-hole binaries with the Einstein Telescope, General Relativity and Gravitation **43**, 485 (2011), arXiv:0907.5450 [astro-ph.CO].

[113] T. Matsubayashi, J. Makino, and T. Ebisuzaki, Evolution of galactic nuclei. 1. orbital evolution of imbh, Astrophys. J. **656**, 879 (2007), arXiv:astro-ph/0511782.

[114] M. Arca-Sedda and A. Gualandris, Gravitational wave sources from inspiralling globular clusters in the Galactic Centre and similar environments, Mon. Not. Roy. Astron. Soc. **477**, 4423 (2018), arXiv:1804.06116 [astro-ph.GA].

[115] J. Bellovary, C. Cleary, F. Munshi, M. Tremmel, C. Christensen, A. Brooks, and T. Quinn, Multimessenger Signatures of Massive Black Holes in Dwarf Galaxies, Mon. Not. Roy. Astron. Soc. **482**, 2913 (2019), arXiv:1806.00471 [astro-ph.GA].

[116] D. Gerosa and M. Fishbach, Hierarchical mergers of stellar-mass black holes and their gravitational-wave signatures, Nature Astron. **5**, 749 (2021), arXiv:2105.03439 [astro-ph.HE].

[117] J. M. Bellovary, M.-M. Mac Low, B. McKernan, and K. E. S. Ford, Migration Traps in Disks Around Supermassive Black Holes, Astrophys. J. Lett. **819**, L17 (2016), arXiv:1511.00005 [astro-ph.GA].

[118] M. J. Graham *et al.*, Candidate Electromagnetic Counterpart to the Binary Black Hole Merger Gravitational Wave Event S190521g, Phys. Rev. Lett. **124**, 251102 (2020), arXiv:2006.14122 [astro-ph.HE].

[119] P. Amaro-Seoane, Detecting Intermediate-Mass Ratio Inspirals From The Ground And Space, Phys. Rev. D **98**, 063018 (2018), arXiv:1807.03824 [astro-ph.HE].

[120] G. Fragione and N. Leigh, Intermediate-Mass Ratio Inspirals in Galactic Nuclei, Mon. Not. Roy. Astron. Soc. **480**, 5160 (2018), arXiv:1807.09281 [astro-ph.GA].

[121] K. Jani, D. Shoemaker, and C. Cutler, Detectability of Intermediate-Mass Black Holes in Multiband Gravitational Wave Astronomy, Nature Astron. **4**, 260 (2019), arXiv:1908.04985 [gr-qc].

[122] P. Amaro-Seoane, J. R. Gair, M. Freitag, M. Coleman Miller, I. Mandel, C. J. Cutler, and S. Babak, Astrophysics, detection and science applications of intermediate- and extreme mass-ratio inspirals, Class. Quant. Grav. **24**, R113 (2007), arXiv:astro-ph/0703495.

[123] E. A. Huerta, J. R. Gair, and D. A. Brown, Importance of including small body spin effects in the modelling of intermediate mass-ratio inspirals. II Accurate parameter extraction of strong sources using higher-order spin effects, Phys. Rev. D **85**, 064023 (2012), arXiv:1111.3243 [gr-qc].

[124] G. A. Piovano, R. Brito, A. Maselli, and P. Pani, Assessing the detectability of the secondary spin in extreme mass-ratio inspirals with fully relativistic numerical waveforms, Phys. Rev. D **104**, 124019 (2021), arXiv:2105.07083 [gr-qc].

[125] O. Burke, G. A. Piovano, N. Warburton, P. Lynch, L. Speri, C. Kavanagh, B. Wardell, A. Pound, L. Durkan, and J. Miller, Accuracy Requirements: Assessing the Importance of First Post-Adiabatic Terms for Small-Mass-Ratio Binaries, arXiv:2310.08927 [gr-qc].

[126] M. C. Miller, Probing general relativity with mergers of supermassive and intermediate-mass black holes, Astrophys. J. **618**, 426 (2004), arXiv:astro-ph/0409331.

[127] C. F. Sopuerta and N. Yunes, Extreme and Intermediate-Mass Ratio Inspirals in Dynamical Chern-Simons Modified Gravity, Phys. Rev. D **80**, 064006 (2009), arXiv:0904.4501 [gr-qc].

[128] N. Dai, Y. Gong, T. Jiang, and D. Liang, Intermediate mass-ratio inspirals with dark matter minispikes, Phys. Rev. D **106**, 064003 (2022), arXiv:2111.13514 [gr-qc].

[129] J. Aasi *et al.* (LIGO Scientific), Advanced LIGO, Class. Quant. Grav. **32**, 074001 (2015), arXiv:1411.4547 [gr-qc].

[130] F. Acernese *et al.* (VIRGO), Advanced Virgo: a second-generation interferometric gravitational wave detector, Class. Quant. Grav. **32**, 024001 (2015), arXiv:1408.3978 [gr-qc].

[131] B. Sathyaprakash *et al.*, Scientific Objectives of Einstein Telescope, Class. Quant. Grav. **29**, 124013 (2012), [Erratum: Class.Quant.Grav. 30, 079501 (2013)], arXiv:1206.0331 [gr-qc].

[132] D. Reitze *et al.*, Cosmic Explorer: The U.S. Contribution to Gravitational-Wave Astronomy beyond LIGO, Bull. Am. Astron. Soc. **51**, 035 (2019), arXiv:1907.04833 [astro-ph.IM].

[133] P. Amaro-Seoane and L. Santamaria, Detection of IMBHs with ground-based gravitational wave observatories: A biography of a binary of black holes, from birth to death, Astrophys. J. **722**, 1197 (2010), arXiv:0910.0254 [astro-ph.CO].

[134] A. Sesana, Prospects for Multiband Gravitational-Wave Astronomy after GW150914, Phys. Rev. Lett. **116**, 231102 (2016), arXiv:1602.06951 [gr-qc].

[135] K. W. K. Wong, E. D. Kovetz, C. Cutler, and E. Berti, Expanding the LISA Horizon from the Ground, Phys. Rev. Lett. **121**, 251102 (2018), arXiv:1808.08247 [astro-ph.HE].

[136] S. Datta, A. Gupta, S. Kastha, K. G. Arun, and B. S. Sathyaprakash, Tests of general relativity using multiband observations of intermediate mass binary black hole mergers, Phys. Rev. D **103**, 024036 (2021), arXiv:2006.12137 [gr-qc].

[137] K. A. Postnov and L. R. Yungelson, The Evolution of Compact Binary Star Systems, Living Rev. Rel. **17**, 3 (2014), arXiv:1403.4754 [astro-ph.HE].

[138] T. Kupfer *et al.*, LISA Galactic binaries with astrometry from Gaia DR3, arXiv:2302.12719 [astro-ph.SR].

[139] J. J. Hermes, M. Kilic, W. R. Brown, D. E. Winget, C. Allende Prieto, A. Gianninas, A. S. Mukadam, A. Cabrera-Lavers, and S. J. Kenyon, Rapid Orbital Decay in the 12.75-minute Binary White Dwarf J0651+2844, Astrophysical Journal Letters **757**, L21 (2012), arXiv:1208.5051 [astro-ph.SR].

[140] K. B. Burdge *et al.*, General relativistic orbital decay in a seven-minute-orbital-period eclipsing binary system, Nature **571**, 528 (2019), arXiv:1907.11291 [astro-ph.SR].

[141] J. Munday *et al.*, Two decades of optical timing of the shortest-period binary star system HM

Cancri, Mon. Not. Roy. Astron. Soc. **518**, 5123 (2022), arXiv:2211.09834 [astro-ph.SR].

[142] A. Stroeer and A. Vecchio, The LISA verification binaries, Class. Quant. Grav. **23**, S809 (2006), arXiv:astro-ph/0605227.

[143] D. Maoz, N. Hallakoun, and C. Badenes, The separation distribution and merger rate of double white dwarfs: improved constraints, MNRAS **476**, 2584 (2018), arXiv:1801.04275 [astro-ph.SR].

[144] W. R. Brown, M. Kilic, A. Kosakowski, J. J. Andrews, C. O. Heinke, M. A. Agüeros, F. Camilo, A. Gianninas, J. J. Hermes, and S. J. Kenyon, The ELM Survey. VIII. Ninety-eight Double White Dwarf Binaries, Astrophysical Journal **889**, 49 (2020), arXiv:2002.00064 [astro-ph.SR].

[145] C. R. Evans, J. Iben, Icko, and L. Smarr, Degenerate Dwarf Binaries as Promising, Detectable Sources of Gravitational Radiation, Astrophysical Journal **323**, 129 (1987).

[146] V. M. Lipunov, K. A. Postnov, and M. E. Prokhorov, The sources of gravitational waves with continuous and discrete spectra, Astronomy & Astrophysics **176**, L1 (1987).

[147] D. Hils, P. L. Bender, and R. F. Webbink, Gravitational Radiation from the Galaxy, Astrophysical Journal **360**, 75 (1990).

[148] A. J. Ruiter, K. Belczynski, M. Benacquista, S. L. Larson, and G. Williams, The LISA Gravitational Wave Foreground: A Study of Double White Dwarfs, Astrophys. J. **717**, 1006 (2010), arXiv:0705.3272 [astro-ph].

[149] G. Nelemans, L. R. Yungelson, and S. F. Portegies Zwart, The gravitational wave signal from the galactic disk population of binaries containing two compact objects, Astron. Astrophys. **375**, 890 (2001), arXiv:astro-ph/0105221.

[150] LISA Science Group, Figures of merit.

[151] V. Korol, N. Hallakoun, S. Toonen, and N. Karnesis, Observationally driven Galactic double white dwarf population for LISA, Mon. Not. Roy. Astron. Soc. **511**, 5936 (2022), arXiv:2109.10972 [astro-ph.HE].

[152] M. Y. M. Lau, I. Mandel, A. Vigna-Gómez, C. J. Neijssel, S. Stevenson, and A. Sesana, Detecting Double Neutron Stars with LISA, Mon. Not. Roy. Astron. Soc. **492**, 3061 (2020), arXiv:1910.12422 [astro-ph.HE].

[153] J. J. Andrews and I. Mandel, Double Neutron Star Populations and Formation Channels, Astrophys. J. Lett. **880**, L8 (2019), arXiv:1904.12745 [astro-ph.HE].

[154] K. Kremer, S. Chatterjee, K. Breivik, C. L. Rodriguez, S. L. Larson, and F. A. Rasio, LISA Sources in Milky Way Globular Clusters, Phys. Rev. Lett. **120**, 191103 (2018), arXiv:1802.05661 [astro-ph.HE].

[155] E. Finch, G. Bartolucci, D. Chucherko, B. G. Patterson, V. Korol, A. Klein, D. Bandopadhyay, H. Middleton, C. J. Moore, and A. Vecchio, Identifying LISA verification binaries among the Galactic population of double white dwarfs, Mon. Not. Roy. Astron. Soc. **522**, 5358 (2023), arXiv:2210.10812 [astro-ph.SR].

[156] V. Paschalidis, M. MacLeod, T. W. Baumgarte, and S. L. Shapiro, Merger of white dwarf-neutron star binaries: Prelude to hydrodynamic simulations in general relativity, Phys. Rev. D **80**, 024006 (2009), arXiv:0910.5719 [astro-ph.HE].

[157] V. Paschalidis, Z. Etienne, Y. T. Liu, and S. L. Shapiro, Head-on collisions of binary white dwarf–neutron stars: Simulations in full general relativity, Phys. Rev. D **83**, 064002 (2011), arXiv:1009.4932 [astro-ph.HE].

[158] V. Paschalidis, Y. T. Liu, Z. Etienne, and S. L. Shapiro, The merger of binary white dwarf–neutron stars: Simulations in full general relativity, Phys. Rev. D **84**, 104032 (2011), arXiv:1109.5177 [astro-ph.HE].

[159] J. P. A. Clark and D. M. Eardley, Evolution of close neutron star binaries., Astrophysical Journal **215**, 311 (1977).

[160] L. Bildsten and C. Cutler, Tidal Interactions of Inspiraling Compact Binaries, Astrophysical Journal **400**, 175 (1992).

[161] W. H. Lee and W. Kluzniak, Newtonian hydrodynamics of the coalescence of black holes with

neutron stars. 1. Tidally locked binaries with a stiff equation of state, Astrophys. J. **526**, 178 (1999), arXiv:astro-ph/9808185.

[162] W. H. Lee and W. Kluzniak, Newtonian hydrodynamics of the coalescence of black holes with neutron stars. 2. Tidally locked binaries with a soft equation of state, Mon. Not. Roy. Astron. Soc. **308**, 780 (1999), arXiv:astro-ph/9904328.

[163] K. Breivik, K. Kremer, M. Bueno, S. L. Larson, S. Coughlin, and V. Kalogera, Characterizing Accreting Double White Dwarf Binaries with the Laser Interferometer Space Antenna and Gaia, Astrophys. J. Lett. **854**, L1 (2018), arXiv:1710.08370 [astro-ph.SR].

[164] S. Toonen, A. Hamers, and S. Portegies Zwart, The evolution of hierarchical triple star-systems, Computational Astrophysics and Cosmology **3**, 6 (2016), arXiv:1612.06172 [astro-ph.SR].

[165] A. S. Rajamuthukumar, A. S. Hamers, P. Neunteufel, R. Pakmor, and S. E. de mink, Triple Evolution: An Important Channel in the Formation of Type Ia Supernovae, Astrophys. J. **950**, 9 (2023), arXiv:2211.04463 [astro-ph.SR].

[166] N. Seto, Detecting Planets around Compact Binaries with Gravitational Wave Detectors in Space, Astrophys. J. Lett. **677**, L55 (2008), arXiv:0802.3411 [astro-ph].

[167] N. Tamanini and C. Danielski, The gravitational-wave detection of exoplanets orbiting white dwarf binaries using LISA, Nature Astron. **3**, 858 (2019), arXiv:1812.04330 [astro-ph.EP].

[168] M. L. Katz, C. Danielski, N. Karnesis, V. Korol, N. Tamanini, N. J. Cornish, and T. B. Littenberg, Bayesian characterization of circumbinary sub-stellar objects with LISA, Mon. Not. Roy. Astron. Soc. **517**, 697 (2022), arXiv:2205.03461 [astro-ph.EP].

[169] J. Crowder and N. Cornish, A Solution to the Galactic Foreground Problem for LISA, Phys. Rev. D **75**, 043008 (2007), arXiv:astro-ph/0611546.

[170] T. B. Littenberg, A detection pipeline for galactic binaries in LISA data, Phys. Rev. D **84**, 063009 (2011), arXiv:1106.6355 [gr-qc].

[171] Y. Bouffanais and E. K. Porter, Detecting compact galactic binaries using a hybrid swarm-based algorithm, Phys. Rev. D **93**, 064020 (2016), arXiv:1509.08867 [gr-qc].

[172] T. Littenberg, N. Cornish, K. Lackeos, and T. Robson, Global Analysis of the Gravitational Wave Signal from Galactic Binaries, Phys. Rev. D **101**, 123021 (2020), arXiv:2004.08464 [gr-qc].

[173] V. Korol, E. M. Rossi, P. J. Groot, G. Nelemans, S. Toonen, and A. G. A. Brown, Prospects for detection of detached double white dwarf binaries with Gaia, LSST and LISA, Mon. Not. Roy. Astron. Soc. **470**, 1894 (2017), arXiv:1703.02555 [astro-ph.HE].

[174] I. Pelisoli, T. R. Marsh, V. S. Dhillon, E. Breedt, A. J. Brown, M. J. Dyer, M. J. Green, P. Kerry, S. P. Littlefair, S. G. Parsons, D. I. Sahman, and J. F. Wild, Found: a rapidly spinning white dwarf in LAMOST J024048.51+195226.9., MNRAS **509**, L31 (2022), arXiv:2108.11396 [astro-ph.SR].

[175] M. Kilic, A. Kosakowski, A. G. Moss, P. Bergeron, and A. A. Conly, An Isolated White Dwarf with a 70 s Spin Period, Astrophysical Journal Letters **923**, L6 (2021), arXiv:2111.14902 [astro-ph.SR].

[176] V. Korol, A. P. Igoshev, S. Toonen, N. Karnesis, C. J. Moore, E. Finch, and A. Klein, Neutron Star - White Dwarf Binaries: Probing Formation Pathways and Natal Kicks with LISA, arXiv:2310.06559 [astro-ph.HE].

[177] A. Vigna-Gómez *et al.*, On the formation history of Galactic double neutron stars, Mon. Not. Roy. Astron. Soc. **481**, 4009 (2018), arXiv:1805.07974 [astro-ph.SR].

[178] T. Wagg, F. S. Broekgaarden, S. E. de Mink, L. A. C. van Son, N. Frankel, and S. Justham, Gravitational Wave Sources in Our Galactic Backyard: Predictions for BHBH, BHNS, and NSNS Binaries Detectable with LISA, Astrophys. J. **937**, 118 (2022), arXiv:2111.13704 [astro-ph.HE].

[179] A. Vigna-Gomez, Table of confirmed binary neutron stars.

[180] S. E. Woosley, Pulsational Pair-Instability Supernovae, Astrophys. J. **836**, 244 (2017), arXiv:1608.08939 [astro-ph.HE].

[181] R. Farmer, M. Renzo, S. E. de Mink, P. Marchant, and S. Justham, Mind the gap: The location of the lower edge of the pair instability supernovae black hole mass gap, arXiv:1910.12874 [astro-ph.SR].

[182] S. E. Woosley and A. Heger, The Pair-Instability Mass Gap for Black Holes, Astrophys. J. Lett. 912, L31 (2021), arXiv:2103.07933 [astro-ph.SR].

[183] I. Mandel, A. Sesana, and A. Vecchio, The astrophysical science case for a decihertz gravitational-wave detector, Class. Quant. Grav. 35, 054004 (2018), arXiv:1710.11187 [astro-ph.HE].

[184] P. C. Peters, Gravitational Radiation and the Motion of Two Point Masses, Phys. Rev. 136, B1224 (1964).

[185] B. P. Abbott et al. (LIGO Scientific, Virgo), Observation of Gravitational Waves from a Binary Black Hole Merger, Phys. Rev. Lett. 116, 061102 (2016), arXiv:1602.03837 [gr-qc].

[186] S. Vitale, R. Lynch, R. Sturani, and P. Graff, Use of gravitational waves to probe the formation channels of compact binaries, Class. Quant. Grav. 34, 03LT01 (2017), arXiv:1503.04307 [gr-qc].

[187] S. Stevenson, C. P. L. Berry, and I. Mandel, Hierarchical analysis of gravitational-wave measurements of binary black hole spin–orbit misalignments, Mon. Not. Roy. Astron. Soc. 471, 2801 (2017), arXiv:1703.06873 [astro-ph.HE].

[188] M. Zevin, C. Pankow, C. L. Rodriguez, L. Sampson, E. Chase, V. Kalogera, and F. A. Rasio, Constraining Formation Models of Binary Black Holes with Gravitational-Wave Observations, Astrophys. J. 846, 82 (2017), arXiv:1704.07379 [astro-ph.HE].

[189] W. M. Farr, S. Stevenson, M. Coleman Miller, I. Mandel, B. Farr, and A. Vecchio, Distinguishing Spin-Aligned and Isotropic Black Hole Populations With Gravitational Waves, Nature 548, 426 (2017), arXiv:1706.01385 [astro-ph.HE].

[190] R. Abbott et al. (KAGRA, VIRGO, LIGO Scientific), Population of Merging Compact Binaries Inferred Using Gravitational Waves through GWTC-3, Phys. Rev. X 13, 011048 (2023), arXiv:2111.03634 [astro-ph.HE].

[191] J. Roulet, T. Venumadhav, B. Zackay, L. Dai, and M. Zaldarriaga, Binary Black Hole Mergers from LIGO/Virgo O1 and O2: Population Inference Combining Confident and Marginal Events, Phys. Rev. D 102, 123022 (2020), arXiv:2008.07014 [astro-ph.HE].

[192] S. Galaudage et al., Building Better Spin Models for Merging Binary Black Holes: Evidence for Nonspinning and Rapidly Spinning Nearly Aligned Subpopulations, Astrophys. J. Lett. 921, L15 (2021), [Erratum: Astrophys.J.Lett. 936, L18 (2022), Erratum: Astrophys.J. 936, L18 (2022)], arXiv:2109.02424 [gr-qc].

[193] T. A. Callister, C.-J. Haster, K. K. Y. Ng, S. Vitale, and W. M. Farr, Who Ordered That? Unequal-mass Binary Black Hole Mergers Have Larger Effective Spins, Astrophys. J. Lett. 922, L5 (2021), arXiv:2106.00521 [astro-ph.HE].

[194] I. M. Romero-Shaw, P. D. Lasky, and E. Thrane, Searching for Eccentricity: Signatures of Dynamical Formation in the First Gravitational-Wave Transient Catalogue of LIGO and Virgo, Mon. Not. Roy. Astron. Soc. 490, 5210 (2019), arXiv:1909.05466 [astro-ph.HE].

[195] B. P. Abbott et al. (LIGO Scientific, Virgo), Astrophysical Implications of the Binary Black-Hole Merger GW150914, Astrophys. J. Lett. 818, L22 (2016), arXiv:1602.03846 [astro-ph.HE].

[196] I. M. Romero-Shaw, K. Kremer, P. D. Lasky, E. Thrane, and J. Samsing, Gravitational waves as a probe of globular cluster formation and evolution, Mon. Not. Roy. Astron. Soc. 506, 2362 (2021), arXiv:2011.14541 [astro-ph.HE].

[197] L. O. McNeill and N. Seto, Probing the formation of double neutron star binaries around 1 mHz with LISA, Phys. Rev. D 106, 123031 (2022), arXiv:2210.04407 [astro-ph.HE].

[198] R. M. O'Leary, B. Kocsis, and A. Loeb, Gravitational waves from scattering of stellar-mass black holes in galactic nuclei, Mon. Not. Roy. Astron. Soc. 395, 2127 (2009), arXiv:0807.2638 [astro-ph].

[199] H. Tagawa, Z. Haiman, and B. Kocsis, Formation and Evolution of Compact Object Binaries in AGN Disks, Astrophys. J. 898, 25 (2020), arXiv:1912.08218 [astro-ph.GA].

[200] Y. Yang *et al.*, Hierarchical Black Hole Mergers in Active Galactic Nuclei, Phys. Rev. Lett. **123**, 181101 (2019), arXiv:1906.09281 [astro-ph.HE].

[201] M. Mapelli, F. Santoliquido, Y. Bouffanais, M. A. Sedda, M. C. Artale, and A. Ballone, Mass and Rate of Hierarchical Black Hole Mergers in Young, Globular and Nuclear Star Clusters, Symmetry **13**, 1678 (2021), arXiv:2007.15022 [astro-ph.HE].

[202] R. Abbott *et al.* (LIGO Scientific, Virgo), GW190814: Gravitational Waves from the Coalescence of a 23 Solar Mass Black Hole with a 2.6 Solar Mass Compact Object, Astrophys. J. Lett. **896**, L44 (2020), arXiv:2006.12611 [astro-ph.HE].

[203] I. Mandel and T. Fragos, An alternative interpretation of GW190412 as a binary black hole merger with a rapidly spinning secondary, Astrophys. J. Lett. **895**, L28 (2020), arXiv:2004.09288 [astro-ph.HE].

[204] M. Fishbach and V. Kalogera, Apples and Oranges: Comparing Black Holes in X-Ray Binaries and Gravitational-wave Sources, Astrophys. J. Lett. **929**, L26 (2022), arXiv:2111.02935 [astro-ph.HE].

[205] I. Mandel and A. Farmer, Merging stellar-mass binary black holes, Phys. Rept. **955**, 1 (2022), arXiv:1806.05820 [astro-ph.HE].

[206] M. Mapelli, Astrophysics of stellar black holes, Proc. Int. Sch. Phys. Fermi **200**, 87 (2020), arXiv:1809.09130 [astro-ph.HE].

[207] C. J. Moore, D. Gerosa, and A. Klein, Are stellar-mass black-hole binaries too quiet for LISA?, Mon. Not. Roy. Astron. Soc. **488**, L94 (2019), arXiv:1905.11998 [astro-ph.HE].

[208] A. Vilenkin and E. P. S. Shellard, *Cosmic Strings and Other Topological Defects* (Cambridge University Press, 2000).

[209] G. F. Smoot *et al.* (COBE), Structure in the COBE differential microwave radiometer first year maps, Astrophys. J. Lett. **396**, L1 (1992).

[210] D. N. Spergel *et al.* (WMAP), Wilkinson Microwave Anisotropy Probe (WMAP) three year results: implications for cosmology, Astrophys. J. Suppl. **170**, 377 (2007), arXiv:astro-ph/0603449.

[211] E. Witten, D-branes and K-theory, JHEP **12**, 019, arXiv:hep-th/9810188.

[212] A. Sen, Stable nonBPS bound states of BPS D-branes, JHEP **08**, 010, arXiv:hep-th/9805019.

[213] P. Horava, Type IIA D-branes, K theory, and matrix theory, Adv. Theor. Math. Phys. **2**, 1373 (1999), arXiv:hep-th/9812135.

[214] G. R. Dvali and S. H. H. Tye, Brane inflation, Phys. Lett. B **450**, 72 (1999), arXiv:hep-ph/9812483.

[215] A. Sen, SO(32) spinors of type I and other solitons on brane - anti-brane pair, JHEP **09**, 023, arXiv:hep-th/9808141.

[216] S. B. Giddings, S. Kachru, and J. Polchinski, Hierarchies from fluxes in string compactifications, Phys. Rev. D **66**, 106006 (2002), arXiv:hep-th/0105097.

[217] N. T. Jones, H. Stoica, and S. H. H. Tye, Brane interaction as the origin of inflation, JHEP **07**, 051, arXiv:hep-th/0203163.

[218] S. Sarangi and S. H. H. Tye, Cosmic string production towards the end of brane inflation, Phys. Lett. B **536**, 185 (2002), arXiv:hep-th/0204074.

[219] S. Kachru, R. Kallosh, A. D. Linde, and S. P. Trivedi, De Sitter vacua in string theory, Phys. Rev. D **68**, 046005 (2003), arXiv:hep-th/0301240.

[220] E. J. Copeland, R. C. Myers, and J. Polchinski, Cosmic F and D strings, JHEP **06**, 013, arXiv:hep-th/0312067.

[221] N. T. Jones, H. Stoica, and S. H. H. Tye, The Production, spectrum and evolution of cosmic strings in brane inflation, Phys. Lett. B **563**, 6 (2003), arXiv:hep-th/0303269.

[222] S. Kachru, R. Kallosh, A. D. Linde, J. M. Maldacena, L. P. McAllister, and S. P. Trivedi, Towards inflation in string theory, JCAP **10**, 013, arXiv:hep-th/0308055.

[223] G. Dvali and A. Vilenkin, Formation and evolution of cosmic D strings, JCAP **03**, 010, arXiv:hep-th/0312007.

[224] S. H. Henry Tye, Brane inflation: String theory viewed from the cosmos, Lect. Notes Phys. **737**, 949 (2008), arXiv:hep-th/0610221.

[225] D. F. Chernoff and S. H. H. Tye, Inflation, string theory and cosmic strings, Int. J. Mod. Phys. D **24**, 1530010 (2015), arXiv:1412.0579 [astro-ph.CO].

[226] D. Baumann and L. McAllister, *Inflation and String Theory*, Cambridge Monographs on Mathematical Physics (Cambridge University Press, 2015) arXiv:1404.2601 [hep-th].

[227] J. A. Dror, T. Hiramatsu, K. Kohri, H. Murayama, and G. White, Testing the Seesaw Mechanism and Leptogenesis with Gravitational Waves, Phys. Rev. Lett. **124**, 041804 (2020), arXiv:1908.03227 [hep-ph].

[228] D. I. Dunsky, A. Ghoshal, H. Murayama, Y. Sakakihara, and G. White, GUTs, hybrid topological defects, and gravitational waves, Phys. Rev. D **106**, 075030 (2022), arXiv:2111.08750 [hep-ph].

[229] R. H. Brandenberger, On the Decay of Cosmic String Loops, Nucl. Phys. B **293**, 812 (1987).

[230] M. Srednicki and S. Theisen, Nongravitational Decay of Cosmic Strings, Phys. Lett. B **189**, 397 (1987).

[231] P. Bhattacharjee, C. T. Hill, and D. N. Schramm, Grand unified theories, topological defects and ultrahigh-energy cosmic rays, Phys. Rev. Lett. **69**, 567 (1992).

[232] T. Damour and A. Vilenkin, Cosmic strings and the string dilaton, Phys. Rev. Lett. **78**, 2288 (1997), arXiv:gr-qc/9610005.

[233] U. F. Wichoski, J. H. MacGibbon, and R. H. Brandenberger, High-energy neutrinos, photons and cosmic ray fluxes from VHS cosmic strings, Phys. Rev. D **65**, 063005 (2002), arXiv:hep-ph/9805419.

[234] M. Peloso and L. Sorbo, Moduli from cosmic strings, Nucl. Phys. B **649**, 88 (2003), arXiv:hep-ph/0205063.

[235] T. Vachaspati, Cosmic Rays from Cosmic Strings with Condensates, Phys. Rev. D **81**, 043531 (2010), arXiv:0911.2655 [astro-ph.CO].

[236] E. Sabancilar, Cosmological Constraints on Strongly Coupled Moduli from Cosmic Strings, Phys. Rev. D **81**, 123502 (2010), arXiv:0910.5544 [hep-ph].

[237] A. J. Long, J. M. Hyde, and T. Vachaspati, Cosmic Strings in Hidden Sectors: 1. Radiation of Standard Model Particles, JCAP **09**, 030, arXiv:1405.7679 [hep-ph].

[238] A. Vilenkin, Gravitational radiation from cosmic strings, Phys. Lett. B **107**, 47 (1981).

[239] T. Vachaspati and A. Vilenkin, Gravitational Radiation from Cosmic Strings, Phys. Rev. D **31**, 3052 (1985).

[240] C. J. Hogan and M. J. Rees, Gravitational interactions of cosmic strings, Nature **311**, 109 (1984).

[241] F. S. Accetta and L. M. Krauss, The stochastic gravitational wave spectrum resulting from cosmic string evolution, Nucl. Phys. B **319**, 747 (1989).

[242] D. P. Bennett and F. R. Bouchet, Constraints on the gravity wave background generated by cosmic strings, Phys. Rev. D **43**, 2733 (1991).

[243] R. R. Caldwell and B. Allen, Cosmological constraints on cosmic string gravitational radiation, Phys. Rev. D **45**, 3447 (1992).

[244] X. Siemens, V. Mandic, and J. Creighton, Gravitational wave stochastic background from cosmic (super)strings, Phys. Rev. Lett. **98**, 111101 (2007), arXiv:astro-ph/0610920.

[245] M. R. DePies and C. J. Hogan, Stochastic Gravitational Wave Background from Light Cosmic Strings, Phys. Rev. D **75**, 125006 (2007), arXiv:astro-ph/0702335.

[246] S. Olmez, V. Mandic, and X. Siemens, Gravitational-Wave Stochastic Background from Kinks and Cusps on Cosmic Strings, Phys. Rev. D **81**, 104028 (2010), arXiv:1004.0890 [astro-ph.CO].

[247] S. A. Sanidas, R. A. Battye, and B. W. Stappers, Constraints on cosmic string tension imposed by the limit on the stochastic gravitational wave background from the European Pulsar Timing Array, Phys. Rev. D **85**, 122003 (2012), arXiv:1201.2419 [astro-ph.CO].

[248] S. A. Sanidas, R. A. Battye, and B. W. Stappers, Projected constraints on the cosmic (super)string tension with future gravitational wave detection experiments, Astrophys. J. **764**, 108 (2013), arXiv:1211.5042 [astro-ph.CO].

[249] P. Binetruy, A. Bohe, C. Caprini, and J.-F. Dufaux, Cosmological Backgrounds of Gravitational Waves and eLISA/NGO: Phase Transitions, Cosmic Strings and Other Sources, JCAP **06**, 027, arXiv:1201.0983 [gr-qc].

[250] S. Kuroyanagi, K. Miyamoto, T. Sekiguchi, K. Takahashi, and J. Silk, Forecast constraints on cosmic strings from future CMB, pulsar timing and gravitational wave direct detection experiments, Phys. Rev. D **87**, 023522 (2013), [Erratum: Phys.Rev.D 87, 069903 (2013)], arXiv:1210.2829 [astro-ph.CO].

[251] S. Kuroyanagi, K. Miyamoto, T. Sekiguchi, K. Takahashi, and J. Silk, Forecast constraints on cosmic string parameters from gravitational wave direct detection experiments, Phys. Rev. D **86**, 023503 (2012), arXiv:1202.3032 [astro-ph.CO].

[252] L. Sousa and P. P. Avelino, Stochastic Gravitational Wave Background generated by Cosmic String Networks: Velocity-Dependent One-Scale model versus Scale-Invariant Evolution, Phys. Rev. D **88**, 023516 (2013), arXiv:1304.2445 [astro-ph.CO].

[253] J. J. Blanco-Pillado, K. D. Olum, and B. Shlaer, The number of cosmic string loops, Phys. Rev. D **89**, 023512 (2014), arXiv:1309.6637 [astro-ph.CO].

[254] L. Sousa and P. P. Avelino, Stochastic gravitational wave background generated by cosmic string networks: The small-loop regime, Phys. Rev. D **89**, 083503 (2014), arXiv:1403.2621 [astro-ph.CO].

[255] J. J. Blanco-Pillado and K. D. Olum, Stochastic gravitational wave background from smoothed cosmic string loops, Phys. Rev. D **96**, 104046 (2017), arXiv:1709.02693 [astro-ph.CO].

[256] D. F. Chernoff and S. H. H. Tye, Detection of Low Tension Cosmic Superstrings, JCAP **05**, 002, arXiv:1712.05060 [astro-ph.CO].

[257] C. Ringeval and T. Suyama, Stochastic gravitational waves from cosmic string loops in scaling, JCAP **12**, 027, arXiv:1709.03845 [astro-ph.CO].

[258] J. J. Blanco-Pillado, K. D. Olum, and X. Siemens, New limits on cosmic strings from gravitational wave observation, Phys. Lett. B **778**, 392 (2018), arXiv:1709.02434 [astro-ph.CO].

[259] Y. Cui, M. Lewicki, D. E. Morrissey, and J. D. Wells, Probing the pre-BBN universe with gravitational waves from cosmic strings, JHEP **01**, 081, arXiv:1808.08968 [hep-ph].

[260] A. C. Jenkins and M. Sakellariadou, Anisotropies in the stochastic gravitational-wave background: Formalism and the cosmic string case, Phys. Rev. D **98**, 063509 (2018), arXiv:1802.06046 [astro-ph.CO].

[261] T. Damour and A. Vilenkin, Gravitational wave bursts from cosmic strings, Phys. Rev. Lett. **85**, 3761 (2000), arXiv:gr-qc/0004075.

[262] T. Damour and A. Vilenkin, Gravitational wave bursts from cusps and kinks on cosmic strings, Phys. Rev. D **64**, 064008 (2001), arXiv:gr-qc/0104026.

[263] P. Binetruy, A. Bohe, T. Hertog, and D. A. Steer, Gravitational Wave Bursts from Cosmic Superstrings with Y-junctions, Phys. Rev. D **80**, 123510 (2009), arXiv:0907.4522 [hep-th].

[264] T. Regimbau, S. Giampanis, X. Siemens, and V. Mandic, The stochastic background from cosmic (super)strings: popcorn and (Gaussian) continuous regimes, Phys. Rev. D **85**, 066001 (2012), arXiv:1111.6638 [astro-ph.CO].

[265] J. Aasi *et al.* (LIGO Scientific, VIRGO), Constraints on cosmic strings from the LIGO-Virgo gravitational-wave detectors, Phys. Rev. Lett. **112**, 131101 (2014), arXiv:1310.2384 [gr-qc].

[266] B. P. Abbott *et al.* (LIGO Scientific, Virgo), Constraints on cosmic strings using data from the first Advanced LIGO observing run, Phys. Rev. D **97**, 102002 (2018), arXiv:1712.01168 [gr-qc].

[267] P. Auclair *et al.* (LISA Cosmology Working Group), Cosmology with the Laser Interferometer Space Antenna, Living Rev. Rel. **26**, 5 (2023), arXiv:2204.05434 [astro-ph.CO].

[268] C. J. A. P. Martins and E. P. S. Shellard, Quantitative string evolution, Phys. Rev. D **54**, 2535 (1996), arXiv:hep-ph/9602271.

[269] C. J. A. P. Martins and E. P. S. Shellard, Extending the velocity dependent one scale string

evolution model, Phys. Rev. D **65**, 043514 (2002), arXiv:hep-ph/0003298.

[270] C. J. A. P. Martins, J. N. Moore, and E. P. S. Shellard, A Unified model for vortex string network evolution, Phys. Rev. Lett. **92**, 251601 (2004), arXiv:hep-ph/0310255.

[271] E. P. S. Shellard, Cosmic String Interactions, Nucl. Phys. B **283**, 624 (1987).

[272] M. G. Jackson, N. T. Jones, and J. Polchinski, Collisions of cosmic F and D-strings, JHEP **10**, 013, arXiv:hep-th/0405229.

[273] D. F. Chernoff, Clustering of Superstring Loops, arXiv:0908.4077 [astro-ph.CO].

[274] C. J. Burden, Gravitational Radiation From a Particular Class of Cosmic Strings, Phys. Lett. B **164**, 277 (1985).

[275] D. Garfinkle and T. Vachaspati, Radiation From Kinky, Cuspless Cosmic Loops, Phys. Rev. D **36**, 2229 (1987).

[276] J. M. Wachter and K. D. Olum, Gravitational backreaction on piecewise linear cosmic string loops, Phys. Rev. D **95**, 023519 (2017), arXiv:1609.01685 [gr-qc].

[277] J. J. Blanco-Pillado, K. D. Olum, and J. M. Wachter, Gravitational backreaction near cosmic string kinks and cusps, Phys. Rev. D **98**, 123507 (2018), arXiv:1808.08254 [gr-qc].

[278] D. F. Chernoff, E. E. Flanagan, and B. Wardell, Gravitational backreaction on a cosmic string: Formalism, Phys. Rev. D **99**, 084036 (2019), arXiv:1808.08631 [gr-qc].

[279] J. J. Blanco-Pillado, K. D. Olum, and J. M. Wachter, Gravitational backreaction simulations of simple cosmic string loops, Phys. Rev. D **100**, 023535 (2019), arXiv:1903.06079 [gr-qc].

[280] A. Vilenkin, Gravitational Field of Vacuum Domain Walls and Strings, Phys. Rev. D **23**, 852 (1981).

[281] C. Hogan and R. Narayan, Gravitational lensing by cosmic strings, MNRAS **211**, 575 (1984).

[282] A. Vilenkin, Cosmic strings as gravitational lenses, Astrophys. J. Lett. **282**, L51 (1984).

[283] A. A. de Laix, Observing long cosmic strings through gravitational lensing, Phys. Rev. D **56**, 6193 (1997), arXiv:astro-ph/9705223.

[284] F. Bernardeau and J.-P. Uzan, Cosmic string lens phenomenology: Model of Poisson energy distribution, Phys. Rev. D **63**, 023005 (2001), arXiv:astro-ph/0004102.

[285] M. Sazhin, G. Longo, J. M. Alcala', R. Silvotti, G. Covone, O. Khovanskaya, M. Pavlov, M. Pannella, M. Radovich, and V. Testa, CSL-1: A chance projection effect or serendipitous discovery of a gravitational lens induced by a cosmic string?, Mon. Not. Roy. Astron. Soc. **343**, 353 (2003), arXiv:astro-ph/0302547.

[286] M. V. Sazhin, M. Capaccioli, G. Longo, M. Paolillo, and O. S. Khovanskaya, The true nature of csl-1, arXiv:astro-ph/0601494.

[287] J. L. Christiansen, E. Albin, K. A. James, J. Goldman, D. Maruyama, and G. F. Smoot, Search for Cosmic Strings in the GOODS Survey, Phys. Rev. D **77**, 123509 (2008), arXiv:0803.0027 [astro-ph].

[288] A. Economou, D. Harari, and M. Sakellariadou, Gravitational effects of traveling waves along global cosmic strings, Phys. Rev. D **45**, 433 (1992).

[289] R. A. Battye, R. R. Caldwell, and E. P. S. Shellard, Gravitational waves from cosmic strings, in *Conference on Topological Defects and CMB* (1997) pp. 11–31, arXiv:astro-ph/9706013.

[290] T. Damour and A. Vilenkin, Gravitational radiation from cosmic (super)strings: Bursts, stochastic background, and observational windows, Phys. Rev. D **71**, 063510 (2005), arXiv:hep-th/0410222.

[291] X. Siemens, J. Creighton, I. Maor, S. Ray Majumder, K. Cannon, and J. Read, Gravitational wave bursts from cosmic (super)strings: Quantitative analysis and constraints, Phys. Rev. D **73**, 105001 (2006), arXiv:gr-qc/0603115.

[292] C. J. Hogan, Gravitational Waves from Light Cosmic Strings: Backgrounds and Bursts with Large Loops, Phys. Rev. D **74**, 043526 (2006), arXiv:astro-ph/0605567.

[293] B. Abbott *et al.* (LIGO Scientific), Coherent searches for periodic gravitational waves from unknown isolated sources and Scorpius X-1: Results from the second LIGO science run, Phys. Rev. D **76**, 082001 (2007), arXiv:gr-qc/0605028.

[294] B. P. Abbott *et al.* (LIGO Scientific), First LIGO search for gravitational wave bursts from cosmic (super)strings, Phys. Rev. D **80**, 062002 (2009), arXiv:0904.4718 [astro-ph.CO].

[295] B. P. Abbott *et al.* (LIGO Scientific, VIRGO), An Upper Limit on the Stochastic Gravitational-Wave Background of Cosmological Origin, Nature **460**, 990 (2009), arXiv:0910.5772 [astro-ph.CO].

[296] B. P. Abbott *et al.* (LIGO Scientific, Virgo), Upper Limits on the Stochastic Gravitational-Wave Background from Advanced LIGO's First Observing Run, Phys. Rev. Lett. **118**, 121101 (2017), [Erratum: Phys.Rev.Lett. 119, 029901 (2017)], arXiv:1612.02029 [gr-qc].

[297] B. P. Abbott *et al.* (LIGO Scientific, Virgo), All-Sky Search for Short Gravitational-Wave Bursts in the Second Advanced LIGO and Advanced Virgo Run, Phys. Rev. D **100**, 024017 (2019), arXiv:1905.03457 [gr-qc].

[298] F. R. Bouchet and D. P. Bennett, Does the Millisecond Pulsar Constrain Cosmic Strings?, Phys. Rev. D **41**, 720 (1990).

[299] V. M. Kaspi, J. H. Taylor, and M. F. Ryba, High - precision timing of millisecond pulsars. 3: Long - term monitoring of PSRs B1855+09 and B1937+21, Astrophys. J. **428**, 713 (1994).

[300] F. A. Jenet, G. B. Hobbs, W. van Straten, R. N. Manchester, M. Bailes, J. P. W. Verbiest, R. T. Edwards, A. W. Hotan, J. M. Sarkissian, and S. M. Ord, Upper bounds on the low-frequency stochastic gravitational wave background from pulsar timing observations: Current limits and future prospects, Astrophys. J. **653**, 1571 (2006), arXiv:astro-ph/0609013.

[301] C. L. Bennett, A. Banday, K. M. Gorski, G. Hinshaw, P. Jackson, P. Keegstra, A. Kogut, G. F. Smoot, D. T. Wilkinson, and E. L. Wright, Four year COBE DMR cosmic microwave background observations: Maps and basic results, Astrophys. J. Lett. **464**, L1 (1996), arXiv:astro-ph/9601067.

[302] L. Pogosian, S. H. H. Tye, I. Wasserman, and M. Wyman, Observational constraints on cosmic string production during brane inflation, Phys. Rev. D **68**, 023506 (2003), [Erratum: Phys.Rev.D 73, 089904 (2006)], arXiv:hep-th/0304188.

[303] L. Pogosian, M. C. Wyman, and I. Wasserman, Observational constraints on cosmic strings: Bayesian analysis in a three dimensional parameter space, JCAP **09**, 008, arXiv:astro-ph/0403268.

[304] S. H. H. Tye, I. Wasserman, and M. Wyman, Scaling of multi-tension cosmic superstring networks, Phys. Rev. D **71**, 103508 (2005), [Erratum: Phys.Rev.D 71, 129906 (2005)], arXiv:astro-ph/0503506.

[305] M. Wyman, L. Pogosian, and I. Wasserman, Bounds on cosmic strings from WMAP and SDSS, Phys. Rev. D **72**, 023513 (2005), [Erratum: Phys.Rev.D 73, 089905 (2006)], arXiv:astro-ph/0503364.

[306] L. Pogosian, I. Wasserman, and M. Wyman, On vector mode contribution to CMB temperature and polarization from local strings, arXiv:astro-ph/0604141.

[307] U. Seljak, A. Slosar, and P. McDonald, Cosmological parameters from combining the Lyman-alpha forest with CMB, galaxy clustering and SN constraints, JCAP **10**, 014, arXiv:astro-ph/0604335.

[308] N. Bevis, M. Hindmarsh, M. Kunz, and J. Urrestilla, CMB polarization power spectra contributions from a network of cosmic strings, Phys. Rev. D **76**, 043005 (2007), arXiv:0704.3800 [astro-ph].

[309] A. A. Fraisse, Limits on Defects Formation and Hybrid Inflationary Models with Three-Year WMAP Observations, JCAP **03**, 008, arXiv:astro-ph/0603589.

[310] L. Pogosian, S. H. H. Tye, I. Wasserman, and M. Wyman, Cosmic Strings as the Source of Small-Scale Microwave Background Anisotropy, JCAP **02**, 013, arXiv:0804.0810 [astro-ph].

[311] P. A. R. Ade *et al.* (Planck), Planck 2013 results. XXV. Searches for cosmic strings and other topological defects, Astron. Astrophys. **571**, A25 (2014), arXiv:1303.5085 [astro-ph.CO].

[312] R. Battye and A. Moss, Updated constraints on the cosmic string tension, Phys. Rev. D **82**, 023521 (2010), arXiv:1005.0479 [astro-ph.CO].

[313] B. P. Abbott *et al.* (LIGO Scientific, Virgo), Search for the isotropic stochastic background using data from Advanced LIGO's second observing run, Phys. Rev. D **100**, 061101 (2019), arXiv:1903.02886 [gr-qc].

[314] R. Abbott *et al.* (LIGO Scientific, Virgo, KAGRA), Constraints on Cosmic Strings Using Data from the Third Advanced LIGO–Virgo Observing Run, Phys. Rev. Lett. **126**, 241102 (2021), arXiv:2101.12248 [gr-qc].

[315] K. G. Arun *et al.* (LISA), New horizons for fundamental physics with LISA, Living Rev. Rel. **25**, 4 (2022), arXiv:2205.01597 [gr-qc].

[316] N. Bartolo *et al.* (LISA Cosmology Working Group), Probing anisotropies of the Stochastic Gravitational Wave Background with LISA, JCAP **11**, 009, arXiv:2201.08782 [astro-ph.CO].

[317] M. R. DePies and C. J. Hogan, Harmonic Gravitational Wave Spectra of Cosmic String Loops in the Galaxy, arXiv:0904.1052 [astro-ph.CO].

[318] Z. Khakhaleva-Li and C. J. Hogan, Will LISA Detect Harmonic Gravitational Waves from Galactic Cosmic String Loops?, arXiv:2006.00438 [astro-ph.CO].

[319] M. Jain and A. Vilenkin, Clustering of cosmic string loops, JCAP **09**, 043, arXiv:2006.15358 [astro-ph.CO].

[320] A. H. Guth, The Inflationary Universe: A Possible Solution to the Horizon and Flatness Problems, Phys. Rev. D **23**, 347 (1981).

[321] A. D. Linde, A New Inflationary Universe Scenario: A Possible Solution of the Horizon, Flatness, Homogeneity, Isotropy and Primordial Monopole Problems, Phys. Lett. B **108**, 389 (1982).

[322] A. Albrecht and P. J. Steinhardt, Cosmology for Grand Unified Theories with Radiatively Induced Symmetry Breaking, Phys. Rev. Lett. **48**, 1220 (1982).

[323] R. Jeannerot, J. Rocher, and M. Sakellariadou, How generic is cosmic string formation in SUSY GUTs, Phys. Rev. D **68**, 103514 (2003), arXiv:hep-ph/0308134.

[324] A. Arvanitaki and S. Dubovsky, Exploring the String Axiverse with Precision Black Hole Physics, Phys. Rev. D **83**, 044026 (2011), arXiv:1004.3558 [hep-th].

[325] N. Yunes and X. Siemens, Gravitational-Wave Tests of General Relativity with Ground-Based Detectors and Pulsar Timing-Arrays, Living Rev. Rel. **16**, 9 (2013), arXiv:1304.3473 [gr-qc].

[326] E. Berti *et al.*, Testing General Relativity with Present and Future Astrophysical Observations, Class. Quant. Grav. **32**, 243001 (2015), arXiv:1501.07274 [gr-qc].

[327] A. Arvanitaki, S. Dimopoulos, S. Dubovsky, N. Kaloper, and J. March-Russell, String Axiverse, Phys. Rev. D **81**, 123530 (2010), arXiv:0905.4720 [hep-th].

[328] R. D. Peccei and H. R. Quinn, CP Conservation in the Presence of Instantons, Phys. Rev. Lett. **38**, 1440 (1977).

[329] L. Hui, J. P. Ostriker, S. Tremaine, and E. Witten, Ultralight scalars as cosmological dark matter, Phys. Rev. D **95**, 043541 (2017), arXiv:1610.08297 [astro-ph.CO].

[330] E. G. M. Ferreira, Ultra-light dark matter, Astron. Astrophys. Rev. **29**, 7 (2021), arXiv:2005.03254 [astro-ph.CO].

[331] D. J. E. Marsh, Axion Cosmology, Phys. Rept. **643**, 1 (2016), arXiv:1510.07633 [astro-ph.CO].

[332] R. Brito, V. Cardoso, and P. Pani, Superradiance: New Frontiers in Black Hole Physics, Lect. Notes Phys. **906**, pp.1 (2015), arXiv:1501.06570 [gr-qc].

[333] G. Bertone *et al.*, Gravitational wave probes of dark matter: challenges and opportunities, SciPost Phys. Core **3**, 007 (2020), arXiv:1907.10610 [astro-ph.CO].

[334] A. Arvanitaki, M. Baryakhtar, and X. Huang, Discovering the QCD Axion with Black Holes and Gravitational Waves, Phys. Rev. D **91**, 084011 (2015), arXiv:1411.2263 [hep-ph].

[335] R. Brito, S. Ghosh, E. Barausse, E. Berti, V. Cardoso, I. Dvorkin, A. Klein, and P. Pani, Gravitational wave searches for ultralight bosons with LIGO and LISA, Phys. Rev. D **96**, 064050 (2017), arXiv:1706.06311 [gr-qc].

[336] R. Brito, S. Ghosh, E. Barausse, E. Berti, V. Cardoso, I. Dvorkin, A. Klein, and P. Pani, Stochastic and resolvable gravitational waves from ultralight bosons, Phys. Rev. Lett. **119**, 131101 (2017), arXiv:1706.05097 [gr-qc].

[337] W. H. Press and S. A. Teukolsky, Floating Orbits, Superradiant Scattering and the Black-hole Bomb, Nature **238**, 211 (1972).

[338] A. A. Starobinsky, Amplification of waves reflected from a rotating "black hole"., Sov. Phys. JETP **37**, 28 (1973).

[339] J. D. Bekenstein, Extraction of energy and charge from a black hole, Phys. Rev. D **7**, 949 (1973).

[340] S. A. Teukolsky and W. H. Press, Perturbations of a rotating black hole. III - Interaction of the hole with gravitational and electromagnet ic radiation, Astrophys. J. **193**, 443 (1974).

[341] S. L. Detweiler, KLEIN-GORDON EQUATION AND ROTATING BLACK HOLES, Phys. Rev. D **22**, 2323 (1980).

[342] Y. Shlapentokh-Rothman, Exponentially growing finite energy solutions for the Klein-Gordon equation on sub-extremal Kerr spacetimes, Commun. Math. Phys. **329**, 859 (2014), arXiv:1302.3448 [gr-qc].

[343] S. R. Dolan, Instability of the massive Klein-Gordon field on the Kerr spacetime, Phys. Rev. D **76**, 084001 (2007), arXiv:0705.2880 [gr-qc].

[344] H. Witek, V. Cardoso, A. Ishibashi, and U. Sperhake, Superradiant instabilities in astrophysical systems, Phys. Rev. D **87**, 043513 (2013), arXiv:1212.0551 [gr-qc].

[345] P. Pani, V. Cardoso, L. Gualtieri, E. Berti, and A. Ishibashi, Black hole bombs and photon mass bounds, Phys. Rev. Lett. **109**, 131102 (2012), arXiv:1209.0465 [gr-qc].

[346] W. E. East, Superradiant instability of massive vector fields around spinning black holes in the relativistic regime, Phys. Rev. D **96**, 024004 (2017), arXiv:1705.01544 [gr-qc].

[347] Z. Wang, T. Helfer, K. Clough, and E. Berti, Superradiance in massive vector fields with spatially varying mass, Phys. Rev. D **105**, 104055 (2022), arXiv:2201.08305 [gr-qc].

[348] K. Clough, P. G. Ferreira, and M. Lagos, Growth of massive scalar hair around a Schwarzschild black hole, Phys. Rev. D **100**, 063014 (2019), arXiv:1904.12783 [gr-qc].

[349] J. Bamber, K. Clough, P. G. Ferreira, L. Hui, and M. Lagos, Growth of accretion driven scalar hair around Kerr black holes, Phys. Rev. D **103**, 044059 (2021), arXiv:2011.07870 [gr-qc].

[350] C. A. R. Herdeiro and E. Radu, Asymptotically flat black holes with scalar hair: a review, Int. J. Mod. Phys. D **24**, 1542014 (2015), arXiv:1504.08209 [gr-qc].

[351] C. A. R. Herdeiro and E. Radu, Kerr black holes with scalar hair, Phys. Rev. Lett. **112**, 221101 (2014), arXiv:1403.2757 [gr-qc].

[352] C. Herdeiro, E. Radu, and H. Rúnarsson, Kerr black holes with Proca hair, Class. Quant. Grav. **33**, 154001 (2016), arXiv:1603.02687 [gr-qc].

[353] N. M. Santos, C. L. Benone, L. C. B. Crispino, C. A. R. Herdeiro, and E. Radu, Black holes with synchronised Proca hair: linear clouds and fundamental non-linear solutions, JHEP **07**, 010, arXiv:2004.09536 [gr-qc].

[354] R. Brito, V. Cardoso, and P. Pani, Black holes as particle detectors: evolution of superradiant instabilities, Class. Quant. Grav. **32**, 134001 (2015), arXiv:1411.0686 [gr-qc].

[355] G. Ficarra, P. Pani, and H. Witek, Impact of multiple modes on the black-hole superradiant instability, Phys. Rev. D **99**, 104019 (2019), arXiv:1812.02758 [gr-qc].

[356] W. E. East and F. Pretorius, Superradiant Instability and Backreaction of Massive Vector Fields around Kerr Black Holes, Phys. Rev. Lett. **119**, 041101 (2017), arXiv:1704.04791 [gr-qc].

[357] H. Yoshino and H. Kodama, Gravitational radiation from an axion cloud around a black hole: Superradiant phase, PTEP **2014**, 043E02 (2014), arXiv:1312.2326 [gr-qc].

[358] H. Okawa, H. Witek, and V. Cardoso, Black holes and fundamental fields in Numerical Relativity: initial data construction and evolution of bound states, Phys. Rev. D **89**, 104032 (2014), arXiv:1401.1548 [gr-qc].

[359] M. Zilhão, H. Witek, and V. Cardoso, Nonlinear interactions between black holes and Proca fields, Class. Quant. Grav. **32**, 234003 (2015), arXiv:1505.00797 [gr-qc].

[360] W. E. East, Massive Boson Superradiant Instability of Black Holes: Nonlinear Growth, Saturation, and Gravitational Radiation, Phys. Rev. Lett. **121**, 131104 (2018), arXiv:1807.00043 [gr-qc].

[361] N. Siemonsen and W. E. East, Gravitational wave signatures of ultralight vector bosons from black hole superradiance, Phys. Rev. D **101**, 024019 (2020), arXiv:1910.09476 [gr-qc].

[362] S. J. Zhu, M. Baryakhtar, M. A. Papa, D. Tsuna, N. Kawanaka, and H.-B. Eggenstein, Characterizing the continuous gravitational-wave signal from boson clouds around Galactic isolated black holes, Phys. Rev. D **102**, 063020 (2020), arXiv:2003.03359 [gr-qc].

[363] R. Brito, S. Grillo, and P. Pani, Black Hole Superradiant Instability from Ultralight Spin-2 Fields, Phys. Rev. Lett. **124**, 211101 (2020), arXiv:2002.04055 [gr-qc].

[364] J. Bamber, J. C. Aurrekoetxea, K. Clough, and P. G. Ferreira, Black hole merger simulations in wave dark matter environments, Phys. Rev. D **107**, 024035 (2023), arXiv:2210.09254 [gr-qc].

[365] C. F. B. Macedo, P. Pani, V. Cardoso, and L. C. B. Crispino, Into the lair: gravitational-wave signatures of dark matter, Astrophys. J. **774**, 48 (2013), arXiv:1302.2646 [gr-qc].

[366] L. K. Wong, Evolution of diffuse scalar clouds around binary black holes, Phys. Rev. D **101**, 124049 (2020), arXiv:2004.03570 [hep-th].

[367] T. Ikeda, L. Bernard, V. Cardoso, and M. Zilhão, Black hole binaries and light fields: Gravitational molecules, Phys. Rev. D **103**, 024020 (2021), arXiv:2010.00008 [gr-qc].

[368] S. Choudhary, N. Sanchis-Gual, A. Gupta, J. C. Degollado, S. Bose, and J. A. Font, Gravitational waves from binary black hole mergers surrounded by scalar field clouds: Numerical simulations and observational implications, Phys. Rev. D **103**, 044032 (2021), arXiv:2010.00935 [gr-qc].

[369] D. Baumann, H. S. Chia, and R. A. Porto, Probing Ultralight Bosons with Binary Black Holes, Phys. Rev. D **99**, 044001 (2019), arXiv:1804.03208 [gr-qc].

[370] D. Baumann, H. S. Chia, J. Stout, and L. ter Haar, The Spectra of Gravitational Atoms, JCAP **12**, 006, arXiv:1908.10370 [gr-qc].

[371] D. Baumann, H. S. Chia, R. A. Porto, and J. Stout, Gravitational Collider Physics, Phys. Rev. D **101**, 083019 (2020), arXiv:1912.04932 [gr-qc].

[372] E. Berti, R. Brito, C. F. B. Macedo, G. Raposo, and J. L. Rosa, Ultralight boson cloud depletion in binary systems, Phys. Rev. D **99**, 104039 (2019), arXiv:1904.03131 [gr-qc].

[373] O. A. Hannuksela, K. W. K. Wong, R. Brito, E. Berti, and T. G. F. Li, Probing the existence of ultralight bosons with a single gravitational-wave measurement, Nature Astron. **3**, 447 (2019), arXiv:1804.09659 [astro-ph.HE].

[374] O. A. Hannuksela, K. C. Y. Ng, and T. G. F. Li, Extreme dark matter tests with extreme mass ratio inspirals, Phys. Rev. D **102**, 103022 (2020), arXiv:1906.11845 [astro-ph.CO].

[375] J. Zhang and H. Yang, Dynamic Signatures of Black Hole Binaries with Superradiant Clouds, Phys. Rev. D **101**, 043020 (2020), arXiv:1907.13582 [gr-qc].

[376] D. Traykova, K. Clough, T. Helfer, E. Berti, P. G. Ferreira, and L. Hui, Dynamical friction from scalar dark matter in the relativistic regime, Phys. Rev. D **104**, 103014 (2021), arXiv:2106.08280 [gr-qc].

[377] V. Cardoso, F. Duque, and T. Ikeda, Tidal effects and disruption in superradiant clouds: a numerical investigation, Phys. Rev. D **101**, 064054 (2020), arXiv:2001.01729 [gr-qc].

[378] M. Goodsell, J. Jaeckel, J. Redondo, and A. Ringwald, Naturally Light Hidden Photons in LARGE Volume String Compactifications, JHEP **11**, 027, arXiv:0909.0515 [hep-ph].

[379] M. Baryakhtar, R. Lasenby, and M. Teo, Black Hole Superradiance Signatures of Ultralight Vectors, Phys. Rev. D **96**, 035019 (2017), arXiv:1704.05081 [hep-ph].

[380] O. J. C. Dias, G. Lingetti, P. Pani, and J. E. Santos, Black hole superradiant instability for massive spin-2 fields, Phys. Rev. D **108**, L041502 (2023), arXiv:2304.01265 [gr-qc].

[381] M. Isi, L. Sun, R. Brito, and A. Melatos, Directed searches for gravitational waves from ultralight bosons, Phys. Rev. D **99**, 084042 (2019), [Erratum: Phys.Rev.D 102, 049901 (2020)], arXiv:1810.03812 [gr-qc].

[382] M. J. Stott, Ultralight Bosonic Field Mass Bounds from Astrophysical Black Hole Spin, arXiv:2009.07206 [hep-ph].

[383] K. K. Y. Ng, M. Isi, C.-J. Haster, and S. Vitale, Multiband gravitational-wave searches for ultralight bosons, Phys. Rev. D **102**, 083020 (2020), arXiv:2007.12793 [gr-qc].

[384] S. W. Hawking, Black holes in the Brans-Dicke theory of gravitation, Commun. Math. Phys. **25**, 167 (1972).

[385] J. D. Bekenstein, Black hole hair: 25 - years after, in *2nd International Sakharov Conference on Physics* (1996) pp. 216–219, arXiv:gr-qc/9605059.

[386] J. W. Moffat, Scalar-tensor-vector gravity theory, JCAP **03**, 004, arXiv:gr-qc/0506021.

[387] V. Cardoso, C. F. B. Macedo, P. Pani, and V. Ferrari, Black holes and gravitational waves in models of minicharged dark matter, JCAP **05**, 054, [Erratum: JCAP 04, E01 (2020)], arXiv:1604.07845 [hep-ph].

[388] J. Preskill, MAGNETIC MONOPOLES IN PARTICLE PHYSICS AND COSMOLOGY, in *Inner Space/ Outer Space: Conference on Physics at the Interface of Astrophysics / Cosmology and Particle Physics* (1984).

[389] J. Fan, A. Katz, L. Randall, and M. Reece, Double-Disk Dark Matter, Phys. Dark Univ. **2**, 139 (2013), arXiv:1303.1521 [astro-ph.CO].

[390] K. Nordtvedt, Equivalence Principle for Massive Bodies. 1. Phenomenology, Phys. Rev. **169**, 1014 (1968).

[391] A. Cardenas-Avendano, S. Nampalliwar, and N. Yunes, Gravitational-wave versus X-ray tests of strong-field gravity, Class. Quant. Grav. **37**, 135008 (2020), arXiv:1912.08062 [gr-qc].

[392] N. Yunes, K. Yagi, and F. Pretorius, Theoretical Physics Implications of the Binary Black-Hole Mergers GW150914 and GW151226, Phys. Rev. D **94**, 084002 (2016), arXiv:1603.08955 [gr-qc].

[393] R. R. Metsaev and A. A. Tseytlin, Order alpha-prime (Two Loop) Equivalence of the String Equations of Motion and the Sigma Model Weyl Invariance Conditions: Dependence on the Dilaton and the Antisymmetric Tensor, Nucl. Phys. B **293**, 385 (1987).

[394] B. A. Campbell, N. Kaloper, and K. A. Olive, Classical hair for Kerr-Newman black holes in string gravity, Phys. Lett. B **285**, 199 (1992).

[395] P. Kanti, N. E. Mavromatos, J. Rizos, K. Tamvakis, and E. Winstanley, Dilatonic black holes in higher curvature string gravity, Phys. Rev. D **54**, 5049 (1996), arXiv:hep-th/9511071.

[396] S. Alexander and N. Yunes, Chern-Simons Modified General Relativity, Phys. Rept. **480**, 1 (2009), arXiv:0907.2562 [hep-th].

[397] J. R. Gair, M. Vallisneri, S. L. Larson, and J. G. Baker, Testing General Relativity with Low-Frequency, Space-Based Gravitational-Wave Detectors, Living Rev. Rel. **16**, 7 (2013), arXiv:1212.5575 [gr-qc].

[398] P. Nicolini, A. Smailagic, and E. Spallucci, Noncommutative geometry inspired Schwarzschild black hole, Phys. Lett. B **632**, 547 (2006), arXiv:gr-qc/0510112.

[399] I. Bena and N. P. Warner, Black holes, black rings and their microstates, Lect. Notes Phys. **755**, 1 (2008), arXiv:hep-th/0701216.

[400] S. B. Giddings, Possible observational windows for quantum effects from black holes, Phys. Rev. D **90**, 124033 (2014), arXiv:1406.7001 [hep-th].

[401] A. S. Koshelev and A. Mazumdar, Do massive compact objects without event horizon exist in infinite derivative gravity?, Phys. Rev. D **96**, 084069 (2017), arXiv:1707.00273 [gr-qc].

[402] J. Abedi, N. Afshordi, N. Oshita, and Q. Wang, Quantum Black Holes in the Sky, Universe **6**, 43 (2020), arXiv:2001.09553 [gr-qc].

[403] S. L. Liebling and C. Palenzuela, Dynamical boson stars, Living Rev. Rel. **26**, 1 (2023), arXiv:1202.5809 [gr-qc].

[404] R. Brito, V. Cardoso, C. A. R. Herdeiro, and E. Radu, Proca stars: Gravitating Bose–Einstein condensates of massive spin 1 particles, Phys. Lett. B **752**, 291 (2016), arXiv:1508.05395 [gr-qc].

[405] G. F. Giudice, M. McCullough, and A. Urbano, Hunting for Dark Particles with Gravitational Waves, JCAP **10**, 001, arXiv:1605.01209 [hep-ph].

[406] R. C. Myers, Pure states don't wear black, Gen. Rel. Grav. **29**, 1217 (1997), arXiv:gr-qc/9705065.

[407] S. R. Das and S. D. Mathur, The quantum physics of black holes: Results from string theory,

Ann. Rev. Nucl. Part. Sci. **50**, 153 (2000), arXiv:gr-qc/0105063.

[408] S. D. Mathur, Fuzzballs and the information paradox: A Summary and conjectures, arXiv:0810.4525 [hep-th].

[409] P. O. Mazur and E. Mottola, Gravitational Condensate Stars: An Alternative to Black Holes, Universe **9**, 88 (2023), arXiv:gr-qc/0109035.

[410] P. O. Mazur and E. Mottola, Gravitational vacuum condensate stars, Proc. Nat. Acad. Sci. **101**, 9545 (2004), arXiv:gr-qc/0407075.

[411] D. A. Feinblum and W. A. McKinley, Stable States of a Scalar Particle in Its Own Gravational Field, Phys. Rev. **168**, 1445 (1968).

[412] D. J. Kaup, Klein-Gordon Geon, Phys. Rev. **172**, 1331 (1968).

[413] R. Ruffini and S. Bonazzola, Systems of selfgravitating particles in general relativity and the concept of an equation of state, Phys. Rev. **187**, 1767 (1969).

[414] E. Seidel and W. M. Suen, Oscillating soliton stars, Phys. Rev. Lett. **66**, 1659 (1991).

[415] A. Einstein and N. Rosen, The Particle Problem in the General Theory of Relativity, Phys. Rev. **48**, 73 (1935).

[416] M. S. Morris and K. S. Thorne, Wormholes in space-time and their use for interstellar travel: A tool for teaching general relativity, Am. J. Phys. **56**, 395 (1988).

[417] T. Damour and S. N. Solodukhin, Wormholes as black hole foils, Phys. Rev. D **76**, 024016 (2007), arXiv:0704.2667 [gr-qc].

[418] S. D. Mathur, The Fuzzball proposal for black holes: An Elementary review, Fortsch. Phys. **53**, 793 (2005), arXiv:hep-th/0502050.

[419] R. L. Bowers and E. P. T. Liang, Anisotropic Spheres in General Relativity, Astrophys. J. **188**, 657 (1974).

[420] E. G. Gimon and P. Horava, Astrophysical violations of the Kerr bound as a possible signature of string theory, Phys. Lett. B **672**, 299 (2009), arXiv:0706.2873 [hep-th].

[421] C. Prescod-Weinstein, N. Afshordi, M. L. Balogh, N. Afshordi, and M. L. Balogh, Stellar Black Holes and the Origin of Cosmic Acceleration, Phys. Rev. D **80**, 043513 (2009), arXiv:0905.3551 [astro-ph.CO].

[422] R. Brustein and A. J. M. Medved, Black holes as collapsed polymers, Fortsch. Phys. **65**, 1600114 (2017), arXiv:1602.07706 [hep-th].

[423] B. Holdom and J. Ren, Not quite a black hole, Phys. Rev. D **95**, 084034 (2017), arXiv:1612.04889 [gr-qc].

[424] L. Buoninfante and A. Mazumdar, Nonlocal star as a blackhole mimicker, Phys. Rev. D **100**, 024031 (2019), arXiv:1903.01542 [gr-qc].

[425] Q. Wang and N. Afshordi, Black hole echology: The observer's manual, Phys. Rev. D **97**, 124044 (2018), arXiv:1803.02845 [gr-qc].

[426] V. Cardoso and P. Pani, Tests for the existence of black holes through gravitational wave echoes, Nature Astron. **1**, 586 (2017), arXiv:1709.01525 [gr-qc].

[427] A. Urbano and H. Veermäe, On gravitational echoes from ultracompact exotic stars, JCAP **04**, 011, arXiv:1810.07137 [gr-qc].

[428] E. Maggio, L. Buoninfante, A. Mazumdar, and P. Pani, How does a dark compact object ringdown?, Phys. Rev. D **102**, 064053 (2020), arXiv:2006.14628 [gr-qc].

[429] V. Cardoso, E. Franzin, and P. Pani, Is the gravitational-wave ringdown a probe of the event horizon?, Phys. Rev. Lett. **116**, 171101 (2016), [Erratum: Phys.Rev.Lett. 117, 089902 (2016)], arXiv:1602.07309 [gr-qc].

[430] V. Cardoso, S. Hopper, C. F. B. Macedo, C. Palenzuela, and P. Pani, Gravitational-wave signatures of exotic compact objects and of quantum corrections at the horizon scale, Phys. Rev. D **94**, 084031 (2016), arXiv:1608.08637 [gr-qc].

[431] R. H. Price and G. Khanna, Gravitational wave sources: reflections and echoes, Class. Quant. Grav. **34**, 225005 (2017), arXiv:1702.04833 [gr-qc].

[432] M. R. Correia and V. Cardoso, Characterization of echoes: A Dyson-series representation of

individual pulses, Phys. Rev. D **97**, 084030 (2018), arXiv:1802.07735 [gr-qc].

[433] C. P. Burgess, R. Plestid, and M. Rummel, Effective Field Theory of Black Hole Echoes, JHEP **09**, 113, arXiv:1808.00847 [gr-qc].

[434] Y.-X. Huang, J.-C. Xu, and S.-Y. Zhou, Fredholm approach to characterize gravitational wave echoes, Phys. Rev. D **101**, 024045 (2020), arXiv:1908.00189 [gr-qc].

[435] N. Oshita, D. Tsuna, and N. Afshordi, Quantum Black Hole Seismology I: Echoes, Ergospheres, and Spectra, Phys. Rev. D **102**, 024045 (2020), arXiv:2001.11642 [gr-qc].

[436] J. L. Friedman, Ergosphere instability, Communications in Mathematical Physics **63**, 243 (1978).

[437] N. Comins and B. F. Schutz, On the Ergoregion Instability, Proceedings of the Royal Society of London Series A **364**, 211 (1978).

[438] S. Yoshida and Y. Eriguchi, Ergoregion instability revisited - a new and general method for numerical analysis of stability, MNRAS **282**, 580 (1996).

[439] K. D. Kokkotas, J. Ruoff, and N. Andersson, The w-mode instability of ultracompact relativistic stars, Phys. Rev. D **70**, 043003 (2004), arXiv:astro-ph/0212429.

[440] V. Cardoso, L. C. B. Crispino, C. F. B. Macedo, H. Okawa, and P. Pani, Light rings as observational evidence for event horizons: long-lived modes, ergoregions and nonlinear instabilities of ultracompact objects, Phys. Rev. D **90**, 044069 (2014), arXiv:1406.5510 [gr-qc].

[441] E. Maggio, P. Pani, and V. Ferrari, Exotic Compact Objects and How to Quench their Ergoregion Instability, Phys. Rev. D **96**, 104047 (2017), arXiv:1703.03696 [gr-qc].

[442] E. Maggio, V. Cardoso, S. R. Dolan, and P. Pani, Ergoregion instability of exotic compact objects: electromagnetic and gravitational perturbations and the role of absorption, Phys. Rev. D **99**, 064007 (2019), arXiv:1807.08840 [gr-qc].

[443] P. V. P. Cunha, E. Berti, and C. A. R. Herdeiro, Light-Ring Stability for Ultracompact Objects, Phys. Rev. Lett. **119**, 251102 (2017), arXiv:1708.04211 [gr-qc].

[444] P. V. P. Cunha, C. Herdeiro, E. Radu, and N. Sanchis-Gual, Exotic Compact Objects and the Fate of the Light-Ring Instability, Phys. Rev. Lett. **130**, 061401 (2023), arXiv:2207.13713 [gr-qc].

[445] V. Cardoso, P. Pani, M. Cadoni, and M. Cavaglia, Ergoregion instability of ultracompact astrophysical objects, Phys. Rev. D **77**, 124044 (2008), arXiv:0709.0532 [gr-qc].

[446] X.-L. Fan and Y.-B. Chen, Stochastic gravitational-wave background from spin loss of black holes, Phys. Rev. D **98**, 044020 (2018), arXiv:1712.00784 [gr-qc].

[447] E. Barausse, R. Brito, V. Cardoso, I. Dvorkin, and P. Pani, The stochastic gravitational-wave background in the absence of horizons, Class. Quant. Grav. **35**, 20LT01 (2018), arXiv:1805.08229 [gr-qc].

[448] E. Maggio, A. Testa, S. Bhagwat, and P. Pani, Analytical model for gravitational-wave echoes from spinning remnants, Phys. Rev. D **100**, 064056 (2019), arXiv:1907.03091 [gr-qc].

[449] E. Maggio, M. van de Meent, and P. Pani, Extreme mass-ratio inspirals around a spinning horizonless compact object, Phys. Rev. D **104**, 104026 (2021), arXiv:2106.07195 [gr-qc].

[450] E. Maggio, P. Pani, and G. Raposo, Testing the nature of dark compact objects with gravitational waves, arXiv:2105.06410 [gr-qc].

[451] K. Glampedakis and G. Pappas, How well can ultracompact bodies imitate black hole ringdowns?, Phys. Rev. D **97**, 041502 (2018), arXiv:1710.02136 [gr-qc].

[452] G. Raposo, P. Pani, and R. Emparan, Exotic compact objects with soft hair, Phys. Rev. D **99**, 104050 (2019), arXiv:1812.07615 [gr-qc].

[453] G. Raposo and P. Pani, Axisymmetric deformations of neutron stars and gravitational-wave astronomy, Phys. Rev. D **102**, 044045 (2020), arXiv:2002.02555 [gr-qc].

[454] M. Bianchi, D. Consoli, A. Grillo, J. F. Morales, P. Pani, and G. Raposo, The multipolar structure of fuzzballs, JHEP **01**, 003, arXiv:2008.01445 [hep-th].

[455] M. Bianchi, D. Consoli, A. Grillo, J. F. Morales, P. Pani, and G. Raposo, Distinguishing fuzzballs from black holes through their multipolar structure, Phys. Rev. Lett. **125**, 221601 (2020),

arXiv:2007.01743 [hep-th].

[456] I. Bena and D. R. Mayerson, Multipole Ratios: A New Window into Black Holes, Phys. Rev. Lett. **125**, 221602 (2020), arXiv:2006.10750 [hep-th].

[457] I. Bena and D. R. Mayerson, Black Holes Lessons from Multipole Ratios, JHEP **03**, 114, arXiv:2007.09152 [hep-th].

[458] C. A. R. Herdeiro, J. Kunz, I. Perapechka, E. Radu, and Y. Shnir, Multipolar boson stars: macroscopic Bose-Einstein condensates akin to hydrogen orbitals, Phys. Lett. B **812**, 136027 (2021), arXiv:2008.10608 [gr-qc].

[459] I. Bah, I. Bena, P. Heidmann, Y. Li, and D. R. Mayerson, Gravitational footprints of black holes and their microstate geometries, JHEP **10**, 138, arXiv:2104.10686 [hep-th].

[460] K. Fransen and D. R. Mayerson, Detecting equatorial symmetry breaking with LISA, Phys. Rev. D **106**, 064035 (2022), arXiv:2201.03569 [gr-qc].

[461] N. Loutrel, R. Brito, A. Maselli, and P. Pani, Inspiraling compact objects with generic deformations, Phys. Rev. D **105**, 124050 (2022), arXiv:2203.01725 [gr-qc].

[462] M. Vaglio, C. Pacilio, A. Maselli, and P. Pani, Multipolar structure of rotating boson stars, Phys. Rev. D **105**, 124020 (2022), arXiv:2203.07442 [gr-qc].

[463] P. Pani and A. Maselli, Love in Extrema Ratio, Int. J. Mod. Phys. D **28**, 1944001 (2019), arXiv:1905.03947 [gr-qc].

[464] G. A. Piovano, A. Maselli, and P. Pani, Constraining the tidal deformability of supermassive objects with extreme mass ratio inspirals and semianalytical frequency-domain waveforms, Phys. Rev. D **107**, 024021 (2023), arXiv:2207.07452 [gr-qc].

[465] LISA Data Challenge Working Group, LISA Data Challenge White Paper.

[466] P. Jaranowski and A. Krolak, Gravitational-Wave Data Analysis. Formalism and Sample Applications: The Gaussian Case, Living Rev. Rel. **8**, 3 (2005), arXiv:0711.1115 [gr-qc].

[467] M. Drago *et al.*, Coherent WaveBurst, a pipeline for unmodeled gravitational-wave data analysis, arXiv:2006.12604 [gr-qc].

[468] J. D. Romano and N. J. Cornish, Detection methods for stochastic gravitational-wave backgrounds: a unified treatment, Living Rev. Rel. **20**, 2 (2017), arXiv:1608.06889 [gr-qc].

[469] S. A. Usman *et al.*, The PyCBC search for gravitational waves from compact binary coalescence, Class. Quant. Grav. **33**, 215004 (2016), arXiv:1508.02357 [gr-qc].

[470] M. L. Katz, Fully automated end-to-end pipeline for massive black hole binary signal extraction from LISA data, Phys. Rev. D **105**, 044055 (2022), arXiv:2111.01064 [gr-qc].

[471] T. B. Littenberg and N. J. Cornish, Prototype global analysis of LISA data with multiple source types, Phys. Rev. D **107**, 063004 (2023), arXiv:2301.03673 [gr-qc].

[472] K. Lackeos, T. B. Littenberg, N. J. Cornish, and J. I. Thorpe, The LISA Data Challenge Radler Analysis and Time-dependent Ultra-compact Binary Catalogues, Astron. Astrophys. **678**, A123 (2023), arXiv:2308.12827 [gr-qc].

[473] A. R. Kaiser and S. T. McWilliams, Sensitivity of present and future detectors across the black-hole binary gravitational wave spectrum, Class. Quant. Grav. **38**, 055009 (2021), arXiv:2010.02135 [gr-qc].

[474] E. E. Flanagan and S. A. Hughes, Measuring gravitational waves from binary black hole coalescences: 2. The Waves' information and its extraction, with and without templates, Phys. Rev. D **57**, 4566 (1998), arXiv:gr-qc/9710129.

[475] L. Lindblom, B. J. Owen, and D. A. Brown, Model Waveform Accuracy Standards for Gravitational Wave Data Analysis, Phys. Rev. D **78**, 124020 (2008), arXiv:0809.3844 [gr-qc].

[476] S. T. McWilliams, B. J. Kelly, and J. G. Baker, Observing mergers of non-spinning black-hole binaries, Phys. Rev. D **82**, 024014 (2010), arXiv:1004.0961 [gr-qc].

[477] A. Sharma and J. Harms, Searching for cosmological gravitational-wave backgrounds with third-generation detectors in the presence of an astrophysical foreground, Phys. Rev. D **102**, 063009 (2020), arXiv:2006.16116 [gr-qc].

[478] Z. Pan and H. Yang, Probing Primordial Stochastic Gravitational Wave Background with

Multi-band Astrophysical Foreground Cleaning, Class. Quant. Grav. **37**, 195020 (2020), arXiv:1910.09637 [astro-ph.CO].

[479] J. R. Gair, L. Barack, T. Creighton, C. Cutler, S. L. Larson, E. S. Phinney, and M. Vallisneri, Event rate estimates for LISA extreme mass ratio capture sources, Class. Quant. Grav. **21**, S1595 (2004), arXiv:gr-qc/0405137.

[480] A. J. K. Chua, C. J. Moore, and J. R. Gair, Augmented kludge waveforms for detecting extreme-mass-ratio inspirals, Phys. Rev. D **96**, 044005 (2017), arXiv:1705.04259 [gr-qc].

[481] J. R. Gair, E. K. Porter, S. Babak, and L. Barack, A Constrained Metropolis-Hastings Search for EMRIs in the Mock LISA Data Challenge 1B, Class. Quant. Grav. **25**, 184030 (2008), arXiv:0804.3322 [gr-qc].

[482] N. J. Cornish, Detection Strategies for Extreme Mass Ratio Inspirals, Class. Quant. Grav. **28**, 094016 (2011), arXiv:0804.3323 [gr-qc].

[483] M. Vallisneri, A LISA Data-Analysis Primer, Class. Quant. Grav. **26**, 094024 (2009), arXiv:0812.0751 [gr-qc].

[484] S. Babak *et al.* (Mock LISA Data Challenge Task Force), Report on the second Mock LISA Data Challenge, Class. Quant. Grav. **25**, 114037 (2008), arXiv:0711.2667 [gr-qc].

[485] S. Babak *et al.*, The Mock LISA Data Challenges: From Challenge 1B to Challenge 3, Class. Quant. Grav. **25**, 184026 (2008), arXiv:0806.2110 [gr-qc].

[486] S. Babak *et al.* (Mock LISA Data Challenge Task Force), The Mock LISA Data Challenges: From Challenge 3 to Challenge 4, Class. Quant. Grav. **27**, 084009 (2010), arXiv:0912.0548 [gr-qc].

[487] M. Vallisneri and N. Yunes, Stealth Bias in Gravitational-Wave Parameter Estimation, Phys. Rev. D **87**, 102002 (2013), arXiv:1301.2627 [gr-qc].

[488] C. Cutler and M. Vallisneri, LISA detections of massive black hole inspirals: Parameter extraction errors due to inaccurate template waveforms, Phys. Rev. D **76**, 104018 (2007), arXiv:0707.2982 [gr-qc].

[489] K. Chatziioannou, A. Klein, N. Yunes, and N. Cornish, Constructing Gravitational Waves from Generic Spin-Precessing Compact Binary Inspirals, Phys. Rev. D **95**, 104004 (2017), arXiv:1703.03967 [gr-qc].

[490] D. Wysocki, J. Lange, and R. O'Shaughnessy, Reconstructing phenomenological distributions of compact binaries via gravitational wave observations, Phys. Rev. D **100**, 043012 (2019), arXiv:1805.06442 [gr-qc].

[491] R. O'Shaughnessy and J. Lange, Some diagnostics for gravitational waveform accuracy , In preparation (2020).

[492] R. N. Lang and S. A. Hughes, Localizing coalescing massive black hole binaries with gravitational waves, Astrophys. J. **677**, 1184 (2008), arXiv:0710.3795 [astro-ph].

[493] E. K. Porter, The Challenges in Gravitational Wave Astronomy for Space-Based Detectors, Astrophys. Space Sci. Proc. **40**, 267 (2015), arXiv:1406.6891 [gr-qc].

[494] N. J. Cornish and K. Shuman, Black Hole Hunting with LISA, Phys. Rev. D **101**, 124008 (2020), arXiv:2005.03610 [gr-qc].

[495] M. L. Katz, S. Marsat, A. J. K. Chua, S. Babak, and S. L. Larson, GPU-accelerated massive black hole binary parameter estimation with LISA, Phys. Rev. D **102**, 023033 (2020), arXiv:2005.01827 [gr-qc].

[496] S. Marsat, J. G. Baker, and T. Dal Canton, Exploring the Bayesian parameter estimation of binary black holes with LISA, Phys. Rev. D **103**, 083011 (2021), arXiv:2003.00357 [gr-qc].

[497] A. Albertini, A. Nagar, A. Pound, N. Warburton, B. Wardell, L. Durkan, and J. Miller, Comparing second-order gravitational self-force, numerical relativity, and effective one body waveforms from inspiralling, quasicircular, and nonspinning black hole binaries, Phys. Rev. D **106**, 084061 (2022), arXiv:2208.01049 [gr-qc].

[498] M. van de Meent and H. P. Pfeiffer, Intermediate mass-ratio black hole binaries: Applicability of small mass-ratio perturbation theory, Phys. Rev. Lett. **125**, 181101 (2020), arXiv:2006.12036

[gr-qc].

[499] M. Alcubierre, *Introduction to 3+1 Numerical Relativity* (2008).

[500] C. Bona, C. Palenzuela-Luque, and C. Bona-Casas, *Elements of Numerical Relativity and Relativistic Hydrodynamics*, Vol. 783 (2009).

[501] T. W. Baumgarte and S. L. Shapiro, *Numerical Relativity: Solving Einstein's Equations on the Computer* (Cambridge University Press, Cambridge, England, 2010).

[502] E. Gourgoulhon, *3+1 Formalism in General Relativity*, Vol. 846 (2012).

[503] M. Shibata, *Numerical Relativity* (2016).

[504] S. G. Hahn and R. W. Lindquist, The two-body problem in geometrodynamics, Annals of Physics **29**, 304 (1964).

[505] L. Smarr, A. Cadez, B. S. DeWitt, and K. Eppley, Collision of Two Black Holes: Theoretical Framework, Phys. Rev. D **14**, 2443 (1976).

[506] F. Pretorius, Evolution of binary black hole spacetimes, Phys. Rev. Lett. **95**, 121101 (2005), arXiv:gr-qc/0507014.

[507] M. Campanelli, C. O. Lousto, P. Marronetti, and Y. Zlochower, Accurate evolutions of orbiting black-hole binaries without excision, Phys. Rev. Lett. **96**, 111101 (2006), arXiv:gr-qc/0511048.

[508] J. G. Baker, J. Centrella, D.-I. Choi, M. Koppitz, and J. van Meter, Gravitational wave extraction from an inspiraling configuration of merging black holes, Phys. Rev. Lett. **96**, 111102 (2006), arXiv:gr-qc/0511103.

[509] L. Lehner, Numerical relativity: A Review, Class. Quant. Grav. **18**, R25 (2001), arXiv:gr-qc/0106072.

[510] J. Centrella, J. G. Baker, B. J. Kelly, and J. R. van Meter, Black-hole binaries, gravitational waves, and numerical relativity, Rev. Mod. Phys. **82**, 3069 (2010), arXiv:1010.5260 [gr-qc].

[511] M. D. Duez and Y. Zlochower, Numerical Relativity of Compact Binaries in the 21st Century, Rept. Prog. Phys. **82**, 016902 (2019), arXiv:1808.06011 [gr-qc].

[512] F. Foucart, P. Laguna, G. Lovelace, D. Radice, and H. Witek, Snowmass2021 Cosmic Frontier White Paper: Numerical relativity for next-generation gravitational-wave probes of fundamental physics, arXiv:2203.08139 [gr-qc].

[513] A. H. Mroue *et al.*, Catalog of 174 Binary Black Hole Simulations for Gravitational Wave Astronomy, Phys. Rev. Lett. **111**, 241104 (2013), arXiv:1304.6077 [gr-qc].

[514] S. Husa, S. Khan, M. Hannam, M. Pürrer, F. Ohme, X. Jiménez Forteza, and A. Bohé, Frequency-domain gravitational waves from nonprecessing black-hole binaries. I. New numerical waveforms and anatomy of the signal, Phys. Rev. D **93**, 044006 (2016), arXiv:1508.07250 [gr-qc].

[515] M. Boyle *et al.*, The SXS Collaboration catalog of binary black hole simulations, Class. Quant. Grav. **36**, 195006 (2019), arXiv:1904.04831 [gr-qc].

[516] E. Hamilton *et al.*, A catalogue of precessing black-hole-binary numerical-relativity simulations, arXiv:2303.05419 [gr-qc].

[517] R. Arnowitt, S. Deser, and C. W. Misner, The dynamics of general relativity, in *Gravitation: An introduction to current research*, edited by L. Witten (Wiley, New York, 1962).

[518] J. W. York, Jr., Kinematics and dynamics of general relativity, in *Sources of Gravitational Radiation*, edited by L. L. Smarr (Cambridge University Press, Cambridge, England, 1979) p. 83.

[519] J. W. York, Jr., Conformal 'thin sandwich' data for the initial-value problem, Phys. Rev. Lett. **82**, 1350 (1999), arXiv:gr-qc/9810051.

[520] H. P. Pfeiffer and J. W. York, Jr., Extrinsic curvature and the Einstein constraints, Phys. Rev. D **67**, 044022 (2003), arXiv:gr-qc/0207095.

[521] S. Brandt and B. Bruegmann, A Simple construction of initial data for multiple black holes, Phys. Rev. Lett. **78**, 3606 (1997), arXiv:gr-qc/9703066.

[522] H. P. Pfeiffer, L. E. Kidder, M. A. Scheel, and S. A. Teukolsky, A Multidomain spectral method for solving elliptic equations, Comput. Phys. Commun. **152**, 253 (2003), arXiv:gr-qc/0202096.

[523] M. Ansorg, B. Bruegmann, and W. Tichy, A Single-domain spectral method for black hole puncture data, Phys. Rev. D **70**, 064011 (2004), arXiv:gr-qc/0404056.

[524] LORENE: Langage Objet pour la RElativité NumériquE, `http://www.lorene.obspm.fr`.

[525] G. Lovelace, R. Owen, H. P. Pfeiffer, and T. Chu, Binary-black-hole initial data with nearly-extremal spins, Phys. Rev. D **78**, 084017 (2008), arXiv:0805.4192 [gr-qc].

[526] F. Foucart, L. E. Kidder, H. P. Pfeiffer, and S. A. Teukolsky, Initial data for black hole-neutron star binaries: A Flexible, high-accuracy spectral method, Phys. Rev. D **77**, 124051 (2008), arXiv:0804.3787 [gr-qc].

[527] P. Grandclement, Kadath: A Spectral solver for theoretical physics, J. Comput. Phys. **229**, 3334 (2010), arXiv:0909.1228 [gr-qc].

[528] I. Ruchlin, J. Healy, C. O. Lousto, and Y. Zlochower, Puncture Initial Data for Black-Hole Binaries with High Spins and High Boosts, Phys. Rev. D **95**, 024033 (2017), arXiv:1410.8607 [gr-qc].

[529] S. Ossokine, F. Foucart, H. P. Pfeiffer, M. Boyle, and B. Szilágyi, Improvements to the construction of binary black hole initial data, Class. Quant. Grav. **32**, 245010 (2015), arXiv:1506.01689 [gr-qc].

[530] T. Dietrich, N. Moldenhauer, N. K. Johnson-McDaniel, S. Bernuzzi, C. M. Markakis, B. Brügmann, and W. Tichy, Binary Neutron Stars with Generic Spin, Eccentricity, Mass ratio, and Compactness - Quasi-equilibrium Sequences and First Evolutions, Phys. Rev. D **92**, 124007 (2015), arXiv:1507.07100 [gr-qc].

[531] A. Rashti, F. M. Fabbri, B. Brügmann, S. V. Chaurasia, T. Dietrich, M. Ujevic, and W. Tichy, New pseudospectral code for the construction of initial data, Phys. Rev. D **105**, 104027 (2022), arXiv:2109.14511 [gr-qc].

[532] T. Assumpcao, L. R. Werneck, T. P. Jacques, and Z. B. Etienne, Fast hyperbolic relaxation elliptic solver for numerical relativity: Conformally flat, binary puncture initial data, Phys. Rev. D **105**, 104037 (2022), arXiv:2111.02424 [gr-qc].

[533] N. L. Vu *et al.*, A scalable elliptic solver with task-based parallelism for the SpECTRE numerical relativity code, Phys. Rev. D **105**, 084027 (2022), arXiv:2111.06767 [gr-qc].

[534] L. J. Papenfort, S. D. Tootle, P. Grandclément, E. R. Most, and L. Rezzolla, New public code for initial data of unequal-mass, spinning compact-object binaries, Phys. Rev. D **104**, 024057 (2021), arXiv:2103.09911 [gr-qc].

[535] F. Pretorius, Numerical relativity using a generalized harmonic decomposition, Class. Quant. Grav. **22**, 425 (2005), arXiv:gr-qc/0407110.

[536] L. Lindblom, M. A. Scheel, L. E. Kidder, R. Owen, and O. Rinne, A New generalized harmonic evolution system, Class. Quant. Grav. **23**, S447 (2006), arXiv:gr-qc/0512093.

[537] B. Szilagyi, L. Lindblom, and M. A. Scheel, Simulations of Binary Black Hole Mergers Using Spectral Methods, Phys. Rev. D **80**, 124010 (2009), arXiv:0909.3557 [gr-qc].

[538] M. Shibata and T. Nakamura, Evolution of three-dimensional gravitational waves: Harmonic slicing case, Phys. Rev. D **52**, 5428 (1995).

[539] T. W. Baumgarte and S. L. Shapiro, On the numerical integration of Einstein's field equations, Phys. Rev. D **59**, 024007 (1998), arXiv:gr-qc/9810065.

[540] C. Bona, T. Ledvinka, C. Palenzuela, and M. Zacek, General covariant evolution formalism for numerical relativity, Phys. Rev. D **67**, 104005 (2003), arXiv:gr-qc/0302083.

[541] S. Bernuzzi and D. Hilditch, Constraint violation in free evolution schemes: Comparing BSSNOK with a conformal decomposition of Z4, Phys. Rev. D **81**, 084003 (2010), arXiv:0912.2920 [gr-qc].

[542] M. Ruiz, D. Hilditch, and S. Bernuzzi, Constraint preserving boundary conditions for the Z4c formulation of general relativity, Phys. Rev. D **83**, 024025 (2011), arXiv:1010.0523 [gr-qc].

[543] A. Weyhausen, S. Bernuzzi, and D. Hilditch, Constraint damping for the Z4c formulation of general relativity, Phys. Rev. D **85**, 024038 (2012), arXiv:1107.5539 [gr-qc].

[544] D. Hilditch, S. Bernuzzi, M. Thierfelder, Z. Cao, W. Tichy, and B. Bruegmann, Compact binary

166

evolutions with the Z4c formulation, Phys. Rev. D **88**, 084057 (2013), arXiv:1212.2901 [gr-qc].

[545] D. Alic, C. Bona-Casas, C. Bona, L. Rezzolla, and C. Palenzuela, Conformal and covariant formulation of the Z4 system with constraint-violation damping, Phys. Rev. D **85**, 064040 (2012), arXiv:1106.2254 [gr-qc].

[546] D. Alic, W. Kastaun, and L. Rezzolla, Constraint damping of the conformal and covariant formulation of the Z4 system in simulations of binary neutron stars, Phys. Rev. D **88**, 064049 (2013), arXiv:1307.7391 [gr-qc].

[547] N. T. Bishop and L. Rezzolla, Extraction of Gravitational Waves in Numerical Relativity, Living Rev. Rel. **19**, 2 (2016), arXiv:1606.02532 [gr-qc].

[548] M. Boyle and A. H. Mroue, Extrapolating gravitational-wave data from numerical simulations, Phys. Rev. D **80**, 124045 (2009), arXiv:0905.3177 [gr-qc].

[549] C. Reisswig and D. Pollney, Notes on the integration of numerical relativity waveforms, Class. Quant. Grav. **28**, 195015 (2011), arXiv:1006.1632 [gr-qc].

[550] N. T. Bishop, R. Gomez, L. Lehner, and J. Winicour, Cauchy-characteristic extraction in numerical relativity, Phys. Rev. D **54**, 6153 (1996), arXiv:gr-qc/9705033.

[551] C. J. Handmer and B. Szilagyi, Spectral Characteristic Evolution: A New Algorithm for Gravitational Wave Propagation, Class. Quant. Grav. **32**, 025008 (2015), arXiv:1406.7029 [gr-qc].

[552] J. Moxon, M. A. Scheel, S. A. Teukolsky, N. Deppe, N. Fischer, F. Hébert, L. E. Kidder, and W. Throwe, SpECTRE Cauchy-characteristic evolution system for rapid, precise waveform extraction, Phys. Rev. D **107**, 064013 (2023), arXiv:2110.08635 [gr-qc].

[553] K. Mitman, J. Moxon, M. A. Scheel, S. A. Teukolsky, M. Boyle, N. Deppe, L. E. Kidder, and W. Throwe, Computation of displacement and spin gravitational memory in numerical relativity, Phys. Rev. D **102**, 104007 (2020), arXiv:2007.11562 [gr-qc].

[554] L. Lehner and O. M. Moreschi, Dealing with delicate issues in waveforms calculations, Phys. Rev. D **76**, 124040 (2007), arXiv:0706.1319 [gr-qc].

[555] K. Mitman *et al.*, Fixing the BMS frame of numerical relativity waveforms with BMS charges, Phys. Rev. D **106**, 084029 (2022), arXiv:2208.04356 [gr-qc].

[556] M. Favata, Nonlinear gravitational-wave memory from binary black hole mergers, Astrophys. J. Lett. **696**, L159 (2009), arXiv:0902.3660 [astro-ph.SR].

[557] C. Talbot, E. Thrane, P. D. Lasky, and F. Lin, Gravitational-wave memory: waveforms and phenomenology, Phys. Rev. D **98**, 064031 (2018), arXiv:1807.00990 [astro-ph.HE].

[558] O. M. Boersma, D. A. Nichols, and P. Schmidt, Forecasts for detecting the gravitational-wave memory effect with Advanced LIGO and Virgo, Phys. Rev. D **101**, 083026 (2020), arXiv:2002.01821 [astro-ph.HE].

[559] N. Khera, B. Krishnan, A. Ashtekar, and T. De Lorenzo, Inferring the gravitational wave memory for binary coalescence events, Phys. Rev. D **103**, 044012 (2021), arXiv:2009.06351 [gr-qc].

[560] K. Mitman *et al.*, Adding gravitational memory to waveform catalogs using BMS balance laws, Phys. Rev. D **103**, 024031 (2021), arXiv:2011.01309 [gr-qc].

[561] X. Liu, X. He, and Z. Cao, Accurate calculation of gravitational wave memory, Phys. Rev. D **103**, 043005 (2021), arXiv:2302.02642 [gr-qc].

[562] J. G. Baker, J. Centrella, D.-I. Choi, M. Koppitz, J. R. van Meter, and M. C. Miller, Getting a kick out of numerical relativity, Astrophys. J. Lett. **653**, L93 (2006), arXiv:astro-ph/0603204.

[563] F. Herrmann, I. Hinder, D. Shoemaker, and P. Laguna, Unequal Mass Binary Black Hole Plunges and Gravitational Recoil, in *New Frontiers in Numerical Relativity (NFNR 2006)* (2006) arXiv:gr-qc/0601026.

[564] M. Campanelli, C. O. Lousto, and Y. Zlochower, Spinning-black-hole binaries: The orbital hang up, Phys. Rev. D **74**, 041501 (2006), arXiv:gr-qc/0604012.

[565] I. Hinder, F. Herrmann, P. Laguna, and D. Shoemaker, Comparisons of eccentric binary black hole simulations with post-Newtonian models, Phys. Rev. D **82**, 024033 (2010), arXiv:0806.1037 [gr-qc].

[566] J. G. Baker, J. R. van Meter, S. T. McWilliams, J. Centrella, and B. J. Kelly, Consistency of post-Newtonian waveforms with numerical relativity, Phys. Rev. Lett. **99**, 181101 (2007), arXiv:gr-qc/0612024.

[567] A. Buonanno, G. B. Cook, and F. Pretorius, Inspiral, merger and ring-down of equal-mass black-hole binaries, Phys. Rev. D **75**, 124018 (2007), arXiv:gr-qc/0610122.

[568] M. Hannam, S. Husa, U. Sperhake, B. Bruegmann, and J. A. Gonzalez, Where post-Newtonian and numerical-relativity waveforms meet, Phys. Rev. D **77**, 044020 (2008), arXiv:0706.1305 [gr-qc].

[569] M. Boyle, D. A. Brown, L. E. Kidder, A. H. Mroue, H. P. Pfeiffer, M. A. Scheel, G. B. Cook, and S. A. Teukolsky, High-accuracy comparison of numerical relativity simulations with post-Newtonian expansions, Phys. Rev. D **76**, 124038 (2007), arXiv:0710.0158 [gr-qc].

[570] J. A. Gonzalez, U. Sperhake, B. Bruegmann, M. Hannam, and S. Husa, Total recoil: The Maximum kick from nonspinning black-hole binary inspiral, Phys. Rev. Lett. **98**, 091101 (2007), arXiv:gr-qc/0610154.

[571] M. Campanelli, C. O. Lousto, Y. Zlochower, and D. Merritt, Large merger recoils and spin flips from generic black-hole binaries, Astrophys. J. Lett. **659**, L5 (2007), arXiv:gr-qc/0701164.

[572] J. A. Gonzalez, M. D. Hannam, U. Sperhake, B. Bruegmann, and S. Husa, Supermassive recoil velocities for binary black-hole mergers with antialigned spins, Phys. Rev. Lett. **98**, 231101 (2007), arXiv:gr-qc/0702052.

[573] M. Campanelli, C. O. Lousto, Y. Zlochower, and D. Merritt, Maximum gravitational recoil, Phys. Rev. Lett. **98**, 231102 (2007), arXiv:gr-qc/0702133.

[574] S. Husa, J. A. Gonzalez, M. Hannam, B. Bruegmann, and U. Sperhake, Reducing phase error in long numerical binary black hole evolutions with sixth order finite differencing, Class. Quant. Grav. **25**, 105006 (2008), arXiv:0706.0740 [gr-qc].

[575] M. A. Scheel, M. Giesler, D. A. Hemberger, G. Lovelace, K. Kuper, M. Boyle, B. Szilágyi, and L. E. Kidder, Improved methods for simulating nearly extremal binary black holes, Class. Quant. Grav. **32**, 105009 (2015), arXiv:1412.1803 [gr-qc].

[576] B. Szilágyi, J. Blackman, A. Buonanno, A. Taracchini, H. P. Pfeiffer, M. A. Scheel, T. Chu, L. E. Kidder, and Y. Pan, Approaching the Post-Newtonian Regime with Numerical Relativity: A Compact-Object Binary Simulation Spanning 350 Gravitational-Wave Cycles, Phys. Rev. Lett. **115**, 031102 (2015), arXiv:1502.04953 [gr-qc].

[577] B. Aylott *et al.*, Status of NINJA: The Numerical INJection Analysis project, Class. Quant. Grav. **26**, 114008 (2009), arXiv:0905.4227 [gr-qc].

[578] P. Ajith *et al.*, The NINJA-2 catalog of hybrid post-Newtonian/numerical-relativity waveforms for non-precessing black-hole binaries, Class. Quant. Grav. **29**, 124001 (2012), [Erratum: Class.Quant.Grav. 30, 199401 (2013)], arXiv:1201.5319 [gr-qc].

[579] I. Hinder *et al.*, Error-analysis and comparison to analytical models of numerical waveforms produced by the NRAR Collaboration, Class. Quant. Grav. **31**, 025012 (2014), arXiv:1307.5307 [gr-qc].

[580] M. Hannam *et al.*, The Samurai Project: Verifying the consistency of black-hole-binary waveforms for gravitational-wave detection, Phys. Rev. D **79**, 084025 (2009), arXiv:0901.2437 [gr-qc].

[581] J. Blackman, S. E. Field, M. A. Scheel, C. R. Galley, C. D. Ott, M. Boyle, L. E. Kidder, H. P. Pfeiffer, and B. Szilágyi, Numerical relativity waveform surrogate model for generically precessing binary black hole mergers, Phys. Rev. D **96**, 024058 (2017), arXiv:1705.07089 [gr-qc].

[582] V. Varma, S. E. Field, M. A. Scheel, J. Blackman, D. Gerosa, L. C. Stein, L. E. Kidder, and H. P. Pfeiffer, Surrogate models for precessing binary black hole simulations with unequal masses, Phys. Rev. Research. **1**, 033015 (2019), arXiv:1905.09300 [gr-qc].

[583] P. Schmidt, I. W. Harry, and H. P. Pfeiffer, Numerical Relativity Injection Infrastructure, arXiv:1703.01076 [gr-qc].

[584] J. Aasi *et al.* (LIGO Scientific, VIRGO, NINJA-2), The NINJA-2 project: Detecting and characterizing gravitational waveforms modelled using numerical binary black hole simulations, Class. Quant. Grav. **31**, 115004 (2014), arXiv:1401.0939 [gr-qc].

[585] B. P. Abbott *et al.* (LIGO Scientific, Virgo), Effects of waveform model systematics on the interpretation of GW150914, Class. Quant. Grav. **34**, 104002 (2017), arXiv:1611.07531 [gr-qc].

[586] B. P. Abbott *et al.* (LIGO Scientific, Virgo), Directly comparing GW150914 with numerical solutions of Einstein's equations for binary black hole coalescence, Phys. Rev. D **94**, 064035 (2016), arXiv:1606.01262 [gr-qc].

[587] J. Lange *et al.*, Parameter estimation method that directly compares gravitational wave observations to numerical relativity, Phys. Rev. D **96**, 104041 (2017), arXiv:1705.09833 [gr-qc].

[588] V. Gayathri, J. Healy, J. Lange, B. O'Brien, M. Szczepanczyk, I. Bartos, M. Campanelli, S. Klimenko, C. O. Lousto, and R. O'Shaughnessy, Eccentricity estimate for black hole mergers with numerical relativity simulations, Nature Astron. **6**, 344 (2022), arXiv:2009.05461 [astro-ph.HE].

[589] E. Barausse and L. Rezzolla, Predicting the direction of the final spin from the coalescence of two black holes, Astrophys. J. Lett. **704**, L40 (2009), arXiv:0904.2577 [gr-qc].

[590] J. Healy, C. O. Lousto, and Y. Zlochower, Remnant mass, spin, and recoil from spin aligned black-hole binaries, Phys. Rev. D **90**, 104004 (2014), arXiv:1406.7295 [gr-qc].

[591] F. Hofmann, E. Barausse, and L. Rezzolla, The final spin from binary black holes in quasi-circular orbits, Astrophys. J. Lett. **825**, L19 (2016), arXiv:1605.01938 [gr-qc].

[592] J. Healy and C. O. Lousto, Remnant of binary black-hole mergers: New simulations and peak luminosity studies, Phys. Rev. D **95**, 024037 (2017), arXiv:1610.09713 [gr-qc].

[593] J. Healy and C. O. Lousto, Hangup effect in unequal mass binary black hole mergers and further studies of their gravitational radiation and remnant properties, Phys. Rev. D **97**, 084002 (2018), arXiv:1801.08162 [gr-qc].

[594] V. Varma, D. Gerosa, L. C. Stein, F. Hébert, and H. Zhang, High-accuracy mass, spin, and recoil predictions of generic black-hole merger remnants, Phys. Rev. Lett. **122**, 011101 (2019), arXiv:1809.09125 [gr-qc].

[595] R. Cotesta, G. Carullo, E. Berti, and V. Cardoso, Analysis of Ringdown Overtones in GW150914, Phys. Rev. Lett. **129**, 111102 (2022), arXiv:2201.00822 [gr-qc].

[596] R. Abbott *et al.* (LIGO Scientific, Virgo), Tests of general relativity with binary black holes from the second LIGO-Virgo gravitational-wave transient catalog, Phys. Rev. D **103**, 122002 (2021), arXiv:2010.14529 [gr-qc].

[597] R. Abbott *et al.* (LIGO Scientific, VIRGO, KAGRA), Tests of General Relativity with GWTC-3, arXiv:2112.06861 [gr-qc].

[598] A. Ghosh, R. Brito, and A. Buonanno, Constraints on quasinormal-mode frequencies with LIGO-Virgo binary–black-hole observations, Phys. Rev. D **103**, 124041 (2021), arXiv:2104.01906 [gr-qc].

[599] T. Islam, Applying higher-modes consistency test on GW190814 : lessons on no-hair theorem, nature of the secondary compact object and waveform modeling, arXiv:2111.00111 [gr-qc].

[600] C. D. Capano, M. Cabero, J. Westerweck, J. Abedi, S. Kastha, A. H. Nitz, Y.-F. Wang, A. B. Nielsen, and B. Krishnan, A multimode quasi-normal spectrum from a perturbed black hole, arXiv:2105.05238 [gr-qc].

[601] E. Finch and C. J. Moore, Searching for a ringdown overtone in GW150914, Phys. Rev. D **106**, 043005 (2022), arXiv:2205.07809 [gr-qc].

[602] M. Isi, W. M. Farr, M. Giesler, M. A. Scheel, and S. A. Teukolsky, Testing the Black-Hole Area Law with GW150914, Phys. Rev. Lett. **127**, 011103 (2021), arXiv:2012.04486 [gr-qc].

[603] D. Gerosa, C. M. Fabbri, and U. Sperhake, The irreducible mass and the horizon area of LIGO's black holes, Class. Quant. Grav. **39**, 175008 (2022), arXiv:2202.08848 [gr-qc].

[604] E. Berti, V. Cardoso, and C. M. Will, On gravitational-wave spectroscopy of massive black holes

169

with the space interferometer LISA, Phys. Rev. D **73**, 064030 (2006), arXiv:gr-qc/0512160.

[605] Z.-j. Cao, H.-J. Yo, and J.-P. Yu, A Reinvestigation of Moving Punctured Black Holes with a New Code, Phys. Rev. D **78**, 124011 (2008), arXiv:0812.0641 [gr-qc].

[606] Z. Cao, P. Galaviz, and L.-F. Li, Binary black hole mergers in $f(R)$ theory, Phys. Rev. D **87**, 104029 (2013), arXiv:1608.07816 [gr-qc].

[607] Z. Cao and D. Hilditch, Numerical stability of the Z4c formulation of general relativity, Phys. Rev. D **85**, 124032 (2012), arXiv:1111.2177 [gr-qc].

[608] B. Bruegmann, J. A. Gonzalez, M. Hannam, S. Husa, U. Sperhake, and W. Tichy, Calibration of Moving Puncture Simulations, Phys. Rev. D **77**, 024027 (2008), arXiv:gr-qc/0610128.

[609] M. Thierfelder, S. Bernuzzi, and B. Bruegmann, Numerical relativity simulations of binary neutron stars, Phys. Rev. D **84**, 044012 (2011), arXiv:1104.4751 [gr-qc].

[610] T. Dietrich, S. Bernuzzi, M. Ujevic, and B. Brügmann, Numerical relativity simulations of neutron star merger remnants using conservative mesh refinement, Phys. Rev. D **91**, 124041 (2015), arXiv:1504.01266 [gr-qc].

[611] T. Dietrich, D. Radice, S. Bernuzzi, F. Zappa, A. Perego, B. Brügmann, S. V. Chaurasia, R. Dudi, W. Tichy, and M. Ujevic, CoRe database of binary neutron star merger waveforms, Class. Quant. Grav. **35**, 24LT01 (2018), arXiv:1806.01625 [gr-qc].

[612] A. Gonzalez *et al.*, Second release of the CoRe database of binary neutron star merger waveforms, Class. Quant. Grav. **40**, 085011 (2023), arXiv:2210.16366 [gr-qc].

[613] M. Bugner, T. Dietrich, S. Bernuzzi, A. Weyhausen, and B. Brügmann, Solving 3D relativistic hydrodynamical problems with weighted essentially nonoscillatory discontinuous Galerkin methods, Phys. Rev. D **94**, 084004 (2016), arXiv:1508.07147 [gr-qc].

[614] D. Hilditch, A. Weyhausen, and B. Brügmann, Pseudospectral method for gravitational wave collapse, Phys. Rev. D **93**, 063006 (2016), arXiv:1504.04732 [gr-qc].

[615] S. Renkhoff, D. Cors, D. Hilditch, and B. Brügmann, Adaptive hp refinement for spectral elements in numerical relativity, Phys. Rev. D **107**, 104043 (2023), arXiv:2302.00575 [gr-qc].

[616] G. Doulis, J. Frauendiener, C. Stevens, and B. Whale, COFFEE – An MPI-parallelized Python package for the numerical evolution of differential equations, SoftwareX **10**, 100283 (2019), arXiv:1903.12482 [cs.MS].

[617] J. Frauendiener and C. Stevens, The non-linear perturbation of a black hole by gravitational waves. I. The Bondi–Sachs mass loss, Class. Quant. Grav. **38**, 194002 (2021), arXiv:2105.09515 [gr-qc].

[618] M. Fernando, D. Neilsen, H. Lim, E. Hirschmann, and H. Sundar, Massively Parallel Simulations of Binary Black Hole Intermediate-Mass-Ratio Inspirals, SIAM J. Sci. Comput. **41**, C97 (2019), arXiv:1807.06128 [gr-qc].

[619] M. Fernando, D. Neilsen, Y. Zlochower, E. W. Hirschmann, and H. Sundar, Massively parallel simulations of binary black holes with adaptive wavelet multiresolution, Phys. Rev. D **107**, 064035 (2023), arXiv:2211.11575 [gr-qc].

[620] F. Loffler *et al.*, The Einstein Toolkit: A Community Computational Infrastructure for Relativistic Astrophysics, Class. Quant. Grav. **29**, 115001 (2012), arXiv:1111.3344 [gr-qc].

[621] Einstein Toolkit.

[622] H. Witek, L. Gualtieri, P. Pani, and T. P. Sotiriou, Black holes and binary mergers in scalar Gauss-Bonnet gravity: scalar field dynamics, Phys. Rev. D **99**, 064035 (2019), arXiv:1810.05177 [gr-qc].

[623] Z. B. Etienne, V. Paschalidis, R. Haas, P. Mösta, and S. L. Shapiro, IllinoisGRMHD: An Open-Source, User-Friendly GRMHD Code for Dynamical Spacetimes, Class. Quant. Grav. **32**, 175009 (2015), arXiv:1501.07276 [astro-ph.HE].

[624] Y. Zlochower, J. G. Baker, M. Campanelli, and C. O. Lousto, Accurate black hole evolutions by fourth-order numerical relativity, Phys. Rev. D **72**, 024021 (2005), arXiv:gr-qc/0505055.

[625] J. Healy, C. O. Lousto, Y. Zlochower, and M. Campanelli, The RIT binary black hole simulations catalog, Class. Quant. Grav. **34**, 224001 (2017), arXiv:1703.03423 [gr-qc].

[626] J. Healy, C. O. Lousto, J. Lange, R. O'Shaughnessy, Y. Zlochower, and M. Campanelli, Second RIT binary black hole simulations catalog and its application to gravitational waves parameter estimation, Phys. Rev. D **100**, 024021 (2019), arXiv:1901.02553 [gr-qc].

[627] J. Healy and C. O. Lousto, Third RIT binary black hole simulations catalog, Phys. Rev. D **102**, 104018 (2020), arXiv:2007.07910 [gr-qc].

[628] J. Healy and C. O. Lousto, Fourth RIT binary black hole simulations catalog: Extension to eccentric orbits, Phys. Rev. D **105**, 124010 (2022), arXiv:2202.00018 [gr-qc].

[629] U. Sperhake, Binary black-hole evolutions of excision and puncture data, Phys. Rev. D **76**, 104015 (2007), arXiv:gr-qc/0606079.

[630] E. Berti, V. Cardoso, L. Gualtieri, M. Horbatsch, and U. Sperhake, Numerical simulations of single and binary black holes in scalar-tensor theories: circumventing the no-hair theorem, Phys. Rev. D **87**, 124020 (2013), arXiv:1304.2836 [gr-qc].

[631] K. Jani, J. Healy, J. A. Clark, L. London, P. Laguna, and D. Shoemaker, Georgia Tech Catalog of Gravitational Waveforms, Class. Quant. Grav. **33**, 204001 (2016), arXiv:1605.03204 [gr-qc].

[632] I. Ruchlin, Z. B. Etienne, and T. W. Baumgarte, SENR/NRPy+: Numerical Relativity in Singular Curvilinear Coordinate Systems, Phys. Rev. D **97**, 064036 (2018), arXiv:1712.07658 [gr-qc].

[633] V. Mewes, Y. Zlochower, M. Campanelli, I. Ruchlin, Z. B. Etienne, and T. W. Baumgarte, Numerical relativity in spherical coordinates with the Einstein Toolkit, Phys. Rev. D **97**, 084059 (2018), arXiv:1802.09625 [gr-qc].

[634] V. Mewes, Y. Zlochower, M. Campanelli, T. W. Baumgarte, Z. B. Etienne, F. G. Lopez Armengol, and F. Cipolletta, Numerical relativity in spherical coordinates: A new dynamical spacetime and general relativistic MHD evolution framework for the Einstein Toolkit, Phys. Rev. D **101**, 104007 (2020), arXiv:2002.06225 [gr-qc].

[635] F. Cipolletta, J. V. Kalinani, B. Giacomazzo, and R. Ciolfi, Spritz: a new fully general-relativistic magnetohydrodynamic code, Class. Quant. Grav. **37**, 135010 (2020), arXiv:1912.04794 [astro-ph.HE].

[636] The Spritz Code, https://zenodo.org/record/4350072.

[637] D. Radice and L. Rezzolla, THC: a new high-order finite-difference high-resolution shock-capturing code for special-relativistic hydrodynamics, Astron. Astrophys. **547**, A26 (2012), arXiv:1206.6502 [astro-ph.IM].

[638] D. Radice, L. Rezzolla, and F. Galeazzi, Beyond second-order convergence in simulations of binary neutron stars in full general-relativity, Mon. Not. Roy. Astron. Soc. **437**, L46 (2014), arXiv:1306.6052 [gr-qc].

[639] D. Radice, L. Rezzolla, and F. Galeazzi, High-Order Fully General-Relativistic Hydrodynamics: new Approaches and Tests, Class. Quant. Grav. **31**, 075012 (2014), arXiv:1312.5004 [gr-qc].

[640] B. Giacomazzo and L. Rezzolla, WhiskyMHD: A New numerical code for general relativistic magnetohydrodynamics, Class. Quant. Grav. **24**, S235 (2007), arXiv:gr-qc/0701109.

[641] Whiskymhd waveforms.

[642] S. Köppel, Towards an exascale code for GRMHD on dynamical spacetimes, J. Phys. Conf. Ser. **1031**, 012017 (2018), arXiv:1711.08221 [gr-qc].

[643] E. R. Most, L. J. Papenfort, and L. Rezzolla, Beyond second-order convergence in simulations of magnetized binary neutron stars with realistic microphysics, Mon. Not. Roy. Astron. Soc. **490**, 3588 (2019), arXiv:1907.10328 [astro-ph.HE].

[644] B. Daszuta, F. Zappa, W. Cook, D. Radice, S. Bernuzzi, and V. Morozova, GR-Athena++: Puncture Evolutions on Vertex-centered Oct-tree Adaptive Mesh Refinement, Astrophys. J. Supp. **257**, 25 (2021), arXiv:2101.08289 [gr-qc].

[645] K. Clough, P. Figueras, H. Finkel, M. Kunesch, E. A. Lim, and S. Tunyasuvunakool, GRChombo : Numerical Relativity with Adaptive Mesh Refinement, Class. Quant. Grav. **32**, 245011 (2015), arXiv:1503.03436 [gr-qc].

[646] GRChombo a new AMR based open-source code for numerical-relativity simulations, https:

//www.grchombo.org.

[647] T. Andrade *et al.*, GRChombo: An adaptable numerical relativity code for fundamental physics, J. Open Source Softw. **6**, 3703 (2021), arXiv:2201.03458 [gr-qc].

[648] http://had.liu.edu/.

[649] S. L. Liebling, The Singularity threshold of the nonlinear sigma model using 3-D adaptive mesh refinement, Phys. Rev. D **66**, 041703 (2002), arXiv:gr-qc/0202093.

[650] L. Lehner, S. L. Liebling, and O. Reula, AMR, stability and higher accuracy, Class. Quant. Grav. **23**, S421 (2006), arXiv:gr-qc/0510111.

[651] Z. B. Etienne, Y. T. Liu, and S. L. Shapiro, Relativistic magnetohydrodynamics in dynamical spacetimes: A new AMR implementation, Phys. Rev. D **82**, 084031 (2010), arXiv:1007.2848 [astro-ph.HE].

[652] L. Sun, M. Ruiz, S. L. Shapiro, and A. Tsokaros, Jet launching from binary neutron star mergers: Incorporating neutrino transport and magnetic fields, Phys. Rev. D **105**, 104028 (2022), arXiv:2202.12901 [astro-ph.HE].

[653] P. Chang and Z. Etienne, General relativistic hydrodynamics on a moving-mesh I: static space–times, Mon. Not. Roy. Astron. Soc. **496**, 206 (2020), arXiv:2002.09613 [gr-qc].

[654] BH@Home, https://blackholesathome.net/.

[655] C. Palenzuela, B. Miñano, D. Viganò, A. Arbona, C. Bona-Casas, A. Rigo, M. Bezares, C. Bona, and J. Massó, A Simflowny-based finite-difference code for high-performance computing in numerical relativity, Class. Quant. Grav. **35**, 185007 (2018), arXiv:1806.04182 [physics.comp-ph].

[656] S. L. Liebling, C. Palenzuela, and L. Lehner, Toward fidelity and scalability in non-vacuum mergers, Class. Quant. Grav. **37**, 135006 (2020), arXiv:2002.07554 [gr-qc].

[657] T. Yamamoto, M. Shibata, and K. Taniguchi, Simulating coalescing compact binaries by a new code SACRA, Phys. Rev. D **78**, 064054 (2008), arXiv:0806.4007 [gr-qc].

[658] K. Kiuchi, K. Kawaguchi, K. Kyutoku, Y. Sekiguchi, M. Shibata, and K. Taniguchi, Sub-radian-accuracy gravitational waveforms of coalescing binary neutron stars in numerical relativity, Phys. Rev. D **96**, 084060 (2017), arXiv:1708.08926 [astro-ph.HE].

[659] H.-J. Kuan, A. T.-L. Lam, D. D. Doneva, S. S. Yazadjiev, M. Shibata, and K. Kiuchi, Dynamical scalarization during neutron star mergers in scalar-Gauss-Bonnet theory, Phys. Rev. D **108**, 063033 (2023), arXiv:2302.11596 [gr-qc].

[660] M. Shibata and D. Traykova, Properties of scalar wave emission in a scalar-tensor theory with kinetic screening, Phys. Rev. D **107**, 044068 (2023), arXiv:2210.12139 [gr-qc].

[661] M. Shibata and H. Yoshino, Bar-mode instability of rapidly spinning black hole in higher dimensions: Numerical simulation in general relativity, Phys. Rev. D **81**, 104035 (2010), arXiv:1004.4970 [gr-qc].

[662] http://www2.yukawa.kyoto-u.ac.jp/~nr_kyoto/SACRA_PUB/catalog.html.

[663] S. Fujibayashi, K. Kiuchi, N. Nishimura, Y. Sekiguchi, and M. Shibata, Mass Ejection from the Remnant of a Binary Neutron Star Merger: Viscous-Radiation Hydrodynamics Study, Astrophys. J. **860**, 64 (2018), arXiv:1711.02093 [astro-ph.HE].

[664] M. Shibata, S. Fujibayashi, and Y. Sekiguchi, Long-term evolution of neutron-star merger remnants in general relativistic resistive magnetohydrodynamics with a mean-field dynamo term, Phys. Rev. D **104**, 063026 (2021), arXiv:2109.08732 [astro-ph.HE].

[665] The Spectral Einstein Code, http://www.black-holes.org/SpEC.html.

[666] http://www.black-holes.org/waveforms.

[667] L. E. Kidder *et al.*, SpECTRE: A Task-based Discontinuous Galerkin Code for Relativistic Astrophysics, J. Comput. Phys. **335**, 84 (2017), arXiv:1609.00098 [astro-ph.HE].

[668] N. Deppe, W. Throwe, L. E. Kidder, N. L. Vu, F. Hébert, J. Moxon, C. Armaza, M. S. Bonilla, Y. Kim, P. Kumar, G. Lovelace, A. Macedo, K. C. Nelli, E. O'Shea, H. P. Pfeiffer, M. A. Scheel, S. A. Teukolsky, N. A. Wittek, *et al.*, SpECTRE v2023.04.07, 10.5281/zenodo.7809262 (2023).

172

[669] S. Rosswog and P. Diener, SPHINCS_BSSN: A general relativistic Smooth Particle Hydrodynamics code for dynamical spacetimes, Class. Quant. Grav. **38**, 115002 (2021), arXiv:2012.13954 [gr-qc].

[670] J. G. Baker, M. Campanelli, F. Pretorius, and Y. Zlochower, Comparisons of binary black hole merger waveforms, Class. Quant. Grav. **24**, S25 (2007), arXiv:gr-qc/0701016.

[671] G. Lovelace *et al.*, Modeling the source of GW150914 with targeted numerical-relativity simulations, Class. Quant. Grav. **33**, 244002 (2016), arXiv:1607.05377 [gr-qc].

[672] Y. Zlochower, M. Ponce, and C. O. Lousto, Accuracy Issues for Numerical Waveforms, Phys. Rev. D **86**, 104056 (2012), arXiv:1208.5494 [gr-qc].

[673] K. Mitman *et al.*, Fixing the BMS frame of numerical relativity waveforms, Phys. Rev. D **104**, 024051 (2021), arXiv:2105.02300 [gr-qc].

[674] G. B. Cook, Three-dimensional initial data for the collision of two black holes. 2: Quasicircular orbits for equal mass black holes, Phys. Rev. D **50**, 5025 (1994), arXiv:gr-qc/9404043.

[675] G. B. Cook, Initial data for numerical relativity, Living Rev. Rel. **3**, 5 (2000), arXiv:gr-qc/0007085.

[676] H. P. Pfeiffer, *Initial data for black hole evolutions*, Ph.D. thesis, Cornell U. (2005), arXiv:gr-qc/0510016.

[677] E. Gourgoulhon, Construction of initial data for 3+1 numerical relativity, J. Phys. Conf. Ser. **91**, 012001 (2007), arXiv:0704.0149 [gr-qc].

[678] G. Lovelace, Reducing spurious gravitational radiation in binary-black-hole simulations by using conformally curved initial data, Class. Quant. Grav. **26**, 114002 (2009), arXiv:0812.3132 [gr-qc].

[679] J. Healy, C. O. Lousto, I. Ruchlin, and Y. Zlochower, Evolutions of unequal mass, highly spinning black hole binaries, Phys. Rev. D **97**, 104026 (2018), arXiv:1711.09041 [gr-qc].

[680] Y. Zlochower, J. Healy, C. O. Lousto, and I. Ruchlin, Evolutions of Nearly Maximally Spinning Black Hole Binaries Using the Moving Puncture Approach, Phys. Rev. D **96**, 044002 (2017), arXiv:1706.01980 [gr-qc].

[681] U. Sperhake, V. Cardoso, C. D. Ott, E. Schnetter, and H. Witek, Extreme black hole simulations: collisions of unequal mass black holes and the point particle limit, Phys. Rev. D **84**, 084038 (2011), arXiv:1105.5391 [gr-qc].

[682] C. O. Lousto and J. Healy, Study of the intermediate mass ratio black hole binary merger up to 1000:1 with numerical relativity, Class. Quant. Grav. **40**, 09LT01 (2023), arXiv:2203.08831 [gr-qc].

[683] C. O. Lousto and J. Healy, Exploring the Small Mass Ratio Binary Black Hole Merger via Zeno's Dichotomy Approach, Phys. Rev. Lett. **125**, 191102 (2020), arXiv:2006.04818 [gr-qc].

[684] N. Rosato, J. Healy, and C. O. Lousto, Adapted gauge to small mass ratio binary black hole evolutions, Phys. Rev. D **103**, 104068 (2021), arXiv:2103.09326 [gr-qc].

[685] M. Dhesi, H. R. Rüter, A. Pound, L. Barack, and H. P. Pfeiffer, Worldtube excision method for intermediate-mass-ratio inspirals: Scalar-field toy model, Phys. Rev. D **104**, 124002 (2021), arXiv:2109.03531 [gr-qc].

[686] N. A. Wittek *et al.*, Worldtube excision method for intermediate-mass-ratio inspirals: Scalar-field model in 3+1 dimensions, Phys. Rev. D **108**, 024041 (2023), arXiv:2304.05329 [gr-qc].

[687] F. Antonini, S. Chatterjee, C. L. Rodriguez, M. Morscher, B. Pattabiraman, V. Kalogera, and F. A. Rasio, Black hole mergers and blue stragglers from hierarchical triples formed in globular clusters, Astrophys. J. **816**, 65 (2016), arXiv:1509.05080 [astro-ph.GA].

[688] G. Fragione and B. Kocsis, Effective spin distribution of black hole mergers in triples, Mon. Not. Roy. Astron. Soc. **493**, 3920 (2020), arXiv:1910.00407 [astro-ph.GA].

[689] G. Fragione, N. Leigh, and R. Perna, Black hole and neutron star mergers in Galactic Nuclei: the role of triples, Mon. Not. Roy. Astron. Soc. **488**, 2825 (2019), arXiv:1903.09160 [astro-ph.GA].

[690] L. Gondán and B. Kocsis, High eccentricities and high masses characterize gravitational-wave captures in galactic nuclei as seen by Earth-based detectors, Mon. Not. Roy. Astron. Soc. **506**,

1665 (2021), arXiv:2011.02507 [astro-ph.HE].

[691] C. L. Rodriguez, P. Amaro-Seoane, S. Chatterjee, K. Kremer, F. A. Rasio, J. Samsing, C. S. Ye, and M. Zevin, Post-Newtonian Dynamics in Dense Star Clusters: Formation, Masses, and Merger Rates of Highly-Eccentric Black Hole Binaries, Phys. Rev. D **98**, 123005 (2018), arXiv:1811.04926 [astro-ph.HE].

[692] G. Fragione and O. Bromberg, Eccentric binary black hole mergers in globular clusters hosting intermediate-mass black holes, Mon. Not. Roy. Astron. Soc. **488**, 4370 (2019), arXiv:1903.09659 [astro-ph.GA].

[693] J. Samsing, I. Bartos, D. J. D'Orazio, Z. Haiman, B. Kocsis, N. W. C. Leigh, B. Liu, M. E. Pessah, and H. Tagawa, AGN as potential factories for eccentric black hole mergers, Nature **603**, 237 (2022), arXiv:2010.09765 [astro-ph.HE].

[694] C. L. Rodriguez, P. Amaro-Seoane, S. Chatterjee, and F. A. Rasio, Post-Newtonian Dynamics in Dense Star Clusters: Highly-Eccentric, Highly-Spinning, and Repeated Binary Black Hole Mergers, Phys. Rev. Lett. **120**, 151101 (2018), arXiv:1712.04937 [astro-ph.HE].

[695] I. Hinder, B. Vaishnav, F. Herrmann, D. Shoemaker, and P. Laguna, Universality and final spin in eccentric binary black hole inspirals, Phys. Rev. D **77**, 081502 (2008), arXiv:0710.5167 [gr-qc].

[696] J. Healy, J. Levin, and D. Shoemaker, Zoom-Whirl Orbits in Black Hole Binaries, Phys. Rev. Lett. **103**, 131101 (2009), arXiv:0907.0671 [gr-qc].

[697] R. Gold and B. Brügmann, Eccentric black hole mergers and zoom-whirl behavior from elliptic inspirals to hyperbolic encounters, Phys. Rev. D **88**, 064051 (2013), arXiv:1209.4085 [gr-qc].

[698] R. Gold and B. Bruegmann, Radiation from low-momentum zoom-whirl orbits, Class. Quant. Grav. **27**, 084035 (2010), arXiv:0911.3862 [gr-qc].

[699] E. A. Huerta *et al.*, Physics of eccentric binary black hole mergers: A numerical relativity perspective, Phys. Rev. D **100**, 064003 (2019), arXiv:1901.07038 [gr-qc].

[700] E. A. Huerta *et al.*, Complete waveform model for compact binaries on eccentric orbits, Phys. Rev. D **95**, 024038 (2017), arXiv:1609.05933 [gr-qc].

[701] A. Ramos-Buades, S. Husa, G. Pratten, H. Estellés, C. García-Quirós, M. Mateu-Lucena, M. Colleoni, and R. Jaume, First survey of spinning eccentric black hole mergers: Numerical relativity simulations, hybrid waveforms, and parameter estimation, Phys. Rev. D **101**, 083015 (2020), arXiv:1909.11011 [gr-qc].

[702] I. Hinder, L. E. Kidder, and H. P. Pfeiffer, Eccentric binary black hole inspiral-merger-ringdown gravitational waveform model from numerical relativity and post-Newtonian theory, Phys. Rev. D **98**, 044015 (2018), arXiv:1709.02007 [gr-qc].

[703] E. A. Huerta *et al.*, Eccentric, nonspinning, inspiral, Gaussian-process merger approximant for the detection and characterization of eccentric binary black hole mergers, Phys. Rev. D **97**, 024031 (2018), arXiv:1711.06276 [gr-qc].

[704] Z. Cao and W.-B. Han, Waveform model for an eccentric binary black hole based on the effective-one-body-numerical-relativity formalism, Phys. Rev. D **96**, 044028 (2017), arXiv:1708.00166 [gr-qc].

[705] D. Chiaramello and A. Nagar, Faithful analytical effective-one-body waveform model for spin-aligned, moderately eccentric, coalescing black hole binaries, Phys. Rev. D **101**, 101501 (2020), arXiv:2001.11736 [gr-qc].

[706] X. Liu, Z. Cao, and L. Shao, Validating the Effective-One-Body Numerical-Relativity Waveform Models for Spin-aligned Binary Black Holes along Eccentric Orbits, Phys. Rev. D **101**, 044049 (2020), arXiv:1910.00784 [gr-qc].

[707] T. Islam, V. Varma, J. Lodman, S. E. Field, G. Khanna, M. A. Scheel, H. P. Pfeiffer, D. Gerosa, and L. E. Kidder, Eccentric binary black hole surrogate models for the gravitational waveform and remnant properties: comparable mass, nonspinning case, Phys. Rev. D **103**, 064022 (2021), arXiv:2101.11798 [gr-qc].

[708] A. Ramos-Buades, M. van de Meent, H. P. Pfeiffer, H. R. Rüter, M. A. Scheel, M. Boyle,

and L. E. Kidder, Eccentric binary black holes: Comparing numerical relativity and small mass-ratio perturbation theory, Phys. Rev. D **106**, 124040 (2022), arXiv:2209.03390 [gr-qc].

[709] J. Healy, F. Herrmann, I. Hinder, D. M. Shoemaker, P. Laguna, and R. A. Matzner, Superkicks in Hyperbolic Encounters of Binary Black Holes, Phys. Rev. Lett. **102**, 041101 (2009), arXiv:0807.3292 [gr-qc].

[710] S. Jaraba and J. Garcia-Bellido, Black hole induced spins from hyperbolic encounters in dense clusters, Phys. Dark Univ. **34**, 100882 (2021), arXiv:2106.01436 [gr-qc].

[711] S. Hopper, A. Nagar, and P. Rettegno, Strong-field scattering of two spinning black holes: Numerics versus analytics, Phys. Rev. D **107**, 124034 (2023), arXiv:2204.10299 [gr-qc].

[712] T. Andrade *et al.*, Towards numerical-relativity informed effective-one-body waveforms for dynamical capture black hole binaries, arXiv:2307.08697 [gr-qc].

[713] A. H. Mroue, H. P. Pfeiffer, L. E. Kidder, and S. A. Teukolsky, Measuring orbital eccentricity and periastron advance in quasi-circular black hole simulations, Phys. Rev. D **82**, 124016 (2010), arXiv:1004.4697 [gr-qc].

[714] S. Habib and E. A. Huerta, Characterization of numerical relativity waveforms of eccentric binary black hole mergers, Phys. Rev. D **100**, 044016 (2019), arXiv:1904.09295 [gr-qc].

[715] A. Ciarfella, J. Healy, C. O. Lousto, and H. Nakano, Eccentricity estimation from initial data for numerical relativity simulations, Phys. Rev. D **106**, 104035 (2022), arXiv:2206.13532 [gr-qc].

[716] M. A. Shaikh, V. Varma, H. P. Pfeiffer, A. Ramos-Buades, and M. van de Meent, Defining eccentricity for gravitational wave astronomy, arXiv:2302.11257 [gr-qc].

[717] J. A. Gonzalez, U. Sperhake, and B. Bruegmann, Black-hole binary simulations: The Mass ratio 10:1, Phys. Rev. D **79**, 124006 (2009), arXiv:0811.3952 [gr-qc].

[718] C. O. Lousto and Y. Zlochower, Orbital Evolution of Extreme-Mass-Ratio Black-Hole Binaries with Numerical Relativity, Phys. Rev. Lett. **106**, 041101 (2011), arXiv:1009.0292 [gr-qc].

[719] S. Khan, S. Husa, M. Hannam, F. Ohme, M. Pürrer, X. Jiménez Forteza, and A. Bohé, Frequency-domain gravitational waves from nonprecessing black-hole binaries. II. A phenomenological model for the advanced detector era, Phys. Rev. D **93**, 044007 (2016), arXiv:1508.07253 [gr-qc].

[720] Y. T. Liu, Z. B. Etienne, and S. L. Shapiro, Evolution of near-extremal-spin black holes using the moving puncture technique, Phys. Rev. D **80**, 121503 (2009), arXiv:1001.4077 [gr-qc].

[721] T. Bode, R. Haas, T. Bogdanovic, P. Laguna, and D. Shoemaker, Relativistic Mergers of Supermassive Black Holes and their Electromagnetic Signatures, Astrophys. J. **715**, 1117 (2010), arXiv:0912.0087 [gr-qc].

[722] J. M. Fedrow, C. D. Ott, U. Sperhake, J. Blackman, R. Haas, C. Reisswig, and A. De Felice, Gravitational Waves from Binary Black Hole Mergers inside Stars, Phys. Rev. Lett. **119**, 171103 (2017), arXiv:1704.07383 [astro-ph.HE].

[723] A. Smith, V. Bromm, and A. Loeb, The first supermassive black holes, Astronomy and Geophysics **58**, 3.22 (2017), arXiv:1703.03083 [astro-ph.GA].

[724] M. Shibata, Y. T. Liu, S. L. Shapiro, and B. C. Stephens, Magnetorotational collapse of massive stellar cores to neutron stars: Simulations in full general relativity, Phys. Rev. D **74**, 104026 (2006), arXiv:astro-ph/0610840.

[725] M. Shibata, Y. Sekiguchi, H. Uchida, and H. Umeda, Gravitational waves from supermassive stars collapsing to a supermassive black hole, Phys. Rev. D **94**, 021501 (2016), arXiv:1606.07147 [astro-ph.HE].

[726] L. Sun, V. Paschalidis, M. Ruiz, and S. L. Shapiro, Magnetorotational Collapse of Supermassive Stars: Black Hole Formation, Gravitational Waves and Jets, Phys. Rev. D **96**, 043006 (2017), arXiv:1704.04502 [astro-ph.HE].

[727] J. C. B. Papaloizou and J. E. Pringle, The dynamical stability of differentially rotating discs with constant specific angular momentum, MNRAS **208**, 721 (1984).

[728] K. Kiuchi, M. Shibata, P. J. Montero, and J. A. Font, Gravitational waves from the Papaloizou-Pringle instability in black hole-torus systems, Phys. Rev. Lett. **106**, 251102

(2011), arXiv:1105.5035 [astro-ph.HE].

[729] E. Wessel, V. Paschalidis, A. Tsokaros, M. Ruiz, and S. L. Shapiro, Gravitational Waves from Disks Around Spinning Black Holes: Simulations in Full General Relativity, Phys. Rev. D **103**, 043013 (2021), arXiv:2011.04077 [astro-ph.HE].

[730] B. Schutz, Discussion on emri/imri using numerical relativity. (2017), 20th Capra Meeting.

[731] Black Hole Perturbation Toolkit, (bhptoolkit.org) ().

[732] J. M. Bowen and J. W. York, Jr., Time asymmetric initial data for black holes and black hole collisions, Phys. Rev. D **21**, 2047 (1980).

[733] G. B. Cook and J. W. York, Jr., Apparent Horizons for Boosted or Spinning Black Holes, Phys. Rev. D **41**, 1077 (1990).

[734] S. Dain, C. O. Lousto, and R. Takahashi, New conformally flat initial data for spinning black holes, Phys. Rev. D **65**, 104038 (2002), arXiv:gr-qc/0201062.

[735] G. Lovelace, M. A. Scheel, and B. Szilagyi, Simulating merging binary black holes with nearly extremal spins, Phys. Rev. D **83**, 024010 (2011), arXiv:1010.2777 [gr-qc].

[736] P. J. Armitage and P. Natarajan, Eccentricity of supermassive black hole binaries coalescing from gas rich mergers, Astrophys. J. **634**, 921 (2005), arXiv:astro-ph/0508493.

[737] A. V. Joshi, S. G. Rosofsky, R. Haas, and E. A. Huerta, Numerical relativity higher order gravitational waveforms of eccentric, spinning, nonprecessing binary black hole mergers, Phys. Rev. D **107**, 064038 (2023), arXiv:2210.01852 [gr-qc].

[738] M. Van De Meent and N. Warburton, Fast Self-forced Inspirals, Class. Quant. Grav. **35**, 144003 (2018), arXiv:1802.05281 [gr-qc].

[739] B. Ireland, O. Birnholtz, H. Nakano, E. West, and M. Campanelli, Eccentric Binary Black Holes with Spin via the Direct Integration of the Post-Newtonian Equations of Motion, Phys. Rev. D **100**, 024015 (2019), arXiv:1904.03443 [gr-qc].

[740] E. A. Huerta, P. Kumar, S. T. McWilliams, R. O'Shaughnessy, and N. Yunes, Accurate and efficient waveforms for compact binaries on eccentric orbits, Phys. Rev. D **90**, 084016 (2014), arXiv:1408.3406 [gr-qc].

[741] B. Moore and N. Yunes, A 3PN Fourier Domain Waveform for Non-Spinning Binaries with Moderate Eccentricity, Class. Quant. Grav. **36**, 185003 (2019), arXiv:1903.05203 [gr-qc].

[742] M. Ebersold, Y. Boetzel, G. Faye, C. K. Mishra, B. R. Iyer, and P. Jetzer, Gravitational-wave amplitudes for compact binaries in eccentric orbits at the third post-Newtonian order: Memory contributions, Phys. Rev. D **100**, 084043 (2019), arXiv:1906.06263 [gr-qc].

[743] T. Hinderer and S. Babak, Foundations of an effective-one-body model for coalescing binaries on eccentric orbits, Phys. Rev. D **96**, 104048 (2017), arXiv:1707.08426 [gr-qc].

[744] M. Hannam, P. Schmidt, A. Bohé, L. Haegel, S. Husa, F. Ohme, G. Pratten, and M. Pürrer, Simple Model of Complete Precessing Black-Hole-Binary Gravitational Waveforms, Phys. Rev. Lett. **113**, 151101 (2014), arXiv:1308.3271 [gr-qc].

[745] A. Bohé *et al.*, Improved effective-one-body model of spinning, nonprecessing binary black holes for the era of gravitational-wave astrophysics with advanced detectors, Phys. Rev. D **95**, 044028 (2017), arXiv:1611.03703 [gr-qc].

[746] A. Buonanno and T. Damour, Effective one-body approach to general relativistic two-body dynamics, Phys. Rev. D **59**, 084006 (1999), arXiv:gr-qc/9811091.

[747] S. Ossokine *et al.*, Multipolar Effective-One-Body Waveforms for Precessing Binary Black Holes: Construction and Validation, Phys. Rev. D **102**, 044055 (2020), arXiv:2004.09442 [gr-qc].

[748] M. Khalil, A. Buonanno, J. Steinhoff, and J. Vines, Radiation-reaction force and multipolar waveforms for eccentric, spin-aligned binaries in the effective-one-body formalism, Phys. Rev. D **104**, 024046 (2021), arXiv:2104.11705 [gr-qc].

[749] A. Ramos-Buades, A. Buonanno, M. Khalil, and S. Ossokine, Effective-one-body multipolar waveforms for eccentric binary black holes with nonprecessing spins, Phys. Rev. D **105**, 044035 (2022), arXiv:2112.06952 [gr-qc].

[750] A. Nagar, A. Bonino, and P. Rettegno, Effective one-body multipolar waveform model for spin-

176

aligned, quasicircular, eccentric, hyperbolic black hole binaries, Phys. Rev. D **103**, 104021 (2021), arXiv:2101.08624 [gr-qc].

[751] R. Gamba, S. Akçay, S. Bernuzzi, and J. Williams, Effective-one-body waveforms for precessing coalescing compact binaries with post-Newtonian twist, Phys. Rev. D **106**, 024020 (2022), arXiv:2111.03675 [gr-qc].

[752] G. Pratten *et al.*, Computationally efficient models for the dominant and subdominant harmonic modes of precessing binary black holes, Phys. Rev. D **103**, 104056 (2021), arXiv:2004.06503 [gr-qc].

[753] G. Pratten, S. Husa, C. Garcia-Quiros, M. Colleoni, A. Ramos-Buades, H. Estelles, and R. Jaume, Setting the cornerstone for a family of models for gravitational waves from compact binaries: The dominant harmonic for nonprecessing quasicircular black holes, Phys. Rev. D **102**, 064001 (2020), arXiv:2001.11412 [gr-qc].

[754] E. Hamilton, L. London, J. E. Thompson, E. Fauchon-Jones, M. Hannam, C. Kalaghatgi, S. Khan, F. Pannarale, and A. Vano-Vinuales, Model of gravitational waves from precessing black-hole binaries through merger and ringdown, Phys. Rev. D **104**, 124027 (2021), arXiv:2107.08876 [gr-qc].

[755] J. Blackman, S. E. Field, C. R. Galley, B. Szilágyi, M. A. Scheel, M. Tiglio, and D. A. Hemberger, Fast and Accurate Prediction of Numerical Relativity Waveforms from Binary Black Hole Coalescences Using Surrogate Models, Phys. Rev. Lett. **115**, 121102 (2015), arXiv:1502.07758 [gr-qc].

[756] J. Yoo, V. Varma, M. Giesler, M. A. Scheel, C.-J. Haster, H. P. Pfeiffer, L. E. Kidder, and M. Boyle, Targeted large mass ratio numerical relativity surrogate waveform model for GW190814, Phys. Rev. D **106**, 044001 (2022), arXiv:2203.10109 [gr-qc].

[757] T. Islam, S. E. Field, S. A. Hughes, G. Khanna, V. Varma, M. Giesler, M. A. Scheel, L. E. Kidder, and H. P. Pfeiffer, Surrogate model for gravitational wave signals from nonspinning, comparable-to large-mass-ratio black hole binaries built on black hole perturbation theory waveforms calibrated to numerical relativity, Phys. Rev. D **106**, 104025 (2022), arXiv:2204.01972 [gr-qc].

[758] L. Blanchet, Gravitational Radiation from Post-Newtonian Sources and Inspiralling Compact Binaries, Living Rev. Rel. **17**, 2 (2014), arXiv:1310.1528 [gr-qc].

[759] B. P. Abbott *et al.* (LIGO Scientific, Virgo), GW170814: A Three-Detector Observation of Gravitational Waves from a Binary Black Hole Coalescence, Phys. Rev. Lett. **119**, 141101 (2017), arXiv:1709.09660 [gr-qc].

[760] B. P. Abbott *et al.* (LIGO Scientific, Virgo), GW170817: Observation of Gravitational Waves from a Binary Neutron Star Inspiral, Phys. Rev. Lett. **119**, 161101 (2017), arXiv:1710.05832 [gr-qc].

[761] B. P. Abbott *et al.* (LIGO Scientific, Virgo), GWTC-1: A Gravitational-Wave Transient Catalog of Compact Binary Mergers Observed by LIGO and Virgo during the First and Second Observing Runs, Phys. Rev. X **9**, 031040 (2019), arXiv:1811.12907 [astro-ph.HE].

[762] B. P. Abbott *et al.* (LIGO Scientific, Virgo), GW190425: Observation of a Compact Binary Coalescence with Total Mass $\sim 3.4 M_\odot$, Astrophys. J. Lett. **892**, L3 (2020), arXiv:2001.01761 [astro-ph.HE].

[763] H. A. Lorentz and J. Droste, De beweging van een stelsel lichamen onder den invloed van hunne onderlinge aantrekking, behandeld volgens de theorie van Einstein I,II, Versl. K. Akad. Wet. Amsterdam **26**, 392 & 649 (1917).

[764] A. Einstein, L. Infeld, and B. Hoffmann, The Gravitational equations and the problem of motion, Annals Math. **39**, 65 (1938).

[765] T. Damour and N. Deruelle, General relativistic celestial mechanics of binary systems I. The post-Newtonian motion, Ann. Inst. Henri Poincaré **43**, 107 (1985).

[766] T. Damour and N. Deruelle, General relativistic celestial mechanics of binary systems II. The post-Newtonian timing formula, Ann. Inst. Henri Poincaré **44**, 263 (1986).

[767] K. Westpfahl and M. Goller, GRAVITATIONAL SCATTERING OF TWO RELATIVISTIC PARTICLES IN POSTLINEAR APPROXIMATION, Lett. Nuovo Cim. **26**, 573 (1979).

[768] K. Westpfahl and H. Hoyler, GRAVITATIONAL BREMSSTRAHLUNG IN POSTLINEAR FAST MOTION APPROXIMATION, Lett. Nuovo Cim. **27**, 581 (1980).

[769] T. Futamase and Y. Itoh, The post-Newtonian approximation for relativistic compact binaries, Living Rev. Rel. **10**, 2 (2007).

[770] L. Blanchet, Post-Newtonian theory and the two-body problem, Fundam. Theor. Phys. **162**, 125 (2011), arXiv:0907.3596 [gr-qc].

[771] G. Schaefer, Post-Newtonian methods: Analytic results on the binary problem, Fundam. Theor. Phys. **162**, 167 (2011), arXiv:0910.2857 [gr-qc].

[772] S. Foffa and R. Sturani, Effective field theory methods to model compact binaries, Class. Quant. Grav. **31**, 043001 (2014), arXiv:1309.3474 [gr-qc].

[773] I. Z. Rothstein, Progress in effective field theory approach to the binary inspiral problem, Gen. Rel. Grav. **46**, 1726 (2014).

[774] R. A. Porto, The effective field theorist's approach to gravitational dynamics, Phys. Rept. **633**, 1 (2016), arXiv:1601.04914 [hep-th].

[775] G. Schäfer and P. Jaranowski, Hamiltonian formulation of general relativity and post-Newtonian dynamics of compact binaries, Living Rev. Rel. **21**, 7 (2018), arXiv:1805.07240 [gr-qc].

[776] M. Levi, Effective Field Theories of Post-Newtonian Gravity: A comprehensive review, Rept. Prog. Phys. **83**, 075901 (2020), arXiv:1807.01699 [hep-th].

[777] M. Maggiore, *Gravitational Waves. Vol. 1: Theory and Experiments* (Oxford University Press, 2007).

[778] E. Poisson and C. M. Will, *Gravity: Newtonian, post-Newtonian, relativistic* (Cambridge University Press, Cambridge, 2014).

[779] J. Garcia-Bellido and S. Nesseris, Gravitational wave bursts from Primordial Black Hole hyperbolic encounters, Phys. Dark Univ. **18**, 123 (2017), arXiv:1706.02111 [astro-ph.CO].

[780] J. García-Bellido and S. Nesseris, Gravitational wave energy emission and detection rates of Primordial Black Hole hyperbolic encounters, Phys. Dark Univ. **21**, 61 (2018), arXiv:1711.09702 [astro-ph.HE].

[781] T. Marchand, Q. Henry, F. Larrouturou, S. Marsat, G. Faye, and L. Blanchet, The mass quadrupole moment of compact binary systems at the fourth post-Newtonian order, Class. Quant. Grav. **37**, 215006 (2020), arXiv:2003.13672 [gr-qc].

[782] Q. Henry, G. Faye, and L. Blanchet, The current-type quadrupole moment and gravitational-wave mode $(\ell, m) = (2, 1)$ of compact binary systems at the third post-Newtonian order, Class. Quant. Grav. **38**, 185004 (2021), arXiv:2105.10876 [gr-qc].

[783] F. Larrouturou, Q. Henry, L. Blanchet, and G. Faye, The quadrupole moment of compact binaries to the fourth post-Newtonian order: I. Non-locality in time and infra-red divergencies, Class. Quant. Grav. **39**, 115007 (2022), arXiv:2110.02240 [gr-qc].

[784] F. Larrouturou, L. Blanchet, Q. Henry, and G. Faye, The quadrupole moment of compact binaries to the fourth post-Newtonian order: II. Dimensional regularization and renormalization, Class. Quant. Grav. **39**, 115008 (2022), arXiv:2110.02243 [gr-qc].

[785] L. Blanchet, G. Faye, and F. Larrouturou, The quadrupole moment of compact binaries to the fourth post-Newtonian order: from source to canonical moment, Class. Quant. Grav. **39**, 195003 (2022), arXiv:2204.11293 [gr-qc].

[786] D. Trestini, F. Larrouturou, and L. Blanchet, The quadrupole moment of compact binaries to the fourth post-Newtonian order: relating the harmonic and radiative metrics, Class. Quant. Grav. **40**, 055006 (2023), arXiv:2209.02719 [gr-qc].

[787] Q. Henry, Complete gravitational-waveform amplitude modes for quasicircular compact binaries to the 3.5PN order, Phys. Rev. D **107**, 044057 (2023), arXiv:2210.15602 [gr-qc].

[788] L. Blanchet, G. Faye, Q. Henry, F. Larrouturou, and D. Trestini, Gravitational-Wave Phasing of Quasicircular Compact Binary Systems to the Fourth-and-a-Half Post-Newtonian Order,

Phys. Rev. Lett. **131**, 121402 (2023), arXiv:2304.11185 [gr-qc].

[789] L. Blanchet, G. Faye, Q. Henry, F. Larrouturou, and D. Trestini, Gravitational-wave flux and quadrupole modes from quasicircular nonspinning compact binaries to the fourth post-Newtonian order, Phys. Rev. D **108**, 064041 (2023), arXiv:2304.11186 [gr-qc].

[790] A. Mangiagli, A. Klein, A. Sesana, E. Barausse, and M. Colpi, Post-Newtonian phase accuracy requirements for stellar black hole binaries with LISA, Phys. Rev. D **99**, 064056 (2019), arXiv:1811.01805 [gr-qc].

[791] A. Buonanno and B. S. Sathyaprakash, Sources of Gravitational Waves: Theory and Observations (2014) arXiv:1410.7832 [gr-qc].

[792] W. D. Goldberger, Les Houches lectures on effective field theories and gravitational radiation, in *Les Houches Summer School - Session 86: Particle Physics and Cosmology: The Fabric of Spacetime* (2007) arXiv:hep-ph/0701129.

[793] P. Jaranowski and G. Schäfer, Dimensional regularization of local singularities in the 4th post-Newtonian two-point-mass Hamiltonian, Phys. Rev. D **87**, 081503 (2013), arXiv:1303.3225 [gr-qc].

[794] P. Jaranowski and G. Schäfer, Derivation of local-in-time fourth post-Newtonian ADM Hamiltonian for spinless compact binaries, Phys. Rev. D **92**, 124043 (2015), arXiv:1508.01016 [gr-qc].

[795] T. Damour, P. Jaranowski, and G. Schäfer, Nonlocal-in-time action for the fourth post-Newtonian conservative dynamics of two-body systems, Phys. Rev. D **89**, 064058 (2014), arXiv:1401.4548 [gr-qc].

[796] T. Damour, P. Jaranowski, and G. Schäfer, Fourth post-Newtonian effective one-body dynamics, Phys. Rev. D **91**, 084024 (2015), arXiv:1502.07245 [gr-qc].

[797] T. Damour, P. Jaranowski, and G. Schäfer, Conservative dynamics of two-body systems at the fourth post-Newtonian approximation of general relativity, Phys. Rev. D **93**, 084014 (2016), arXiv:1601.01283 [gr-qc].

[798] L. Bernard, L. Blanchet, A. Bohé, G. Faye, and S. Marsat, Fokker action of nonspinning compact binaries at the fourth post-Newtonian approximation, Phys. Rev. D **93**, 084037 (2016), arXiv:1512.02876 [gr-qc].

[799] L. Bernard, L. Blanchet, A. Bohé, G. Faye, and S. Marsat, Energy and periastron advance of compact binaries on circular orbits at the fourth post-Newtonian order, Phys. Rev. D **95**, 044026 (2017), arXiv:1610.07934 [gr-qc].

[800] L. Bernard, L. Blanchet, A. Bohé, G. Faye, and S. Marsat, Dimensional regularization of the IR divergences in the Fokker action of point-particle binaries at the fourth post-Newtonian order, Phys. Rev. D **96**, 104043 (2017), arXiv:1706.08480 [gr-qc].

[801] T. Marchand, L. Bernard, L. Blanchet, and G. Faye, Ambiguity-Free Completion of the Equations of Motion of Compact Binary Systems at the Fourth Post-Newtonian Order, Phys. Rev. D **97**, 044023 (2018), arXiv:1707.09289 [gr-qc].

[802] L. Bernard, L. Blanchet, G. Faye, and T. Marchand, Center-of-Mass Equations of Motion and Conserved Integrals of Compact Binary Systems at the Fourth Post-Newtonian Order, Phys. Rev. D **97**, 044037 (2018), arXiv:1711.00283 [gr-qc].

[803] S. Foffa and R. Sturani, Dynamics of the gravitational two-body problem at fourth post-Newtonian order and at quadratic order in the Newton constant, Phys. Rev. D **87**, 064011 (2013), arXiv:1206.7087 [gr-qc].

[804] S. Foffa and R. Sturani, Tail terms in gravitational radiation reaction via effective field theory, Phys. Rev. D **87**, 044056 (2013), arXiv:1111.5488 [gr-qc].

[805] C. R. Galley, A. K. Leibovich, R. A. Porto, and A. Ross, Tail effect in gravitational radiation reaction: Time nonlocality and renormalization group evolution, Phys. Rev. D **93**, 124010 (2016), arXiv:1511.07379 [gr-qc].

[806] S. Foffa and R. Sturani, Conservative dynamics of binary systems to fourth Post-Newtonian order in the EFT approach I: Regularized Lagrangian, Phys. Rev. D **100**, 024047 (2019),

arXiv:1903.05113 [gr-qc].

[807] S. Foffa, R. A. Porto, I. Rothstein, and R. Sturani, Conservative dynamics of binary systems to fourth Post-Newtonian order in the EFT approach II: Renormalized Lagrangian, Phys. Rev. D **100**, 024048 (2019), arXiv:1903.05118 [gr-qc].

[808] J. Blümlein, A. Maier, P. Marquard, and G. Schäfer, Fourth post-Newtonian Hamiltonian dynamics of two-body systems from an effective field theory approach, Nucl. Phys. B **955**, 115041 (2020), arXiv:2003.01692 [gr-qc].

[809] D. Bini, T. Damour, and A. Geralico, Sixth post-Newtonian local-in-time dynamics of binary systems, Phys. Rev. D **102**, 024061 (2020), arXiv:2004.05407 [gr-qc].

[810] L. Blanchet, S. Foffa, F. Larrouturou, and R. Sturani, Logarithmic tail contributions to the energy function of circular compact binaries, Phys. Rev. D **101**, 084045 (2020), arXiv:1912.12359 [gr-qc].

[811] A. Einstein, Über Gravitationswellen, Sitzungsber. Preuss. Akad. Wiss. Berlin (Math. Phys.) **1918**, 154 (1918).

[812] L. D. Landau and E. M. Lifschits, *The Classical Theory of Fields*, Course of Theoretical Physics, Vol. Volume 2 (Pergamon Press, Oxford, 1975).

[813] K. S. Thorne, Multipole Expansions of Gravitational Radiation, Rev. Mod. Phys. **52**, 299 (1980).

[814] T. Marchand, L. Blanchet, and G. Faye, Gravitational-wave tail effects to quartic non-linear order, Class. Quant. Grav. **33**, 244003 (2016), arXiv:1607.07601 [gr-qc].

[815] F. Messina and A. Nagar, Parametrized-4.5PN TaylorF2 approximants and tail effects to quartic nonlinear order from the effective one body formalism, Phys. Rev. D **95**, 124001 (2017), [Erratum: Phys.Rev.D 96, 049907 (2017)], arXiv:1703.08107 [gr-qc].

[816] D. Trestini and L. Blanchet, Gravitational-wave tails of memory, Phys. Rev. D **107**, 104048 (2023), arXiv:2301.09395 [gr-qc].

[817] G. Faye, L. Blanchet, and B. R. Iyer, Non-linear multipole interactions and gravitational-wave octupole modes for inspiralling compact binaries to third-and-a-half post-Newtonian order, Class. Quant. Grav. **32**, 045016 (2015), arXiv:1409.3546 [gr-qc].

[818] L. Blanchet, G. Faye, B. R. Iyer, and S. Sinha, The Third post-Newtonian gravitational wave polarisations and associated spherical harmonic modes for inspiralling compact binaries in quasi-circular orbits, Class. Quant. Grav. **25**, 165003 (2008), [Erratum: Class.Quant.Grav. 29, 239501 (2012)], arXiv:0802.1249 [gr-qc].

[819] E. Poisson and M. Sasaki, Gravitational radiation from a particle in circular orbit around a black hole. 5: Black hole absorption and tail corrections, Phys. Rev. D **51**, 5753 (1995), arXiv:gr-qc/9412027.

[820] H. Tagoshi, S. Mano, and E. Takasugi, PostNewtonian expansion of gravitational waves from a particle in circular orbits around a rotating black hole: Effects of black hole absorption, Prog. Theor. Phys. **98**, 829 (1997), arXiv:gr-qc/9711072.

[821] K. Alvi, Energy and angular momentum flow into a black hole in a binary, Phys. Rev. D **64**, 104020 (2001), arXiv:gr-qc/0107080.

[822] R. A. Porto, Absorption effects due to spin in the worldline approach to black hole dynamics, Phys. Rev. D **77**, 064026 (2008), arXiv:0710.5150 [hep-th].

[823] K. Chatziioannou, E. Poisson, and N. Yunes, Tidal heating and torquing of a Kerr black hole to next-to-leading order in the tidal coupling, Phys. Rev. D **87**, 044022 (2013), arXiv:1211.1686 [gr-qc].

[824] C. M. Will and A. G. Wiseman, Gravitational radiation from compact binary systems: Gravitational wave forms and energy loss to second postNewtonian order, Phys. Rev. D **54**, 4813 (1996), arXiv:gr-qc/9608012.

[825] A. K. Leibovich, N. T. Maia, I. Z. Rothstein, and Z. Yang, Second post-Newtonian order radiative dynamics of inspiralling compact binaries in the Effective Field Theory approach, Phys. Rev. D **101**, 084058 (2020), arXiv:1912.12546 [gr-qc].

[826] G. Compère, R. Oliveri, and A. Seraj, The Poincaré and BMS flux-balance laws with application

to binary systems, JHEP **10**, 116, arXiv:1912.03164 [gr-qc].

[827] L. Blanchet, G. Compère, G. Faye, R. Oliveri, and A. Seraj, Multipole expansion of gravitational waves: from harmonic to Bondi coordinates, JHEP **02**, 029, arXiv:2011.10000 [gr-qc].

[828] L. Blanchet, G. Compère, G. Faye, R. Oliveri, and A. Seraj, Multipole expansion of gravitational waves: memory effects and Bondi aspects, JHEP **07**, 123, arXiv:2303.07732 [gr-qc].

[829] B. M. Barker and R. F. O'Connell, Gravitational Two-Body Problem with Arbitrary Masses, Spins, and Quadrupole Moments, Phys. Rev. D **12**, 329 (1975).

[830] T. Damour, Probléme des deux corps et freinage de rayonnement en relativité générale, C. R. Acad. Sci. Paris Sér. II **294**, 1355 (1982).

[831] C. M. Will, Post-Newtonian gravitational radiation and equations of motion via direct integration of the relaxed Einstein equations. III. Radiation reaction for binary systems with spinning bodies, Phys. Rev. D **71**, 084027 (2005), arXiv:gr-qc/0502039.

[832] M. Mathisson, Neue mechanik materieller systemes, Acta Phys. Polon. **6**, 163 (1937).

[833] W. Tulczyjew, Equations of motion of rotating bodies in general relativity theory, Acta Phys. Polon. **18**, 37 (1959), [Erratum: Acta Phys. Polon. **18**, 534 (1959)].

[834] A. Papapetrou, Spinning test particles in general relativity. 1., Proc. Roy. Soc. Lond. A **209**, 248 (1951).

[835] W. G. Dixon, Dynamics of Extended Bodies in General Relativity. III. Equations of Motion, Philosophical Transactions of the Royal Society of London Series A **277**, 59 (1974).

[836] H. Tagoshi, A. Ohashi, and B. J. Owen, Gravitational field and equations of motion of spinning compact binaries to 2.5 postNewtonian order, Phys. Rev. D **63**, 044006 (2001), arXiv:gr-qc/0010014.

[837] G. Faye, L. Blanchet, and A. Buonanno, Higher-order spin effects in the dynamics of compact binaries. I. Equations of motion, Phys. Rev. D **74**, 104033 (2006), arXiv:gr-qc/0605139.

[838] S. Marsat, A. Bohe, G. Faye, and L. Blanchet, Next-to-next-to-leading order spin-orbit effects in the equations of motion of compact binary systems, Class. Quant. Grav. **30**, 055007 (2013), arXiv:1210.4143 [gr-qc].

[839] A. Bohe, S. Marsat, G. Faye, and L. Blanchet, Next-to-next-to-leading order spin-orbit effects in the near-zone metric and precession equations of compact binaries, Class. Quant. Grav. **30**, 075017 (2013), arXiv:1212.5520 [gr-qc].

[840] A. Bohé, G. Faye, S. Marsat, and E. K. Porter, Quadratic-in-spin effects in the orbital dynamics and gravitational-wave energy flux of compact binaries at the 3PN order, Class. Quant. Grav. **32**, 195010 (2015), arXiv:1501.01529 [gr-qc].

[841] R. A. Porto and I. Z. Rothstein, The Hyperfine Einstein-Infeld-Hoffmann potential, Phys. Rev. Lett. **97**, 021101 (2006), arXiv:gr-qc/0604099.

[842] R. A. Porto, Post-Newtonian corrections to the motion of spinning bodies in NRGR, Phys. Rev. D **73**, 104031 (2006), arXiv:gr-qc/0511061.

[843] M. Levi and J. Steinhoff, Spinning gravitating objects in the effective field theory in the post-Newtonian scheme, JHEP **09**, 219, arXiv:1501.04956 [gr-qc].

[844] R. A. Porto and I. Z. Rothstein, Spin(1)Spin(2) Effects in the Motion of Inspiralling Compact Binaries at Third Order in the Post-Newtonian Expansion, Phys. Rev. D **78**, 044012 (2008), [Erratum: Phys.Rev.D 81, 029904 (2010)], arXiv:0802.0720 [gr-qc].

[845] M. Levi, Next to Leading Order gravitational Spin1-Spin2 coupling with Kaluza-Klein reduction, Phys. Rev. D **82**, 064029 (2010), arXiv:0802.1508 [gr-qc].

[846] R. A. Porto and I. Z. Rothstein, Next to Leading Order Spin(1)Spin(1) Effects in the Motion of Inspiralling Compact Binaries, Phys. Rev. D **78**, 044013 (2008), [Erratum: Phys.Rev.D 81, 029905 (2010)], arXiv:0804.0260 [gr-qc].

[847] M. Levi, Next to Leading Order gravitational Spin-Orbit coupling in an Effective Field Theory approach, Phys. Rev. D **82**, 104004 (2010), arXiv:1006.4139 [gr-qc].

[848] R. A. Porto, Next to leading order spin-orbit effects in the motion of inspiralling compact binaries, Class. Quant. Grav. **27**, 205001 (2010), arXiv:1005.5730 [gr-qc].

[849] J. Steinhoff, S. Hergt, and G. Schaefer, On the next-to-leading order gravitational spin(1)-spin(2) dynamics, Phys. Rev. D **77**, 081501 (2008), arXiv:0712.1716 [gr-qc].

[850] J. Steinhoff, S. Hergt, and G. Schaefer, Spin-squared Hamiltonian of next-to-leading order gravitational interaction, Phys. Rev. D **78**, 101503 (2008), arXiv:0809.2200 [gr-qc].

[851] J. Steinhoff, G. Schaefer, and S. Hergt, ADM canonical formalism for gravitating spinning objects, Phys. Rev. D **77**, 104018 (2008), arXiv:0805.3136 [gr-qc].

[852] J. Steinhoff and G. Schaefer, Canonical formulation of self-gravitating spinning-object systems, EPL **87**, 50004 (2009), arXiv:0907.1967 [gr-qc].

[853] J. Hartung and J. Steinhoff, Next-to-next-to-leading order post-Newtonian spin-orbit Hamiltonian for self-gravitating binaries, Annalen Phys. **523**, 783 (2011), arXiv:1104.3079 [gr-qc].

[854] J. Hartung, J. Steinhoff, and G. Schafer, Next-to-next-to-leading order post-Newtonian linear-in-spin binary Hamiltonians, Annalen Phys. **525**, 359 (2013), arXiv:1302.6723 [gr-qc].

[855] J. Hartung and J. Steinhoff, Next-to-next-to-leading order post-Newtonian spin(1)-spin(2) Hamiltonian for self-gravitating binaries, Annalen Phys. **523**, 919 (2011), arXiv:1107.4294 [gr-qc].

[856] S. Hergt, J. Steinhoff, and G. Schaefer, Reduced Hamiltonian for next-to-leading order Spin-Squared Dynamics of General Compact Binaries, Class. Quant. Grav. **27**, 135007 (2010), arXiv:1002.2093 [gr-qc].

[857] M. Levi, Binary dynamics from spin1-spin2 coupling at fourth post-Newtonian order, Phys. Rev. D **85**, 064043 (2012), arXiv:1107.4322 [gr-qc].

[858] J. Vines and J. Steinhoff, Spin-multipole effects in binary black holes and the test-body limit, Phys. Rev. D **97**, 064010 (2018), arXiv:1606.08832 [gr-qc].

[859] M. Levi and J. Steinhoff, Leading order finite size effects with spins for inspiralling compact binaries, JHEP **06**, 059, arXiv:1410.2601 [gr-qc].

[860] M. Levi, S. Mougiakakos, and M. Vieira, Gravitational cubic-in-spin interaction at the next-to-leading post-Newtonian order, JHEP **01**, 036, arXiv:1912.06276 [hep-th].

[861] M. Levi and F. Teng, NLO gravitational quartic-in-spin interaction, JHEP **01**, 066, arXiv:2008.12280 [hep-th].

[862] J.-W. Kim, M. Levi, and Z. Yin, N^{3}LO spin-orbit interaction via the EFT of spinning gravitating objects, JHEP **05**, 184, arXiv:2208.14949 [hep-th].

[863] J.-W. Kim, M. Levi, and Z. Yin, N^{3}LO quadratic-in-spin interactions for generic compact binaries, JHEP **03**, 098, arXiv:2209.09235 [hep-th].

[864] J. Zeng and C. M. Will, Application of energy and angular momentum balance to gravitational radiation reaction for binary systems with spin-orbit coupling, Gen. Rel. Grav. **39**, 1661 (2007), arXiv:0704.2720 [gr-qc].

[865] H. Wang and C. M. Will, Post-Newtonian gravitational radiation and equations of motion via direct integration of the relaxed Einstein equations. IV. Radiation reaction for binary systems with spin-spin coupling, Phys. Rev. D **75**, 064017 (2007), arXiv:gr-qc/0701047.

[866] N. T. Maia, C. R. Galley, A. K. Leibovich, and R. A. Porto, Radiation reaction for spinning bodies in effective field theory I: Spin-orbit effects, Phys. Rev. D **96**, 084064 (2017), arXiv:1705.07934 [gr-qc].

[867] N. T. Maia, C. R. Galley, A. K. Leibovich, and R. A. Porto, Radiation reaction for spinning bodies in effective field theory II: Spin-spin effects, Phys. Rev. D **96**, 084065 (2017), arXiv:1705.07938 [gr-qc].

[868] N. Siemonsen, J. Steinhoff, and J. Vines, Gravitational waves from spinning binary black holes at the leading post-Newtonian orders at all orders in spin, Phys. Rev. D **97**, 124046 (2018), arXiv:1712.08603 [gr-qc].

[869] H. Wang, J. Steinhoff, J. Zeng, and G. Schafer, Leading-order spin-orbit and spin(1)-spin(2) radiation-reaction Hamiltonians, Phys. Rev. D **84**, 124005 (2011), arXiv:1109.1182 [gr-qc].

[870] L. Blanchet, On the multipole expansion of the gravitational field, Class. Quant. Grav. **15**, 1971

(1998), arXiv:gr-qc/9801101.

[871] A. Ross, Multipole expansion at the level of the action, Phys. Rev. D **85**, 125033 (2012), arXiv:1202.4750 [gr-qc].

[872] R. A. Porto, A. Ross, and I. Z. Rothstein, Spin induced multipole moments for the gravitational wave amplitude from binary inspirals to 2.5 Post-Newtonian order, JCAP **09**, 028, arXiv:1203.2962 [gr-qc].

[873] L. Blanchet, A. Buonanno, and G. Faye, Tail-induced spin-orbit effect in the gravitational radiation of compact binaries, Phys. Rev. D **84**, 064041 (2011), arXiv:1104.5659 [gr-qc].

[874] S. Marsat, A. Bohé, L. Blanchet, and A. Buonanno, Next-to-leading tail-induced spin–orbit effects in the gravitational radiation flux of compact binaries, Class. Quant. Grav. **31**, 025023 (2014), arXiv:1307.6793 [gr-qc].

[875] G. Cho, R. A. Porto, and Z. Yang, Gravitational radiation from inspiralling compact objects: Spin effects to the fourth post-Newtonian order, Phys. Rev. D **106**, L101501 (2022), arXiv:2201.05138 [gr-qc].

[876] A. Bohé, S. Marsat, and L. Blanchet, Next-to-next-to-leading order spin–orbit effects in the gravitational wave flux and orbital phasing of compact binaries, Class. Quant. Grav. **30**, 135009 (2013), arXiv:1303.7412 [gr-qc].

[877] L. E. Kidder, C. M. Will, and A. G. Wiseman, Spin effects in the inspiral of coalescing compact binaries, Phys. Rev. D **47**, R4183 (1993), arXiv:gr-qc/9211025.

[878] L. E. Kidder, Coalescing binary systems of compact objects to postNewtonian 5/2 order. 5. Spin effects, Phys. Rev. D **52**, 821 (1995), arXiv:gr-qc/9506022.

[879] L. Blanchet, A. Buonanno, and G. Faye, Higher-order spin effects in the dynamics of compact binaries. II. Radiation field, Phys. Rev. D **74**, 104034 (2006), [Erratum: Phys.Rev.D 75, 049903 (2007), Erratum: Phys.Rev.D 81, 089901 (2010)], arXiv:gr-qc/0605140.

[880] S. Marsat, Cubic order spin effects in the dynamics and gravitational wave energy flux of compact object binaries, Class. Quant. Grav. **32**, 085008 (2015), arXiv:1411.4118 [gr-qc].

[881] R. A. Porto, A. Ross, and I. Z. Rothstein, Spin induced multipole moments for the gravitational wave flux from binary inspirals to third Post-Newtonian order, JCAP **03**, 009, arXiv:1007.1312 [gr-qc].

[882] Q. Henry, S. Marsat, and M. Khalil, Spin contributions to the gravitational-waveform modes for spin-aligned binaries at the 3.5PN order, Phys. Rev. D **106**, 124018 (2022), arXiv:2209.00374 [gr-qc].

[883] A. Buonanno, G. Faye, and T. Hinderer, Spin effects on gravitational waves from inspiraling compact binaries at second post-Newtonian order, Phys. Rev. D **87**, 044009 (2013), arXiv:1209.6349 [gr-qc].

[884] K. G. Arun, A. Buonanno, G. Faye, and E. Ochsner, Higher-order spin effects in the amplitude and phase of gravitational waveforms emitted by inspiraling compact binaries: Ready-to-use gravitational waveforms, Phys. Rev. D **79**, 104023 (2009), [Erratum: Phys.Rev.D 84, 049901 (2011)], arXiv:0810.5336 [gr-qc].

[885] T. Damour, A. Gopakumar, and B. R. Iyer, Phasing of gravitational waves from inspiralling eccentric binaries, Phys. Rev. D **70**, 064028 (2004), arXiv:gr-qc/0404128.

[886] R.-M. Memmesheimer, A. Gopakumar, and G. Schaefer, Third post-Newtonian accurate generalized quasi-Keplerian parametrization for compact binaries in eccentric orbits, Phys. Rev. D **70**, 104011 (2004), arXiv:gr-qc/0407049.

[887] K. G. Arun, L. Blanchet, B. R. Iyer, and M. S. S. Qusailah, Tail effects in the 3PN gravitational wave energy flux of compact binaries in quasi-elliptical orbits, Phys. Rev. D **77**, 064034 (2008), arXiv:0711.0250 [gr-qc].

[888] K. G. Arun, L. Blanchet, B. R. Iyer, and M. S. S. Qusailah, Inspiralling compact binaries in quasi-elliptical orbits: The Complete 3PN energy flux, Phys. Rev. D **77**, 064035 (2008), arXiv:0711.0302 [gr-qc].

[889] K. G. Arun, L. Blanchet, B. R. Iyer, and S. Sinha, Third post-Newtonian angular momentum

flux and the secular evolution of orbital elements for inspiralling compact binaries in quasi-elliptical orbits, Phys. Rev. D **80**, 124018 (2009), arXiv:0908.3854 [gr-qc].

[890] G. Cho, S. Tanay, A. Gopakumar, and H. M. Lee, Generalized quasi-Keplerian solution for eccentric, nonspinning compact binaries at 4PN order and the associated inspiral-merger-ringdown waveform, Phys. Rev. D **105**, 064010 (2022), arXiv:2110.09608 [gr-qc].

[891] C. K. Mishra, K. G. Arun, and B. R. Iyer, Third post-Newtonian gravitational waveforms for compact binary systems in general orbits: Instantaneous terms, Phys. Rev. D **91**, 084040 (2015), arXiv:1501.07096 [gr-qc].

[892] Y. Boetzel, C. K. Mishra, G. Faye, A. Gopakumar, and B. R. Iyer, Gravitational-wave amplitudes for compact binaries in eccentric orbits at the third post-Newtonian order: Tail contributions and postadiabatic corrections, Phys. Rev. D **100**, 044018 (2019), arXiv:1904.11814 [gr-qc].

[893] C. Konigsdorffer and A. Gopakumar, Phasing of gravitational waves from inspiralling eccentric binaries at the third-and-a-half post-Newtonian order, Phys. Rev. D **73**, 124012 (2006), arXiv:gr-qc/0603056.

[894] B. Moore, M. Favata, K. G. Arun, and C. K. Mishra, Gravitational-wave phasing for low-eccentricity inspiralling compact binaries to 3PN order, Phys. Rev. D **93**, 124061 (2016), arXiv:1605.00304 [gr-qc].

[895] A. Klein and P. Jetzer, Spin effects in the phasing of gravitational waves from binaries on eccentric orbits, Phys. Rev. D **81**, 124001 (2010), arXiv:1005.2046 [gr-qc].

[896] M. Tessmer, J. Hartung, and G. Schafer, Motion and gravitational wave forms of eccentric compact binaries with orbital-angular-momentum-aligned spins under next-to-leading order in spin-orbit and leading order in spin(1)-spin(2) and spin-squared couplings, Class. Quant. Grav. **27**, 165005 (2010), arXiv:1003.2735 [gr-qc].

[897] M. Tessmer, J. Hartung, and G. Schafer, Aligned Spins: Orbital Elements, Decaying Orbits, and Last Stable Circular Orbit to high post-Newtonian Orders, Class. Quant. Grav. **30**, 015007 (2013), arXiv:1207.6961 [gr-qc].

[898] Q. Henry and M. Khalil, Spin effects in gravitational waveforms and fluxes for binaries on eccentric orbits to the third post-Newtonian order, arXiv:2308.13606 [gr-qc].

[899] A. Klein, EFPE: Efficient fully precessing eccentric gravitational waveforms for binaries with long inspirals, arXiv:2106.10291 [gr-qc].

[900] K. Paul and C. K. Mishra, Spin effects in spherical harmonic modes of gravitational waves from eccentric compact binary inspirals, Phys. Rev. D **108**, 024023 (2023), arXiv:2211.04155 [gr-qc].

[901] N. Yunes, K. G. Arun, E. Berti, and C. M. Will, Post-Circular Expansion of Eccentric Binary Inspirals: Fourier-Domain Waveforms in the Stationary Phase Approximation, Phys. Rev. D **80**, 084001 (2009), [Erratum: Phys.Rev.D 89, 109901 (2014)], arXiv:0906.0313 [gr-qc].

[902] S. Tanay, M. Haney, and A. Gopakumar, Frequency and time domain inspiral templates for comparable mass compact binaries in eccentric orbits, Phys. Rev. D **93**, 064031 (2016), arXiv:1602.03081 [gr-qc].

[903] S. Tiwari, G. Achamveedu, M. Haney, and P. Hemantakumar, Ready-to-use Fourier domain templates for compact binaries inspiraling along moderately eccentric orbits, Phys. Rev. D **99**, 124008 (2019), arXiv:1905.07956 [gr-qc].

[904] B. Moore, T. Robson, N. Loutrel, and N. Yunes, Towards a Fourier domain waveform for non-spinning binaries with arbitrary eccentricity, Class. Quant. Grav. **35**, 235006 (2018), arXiv:1807.07163 [gr-qc].

[905] A. Klein, Y. Boetzel, A. Gopakumar, P. Jetzer, and L. de Vittori, Fourier domain gravitational waveforms for precessing eccentric binaries, Phys. Rev. D **98**, 104043 (2018), arXiv:1801.08542 [gr-qc].

[906] T. Damour, Gravitational scattering, post-Minkowskian approximation and Effective One-Body theory, Phys. Rev. D **94**, 104015 (2016), arXiv:1609.00354 [gr-qc].

[907] T. Damour, High-energy gravitational scattering and the general relativistic two-body problem,

Phys. Rev. D **97**, 044038 (2018), arXiv:1710.10599 [gr-qc].

[908] A. Antonelli, A. Buonanno, J. Steinhoff, M. van de Meent, and J. Vines, Energetics of two-body Hamiltonians in post-Minkowskian gravity, Phys. Rev. D **99**, 104004 (2019), arXiv:1901.07102 [gr-qc].

[909] G. Kälin and R. A. Porto, From Boundary Data to Bound States, JHEP **01**, 072, arXiv:1910.03008 [hep-th].

[910] G. Kälin and R. A. Porto, From boundary data to bound states. Part II. Scattering angle to dynamical invariants (with twist), JHEP **02**, 120, arXiv:1911.09130 [hep-th].

[911] N. E. J. Bjerrum-Bohr, A. Cristofoli, and P. H. Damgaard, Post-Minkowskian Scattering Angle in Einstein Gravity, JHEP **08**, 038, arXiv:1910.09366 [hep-th].

[912] G. Cho, G. Kälin, and R. A. Porto, From boundary data to bound states. Part III. Radiative effects, JHEP **04**, 154, [Erratum: JHEP 07, 002 (2022)], arXiv:2112.03976 [hep-th].

[913] M. V. S. Saketh, J. Vines, J. Steinhoff, and A. Buonanno, Conservative and radiative dynamics in classical relativistic scattering and bound systems, Phys. Rev. Res. **4**, 013127 (2022), arXiv:2109.05994 [gr-qc].

[914] N. Arkani-Hamed, T.-C. Huang, and Y.-t. Huang, Scattering amplitudes for all masses and spins, JHEP **11**, 070, arXiv:1709.04891 [hep-th].

[915] Z. Bern, C. Cheung, R. Roiban, C.-H. Shen, M. P. Solon, and M. Zeng, Black Hole Binary Dynamics from the Double Copy and Effective Theory, JHEP **10**, 206, arXiv:1908.01493 [hep-th].

[916] Z. Bern, C. Cheung, R. Roiban, C.-H. Shen, M. P. Solon, and M. Zeng, Scattering Amplitudes and the Conservative Hamiltonian for Binary Systems at Third Post-Minkowskian Order, Phys. Rev. Lett. **122**, 201603 (2019), arXiv:1901.04424 [hep-th].

[917] G. Kälin, Z. Liu, and R. A. Porto, Conservative Dynamics of Binary Systems to Third Post-Minkowskian Order from the Effective Field Theory Approach, Phys. Rev. Lett. **125**, 261103 (2020), arXiv:2007.04977 [hep-th].

[918] C. Cheung and M. P. Solon, Classical gravitational scattering at $\mathcal{O}(\mathrm{G}^3)$ from Feynman diagrams, JHEP **06**, 144, arXiv:2003.08351 [hep-th].

[919] C. Cheung, I. Z. Rothstein, and M. P. Solon, From Scattering Amplitudes to Classical Potentials in the Post-Minkowskian Expansion, Phys. Rev. Lett. **121**, 251101 (2018), arXiv:1808.02489 [hep-th].

[920] N. E. J. Bjerrum-Bohr, P. H. Damgaard, G. Festuccia, L. Planté, and P. Vanhove, General Relativity from Scattering Amplitudes, Phys. Rev. Lett. **121**, 171601 (2018), arXiv:1806.04920 [hep-th].

[921] A. Cristofoli, P. H. Damgaard, P. Di Vecchia, and C. Heissenberg, Second-order Post-Minkowskian scattering in arbitrary dimensions, JHEP **07**, 122, arXiv:2003.10274 [hep-th].

[922] D. A. Kosower, B. Maybee, and D. O'Connell, Amplitudes, Observables, and Classical Scattering, JHEP **02**, 137, arXiv:1811.10950 [hep-th].

[923] G. Kälin and R. A. Porto, Post-Minkowskian Effective Field Theory for Conservative Binary Dynamics, JHEP **11**, 106, arXiv:2006.01184 [hep-th].

[924] Z. Bern, J. Parra-Martinez, R. Roiban, M. S. Ruf, C.-H. Shen, M. P. Solon, and M. Zeng, Scattering Amplitudes and Conservative Binary Dynamics at $\mathcal{O}(G^4)$, Phys. Rev. Lett. **126**, 171601 (2021), arXiv:2101.07254 [hep-th].

[925] Z. Bern, J. Parra-Martinez, R. Roiban, M. S. Ruf, C.-H. Shen, M. P. Solon, and M. Zeng, Scattering Amplitudes, the Tail Effect, and Conservative Binary Dynamics at O(G4), Phys. Rev. Lett. **128**, 161103 (2022), arXiv:2112.10750 [hep-th].

[926] C. Dlapa, G. Kälin, Z. Liu, and R. A. Porto, Dynamics of binary systems to fourth Post-Minkowskian order from the effective field theory approach, Phys. Lett. B **831**, 137203 (2022), arXiv:2106.08276 [hep-th].

[927] C. Dlapa, G. Kälin, Z. Liu, and R. A. Porto, Conservative Dynamics of Binary Systems at Fourth Post-Minkowskian Order in the Large-Eccentricity Expansion, Phys. Rev. Lett. **128**,

161104 (2022), arXiv:2112.11296 [hep-th].

[928] G. Kälin, J. Neef, and R. A. Porto, Radiation-reaction in the Effective Field Theory approach to Post-Minkowskian dynamics, JHEP **01**, 140, arXiv:2207.00580 [hep-th].

[929] C. Dlapa, G. Kälin, Z. Liu, J. Neef, and R. A. Porto, Radiation Reaction and Gravitational Waves at Fourth Post-Minkowskian Order, Phys. Rev. Lett. **130**, 101401 (2023), arXiv:2210.05541 [hep-th].

[930] G. Mogull, J. Plefka, and J. Steinhoff, Classical black hole scattering from a worldline quantum field theory, JHEP **02**, 048, arXiv:2010.02865 [hep-th].

[931] G. U. Jakobsen, G. Mogull, J. Plefka, and J. Steinhoff, Classical Gravitational Bremsstrahlung from a Worldline Quantum Field Theory, Phys. Rev. Lett. **126**, 201103 (2021), arXiv:2101.12688 [gr-qc].

[932] S. Mougiakakos, M. M. Riva, and F. Vernizzi, Gravitational Bremsstrahlung in the post-Minkowskian effective field theory, Phys. Rev. D **104**, 024041 (2021), arXiv:2102.08339 [gr-qc].

[933] T. Damour, Radiative contribution to classical gravitational scattering at the third order in G, Phys. Rev. D **102**, 124008 (2020), arXiv:2010.01641 [gr-qc].

[934] N. E. J. Bjerrum-Bohr, P. H. Damgaard, L. Planté, and P. Vanhove, The amplitude for classical gravitational scattering at third Post-Minkowskian order, JHEP **08**, 172, arXiv:2105.05218 [hep-th].

[935] E. Herrmann, J. Parra-Martinez, M. S. Ruf, and M. Zeng, Radiative classical gravitational observables at $\mathcal{O}(G^3)$ from scattering amplitudes, JHEP **10**, 148, arXiv:2104.03957 [hep-th].

[936] E. Herrmann, J. Parra-Martinez, M. S. Ruf, and M. Zeng, Gravitational Bremsstrahlung from Reverse Unitarity, Phys. Rev. Lett. **126**, 201602 (2021), arXiv:2101.07255 [hep-th].

[937] P. Di Vecchia, C. Heissenberg, R. Russo, and G. Veneziano, The eikonal approach to gravitational scattering and radiation at $\mathcal{O}(G^3)$, JHEP **07**, 169, arXiv:2104.03256 [hep-th].

[938] P. Di Vecchia, C. Heissenberg, R. Russo, and G. Veneziano, Radiation Reaction from Soft Theorems, Phys. Lett. B **818**, 136379 (2021), arXiv:2101.05772 [hep-th].

[939] P. Di Vecchia, C. Heissenberg, R. Russo, and G. Veneziano, Universality of ultra-relativistic gravitational scattering, Phys. Lett. B **811**, 135924 (2020), arXiv:2008.12743 [hep-th].

[940] A. Brandhuber, G. Chen, G. Travaglini, and C. Wen, Classical gravitational scattering from a gauge-invariant double copy, JHEP **10**, 118, arXiv:2108.04216 [hep-th].

[941] P. H. Damgaard, L. Plante, and P. Vanhove, On an exponential representation of the gravitational S-matrix, JHEP **11**, 213, arXiv:2107.12891 [hep-th].

[942] M. M. Riva and F. Vernizzi, Radiated momentum in the post-Minkowskian worldline approach via reverse unitarity, JHEP **11**, 228, arXiv:2110.10140 [hep-th].

[943] A. V. Manohar, A. K. Ridgway, and C.-H. Shen, Radiated Angular Momentum and Dissipative Effects in Classical Scattering, Phys. Rev. Lett. **129**, 121601 (2022), arXiv:2203.04283 [hep-th].

[944] D. Bini, T. Damour, A. Geralico, S. Laporta, and P. Mastrolia, Gravitational dynamics at $O(G^6)$: perturbative gravitational scattering meets experimental mathematics, arXiv:2008.09389 [gr-qc].

[945] D. Bini, T. Damour, and A. Geralico, Radiative contributions to gravitational scattering, Phys. Rev. D **104**, 084031 (2021), arXiv:2107.08896 [gr-qc].

[946] D. Bini and A. Geralico, Higher-order tail contributions to the energy and angular momentum fluxes in a two-body scattering process, Phys. Rev. D **104**, 104020 (2021), arXiv:2108.05445 [gr-qc].

[947] D. Bini and A. Geralico, Frequency domain analysis of the gravitational wave energy loss in hyperbolic encounters, Phys. Rev. D **104**, 104019 (2021), arXiv:2108.02472 [gr-qc].

[948] D. Bini and A. Geralico, Momentum recoil in the relativistic two-body problem: Higher-order tails, Phys. Rev. D **105**, 084028 (2022), arXiv:2202.03037 [gr-qc].

[949] D. Bini and A. Geralico, Multipolar invariants and the eccentricity enhancement function parametrization of gravitational radiation, Phys. Rev. D **105**, 124001 (2022), arXiv:2204.08077 [gr-qc].

[950] D. Bini, T. Damour, and A. Geralico, Radiated momentum and radiation reaction in gravitational two-body scattering including time-asymmetric effects, Phys. Rev. D **107**, 024012 (2023), arXiv:2210.07165 [gr-qc].

[951] D. Bini and T. Damour, Gravitational spin-orbit coupling in binary systems at the second post-Minkowskian approximation, Phys. Rev. D **98**, 044036 (2018), arXiv:1805.10809 [gr-qc].

[952] D. Bini and T. Damour, Gravitational spin-orbit coupling in binary systems, post-Minkowskian approximation and effective one-body theory, Phys. Rev. D **96**, 104038 (2017), arXiv:1709.00590 [gr-qc].

[953] D. Kosmopoulos and A. Luna, Quadratic-in-spin Hamiltonian at $\mathcal{O}(G^2)$ from scattering amplitudes, JHEP **07**, 037, arXiv:2102.10137 [hep-th].

[954] Z. Liu, R. A. Porto, and Z. Yang, Spin Effects in the Effective Field Theory Approach to Post-Minkowskian Conservative Dynamics, JHEP **06**, 012, arXiv:2102.10059 [hep-th].

[955] M.-Z. Chung, Y.-t. Huang, J.-W. Kim, and S. Lee, Complete Hamiltonian for spinning binary systems at first post-Minkowskian order, JHEP **05**, 105, arXiv:2003.06600 [hep-th].

[956] Z. Bern, A. Luna, R. Roiban, C.-H. Shen, and M. Zeng, Spinning black hole binary dynamics, scattering amplitudes, and effective field theory, Phys. Rev. D **104**, 065014 (2021), arXiv:2005.03071 [hep-th].

[957] Y. F. Bautista, A. Guevara, C. Kavanagh, and J. Vines, Scattering in black hole backgrounds and higher-spin amplitudes. Part I, JHEP **03**, 136, arXiv:2107.10179 [hep-th].

[958] G. U. Jakobsen, G. Mogull, J. Plefka, and J. Steinhoff, Gravitational Bremsstrahlung and Hidden Supersymmetry of Spinning Bodies, Phys. Rev. Lett. **128**, 011101 (2022), arXiv:2106.10256 [hep-th].

[959] G. U. Jakobsen, G. Mogull, J. Plefka, and J. Steinhoff, SUSY in the sky with gravitons, JHEP **01**, 027, arXiv:2109.04465 [hep-th].

[960] G. U. Jakobsen and G. Mogull, Linear response, Hamiltonian, and radiative spinning two-body dynamics, Phys. Rev. D **107**, 044033 (2023), arXiv:2210.06451 [hep-th].

[961] J. Vines, Scattering of two spinning black holes in post-Minkowskian gravity, to all orders in spin, and effective-one-body mappings, Class. Quant. Grav. **35**, 084002 (2018), arXiv:1709.06016 [gr-qc].

[962] R. Aoude, K. Haddad, and A. Helset, Classical Gravitational Spinning-Spinless Scattering at O(G2S∞), Phys. Rev. Lett. **129**, 141102 (2022), arXiv:2205.02809 [hep-th].

[963] B. Maybee, D. O'Connell, and J. Vines, Observables and amplitudes for spinning particles and black holes, JHEP **12**, 156, arXiv:1906.09260 [hep-th].

[964] A. Guevara, A. Ochirov, and J. Vines, Black-hole scattering with general spin directions from minimal-coupling amplitudes, Phys. Rev. D **100**, 104024 (2019), arXiv:1906.10071 [hep-th].

[965] C. Cheung and M. P. Solon, Tidal Effects in the Post-Minkowskian Expansion, Phys. Rev. Lett. **125**, 191601 (2020), arXiv:2006.06665 [hep-th].

[966] D. Bini, T. Damour, and A. Geralico, Scattering of tidally interacting bodies in post-Minkowskian gravity, Phys. Rev. D **101**, 044039 (2020), arXiv:2001.00352 [gr-qc].

[967] C. Cheung, N. Shah, and M. P. Solon, Mining the Geodesic Equation for Scattering Data, Phys. Rev. D **103**, 024030 (2021), arXiv:2010.08568 [hep-th].

[968] Z. Bern, J. Parra-Martinez, R. Roiban, E. Sawyer, and C.-H. Shen, Leading Nonlinear Tidal Effects and Scattering Amplitudes, JHEP **05**, 188, arXiv:2010.08559 [hep-th].

[969] G. Kälin, Z. Liu, and R. A. Porto, Conservative Tidal Effects in Compact Binary Systems to Next-to-Leading Post-Minkowskian Order, Phys. Rev. D **102**, 124025 (2020), arXiv:2008.06047 [hep-th].

[970] R. Aoude, K. Haddad, and A. Helset, Tidal effects for spinning particles, JHEP **03**, 097, arXiv:2012.05256 [hep-th].

[971] K. Haddad and A. Helset, Tidal effects in quantum field theory, JHEP **12**, 024, arXiv:2008.04920 [hep-th].

[972] S. Mougiakakos, M. M. Riva, and F. Vernizzi, Gravitational Bremsstrahlung with Tidal Effects

in the Post-Minkowskian Expansion, Phys. Rev. Lett. **129**, 121101 (2022), arXiv:2204.06556 [hep-th].

[973] A. Cristofoli, N. E. J. Bjerrum-Bohr, P. H. Damgaard, and P. Vanhove, Post-Minkowskian Hamiltonians in general relativity, Phys. Rev. D **100**, 084040 (2019), arXiv:1906.01579 [hep-th].

[974] J. Vines, J. Steinhoff, and A. Buonanno, Spinning-black-hole scattering and the test-black-hole limit at second post-Minkowskian order, Phys. Rev. D **99**, 064054 (2019), arXiv:1812.00956 [gr-qc].

[975] A. Antonelli, M. van de Meent, A. Buonanno, J. Steinhoff, and J. Vines, Quasicircular inspirals and plunges from nonspinning effective-one-body Hamiltonians with gravitational self-force information, Phys. Rev. D **101**, 024024 (2020), arXiv:1907.11597 [gr-qc].

[976] P. H. Damgaard and P. Vanhove, Remodeling the effective one-body formalism in post-Minkowskian gravity, Phys. Rev. D **104**, 104029 (2021), arXiv:2108.11248 [hep-th].

[977] M. Khalil, A. Buonanno, J. Steinhoff, and J. Vines, Energetics and scattering of gravitational two-body systems at fourth post-Minkowskian order, Phys. Rev. D **106**, 024042 (2022), arXiv:2204.05047 [gr-qc].

[978] T. Damour and P. Rettegno, Strong-field scattering of two black holes: Numerical relativity meets post-Minkowskian gravity, Phys. Rev. D **107**, 064051 (2023), arXiv:2211.01399 [gr-qc].

[979] D. Bini, T. Damour, and A. Geralico, Novel approach to binary dynamics: application to the fifth post-Newtonian level, Phys. Rev. Lett. **123**, 231104 (2019), arXiv:1909.02375 [gr-qc].

[980] D. Bini, T. Damour, and A. Geralico, Binary dynamics at the fifth and fifth-and-a-half post-Newtonian orders, Phys. Rev. D **102**, 024062 (2020), arXiv:2003.11891 [gr-qc].

[981] D. Bini, T. Damour, and A. Geralico, Sixth post-Newtonian nonlocal-in-time dynamics of binary systems, Phys. Rev. D **102**, 084047 (2020), arXiv:2007.11239 [gr-qc].

[982] J. Blümlein, A. Maier, P. Marquard, and G. Schäfer, The fifth-order post-Newtonian Hamiltonian dynamics of two-body systems from an effective field theory approach, Nucl. Phys. B **983**, 115900 (2022), [Erratum: Nucl.Phys.B 985, 115991 (2022)], arXiv:2110.13822 [gr-qc].

[983] J. Blümlein, A. Maier, P. Marquard, and G. Schäfer, Testing binary dynamics in gravity at the sixth post-Newtonian level, Phys. Lett. B **807**, 135496 (2020), arXiv:2003.07145 [gr-qc].

[984] A. Antonelli, C. Kavanagh, M. Khalil, J. Steinhoff, and J. Vines, Gravitational spin-orbit coupling through third-subleading post-Newtonian order: from first-order self-force to arbitrary mass ratios, Phys. Rev. Lett. **125**, 011103 (2020), arXiv:2003.11391 [gr-qc].

[985] A. Antonelli, C. Kavanagh, M. Khalil, J. Steinhoff, and J. Vines, Gravitational spin-orbit and aligned spin$_1$-spin$_2$ couplings through third-subleading post-Newtonian orders, Phys. Rev. D **102**, 124024 (2020), arXiv:2010.02018 [gr-qc].

[986] N. Siemonsen and J. Vines, Test black holes, scattering amplitudes and perturbations of Kerr spacetime, Phys. Rev. D **101**, 064066 (2020), arXiv:1909.07361 [gr-qc].

[987] T. Damour, Classical and quantum scattering in post-Minkowskian gravity, Phys. Rev. D **102**, 024060 (2020), arXiv:1912.02139 [gr-qc].

[988] A. Le Tiec, L. Blanchet, and B. F. Whiting, The First Law of Binary Black Hole Mechanics in General Relativity and Post-Newtonian Theory, Phys. Rev. D **85**, 064039 (2012), arXiv:1111.5378 [gr-qc].

[989] J. L. Friedman, K. Uryu, and M. Shibata, Thermodynamics of binary black holes and neutron stars, Phys. Rev. D **65**, 064035 (2002), [Erratum: Phys.Rev.D 70, 129904 (2004)], arXiv:gr-qc/0108070.

[990] A. Le Tiec, First Law of Mechanics for Compact Binaries on Eccentric Orbits, Phys. Rev. D **92**, 084021 (2015), arXiv:1506.05648 [gr-qc].

[991] L. Blanchet and A. Le Tiec, First Law of Compact Binary Mechanics with Gravitational-Wave Tails, Class. Quant. Grav. **34**, 164001 (2017), arXiv:1702.06839 [gr-qc].

[992] L. Blanchet, A. Buonanno, and A. Le Tiec, First law of mechanics for black hole binaries with

spins, Phys. Rev. D **87**, 024030 (2013), arXiv:1211.1060 [gr-qc].

[993] A. Le Tiec, A Note on Celestial Mechanics in Kerr Spacetime, Class. Quant. Grav. **31**, 097001 (2014), arXiv:1311.3836 [gr-qc].

[994] R. Fujita, S. Isoyama, A. Le Tiec, H. Nakano, N. Sago, and T. Tanaka, Hamiltonian Formulation of the Conservative Self-Force Dynamics in the Kerr Geometry, Class. Quant. Grav. **34**, 134001 (2017), arXiv:1612.02504 [gr-qc].

[995] P. Jaranowski and G. Schafer, Towards the 4th post-Newtonian Hamiltonian for two-point-mass systems, Phys. Rev. D **86**, 061503 (2012), arXiv:1207.5448 [gr-qc].

[996] A. Le Tiec, E. Barausse, and A. Buonanno, Gravitational Self-Force Correction to the Binding Energy of Compact Binary Systems, Phys. Rev. Lett. **108**, 131103 (2012), arXiv:1111.5609 [gr-qc].

[997] S. Akcay, L. Barack, T. Damour, and N. Sago, Gravitational self-force and the effective-one-body formalism between the innermost stable circular orbit and the light ring, Phys. Rev. D **86**, 104041 (2012), arXiv:1209.0964 [gr-qc].

[998] S. Isoyama, L. Barack, S. R. Dolan, A. Le Tiec, H. Nakano, A. G. Shah, T. Tanaka, and N. Warburton, Gravitational Self-Force Correction to the Innermost Stable Circular Equatorial Orbit of a Kerr Black Hole, Phys. Rev. Lett. **113**, 161101 (2014), arXiv:1404.6133 [gr-qc].

[999] M. van de Meent, Self-force corrections to the periapsis advance around a spinning black hole, Phys. Rev. Lett. **118**, 011101 (2017), arXiv:1610.03497 [gr-qc].

[1000] E. Barausse, A. Buonanno, and A. Le Tiec, The complete non-spinning effective-one-body metric at linear order in the mass ratio, Phys. Rev. D **85**, 064010 (2012), arXiv:1111.5610 [gr-qc].

[1001] S. Akcay and M. van de Meent, Numerical computation of the effective-one-body potential q using self-force results, Phys. Rev. D **93**, 064063 (2016), arXiv:1512.03392 [gr-qc].

[1002] D. Bini, T. Damour, and A. Geralico, Confirming and improving post-Newtonian and effective-one-body results from self-force computations along eccentric orbits around a Schwarzschild black hole, Phys. Rev. D **93**, 064023 (2016), arXiv:1511.04533 [gr-qc].

[1003] D. Bini, T. Damour, and a. Geralico, New gravitational self-force analytical results for eccentric orbits around a Schwarzschild black hole, Phys. Rev. D **93**, 104017 (2016), arXiv:1601.02988 [gr-qc].

[1004] D. Bini, T. Damour, and A. Geralico, Spin-dependent two-body interactions from gravitational self-force computations, Phys. Rev. D **92**, 124058 (2015), [Erratum: Phys.Rev.D 93, 109902 (2016)], arXiv:1510.06230 [gr-qc].

[1005] M. Colleoni, L. Barack, A. G. Shah, and M. van de Meent, Self-force as a cosmic censor in the Kerr overspinning problem, Phys. Rev. D **92**, 084044 (2015), arXiv:1508.04031 [gr-qc].

[1006] A. Zimmerman, A. G. M. Lewis, and H. P. Pfeiffer, Redshift factor and the first law of binary black hole mechanics in numerical simulations, Phys. Rev. Lett. **117**, 191101 (2016), arXiv:1606.08056 [gr-qc].

[1007] A. Le Tiec and P. Grandclément, Horizon Surface Gravity in Corotating Black Hole Binaries, Class. Quant. Grav. **35**, 144002 (2018), arXiv:1710.03673 [gr-qc].

[1008] L. Barack, M. Colleoni, T. Damour, S. Isoyama, and N. Sago, Self-force effects on the marginally bound zoom-whirl orbit in Schwarzschild spacetime, Phys. Rev. D **100**, 124015 (2019), arXiv:1909.06103 [gr-qc].

[1009] A. Pound, B. Wardell, N. Warburton, and J. Miller, Second-Order Self-Force Calculation of Gravitational Binding Energy in Compact Binaries, Phys. Rev. Lett. **124**, 021101 (2020), arXiv:1908.07419 [gr-qc].

[1010] P. Ramond and A. Le Tiec, Multipolar Particles in Helically Symmetric Spacetimes, Class. Quant. Grav. **38**, 135022 (2021), arXiv:2005.00602 [gr-qc].

[1011] P. Ramond and A. Le Tiec, First law of mechanics for spinning compact binaries: Dipolar order, Phys. Rev. D **106**, 044057 (2022), arXiv:2202.09345 [gr-qc].

[1012] B. C. Mundim, H. Nakano, N. Yunes, M. Campanelli, S. C. Noble, and Y. Zlochower,

Approximate black hole binary spacetime via asymptotic matching, Phys. Rev. D **89**, 084008 (2014), arXiv:1312.6731 [gr-qc].

[1013] S. C. Noble, B. C. Mundim, H. Nakano, J. H. Krolik, M. Campanelli, Y. Zlochower, and N. Yunes, Circumbinary MHD Accretion into Inspiraling Binary Black Holes, Astrophys. J. **755**, 51 (2012), arXiv:1204.1073 [astro-ph.HE].

[1014] M. Zilhão, S. C. Noble, M. Campanelli, and Y. Zlochower, Resolving the relative influence of strong field spacetime dynamics and MHD on circumbinary disk physics, Phys. Rev. D **91**, 024034 (2015), arXiv:1409.4787 [gr-qc].

[1015] L. Gallouin, H. Nakano, N. Yunes, and M. Campanelli, Asymptotically Matched Spacetime Metric for Non-Precessing, Spinning Black Hole Binaries, Class. Quant. Grav. **29**, 235013 (2012), arXiv:1208.6489 [gr-qc].

[1016] B. Ireland, B. C. Mundim, H. Nakano, and M. Campanelli, Inspiralling, nonprecessing, spinning black hole binary spacetime via asymptotic matching, Phys. Rev. D **93**, 104057 (2016), arXiv:1512.05650 [gr-qc].

[1017] H. Nakano, B. Ireland, M. Campanelli, and E. J. West, Spinning, Precessing, Black Hole Binary Spacetime via Asymptotic Matching, Class. Quant. Grav. **33**, 247001 (2016), arXiv:1608.01033 [gr-qc].

[1018] A. Kuntz, Precession resonances in hierarchical triple systems, Phys. Rev. D **105**, 024017 (2022), arXiv:2112.05167 [gr-qc].

[1019] Y. Kozai, Secular perturbations of asteroids with high inclination and eccentricity, Astron. J. **67**, 591 (1962).

[1020] M. L. Lidov, The evolution of orbits of artificial satellites of planets under the action of gravitational perturbations of external bodies, Planet. Space Sci. **9**, 719 (1962).

[1021] M. Bonetti, F. Haardt, A. Sesana, and E. Barausse, Post-Newtonian evolution of massive black hole triplets in galactic nuclei – I. Numerical implementation and tests, Mon. Not. Roy. Astron. Soc. **461**, 4419 (2016), arXiv:1604.08770 [astro-ph.GA].

[1022] M. Bonetti, E. Barausse, G. Faye, F. Haardt, and A. Sesana, About gravitational-wave generation by a three-body system, Class. Quant. Grav. **34**, 215004 (2017), arXiv:1707.04902 [gr-qc].

[1023] C. M. Will, Higher-order effects in the dynamics of hierarchical triple systems. Quadrupole-squared terms, Phys. Rev. D **103**, 063003 (2021), arXiv:2011.13286 [astro-ph.EP].

[1024] A. Kuntz, F. Serra, and E. Trincherini, Effective two-body approach to the hierarchical three-body problem, Phys. Rev. D **104**, 024016 (2021), arXiv:2104.13387 [hep-th].

[1025] A. Kuntz, F. Serra, and E. Trincherini, Effective two-body approach to the hierarchical three-body problem: Quadrupole to 1PN, Phys. Rev. D **107**, 044011 (2023), arXiv:2210.13493 [gr-qc].

[1026] T. Damour, GRAVITATIONAL RADIATION AND THE MOTION OF COMPACT BODIES, in *Les Houches Summer School on Gravitational Radiation* (1982).

[1027] E. E. Flanagan and T. Hinderer, Constraining neutron star tidal Love numbers with gravitational wave detectors, Phys. Rev. D **77**, 021502 (2008), arXiv:0709.1915 [astro-ph].

[1028] T. Damour, A. Nagar, and L. Villain, Measurability of the tidal polarizability of neutron stars in late-inspiral gravitational-wave signals, Phys. Rev. D **85**, 123007 (2012), arXiv:1203.4352 [gr-qc].

[1029] D. Bini, T. Damour, and G. Faye, Effective action approach to higher-order relativistic tidal interactions in binary systems and their effective one body description, Phys. Rev. D **85**, 124034 (2012), arXiv:1202.3565 [gr-qc].

[1030] Q. Henry, G. Faye, and L. Blanchet, Tidal effects in the gravitational-wave phase evolution of compact binary systems to next-to-next-to-leading post-Newtonian order, Phys. Rev. D **102**, 044033 (2020), arXiv:2005.13367 [gr-qc].

[1031] J. D. Brown and J. W. York, Jr., Quasilocal energy and conserved charges derived from the gravitational action, Phys. Rev. D **47**, 1407 (1993), arXiv:gr-qc/9209012.

[1032] A. Ashtekar, C. Beetle, and J. Lewandowski, Mechanics of rotating isolated horizons, Phys. Rev. D **64**, 044016 (2001), arXiv:gr-qc/0103026.

[1033] R. Owen, A. S. Fox, J. A. Freiberg, and T. P. Jacques, Black Hole Spin Axis in Numerical Relativity, Phys. Rev. D **99**, 084031 (2019), arXiv:1708.07325 [gr-qc].

[1034] E. Poisson, A. Pound, and I. Vega, The Motion of point particles in curved spacetime, Living Rev. Rel. **14**, 7 (2011), arXiv:1102.0529 [gr-qc].

[1035] A. I. Harte, Motion in classical field theories and the foundations of the self-force problem, Fund. Theor. Phys. **179**, 327 (2015), arXiv:1405.5077 [gr-qc].

[1036] A. Pound, Motion of small objects in curved spacetimes: An introduction to gravitational self-force, Fund. Theor. Phys. **179**, 399 (2015), arXiv:1506.06245 [gr-qc].

[1037] A. Pound and B. Wardell, Black hole perturbation theory and gravitational self-force, arXiv:2101.04592 [gr-qc].

[1038] C. R. Galley and B. L. Hu, Self-force on extreme mass ratio inspirals via curved spacetime effective field theory, Phys. Rev. D **79**, 064002 (2009), arXiv:0801.0900 [gr-qc].

[1039] Y. Mino, M. Sasaki, and T. Tanaka, Gravitational radiation reaction to a particle motion, Phys. Rev. D **55**, 3457 (1997), arXiv:gr-qc/9606018.

[1040] T. C. Quinn and R. M. Wald, An Axiomatic approach to electromagnetic and gravitational radiation reaction of particles in curved space-time, Phys. Rev. D **56**, 3381 (1997), arXiv:gr-qc/9610053.

[1041] S. L. Detweiler, Radiation reaction and the selfforce for a point mass in general relativity, Phys. Rev. Lett. **86**, 1931 (2001), arXiv:gr-qc/0011039.

[1042] S. L. Detweiler and B. F. Whiting, Selfforce via a Green's function decomposition, Phys. Rev. D **67**, 024025 (2003), arXiv:gr-qc/0202086.

[1043] S. E. Gralla and R. M. Wald, A Rigorous Derivation of Gravitational Self-force, Class. Quant. Grav. **25**, 205009 (2008), [Erratum: Class.Quant.Grav. 28, 159501 (2011)], arXiv:0806.3293 [gr-qc].

[1044] A. Pound, Self-consistent gravitational self-force, Phys. Rev. D **81**, 024023 (2010), arXiv:0907.5197 [gr-qc].

[1045] S. E. Gralla, Gauge and Averaging in Gravitational Self-force, Phys. Rev. D **84**, 084050 (2011), arXiv:1104.5635 [gr-qc].

[1046] A. I. Harte, Mechanics of extended masses in general relativity, Class. Quant. Grav. **29**, 055012 (2012), arXiv:1103.0543 [gr-qc].

[1047] S. Detweiler, Gravitational radiation reaction and second order perturbation theory, Phys. Rev. D **85**, 044048 (2012), arXiv:1107.2098 [gr-qc].

[1048] A. Pound, Second-order gravitational self-force, Phys. Rev. Lett. **109**, 051101 (2012), arXiv:1201.5089 [gr-qc].

[1049] S. E. Gralla, Second Order Gravitational Self Force, Phys. Rev. D **85**, 124011 (2012), arXiv:1203.3189 [gr-qc].

[1050] A. Pound, Nonlinear gravitational self-force: second-order equation of motion, Phys. Rev. D **95**, 104056 (2017), arXiv:1703.02836 [gr-qc].

[1051] S. D. Upton and A. Pound, Second-order gravitational self-force in a highly regular gauge, Phys. Rev. D **103**, 124016 (2021), arXiv:2101.11409 [gr-qc].

[1052] L. Barack, D. A. Golbourn, and N. Sago, m-Mode Regularization Scheme for the Self Force in Kerr Spacetime, Phys. Rev. D **76**, 124036 (2007), arXiv:0709.4588 [gr-qc].

[1053] I. Vega and S. L. Detweiler, Regularization of fields for self-force problems in curved spacetime: Foundations and a time-domain application, Phys. Rev. D **77**, 084008 (2008), arXiv:0712.4405 [gr-qc].

[1054] L. Barack and A. Ori, Mode sum regularization approach for the selfforce in black hole spacetime, Phys. Rev. D **61**, 061502 (2000), arXiv:gr-qc/9912010.

[1055] L. Barack and A. Ori, Regularization parameters for the selfforce in Schwarzschild spacetime. 2. Gravitational and electromagnetic cases, Phys. Rev. D **67**, 024029 (2003), arXiv:gr-

qc/0209072.

[1056] L. Barack and A. Ori, Gravitational selfforce on a particle orbiting a Kerr black hole, Phys. Rev. Lett. **90**, 111101 (2003), arXiv:gr-qc/0212103.

[1057] L. Barack, Y. Mino, H. Nakano, A. Ori, and M. Sasaki, Calculating the gravitational selfforce in Schwarzschild space-time, Phys. Rev. Lett. **88**, 091101 (2002), arXiv:gr-qc/0111001.

[1058] M. Casals, S. R. Dolan, A. C. Ottewill, and B. Wardell, Self-Force Calculations with Matched Expansions and Quasinormal Mode Sums, Phys. Rev. D **79**, 124043 (2009), arXiv:0903.0395 [gr-qc].

[1059] B. Wardell, C. R. Galley, A. Zenginoğlu, M. Casals, S. R. Dolan, and A. C. Ottewill, Self-force via Green functions and worldline integration, Phys. Rev. D **89**, 084021 (2014), arXiv:1401.1506 [gr-qc].

[1060] L. Barack, Gravitational self force in extreme mass-ratio inspirals, Class. Quant. Grav. **26**, 213001 (2009), arXiv:0908.1664 [gr-qc].

[1061] B. Wardell and N. Warburton, Applying the effective-source approach to frequency-domain self-force calculations: Lorenz-gauge gravitational perturbations, Phys. Rev. D **92**, 084019 (2015), arXiv:1505.07841 [gr-qc].

[1062] T. Regge and J. A. Wheeler, Stability of a Schwarzschild singularity, Phys. Rev. **108**, 1063 (1957).

[1063] F. J. Zerilli, Gravitational field of a particle falling in a schwarzschild geometry analyzed in tensor harmonics, Phys. Rev. D **2**, 2141 (1970).

[1064] S. A. Teukolsky, Perturbations of a rotating black hole. 1. Fundamental equations for gravitational electromagnetic and neutrino field perturbations, Astrophys. J. **185**, 635 (1973).

[1065] R. M. Wald, On perturbations of a Kerr black hole, Journal of Mathematical Physics **14**, 1453 (1973).

[1066] P. L. Chrzanowski, Vector Potential and Metric Perturbations of a Rotating Black Hole, Phys. Rev. D **11**, 2042 (1975).

[1067] R. M. Wald, Construction of Solutions of Gravitational, Electromagnetic, Or Other Perturbation Equations from Solutions of Decoupled Equations, Phys. Rev. Lett. **41**, 203 (1978).

[1068] L. S. Kegeles and J. M. Cohen, CONSTRUCTIVE PROCEDURE FOR PERTURBATIONS OF SPACE-TIMES, Phys. Rev. D **19**, 1641 (1979).

[1069] M. Sasaki and H. Tagoshi, Analytic black hole perturbation approach to gravitational radiation, Living Rev. Rel. **6**, 6 (2003), arXiv:gr-qc/0306120.

[1070] K. Martel and E. Poisson, Gravitational perturbations of the Schwarzschild spacetime: A Practical covariant and gauge-invariant formalism, Phys. Rev. D **71**, 104003 (2005), arXiv:gr-qc/0502028.

[1071] L. Barack and C. O. Lousto, Perturbations of Schwarzschild black holes in the Lorenz gauge: Formulation and numerical implementation, Phys. Rev. D **72**, 104026 (2005), arXiv:gr-qc/0510019.

[1072] W. Schmidt, Celestial mechanics in Kerr space-time, Class. Quant. Grav. **19**, 2743 (2002), arXiv:gr-qc/0202090.

[1073] Y. Mino, Perturbative approach to an orbital evolution around a supermassive black hole, Phys. Rev. D **67**, 084027 (2003), arXiv:gr-qc/0302075.

[1074] R. Fujita and W. Hikida, Analytical solutions of bound timelike geodesic orbits in Kerr spacetime, Class. Quant. Grav. **26**, 135002 (2009), arXiv:0906.1420 [gr-qc].

[1075] R. Grossman, J. Levin, and G. Perez-Giz, The harmonic structure of generic Kerr orbits, Phys. Rev. D **85**, 023012 (2012), arXiv:1105.5811 [gr-qc].

[1076] Y. Mino and R. Price, Two-timescale adiabatic expansion of a scalar field model, Phys. Rev. D **77**, 064001 (2008), arXiv:0801.0179 [gr-qc].

[1077] T. Hinderer and E. E. Flanagan, Two timescale analysis of extreme mass ratio inspirals in Kerr. I. Orbital Motion, Phys. Rev. D **78**, 064028 (2008), arXiv:0805.3337 [gr-qc].

[1078] A. Pound, Singular perturbation techniques in the gravitational self-force problem, Phys. Rev.

D **81**, 124009 (2010), arXiv:1003.3954 [gr-qc].

[1079] A. Pound, Second-order perturbation theory: problems on large scales, Phys. Rev. D **92**, 104047 (2015), arXiv:1510.05172 [gr-qc].

[1080] J. Miller and A. Pound, Two-timescale evolution of extreme-mass-ratio inspirals: waveform generation scheme for quasicircular orbits in Schwarzschild spacetime, Phys. Rev. D **103**, 064048 (2021), arXiv:2006.11263 [gr-qc].

[1081] E. Flanagan, T. Hinderer, J. Moxon, and A. Pound, The two-body problem in general relativity in the extreme-mass-ratio limit via multiscale expansions: Foundations (in preparation).

[1082] P. Lynch, M. van de Meent, and N. Warburton, Eccentric self-forced inspirals into a rotating black hole, Class. Quant. Grav. **39**, 145004 (2022), arXiv:2112.05651 [gr-qc].

[1083] S. Hopper, Unbound motion on a Schwarzschild background: Practical approaches to frequency domain computations, Phys. Rev. D **97**, 064007 (2018), arXiv:1706.05455 [gr-qc].

[1084] S. Hopper and V. Cardoso, Scattering of point particles by black holes: gravitational radiation, Phys. Rev. D **97**, 044031 (2018), arXiv:1706.02791 [gr-qc].

[1085] O. Long and L. Barack, Time-domain metric reconstruction for hyperbolic scattering, Phys. Rev. D **104**, 024014 (2021), arXiv:2105.05630 [gr-qc].

[1086] L. Barack and O. Long, Self-force correction to the deflection angle in black-hole scattering: A scalar charge toy model, Phys. Rev. D **106**, 104031 (2022), arXiv:2209.03740 [gr-qc].

[1087] O. Long, *Self-force in hyperbolic black hole encounters*, Ph.D. thesis, Southampton U. (2022), arXiv:2209.03836 [gr-qc].

[1088] A. Buonanno and T. Damour, Transition from inspiral to plunge in binary black hole coalescences, Phys. Rev. D **62**, 064015 (2000), arXiv:gr-qc/0001013.

[1089] A. Ori and K. S. Thorne, The Transition from inspiral to plunge for a compact body in a circular equatorial orbit around a massive, spinning black hole, Phys. Rev. D **62**, 124022 (2000), arXiv:gr-qc/0003032.

[1090] A. Apte and S. A. Hughes, Exciting black hole modes via misaligned coalescences: I. Inspiral, transition, and plunge trajectories using a generalized Ori-Thorne procedure, Phys. Rev. D **100**, 084031 (2019), arXiv:1901.05901 [gr-qc].

[1091] O. Burke, J. R. Gair, and J. Simón, Transition from Inspiral to Plunge: A Complete Near-Extremal Trajectory and Associated Waveform, Phys. Rev. D **101**, 064026 (2020), arXiv:1909.12846 [gr-qc].

[1092] G. Compère, K. Fransen, and C. Jonas, Transition from inspiral to plunge into a highly spinning black hole, Class. Quant. Grav. **37**, 095013 (2020), arXiv:1909.12848 [gr-qc].

[1093] G. Compère and L. Küchler, Asymptotically matched quasi-circular inspiral and transition-to-plunge in the small mass ratio expansion, SciPost Phys. **13**, 043 (2022), arXiv:2112.02114 [gr-qc].

[1094] T. Tanaka, Gravitational radiation reaction, Prog. Theor. Phys. Suppl. **163**, 120 (2006), arXiv:gr-qc/0508114.

[1095] E. E. Flanagan and T. Hinderer, Transient resonances in the inspirals of point particles into black holes, Phys. Rev. Lett. **109**, 071102 (2012), arXiv:1009.4923 [gr-qc].

[1096] G. Lukes-Gerakopoulos and V. Witzany, Non-linear effects in EMRI dynamics and their imprints on gravitational waves, arXiv:2103.06724 [gr-qc].

[1097] Black Hole Perturbation Club, (sites.google.com/view/bhpc1996/home) ().

[1098] M. L. Katz, A. J. K. Chua, L. Speri, N. Warburton, and S. A. Hughes, Fast extreme-mass-ratio-inspiral waveforms: New tools for millihertz gravitational-wave data analysis, Phys. Rev. D **104**, 064047 (2021), arXiv:2104.04582 [gr-qc].

[1099] M. J. Fitchett and S. L. Detweiler, Linear momentum and gravitational-waves - circular orbits around a schwarzschild black-hole, Mon. Not. Roy. Astron. Soc. **211**, 933 (1984).

[1100] P. Anninos, R. H. Price, J. Pullin, E. Seidel, and W.-M. Suen, Headon collision of two black holes: Comparison of different approaches, Phys. Rev. D **52**, 4462 (1995), arXiv:gr-qc/9505042.

[1101] M. Favata, S. A. Hughes, and D. E. Holz, How black holes get their kicks: Gravitational radiation

193

recoil revisited, Astrophys. J. Lett. **607**, L5 (2004), arXiv:astro-ph/0402056.

[1102] A. Le Tiec, A. H. Mroue, L. Barack, A. Buonanno, H. P. Pfeiffer, N. Sago, and A. Taracchini, Periastron Advance in Black Hole Binaries, Phys. Rev. Lett. **107**, 141101 (2011), arXiv:1106.3278 [gr-qc].

[1103] A. Le Tiec *et al.*, Periastron Advance in Spinning Black Hole Binaries: Gravitational Self-Force from Numerical Relativity, Phys. Rev. D **88**, 124027 (2013), arXiv:1309.0541 [gr-qc].

[1104] A. Nagar, Gravitational recoil in nonspinning black hole binaries: the span of test-mass results, Phys. Rev. D **88**, 121501 (2013), arXiv:1306.6299 [gr-qc].

[1105] N. E. M. Rifat, S. E. Field, G. Khanna, and V. Varma, Surrogate model for gravitational wave signals from comparable and large-mass-ratio black hole binaries, Phys. Rev. D **101**, 081502 (2020), arXiv:1910.10473 [gr-qc].

[1106] N. Warburton, A. Pound, B. Wardell, J. Miller, and L. Durkan, Gravitational-Wave Energy Flux for Compact Binaries through Second Order in the Mass Ratio, Phys. Rev. Lett. **127**, 151102 (2021), arXiv:2107.01298 [gr-qc].

[1107] B. Wardell, A. Pound, N. Warburton, J. Miller, L. Durkan, and A. Le Tiec, Gravitational Waveforms for Compact Binaries from Second-Order Self-Force Theory, Phys. Rev. Lett. **130**, 241402 (2023), arXiv:2112.12265 [gr-qc].

[1108] A. Le Tiec, The Overlap of Numerical Relativity, Perturbation Theory and Post-Newtonian Theory in the Binary Black Hole Problem, Int. J. Mod. Phys. D **23**, 1430022 (2014), arXiv:1408.5505 [gr-qc].

[1109] E. Gourgoulhon, A. Le Tiec, F. H. Vincent, and N. Warburton, Gravitational waves from bodies orbiting the Galactic Center black hole and their detectability by LISA, Astron. Astrophys. **627**, A92 (2019), arXiv:1903.02049 [gr-qc].

[1110] J. Steinhoff and D. Puetzfeld, Influence of internal structure on the motion of test bodies in extreme mass ratio situations, Phys. Rev. D **86**, 044033 (2012), arXiv:1205.3926 [gr-qc].

[1111] Y. Mino, Self-force in the radiation reaction formula, Prog. Theor. Phys. **113**, 733 (2005), arXiv:gr-qc/0506003.

[1112] S. A. Hughes, S. Drasco, E. E. Flanagan, and J. Franklin, Gravitational radiation reaction and inspiral waveforms in the adiabatic limit, Phys. Rev. Lett. **94**, 221101 (2005), arXiv:gr-qc/0504015.

[1113] P. A. Sundararajan, G. Khanna, S. A. Hughes, and S. Drasco, Towards adiabatic waveforms for inspiral into Kerr black holes: II. Dynamical sources and generic orbits, Phys. Rev. D **78**, 024022 (2008), arXiv:0803.0317 [gr-qc].

[1114] E. Barausse, A. Buonanno, S. A. Hughes, G. Khanna, S. O'Sullivan, and Y. Pan, Modeling multipolar gravitational-wave emission from small mass-ratio mergers, Phys. Rev. D **85**, 024046 (2012), arXiv:1110.3081 [gr-qc].

[1115] A. Taracchini, A. Buonanno, G. Khanna, and S. A. Hughes, Small mass plunging into a Kerr black hole: Anatomy of the inspiral-merger-ringdown waveforms, Phys. Rev. D **90**, 084025 (2014), arXiv:1404.1819 [gr-qc].

[1116] E. Harms, S. Bernuzzi, A. Nagar, and A. Zenginoglu, A new gravitational wave generation algorithm for particle perturbations of the Kerr spacetime, Class. Quant. Grav. **31**, 245004 (2014), arXiv:1406.5983 [gr-qc].

[1117] D. V. Gal'tsov, Radiation reaction in the Kerr gravitational field, J. Phys. A **15**, 3737 (1982).

[1118] S. Drasco, E. E. Flanagan, and S. A. Hughes, Computing inspirals in Kerr in the adiabatic regime. I. The Scalar case, Class. Quant. Grav. **22**, S801 (2005), arXiv:gr-qc/0505075.

[1119] N. Sago, T. Tanaka, W. Hikida, and H. Nakano, Adiabatic radiation reaction to the orbits in Kerr spacetime, Prog. Theor. Phys. **114**, 509 (2005), arXiv:gr-qc/0506092.

[1120] S. Isoyama, R. Fujita, H. Nakano, N. Sago, and T. Tanaka, Evolution of the Carter constant for resonant inspirals into a Kerr black hole: I. The scalar case, PTEP **2013**, 063E01 (2013), arXiv:1302.4035 [gr-qc].

[1121] S. Isoyama, R. Fujita, H. Nakano, N. Sago, and T. Tanaka, "Flux-balance formulae" for extreme

194

mass-ratio inspirals, PTEP **2019**, 013E01 (2019), arXiv:1809.11118 [gr-qc].

[1122] W. H. Press and S. A. Teukolsky, Perturbations of a Rotating Black Hole. II. Dynamical Stability of the Kerr Metric, Astrophys. J. **185**, 649 (1973).

[1123] T. Nakamura, K. Oohara, and Y. Kojima, General Relativistic Collapse to Black Holes and Gravitational Waves from Black Holes, Prog. Theor. Phys. Suppl. **90**, 1 (1987).

[1124] K. Martel, Gravitational wave forms from a point particle orbiting a Schwarzschild black hole, Phys. Rev. D **69**, 044025 (2004), arXiv:gr-qc/0311017.

[1125] E. Poisson, Absorption of mass and angular momentum by a black hole: Time-domain formalisms for gravitational perturbations, and the small-hole / slow-motion approximation, Phys. Rev. D **70**, 084044 (2004), arXiv:gr-qc/0407050.

[1126] P. A. Sundararajan, G. Khanna, and S. A. Hughes, Towards adiabatic waveforms for inspiral into Kerr black holes. I. A New model of the source for the time domain perturbation equation, Phys. Rev. D **76**, 104005 (2007), arXiv:gr-qc/0703028.

[1127] A. Zenginoglu and G. Khanna, Null infinity waveforms from extreme-mass-ratio inspirals in Kerr spacetime, Phys. Rev. X **1**, 021017 (2011), arXiv:1108.1816 [gr-qc].

[1128] S. A. Hughes, The Evolution of circular, nonequatorial orbits of Kerr black holes due to gravitational wave emission, Phys. Rev. D **61**, 084004 (2000), [Erratum: Phys.Rev.D 63, 049902 (2001), Erratum: Phys.Rev.D 65, 069902 (2002), Erratum: Phys.Rev.D 67, 089901 (2003), Erratum: Phys.Rev.D 78, 109902 (2008), Erratum: Phys.Rev.D 90, 109904 (2014)], arXiv:gr-qc/9910091.

[1129] K. Glampedakis and D. Kennefick, Zoom and whirl: Eccentric equatorial orbits around spinning black holes and their evolution under gravitational radiation reaction, Phys. Rev. D **66**, 044002 (2002), arXiv:gr-qc/0203086.

[1130] S. Drasco and S. A. Hughes, Gravitational wave snapshots of generic extreme mass ratio inspirals, Phys. Rev. D **73**, 024027 (2006), [Erratum: Phys.Rev.D 88, 109905 (2013), Erratum: Phys.Rev.D 90, 109905 (2014)], arXiv:gr-qc/0509101.

[1131] R. Fujita, W. Hikida, and H. Tagoshi, An Efficient Numerical Method for Computing Gravitational Waves Induced by a Particle Moving on Eccentric Inclined Orbits around a Kerr Black Hole, Prog. Theor. Phys. **121**, 843 (2009), arXiv:0904.3810 [gr-qc].

[1132] S. Mano, H. Suzuki, and E. Takasugi, Analytic solutions of the Teukolsky equation and their low frequency expansions, Prog. Theor. Phys. **95**, 1079 (1996), arXiv:gr-qc/9603020.

[1133] Y. Mino, M. Sasaki, M. Shibata, H. Tagoshi, and T. Tanaka, Black hole perturbation: Chapter 1, Prog. Theor. Phys. Suppl. **128**, 1 (1997), arXiv:gr-qc/9712057.

[1134] R. Fujita, Gravitational Waves from a Particle in Circular Orbits around a Schwarzschild Black Hole to the 22nd Post-Newtonian Order, Prog. Theor. Phys. **128**, 971 (2012), arXiv:1211.5535 [gr-qc].

[1135] R. Fujita, Gravitational Waves from a Particle in Circular Orbits around a Rotating Black Hole to the 11th Post-Newtonian Order, PTEP **2015**, 033E01 (2015), arXiv:1412.5689 [gr-qc].

[1136] A. G. Shah, Gravitational-wave flux for a particle orbiting a Kerr black hole to 20th post-Newtonian order: a numerical approach, Phys. Rev. D **90**, 044025 (2014), arXiv:1403.2697 [gr-qc].

[1137] H. Tagoshi, PostNewtonian expansion of gravitational waves from a particle in slightly eccentric orbit around a rotating black hole, Prog. Theor. Phys. **93**, 307 (1995), [Erratum: Prog.Theor.Phys. 118, 577–579 (2007)].

[1138] C. Munna, C. R. Evans, S. Hopper, and E. Forseth, Determination of new coefficients in the angular momentum and energy fluxes at infinity to 9PN order for eccentric Schwarzschild extreme-mass-ratio inspirals using mode-by-mode fitting, Phys. Rev. D **102**, 024047 (2020), arXiv:2005.03044 [gr-qc].

[1139] C. Munna and C. R. Evans, Eccentric-orbit extreme-mass-ratio-inspiral radiation II: 1PN correction to leading-logarithm and subleading-logarithm flux sequences and the entire perturbative 4PN flux, Phys. Rev. D **102**, 104006 (2020), arXiv:2009.01254 [gr-qc].

195

[1140] N. Sago, T. Tanaka, W. Hikida, K. Ganz, and H. Nakano, The Adiabatic evolution of orbital parameters in the Kerr spacetime, Prog. Theor. Phys. **115**, 873 (2006), arXiv:gr-qc/0511151.

[1141] K. Ganz, W. Hikida, H. Nakano, N. Sago, and T. Tanaka, Adiabatic Evolution of Three 'Constants' of Motion for Greatly Inclined Orbits in Kerr Spacetime, Prog. Theor. Phys. **117**, 1041 (2007), arXiv:gr-qc/0702054.

[1142] N. Sago and R. Fujita, Calculation of radiation reaction effect on orbital parameters in Kerr spacetime, PTEP **2015**, 073E03 (2015), arXiv:1505.01600 [gr-qc].

[1143] C. Cutler, D. Kennefick, and E. Poisson, Gravitational radiation reaction for bound motion around a Schwarzschild black hole, Phys. Rev. D **50**, 3816 (1994).

[1144] S. A. Hughes, Evolution of circular, nonequatorial orbits of Kerr black holes due to gravitational wave emission. II. Inspiral trajectories and gravitational wave forms, Phys. Rev. D **64**, 064004 (2001), [Erratum: Phys.Rev.D 88, 109902 (2013)], arXiv:gr-qc/0104041.

[1145] R. Fujita and B. R. Iyer, Spherical harmonic modes of 5.5 post-Newtonian gravitational wave polarisations and associated factorised resummed waveforms for a particle in circular orbit around a Schwarzschild black hole, Phys. Rev. D **82**, 044051 (2010), arXiv:1005.2266 [gr-qc].

[1146] Y. Pan, A. Buonanno, R. Fujita, E. Racine, and H. Tagoshi, Post-Newtonian factorized multipolar waveforms for spinning, non-precessing black-hole binaries, Phys. Rev. D **83**, 064003 (2011), [Erratum: Phys.Rev.D 87, 109901 (2013)], arXiv:1006.0431 [gr-qc].

[1147] S. E. Gralla, S. A. Hughes, and N. Warburton, Inspiral into Gargantua, Class. Quant. Grav. **33**, 155002 (2016), [Erratum: Class.Quant.Grav. 37, 109501 (2020)], arXiv:1603.01221 [gr-qc].

[1148] A. J. K. Chua, M. L. Katz, N. Warburton, and S. A. Hughes, Rapid generation of fully relativistic extreme-mass-ratio-inspiral waveform templates for LISA data analysis, Phys. Rev. Lett. **126**, 051102 (2021), arXiv:2008.06071 [gr-qc].

[1149] R. Fujita and M. Shibata, Extreme mass ratio inspirals on the equatorial plane in the adiabatic order, Phys. Rev. D **102**, 064005 (2020), arXiv:2008.13554 [gr-qc].

[1150] S. A. Hughes, N. Warburton, G. Khanna, A. J. K. Chua, and M. L. Katz, Adiabatic waveforms for extreme mass-ratio inspirals via multivoice decomposition in time and frequency, Phys. Rev. D **103**, 104014 (2021), [Erratum: Phys.Rev.D 107, 089901 (2023)], arXiv:2102.02713 [gr-qc].

[1151] S. Isoyama, R. Fujita, A. J. K. Chua, H. Nakano, A. Pound, and N. Sago, Adiabatic Waveforms from Extreme-Mass-Ratio Inspirals: An Analytical Approach, Phys. Rev. Lett. **128**, 231101 (2022), arXiv:2111.05288 [gr-qc].

[1152] L. Barack and C. Cutler, LISA capture sources: Approximate waveforms, signal-to-noise ratios, and parameter estimation accuracy, Phys. Rev. D **69**, 082005 (2004), arXiv:gr-qc/0310125.

[1153] S. Babak, H. Fang, J. R. Gair, K. Glampedakis, and S. A. Hughes, 'Kludge' gravitational waveforms for a test-body orbiting a Kerr black hole, Phys. Rev. D **75**, 024005 (2007), [Erratum: Phys.Rev.D 77, 04990 (2008)], arXiv:gr-qc/0607007.

[1154] A. J. K. Chua and J. R. Gair, Improved analytic extreme-mass-ratio inspiral model for scoping out eLISA data analysis, Class. Quant. Grav. **32**, 232002 (2015), arXiv:1510.06245 [gr-qc].

[1155] EMRI Kludge Suite, (github.com/alvincjk/EMRI_Kludge_Suite).

[1156] L. Barack and N. Sago, Gravitational self force on a particle in circular orbit around a Schwarzschild black hole, Phys. Rev. D **75**, 064021 (2007), arXiv:gr-qc/0701069.

[1157] L. Barack and N. Sago, Gravitational self-force on a particle in eccentric orbit around a Schwarzschild black hole, Phys. Rev. D **81**, 084021 (2010), arXiv:1002.2386 [gr-qc].

[1158] S. R. Dolan and L. Barack, Self-force via m-mode regularization and 2+1D evolution: III. Gravitational field on Schwarzschild spacetime, Phys. Rev. D **87**, 084066 (2013), arXiv:1211.4586 [gr-qc].

[1159] S. Akcay, N. Warburton, and L. Barack, Frequency-domain algorithm for the Lorenz-gauge gravitational self-force, Phys. Rev. D **88**, 104009 (2013), arXiv:1308.5223 [gr-qc].

[1160] T. Osburn, E. Forseth, C. R. Evans, and S. Hopper, Lorenz gauge gravitational self-force calculations of eccentric binaries using a frequency domain procedure, Phys. Rev. D **90**, 104031

(2014), arXiv:1409.4419 [gr-qc].

[1161] T. S. Keidl, A. G. Shah, J. L. Friedman, D.-H. Kim, and L. R. Price, Gravitational Self-force in a Radiation Gauge, Phys. Rev. D **82**, 124012 (2010), [Erratum: Phys.Rev.D 90, 109902 (2014)], arXiv:1004.2276 [gr-qc].

[1162] A. G. Shah, T. S. Keidl, J. L. Friedman, D.-H. Kim, and L. R. Price, Conservative, gravitational self-force for a particle in circular orbit around a Schwarzschild black hole in a Radiation Gauge, Phys. Rev. D **83**, 064018 (2011), arXiv:1009.4876 [gr-qc].

[1163] A. Pound, C. Merlin, and L. Barack, Gravitational self-force from radiation-gauge metric perturbations, Phys. Rev. D **89**, 024009 (2014), arXiv:1310.1513 [gr-qc].

[1164] C. Merlin and A. G. Shah, Self-force from reconstructed metric perturbations: numerical implementation in Schwarzschild spacetime, Phys. Rev. D **91**, 024005 (2015), arXiv:1410.2998 [gr-qc].

[1165] M. van de Meent and A. G. Shah, Metric perturbations produced by eccentric equatorial orbits around a Kerr black hole, Phys. Rev. D **92**, 064025 (2015), arXiv:1506.04755 [gr-qc].

[1166] M. van de Meent, Gravitational self-force on eccentric equatorial orbits around a Kerr black hole, Phys. Rev. D **94**, 044034 (2016), arXiv:1606.06297 [gr-qc].

[1167] C. Merlin, A. Ori, L. Barack, A. Pound, and M. van de Meent, Completion of metric reconstruction for a particle orbiting a Kerr black hole, Phys. Rev. D **94**, 104066 (2016), arXiv:1609.01227 [gr-qc].

[1168] M. van De Meent, The mass and angular momentum of reconstructed metric perturbations, Class. Quant. Grav. **34**, 124003 (2017), arXiv:1702.00969 [gr-qc].

[1169] M. van de Meent, Gravitational self-force on generic bound geodesics in Kerr spacetime, Phys. Rev. D **97**, 104033 (2018), arXiv:1711.09607 [gr-qc].

[1170] V. Toomani, P. Zimmerman, A. Spiers, S. Hollands, A. Pound, and S. R. Green, New metric reconstruction scheme for gravitational self-force calculations, Class. Quant. Grav. **39**, 015019 (2022), arXiv:2108.04273 [gr-qc].

[1171] S. R. Dolan, C. Kavanagh, and B. Wardell, Gravitational Perturbations of Rotating Black Holes in Lorenz Gauge, Phys. Rev. Lett. **128**, 151101 (2022), arXiv:2108.06344 [gr-qc].

[1172] R. Panosso Macedo, B. Leather, N. Warburton, B. Wardell, and A. Zenginoğlu, Hyperboloidal method for frequency-domain self-force calculations, Phys. Rev. D **105**, 104033 (2022), arXiv:2202.01794 [gr-qc].

[1173] A. G. Shah, J. L. Friedman, and T. S. Keidl, EMRI corrections to the angular velocity and redshift factor of a mass in circular orbit about a Kerr black hole, Phys. Rev. D **86**, 084059 (2012), arXiv:1207.5595 [gr-qc].

[1174] A. G. Shah, J. L. Friedman, and B. F. Whiting, Finding high-order analytic post-Newtonian parameters from a high-precision numerical self-force calculation, Phys. Rev. D **89**, 064042 (2014), arXiv:1312.1952 [gr-qc].

[1175] D. Bini and T. Damour, Analytic determination of the eight-and-a-half post-Newtonian self-force contributions to the two-body gravitational interaction potential, Phys. Rev. D **89**, 104047 (2014), arXiv:1403.2366 [gr-qc].

[1176] S. Hopper, C. Kavanagh, and A. C. Ottewill, Analytic self-force calculations in the post-Newtonian regime: eccentric orbits on a Schwarzschild background, Phys. Rev. D **93**, 044010 (2016), arXiv:1512.01556 [gr-qc].

[1177] C. Kavanagh, A. C. Ottewill, and B. Wardell, Analytical high-order post-Newtonian expansions for spinning extreme mass ratio binaries, Phys. Rev. D **93**, 124038 (2016), arXiv:1601.03394 [gr-qc].

[1178] D. Bini, T. Damour, A. Geralico, and C. Kavanagh, Detweiler's redshift invariant for spinning particles along circular orbits on a Schwarzschild background, Phys. Rev. D **97**, 104022 (2018), arXiv:1801.09616 [gr-qc].

[1179] D. Bini and A. Geralico, New gravitational self-force analytical results for eccentric equatorial orbits around a Kerr black hole: redshift invariant, Phys. Rev. D **100**, 104002 (2019),

197

arXiv:1907.11080 [gr-qc].

[1180] D. Bini and A. Geralico, Analytical determination of the periastron advance in spinning binaries from self-force computations, Phys. Rev. D **100**, 121502 (2019), arXiv:1907.11083 [gr-qc].

[1181] P. Nolan, C. Kavanagh, S. R. Dolan, A. C. Ottewill, N. Warburton, and B. Wardell, Octupolar invariants for compact binaries on quasicircular orbits, Phys. Rev. D **92**, 123008 (2015), arXiv:1505.04447 [gr-qc].

[1182] A. G. Shah and A. Pound, Linear-in-mass-ratio contribution to spin precession and tidal invariants in Schwarzschild spacetime at very high post-Newtonian order, Phys. Rev. D **91**, 124022 (2015), arXiv:1503.02414 [gr-qc].

[1183] D. Bini and A. Geralico, Tidal invariants along the worldline of an extended body in Kerr spacetime, Phys. Rev. D **91**, 084012 (2015), arXiv:1806.07696 [gr-qc].

[1184] D. Bini, T. Damour, A. Geralico, C. Kavanagh, and M. van de Meent, Gravitational self-force corrections to gyroscope precession along circular orbits in the Kerr spacetime, Phys. Rev. D **98**, 104062 (2018), arXiv:1809.02516 [gr-qc].

[1185] D. Bini and A. Geralico, New gravitational self-force analytical results for eccentric equatorial orbits around a Kerr black hole: gyroscope precession, Phys. Rev. D **100**, 104003 (2019), arXiv:1907.11082 [gr-qc].

[1186] C. Munna and C. R. Evans, Post-Newtonian expansion of the spin-precession invariant for eccentric-orbit nonspinning extreme-mass-ratio inspirals to 9PN and e16, Phys. Rev. D **106**, 044058 (2022), arXiv:2206.04085 [gr-qc].

[1187] L. Barack and P. Giudice, Time-domain metric reconstruction for self-force applications, Phys. Rev. D **95**, 104033 (2017), arXiv:1702.04204 [gr-qc].

[1188] S. A. Hughes, (Sort of) testing relativity with extreme mass ratio inspirals, AIP Conf. Proc. **873**, 233 (2006), arXiv:gr-qc/0608140.

[1189] P. Canizares and C. F. Sopuerta, Simulations of Extreme-Mass-Ratio Inspirals Using Pseudospectral Methods, J. Phys. Conf. Ser. **154**, 012053 (2009), arXiv:0811.0294 [gr-qc].

[1190] P. Canizares and C. F. Sopuerta, Modelling Extreme-Mass-Ratio Inspirals using Pseudospectral Methods, in *12th Marcel Grossmann Meeting on General Relativity* (2010) pp. 841–843, arXiv:1001.4697 [gr-qc].

[1191] P. Canizares and C. F. Sopuerta, Time-domain modelling of Extreme-Mass-Ratio Inspirals for the Laser Interferometer Space Antenna, J. Phys. Conf. Ser. **314**, 012075 (2011), arXiv:1103.2149 [gr-qc].

[1192] S. E. Field, J. S. Hesthaven, and S. R. Lau, Discontinuous Galerkin method for computing gravitational waveforms from extreme mass ratio binaries, Class. Quant. Grav. **26**, 165010 (2009), arXiv:0902.1287 [gr-qc].

[1193] P. Diener, I. Vega, B. Wardell, and S. Detweiler, Self-consistent orbital evolution of a particle around a Schwarzschild black hole, Phys. Rev. Lett. **108**, 191102 (2012), arXiv:1112.4821 [gr-qc].

[1194] C. Markakis, M. F. O'Boyle, P. D. Brubeck, and L. Barack, Discontinuous collocation methods and gravitational self-force applications, Class. Quant. Grav. **38**, 075031 (2021), arXiv:1406.4865 [math.NA].

[1195] L. J. G. Da Silva, R. Panosso Macedo, J. E. Thompson, J. A. V. Kroon, L. Durkan, and O. Long, Hyperboloidal discontinuous time-symmetric numerical algorithm with higher order jumps for gravitational self-force computations in the time domain, arXiv:2306.13153 [gr-qc].

[1196] M. Vishal, S. E. Field, K. Rink, S. Gottlieb, and G. Khanna, Towards exponentially-convergent simulations of extreme-mass-ratio inspirals: A time-domain solver for the scalar Teukolsky equation with singular source terms, arXiv:2307.01349 [gr-qc].

[1197] M. F. O'Boyle, C. Markakis, L. J. G. Da Silva, R. Panosso Macedo, and J. A. V. Kroon, Conservative Evolution of Black Hole Perturbations with Time-Symmetric Numerical Methods, arXiv:2210.02550 [gr-qc].

[1198] C. Markakis, S. Bray, and A. Zenginoğlu, Symmetric integration of the 1+1 Teukolsky equation

on hyperboloidal foliations of Kerr spacetimes, arXiv:2303.08153 [gr-qc].

[1199] M. F. O'Boyle and C. Markakis, Discontinuous collocation and symmetric integration methods for distributionally-sourced hyperboloidal partial differential equations, arXiv:2308.02385 [math.NA].

[1200] M. Casals, S. Dolan, A. C. Ottewill, and B. Wardell, Self-Force and Green Function in Schwarzschild spacetime via Quasinormal Modes and Branch Cut, Phys. Rev. D **88**, 044022 (2013), arXiv:1306.0884 [gr-qc].

[1201] M. Casals, B. C. Nolan, A. C. Ottewill, and B. Wardell, Regularized calculation of the retarded Green function in a Schwarzschild spacetime, Phys. Rev. D **100**, 104037 (2019), arXiv:1910.02567 [gr-qc].

[1202] H. Yang, F. Zhang, A. Zimmerman, and Y. Chen, Scalar Green function of the Kerr spacetime, Phys. Rev. D **89**, 064014 (2014), arXiv:1311.3380 [gr-qc].

[1203] C. O'Toole, A. Ottewill, and B. Wardell, Characteristic formulation of the Regge-Wheeler and Zerilli Green functions, Phys. Rev. D **103**, 124022 (2021), arXiv:2010.15818 [gr-qc].

[1204] N. Warburton, S. Akcay, L. Barack, J. R. Gair, and N. Sago, Evolution of inspiral orbits around a Schwarzschild black hole, Phys. Rev. D **85**, 061501 (2012), arXiv:1111.6908 [gr-qc].

[1205] T. Osburn, N. Warburton, and C. R. Evans, Highly eccentric inspirals into a black hole, Phys. Rev. D **93**, 064024 (2016), arXiv:1511.01498 [gr-qc].

[1206] P. Lynch, M. van de Meent, and N. Warburton, Self-forced inspirals with spin-orbit precession, arXiv:2305.10533 [gr-qc].

[1207] K. A. Lackeos and L. M. Burko, Self-forced gravitational waveforms for Extreme and Intermediate mass ratio inspirals, Phys. Rev. D **86**, 084055 (2012), arXiv:1206.1452 [gr-qc].

[1208] E. Rosenthal, Second-order gravitational self-force, Phys. Rev. D **74**, 084018 (2006), arXiv:gr-qc/0609069.

[1209] A. Pound, Nonlinear gravitational self-force. I. Field outside a small body, Phys. Rev. D **86**, 084019 (2012), arXiv:1206.6538 [gr-qc].

[1210] A. Pound, Gauge and motion in perturbation theory, Phys. Rev. D **92**, 044021 (2015), arXiv:1506.02894 [gr-qc].

[1211] A. Pound and J. Miller, Practical, covariant puncture for second-order self-force calculations, Phys. Rev. D **89**, 104020 (2014), arXiv:1403.1843 [gr-qc].

[1212] N. Warburton and B. Wardell, Applying the effective-source approach to frequency-domain self-force calculations, Phys. Rev. D **89**, 044046 (2014), arXiv:1311.3104 [gr-qc].

[1213] J. Miller, B. Wardell, and A. Pound, Second-order perturbation theory: the problem of infinite mode coupling, Phys. Rev. D **94**, 104018 (2016), arXiv:1608.06783 [gr-qc].

[1214] J. Miller, *The second-order gravitational self-force*, Ph.D. thesis, Southampton U. (2017).

[1215] L. Durkan and N. Warburton, Slow evolution of the metric perturbation due to a quasicircular inspiral into a Schwarzschild black hole, Phys. Rev. D **106**, 084023 (2022), arXiv:2206.08179 [gr-qc].

[1216] A. Spiers, A. Pound, and B. Wardell, Second-order perturbations of the Schwarzschild spacetime: practical, covariant and gauge-invariant formalisms, arXiv:2306.17847 [gr-qc].

[1217] J. Mathews, Spin effects in post-adiabatic waveforms, talk given at the 25th Capra Meeting, Jun 2022. Available at https://www.caprameeting.org/previous-meetings-archive/25th-capra/timetable.

[1218] J. Brink, M. Geyer, and T. Hinderer, Orbital resonances around Black holes, Phys. Rev. Lett. **114**, 081102 (2015), arXiv:1304.0330 [gr-qc].

[1219] J. Brink, M. Geyer, and T. Hinderer, Astrophysics of resonant orbits in the Kerr metric, Phys. Rev. D **91**, 083001 (2015), arXiv:1501.07728 [gr-qc].

[1220] J. Levin and G. Perez-Giz, A Periodic Table for Black Hole Orbits, Phys. Rev. D **77**, 103005 (2008), arXiv:0802.0459 [gr-qc].

[1221] T. A. Apostolatos, G. Lukes-Gerakopoulos, and G. Contopoulos, How to Observe a Non-Kerr Spacetime Using Gravitational Waves, Phys. Rev. Lett. **103**, 111101 (2009), arXiv:0906.0093

[gr-qc].

[1222] U. Ruangsri and S. A. Hughes, Census of transient orbital resonances encountered during binary inspiral, Phys. Rev. D **89**, 084036 (2014), arXiv:1307.6483 [gr-qc].

[1223] D. P. Mihaylov and J. R. Gair, Transition of EMRIs through resonance: corrections to higher order in the on-resonance flux modification, J. Math. Phys. **58**, 112501 (2017), arXiv:1706.06639 [gr-qc].

[1224] J. Gair, N. Yunes, and C. M. Bender, Resonances in Extreme Mass-Ratio Inspirals: Asymptotic and Hyperasymptotic Analysis, J. Math. Phys. **53**, 032503 (2012), arXiv:1111.3605 [gr-qc].

[1225] E. E. Flanagan, S. A. Hughes, and U. Ruangsri, Resonantly enhanced and diminished strong-field gravitational-wave fluxes, Phys. Rev. D **89**, 084028 (2014), arXiv:1208.3906 [gr-qc].

[1226] M. van de Meent, Conditions for Sustained Orbital Resonances in Extreme Mass Ratio Inspirals, Phys. Rev. D **89**, 084033 (2014), arXiv:1311.4457 [gr-qc].

[1227] A. G. M. Lewis, A. Zimmerman, and H. P. Pfeiffer, Fundamental frequencies and resonances from eccentric and precessing binary black hole inspirals, Class. Quant. Grav. **34**, 124001 (2017), arXiv:1611.03418 [gr-qc].

[1228] Z. Nasipak and C. R. Evans, Resonant self-force effects in extreme-mass-ratio binaries: A scalar model, Phys. Rev. D **104**, 084011 (2021), arXiv:2105.15188 [gr-qc].

[1229] Z. Nasipak, Adiabatic evolution due to the conservative scalar self-force during orbital resonances, Phys. Rev. D **106**, 064042 (2022), arXiv:2207.02224 [gr-qc].

[1230] C. M. Hirata, Resonant recoil in extreme mass ratio binary black hole mergers, Phys. Rev. D **83**, 104024 (2011), arXiv:1011.4987 [gr-qc].

[1231] M. van de Meent, Resonantly enhanced kicks from equatorial small mass-ratio inspirals, Phys. Rev. D **90**, 044027 (2014), arXiv:1406.2594 [gr-qc].

[1232] A. Buonanno, Y. Chen, and T. Damour, Transition from inspiral to plunge in precessing binaries of spinning black holes, Phys. Rev. D **74**, 104005 (2006), arXiv:gr-qc/0508067.

[1233] A. Nagar, T. Damour, and A. Tartaglia, Binary black hole merger in the extreme mass ratio limit, Class. Quant. Grav. **24**, S109 (2007), arXiv:gr-qc/0612096.

[1234] T. Damour and A. Nagar, Faithful effective-one-body waveforms of small-mass-ratio coalescing black-hole binaries, Phys. Rev. D **76**, 064028 (2007), arXiv:0705.2519 [gr-qc].

[1235] T. Damour and A. Nagar, An Improved analytical description of inspiralling and coalescing black-hole binaries, Phys. Rev. D **79**, 081503 (2009), arXiv:0902.0136 [gr-qc].

[1236] S. Bernuzzi and A. Nagar, Binary black hole merger in the extreme-mass-ratio limit: a multipolar analysis, Phys. Rev. D **81**, 084056 (2010), arXiv:1003.0597 [gr-qc].

[1237] S. Bernuzzi, A. Nagar, and A. Zenginoglu, Binary black hole coalescence in the extreme-mass-ratio limit: testing and improving the effective-one-body multipolar waveform, Phys. Rev. D **83**, 064010 (2011), arXiv:1012.2456 [gr-qc].

[1238] S. Bernuzzi, A. Nagar, and A. Zenginoglu, Binary black hole coalescence in the large-mass-ratio limit: the hyperboloidal layer method and waveforms at null infinity, Phys. Rev. D **84**, 084026 (2011), arXiv:1107.5402 [gr-qc].

[1239] Y. Pan, A. Buonanno, A. Taracchini, L. E. Kidder, A. H. Mroué, H. P. Pfeiffer, M. A. Scheel, and B. Szilágyi, Inspiral-merger-ringdown waveforms of spinning, precessing black-hole binaries in the effective-one-body formalism, Phys. Rev. D **89**, 084006 (2014), arXiv:1307.6232 [gr-qc].

[1240] P. A. Sundararajan, The Transition from adiabatic inspiral to geodesic plunge for a compact object around a massive Kerr black hole: Generic orbits, Phys. Rev. D **77**, 124050 (2008), arXiv:0803.4482 [gr-qc].

[1241] M. Kesden, Transition from adiabatic inspiral to plunge into a spinning black hole, Phys. Rev. D **83**, 104011 (2011), arXiv:1101.3749 [gr-qc].

[1242] A. Folacci and M. Ould El Hadj, Multipolar gravitational waveforms and ringdowns generated during the plunge from the innermost stable circular orbit into a Schwarzschild black hole, Phys. Rev. D **98**, 084008 (2018), arXiv:1806.01577 [gr-qc].

[1243] B. Rom and R. Sari, Extreme mass-ratio binary black hole merger: Characteristics of the test-

200

particle limit, Phys. Rev. D **106**, 104040 (2022), arXiv:2204.11738 [gr-qc].

[1244] G. Compère and L. Küchler, Self-consistent adiabatic inspiral and transition motion, Phys. Rev. Lett. **126**, 241106 (2021), arXiv:2102.12747 [gr-qc].

[1245] L. Küchler, Inspiral, transition and plunge in the small mass ratio expansion, talk given at the 25th Capra Meeting, Jun 2022. Available at https://www.caprameeting.org/previous-meetings-archive/25th-capra/timetable.

[1246] W. G. Dixon, Dynamics of extended bodies in general relativity. I. Momentum and angular momentum, Proc. Roy. Soc. Lond. A **314**, 499 (1970).

[1247] W. G. Dixon, Dynamics of extended bodies in general relativity. II. Moments of the charge-current vector, Proc. Roy. Soc. Lond. A **319**, 509 (1970).

[1248] K. S. Thorne and J. B. Hartle, Laws of motion and precession for black holes and other bodies, Phys. Rev. D **31**, 1815 (1984).

[1249] J. Mathews, A. Pound, and B. Wardell, Self-force calculations with a spinning secondary, Phys. Rev. D **105**, 084031 (2022), arXiv:2112.13069 [gr-qc].

[1250] S. Suzuki and K.-i. Maeda, Chaos in Schwarzschild space-time: The motion of a spinning particle, Phys. Rev. D **55**, 4848 (1997), arXiv:gr-qc/9604020.

[1251] R. Rudiger, Conserved Quantities of Spinning Test Particles in General Relativity. II, Proceedings of the Royal Society of London Series A **385**, 229 (1983).

[1252] S. Suzuki and K.-i. Maeda, Signature of chaos in gravitational waves from a spinning particle, Phys. Rev. D **61**, 024005 (2000), arXiv:gr-qc/9910064.

[1253] U. Ruangsri, S. J. Vigeland, and S. A. Hughes, Gyroscopes orbiting black holes: A frequency-domain approach to precession and spin-curvature coupling for spinning bodies on generic Kerr orbits, Phys. Rev. D **94**, 044008 (2016), arXiv:1512.00376 [gr-qc].

[1254] O. Zelenka, G. Lukes-Gerakopoulos, V. Witzany, and O. Kopáček, Growth of resonances and chaos for a spinning test particle in the Schwarzschild background, Phys. Rev. D **101**, 024037 (2020), arXiv:1911.00414 [gr-qc].

[1255] V. Witzany, A. Pound, and L. Barack, Finite-size effects in large mass ratio inspirals, Unpublished manuscript (2020).

[1256] S. Akcay, S. R. Dolan, C. Kavanagh, J. Moxon, N. Warburton, and B. Wardell, Dissipation in extreme-mass ratio binaries with a spinning secondary, Phys. Rev. D **102**, 064013 (2020), arXiv:1912.09461 [gr-qc].

[1257] Y. Mino, M. Shibata, and T. Tanaka, Gravitational waves induced by a spinning particle falling into a rotating black hole, Phys. Rev. D **53**, 622 (1996), [Erratum: Phys.Rev.D 59, 047502 (1999)].

[1258] T. Tanaka, Y. Mino, M. Sasaki, and M. Shibata, Gravitational waves from a spinning particle in circular orbits around a rotating black hole, Phys. Rev. D **54**, 3762 (1996), arXiv:gr-qc/9602038.

[1259] W.-B. Han, Gravitational Radiations from a Spinning Compact Object around a supermassive Kerr black hole in circular orbit, Phys. Rev. D **82**, 084013 (2010), arXiv:1008.3324 [gr-qc].

[1260] E. Harms, G. Lukes-Gerakopoulos, S. Bernuzzi, and A. Nagar, Asymptotic gravitational wave fluxes from a spinning particle in circular equatorial orbits around a rotating black hole, Phys. Rev. D **93**, 044015 (2016), [Addendum: Phys.Rev.D 100, 129901 (2019)], arXiv:1510.05548 [gr-qc].

[1261] E. Harms, G. Lukes-Gerakopoulos, S. Bernuzzi, and A. Nagar, Spinning test body orbiting around a Schwarzschild black hole: Circular dynamics and gravitational-wave fluxes, Phys. Rev. D **94**, 104010 (2016), arXiv:1609.00356 [gr-qc].

[1262] G. Lukes-Gerakopoulos, E. Harms, S. Bernuzzi, and A. Nagar, Spinning test-body orbiting around a Kerr black hole: circular dynamics and gravitational-wave fluxes, Phys. Rev. D **96**, 064051 (2017), arXiv:1707.07537 [gr-qc].

[1263] A. Nagar, F. Messina, C. Kavanagh, G. Lukes-Gerakopoulos, N. Warburton, S. Bernuzzi, and E. Harms, Factorization and resummation: A new paradigm to improve gravitational

wave amplitudes. III: the spinning test-body terms, Phys. Rev. D **100**, 104056 (2019), arXiv:1907.12233 [gr-qc].

[1264] G. A. Piovano, A. Maselli, and P. Pani, Extreme mass ratio inspirals with spinning secondary: a detailed study of equatorial circular motion, Phys. Rev. D **102**, 024041 (2020), arXiv:2004.02654 [gr-qc].

[1265] V. Skoupý and G. Lukes-Gerakopoulos, Spinning test body orbiting around a Kerr black hole: Eccentric equatorial orbits and their asymptotic gravitational-wave fluxes, Phys. Rev. D **103**, 104045 (2021), arXiv:2102.04819 [gr-qc].

[1266] N. Warburton, T. Osburn, and C. R. Evans, Evolution of small-mass-ratio binaries with a spinning secondary, Phys. Rev. D **96**, 084057 (2017), arXiv:1708.03720 [gr-qc].

[1267] V. Skoupý and G. Lukes-Gerakopoulos, Adiabatic equatorial inspirals of a spinning body into a Kerr black hole, Phys. Rev. D **105**, 084033 (2022), arXiv:2201.07044 [gr-qc].

[1268] L. V. Drummond and S. A. Hughes, Precisely computing bound orbits of spinning bodies around black holes. I. General framework and results for nearly equatorial orbits, Phys. Rev. D **105**, 124040 (2022), arXiv:2201.13334 [gr-qc].

[1269] L. V. Drummond and S. A. Hughes, Precisely computing bound orbits of spinning bodies around black holes. II. Generic orbits, Phys. Rev. D **105**, 124041 (2022), arXiv:2201.13335 [gr-qc].

[1270] T. Binnington and E. Poisson, Relativistic theory of tidal Love numbers, Phys. Rev. D **80**, 084018 (2009), arXiv:0906.1366 [gr-qc].

[1271] H. Yang and M. Casals, General Relativistic Dynamics of an Extreme Mass-Ratio Binary interacting with an External Body, Phys. Rev. D **96**, 083015 (2017), arXiv:1704.02022 [gr-qc].

[1272] H. Yang, B. Bonga, Z. Peng, and G. Li, Relativistic Mean Motion Resonance, Phys. Rev. D **100**, 124056 (2019), arXiv:1910.07337 [gr-qc].

[1273] P. Gupta, B. Bonga, A. J. K. Chua, and T. Tanaka, Importance of tidal resonances in extreme-mass-ratio inspirals, Phys. Rev. D **104**, 044056 (2021), arXiv:2104.03422 [gr-qc].

[1274] P. Gupta, T. Kakehi, and T. Tanaka, Resonant jumps induced by stationary tidal perturbation: a two-for-one deal, Class. Quant. Grav. **39**, 245005 (2022), arXiv:2207.13369 [gr-qc].

[1275] E. Barausse and L. Rezzolla, The Influence of the hydrodynamic drag from an accretion torus on extreme mass-ratio inspirals, Phys. Rev. D **77**, 104027 (2008), arXiv:0711.4558 [gr-qc].

[1276] P. Suková, M. Zajaček, V. Witzany, and V. Karas, Stellar Transits across a Magnetized Accretion Torus as a Mechanism for Plasmoid Ejection, Astrophys. J. **917**, 43 (2021), arXiv:2102.08135 [astro-ph.HE].

[1277] L. Speri, A. Antonelli, L. Sberna, S. Babak, E. Barausse, J. R. Gair, and M. L. Katz, Probing Accretion Physics with Gravitational Waves, Phys. Rev. X **13**, 021035 (2023), arXiv:2207.10086 [gr-qc].

[1278] V. Cardoso, K. Destounis, F. Duque, R. Panosso Macedo, and A. Maselli, Gravitational Waves from Extreme-Mass-Ratio Systems in Astrophysical Environments, Phys. Rev. Lett. **129**, 241103 (2022), arXiv:2210.01133 [gr-qc].

[1279] K. Destounis, A. Kulathingal, K. D. Kokkotas, and G. O. Papadopoulos, Gravitational-wave imprints of compact and galactic-scale environments in extreme-mass-ratio binaries, Phys. Rev. D **107**, 084027 (2023), arXiv:2210.09357 [gr-qc].

[1280] E. Barausse, L. Rezzolla, D. Petroff, and M. Ansorg, Gravitational waves from Extreme Mass Ratio Inspirals in non-pure Kerr spacetimes, Phys. Rev. D **75**, 064026 (2007), arXiv:gr-qc/0612123.

[1281] J. P. S. Lemos and P. S. Letelier, Exact general relativistic thin disks around black holes, Phys. Rev. D **49**, 5135 (1994).

[1282] M. Basovník and O. Semerák, Geometry of deformed black holes. II. Schwarzschild hole surrounded by a Bach-Weyl ring, Phys. Rev. D **94**, 044007 (2016), arXiv:1608.05961 [gr-qc].

[1283] O. Semerák and P. Čížek, Rotating Disc around a Schwarzschild Black Hole, Universe **6**, 27 (2020).

[1284] O. Semerák and P. Suková, On geodesic dynamics in deformed black-hole fields, Fund. Theor.

202

Phys. **179**, 561 (2015), arXiv:1509.08536 [gr-qc].

[1285] N. Yunes and J. Gonzalez, Metric of a tidally perturbed spinning black hole, Phys. Rev. D **73**, 024010 (2006), [Erratum: Phys.Rev.D 89, 089902 (2014)], arXiv:gr-qc/0510076.

[1286] A. Le Tiec, M. Casals, and E. Franzin, Tidal Love Numbers of Kerr Black Holes, Phys. Rev. D **103**, 084021 (2021), arXiv:2010.15795 [gr-qc].

[1287] L. Polcar, G. Lukes-Gerakopoulos, and V. Witzany, Extreme mass ratio inspirals into black holes surrounded by matter, Phys. Rev. D **106**, 044069 (2022), arXiv:2205.08516 [gr-qc].

[1288] L. Barack, A. Ori, and N. Sago, Frequency-domain calculation of the self force: The High-frequency problem and its resolution, Phys. Rev. D **78**, 084021 (2008), arXiv:0808.2315 [gr-qc].

[1289] N. Warburton and L. Barack, Self force on a scalar charge in Kerr spacetime: eccentric equatorial orbits, Phys. Rev. D **83**, 124038 (2011), arXiv:1103.0287 [gr-qc].

[1290] S. Hopper and C. R. Evans, Metric perturbations from eccentric orbits on a Schwarzschild black hole: I. Odd-parity Regge-Wheeler to Lorenz gauge transformation and two new methods to circumvent the Gibbs phenomenon, Phys. Rev. D **87**, 064008 (2013), arXiv:1210.7969 [gr-qc].

[1291] B. Leather and N. Warburton, Applying the effective-source approach to frequency-domain self-force calculations for eccentric orbits, Phys. Rev. D **108**, 084045 (2023), arXiv:2306.17221 [gr-qc].

[1292] M. Campanelli and C. O. Lousto, Second order gauge invariant gravitational perturbations of a Kerr black hole, Phys. Rev. D **59**, 124022 (1999), arXiv:gr-qc/9811019.

[1293] S. R. Green, S. Hollands, and P. Zimmerman, Teukolsky formalism for nonlinear Kerr perturbations, Class. Quant. Grav. **37**, 075001 (2020), arXiv:1908.09095 [gr-qc].

[1294] A. Spiers, A. Pound, and J. Moxon, Second-order Teukolsky formalism in Kerr spacetime: Formulation and nonlinear source, Phys. Rev. D **108**, 064002 (2023), arXiv:2305.19332 [gr-qc].

[1295] J. Moxon, A. Grant, E. E. Flanagan, A. Pound, Z. Sam, and J. E. Thompson, Energy and angular momentum balance laws in second-order self-force theory, in preparation.

[1296] T. Osburn and N. Nishimura, New self-force method via elliptic partial differential equations for Kerr inspiral models, Phys. Rev. D **106**, 044056 (2022), arXiv:2206.07031 [gr-qc].

[1297] S. R. Dolan, L. Durkan, C. Kavanagh, and B. Wardell, Metric perturbations of Kerr spacetime in Lorenz gauge: Circular equatorial orbits, arXiv:2306.16459 [gr-qc].

[1298] W.-B. Han and Z. Cao, Constructing EOB dynamics with numerical energy flux for intermediate-mass-ratio inspirals, Phys. Rev. D **84**, 044014 (2011), arXiv:1108.0995 [gr-qc].

[1299] W.-B. Han, Gravitational waves from extreme-mass-ratio inspirals in equatorially eccentric orbits, Int. J. Mod. Phys. D **23**, 1450064 (2014).

[1300] W.-B. Han, Fast evolution and waveform generator for extreme-mass-ratio inspirals in equatorial-circular orbits, Class. Quant. Grav. **33**, 065009 (2016), arXiv:1609.06817 [gr-qc].

[1301] W.-B. Han, Z. Cao, and Y.-M. Hu, Excitation of high frequency voices from intermediate-mass-ratio inspirals with large eccentricity, Class. Quant. Grav. **34**, 225010 (2017), arXiv:1710.00147 [gr-qc].

[1302] C. Zhang, W.-B. Han, and S.-C. Yang, Analytical effective one-body formalism for extreme-mass-ratio inspirals with eccentric orbits, Commun. Theor. Phys. **73**, 085401 (2021), arXiv:2001.06763 [gr-qc].

[1303] C. Zhang, W.-B. Han, X.-Y. Zhong, and G. Wang, Geometrized effective-one-body formalism for extreme-mass-ratio limits: Generic orbits, Phys. Rev. D **104**, 024050 (2021), arXiv:2102.05391 [gr-qc].

[1304] P. Shen, W.-B. Han, C. Zhang, S.-C. Yang, X.-Y. Zhong, Y. Jiang, and Q. Cui, Influence of mass-ratio corrections in extreme-mass-ratio inspirals for testing general relativity, Phys. Rev. D **108**, 064015 (2023), arXiv:2303.13749 [gr-qc].

[1305] P. Canizares, C. F. Sopuerta, and J. L. Jaramillo, Pseudospectral Collocation Methods for the Computation of the Self-Force on a Charged Particle: Generic Orbits around a Schwarzschild Black Hole, Phys. Rev. D **82**, 044023 (2010), arXiv:1006.3201 [gr-qc].

[1306] K. Destounis, A. G. Suvorov, and K. D. Kokkotas, Gravitational-wave glitches in chaotic extreme-mass-ratio inspirals, Phys. Rev. Lett. **126**, 141102 (2021), arXiv:2103.05643 [gr-qc].

[1307] R. Gonzo and C. Shi, Boundary to bound dictionary for generic Kerr orbits, arXiv:2304.06066 [hep-th].

[1308] L. Barack *et al.*, Comparison of post-Minkowskian and self-force expansions: Scattering in a scalar charge toy model, Phys. Rev. D **108**, 024025 (2023), arXiv:2304.09200 [hep-th].

[1309] C. Whittall and L. Barack, Frequency-domain approach to self-force in hyperbolic scattering, Phys. Rev. D **108**, 064017 (2023), arXiv:2305.09724 [gr-qc].

[1310] P. T. Chrusciel, J. Lopes Costa, and M. Heusler, Stationary Black Holes: Uniqueness and Beyond, Living Rev. Rel. **15**, 7 (2012), arXiv:1205.6112 [gr-qc].

[1311] F. J. Zerilli, Effective potential for even parity Regge-Wheeler gravitational perturbation equations, Phys. Rev. Lett. **24**, 737 (1970).

[1312] S. A. Teukolsky, Rotating black holes - separable wave equations for gravitational and electromagnetic perturbations, Phys. Rev. Lett. **29**, 1114 (1972).

[1313] W. H. Press, Long Wave Trains of Gravitational Waves from a Vibrating Black Hole, Astrophys. J. Lett. **170**, L105 (1971).

[1314] S. Chandrasekhar and S. L. Detweiler, The quasi-normal modes of the Schwarzschild black hole, Proc. Roy. Soc. Lond. A **344**, 441 (1975).

[1315] K. D. Kokkotas and B. G. Schmidt, Quasinormal modes of stars and black holes, Living Rev. Rel. **2**, 2 (1999), arXiv:gr-qc/9909058.

[1316] H.-P. Nollert, TOPICAL REVIEW: Quasinormal modes: the characteristic 'sound' of black holes and neutron stars, Class. Quant. Grav. **16**, R159 (1999).

[1317] E. Berti, V. Cardoso, and A. O. Starinets, Quasinormal modes of black holes and black branes, Class. Quant. Grav. **26**, 163001 (2009), arXiv:0905.2975 [gr-qc].

[1318] E. Berti, K. Yagi, H. Yang, and N. Yunes, Extreme Gravity Tests with Gravitational Waves from Compact Binary Coalescences: (II) Ringdown, Gen. Rel. Grav. **50**, 49 (2018), arXiv:1801.03587 [gr-qc].

[1319] B. P. Jensen and P. Candelas, The Schwarzschild Radial Functions, Phys. Rev. D **33**, 1590 (1986), [Erratum: Phys.Rev.D 35, 4041 (1987)].

[1320] E. W. Leaver, Spectral decomposition of the perturbation response of the Schwarzschild geometry, Phys. Rev. D **34**, 384 (1986).

[1321] R. H. Price, Nonspherical perturbations of relativistic gravitational collapse. 1. Scalar and gravitational perturbations, Phys. Rev. D **5**, 2419 (1972).

[1322] S. L. Detweiler, BLACK HOLES AND GRAVITATIONAL WAVES. III. THE RESONANT FREQUENCIES OF ROTATING HOLES, Astrophys. J. **239**, 292 (1980).

[1323] O. Dreyer, B. J. Kelly, B. Krishnan, L. S. Finn, D. Garrison, and R. Lopez-Aleman, Black hole spectroscopy: Testing general relativity through gravitational wave observations, Class. Quant. Grav. **21**, 787 (2004), arXiv:gr-qc/0309007.

[1324] M. Isi, M. Giesler, W. M. Farr, M. A. Scheel, and S. A. Teukolsky, Testing the no-hair theorem with GW150914, Phys. Rev. Lett. **123**, 111102 (2019), arXiv:1905.00869 [gr-qc].

[1325] E. Berti, J. Cardoso, V. Cardoso, and M. Cavaglia, Matched-filtering and parameter estimation of ringdown waveforms, Phys. Rev. D **76**, 104044 (2007), arXiv:0707.1202 [gr-qc].

[1326] E. Berti, A. Sesana, E. Barausse, V. Cardoso, and K. Belczynski, Spectroscopy of Kerr black holes with Earth- and space-based interferometers, Phys. Rev. Lett. **117**, 101102 (2016), arXiv:1605.09286 [gr-qc].

[1327] G. Compère, K. Fransen, T. Hertog, and J. Long, Gravitational waves from plunges into Gargantua, Class. Quant. Grav. **35**, 104002 (2018), arXiv:1712.07130 [gr-qc].

[1328] N. Oshita and D. Tsuna, Slowly Decaying Ringdown of a Rapidly Spinning Black Hole: Probing the No-Hair Theorem by Small Mass-Ratio Mergers with LISA, arXiv:2210.14049 [gr-qc].

[1329] V. Baibhav, E. Berti, and V. Cardoso, LISA parameter estimation and source localization with higher harmonics of the ringdown, Phys. Rev. D **101**, 084053 (2020), arXiv:2001.10011 [gr-qc].

[1330] E. W. Leaver, An Analytic representation for the quasi normal modes of Kerr black holes, Proc. Roy. Soc. Lond. A **402**, 285 (1985).

[1331] H.-P. Nollert, Quasinormal modes of Schwarzschild black holes: The determination of quasinormal frequencies with very large imaginary parts, Phys. Rev. D **47**, 5253 (1993).

[1332] H. Onozawa, A Detailed study of quasinormal frequencies of the Kerr black hole, Phys. Rev. D **55**, 3593 (1997), arXiv:gr-qc/9610048.

[1333] Emanuele Berti's ringdown web page, (eberti2/ringdown/).

[1334] G. B. Cook and M. Zalutskiy, Gravitational perturbations of the Kerr geometry: High-accuracy study, Phys. Rev. D **90**, 124021 (2014), arXiv:1410.7698 [gr-qc].

[1335] L. C. Stein, qnm: A Python package for calculating Kerr quasinormal modes, separation constants, and spherical-spheroidal mixing coefficients, J. Open Source Softw. **4**, 1683 (2019), arXiv:1908.10377 [gr-qc].

[1336] H.-J. Blome and B. Mashhoon, Quasi-normal oscillations of a schwarzschild black hole, Physics Letters A **100**, 231 (1984).

[1337] B. F. Schutz and C. M. Will, BLACK HOLE NORMAL MODES: A SEMIANALYTIC APPROACH, Astrophys. J. Lett. **291**, L33 (1985).

[1338] E. Seidel and S. Iyer, BLACK HOLE NORMAL MODES: A WKB APPROACH. 4. KERR BLACK HOLES, Phys. Rev. D **41**, 374 (1990).

[1339] K. D. Kokkotas, Normal modes of the Kerr black hole, Class. Quant. Grav. **8**, 2217 (1991).

[1340] S. R. Dolan and A. C. Ottewill, On an Expansion Method for Black Hole Quasinormal Modes and Regge Poles, Class. Quant. Grav. **26**, 225003 (2009), arXiv:0908.0329 [gr-qc].

[1341] S. R. Dolan, The Quasinormal Mode Spectrum of a Kerr Black Hole in the Eikonal Limit, Phys. Rev. D **82**, 104003 (2010), arXiv:1007.5097 [gr-qc].

[1342] L. Magaña Zertuche *et al.*, High precision ringdown modeling: Multimode fits and BMS frames, Phys. Rev. D **105**, 104015 (2022), arXiv:2110.15922 [gr-qc].

[1343] E. Hamilton, L. London, and M. Hannam, Ringdown frequencies in black holes formed from precessing black-hole binaries, Phys. Rev. D **107**, 104035 (2023), arXiv:2301.06558 [gr-qc].

[1344] D. Gerosa and C. J. Moore, Black hole kicks as new gravitational wave observables, Phys. Rev. Lett. **117**, 011101 (2016), arXiv:1606.04226 [gr-qc].

[1345] E. Berti and V. Cardoso, Quasinormal ringing of Kerr black holes. I. The Excitation factors, Phys. Rev. D **74**, 104020 (2006), arXiv:gr-qc/0605118.

[1346] I. Kamaretsos, M. Hannam, S. Husa, and B. S. Sathyaprakash, Black-hole hair loss: learning about binary progenitors from ringdown signals, Phys. Rev. D **85**, 024018 (2012), arXiv:1107.0854 [gr-qc].

[1347] I. Kamaretsos, M. Hannam, and B. Sathyaprakash, Is black-hole ringdown a memory of its progenitor?, Phys. Rev. Lett. **109**, 141102 (2012), arXiv:1207.0399 [gr-qc].

[1348] E. Berti, V. Cardoso, J. A. Gonzalez, U. Sperhake, M. Hannam, S. Husa, and B. Bruegmann, Inspiral, merger and ringdown of unequal mass black hole binaries: A Multipolar analysis, Phys. Rev. D **76**, 064034 (2007), arXiv:gr-qc/0703053.

[1349] L. London, D. Shoemaker, and J. Healy, Modeling ringdown: Beyond the fundamental quasinormal modes, Phys. Rev. D **90**, 124032 (2014), [Erratum: Phys.Rev.D 94, 069902 (2016)], arXiv:1404.3197 [gr-qc].

[1350] V. Baibhav, E. Berti, V. Cardoso, and G. Khanna, Black Hole Spectroscopy: Systematic Errors and Ringdown Energy Estimates, Phys. Rev. D **97**, 044048 (2018), arXiv:1710.02156 [gr-qc].

[1351] L. T. London, Modeling ringdown. II. Aligned-spin binary black holes, implications for data analysis and fundamental theory, Phys. Rev. D **102**, 084052 (2020), arXiv:1801.08208 [gr-qc].

[1352] X. J. Forteza, S. Bhagwat, S. Kumar, and P. Pani, Novel Ringdown Amplitude-Phase Consistency Test, Phys. Rev. Lett. **130**, 021001 (2023), arXiv:2205.14910 [gr-qc].

[1353] V. Baibhav, M. H.-Y. Cheung, E. Berti, V. Cardoso, G. Carullo, R. Cotesta, W. Del Pozzo, and F. Duque, Agnostic black hole spectroscopy: quasinormal mode content of numerical relativity waveforms and limits of validity of linear perturbation theory, arXiv:2302.03050 [gr-qc].

[1354] H. Lim, G. Khanna, A. Apte, and S. A. Hughes, Exciting black hole modes via misaligned coalescences: II. The mode content of late-time coalescence waveforms, Phys. Rev. D **100**, 084032 (2019), arXiv:1901.05902 [gr-qc].

[1355] S. A. Hughes, A. Apte, G. Khanna, and H. Lim, Learning about black hole binaries from their ringdown spectra, Phys. Rev. Lett. **123**, 161101 (2019), arXiv:1901.05900 [gr-qc].

[1356] H. Lim, S. A. Hughes, and G. Khanna, Measuring quasinormal mode amplitudes with misaligned binary black hole ringdowns, Phys. Rev. D **105**, 124030 (2022), arXiv:2204.06007 [gr-qc].

[1357] M. Giesler, M. Isi, M. A. Scheel, and S. Teukolsky, Black Hole Ringdown: The Importance of Overtones, Phys. Rev. X **9**, 041060 (2019), arXiv:1903.08284 [gr-qc].

[1358] G. B. Cook, Aspects of multimode Kerr ringdown fitting, Phys. Rev. D **102**, 024027 (2020), arXiv:2004.08347 [gr-qc].

[1359] X. Jiménez Forteza, S. Bhagwat, P. Pani, and V. Ferrari, Spectroscopy of binary black hole ringdown using overtones and angular modes, Phys. Rev. D **102**, 044053 (2020), arXiv:2005.03260 [gr-qc].

[1360] I. Ota and C. Chirenti, Black hole spectroscopy horizons for current and future gravitational wave detectors, Phys. Rev. D **105**, 044015 (2022), arXiv:2108.01774 [gr-qc].

[1361] X. Li, L. Sun, R. K. L. Lo, E. Payne, and Y. Chen, Angular emission patterns of remnant black holes, Phys. Rev. D **105**, 024016 (2022), arXiv:2110.03116 [gr-qc].

[1362] S. Bhagwat, X. J. Forteza, P. Pani, and V. Ferrari, Ringdown overtones, black hole spectroscopy, and no-hair theorem tests, Phys. Rev. D **101**, 044033 (2020), arXiv:1910.08708 [gr-qc].

[1363] X. J. Forteza and P. Mourier, High-overtone fits to numerical relativity ringdowns: Beyond the dismissed n=8 special tone, Phys. Rev. D **104**, 124072 (2021), arXiv:2107.11829 [gr-qc].

[1364] K. Mitman *et al.*, Nonlinearities in Black Hole Ringdowns, Phys. Rev. Lett. **130**, 081402 (2023), arXiv:2208.07380 [gr-qc].

[1365] S. Ma, K. Mitman, L. Sun, N. Deppe, F. Hébert, L. E. Kidder, J. Moxon, W. Throwe, N. L. Vu, and Y. Chen, Quasinormal-mode filters: A new approach to analyze the gravitational-wave ringdown of binary black-hole mergers, Phys. Rev. D **106**, 084036 (2022), arXiv:2207.10870 [gr-qc].

[1366] S. Ma, L. Sun, and Y. Chen, Using rational filters to uncover the first ringdown overtone in GW150914, Phys. Rev. D **107**, 084010 (2023), arXiv:2301.06639 [gr-qc].

[1367] S. Ma, L. Sun, and Y. Chen, Black Hole Spectroscopy by Mode Cleaning, Phys. Rev. Lett. **130**, 141401 (2023), arXiv:2301.06705 [gr-qc].

[1368] P. J. Nee, S. H. Völkel, and H. P. Pfeiffer, Role of black hole quasinormal mode overtones for ringdown analysis, Phys. Rev. D **108**, 044032 (2023), arXiv:2302.06634 [gr-qc].

[1369] H. Zhu, J. L. Ripley, A. Cárdenas-Avendaño, and F. Pretorius, Challenges in Quasinormal Mode Extraction: Perspectives from Numerical solutions to the Teukolsky Equation, arXiv:2309.13204 [gr-qc].

[1370] L. Barack, Late time decay of scalar, electromagnetic, and gravitational perturbations outside rotating black holes, Phys. Rev. D **61**, 024026 (2000), arXiv:gr-qc/9908005.

[1371] M. Tiglio, L. E. Kidder, and S. A. Teukolsky, High accuracy simulations of Kerr tails: Coordinate dependence and higher multipoles, Class. Quant. Grav. **25**, 105022 (2008), arXiv:0712.2472 [gr-qc].

[1372] R. J. Gleiser, C. O. Nicasio, R. H. Price, and J. Pullin, Second order perturbations of a Schwarzschild black hole, Class. Quant. Grav. **13**, L117 (1996), arXiv:gr-qc/9510049.

[1373] D. Brizuela, J. M. Martin-Garcia, and M. Tiglio, A Complete gauge-invariant formalism for arbitrary second-order perturbations of a Schwarzschild black hole, Phys. Rev. D **80**, 024021 (2009), arXiv:0903.1134 [gr-qc].

[1374] H. Nakano and K. Ioka, Second Order Quasi-Normal Mode of the Schwarzschild Black Hole, Phys. Rev. D **76**, 084007 (2007), arXiv:0708.0450 [gr-qc].

[1375] E. Pazos, D. Brizuela, J. M. Martin-Garcia, and M. Tiglio, Mode coupling of Schwarzschild perturbations: Ringdown frequencies, Phys. Rev. D **82**, 104028 (2010), arXiv:1009.4665 [gr-

qc].

[1376] N. Loutrel, J. L. Ripley, E. Giorgi, and F. Pretorius, Second Order Perturbations of Kerr Black Holes: Reconstruction of the Metric, Phys. Rev. D **103**, 104017 (2021), arXiv:2008.11770 [gr-qc].

[1377] M. Lagos and L. Hui, Generation and propagation of nonlinear quasinormal modes of a Schwarzschild black hole, Phys. Rev. D **107**, 044040 (2023), arXiv:2208.07379 [gr-qc].

[1378] B. Bucciotti, A. Kuntz, F. Serra, and E. Trincherini, Nonlinear Quasi-Normal Modes: Uniform Approximation, arXiv:2309.08501 [hep-th].

[1379] L. Sberna, P. Bosch, W. E. East, S. R. Green, and L. Lehner, Nonlinear effects in the black hole ringdown: Absorption-induced mode excitation, Phys. Rev. D **105**, 064046 (2022), arXiv:2112.11168 [gr-qc].

[1380] J. L. Ripley, N. Loutrel, E. Giorgi, and F. Pretorius, Numerical computation of second order vacuum perturbations of Kerr black holes, Phys. Rev. D **103**, 104018 (2021), arXiv:2010.00162 [gr-qc].

[1381] M. H.-Y. Cheung *et al.*, Nonlinear Effects in Black Hole Ringdown, Phys. Rev. Lett. **130**, 081401 (2023), arXiv:2208.07374 [gr-qc].

[1382] N. Khera, A. Ribes Metidieri, B. Bonga, X. J. Forteza, B. Krishnan, E. Poisson, D. Pook-Kolb, E. Schnetter, and H. Yang, Nonlinearities at Black Hole Horizons, arXiv:2306.11142 [gr-qc].

[1383] S. R. Green, S. Hollands, L. Sberna, V. Toomani, and P. Zimmerman, Conserved currents for a Kerr black hole and orthogonality of quasinormal modes, Phys. Rev. D **107**, 064030 (2023), arXiv:2210.15935 [gr-qc].

[1384] E. Cannizzaro, L. Sberna, S. R. Green, and S. Hollands, Relativistic perturbation theory for black-hole boson clouds, arXiv:2309.10021 [gr-qc].

[1385] L. T. London, Biorthogonal harmonics for the decomposition of gravitational radiation. I. Angular modes, completeness, and the introduction of adjoint-spheroidal harmonics, Phys. Rev. D **107**, 044056 (2023), arXiv:2006.11449 [gr-qc].

[1386] N. Oshita, Thermal ringdown of a Kerr black hole: overtone excitation, Fermi-Dirac statistics and greybody factor, JCAP **04**, 013, arXiv:2208.02923 [gr-qc].

[1387] H.-P. Nollert, About the significance of quasinormal modes of black holes, Phys. Rev. D **53**, 4397 (1996), arXiv:gr-qc/9602032.

[1388] J. M. Aguirregabiria and C. V. Vishveshwara, Scattering by black holes: A Simulated potential approach, Phys. Lett. A **210**, 251 (1996).

[1389] C. V. Vishveshwara, On the black hole trail...: A personal journey, Curr. Sci. **71**, 824 (1996).

[1390] J. L. Jaramillo, R. Panosso Macedo, and L. Al Sheikh, Pseudospectrum and Black Hole Quasinormal Mode Instability, Phys. Rev. X **11**, 031003 (2021), arXiv:2004.06434 [gr-qc].

[1391] J. L. Jaramillo, R. Panosso Macedo, and L. A. Sheikh, Gravitational Wave Signatures of Black Hole Quasinormal Mode Instability, Phys. Rev. Lett. **128**, 211102 (2022), arXiv:2105.03451 [gr-qc].

[1392] M. H.-Y. Cheung, K. Destounis, R. P. Macedo, E. Berti, and V. Cardoso, Destabilizing the Fundamental Mode of Black Holes: The Elephant and the Flea, Phys. Rev. Lett. **128**, 111103 (2022), arXiv:2111.05415 [gr-qc].

[1393] R. A. Konoplya and A. Zhidenko, General black-hole metric mimicking Schwarzschild spacetime, JCAP **08**, 008, arXiv:2303.03130 [gr-qc].

[1394] H. Yang, A. Zimmerman, and L. Lehner, Turbulent Black Holes, Phys. Rev. Lett. **114**, 081101 (2015), arXiv:1402.4859 [gr-qc].

[1395] S. Aretakis, Decay of Axisymmetric Solutions of the Wave Equation on Extreme Kerr Backgrounds, J. Funct. Anal. **263**, 2770 (2012), arXiv:1110.2006 [gr-qc].

[1396] J. Redondo-Yuste, G. Carullo, J. L. Ripley, E. Berti, and V. Cardoso, Spin dependence of black hole ringdown nonlinearities, arXiv:2308.14796 [gr-qc].

[1397] T. Damour, P. Jaranowski, and G. Schaefer, On the determination of the last stable orbit for circular general relativistic binaries at the third postNewtonian approximation, Phys. Rev. D

62, 084011 (2000), arXiv:gr-qc/0005034.

[1398] T. Damour, Coalescence of two spinning black holes: an effective one-body approach, Phys. Rev. D **64**, 124013 (2001), arXiv:gr-qc/0103018.

[1399] T. Damour, Introductory lectures on the Effective One Body formalism, Int. J. Mod. Phys. A **23**, 1130 (2008), arXiv:0802.4047 [gr-qc].

[1400] E. Brezin, C. Itzykson, and J. Zinn-Justin, Relativistic balmer formula including recoil effects, Phys. Rev. D **1**, 2349 (1970).

[1401] T. Damour, P. Jaranowski, and G. Schaefer, Effective one body approach to the dynamics of two spinning black holes with next-to-leading order spin-orbit coupling, Phys. Rev. D **78**, 024009 (2008), arXiv:0803.0915 [gr-qc].

[1402] A. Nagar, Effective one body Hamiltonian of two spinning black-holes with next-to-next-to-leading order spin-orbit coupling, Phys. Rev. D **84**, 084028 (2011), [Erratum: Phys.Rev.D 88, 089901 (2013)], arXiv:1106.4349 [gr-qc].

[1403] T. Damour and A. Nagar, New effective-one-body description of coalescing nonprecessing spinning black-hole binaries, Phys. Rev. D **90**, 044018 (2014), arXiv:1406.6913 [gr-qc].

[1404] S. Balmelli and T. Damour, New effective-one-body Hamiltonian with next-to-leading order spin-spin coupling, Phys. Rev. D **92**, 124022 (2015), arXiv:1509.08135 [gr-qc].

[1405] E. Barausse, E. Racine, and A. Buonanno, Hamiltonian of a spinning test-particle in curved spacetime, Phys. Rev. D **80**, 104025 (2009), [Erratum: Phys.Rev.D 85, 069904 (2012)], arXiv:0907.4745 [gr-qc].

[1406] E. Barausse and A. Buonanno, An Improved effective-one-body Hamiltonian for spinning black-hole binaries, Phys. Rev. D **81**, 084024 (2010), arXiv:0912.3517 [gr-qc].

[1407] E. Barausse and A. Buonanno, Extending the effective-one-body Hamiltonian of black-hole binaries to include next-to-next-to-leading spin-orbit couplings, Phys. Rev. D **84**, 104027 (2011), arXiv:1107.2904 [gr-qc].

[1408] P. Rettegno, F. Martinetti, A. Nagar, D. Bini, G. Riemenschneider, and T. Damour, Comparing Effective One Body Hamiltonians for spin-aligned coalescing binaries, Phys. Rev. D **101**, 104027 (2020), arXiv:1911.10818 [gr-qc].

[1409] M. Khalil, J. Steinhoff, J. Vines, and A. Buonanno, Fourth post-Newtonian effective-one-body Hamiltonians with generic spins, Phys. Rev. D **101**, 104034 (2020), arXiv:2003.04469 [gr-qc].

[1410] T. Damour, B. R. Iyer, and B. S. Sathyaprakash, Improved filters for gravitational waves from inspiralling compact binaries, Phys. Rev. D **57**, 885 (1998), arXiv:gr-qc/9708034.

[1411] T. Damour, B. R. Iyer, and A. Nagar, Improved resummation of post-Newtonian multipolar waveforms from circularized compact binaries, Phys. Rev. D **79**, 064004 (2009), arXiv:0811.2069 [gr-qc].

[1412] A. Taracchini, Y. Pan, A. Buonanno, E. Barausse, M. Boyle, T. Chu, G. Lovelace, H. P. Pfeiffer, and M. A. Scheel, Prototype effective-one-body model for nonprecessing spinning inspiral-merger-ringdown waveforms, Phys. Rev. D **86**, 024011 (2012), arXiv:1202.0790 [gr-qc].

[1413] A. Taracchini *et al.*, Effective-one-body model for black-hole binaries with generic mass ratios and spins, Phys. Rev. D **89**, 061502 (2014), arXiv:1311.2544 [gr-qc].

[1414] A. Nagar and A. Shah, Factorization and resummation: A new paradigm to improve gravitational wave amplitudes, Phys. Rev. D **94**, 104017 (2016), arXiv:1606.00207 [gr-qc].

[1415] F. Messina, A. Maldarella, and A. Nagar, Factorization and resummation: A new paradigm to improve gravitational wave amplitudes. II: the higher multipolar modes, Phys. Rev. D **97**, 084016 (2018), arXiv:1801.02366 [gr-qc].

[1416] R. Cotesta, A. Buonanno, A. Bohé, A. Taracchini, I. Hinder, and S. Ossokine, Enriching the Symphony of Gravitational Waves from Binary Black Holes by Tuning Higher Harmonics, Phys. Rev. D **98**, 084028 (2018), arXiv:1803.10701 [gr-qc].

[1417] L. Pompili *et al.*, Laying the foundation of the effective-one-body waveform models SEOBNRv5: improved accuracy and efficiency for spinning non-precessing binary black holes, arXiv:2303.18039 [gr-qc].

208

[1418] M. van de Meent, A. Buonanno, D. P. Mihaylov, S. Ossokine, L. Pompili, N. Warburton, A. Pound, B. Wardell, L. Durkan, and J. Miller, Enhancing the SEOBNRv5 effective-one-body waveform model with second-order gravitational self-force fluxes, arXiv:2303.18026 [gr-qc].

[1419] T. Damour, B. R. Iyer, P. Jaranowski, and B. S. Sathyaprakash, Gravitational waves from black hole binary inspiral and merger: The Span of third postNewtonian effective one-body templates, Phys. Rev. D 67, 064028 (2003), arXiv:gr-qc/0211041.

[1420] M. Davis, R. Ruffini, J. Tiomno, and F. Zerilli, Can synchrotron gravitational radiation exist?, Phys. Rev. Lett. 28, 1352 (1972).

[1421] R. H. Price and J. Pullin, Colliding black holes: The Close limit, Phys. Rev. Lett. 72, 3297 (1994), arXiv:gr-qc/9402039.

[1422] A. Buonanno, Y. Pan, J. G. Baker, J. Centrella, B. J. Kelly, S. T. McWilliams, and J. R. van Meter, Toward faithful templates for non-spinning binary black holes using the effective-one-body approach, Phys. Rev. D 76, 104049 (2007), arXiv:0706.3732 [gr-qc].

[1423] Y. Pan, A. Buonanno, M. Boyle, L. T. Buchman, L. E. Kidder, H. P. Pfeiffer, and M. A. Scheel, Inspiral-merger-ringdown multipolar waveforms of nonspinning black-hole binaries using the effective-one-body formalism, Phys. Rev. D 84, 124052 (2011), arXiv:1106.1021 [gr-qc].

[1424] T. Damour, A. Nagar, and S. Bernuzzi, Improved effective-one-body description of coalescing nonspinning black-hole binaries and its numerical-relativity completion, Phys. Rev. D 87, 084035 (2013), arXiv:1212.4357 [gr-qc].

[1425] S. Babak, A. Taracchini, and A. Buonanno, Validating the effective-one-body model of spinning, precessing binary black holes against numerical relativity, Phys. Rev. D 95, 024010 (2017), arXiv:1607.05661 [gr-qc].

[1426] T. Damour and A. Nagar, A new analytic representation of the ringdown waveform of coalescing spinning black hole binaries, Phys. Rev. D 90, 024054 (2014), arXiv:1406.0401 [gr-qc].

[1427] J. G. Baker, W. D. Boggs, J. Centrella, B. J. Kelly, S. T. McWilliams, and J. R. van Meter, Mergers of non-spinning black-hole binaries: Gravitational radiation characteristics, Phys. Rev. D 78, 044046 (2008), arXiv:0805.1428 [gr-qc].

[1428] X. Jiménez-Forteza, D. Keitel, S. Husa, M. Hannam, S. Khan, and M. Pürrer, Hierarchical data-driven approach to fitting numerical relativity data for nonprecessing binary black holes with an application to final spin and radiated energy, Phys. Rev. D 95, 064024 (2017), arXiv:1611.00332 [gr-qc].

[1429] A. Ramos-Buades, A. Buonanno, H. Estellés, M. Khalil, D. P. Mihaylov, S. Ossokine, L. Pompili, and M. Shiferaw, SEOBNRv5PHM: Next generation of accurate and efficient multipolar precessing-spin effective-one-body waveforms for binary black holes, arXiv:2303.18046 [gr-qc].

[1430] A. Nagar *et al.*, Time-domain effective-one-body gravitational waveforms for coalescing compact binaries with nonprecessing spins, tides and self-spin effects, Phys. Rev. D 98, 104052 (2018), arXiv:1806.01772 [gr-qc].

[1431] A. Nagar, G. Riemenschneider, G. Pratten, P. Rettegno, and F. Messina, Multipolar effective one body waveform model for spin-aligned black hole binaries, Phys. Rev. D 102, 024077 (2020), arXiv:2001.09082 [gr-qc].

[1432] M. Boyle, A. Buonanno, L. E. Kidder, A. H. Mroue, Y. Pan, H. P. Pfeiffer, and M. A. Scheel, High-accuracy numerical simulation of black-hole binaries: Computation of the gravitational-wave energy flux and comparisons with post-Newtonian approximants, Phys. Rev. D 78, 104020 (2008), arXiv:0804.4184 [gr-qc].

[1433] T. Damour, A. Nagar, D. Pollney, and C. Reisswig, Energy versus Angular Momentum in Black Hole Binaries, Phys. Rev. Lett. 108, 131101 (2012), arXiv:1110.2938 [gr-qc].

[1434] S. Bernuzzi, A. Nagar, T. Dietrich, and T. Damour, Modeling the Dynamics of Tidally Interacting Binary Neutron Stars up to the Merger, Phys. Rev. Lett. 114, 161103 (2015), arXiv:1412.4553 [gr-qc].

[1435] S. Ossokine, T. Dietrich, E. Foley, R. Katebi, and G. Lovelace, Assessing the Energetics of Spinning Binary Black Hole Systems, Phys. Rev. D 98, 104057 (2018), arXiv:1712.06533 [gr-

qc].

[1436] T. Hinderer *et al.*, Periastron advance in spinning black hole binaries: comparing effective-one-body and Numerical Relativity, Phys. Rev. D **88**, 084005 (2013), arXiv:1309.0544 [gr-qc].

[1437] T. Damour, F. Guercilena, I. Hinder, S. Hopper, A. Nagar, and L. Rezzolla, Strong-Field Scattering of Two Black Holes: Numerics Versus Analytics, Phys. Rev. D **89**, 081503 (2014), arXiv:1402.7307 [gr-qc].

[1438] C. Devine, Z. B. Etienne, and S. T. McWilliams, Optimizing spinning time-domain gravitational waveforms for Advanced LIGO data analysis, Class. Quant. Grav. **33**, 125025 (2016), arXiv:1601.03393 [astro-ph.HE].

[1439] T. D. Knowles, C. Devine, D. A. Buch, S. A. Bilgili, T. R. Adams, Z. B. Etienne, and S. T. Mcwilliams, Improving performance of SEOBNRv3 by ∼300x, Class. Quant. Grav. **35**, 155003 (2018), arXiv:1803.06346 [gr-qc].

[1440] A. Nagar and P. Rettegno, Efficient effective one body time-domain gravitational waveforms, Phys. Rev. D **99**, 021501 (2019), arXiv:1805.03891 [gr-qc].

[1441] R. Gamba, S. Bernuzzi, and A. Nagar, Fast, faithful, frequency-domain effective-one-body waveforms for compact binary coalescences, Phys. Rev. D **104**, 084058 (2021), arXiv:2012.00027 [gr-qc].

[1442] S. E. Field, C. R. Galley, J. S. Hesthaven, J. Kaye, and M. Tiglio, Fast prediction and evaluation of gravitational waveforms using surrogate models, Phys. Rev. X **4**, 031006 (2014), arXiv:1308.3565 [gr-qc].

[1443] M. Pürrer, Frequency domain reduced order models for gravitational waves from aligned-spin compact binaries, Class. Quant. Grav. **31**, 195010 (2014), arXiv:1402.4146 [gr-qc].

[1444] M. Pürrer, Frequency domain reduced order model of aligned-spin effective-one-body waveforms with generic mass-ratios and spins, Phys. Rev. D **93**, 064041 (2016), arXiv:1512.02248 [gr-qc].

[1445] B. D. Lackey, S. Bernuzzi, C. R. Galley, J. Meidam, and C. Van Den Broeck, Effective-one-body waveforms for binary neutron stars using surrogate models, Phys. Rev. D **95**, 104036 (2017), arXiv:1610.04742 [gr-qc].

[1446] B. D. Lackey, M. Pürrer, A. Taracchini, and S. Marsat, Surrogate model for an aligned-spin effective one body waveform model of binary neutron star inspirals using Gaussian process regression, Phys. Rev. D **100**, 024002 (2019), arXiv:1812.08643 [gr-qc].

[1447] R. Cotesta, S. Marsat, and M. Pürrer, Frequency domain reduced order model of aligned-spin effective-one-body waveforms with higher-order modes, Phys. Rev. D **101**, 124040 (2020), arXiv:2003.12079 [gr-qc].

[1448] B. Gadre, M. Pürrer, S. E. Field, S. Ossokine, and V. Varma, A fully precessing higher-mode surrogate model of effective-one-body waveforms, arXiv:2203.00381 [gr-qc].

[1449] J. Tissino, G. Carullo, M. Breschi, R. Gamba, S. Schmidt, and S. Bernuzzi, Combining effective-one-body accuracy and reduced-order-quadrature speed for binary neutron star merger parameter estimation with machine learning, Phys. Rev. D **107**, 084037 (2023), arXiv:2210.15684 [gr-qc].

[1450] S. Khan and R. Green, Gravitational-wave surrogate models powered by artificial neural networks, Phys. Rev. D **103**, 064015 (2021), arXiv:2008.12932 [gr-qc].

[1451] L. M. Thomas, G. Pratten, and P. Schmidt, Accelerating multimodal gravitational waveforms from precessing compact binaries with artificial neural networks, Phys. Rev. D **106**, 104029 (2022), arXiv:2205.14066 [gr-qc].

[1452] D. P. Mihaylov, S. Ossokine, A. Buonanno, and A. Ghosh, Fast post-adiabatic waveforms in the time domain: Applications to compact binary coalescences in LIGO and Virgo, Phys. Rev. D **104**, 124087 (2021), arXiv:2105.06983 [gr-qc].

[1453] S. Schmidt, M. Breschi, R. Gamba, G. Pagano, P. Rettegno, G. Riemenschneider, S. Bernuzzi, A. Nagar, and W. Del Pozzo, Machine Learning Gravitational Waves from Binary Black Hole Mergers, Phys. Rev. D **103**, 043020 (2021), arXiv:2011.01958 [gr-qc].

[1454] M. Dax, S. R. Green, J. Gair, M. Pürrer, J. Wildberger, J. H. Macke, A. Buonanno,

210

and B. Schölkopf, Neural Importance Sampling for Rapid and Reliable Gravitational-Wave Inference, Phys. Rev. Lett. **130**, 171403 (2023), arXiv:2210.05686 [gr-qc].

[1455] G. Morrás, J. García-Bellido, and S. Nesseris, Search for black hole hyperbolic encounters with gravitational wave detectors, Phys. Dark Univ. **35**, 100932 (2022), arXiv:2110.08000 [astro-ph.HE].

[1456] T. Damour and A. Nagar, Comparing Effective-One-Body gravitational waveforms to accurate numerical data, Phys. Rev. D **77**, 024043 (2008), arXiv:0711.2628 [gr-qc].

[1457] A. Buonanno, Y. Pan, H. P. Pfeiffer, M. A. Scheel, L. T. Buchman, and L. E. Kidder, Effective-one-body waveforms calibrated to numerical relativity simulations: Coalescence of non-spinning, equal-mass black holes, Phys. Rev. D **79**, 124028 (2009), arXiv:0902.0790 [gr-qc].

[1458] A. Nagar, G. Pratten, G. Riemenschneider, and R. Gamba, Multipolar effective one body model for nonspinning black hole binaries, Phys. Rev. D **101**, 024041 (2020), arXiv:1904.09550 [gr-qc].

[1459] T. Damour, A. Nagar, E. N. Dorband, D. Pollney, and L. Rezzolla, Faithful Effective-One-Body waveforms of equal-mass coalescing black-hole binaries, Phys. Rev. D **77**, 084017 (2008), arXiv:0712.3003 [gr-qc].

[1460] Y. Pan, A. Buonanno, L. T. Buchman, T. Chu, L. E. Kidder, H. P. Pfeiffer, and M. A. Scheel, Effective-one-body waveforms calibrated to numerical relativity simulations: coalescence of non-precessing, spinning, equal-mass black holes, Phys. Rev. D **81**, 084041 (2010), arXiv:0912.3466 [gr-qc].

[1461] T. Damour, A. Nagar, M. Hannam, S. Husa, and B. Bruegmann, Accurate Effective-One-Body waveforms of inspiralling and coalescing black-hole binaries, Phys. Rev. D **78**, 044039 (2008), arXiv:0803.3162 [gr-qc].

[1462] S. Balmelli and P. Jetzer, Effective-one-body Hamiltonian with next-to-leading order spin-spin coupling, Phys. Rev. D **91**, 064011 (2015), arXiv:1502.01343 [gr-qc].

[1463] A. Nagar, F. Messina, P. Rettegno, D. Bini, T. Damour, A. Geralico, S. Akcay, and S. Bernuzzi, Nonlinear-in-spin effects in effective-one-body waveform models of spin-aligned, inspiralling, neutron star binaries, Phys. Rev. D **99**, 044007 (2019), arXiv:1812.07923 [gr-qc].

[1464] S. Akcay, R. Gamba, and S. Bernuzzi, Hybrid post-Newtonian effective-one-body scheme for spin-precessing compact-binary waveforms up to merger, Phys. Rev. D **103**, 024014 (2021), arXiv:2005.05338 [gr-qc].

[1465] D. Bini and T. Damour, Gravitational radiation reaction along general orbits in the effective one-body formalism, Phys. Rev. D **86**, 124012 (2012), arXiv:1210.2834 [gr-qc].

[1466] S. Albanesi, A. Placidi, A. Nagar, M. Orselli, and S. Bernuzzi, New avenue for accurate analytical waveforms and fluxes for eccentric compact binaries, Phys. Rev. D **105**, L121503 (2022), arXiv:2203.16286 [gr-qc].

[1467] T. Hinderer *et al.*, Effects of neutron-star dynamic tides on gravitational waveforms within the effective-one-body approach, Phys. Rev. Lett. **116**, 181101 (2016), arXiv:1602.00599 [gr-qc].

[1468] J. Steinhoff, T. Hinderer, A. Buonanno, and A. Taracchini, Dynamical Tides in General Relativity: Effective Action and Effective-One-Body Hamiltonian, Phys. Rev. D **94**, 104028 (2016), arXiv:1608.01907 [gr-qc].

[1469] S. Akcay, S. Bernuzzi, F. Messina, A. Nagar, N. Ortiz, and P. Rettegno, Effective-one-body multipolar waveform for tidally interacting binary neutron stars up to merger, Phys. Rev. D **99**, 044051 (2019), arXiv:1812.02744 [gr-qc].

[1470] J. Steinhoff, T. Hinderer, T. Dietrich, and F. Foucart, Spin effects on neutron star fundamental-mode dynamical tides: Phenomenology and comparison to numerical simulations, Phys. Rev. Res. **3**, 033129 (2021), arXiv:2103.06100 [gr-qc].

[1471] A. Matas *et al.*, Aligned-spin neutron-star–black-hole waveform model based on the effective-one-body approach and numerical-relativity simulations, Phys. Rev. D **102**, 043023 (2020), arXiv:2004.10001 [gr-qc].

[1472] A. Gonzalez, R. Gamba, M. Breschi, F. Zappa, G. Carullo, S. Bernuzzi, and A. Nagar, Numerical-relativity-informed effective-one-body model for black-hole–neutron-star mergers with higher modes and spin precession, Phys. Rev. D **107**, 084026 (2023), arXiv:2212.03909 [gr-qc].

[1473] T. Damour, Gravitational Self Force in a Schwarzschild Background and the Effective One Body Formalism, Phys. Rev. D **81**, 024017 (2010), arXiv:0910.5533 [gr-qc].

[1474] N. Yunes, A. Buonanno, S. A. Hughes, M. Coleman Miller, and Y. Pan, Modeling Extreme Mass Ratio Inspirals within the Effective-One-Body Approach, Phys. Rev. Lett. **104**, 091102 (2010), arXiv:0909.4263 [gr-qc].

[1475] N. Yunes, A. Buonanno, S. A. Hughes, Y. Pan, E. Barausse, M. C. Miller, and W. Throwe, Extreme Mass-Ratio Inspirals in the Effective-One-Body Approach: Quasi-Circular, Equatorial Orbits around a Spinning Black Hole, Phys. Rev. D **83**, 044044 (2011), [Erratum: Phys.Rev.D 88, 109904 (2013)], arXiv:1009.6013 [gr-qc].

[1476] A. Nagar and S. Albanesi, Toward a gravitational self-force-informed effective-one-body waveform model for nonprecessing, eccentric, large-mass-ratio inspirals, Phys. Rev. D **106**, 064049 (2022), arXiv:2207.14002 [gr-qc].

[1477] A. Albertini, A. Nagar, A. Pound, N. Warburton, B. Wardell, L. Durkan, and J. Miller, Comparing second-order gravitational self-force and effective one body waveforms from inspiralling, quasicircular and nonspinning black hole binaries. II. The large-mass-ratio case, Phys. Rev. D **106**, 084062 (2022), arXiv:2208.02055 [gr-qc].

[1478] D. P. Mihaylov, S. Ossokine, A. Buonanno, H. Estelles, L. Pompili, M. Pürrer, and A. Ramos-Buades, pySEOBNR: a software package for the next generation of effective-one-body multipolar waveform models, arXiv:2303.18203 [gr-qc].

[1479] LIGO Scientific Collaboration, LIGO Algorithm Library - LALSuite, free software (GPL), https://doi.org/10.7935/GT1W-FZ16 (2020).

[1480] E. Ochsner, *Improving analytical templates and searching for gravitational waves from coalescing black hole binaries*, Ph.D. thesis, Maryland U., College Park (2010).

[1481] J. Abadie *et al.* (LIGO Scientific, VIRGO), Search for gravitational waves from binary black hole inspiral, merger and ringdown, Phys. Rev. D **83**, 122005 (2011), [Erratum: Phys.Rev.D 86, 069903 (2012)], arXiv:1102.3781 [gr-qc].

[1482] J. Abadie *et al.* (LIGO Scientific, VIRGO), Search for Gravitational Waves from Low Mass Compact Binary Coalescence in LIGO's Sixth Science Run and Virgo's Science Runs 2 and 3, Phys. Rev. D **85**, 082002 (2012), arXiv:1111.7314 [gr-qc].

[1483] J. Aasi *et al.* (LIGO Scientific, VIRGO), Search for gravitational waves from binary black hole inspiral, merger, and ringdown in LIGO-Virgo data from 2009–2010, Phys. Rev. D **87**, 022002 (2013), arXiv:1209.6533 [gr-qc].

[1484] A. Buonanno, Y.-b. Chen, and M. Vallisneri, Detecting gravitational waves from precessing binaries of spinning compact objects: Adiabatic limit, Phys. Rev. D **67**, 104025 (2003), [Erratum: Phys.Rev.D 74, 029904 (2006)], arXiv:gr-qc/0211087.

[1485] P. Schmidt, M. Hannam, S. Husa, and P. Ajith, Tracking the precession of compact binaries from their gravitational-wave signal, Phys. Rev. D **84**, 024046 (2011), arXiv:1012.2879 [gr-qc].

[1486] X. Liu, Z. Cao, and Z.-H. Zhu, A higher-multipole gravitational waveform model for an eccentric binary black holes based on the effective-one-body-numerical-relativity formalism, Class. Quant. Grav. **39**, 035009 (2022), arXiv:2102.08614 [gr-qc].

[1487] R. Abbott *et al.* (LIGO Scientific, Virgo), GWTC-2: Compact Binary Coalescences Observed by LIGO and Virgo During the First Half of the Third Observing Run, Phys. Rev. X **11**, 021053 (2021), arXiv:2010.14527 [gr-qc].

[1488] R. Abbott *et al.* (LIGO Scientific, Virgo), GW190412: Observation of a Binary-Black-Hole Coalescence with Asymmetric Masses, Phys. Rev. D **102**, 043015 (2020), arXiv:2004.08342 [astro-ph.HE].

[1489] M. Khalil, A. Buonanno, H. Estelles, D. P. Mihaylov, S. Ossokine, L. Pompili, and A. Ramos-Buades, Theoretical groundwork supporting the precessing-spin two-body dynamics of the

effective-one-body waveform models SEOBNRv5, arXiv:2303.18143 [gr-qc].

[1490] H. Estellés, A. Ramos-Buades, S. Husa, C. García-Quirós, M. Colleoni, L. Haegel, and R. Jaume, Phenomenological time domain model for dominant quadrupole gravitational wave signal of coalescing binary black holes, Phys. Rev. D **103**, 124060 (2021), arXiv:2004.08302 [gr-qc].

[1491] K. Ackley *et al.*, Neutron Star Extreme Matter Observatory: A kilohertz-band gravitational-wave detector in the global network, Publ. Astron. Soc. Austral. **37**, e047 (2020), arXiv:2007.03128 [astro-ph.HE].

[1492] V. Varma, S. E. Field, M. A. Scheel, J. Blackman, L. E. Kidder, and H. P. Pfeiffer, Surrogate model of hybridized numerical relativity binary black hole waveforms, Phys. Rev. D **99**, 064045 (2019), arXiv:1812.07865 [gr-qc].

[1493] J. Yoo *et al.*, Numerical relativity surrogate model with memory effects and post-Newtonian hybridization, Phys. Rev. D **108**, 064027 (2023), arXiv:2306.03148 [gr-qc].

[1494] H. Estellés, S. Husa, M. Colleoni, D. Keitel, M. Mateu-Lucena, C. García-Quirós, A. Ramos-Buades, and A. Borchers, Time-domain phenomenological model of gravitational-wave subdominant harmonics for quasicircular nonprecessing binary black hole coalescences, Phys. Rev. D **105**, 084039 (2022), arXiv:2012.11923 [gr-qc].

[1495] T. Damour, E. Gourgoulhon, and P. Grandclement, Circular orbits of corotating binary black holes: Comparison between analytical and numerical results, Phys. Rev. D **66**, 024007 (2002), arXiv:gr-qc/0204011.

[1496] G. Riemenschneider, P. Rettegno, M. Breschi, A. Albertini, R. Gamba, S. Bernuzzi, and A. Nagar, Assessment of consistent next-to-quasicircular corrections and postadiabatic approximation in effective-one-body multipolar waveforms for binary black hole coalescences, Phys. Rev. D **104**, 104045 (2021), arXiv:2104.07533 [gr-qc].

[1497] A. Nagar, P. Rettegno, R. Gamba, A. Albertini, and S. Bernuzzi, TEOBResumS: Analytic systematics in next-generation of effective-one-body gravitational waveform models for future observations, arXiv:2304.09662 [gr-qc].

[1498] A. Nagar and P. Rettegno, Next generation: Impact of high-order analytical information on effective one body waveform models for noncircularized, spin-aligned black hole binaries, Phys. Rev. D **104**, 104004 (2021), arXiv:2108.02043 [gr-qc].

[1499] A. Bonino, R. Gamba, P. Schmidt, A. Nagar, G. Pratten, M. Breschi, P. Rettegno, and S. Bernuzzi, Inferring eccentricity evolution from observations of coalescing binary black holes, Phys. Rev. D **107**, 064024 (2023), arXiv:2207.10474 [gr-qc].

[1500] A. Nagar, P. Rettegno, R. Gamba, and S. Bernuzzi, Effective-one-body waveforms from dynamical captures in black hole binaries, Phys. Rev. D **103**, 064013 (2021), arXiv:2009.12857 [gr-qc].

[1501] R. Gamba, M. Breschi, G. Carullo, S. Albanesi, P. Rettegno, S. Bernuzzi, and A. Nagar, GW190521 as a dynamical capture of two nonspinning black holes, Nature Astron. **7**, 11 (2023), arXiv:2106.05575 [gr-qc].

[1502] F.-L. Julié and N. Deruelle, Two-body problem in Scalar-Tensor theories as a deformation of General Relativity : an Effective-One-Body approach, Phys. Rev. D **95**, 124054 (2017), arXiv:1703.05360 [gr-qc].

[1503] F.-L. Julié, Reducing the two-body problem in scalar-tensor theories to the motion of a test particle : a scalar-tensor effective-one-body approach, Phys. Rev. D **97**, 024047 (2018), arXiv:1709.09742 [gr-qc].

[1504] T. Jain, P. Rettegno, M. Agathos, A. Nagar, and L. Turco, Effective-one-body Hamiltonian in scalar-tensor gravity at third post-Newtonian order, Phys. Rev. D **107**, 084017 (2023), arXiv:2211.15580 [gr-qc].

[1505] T. Jain, Nonlocal-in-time effective one body Hamiltonian in scalar-tensor gravity at third post-Newtonian order, Phys. Rev. D **107**, 084018 (2023), arXiv:2301.01070 [gr-qc].

[1506] T. Jain, Gravitational scattering upto third post-Newtonian approximation for conservative dynamics: Scalar-Tensor theories, arXiv:2304.09052 [gr-qc].

[1507] T. Damour, P. Jaranowski, and G. Schaefer, Hamiltonian of two spinning compact bodies with next-to-leading order gravitational spin-orbit coupling, Phys. Rev. D **77**, 064032 (2008), arXiv:0711.1048 [gr-qc].

[1508] A. Placidi, S. Albanesi, A. Nagar, M. Orselli, S. Bernuzzi, and G. Grignani, Exploiting Newton-factorized, 2PN-accurate waveform multipoles in effective-one-body models for spin-aligned noncircularized binaries, Phys. Rev. D **105**, 104030 (2022), arXiv:2112.05448 [gr-qc].

[1509] S. Albanesi, A. Nagar, and S. Bernuzzi, Effective one-body model for extreme-mass-ratio spinning binaries on eccentric equatorial orbits: Testing radiation reaction and waveform, Phys. Rev. D **104**, 024067 (2021), arXiv:2104.10559 [gr-qc].

[1510] S. Albanesi, A. Nagar, S. Bernuzzi, A. Placidi, and M. Orselli, Assessment of effective-one-body radiation reactions for generic planar orbits, Phys. Rev. D **105**, 104031 (2022), arXiv:2202.10063 [gr-qc].

[1511] H. Estellés, M. Colleoni, C. García-Quirós, S. Husa, D. Keitel, M. Mateu-Lucena, M. d. L. Planas, and A. Ramos-Buades, New twists in compact binary waveform modeling: A fast time-domain model for precession, Phys. Rev. D **105**, 084040 (2022), arXiv:2105.05872 [gr-qc].

[1512] M. Cabero, A. B. Nielsen, A. P. Lundgren, and C. D. Capano, Minimum energy and the end of the inspiral in the post-Newtonian approximation, Phys. Rev. D **95**, 064016 (2017), arXiv:1602.03134 [gr-qc].

[1513] P. Ajith *et al.*, Phenomenological template family for black-hole coalescence waveforms, Class. Quant. Grav. **24**, S689 (2007), arXiv:0704.3764 [gr-qc].

[1514] P. Ajith *et al.*, A Template bank for gravitational waveforms from coalescing binary black holes. I. Non-spinning binaries, Phys. Rev. D **77**, 104017 (2008), [Erratum: Phys.Rev.D 79, 129901 (2009)], arXiv:0710.2335 [gr-qc].

[1515] P. Ajith *et al.*, Inspiral-merger-ringdown waveforms for black-hole binaries with non-precessing spins, Phys. Rev. Lett. **106**, 241101 (2011), arXiv:0909.2867 [gr-qc].

[1516] L. Santamaria *et al.*, Matching post-Newtonian and numerical relativity waveforms: systematic errors and a new phenomenological model for non-precessing black hole binaries, Phys. Rev. D **82**, 064016 (2010), arXiv:1005.3306 [gr-qc].

[1517] A. Bohé, M. Hannam, S. Husa, F. Ohme, M. Puerrer, and P. Schmidt, *PhenomPv2 - Technical Notes for LAL Implementation*, Tech. Rep. LIGO-T1500602 (LIGO Project, 2016).

[1518] L. London, S. Khan, E. Fauchon-Jones, C. García, M. Hannam, S. Husa, X. Jiménez-Forteza, C. Kalaghatgi, F. Ohme, and F. Pannarale, First higher-multipole model of gravitational waves from spinning and coalescing black-hole binaries, Phys. Rev. Lett. **120**, 161102 (2018), arXiv:1708.00404 [gr-qc].

[1519] S. Khan, K. Chatziioannou, M. Hannam, and F. Ohme, Phenomenological model for the gravitational-wave signal from precessing binary black holes with two-spin effects, Phys. Rev. D **100**, 024059 (2019), arXiv:1809.10113 [gr-qc].

[1520] S. Khan, F. Ohme, K. Chatziioannou, and M. Hannam, Including higher order multipoles in gravitational-wave models for precessing binary black holes, Phys. Rev. D **101**, 024056 (2020), arXiv:1911.06050 [gr-qc].

[1521] T. Dietrich *et al.*, Matter imprints in waveform models for neutron star binaries: Tidal and self-spin effects, Phys. Rev. D **99**, 024029 (2019), arXiv:1804.02235 [gr-qc].

[1522] T. Dietrich, A. Samajdar, S. Khan, N. K. Johnson-McDaniel, R. Dudi, and W. Tichy, Improving the NRTidal model for binary neutron star systems, Phys. Rev. D **100**, 044003 (2019), arXiv:1905.06011 [gr-qc].

[1523] J. E. Thompson, E. Fauchon-Jones, S. Khan, E. Nitoglia, F. Pannarale, T. Dietrich, and M. Hannam, Modeling the gravitational wave signature of neutron star black hole coalescences, Phys. Rev. D **101**, 124059 (2020), arXiv:2002.08383 [gr-qc].

[1524] C. García-Quirós, M. Colleoni, S. Husa, H. Estellés, G. Pratten, A. Ramos-Buades, M. Mateu-Lucena, and R. Jaume, Multimode frequency-domain model for the gravitational wave signal

214

from nonprecessing black-hole binaries, Phys. Rev. D **102**, 064002 (2020), arXiv:2001.10914 [gr-qc].

[1525] C. García-Quirós, S. Husa, M. Mateu-Lucena, and A. Borchers, Accelerating the evaluation of inspiral–merger–ringdown waveforms with adapted grids, Class. Quant. Grav. **38**, 015006 (2021), arXiv:2001.10897 [gr-qc].

[1526] S. Marsat, L. Blanchet, A. Bohe, and G. Faye, Gravitational waves from spinning compact object binaries: New post-Newtonian results (2013) arXiv:1312.5375 [gr-qc].

[1527] S. Marsat and J. G. Baker, Fourier-domain modulations and delays of gravitational-wave signals, arXiv:1806.10734 [gr-qc].

[1528] A. Ramos-Buades, P. Schmidt, G. Pratten, and S. Husa, Validity of common modeling approximations for precessing binary black holes with higher-order modes, Phys. Rev. D **101**, 103014 (2020), arXiv:2001.10936 [gr-qc].

[1529] S. Babak and A. Petiteau, Lisa data challenge manual, Available at https://https://lisa-ldc.lal.in2p3.fr/static/data/pdf/LDC-manual-002.pdf .

[1530] B. P. Abbott *et al.* (LIGO Scientific, Virgo), Properties of the Binary Black Hole Merger GW150914, Phys. Rev. Lett. **116**, 241102 (2016), arXiv:1602.03840 [gr-qc].

[1531] S. Vinciguerra, J. Veitch, and I. Mandel, Accelerating gravitational wave parameter estimation with multi-band template interpolation, Class. Quant. Grav. **34**, 115006 (2017), arXiv:1703.02062 [gr-qc].

[1532] B. Bruegmann, J. A. Gonzalez, M. Hannam, S. Husa, and U. Sperhake, Exploring black hole superkicks, Phys. Rev. D **77**, 124047 (2008), arXiv:0707.0135 [gr-qc].

[1533] C. Kalaghatgi and M. Hannam, Investigating the effect of in-plane spin directions for precessing binary black hole systems, Phys. Rev. D **103**, 024024 (2021), arXiv:2008.09957 [gr-qc].

[1534] C. R. Galley and I. Z. Rothstein, Deriving analytic solutions for compact binary inspirals without recourse to adiabatic approximations, Phys. Rev. D **95**, 104054 (2017), arXiv:1609.08268 [gr-qc].

[1535] Z. Yang and A. K. Leibovich, Analytic Solutions to Compact Binary Inspirals With Leading Order Spin-Orbit Contribution Using The Dynamical Renormalization Group, Phys. Rev. D **100**, 084021 (2019), arXiv:1908.05688 [gr-qc].

[1536] J. Blackman, S. E. Field, M. A. Scheel, C. R. Galley, D. A. Hemberger, P. Schmidt, and R. Smith, A Surrogate Model of Gravitational Waveforms from Numerical Relativity Simulations of Precessing Binary Black Hole Mergers, Phys. Rev. D **95**, 104023 (2017), arXiv:1701.00550 [gr-qc].

[1537] C. Prud'homme, Y. Maday, A. T. Patera, G. Turinici, D. V. Rovas, K. Veroy, and L. Machiels, Reliable real-time solution of parametrized partial differential equations: Reduced-basis output bound methods, J. Fluids Eng. **124**, 70 (2001).

[1538] M. Barrault, Y. Maday, N. C. Nguyen, and A. T. Patera, An 'empirical interpolation'method: application to efficient reduced-basis discretization of partial differential equations, Comptes Rendus Mathematique **339**, 667 (2004).

[1539] P. Binev, A. Cohen, W. Dahmen, R. A. DeVore, G. Petrova, and P. Wojtaszczyk, Convergence rates for greedy algorithms in reduced basis methods., SIAM J. Math. Analysis **43**, 1457 (2011).

[1540] R. DeVore, G. Petrova, and P. Wojtaszczyk, Greedy algorithms for reduced bases in Banach spaces, Constructive Approximation **37**, 455 (2013).

[1541] Y. Maday, A. T. Patera, and G. Turinici, A priori convergence theory for reduced-basis approximations of single-parameter elliptic partial differential equations, J. Sci. Comput. **17**, 437 (2002).

[1542] A. Quarteroni, G. Rozza, and A. Manzoni, Certified reduced basis approximation for parametrized partial differential equations and applications, Journal of Mathematics in Industry **1**, 1 (2011).

[1543] K. Cannon, J. D. Emberson, C. Hanna, D. Keppel, and H. Pfeiffer, Interpolation in waveform

space: enhancing the accuracy of gravitational waveform families using numerical relativity, Phys. Rev. D **87**, 044008 (2013), arXiv:1211.7095 [gr-qc].

[1544] K. Cannon, A. Chapman, C. Hanna, D. Keppel, A. C. Searle, and A. J. Weinstein, Singular value decomposition applied to compact binary coalescence gravitational-wave signals, Phys. Rev. D **82**, 044025 (2010), arXiv:1005.0012 [gr-qc].

[1545] K. Cannon, C. Hanna, and D. Keppel, Efficiently enclosing the compact binary parameter space by singular-value decomposition, Phys. Rev. D **84**, 084003 (2011), arXiv:1101.4939 [gr-qc].

[1546] K. Cannon, C. Hanna, and D. Keppel, Interpolating compact binary waveforms using the singular value decomposition, Phys. Rev. D **85**, 081504 (2012), arXiv:1108.5618 [gr-qc].

[1547] S. E. Field, C. R. Galley, F. Herrmann, J. S. Hesthaven, E. Ochsner, and M. Tiglio, Reduced basis catalogs for gravitational wave templates, Phys. Rev. Lett. **106**, 221102 (2011), arXiv:1101.3765 [gr-qc].

[1548] F. Herrmann, S. E. Field, C. R. Galley, E. Ochsner, and M. Tiglio, Towards beating the curse of dimensionality for gravitational waves using Reduced Basis, Phys. Rev. D **86**, 084046 (2012), arXiv:1205.6009 [gr-qc].

[1549] Z. Doctor, B. Farr, D. E. Holz, and M. Pürrer, Statistical Gravitational Waveform Models: What to Simulate Next?, Phys. Rev. D **96**, 123011 (2017), arXiv:1706.05408 [astro-ph.HE].

[1550] A. J. K. Chua, C. R. Galley, and M. Vallisneri, Reduced-order modeling with artificial neurons for gravitational-wave inference, Phys. Rev. Lett. **122**, 211101 (2019), arXiv:1811.05491 [astro-ph.IM].

[1551] A. Khan, E. A. Huerta, and H. Zheng, Interpretable AI forecasting for numerical relativity waveforms of quasicircular, spinning, nonprecessing binary black hole mergers, Phys. Rev. D **105**, 024024 (2022), arXiv:2110.06968 [gr-qc].

[1552] Y. Setyawati, M. Pürrer, and F. Ohme, Regression methods in waveform modeling: a comparative study, Class. Quant. Grav. **37**, 075012 (2020), arXiv:1909.10986 [astro-ph.IM].

[1553] S. Caudill, S. E. Field, C. R. Galley, F. Herrmann, and M. Tiglio, Reduced Basis representations of multi-mode black hole ringdown gravitational waves, Class. Quant. Grav. **29**, 095016 (2012), arXiv:1109.5642 [gr-qc].

[1554] K. Barkett, Y. Chen, M. A. Scheel, and V. Varma, Gravitational waveforms of binary neutron star inspirals using post-Newtonian tidal splicing, Phys. Rev. D **102**, 024031 (2020), arXiv:1911.10440 [gr-qc].

[1555] P. Kumar, J. Blackman, S. E. Field, M. Scheel, C. R. Galley, M. Boyle, L. E. Kidder, H. P. Pfeiffer, B. Szilagyi, and S. A. Teukolsky, Constraining the parameters of GW150914 and GW170104 with numerical relativity surrogates, Phys. Rev. D **99**, 124005 (2019), arXiv:1808.08004 [gr-qc].

[1556] S. Biscoveanu, M. Isi, S. Vitale, and V. Varma, New Spin on LIGO-Virgo Binary Black Holes, Phys. Rev. Lett. **126**, 171103 (2021), arXiv:2007.09156 [astro-ph.HE].

[1557] T. Islam, A. Vajpeyi, F. H. Shaik, C.-J. Haster, V. Varma, S. E. Field, J. Lange, R. O'Shaughnessy, and R. Smith, Analysis of GWTC-3 with fully precessing numerical relativity surrogate models, arXiv:2309.14473 [gr-qc].

[1558] J. Blackman, B. Szilagyi, C. R. Galley, and M. Tiglio, Sparse Representations of Gravitational Waves from Precessing Compact Binaries, Phys. Rev. Lett. **113**, 021101 (2014), arXiv:1401.7038 [gr-qc].

[1559] C. Talbot, R. Smith, E. Thrane, and G. B. Poole, Parallelized Inference for Gravitational-Wave Astronomy, Phys. Rev. D **100**, 043030 (2019), arXiv:1904.02863 [astro-ph.IM].

[1560] J. McKennon, G. Forrester, and G. Khanna, High Accuracy Gravitational Waveforms from Black Hole Binary Inspirals Using OpenCL, arXiv:1206.0270 [gr-qc].

[1561] G. Khanna and J. McKennon, Numerical modeling of gravitational wave sources accelerated by OpenCL, Comput. Phys. Commun. **181**, 1605 (2010), arXiv:1001.3631 [gr-qc].

[1562] S. E. Field, S. Gottlieb, Z. J. Grant, L. F. Isherwood, and G. Khanna, A GPU-accelerated mixed-precision WENO method for extremal black hole and gravitational wave physics computations,

Appl. Math. Comput. **5**, 97 (2023), arXiv:2010.04760 [math.NA].

[1563] S. Mirshekari, N. Yunes, and C. M. Will, Constraining Generic Lorentz Violation and the Speed of the Graviton with Gravitational Waves, Phys. Rev. D **85**, 024041 (2012), arXiv:1110.2720 [gr-qc].

[1564] I. D. Saltas, I. Sawicki, L. Amendola, and M. Kunz, Anisotropic Stress as a Signature of Nonstandard Propagation of Gravitational Waves, Phys. Rev. Lett. **113**, 191101 (2014), arXiv:1406.7139 [astro-ph.CO].

[1565] E. Belgacem, Y. Dirian, S. Foffa, and M. Maggiore, Gravitational-wave luminosity distance in modified gravity theories, Phys. Rev. D **97**, 104066 (2018), arXiv:1712.08108 [astro-ph.CO].

[1566] E. Belgacem *et al.* (LISA Cosmology Working Group), Testing modified gravity at cosmological distances with LISA standard sirens, JCAP **07**, 024, arXiv:1906.01593 [astro-ph.CO].

[1567] A. Bonilla, R. D'Agostino, R. C. Nunes, and J. C. N. de Araujo, Forecasts on the speed of gravitational waves at high z, JCAP **03**, 015, arXiv:1910.05631 [gr-qc].

[1568] R. D'Agostino and R. C. Nunes, Probing observational bounds on scalar-tensor theories from standard sirens, Phys. Rev. D **100**, 044041 (2019), arXiv:1907.05516 [gr-qc].

[1569] A. Allahyari, R. C. Nunes, and D. F. Mota, No slip gravity in light of LISA standard sirens, Mon. Not. Roy. Astron. Soc. **514**, 1274 (2022), arXiv:2110.07634 [astro-ph.CO].

[1570] R. D'Agostino and R. C. Nunes, Forecasting constraints on deviations from general relativity in f(Q) gravity with standard sirens, Phys. Rev. D **106**, 124053 (2022), arXiv:2210.11935 [gr-qc].

[1571] J. Healy, T. Bode, R. Haas, E. Pazos, P. Laguna, D. Shoemaker, and N. Yunes, Late Inspiral and Merger of Binary Black Holes in Scalar-Tensor Theories of Gravity, Class. Quant. Grav. **29**, 232002 (2012), arXiv:1112.3928 [gr-qc].

[1572] M. Okounkova, L. C. Stein, M. A. Scheel, and D. A. Hemberger, Numerical binary black hole mergers in dynamical Chern-Simons gravity: Scalar field, Phys. Rev. D **96**, 044020 (2017), arXiv:1705.07924 [gr-qc].

[1573] E. W. Hirschmann, L. Lehner, S. L. Liebling, and C. Palenzuela, Black Hole Dynamics in Einstein-Maxwell-Dilaton Theory, Phys. Rev. D **97**, 064032 (2018), arXiv:1706.09875 [gr-qc].

[1574] M. Okounkova, L. C. Stein, M. A. Scheel, and S. A. Teukolsky, Numerical binary black hole collisions in dynamical Chern-Simons gravity, Phys. Rev. D **100**, 104026 (2019), arXiv:1906.08789 [gr-qc].

[1575] M. Okounkova, L. C. Stein, J. Moxon, M. A. Scheel, and S. A. Teukolsky, Numerical relativity simulation of GW150914 beyond general relativity, Phys. Rev. D **101**, 104016 (2020), arXiv:1911.02588 [gr-qc].

[1576] W. E. East and J. L. Ripley, Evolution of Einstein-scalar-Gauss-Bonnet gravity using a modified harmonic formulation, Phys. Rev. D **103**, 044040 (2021), arXiv:2011.03547 [gr-qc].

[1577] P. Figueras and T. França, Black hole binaries in cubic Horndeski theories, Phys. Rev. D **105**, 124004 (2022), arXiv:2112.15529 [gr-qc].

[1578] W. E. East and J. L. Ripley, Dynamics of Spontaneous Black Hole Scalarization and Mergers in Einstein-Scalar-Gauss-Bonnet Gravity, Phys. Rev. Lett. **127**, 101102 (2021), arXiv:2105.08571 [gr-qc].

[1579] L. Aresté Saló, K. Clough, and P. Figueras, Well-Posedness of the Four-Derivative Scalar-Tensor Theory of Gravity in Singularity Avoiding Coordinates, Phys. Rev. Lett. **129**, 261104 (2022), arXiv:2208.14470 [gr-qc].

[1580] J. L. Ripley, Numerical relativity for Horndeski gravity, Int. J. Mod. Phys. D **31**, 2230017 (2022), arXiv:2207.13074 [gr-qc].

[1581] R. Cayuso, P. Figueras, T. França, and L. Lehner, Modelling self-consistently beyond General Relativity, arXiv:2303.07246 [gr-qc].

[1582] M. Salgado, D. Martinez-del Rio, M. Alcubierre, and D. Nunez, Hyperbolicity of scalar-tensor theories of gravity, Phys. Rev. D **77**, 104010 (2008), arXiv:0801.2372 [gr-qc].

[1583] T. P. Sotiriou and V. Faraoni, Black holes in scalar-tensor gravity, Phys. Rev. Lett. **108**, 081103 (2012), arXiv:1109.6324 [gr-qc].

217

[1584] O. Sarbach and M. Tiglio, Continuum and Discrete Initial-Boundary-Value Problems and Einstein's Field Equations, Living Rev. Rel. **15**, 9 (2012), arXiv:1203.6443 [gr-qc].

[1585] D. Hilditch, An Introduction to Well-posedness and Free-evolution, Int. J. Mod. Phys. A **28**, 1340015 (2013), arXiv:1309.2012 [gr-qc].

[1586] T. Delsate, D. Hilditch, and H. Witek, Initial value formulation of dynamical Chern-Simons gravity, Phys. Rev. D **91**, 024027 (2015), arXiv:1407.6727 [gr-qc].

[1587] G. Papallo and H. S. Reall, On the local well-posedness of Lovelock and Horndeski theories, Phys. Rev. D **96**, 044019 (2017), arXiv:1705.04370 [gr-qc].

[1588] G. Papallo, On the hyperbolicity of the most general Horndeski theory, Phys. Rev. D **96**, 124036 (2017), arXiv:1710.10155 [gr-qc].

[1589] J. Cayuso, N. Ortiz, and L. Lehner, Fixing extensions to general relativity in the nonlinear regime, Phys. Rev. D **96**, 084043 (2017), arXiv:1706.07421 [gr-qc].

[1590] O. Sarbach, E. Barausse, and J. A. Preciado-López, Well-posed Cauchy formulation for Einstein-æther theory, Class. Quant. Grav. **36**, 165007 (2019), arXiv:1902.05130 [gr-qc].

[1591] J. L. Ripley and F. Pretorius, Hyperbolicity in Spherical Gravitational Collapse in a Horndeski Theory, Phys. Rev. D **99**, 084014 (2019), arXiv:1902.01468 [gr-qc].

[1592] J. L. Ripley and F. Pretorius, Gravitational collapse in Einstein dilaton-Gauss–Bonnet gravity, Class. Quant. Grav. **36**, 134001 (2019), arXiv:1903.07543 [gr-qc].

[1593] A. D. Kovács, Well-posedness of cubic Horndeski theories, Phys. Rev. D **100**, 024005 (2019), arXiv:1904.00963 [gr-qc].

[1594] A. D. Kovács and H. S. Reall, Well-Posed Formulation of Scalar-Tensor Effective Field Theory, Phys. Rev. Lett. **124**, 221101 (2020), arXiv:2003.04327 [gr-qc].

[1595] A. D. Kovács and H. S. Reall, Well-posed formulation of Lovelock and Horndeski theories, Phys. Rev. D **101**, 124003 (2020), arXiv:2003.08398 [gr-qc].

[1596] H. Witek, L. Gualtieri, and P. Pani, Towards numerical relativity in scalar Gauss-Bonnet gravity: $3 + 1$ decomposition beyond the small-coupling limit, Phys. Rev. D **101**, 124055 (2020), arXiv:2004.00009 [gr-qc].

[1597] F.-L. Julié and E. Berti, $d + 1$ formalism in Einstein-scalar-Gauss-Bonnet gravity, Phys. Rev. D **101**, 124045 (2020), arXiv:2004.00003 [gr-qc].

[1598] M. Bezares, M. Crisostomi, C. Palenzuela, and E. Barausse, K-dynamics: well-posed 1+1 evolutions in K-essence, JCAP **03**, 072, arXiv:2008.07546 [gr-qc].

[1599] L. ter Haar, M. Bezares, M. Crisostomi, E. Barausse, and C. Palenzuela, Dynamics of Screening in Modified Gravity, Phys. Rev. Lett. **126**, 091102 (2021), arXiv:2009.03354 [gr-qc].

[1600] H. O. Silva, H. Witek, M. Elley, and N. Yunes, Dynamical Descalarization in Binary Black Hole Mergers, Phys. Rev. Lett. **127**, 031101 (2021), arXiv:2012.10436 [gr-qc].

[1601] E. Barausse, M. Bezares, M. Crisostomi, and G. Lara, The well-posedness of the Cauchy problem for self-interacting vector fields, JCAP **11**, 050, arXiv:2207.00443 [gr-qc].

[1602] C. de Rham, J. Kożuszek, A. J. Tolley, and T. Wiseman, Dynamical formulation of ghost-free massive gravity, Phys. Rev. D **108**, 084052 (2023), arXiv:2302.04876 [hep-th].

[1603] R. Benkel, T. P. Sotiriou, and H. Witek, Black hole hair formation in shift-symmetric generalised scalar-tensor gravity, Class. Quant. Grav. **34**, 064001 (2017), arXiv:1610.09168 [gr-qc].

[1604] R. Benkel, T. P. Sotiriou, and H. Witek, Dynamical scalar hair formation around a Schwarzschild black hole, Phys. Rev. D **94**, 121503 (2016), arXiv:1612.08184 [gr-qc].

[1605] D. D. Doneva, A. Vañó Viñuales, and S. S. Yazadjiev, Dynamical descalarization with a jump during a black hole merger, Phys. Rev. D **106**, L061502 (2022), arXiv:2204.05333 [gr-qc].

[1606] G. Allwright and L. Lehner, Towards the nonlinear regime in extensions to GR: assessing possible options, Class. Quant. Grav. **36**, 084001 (2019), arXiv:1808.07897 [gr-qc].

[1607] R. Cayuso and L. Lehner, Nonlinear, noniterative treatment of EFT-motivated gravity, Phys. Rev. D **102**, 084008 (2020), arXiv:2005.13720 [gr-qc].

[1608] N. Franchini, M. Bezares, E. Barausse, and L. Lehner, Fixing the dynamical evolution in scalar-Gauss-Bonnet gravity, Phys. Rev. D **106**, 064061 (2022), arXiv:2206.00014 [gr-qc].

[1609] M. Okounkova, Numerical relativity simulation of GW150914 in Einstein dilaton Gauss-Bonnet gravity, Phys. Rev. D **102**, 084046 (2020), arXiv:2001.03571 [gr-qc].

[1610] M. Elley, H. O. Silva, H. Witek, and N. Yunes, Spin-induced dynamical scalarization, descalarization, and stealthness in scalar-Gauss-Bonnet gravity during a black hole coalescence, Phys. Rev. D **106**, 044018 (2022), arXiv:2205.06240 [gr-qc].

[1611] M. B. Green and J. H. Schwarz, Anomaly Cancellation in Supersymmetric D=10 Gauge Theory and Superstring Theory, Phys. Lett. B **149**, 117 (1984).

[1612] V. Taveras and N. Yunes, The Barbero-Immirzi Parameter as a Scalar Field: K-Inflation from Loop Quantum Gravity?, Phys. Rev. D **78**, 064070 (2008), arXiv:0807.2652 [gr-qc].

[1613] S. Mercuri and V. Taveras, Interaction of the Barbero-Immirzi Field with Matter and Pseudo-Scalar Perturbations, Phys. Rev. D **80**, 104007 (2009), arXiv:0903.4407 [gr-qc].

[1614] D. J. Gross and J. H. Sloan, The quartic effective action for the heterotic string, Nuclear Physics B **291**, 41 (1987).

[1615] F. Moura and R. Schiappa, Higher-derivative corrected black holes: Perturbative stability and absorption cross-section in heterotic string theory, Class. Quant. Grav. **24**, 361 (2007), arXiv:hep-th/0605001.

[1616] D. D. Doneva and S. S. Yazadjiev, New Gauss-Bonnet Black Holes with Curvature-Induced Scalarization in Extended Scalar-Tensor Theories, Phys. Rev. Lett. **120**, 131103 (2018), arXiv:1711.01187 [gr-qc].

[1617] H. O. Silva, J. Sakstein, L. Gualtieri, T. P. Sotiriou, and E. Berti, Spontaneous scalarization of black holes and compact stars from a Gauss-Bonnet coupling, Phys. Rev. Lett. **120**, 131104 (2018), arXiv:1711.02080 [gr-qc].

[1618] G. Antoniou, A. Bakopoulos, and P. Kanti, Evasion of No-Hair Theorems and Novel Black-Hole Solutions in Gauss-Bonnet Theories, Phys. Rev. Lett. **120**, 131102 (2018), arXiv:1711.03390 [hep-th].

[1619] D. D. Doneva, F. M. Ramazanoğlu, H. O. Silva, T. P. Sotiriou, and S. S. Yazadjiev, Scalarization, arXiv:2211.01766 [gr-qc].

[1620] A. Dima, E. Barausse, N. Franchini, and T. P. Sotiriou, Spin-induced black hole spontaneous scalarization, Phys. Rev. Lett. **125**, 231101 (2020), arXiv:2006.03095 [gr-qc].

[1621] C. A. R. Herdeiro, E. Radu, H. O. Silva, T. P. Sotiriou, and N. Yunes, Spin-induced scalarized black holes, Phys. Rev. Lett. **126**, 011103 (2021), arXiv:2009.03904 [gr-qc].

[1622] S. Hod, Onset of spontaneous scalarization in spinning Gauss-Bonnet black holes, Phys. Rev. D **102**, 084060 (2020), arXiv:2006.09399 [gr-qc].

[1623] E. Berti, L. G. Collodel, B. Kleihaus, and J. Kunz, Spin-induced black-hole scalarization in Einstein-scalar-Gauss-Bonnet theory, Phys. Rev. Lett. **126**, 011104 (2021), arXiv:2009.03905 [gr-qc].

[1624] D. D. Doneva and S. S. Yazadjiev, Dynamics of the nonrotating and rotating black hole scalarization, Phys. Rev. D **103**, 064024 (2021), arXiv:2101.03514 [gr-qc].

[1625] D. D. Doneva and S. S. Yazadjiev, Spontaneously scalarized black holes in dynamical Chern-Simons gravity: dynamics and equilibrium solutions, Phys. Rev. D **103**, 083007 (2021), arXiv:2102.03940 [gr-qc].

[1626] M. Okounkova, M. Isi, K. Chatziioannou, and W. M. Farr, Gravitational wave inference on a numerical-relativity simulation of a black hole merger beyond general relativity, Phys. Rev. D **107**, 024046 (2023), arXiv:2208.02805 [gr-qc].

[1627] J. T. Gálvez Ghersi and L. C. Stein, Numerical renormalization-group-based approach to secular perturbation theory, Phys. Rev. E **104**, 034219 (2021), arXiv:2106.08410 [hep-th].

[1628] F. Thaalba, M. Bezares, N. Franchini, and T. P. Sotiriou, Spherical collapse in scalar-Gauss-Bonnet gravity: taming ill-posedness with a Ricci coupling, arXiv:2306.01695 [gr-qc].

[1629] M. Bezares, L. ter Haar, M. Crisostomi, E. Barausse, and C. Palenzuela, Kinetic screening in nonlinear stellar oscillations and gravitational collapse, Phys. Rev. D **104**, 044022 (2021), arXiv:2105.13992 [gr-qc].

219

[1630] A. Coates and F. M. Ramazanoğlu, Treatments and placebos for the pathologies of effective field theories, arXiv:2307.07743 [gr-qc].

[1631] A. Held and H. Lim, Nonlinear Evolution of Quadratic Gravity in 3+1 Dimensions, arXiv:2306.04725 [gr-qc].

[1632] M. Corman, J. L. Ripley, and W. E. East, Nonlinear studies of binary black hole mergers in Einstein-scalar-Gauss-Bonnet gravity, Phys. Rev. D **107**, 024014 (2023), arXiv:2210.09235 [gr-qc].

[1633] W. E. East and F. Pretorius, Binary neutron star mergers in Einstein-scalar-Gauss-Bonnet gravity, Phys. Rev. D **106**, 104055 (2022), arXiv:2208.09488 [gr-qc].

[1634] D. D. Doneva, L. Aresté Saló, K. Clough, P. Figueras, and S. S. Yazadjiev, Testing the limits of scalar-Gauss-Bonnet gravity through nonlinear evolutions of spin-induced scalarization, Phys. Rev. D **108**, 084017 (2023), arXiv:2307.06474 [gr-qc].

[1635] M. Zilhao, V. Cardoso, C. Herdeiro, L. Lehner, and U. Sperhake, Collisions of charged black holes, Phys. Rev. D **85**, 124062 (2012), arXiv:1205.1063 [gr-qc].

[1636] M. Zilhão, V. Cardoso, C. Herdeiro, L. Lehner, and U. Sperhake, Collisions of oppositely charged black holes, Phys. Rev. D **89**, 044008 (2014), arXiv:1311.6483 [gr-qc].

[1637] G. Bozzola and V. Paschalidis, Initial data for general relativistic simulations of multiple electrically charged black holes with linear and angular momenta, Phys. Rev. D **99**, 104044 (2019), arXiv:1903.01036 [gr-qc].

[1638] G. Bozzola and V. Paschalidis, General Relativistic Simulations of the Quasicircular Inspiral and Merger of Charged Black Holes: GW150914 and Fundamental Physics Implications, Phys. Rev. Lett. **126**, 041103 (2021), arXiv:2006.15764 [gr-qc].

[1639] R. Luna, G. Bozzola, V. Cardoso, V. Paschalidis, and M. Zilhão, Kicks in charged black hole binaries, Phys. Rev. D **106**, 084017 (2022), arXiv:2207.06429 [gr-qc].

[1640] P. G. S. Fernandes, C. A. R. Herdeiro, A. M. Pombo, E. Radu, and N. Sanchis-Gual, Spontaneous Scalarisation of Charged Black Holes: Coupling Dependence and Dynamical Features, Class. Quant. Grav. **36**, 134002 (2019), [Erratum: Class.Quant.Grav. 37, 049501 (2020)], arXiv:1902.05079 [gr-qc].

[1641] M. Alcubierre, J. C. Degollado, and M. Salgado, The Einstein-Maxwell system in 3+1 form and initial data for multiple charged black holes, Phys. Rev. D **80**, 104022 (2009), arXiv:0907.1151 [gr-qc].

[1642] J. Barranco, A. Bernal, J. C. Degollado, A. Diez-Tejedor, M. Megevand, M. Alcubierre, D. Núñez, and O. Sarbach, Schwarzschild scalar wigs: spectral analysis and late time behavior, Phys. Rev. D **89**, 083006 (2014), arXiv:1312.5808 [gr-qc].

[1643] H. Okawa and V. Cardoso, Black holes and fundamental fields: Hair, kicks, and a gravitational Magnus effect, Phys. Rev. D **90**, 104040 (2014), arXiv:1405.4861 [gr-qc].

[1644] H. Okawa, Nonlinear evolutions of bosonic clouds around black holes, Class. Quant. Grav. **32**, 214003 (2015).

[1645] N. Sanchis-Gual, J. C. Degollado, P. J. Montero, J. A. Font, and V. Mewes, Quasistationary solutions of self-gravitating scalar fields around collapsing stars, Phys. Rev. D **92**, 083001 (2015), arXiv:1507.08437 [gr-qc].

[1646] N. Sanchis-Gual, J. C. Degollado, P. Izquierdo, J. A. Font, and P. J. Montero, Quasistationary solutions of scalar fields around accreting black holes, Phys. Rev. D **94**, 043004 (2016), arXiv:1606.05146 [gr-qc].

[1647] K. Clough, T. Helfer, H. Witek, and E. Berti, Ghost Instabilities in Self-Interacting Vector Fields: The Problem with Proca Fields, Phys. Rev. Lett. **129**, 151102 (2022), arXiv:2204.10868 [gr-qc].

[1648] W. E. East, Vortex String Formation in Black Hole Superradiance of a Dark Photon with the Higgs Mechanism, Phys. Rev. Lett. **129**, 141103 (2022), arXiv:2205.03417 [hep-ph].

[1649] L. Bernard, V. Cardoso, T. Ikeda, and M. Zilhão, Physics of black hole binaries: Geodesics, relaxation modes, and energy extraction, Phys. Rev. D **100**, 044002 (2019), arXiv:1905.05204

[gr-qc].

[1650] Y.-P. Zhang, M. Gracia-Linares, P. Laguna, D. Shoemaker, and Y.-X. Liu, Gravitational recoil from binary black hole mergers in scalar field clouds, Phys. Rev. D **107**, 044039 (2023), arXiv:2209.11814 [gr-qc].

[1651] Cheng-Hsin Cheng and Giuseppe Ficarra and Helvi Witek, Binary black holes in dark matter environments (2023), in prep.

[1652] C. Palenzuela, I. Olabarrieta, L. Lehner, and S. L. Liebling, Head-on collisions of boson stars, Phys. Rev. D **75**, 064005 (2007), arXiv:gr-qc/0612067.

[1653] C. Palenzuela, L. Lehner, and S. L. Liebling, Orbital Dynamics of Binary Boson Star Systems, Phys. Rev. D **77**, 044036 (2008), arXiv:0706.2435 [gr-qc].

[1654] M. W. Choptuik and F. Pretorius, Ultra Relativistic Particle Collisions, Phys. Rev. Lett. **104**, 111101 (2010), arXiv:0908.1780 [gr-qc].

[1655] R. Brito, V. Cardoso, and H. Okawa, Accretion of dark matter by stars, Phys. Rev. Lett. **115**, 111301 (2015), arXiv:1508.04773 [gr-qc].

[1656] R. Brito, V. Cardoso, C. F. B. Macedo, H. Okawa, and C. Palenzuela, Interaction between bosonic dark matter and stars, Phys. Rev. D **93**, 044045 (2016), arXiv:1512.00466 [astro-ph.SR].

[1657] M. Bezares, C. Palenzuela, and C. Bona, Final fate of compact boson star mergers, Phys. Rev. D **95**, 124005 (2017), arXiv:1705.01071 [gr-qc].

[1658] C. Palenzuela, P. Pani, M. Bezares, V. Cardoso, L. Lehner, and S. Liebling, Gravitational Wave Signatures of Highly Compact Boson Star Binaries, Phys. Rev. D **96**, 104058 (2017), arXiv:1710.09432 [gr-qc].

[1659] M. Bezares and C. Palenzuela, Gravitational Waves from Dark Boson Star binary mergers, Class. Quant. Grav. **35**, 234002 (2018), arXiv:1808.10732 [gr-qc].

[1660] T. Helfer, E. A. Lim, M. A. G. Garcia, and M. A. Amin, Gravitational Wave Emission from Collisions of Compact Scalar Solitons, Phys. Rev. D **99**, 044046 (2019), arXiv:1802.06733 [gr-qc].

[1661] J. Y. Widdicombe, T. Helfer, and E. A. Lim, Black hole formation in relativistic Oscillaton collisions, JCAP **01**, 027, arXiv:1910.01950 [astro-ph.CO].

[1662] N. Sanchis-Gual, C. Herdeiro, J. A. Font, E. Radu, and F. Di Giovanni, Head-on collisions and orbital mergers of Proca stars, Phys. Rev. D **99**, 024017 (2019), arXiv:1806.07779 [gr-qc].

[1663] J. Calderón Bustillo, N. Sanchis-Gual, A. Torres-Forné, J. A. Font, A. Vajpeyi, R. Smith, C. Herdeiro, E. Radu, and S. H. W. Leong, GW190521 as a Merger of Proca Stars: A Potential New Vector Boson of 8.7×10^{-13} eV, Phys. Rev. Lett. **126**, 081101 (2021), arXiv:2009.05376 [gr-qc].

[1664] M. Bezares, M. Bošković, S. Liebling, C. Palenzuela, P. Pani, and E. Barausse, Gravitational waves and kicks from the merger of unequal mass, highly compact boson stars, Phys. Rev. D **105**, 064067 (2022), arXiv:2201.06113 [gr-qc].

[1665] J. Calderon Bustillo, N. Sanchis-Gual, S. H. W. Leong, K. Chandra, A. Torres-Forne, J. A. Font, C. Herdeiro, E. Radu, I. C. F. Wong, and T. G. F. Li, Searching for vector boson-star mergers within LIGO-Virgo intermediate-mass black-hole merger candidates, arXiv:2206.02551 [gr-qc].

[1666] N. Sanchis-Gual, J. Calderón Bustillo, C. Herdeiro, E. Radu, J. A. Font, S. H. W. Leong, and A. Torres-Forné, Impact of the wavelike nature of Proca stars on their gravitational-wave emission, Phys. Rev. D **106**, 124011 (2022), arXiv:2208.11717 [gr-qc].

[1667] N. Sanchis-Gual, M. Zilhão, and V. Cardoso, Electromagnetic emission from axionic boson star collisions, Phys. Rev. D **106**, 064034 (2022), arXiv:2207.05494 [gr-qc].

[1668] V. Jaramillo, N. Sanchis-Gual, J. Barranco, A. Bernal, J. C. Degollado, C. Herdeiro, M. Megevand, and D. Núñez, Head-on collisions of ℓ-boson stars, Phys. Rev. D **105**, 104057 (2022), arXiv:2202.00696 [gr-qc].

[1669] F. F. Freitas, C. A. R. Herdeiro, A. P. Morais, A. Onofre, R. Pasechnik, E. Radu, N. Sanchis-Gual, and R. Santos, Generating gravitational waveform libraries of exotic compact binaries

with deep learning, arXiv:2203.01267 [gr-qc].

[1670] R. Croft, T. Helfer, B.-X. Ge, M. Radia, T. Evstafyeva, E. A. Lim, U. Sperhake, and K. Clough, The gravitational afterglow of boson stars, Class. Quant. Grav. **40**, 065001 (2023), arXiv:2207.05690 [gr-qc].

[1671] T. Evstafyeva, U. Sperhake, T. Helfer, R. Croft, M. Radia, B.-X. Ge, and E. A. Lim, Unequal-mass boson-star binaries: initial data and merger dynamics, Class. Quant. Grav. **40**, 085009 (2023), arXiv:2212.08023 [gr-qc].

[1672] N. Siemonsen and W. E. East, Binary boson stars: Merger dynamics and formation of rotating remnant stars, Phys. Rev. D **107**, 124018 (2023), arXiv:2302.06627 [gr-qc].

[1673] T. Dietrich, S. Ossokine, and K. Clough, Full 3D numerical relativity simulations of neutron star–boson star collisions with BAM, Class. Quant. Grav. **36**, 025002 (2019), arXiv:1807.06959 [gr-qc].

[1674] K. Clough, T. Dietrich, and J. C. Niemeyer, Axion star collisions with black holes and neutron stars in full 3D numerical relativity, Phys. Rev. D **98**, 083020 (2018), arXiv:1808.04668 [gr-qc].

[1675] M. Bezares, D. Viganò, and C. Palenzuela, Gravitational wave signatures of dark matter cores in binary neutron star mergers by using numerical simulations, Phys. Rev. D **100**, 044049 (2019), arXiv:1905.08551 [gr-qc].

[1676] A. Tsokaros, M. Ruiz, S. L. Shapiro, L. Sun, and K. Uryū, Great Impostors: Extremely Compact, Merging Binary Neutron Stars in the Mass Gap Posing as Binary Black Holes, Phys. Rev. Lett. **124**, 071101 (2020), arXiv:1911.06865 [astro-ph.HE].

[1677] A. Tsokaros, M. Ruiz, L. Sun, S. L. Shapiro, and K. Uryū, Dynamically stable ergostars exist: General relativistic models and simulations, Phys. Rev. Lett. **123**, 231103 (2019), arXiv:1907.03765 [gr-qc].

[1678] T. Helfer, U. Sperhake, R. Croft, M. Radia, B.-X. Ge, and E. A. Lim, Malaise and remedy of binary boson-star initial data, Class. Quant. Grav. **39**, 074001 (2022), arXiv:2108.11995 [gr-qc].

[1679] J. C. Aurrekoetxea, K. Clough, and E. A. Lim, CTTK: a new method to solve the initial data constraints in numerical relativity, Class. Quant. Grav. **40**, 075003 (2023), arXiv:2207.03125 [gr-qc].

[1680] S. Tahura and K. Yagi, Parameterized Post-Einsteinian Gravitational Waveforms in Various Modified Theories of Gravity, Phys. Rev. D **98**, 084042 (2018), [Erratum: Phys.Rev.D 101, 109902 (2020)], arXiv:1809.00259 [gr-qc].

[1681] S. Mirshekari and C. M. Will, Compact binary systems in scalar-tensor gravity: Equations of motion to 2.5 post-Newtonian order, Phys. Rev. D **87**, 084070 (2013), arXiv:1301.4680 [gr-qc].

[1682] L. Bernard, Dynamics of compact binary systems in scalar-tensor theories: Equations of motion to the third post-Newtonian order, Phys. Rev. D **98**, 044004 (2018), arXiv:1802.10201 [gr-qc].

[1683] L. Bernard, Dynamics of compact binary systems in scalar-tensor theories: II. Center-of-mass and conserved quantities to 3PN order, Phys. Rev. D **99**, 044047 (2019), arXiv:1812.04169 [gr-qc].

[1684] L. Bernard, L. Bernard, and L. Bernard, Dipolar tidal effects in scalar-tensor theories, Phys. Rev. D **101**, 021501 (2020), [Erratum: Phys.Rev.D 107, 069901 (2023)], arXiv:1906.10735 [gr-qc].

[1685] I. van Gemeren, B. Shiralilou, and T. Hinderer, Dipolar tidal effects in gravitational waves from scalarized black hole binary inspirals in quadratic gravity, Phys. Rev. D **108**, 024026 (2023), arXiv:2302.08480 [gr-qc].

[1686] R. N. Lang, Compact binary systems in scalar-tensor gravity. II. Tensor gravitational waves to second post-Newtonian order, Phys. Rev. D **89**, 084014 (2014), arXiv:1310.3320 [gr-qc].

[1687] R. N. Lang, Compact binary systems in scalar-tensor gravity. III. Scalar waves and energy flux, Phys. Rev. D **91**, 084027 (2015), arXiv:1411.3073 [gr-qc].

[1688] L. Bernard, L. Blanchet, and D. Trestini, Gravitational waves in scalar-tensor theory to one-and-a-half post-Newtonian order, JCAP **08** (08), 008, arXiv:2201.10924 [gr-qc].

[1689] N. Sennett, S. Marsat, and A. Buonanno, Gravitational waveforms in scalar-tensor gravity at 2PN relative order, Phys. Rev. D **94**, 084003 (2016), arXiv:1607.01420 [gr-qc].

[1690] F.-L. Julié, On the motion of hairy black holes in Einstein-Maxwell-dilaton theories, JCAP **01**, 026, arXiv:1711.10769 [gr-qc].

[1691] F.-L. Julié, Gravitational radiation from compact binary systems in Einstein-Maxwell-dilaton theories, JCAP **10**, 033, arXiv:1809.05041 [gr-qc].

[1692] F.-L. Julié and E. Berti, Post-Newtonian dynamics and black hole thermodynamics in Einstein-scalar-Gauss-Bonnet gravity, Phys. Rev. D **100**, 104061 (2019), arXiv:1909.05258 [gr-qc].

[1693] B. Shiralilou, T. Hinderer, S. Nissanke, N. Ortiz, and H. Witek, Nonlinear curvature effects in gravitational waves from inspiralling black hole binaries, Phys. Rev. D **103**, L121503 (2021), arXiv:2012.09162 [gr-qc].

[1694] B. Shiralilou, T. Hinderer, S. M. Nissanke, N. Ortiz, and H. Witek, Post-Newtonian gravitational and scalar waves in scalar-Gauss–Bonnet gravity, Class. Quant. Grav. **39**, 035002 (2022), arXiv:2105.13972 [gr-qc].

[1695] T. Kobayashi, Horndeski theory and beyond: a review, Rept. Prog. Phys. **82**, 086901 (2019), arXiv:1901.07183 [gr-qc].

[1696] Y.-Z. Chu and M. Trodden, Retarded Green's function of a Vainshtein system and Galileon waves, Phys. Rev. D **87**, 024011 (2013), arXiv:1210.6651 [astro-ph.CO].

[1697] C. de Rham, A. Matas, and A. J. Tolley, Galileon Radiation from Binary Systems, Phys. Rev. D **87**, 064024 (2013), arXiv:1212.5212 [hep-th].

[1698] C. de Rham, A. J. Tolley, and D. H. Wesley, Vainshtein Mechanism in Binary Pulsars, Phys. Rev. D **87**, 044025 (2013), arXiv:1208.0580 [gr-qc].

[1699] E. Barausse and K. Yagi, Gravitation-Wave Emission in Shift-Symmetric Horndeski Theories, Phys. Rev. Lett. **115**, 211105 (2015), arXiv:1509.04539 [gr-qc].

[1700] R. McManus, L. Lombriser, and J. Peñarrubia, Parameterised Post-Newtonian Expansion in Screened Regions, JCAP **12**, 031, arXiv:1705.05324 [gr-qc].

[1701] F. Dar, C. De Rham, J. T. Deskins, J. T. Giblin, and A. J. Tolley, Scalar Gravitational Radiation from Binaries: Vainshtein Mechanism in Time-dependent Systems, Class. Quant. Grav. **36**, 025008 (2019), arXiv:1808.02165 [hep-th].

[1702] A. Kuntz, F. Piazza, and F. Vernizzi, Effective field theory for gravitational radiation in scalar-tensor gravity, JCAP **05**, 052, arXiv:1902.04941 [gr-qc].

[1703] P. Brax, L. Heisenberg, and A. Kuntz, Unveiling the Galileon in a three-body system : scalar and gravitational wave production, JCAP **05**, 012, arXiv:2002.12590 [gr-qc].

[1704] N. Yunes and F. Pretorius, Fundamental Theoretical Bias in Gravitational Wave Astrophysics and the Parameterized Post-Einsteinian Framework, Phys. Rev. D **80**, 122003 (2009), arXiv:0909.3328 [gr-qc].

[1705] M. Agathos, W. Del Pozzo, T. G. F. Li, C. Van Den Broeck, J. Veitch, and S. Vitale, TIGER: A data analysis pipeline for testing the strong-field dynamics of general relativity with gravitational wave signals from coalescing compact binaries, Phys. Rev. D **89**, 082001 (2014), arXiv:1311.0420 [gr-qc].

[1706] A. K. Mehta, A. Buonanno, R. Cotesta, A. Ghosh, N. Sennett, and J. Steinhoff, Tests of general relativity with gravitational-wave observations using a flexible theory-independent method, Phys. Rev. D **107**, 044020 (2023), arXiv:2203.13937 [gr-qc].

[1707] E. Barausse, N. Yunes, and K. Chamberlain, Theory-Agnostic Constraints on Black-Hole Dipole Radiation with Multiband Gravitational-Wave Astrophysics, Phys. Rev. Lett. **116**, 241104 (2016), arXiv:1603.04075 [gr-qc].

[1708] K. Yagi, L. C. Stein, N. Yunes, and T. Tanaka, Post-Newtonian, Quasi-Circular Binary Inspirals in Quadratic Modified Gravity, Phys. Rev. D **85**, 064022 (2012), [Erratum: Phys.Rev.D 93, 029902 (2016)], arXiv:1110.5950 [gr-qc].

[1709] K. Yagi, L. C. Stein, and N. Yunes, Challenging the Presence of Scalar Charge and Dipolar Radiation in Binary Pulsars, Phys. Rev. D **93**, 024010 (2016), arXiv:1510.02152 [gr-qc].

223

[1710] N. Yunes, F. Pretorius, and D. Spergel, Constraining the evolutionary history of Newton's constant with gravitational wave observations, Phys. Rev. D **81**, 064018 (2010), arXiv:0912.2724 [gr-qc].

[1711] N. Yunes, R. O'Shaughnessy, B. J. Owen, and S. Alexander, Testing gravitational parity violation with coincident gravitational waves and short gamma-ray bursts, Phys. Rev. D **82**, 064017 (2010), arXiv:1005.3310 [gr-qc].

[1712] K. Yagi, N. Tanahashi, and T. Tanaka, Probing the size of extra dimension with gravitational wave astronomy, Phys. Rev. D **83**, 084036 (2011), arXiv:1101.4997 [gr-qc].

[1713] N. Yunes and L. C. Stein, Non-Spinning Black Holes in Alternative Theories of Gravity, Phys. Rev. D **83**, 104002 (2011), arXiv:1101.2921 [gr-qc].

[1714] S. Vigeland, N. Yunes, and L. Stein, Bumpy Black Holes in Alternate Theories of Gravity, Phys. Rev. D **83**, 104027 (2011), arXiv:1102.3706 [gr-qc].

[1715] Z. Carson and K. Yagi, Parametrized and inspiral-merger-ringdown consistency tests of gravity with multiband gravitational wave observations, Phys. Rev. D **101**, 044047 (2020), arXiv:1911.05258 [gr-qc].

[1716] S. E. Perkins, N. Yunes, and E. Berti, Probing Fundamental Physics with Gravitational Waves: The Next Generation, Phys. Rev. D **103**, 044024 (2021), arXiv:2010.09010 [gr-qc].

[1717] S. Mezzasoma and N. Yunes, Theory-agnostic framework for inspiral tests of general relativity with higher-harmonic gravitational waves, Phys. Rev. D **106**, 024026 (2022), arXiv:2203.15934 [gr-qc].

[1718] N. Loutrel, P. Pani, and N. Yunes, Parametrized post-Einsteinian framework for precessing binaries, Phys. Rev. D **107**, 044046 (2023), arXiv:2210.10571 [gr-qc].

[1719] N. Loutrel and N. Yunes, Parity violation in spin-precessing binaries: Gravitational waves from the inspiral of black holes in dynamical Chern-Simons gravity, Phys. Rev. D **106**, 064009 (2022), arXiv:2205.02675 [gr-qc].

[1720] A. J. K. Chua and M. Vallisneri, On parametric tests of relativity with false degrees of freedom, arXiv:2006.08918 [gr-qc].

[1721] R. Nair, S. Perkins, H. O. Silva, and N. Yunes, Fundamental Physics Implications for Higher-Curvature Theories from Binary Black Hole Signals in the LIGO-Virgo Catalog GWTC-1, Phys. Rev. Lett. **123**, 191101 (2019), arXiv:1905.00870 [gr-qc].

[1722] S. E. Perkins, R. Nair, H. O. Silva, and N. Yunes, Improved gravitational-wave constraints on higher-order curvature theories of gravity, Phys. Rev. D **104**, 024060 (2021), arXiv:2104.11189 [gr-qc].

[1723] K. Eda, Y. Itoh, S. Kuroyanagi, and J. Silk, New Probe of Dark-Matter Properties: Gravitational Waves from an Intermediate-Mass Black Hole Embedded in a Dark-Matter Minispike, Phys. Rev. Lett. **110**, 221101 (2013), arXiv:1301.5971 [gr-qc].

[1724] V. Cardoso and A. Maselli, Constraints on the astrophysical environment of binaries with gravitational-wave observations, Astron. Astrophys. **644**, A147 (2020), arXiv:1909.05870 [astro-ph.HE].

[1725] S. Chandrasekhar, Dynamical Friction. I. General Considerations: the Coefficient of Dynamical Friction, Astrophys. J. **97**, 255 (1943).

[1726] L. Annulli, V. Cardoso, and R. Vicente, Stirred and shaken: Dynamical behavior of boson stars and dark matter cores, Phys. Lett. B **811**, 135944 (2020), arXiv:2007.03700 [astro-ph.HE].

[1727] L. Annulli, V. Cardoso, and R. Vicente, Response of ultralight dark matter to supermassive black holes and binaries, Phys. Rev. D **102**, 063022 (2020), arXiv:2009.00012 [gr-qc].

[1728] J. Zhang and H. Yang, Gravitational floating orbits around hairy black holes, Phys. Rev. D **99**, 064018 (2019), arXiv:1808.02905 [gr-qc].

[1729] T. Takahashi and T. Tanaka, Axion clouds may survive the perturbative tidal interaction over the early inspiral phase of black hole binaries, JCAP **10**, 031, arXiv:2106.08836 [gr-qc].

[1730] T. Takahashi, H. Omiya, and T. Tanaka, Axion cloud evaporation during inspiral of black hole binaries: The effects of backreaction and radiation, PTEP **2022**, 043E01 (2022),

arXiv:2112.05774 [gr-qc].

[1731] X. Tong, Y. Wang, and H.-Y. Zhu, Termination of superradiance from a binary companion, Phys. Rev. D **106**, 043002 (2022), arXiv:2205.10527 [gr-qc].

[1732] V. Cardoso, S. Chakrabarti, P. Pani, E. Berti, and L. Gualtieri, Floating and sinking: The Imprint of massive scalars around rotating black holes, Phys. Rev. Lett. **107**, 241101 (2011), arXiv:1109.6021 [gr-qc].

[1733] M. C. Ferreira, C. F. B. Macedo, and V. Cardoso, Orbital fingerprints of ultralight scalar fields around black holes, Phys. Rev. D **96**, 083017 (2017), arXiv:1710.00830 [gr-qc].

[1734] D. Baumann, G. Bertone, J. Stout, and G. M. Tomaselli, Ionization of gravitational atoms, Phys. Rev. D **105**, 115036 (2022), arXiv:2112.14777 [gr-qc].

[1735] D. Baumann, G. Bertone, J. Stout, and G. M. Tomaselli, Sharp Signals of Boson Clouds in Black Hole Binary Inspirals, Phys. Rev. Lett. **128**, 221102 (2022), arXiv:2206.01212 [gr-qc].

[1736] G. M. Tomaselli, T. F. M. Spieksma, and G. Bertone, Dynamical friction in gravitational atoms, JCAP **07**, 070, arXiv:2305.15460 [gr-qc].

[1737] L. K. Wong, Superradiant scattering by a black hole binary, Phys. Rev. D **100**, 044051 (2019), arXiv:1905.08543 [hep-th].

[1738] E. Poisson, Gravitational waves from inspiraling compact binaries: The Quadrupole moment term, Phys. Rev. D **57**, 5287 (1998), arXiv:gr-qc/9709032.

[1739] E. Poisson, Tidal interaction of black holes and Newtonian viscous bodies, Phys. Rev. D **80**, 064029 (2009), arXiv:0907.0874 [gr-qc].

[1740] V. Cardoso and P. Pani, Tidal acceleration of black holes and superradiance, Class. Quant. Grav. **30**, 045011 (2013), arXiv:1205.3184 [gr-qc].

[1741] E. Poisson and E. Corrigan, Nonrotating black hole in a post-Newtonian tidal environment II, Phys. Rev. D **97**, 124048 (2018), arXiv:1804.01848 [gr-qc].

[1742] A. Maselli, P. Pani, V. Cardoso, T. Abdelsalhin, L. Gualtieri, and V. Ferrari, Probing Planckian corrections at the horizon scale with LISA binaries, Phys. Rev. Lett. **120**, 081101 (2018), arXiv:1703.10612 [gr-qc].

[1743] N. Oshita, Q. Wang, and N. Afshordi, On Reflectivity of Quantum Black Hole Horizons, JCAP **04**, 016, arXiv:1905.00464 [hep-th].

[1744] S. Datta, R. Brito, S. Bose, P. Pani, and S. A. Hughes, Tidal heating as a discriminator for horizons in extreme mass ratio inspirals, Phys. Rev. D **101**, 044004 (2020), arXiv:1910.07841 [gr-qc].

[1745] S. Datta, Tidal heating of Quantum Black Holes and their imprints on gravitational waves, Phys. Rev. D **102**, 064040 (2020), arXiv:2002.04480 [gr-qc].

[1746] V. Cardoso, E. Franzin, A. Maselli, P. Pani, and G. Raposo, Testing strong-field gravity with tidal Love numbers, Phys. Rev. D **95**, 084014 (2017), [Addendum: Phys.Rev.D 95, 089901 (2017)], arXiv:1701.01116 [gr-qc].

[1747] C. Pacilio, M. Vaglio, A. Maselli, and P. Pani, Gravitational-wave detectors as particle-physics laboratories: Constraining scalar interactions with a coherent inspiral model of boson-star binaries, Phys. Rev. D **102**, 083002 (2020), arXiv:2007.05264 [gr-qc].

[1748] M. Vaglio, C. Pacilio, A. Maselli, and P. Pani, Bayesian parameter estimation on boson-star binary signals with a coherent inspiral template and spin-dependent quadrupolar corrections, Phys. Rev. D **108**, 023021 (2023), arXiv:2302.13954 [gr-qc].

[1749] V. Baibhav and E. Berti, Multimode black hole spectroscopy, Phys. Rev. D **99**, 024005 (2019), arXiv:1809.03500 [gr-qc].

[1750] S. Gossan, J. Veitch, and B. S. Sathyaprakash, Bayesian model selection for testing the no-hair theorem with black hole ringdowns, Phys. Rev. D **85**, 124056 (2012), arXiv:1111.5819 [gr-qc].

[1751] J. Meidam, M. Agathos, C. Van Den Broeck, J. Veitch, and B. S. Sathyaprakash, Testing the no-hair theorem with black hole ringdowns using TIGER, Phys. Rev. D **90**, 064009 (2014), arXiv:1406.3201 [gr-qc].

[1752] R. Brito, A. Buonanno, and V. Raymond, Black-hole Spectroscopy by Making Full Use of

Gravitational-Wave Modeling, Phys. Rev. D **98**, 084038 (2018), arXiv:1805.00293 [gr-qc].

[1753] G. Carullo *et al.*, Empirical tests of the black hole no-hair conjecture using gravitational-wave observations, Phys. Rev. D **98**, 104020 (2018), arXiv:1805.04760 [gr-qc].

[1754] G. Carullo, W. Del Pozzo, and J. Veitch, Observational Black Hole Spectroscopy: A time-domain multimode analysis of GW150914, Phys. Rev. D **99**, 123029 (2019), [Erratum: Phys.Rev.D 100, 089903 (2019)], arXiv:1902.07527 [gr-qc].

[1755] A. Maselli, P. Pani, L. Gualtieri, and E. Berti, Parametrized ringdown spin expansion coefficients: a data-analysis framework for black-hole spectroscopy with multiple events, Phys. Rev. D **101**, 024043 (2020), arXiv:1910.12893 [gr-qc].

[1756] J. Bao, C. Shi, H. Wang, J.-d. Zhang, Y. Hu, J. Mei, and J. Luo, Constraining modified gravity with ringdown signals: an explicit example, Phys. Rev. D **100**, 084024 (2019), arXiv:1905.11674 [gr-qc].

[1757] I. Ota and C. Chirenti, Overtones or higher harmonics? Prospects for testing the no-hair theorem with gravitational wave detections, Phys. Rev. D **101**, 104005 (2020), arXiv:1911.00440 [gr-qc].

[1758] S. Bhagwat, C. Pacilio, E. Barausse, and P. Pani, Landscape of massive black-hole spectroscopy with LISA and the Einstein Telescope, Phys. Rev. D **105**, 124063 (2022), arXiv:2201.00023 [gr-qc].

[1759] L. London and E. Fauchon-Jones, On modeling for Kerr black holes: Basis learning, QNM frequencies, and spherical-spheroidal mixing coefficients, Class. Quant. Grav. **36**, 235015 (2019), arXiv:1810.03550 [gr-qc].

[1760] A. Dhani, Importance of mirror modes in binary black hole ringdown waveform, Phys. Rev. D **103**, 104048 (2021), arXiv:2010.08602 [gr-qc].

[1761] E. Finch and C. J. Moore, Modeling the ringdown from precessing black hole binaries, Phys. Rev. D **103**, 084048 (2021), arXiv:2102.07794 [gr-qc].

[1762] O. J. C. Dias, M. Godazgar, and J. E. Santos, Linear Mode Stability of the Kerr-Newman Black Hole and Its Quasinormal Modes, Phys. Rev. Lett. **114**, 151101 (2015), arXiv:1501.04625 [gr-qc].

[1763] O. J. C. Dias, M. Godazgar, J. E. Santos, G. Carullo, W. Del Pozzo, and D. Laghi, Eigenvalue repulsions in the quasinormal spectra of the Kerr-Newman black hole, Phys. Rev. D **105**, 084044 (2022), arXiv:2109.13949 [gr-qc].

[1764] O. J. C. Dias, M. Godazgar, and J. E. Santos, Eigenvalue repulsions and quasinormal mode spectra of Kerr-Newman: an extended study, JHEP **07**, 076, arXiv:2205.13072 [gr-qc].

[1765] D. Li, P. Wagle, Y. Chen, and N. Yunes, Perturbations of Spinning Black Holes beyond General Relativity: Modified Teukolsky Equation, Phys. Rev. X **13**, 021029 (2023), arXiv:2206.10652 [gr-qc].

[1766] A. K.-W. Chung, P. Wagle, and N. Yunes, Spectral method for the gravitational perturbations of black holes: Schwarzschild background case, Phys. Rev. D **107**, 124032 (2023), arXiv:2302.11624 [gr-qc].

[1767] P. Pani, C. F. B. Macedo, L. C. B. Crispino, and V. Cardoso, Slowly rotating black holes in alternative theories of gravity, Phys. Rev. D **84**, 087501 (2011), arXiv:1109.3996 [gr-qc].

[1768] D. Ayzenberg and N. Yunes, Slowly-Rotating Black Holes in Einstein-Dilaton-Gauss-Bonnet Gravity: Quadratic Order in Spin Solutions, Phys. Rev. D **90**, 044066 (2014), [Erratum: Phys.Rev.D 91, 069905 (2015)], arXiv:1405.2133 [gr-qc].

[1769] A. Maselli, P. Pani, L. Gualtieri, and V. Ferrari, Rotating black holes in Einstein-Dilaton-Gauss-Bonnet gravity with finite coupling, Phys. Rev. D **92**, 083014 (2015), arXiv:1507.00680 [gr-qc].

[1770] V. Cardoso, M. Kimura, A. Maselli, and L. Senatore, Black Holes in an Effective Field Theory Extension of General Relativity, Phys. Rev. Lett. **121**, 251105 (2018), arXiv:1808.08962 [gr-qc].

[1771] P. A. Cano, A. Deich, and N. Yunes, Accuracy of the slow-rotation approximation for black holes in modified gravity in light of astrophysical observables, arXiv:2305.15341 [gr-qc].

[1772] B. Kleihaus, J. Kunz, and E. Radu, Rotating Black Holes in Dilatonic Einstein-Gauss-Bonnet

Theory, Phys. Rev. Lett. **106**, 151104 (2011), arXiv:1101.2868 [gr-qc].

[1773] L. C. Stein, Rapidly rotating black holes in dynamical Chern-Simons gravity: Decoupling limit solutions and breakdown, Phys. Rev. D **90**, 044061 (2014), arXiv:1407.2350 [gr-qc].

[1774] P. V. P. Cunha, C. A. R. Herdeiro, and E. Radu, Spontaneously Scalarized Kerr Black Holes in Extended Scalar-Tensor–Gauss-Bonnet Gravity, Phys. Rev. Lett. **123**, 011101 (2019), arXiv:1904.09997 [gr-qc].

[1775] A. Sullivan, N. Yunes, and T. P. Sotiriou, Numerical black hole solutions in modified gravity theories: Spherical symmetry case, Phys. Rev. D **101**, 044024 (2020), arXiv:1903.02624 [gr-qc].

[1776] A. Sullivan, N. Yunes, and T. P. Sotiriou, Numerical black hole solutions in modified gravity theories: Axial symmetry case, Phys. Rev. D **103**, 124058 (2021), arXiv:2009.10614 [gr-qc].

[1777] C. B. Owen, N. Yunes, and H. Witek, Petrov type, principal null directions, and Killing tensors of slowly rotating black holes in quadratic gravity, Phys. Rev. D **103**, 124057 (2021), arXiv:2103.15891 [gr-qc].

[1778] E. Barausse and T. P. Sotiriou, Perturbed Kerr Black Holes can probe deviations from General Relativity, Phys. Rev. Lett. **101**, 099001 (2008), arXiv:0803.3433 [gr-qc].

[1779] C. Molina, P. Pani, V. Cardoso, and L. Gualtieri, Gravitational signature of Schwarzschild black holes in dynamical Chern-Simons gravity, Phys. Rev. D **81**, 124021 (2010), arXiv:1004.4007 [gr-qc].

[1780] J. L. Blázquez-Salcedo, C. F. B. Macedo, V. Cardoso, V. Ferrari, L. Gualtieri, F. S. Khoo, J. Kunz, and P. Pani, Perturbed black holes in Einstein-dilaton-Gauss-Bonnet gravity: Stability, ringdown, and gravitational-wave emission, Phys. Rev. D **94**, 104024 (2016), arXiv:1609.01286 [gr-qc].

[1781] O. J. Tattersall, P. G. Ferreira, and M. Lagos, General theories of linear gravitational perturbations to a Schwarzschild Black Hole, Phys. Rev. D **97**, 044021 (2018), arXiv:1711.01992 [gr-qc].

[1782] G. Franciolini, L. Hui, R. Penco, L. Santoni, and E. Trincherini, Effective Field Theory of Black Hole Quasinormal Modes in Scalar-Tensor Theories, JHEP **02**, 127, arXiv:1810.07706 [hep-th].

[1783] R. McManus, E. Berti, C. F. B. Macedo, M. Kimura, A. Maselli, and V. Cardoso, Parametrized black hole quasinormal ringdown. II. Coupled equations and quadratic corrections for nonrotating black holes, Phys. Rev. D **100**, 044061 (2019), arXiv:1906.05155 [gr-qc].

[1784] K. Glampedakis and H. O. Silva, Eikonal quasinormal modes of black holes beyond General Relativity, Phys. Rev. D **100**, 044040 (2019), arXiv:1906.05455 [gr-qc].

[1785] V. Cardoso, M. Kimura, A. Maselli, E. Berti, C. F. B. Macedo, and R. McManus, Parametrized black hole quasinormal ringdown: Decoupled equations for nonrotating black holes, Phys. Rev. D **99**, 104077 (2019), arXiv:1901.01265 [gr-qc].

[1786] H. O. Silva and K. Glampedakis, Eikonal quasinormal modes of black holes beyond general relativity. II. Generalized scalar-tensor perturbations, Phys. Rev. D **101**, 044051 (2020), arXiv:1912.09286 [gr-qc].

[1787] L. Pierini and L. Gualtieri, Quasi-normal modes of rotating black holes in Einstein-dilaton Gauss-Bonnet gravity: the first order in rotation, Phys. Rev. D **103**, 124017 (2021), arXiv:2103.09870 [gr-qc].

[1788] L. Pierini and L. Gualtieri, Quasinormal modes of rotating black holes in Einstein-dilaton Gauss-Bonnet gravity: The second order in rotation, Phys. Rev. D **106**, 104009 (2022), arXiv:2207.11267 [gr-qc].

[1789] P. A. Cano, K. Fransen, and T. Hertog, Ringing of rotating black holes in higher-derivative gravity, Phys. Rev. D **102**, 044047 (2020), arXiv:2005.03671 [gr-qc].

[1790] A. Hussain and A. Zimmerman, Approach to computing spectral shifts for black holes beyond Kerr, Phys. Rev. D **106**, 104018 (2022), arXiv:2206.10653 [gr-qc].

[1791] R. Ghosh, N. Franchini, S. H. Völkel, and E. Barausse, Quasinormal modes of nonseparable perturbation equations: The scalar non-Kerr case, Phys. Rev. D **108**, 024038 (2023), arXiv:2303.00088 [gr-qc].

227

[1792] P. A. Cano, K. Fransen, T. Hertog, and S. Maenaut, Universal Teukolsky equations and black hole perturbations in higher-derivative gravity, Phys. Rev. D **108**, 024040 (2023), arXiv:2304.02663 [gr-qc].

[1793] P. A. Cano, K. Fransen, T. Hertog, and S. Maenaut, Quasinormal modes of rotating black holes in higher-derivative gravity, arXiv:2307.07431 [gr-qc].

[1794] E. Berti and V. Cardoso, Supermassive black holes or boson stars? Hair counting with gravitational wave detectors, Int. J. Mod. Phys. D **15**, 2209 (2006), arXiv:gr-qc/0605101.

[1795] C. F. B. Macedo, P. Pani, V. Cardoso, and L. C. B. Crispino, Astrophysical signatures of boson stars: quasinormal modes and inspiral resonances, Phys. Rev. D **88**, 064046 (2013), arXiv:1307.4812 [gr-qc].

[1796] C. B. M. H. Chirenti and L. Rezzolla, How to tell a gravastar from a black hole, Class. Quant. Grav. **24**, 4191 (2007), arXiv:0706.1513 [gr-qc].

[1797] P. Pani, E. Berti, V. Cardoso, Y. Chen, and R. Norte, Gravitational wave signatures of the absence of an event horizon. I. Nonradial oscillations of a thin-shell gravastar, Phys. Rev. D **80**, 124047 (2009), arXiv:0909.0287 [gr-qc].

[1798] C. Chirenti and L. Rezzolla, Did GW150914 produce a rotating gravastar?, Phys. Rev. D **94**, 084016 (2016), arXiv:1602.08759 [gr-qc].

[1799] S. H. Völkel and K. D. Kokkotas, A Semi-analytic Study of Axial Perturbations of Ultra Compact Stars, Class. Quant. Grav. **34**, 125006 (2017), arXiv:1703.08156 [gr-qc].

[1800] R. A. Konoplya and A. Zhidenko, Wormholes versus black holes: quasinormal ringing at early and late times, JCAP **12**, 043, arXiv:1606.00517 [gr-qc].

[1801] P. Bueno, P. A. Cano, F. Goelen, T. Hertog, and B. Vercnocke, Echoes of Kerr-like wormholes, Phys. Rev. D **97**, 024040 (2018), arXiv:1711.00391 [gr-qc].

[1802] V. Cardoso, O. J. C. Dias, J. L. Hovdebo, and R. C. Myers, Instability of non-supersymmetric smooth geometries, Phys. Rev. D **73**, 064031 (2006), arXiv:hep-th/0512277.

[1803] F. C. Eperon, H. S. Reall, and J. E. Santos, Instability of supersymmetric microstate geometries, JHEP **10**, 031, arXiv:1607.06828 [hep-th].

[1804] C. Barceló, R. Carballo-Rubio, and L. J. Garay, Gravitational wave echoes from macroscopic quantum gravity effects, JHEP **05**, 054, arXiv:1701.09156 [gr-qc].

[1805] R. Brustein, A. J. M. Medved, and K. Yagi, When black holes collide: Probing the interior composition by the spectrum of ringdown modes and emitted gravitational waves, Phys. Rev. D **96**, 064033 (2017), arXiv:1704.05789 [gr-qc].

[1806] Q. Wang, N. Oshita, and N. Afshordi, Echoes from Quantum Black Holes, Phys. Rev. D **101**, 024031 (2020), arXiv:1905.00446 [gr-qc].

[1807] S. Chakraborty, E. Maggio, A. Mazumdar, and P. Pani, Implications of the quantum nature of the black hole horizon on the gravitational-wave ringdown, Phys. Rev. D **106**, 024041 (2022), arXiv:2202.09111 [gr-qc].

[1808] V. Ferrari and K. D. Kokkotas, Scattering of particles by neutron stars: Time evolutions for axial perturbations, Phys. Rev. D **62**, 107504 (2000), arXiv:gr-qc/0008057.

[1809] P. Pani and V. Ferrari, On gravitational-wave echoes from neutron-star binary coalescences, Class. Quant. Grav. **35**, 15LT01 (2018), arXiv:1804.01444 [gr-qc].

[1810] J. Abedi, H. Dykaar, and N. Afshordi, Echoes from the Abyss: Tentative evidence for Planck-scale structure at black hole horizons, Phys. Rev. D **96**, 082004 (2017), arXiv:1612.00266 [gr-qc].

[1811] H. Nakano, N. Sago, H. Tagoshi, and T. Tanaka, Black hole ringdown echoes and howls, PTEP **2017**, 071E01 (2017), arXiv:1704.07175 [gr-qc].

[1812] A. Maselli, S. H. Völkel, and K. D. Kokkotas, Parameter estimation of gravitational wave echoes from exotic compact objects, Phys. Rev. D **96**, 064045 (2017), arXiv:1708.02217 [gr-qc].

[1813] L. F. Longo Micchi, N. Afshordi, and C. Chirenti, How loud are echoes from exotic compact objects?, Phys. Rev. D **103**, 044028 (2021), arXiv:2010.14578 [gr-qc].

[1814] S. Ma, Q. Wang, N. Deppe, F. Hébert, L. E. Kidder, J. Moxon, W. Throwe, N. L. Vu,

228

M. A. Scheel, and Y. Chen, Gravitational-wave echoes from numerical-relativity waveforms via spacetime construction near merging compact objects, Phys. Rev. D **105**, 104007 (2022), arXiv:2203.03174 [gr-qc].

[1815] X.-Y. Zhong, W.-B. Han, Y. Jiang, P. Shen, S.-C. Yang, and C. Zhang, Detecting properties of echoes from the inspiraling stage with ground-based detectors, Eur. Phys. J. Plus **138**, 761 (2023), arXiv:2212.11175 [gr-qc].

[1816] L. Annulli, V. Cardoso, and L. Gualtieri, Applications of the close-limit approximation: horizonless compact objects and scalar fields, Class. Quant. Grav. **39**, 105005 (2022), arXiv:2104.11236 [gr-qc].

[1817] Z. Mark, A. Zimmerman, S. M. Du, and Y. Chen, A recipe for echoes from exotic compact objects, Phys. Rev. D **96**, 084002 (2017), arXiv:1706.06155 [gr-qc].

[1818] A. Testa and P. Pani, Analytical template for gravitational-wave echoes: signal characterization and prospects of detection with current and future interferometers, Phys. Rev. D **98**, 044018 (2018), arXiv:1806.04253 [gr-qc].

[1819] S. Xin, B. Chen, R. K. L. Lo, L. Sun, W.-B. Han, X. Zhong, M. Srivastava, S. Ma, Q. Wang, and Y. Chen, Gravitational-wave echoes from spinning exotic compact objects: Numerical waveforms from the Teukolsky equation, Phys. Rev. D **104**, 104005 (2021), arXiv:2105.12313 [gr-qc].

[1820] P. Pani, V. Cardoso, and L. Gualtieri, Gravitational waves from extreme mass-ratio inspirals in Dynamical Chern-Simons gravity, Phys. Rev. D **83**, 104048 (2011), arXiv:1104.1183 [gr-qc].

[1821] N. Yunes, P. Pani, and V. Cardoso, Gravitational Waves from Quasicircular Extreme Mass-Ratio Inspirals as Probes of Scalar-Tensor Theories, Phys. Rev. D **85**, 102003 (2012), arXiv:1112.3351 [gr-qc].

[1822] P. Canizares, J. R. Gair, and C. F. Sopuerta, Testing Chern-Simons Modified Gravity with Gravitational-Wave Detections of Extreme-Mass-Ratio Binaries, Phys. Rev. D **86**, 044010 (2012), arXiv:1205.1253 [gr-qc].

[1823] R. Fujita and V. Cardoso, Ultralight scalars and resonances in black-hole physics, Phys. Rev. D **95**, 044016 (2017), arXiv:1612.00978 [gr-qc].

[1824] V. Cardoso, G. Castro, and A. Maselli, Gravitational waves in massive gravity theories: waveforms, fluxes and constraints from extreme-mass-ratio mergers, Phys. Rev. Lett. **121**, 251103 (2018), arXiv:1809.00673 [gr-qc].

[1825] P. Zimmerman, Gravitational self-force in scalar-tensor gravity, Phys. Rev. D **92**, 064051 (2015), arXiv:1507.04076 [gr-qc].

[1826] A. Spiers, A. Maselli, and T. P. Sotiriou, Measuring scalar charge with compact binaries: High accuracy modelling with self-force, arXiv:2310.02315 [gr-qc].

[1827] A. Maselli, N. Franchini, L. Gualtieri, and T. P. Sotiriou, Detecting scalar fields with Extreme Mass Ratio Inspirals, Phys. Rev. Lett. **125**, 141101 (2020), arXiv:2004.11895 [gr-qc].

[1828] A. Maselli, N. Franchini, L. Gualtieri, T. P. Sotiriou, S. Barsanti, and P. Pani, Detecting fundamental fields with LISA observations of gravitational waves from extreme mass-ratio inspirals, Nature Astron. **6**, 464 (2022), arXiv:2106.11325 [gr-qc].

[1829] S. Barsanti, N. Franchini, L. Gualtieri, A. Maselli, and T. P. Sotiriou, Extreme mass-ratio inspirals as probes of scalar fields: Eccentric equatorial orbits around Kerr black holes, Phys. Rev. D **106**, 044029 (2022), arXiv:2203.05003 [gr-qc].

[1830] C. Zhang, Y. Gong, D. Liang, and B. Wang, Gravitational waves from eccentric extreme mass-ratio inspirals as probes of scalar fields, JCAP **06**, 054, arXiv:2210.11121 [gr-qc].

[1831] H. Guo, Y. Liu, C. Zhang, Y. Gong, W.-L. Qian, and R.-H. Yue, Detection of scalar fields by extreme mass ratio inspirals with a Kerr black hole, Phys. Rev. D **106**, 024047 (2022), arXiv:2201.10748 [gr-qc].

[1832] L. Barack and L. M. Burko, Radiation reaction force on a particle plunging into a black hole, Phys. Rev. D **62**, 084040 (2000), arXiv:gr-qc/0007033.

[1833] S. L. Detweiler, E. Messaritaki, and B. F. Whiting, Selfforce of a scalar field for circular orbits

about a Schwarzschild black hole, Phys. Rev. D **67**, 104016 (2003), arXiv:gr-qc/0205079.

[1834] L. M. Diaz-Rivera, E. Messaritaki, B. F. Whiting, and S. L. Detweiler, Scalar field self-force effects on orbits about a Schwarzschild black hole, Phys. Rev. D **70**, 124018 (2004), arXiv:gr-qc/0410011.

[1835] N. Warburton and L. Barack, Self force on a scalar charge in Kerr spacetime: circular equatorial orbits, Phys. Rev. D **81**, 084039 (2010), arXiv:1003.1860 [gr-qc].

[1836] N. Warburton, Self force on a scalar charge in Kerr spacetime: inclined circular orbits, Phys. Rev. D **91**, 024045 (2015), arXiv:1408.2885 [gr-qc].

[1837] S. E. Gralla, A. P. Porfyriadis, and N. Warburton, Particle on the Innermost Stable Circular Orbit of a Rapidly Spinning Black Hole, Phys. Rev. D **92**, 064029 (2015), arXiv:1506.08496 [gr-qc].

[1838] J. Castillo, I. Vega, and B. Wardell, Self-force on a scalar charge in a circular orbit about a Reissner-Nordström black hole, Phys. Rev. D **98**, 024024 (2018), arXiv:1804.09224 [gr-qc].

[1839] Z. Nasipak, T. Osburn, and C. R. Evans, Repeated faint quasinormal bursts in extreme-mass-ratio inspiral waveforms: Evidence from frequency-domain scalar self-force calculations on generic Kerr orbits, Phys. Rev. D **100**, 064008 (2019), arXiv:1905.13237 [gr-qc].

[1840] G. Compère, K. Fransen, T. Hertog, and Y. Liu, Scalar Self-Force for High Spin Black Holes, Phys. Rev. D **101**, 064006 (2020), arXiv:1910.02081 [gr-qc].

[1841] A. Heffernan, Regularization of a scalar charged particle for generic orbits in Kerr spacetime, Phys. Rev. D **106**, 064031 (2022), arXiv:2107.14750 [gr-qc].

[1842] K. Eda, Y. Itoh, S. Kuroyanagi, and J. Silk, Gravitational waves as a probe of dark matter minispikes, Phys. Rev. D **91**, 044045 (2015), arXiv:1408.3534 [gr-qc].

[1843] R. Vicente and V. Cardoso, Dynamical friction of black holes in ultralight dark matter, Phys. Rev. D **105**, 083008 (2022), arXiv:2201.08854 [gr-qc].

[1844] X.-J. Yue and W.-B. Han, Gravitational waves with dark matter minispikes: the combined effect, Phys. Rev. D **97**, 064003 (2018), arXiv:1711.09706 [gr-qc].

[1845] G. D. Quinlan, L. Hernquist, and S. Sigurdsson, Models of Galaxies with Central Black Holes: Adiabatic Growth in Spherical Galaxies, Astrophys. J. **440**, 554 (1995), arXiv:astro-ph/9407005.

[1846] P. Gondolo and J. Silk, Dark matter annihilation at the galactic center, Phys. Rev. Lett. **83**, 1719 (1999), arXiv:astro-ph/9906391.

[1847] P. Ullio, H. Zhao, and M. Kamionkowski, A Dark matter spike at the galactic center?, Phys. Rev. D **64**, 043504 (2001), arXiv:astro-ph/0101481.

[1848] H. Kim, A. Lenoci, I. Stomberg, and X. Xue, Adiabatically compressed wave dark matter halo and intermediate-mass-ratio inspirals, Phys. Rev. D **107**, 083005 (2023), arXiv:2212.07528 [astro-ph.GA].

[1849] L. G. Collodel, D. D. Doneva, and S. S. Yazadjiev, Equatorial extreme-mass-ratio inspirals in Kerr black holes with scalar hair spacetimes, Phys. Rev. D **105**, 044036 (2022), arXiv:2108.11658 [gr-qc].

[1850] J. F. M. Delgado, C. A. R. Herdeiro, and E. Radu, EMRIs around j = 1 black holes with synchronised hair, JCAP **10**, 029, arXiv:2305.02333 [gr-qc].

[1851] A. Coogan, G. Bertone, D. Gaggero, B. J. Kavanagh, and D. A. Nichols, Measuring the dark matter environments of black hole binaries with gravitational waves, Phys. Rev. D **105**, 043009 (2022), arXiv:2108.04154 [gr-qc].

[1852] P. S. Cole, G. Bertone, A. Coogan, D. Gaggero, T. Karydas, B. J. Kavanagh, T. F. M. Spieksma, and G. M. Tomaselli, Distinguishing environmental effects on binary black hole gravitational waveforms, Nature Astron. **7**, 943 (2023), arXiv:2211.01362 [gr-qc].

[1853] N. Becker and L. Sagunski, Comparing accretion disks and dark matter spikes in intermediate mass ratio inspirals, Phys. Rev. D **107**, 083003 (2023), arXiv:2211.05145 [gr-qc].

[1854] X.-J. Yue, W.-B. Han, and X. Chen, Dark matter: an efficient catalyst for intermediate-mass-ratio-inspiral events, Astrophys. J. **874**, 34 (2019), arXiv:1802.03739 [gr-qc].

[1855] B. J. Kavanagh, D. A. Nichols, G. Bertone, and D. Gaggero, Detecting dark matter around black holes with gravitational waves: Effects of dark-matter dynamics on the gravitational waveform, Phys. Rev. D **102**, 083006 (2020), arXiv:2002.12811 [gr-qc].

[1856] N. Speeney, A. Antonelli, V. Baibhav, and E. Berti, Impact of relativistic corrections on the detectability of dark-matter spikes with gravitational waves, Phys. Rev. D **106**, 044027 (2022), arXiv:2204.12508 [gr-qc].

[1857] V. Cardoso, K. Destounis, F. Duque, R. P. Macedo, and A. Maselli, Black holes in galaxies: Environmental impact on gravitational-wave generation and propagation, Phys. Rev. D **105**, L061501 (2022), arXiv:2109.00005 [gr-qc].

[1858] R. Brito and S. Shah, Extreme mass-ratio inspirals into black holes surrounded by scalar clouds, Phys. Rev. D **108**, 084019 (2023), arXiv:2307.16093 [gr-qc].

[1859] N. Siemonsen, T. May, and W. E. East, Modeling the black hole superradiance gravitational waveform, Phys. Rev. D **107**, 104003 (2023), arXiv:2211.03845 [gr-qc].

[1860] V. S. Manko and I. D. Novikov, Generalizations of the Kerr and Kerr-Newman metrics possessing an arbitrary set of mass-multipole moments, Classical and Quantum Gravity **9**, 2477 (1992).

[1861] N. A. Collins and S. A. Hughes, Towards a formalism for mapping the space-times of massive compact objects: Bumpy black holes and their orbits, Phys. Rev. D **69**, 124022 (2004), arXiv:gr-qc/0402063.

[1862] C. J. Moore, A. J. K. Chua, and J. R. Gair, Gravitational waves from extreme mass ratio inspirals around bumpy black holes, Class. Quant. Grav. **34**, 195009 (2017), arXiv:1707.00712 [gr-qc].

[1863] S. Xin, W.-B. Han, and S.-C. Yang, Gravitational waves from extreme-mass-ratio inspirals using general parametrized metrics, Phys. Rev. D **100**, 084055 (2019), arXiv:1812.04185 [gr-qc].

[1864] R. Jackiw and S. Y. Pi, Chern-Simons modification of general relativity, Phys. Rev. D **68**, 104012 (2003), arXiv:gr-qc/0308071.

[1865] N. Yunes and F. Pretorius, Dynamical Chern-Simons Modified Gravity. I. Spinning Black Holes in the Slow-Rotation Approximation, Phys. Rev. D **79**, 084043 (2009), arXiv:0902.4669 [gr-qc].

[1866] T. Damour and A. Nagar, Relativistic tidal properties of neutron stars, Phys. Rev. D **80**, 084035 (2009), arXiv:0906.0096 [gr-qc].

[1867] A. Le Tiec and M. Casals, Spinning Black Holes Fall in Love, Phys. Rev. Lett. **126**, 131102 (2021), arXiv:2007.00214 [gr-qc].

[1868] B. Kol and M. Smolkin, Black hole stereotyping: Induced gravito-static polarization, JHEP **02**, 010, arXiv:1110.3764 [hep-th].

[1869] S. Chakrabarti, T. Delsate, and J. Steinhoff, New perspectives on neutron star and black hole spectroscopy and dynamic tides, arXiv:1304.2228 [gr-qc].

[1870] N. Gürlebeck, No-hair theorem for Black Holes in Astrophysical Environments, Phys. Rev. Lett. **114**, 151102 (2015), arXiv:1503.03240 [gr-qc].

[1871] P. Pani, I-Love-Q relations for gravastars and the approach to the black-hole limit, Phys. Rev. D **92**, 124030 (2015), [Erratum: Phys.Rev.D 95, 049902 (2017)], arXiv:1506.06050 [gr-qc].

[1872] S. Datta, Probing horizon scale quantum effects with Love, Class. Quant. Grav. **39**, 225016 (2022), arXiv:2107.07258 [gr-qc].

[1873] B. Carter, Global structure of the Kerr family of gravitational fields, Phys. Rev. **174**, 1559 (1968).

[1874] J. R. Gair, C. Li, and I. Mandel, Observable Properties of Orbits in Exact Bumpy Spacetimes, Phys. Rev. D **77**, 024035 (2008), arXiv:0708.0628 [gr-qc].

[1875] G. Lukes-Gerakopoulos and O. Kopáček, Recurrence Analysis as a tool to study chaotic dynamics of extreme mass ratio inspiral in signal with noise, Int. J. Mod. Phys. D **27**, 1850010 (2017), arXiv:1709.08446 [gr-qc].

[1876] K. Destounis, A. G. Suvorov, and K. D. Kokkotas, Testing spacetime symmetry through gravitational waves from extreme-mass-ratio inspirals, Phys. Rev. D **102**, 064041 (2020), arXiv:2009.00028 [gr-qc].

[1877] K. Destounis and K. D. Kokkotas, Gravitational-wave glitches: Resonant islands and frequency jumps in nonintegrable extreme-mass-ratio inspirals, Phys. Rev. D **104**, 064023 (2021), arXiv:2108.02782 [gr-qc].

[1878] G. Lukes-Gerakopoulos, T. A. Apostolatos, and G. Contopoulos, Observable signature of a background deviating from the Kerr metric, Phys. Rev. D **81**, 124005 (2010), arXiv:1003.3120 [gr-qc].

[1879] K. Glampedakis, S. A. Hughes, and D. Kennefick, Approximating the inspiral of test bodies into Kerr black holes, Phys. Rev. D **66**, 064005 (2002), arXiv:gr-qc/0205033.

[1880] A. J. K. Chua, S. Hee, W. J. Handley, E. Higson, C. J. Moore, J. R. Gair, M. P. Hobson, and A. N. Lasenby, Towards a framework for testing general relativity with extreme-mass-ratio-inspiral observations, Mon. Not. Roy. Astron. Soc. **478**, 28 (2018), arXiv:1803.10210 [gr-qc].

[1881] K. Destounis, F. Angeloni, M. Vaglio, and P. Pani, Extreme-mass-ratio inspirals into rotating boson stars: nonintegrability, chaos, and transient resonances, arXiv:2305.05691 [gr-qc].

[1882] C. Li and G. Lovelace, A Generalization of Ryan's theorem: Probing tidal coupling with gravitational waves from nearly circular, nearly equatorial, extreme-mass-ratio inspirals, Phys. Rev. D **77**, 064022 (2008), arXiv:gr-qc/0702146.

[1883] V. Cardoso, A. del Rio, and M. Kimura, Distinguishing black holes from horizonless objects through the excitation of resonances during inspiral, Phys. Rev. D **100**, 084046 (2019), [Erratum: Phys.Rev.D 101, 069902 (2020)], arXiv:1907.01561 [gr-qc].

[1884] N. Sago and T. Tanaka, Oscillations in the extreme mass-ratio inspiral gravitational wave phase correction as a probe of a reflective boundary of the central black hole, Phys. Rev. D **104**, 064009 (2021), arXiv:2106.07123 [gr-qc].

[1885] N. Sago and T. Tanaka, Efficient search method of anomalous reflection by the central object in an extreme mass-ratio inspiral system by future space gravitational wave detectors, Phys. Rev. D **106**, 024032 (2022), arXiv:2202.04249 [gr-qc].

[1886] P. Pani, E. Berti, V. Cardoso, Y. Chen, and R. Norte, Gravitational-wave signatures of the absence of an event horizon. II. Extreme mass ratio inspirals in the spacetime of a thin-shell gravastar, Phys. Rev. D **81**, 084011 (2010), arXiv:1001.3031 [gr-qc].

[1887] Y. Asali, P. T. H. Pang, A. Samajdar, and C. Van Den Broeck, Probing resonant excitations in exotic compact objects via gravitational waves, Phys. Rev. D **102**, 024016 (2020), arXiv:2004.05128 [gr-qc].

[1888] K. Fransen, G. Koekoek, R. Tielemans, and B. Vercnocke, Modeling and detecting resonant tides of exotic compact objects, Phys. Rev. D **104**, 044044 (2021), arXiv:2005.12286 [gr-qc].

[1889] V. Cardoso and F. Duque, Resonances, black hole mimickers, and the greenhouse effect: Consequences for gravitational-wave physics, Phys. Rev. D **105**, 104023 (2022), arXiv:2204.05315 [gr-qc].

[1890] M. Kesden, J. Gair, and M. Kamionkowski, Gravitational-wave signature of an inspiral into a supermassive horizonless object, Phys. Rev. D **71**, 044015 (2005), arXiv:astro-ph/0411478.

[1891] B. P. Abbott *et al.* (LIGO Scientific, Virgo), Tests of General Relativity with GW170817, Phys. Rev. Lett. **123**, 011102 (2019), arXiv:1811.00364 [gr-qc].

[1892] N. Sennett, R. Brito, A. Buonanno, V. Gorbenko, and L. Senatore, Gravitational-Wave Constraints on an Effective Field-Theory Extension of General Relativity, Phys. Rev. D **102**, 044056 (2020), arXiv:1912.09917 [gr-qc].

[1893] H. O. Silva, A. Ghosh, and A. Buonanno, Black-hole ringdown as a probe of higher-curvature gravity theories, Phys. Rev. D **107**, 044030 (2023), arXiv:2205.05132 [gr-qc].

[1894] E. Maggio, H. O. Silva, A. Buonanno, and A. Ghosh, Tests of general relativity in the nonlinear regime: A parametrized plunge-merger-ringdown gravitational waveform model, Phys. Rev. D **108**, 024043 (2023), arXiv:2212.09655 [gr-qc].

[1895] F.-L. Julié, V. Baibhav, E. Berti, and A. Buonanno, Third post-Newtonian effective-one-body Hamiltonian in scalar-tensor and Einstein-scalar-Gauss-Bonnet gravity, Phys. Rev. D **107**, 104044 (2023), arXiv:2212.13802 [gr-qc].

[1896] M. Khalil, N. Sennett, J. Steinhoff, J. Vines, and A. Buonanno, Hairy binary black holes in Einstein-Maxwell-dilaton theory and their effective-one-body description, Phys. Rev. D **98**, 104010 (2018), arXiv:1809.03109 [gr-qc].

[1897] A. Kuntz, Two-body potential of Vainshtein screened theories, Phys. Rev. D **100**, 024024 (2019), arXiv:1905.07340 [gr-qc].

[1898] T. Damour and A. Nagar, Effective One Body description of tidal effects in inspiralling compact binaries, Phys. Rev. D **81**, 084016 (2010), arXiv:0911.5041 [gr-qc].

[1899] S. Bernuzzi, A. Nagar, M. Thierfelder, and B. Brugmann, Tidal effects in binary neutron star coalescence, Phys. Rev. D **86**, 044030 (2012), arXiv:1205.3403 [gr-qc].

[1900] D. Bini and T. Damour, Gravitational self-force corrections to two-body tidal interactions and the effective one-body formalism, Phys. Rev. D **90**, 124037 (2014), arXiv:1409.6933 [gr-qc].

[1901] S. Bernuzzi, A. Nagar, S. Balmelli, T. Dietrich, and M. Ujevic, Quasiuniversal properties of neutron star mergers, Phys. Rev. Lett. **112**, 201101 (2014), arXiv:1402.6244 [gr-qc].

[1902] R. Gamba and S. Bernuzzi, Resonant tides in binary neutron star mergers: Analytical-numerical relativity study, Phys. Rev. D **107**, 044014 (2023), arXiv:2207.13106 [gr-qc].

[1903] M. K. Mandal, P. Mastrolia, H. O. Silva, R. Patil, and J. Steinhoff, Gravitoelectric dynamical tides at second post-Newtonian order, arXiv:2304.02030 [hep-th].

[1904] P. K. Gupta, J. Steinhoff, and T. Hinderer, Relativistic effective action of dynamical gravitomagnetic tides for slowly rotating neutron stars, Phys. Rev. Res. **3**, 013147 (2021), arXiv:2011.03508 [gr-qc].

[1905] N. V. Krishnendu, K. G. Arun, and C. K. Mishra, Testing the binary black hole nature of a compact binary coalescence, Phys. Rev. Lett. **119**, 091101 (2017), arXiv:1701.06318 [gr-qc].

[1906] T. Dietrich, S. Bernuzzi, and W. Tichy, Closed-form tidal approximants for binary neutron star gravitational waveforms constructed from high-resolution numerical relativity simulations, Phys. Rev. D **96**, 121501 (2017), arXiv:1706.02969 [gr-qc].

[1907] M. Breschi, S. Bernuzzi, F. Zappa, M. Agathos, A. Perego, D. Radice, and A. Nagar, kiloHertz gravitational waves from binary neutron star remnants: time-domain model and constraints on extreme matter, Phys. Rev. D **100**, 104029 (2019), arXiv:1908.11418 [gr-qc].

[1908] S. Bernuzzi, T. Dietrich, and A. Nagar, Modeling the complete gravitational wave spectrum of neutron star mergers, Phys. Rev. Lett. **115**, 091101 (2015), arXiv:1504.01764 [gr-qc].

[1909] M. Breschi, R. Gamba, S. Borhanian, G. Carullo, and S. Bernuzzi, Kilohertz Gravitational Waves from Binary Neutron Star Mergers: Inference of Postmerger Signals with the Einstein Telescope, arXiv:2205.09979 [gr-qc].

[1910] F. Zappa, S. Bernuzzi, F. Pannarale, M. Mapelli, and N. Giacobbo, Black-Hole Remnants from Black-Hole–Neutron-Star Mergers, Phys. Rev. Lett. **123**, 041102 (2019), arXiv:1903.11622 [gr-qc].

[1911] A. Toubiana, S. Babak, E. Barausse, and L. Lehner, Modeling gravitational waves from exotic compact objects, Phys. Rev. D **103**, 064042 (2021), arXiv:2011.12122 [gr-qc].

[1912] K. Takami, L. Rezzolla, and L. Baiotti, Spectral properties of the post-merger gravitational-wave signal from binary neutron stars, Phys. Rev. D **91**, 064001 (2015), arXiv:1412.3240 [gr-qc].

[1913] B. P. Abbott *et al.* (LIGO Scientific, Virgo), Tests of general relativity with GW150914, Phys. Rev. Lett. **116**, 221101 (2016), [Erratum: Phys.Rev.Lett. 121, 129902 (2018)], arXiv:1602.03841 [gr-qc].

[1914] B. P. Abbott *et al.* (LIGO Scientific, Virgo), Tests of General Relativity with the Binary Black Hole Signals from the LIGO-Virgo Catalog GWTC-1, Phys. Rev. D **100**, 104036 (2019), arXiv:1903.04467 [gr-qc].

[1915] N. V. Krishnendu, M. Saleem, A. Samajdar, K. G. Arun, W. Del Pozzo, and C. K. Mishra, Constraints on the binary black hole nature of GW151226 and GW170608 from the measurement of spin-induced quadrupole moments, Phys. Rev. D **100**, 104019 (2019), arXiv:1908.02247 [gr-qc].

[1916] S. Weinberg, *Gravitation and Cosmology: Principles and Applications of the General Theory of*

Relativity (John Wiley and Sons, New York, 1972).

[1917] D. Garfinkle and T. Vachaspati, FIELDS DUE TO KINKY, CUSPLESS, COSMIC LOOPS, Phys. Rev. D **37**, 257 (1988).

[1918] T. Vachaspati, Gravity of Cosmic Loops, Phys. Rev. D **35**, 1767 (1987).

[1919] B. Allen and E. P. S. Shellard, Gravitational radiation from cosmic strings, Phys. Rev. D **45**, 1898 (1992).

[1920] B. Allen, P. Casper, and A. Ottewill, Closed form expression for the momentum radiated from cosmic string loops, Phys. Rev. D **51**, 1546 (1995), arXiv:gr-qc/9407023.

[1921] B. Allen and P. Casper, A Closed form expression for the gravitational radiation rate from cosmic strings, Phys. Rev. D **50**, 2496 (1994), arXiv:gr-qc/9405005.

[1922] P. Casper and B. Allen, Gravitational radiation from realistic cosmic string loops, Phys. Rev. D **52**, 4337 (1995), arXiv:gr-qc/9505018.

[1923] B. Allen and A. C. Ottewill, Wave forms for gravitational radiation from cosmic string loops, Phys. Rev. D **63**, 063507 (2001), arXiv:gr-qc/0009091.

[1924] N. Suresh and D. F. Chernoff, Modeling the Beam of Gravitational Radiation from a Cosmic String Loop, arXiv:2310.00825 [astro-ph.CO].

[1925] J. Shapiro Key and N. J. Cornish, Characterizing the Gravitational Wave Signature from Cosmic String Cusps, Phys. Rev. D **79**, 043014 (2009), arXiv:0812.1590 [gr-qc].

[1926] D. Austin, E. J. Copeland, and T. W. B. Kibble, Evolution of cosmic string configurations, Phys. Rev. D **48**, 5594 (1993), arXiv:hep-ph/9307325.

[1927] J. Polchinski and J. V. Rocha, Cosmic string structure at the gravitational radiation scale, Phys. Rev. D **75**, 123503 (2007), arXiv:gr-qc/0702055.

[1928] C. J. A. P. Martins, E. P. S. Shellard, and J. P. P. Vieira, Models for Small-Scale Structure on Cosmic Strings: Mathematical Formalism, Phys. Rev. D **90**, 043518 (2014), arXiv:1405.7722 [hep-ph].

[1929] J. P. P. Vieira, C. J. A. P. Martins, and E. P. S. Shellard, Models for small-scale structure on cosmic strings. II. Scaling and its stability, Phys. Rev. D **94**, 096005 (2016), [Erratum: Phys.Rev.D 94, 099907 (2016)], arXiv:1611.06103 [astro-ph.CO].

[1930] C. J. A. P. Martins, P. Peter, I. Y. Rybak, and E. P. S. Shellard, Generalized velocity-dependent one-scale model for current-carrying strings, Phys. Rev. D **103**, 043538 (2021), arXiv:2011.09700 [astro-ph.CO].

[1931] D. P. Bennett and F. R. Bouchet, Cosmic string evolution, Phys. Rev. Lett. **63**, 2776 (1989).

[1932] J. M. Quashnock and D. N. Spergel, Gravitational Selfinteractions of Cosmic Strings, Phys. Rev. D **42**, 2505 (1990).

[1933] X. Siemens and K. D. Olum, Gravitational radiation and the small-scale structure of cosmic strings, Nucl. Phys. B **611**, 125 (2001), [Erratum: Nucl.Phys.B 645, 367–367 (2002)], arXiv:gr-qc/0104085.

[1934] X. Siemens, K. D. Olum, and A. Vilenkin, On the size of the smallest scales in cosmic string networks, Phys. Rev. D **66**, 043501 (2002), arXiv:gr-qc/0203006.

[1935] X. Siemens and K. D. Olum, Cosmic string cusps with small scale structure: Their forms and gravitational wave forms, Phys. Rev. D **68**, 085017 (2003), arXiv:gr-qc/0307113.

[1936] M. J. Stott, T. Elghozi, and M. Sakellariadou, Gravitational Wave Bursts from Cosmic String Cusps and Pseudocusps, Phys. Rev. D **96**, 023533 (2017), arXiv:1612.07599 [hep-th].

[1937] J. J. Blanco-Pillado and K. D. Olum, Form of cosmic string cusps, Phys. Rev. D **59**, 063508 (1999), [Erratum: Phys.Rev.D 103, 029902 (2021)], arXiv:gr-qc/9810005.

[1938] E. O'Callaghan, S. Chadburn, G. Geshnizjani, R. Gregory, and I. Zavala, The effect of extra dimensions on gravity wave bursts from cosmic string cusps, JCAP **09**, 013, arXiv:1005.3220 [hep-th].

[1939] A. C. Jenkins and M. Sakellariadou, Primordial black holes from cusp collapse on cosmic strings, arXiv:2006.16249 [astro-ph.CO].

[1940] T. Helfer, J. C. Aurrekoetxea, and E. A. Lim, Cosmic String Loop Collapse in Full General

Relativity, Phys. Rev. D **99**, 104028 (2019), arXiv:1808.06678 [gr-qc].

[1941] J. C. Aurrekoetxea, T. Helfer, and E. A. Lim, Coherent Gravitational Waveforms and Memory from Cosmic String Loops, Class. Quant. Grav. **37**, 204001 (2020), arXiv:2002.05177 [gr-qc].

[1942] D. Garfinkle and T. Vachaspati, Cosmic string traveling waves, Phys. Rev. D **42**, 1960 (1990).

[1943] M. Kölsch, T. Dietrich, M. Ujevic, and B. Bruegmann, Investigating the mass-ratio dependence of the prompt-collapse threshold with numerical-relativity simulations, Phys. Rev. D **106**, 044026 (2022), arXiv:2112.11851 [gr-qc].

[1944] S. V. Chaurasia, T. Dietrich, and S. Rosswog, Black hole-neutron star simulations with the BAM code: First tests and simulations, Phys. Rev. D **104**, 084010 (2021), arXiv:2107.08752 [gr-qc].

[1945] H. Gieg, F. Schianchi, T. Dietrich, and M. Ujevic, Incorporating a Radiative Hydrodynamics Scheme in the Numerical-Relativity Code BAM, Universe **8**, 370 (2022), arXiv:2206.01337 [gr-qc].

[1946] G. Doulis, F. Atteneder, S. Bernuzzi, and B. Brügmann, Entropy-limited higher-order central scheme for neutron star merger simulations, Phys. Rev. D **106**, 024001 (2022), arXiv:2202.08839 [gr-qc].

[1947] I. S. Fernández, S. Renkhoff, D. Cors, B. Bruegmann, and D. Hilditch, Evolution of Brill waves with an adaptive pseudospectral method, Phys. Rev. D **106**, 024036 (2022), arXiv:2205.04379 [gr-qc].

[1948] M. K. Bhattacharyya, D. Hilditch, K. Rajesh Nayak, S. Renkhoff, H. R. Rüter, and B. Brügmann, Implementation of the dual foliation generalized harmonic gauge formulation with application to spherical black hole excision, Phys. Rev. D **103**, 064072 (2021), arXiv:2101.12094 [gr-qc].

[1949] M. Fernando, D. Neilsen, E. W. Hirschmann, and H. Sundar, A scalable framework for adaptive computational general relativity on heterogeneous clusters, in *Proceedings of the ACM International Conference on Supercomputing*, ICS '19 (Association for Computing Machinery, New York, NY, USA, 2019) p. 1–12.

[1950] M. Fernando, D. Duplyakin, and H. Sundar, Machine and application aware partitioning for adaptive mesh refinement applications, in *Proceedings of the 26th International Symposium on High-Performance Parallel and Distributed Computing*, HPDC '17 (Association for Computing Machinery, New York, NY, USA, 2017) p. 231–242.

[1951] Cactus developers, Cactus Computational Toolkit.

[1952] E. Schnetter, S. H. Hawley, and I. Hawke, Evolutions in 3-D numerical relativity using fixed mesh refinement, Class. Quant. Grav. **21**, 1465 (2004), arXiv:gr-qc/0310042.

[1953] Carpet developers, Carpet: Adaptive mesh refinement for the Cactus framework.

[1954] R. Haas, C.-H. Cheng, P. Diener, Z. Etienne, G. Ficarra, T. Ikeda, H. Kalyanaraman, N. Kuo, L. Leung, C. Tian, B.-J. Tsao, A. Wen, M. Alcubierre, D. Alic, G. Allen, M. Ansorg, M. Babiuc-Hamilton, L. Baiotti, W. Benger, E. Bentivegna, S. Bernuzzi, T. Bode, G. Bozzola, S. R. Brandt, B. Brendal, B. Bruegmann, M. Campanelli, F. Cipolletta, G. Corvino, S. Cupp, R. D. Pietri, A. Dima, H. Dimmelmeier, R. Dooley, N. Dorband, M. Elley, Y. E. Khamra, J. Faber, T. Font, J. Frieben, B. Giacomazzo, T. Goodale, C. Gundlach, I. Hawke, S. Hawley, I. Hinder, E. A. Huerta, S. Husa, S. Iyer, L. Ji, D. Johnson, A. V. Joshi, A. Kankani, W. Kastaun, T. Kellermann, A. Knapp, M. Koppitz, P. Laguna, G. Lanferman, P. Lasky, F. Löffler, H. Macpherson, J. Masso, L. Menger, A. Merzky, J. M. Miller, M. Miller, P. Moesta, P. Montero, B. Mundim, P. Nelson, A. Nerozzi, S. C. Noble, C. Ott, R. Paruchuri, D. Pollney, D. Price, D. Radice, T. Radke, C. Reisswig, L. Rezzolla, C. B. Richards, D. Rideout, M. Ripeanu, L. Sala, J. A. Schewtschenko, E. Schnetter, B. Schutz, E. Seidel, E. Seidel, J. Shalf, K. Sible, U. Sperhake, N. Stergioulas, W.-M. Suen, B. Szilagyi, R. Takahashi, M. Thomas, J. Thornburg, M. Tobias, A. Tonita, P. Walker, M.-B. Wan, B. Wardell, L. Werneck, H. Witek, M. Zilhão, B. Zink, and Y. Zlochower, The einstein toolkit (2022), to find out more, visit http://einsteintoolkit.org.

[1955] W. Zhang, A. Almgren, V. Beckner, J. Bell, J. Blaschke, C. Chan, M. Day, B. Friesen, K. Gott,

D. Graves, M. Katz, A. Myers, T. Nguyen, A. Nonaka, M. Rosso, S. Williams, and M. Zingale, AMReX: a framework for block-structured adaptive mesh refinement, Journal of Open Source Software **4**, 1370 (2019).

[1956] W. F. Godoy, N. Podhorszki, R. Wang, C. Atkins, G. Eisenhauer, J. Gu, P. Davis, J. Choi, K. Germaschewski, K. Huck, A. Huebl, M. Kim, J. Kress, T. Kurc, Q. Liu, J. Logan, K. Mehta, G. Ostrouchov, M. Parashar, F. Poeschel, D. Pugmire, E. Suchyta, K. Takahashi, N. Thompson, S. Tsutsumi, L. Wan, M. Wolf, K. Wu, and S. Klasky, Adios 2: The adaptable input output system. a framework for high-performance data management, SoftwareX **12**, 100561 (2020).

[1957] S. Balay, S. Abhyankar, M. F. Adams, S. Benson, J. Brown, P. Brune, K. Buschelman, E. M. Constantinescu, L. Dalcin, A. Dener, V. Eijkhout, J. Faibussowitsch, W. D. Gropp, V. Hapla, T. Isaac, P. Jolivet, D. Karpeev, D. Kaushik, M. G. Knepley, F. Kong, S. Kruger, D. A. May, L. C. McInnes, R. T. Mills, L. Mitchell, T. Munson, J. E. Roman, K. Rupp, P. Sanan, J. Sarich, B. F. Smith, S. Zampini, H. Zhang, H. Zhang, and J. Zhang, PETSc Web page, https://petsc.org/ (2022).

[1958] S. Shankar, P. Mösta, S. R. Brandt, R. Haas, E. Schnetter, and Y. de Graaf, GRaM-X: a new GPU-accelerated dynamical spacetime GRMHD code for Exascale computing with the Einstein Toolkit, Class. Quant. Grav. **40**, 205009 (2023), arXiv:2210.17509 [astro-ph.IM].

[1959] J. M. Stone, K. Tomida, C. J. White, and K. G. Felker, The Athena++ Adaptive Mesh Refinement Framework: Design and Magnetohydrodynamic Solvers, ApJS **249**, 4 (2020), arXiv:2005.06651 [astro-ph.IM].

[1960] Optimization of finite-differencing kernels for numerical relativity applications, J. Low Power Electron. Appl. **8(2)**, 15 (2018).

[1961] M. Adams, P. Colella, D. T. Graves, J. Johnson, N. Keen, T. J. Ligocki, D. F. Martin, P. McCorquodale, D. Modiano, P. Schwartz, T. Sternberg, and B. V. Straalen, `Chombo` software package for amr applications - design document.

[1962] P. Figueras and T. França, Gravitational Collapse in Cubic Horndeski Theories, Class. Quant. Grav. **37**, 225009 (2020), arXiv:2006.09414 [gr-qc].

[1963] M. D. Duez, Y. T. Liu, S. L. Shapiro, and B. C. Stephens, Relativistic magnetohydrodynamics in dynamical spacetimes: Numerical methods and tests, Phys. Rev. D **72**, 024028 (2005), arXiv:astro-ph/0503420.

[1964] D. Viganò, R. Aguilera-Miret, F. Carrasco, B. Miñano, and C. Palenzuela, General relativistic MHD large eddy simulations with gradient subgrid-scale model, Phys. Rev. D **101**, 123019 (2020), arXiv:2004.00870 [gr-qc].

[1965] M. Bezares, R. Aguilera-Miret, L. ter Haar, M. Crisostomi, C. Palenzuela, and E. Barausse, No Evidence of Kinetic Screening in Simulations of Merging Binary Neutron Stars beyond General Relativity, Phys. Rev. Lett. **128**, 091103 (2022), arXiv:2107.05648 [gr-qc].

[1966] A. T. L. Lam, M. Shibata, and K. Kiuchi, Numerical-relativity simulation for tidal disruption of white dwarfs by a supermassive black hole, Phys. Rev. D **107**, 043033 (2023), arXiv:2212.10891 [astro-ph.HE].

[1967] Y. Sekiguchi, K. Kiuchi, K. Kyutoku, and M. Shibata, Current Status of Numerical-Relativity Simulations in Kyoto, PTEP **2012**, 01A304 (2012), arXiv:1206.5927 [astro-ph.HE].

[1968] M. Shibata and Y.-i. Sekiguchi, Magnetohydrodynamics in full general relativity: Formulation and tests, Phys. Rev. D **72**, 044014 (2005), arXiv:astro-ph/0507383.

[1969] K. Kiuchi, L. E. Held, Y. Sekiguchi, and M. Shibata, Implementation of advanced Riemann solvers in a neutrino-radiation magnetohydrodynamics code in numerical relativity and its application to a binary neutron star merger, Phys. Rev. D **106**, 124041 (2022), arXiv:2205.04487 [astro-ph.HE].

[1970] M. Shibata, K. Kiuchi, and Y.-i. Sekiguchi, General relativistic viscous hydrodynamics of differentially rotating neutron stars, Phys. Rev. D **95**, 083005 (2017), arXiv:1703.10303 [astro-ph.HE].

[1971] H. Uchida, M. Shibata, T. Yoshida, Y. Sekiguchi, and H. Umeda, Gravitational Collapse of Rotating Supermassive Stars including Nuclear Burning Effects, Phys. Rev. D **96**, 083016 (2017), [Erratum: Phys.Rev.D 98, 129901 (2018)], arXiv:1704.00433 [astro-ph.HE].

[1972] S. Fujibayashi, K. Kiuchi, S. Wanajo, K. Kyutoku, Y. Sekiguchi, and M. Shibata, Comprehensive Study of Mass Ejection and Nucleosynthesis in Binary Neutron Star Mergers Leaving Short-lived Massive Neutron Stars, Astrophys. J. **942**, 39 (2023), arXiv:2205.05557 [astro-ph.HE].

[1973] S. Fujibayashi, A. T.-L. Lam, M. Shibata, and Y. Sekiguchi, Supernova-like explosion of massive rotating stars from disks surrounding a black hole, arXiv:2309.02161 [astro-ph.HE].

[1974] H. P. Pfeiffer, D. A. Brown, L. E. Kidder, L. Lindblom, G. Lovelace, and M. A. Scheel, Reducing orbital eccentricity in binary black hole simulations, Class. Quant. Grav. **24**, S59 (2007), arXiv:gr-qc/0702106.

[1975] A. Buonanno, L. E. Kidder, A. H. Mroue, H. P. Pfeiffer, and A. Taracchini, Reducing orbital eccentricity of precessing black-hole binaries, Phys. Rev. D **83**, 104034 (2011), arXiv:1012.1549 [gr-qc].

[1976] A. H. Mroue and H. P. Pfeiffer, Precessing Binary Black Holes Simulations: Quasicircular Initial Data, arXiv:1210.2958 [gr-qc].

[1977] O. Rinne, Stable radiation-controlling boundary conditions for the generalized harmonic Einstein equations, Class. Quant. Grav. **23**, 6275 (2006), arXiv:gr-qc/0606053.

[1978] O. Rinne, L. Lindblom, and M. A. Scheel, Testing outer boundary treatments for the Einstein equations, Class. Quant. Grav. **24**, 4053 (2007), arXiv:0704.0782 [gr-qc].

[1979] B. Szilágyi, Key Elements of Robustness in Binary Black Hole Evolutions using Spectral Methods, Int. J. Mod. Phys. D **23**, 1430014 (2014), arXiv:1405.3693 [gr-qc].

[1980] N. W. Taylor, M. Boyle, C. Reisswig, M. A. Scheel, T. Chu, L. E. Kidder, and B. Szilágyi, Comparing Gravitational Waveform Extrapolation to Cauchy-Characteristic Extraction in Binary Black Hole Simulations, Phys. Rev. D **88**, 124010 (2013), arXiv:1309.3605 [gr-qc].

[1981] C. J. Woodford, M. Boyle, and H. P. Pfeiffer, Compact Binary Waveform Center-of-Mass Corrections, Phys. Rev. D **100**, 124010 (2019), arXiv:1904.04842 [gr-qc].

[1982] G. Lovelace *et al.*, Nearly extremal apparent horizons in simulations of merging black holes, Class. Quant. Grav. **32**, 065007 (2015), arXiv:1411.7297 [gr-qc].

[1983] N. Deppe, F. Hébert, L. E. Kidder, and S. A. Teukolsky, A high-order shock capturing discontinuous Galerkin–finite difference hybrid method for GRMHD, Class. Quant. Grav. **39**, 195001 (2022), arXiv:2109.11645 [gr-qc].

[1984] N. Deppe *et al.*, Simulating magnetized neutron stars with discontinuous Galerkin methods, Phys. Rev. D **105**, 123031 (2022), arXiv:2109.12033 [gr-qc].

[1985] I. Legred, Y. Kim, N. Deppe, K. Chatziioannou, F. Foucart, F. Hébert, and L. E. Kidder, Simulating neutron stars with a flexible enthalpy-based equation of state parametrization in spectre, Phys. Rev. D **107**, 123017 (2023), arXiv:2301.13818 [astro-ph.HE].

[1986] N. L. Fischer and H. P. Pfeiffer, Unified discontinuous Galerkin scheme for a large class of elliptic equations, Phys. Rev. D **105**, 024034 (2022), arXiv:2108.05826 [math.NA].

[1987] N. L. Vu *et al.*, High-accuracy numerical models of Brownian thermal noise in thin mirror coatings, Class. Quant. Grav. **40**, 025015 (2023), arXiv:2111.06893 [astro-ph.IM].

[1988] F. Cipolletta, J. V. Kalinani, E. Giangrandi, B. Giacomazzo, R. Ciolfi, L. Sala, and B. Giudici, Spritz: General Relativistic Magnetohydrodynamics with Neutrinos, Class. Quant. Grav. **38**, 085021 (2021), arXiv:2012.10174 [astro-ph.HE].

[1989] J. V. Kalinani, R. Ciolfi, W. Kastaun, B. Giacomazzo, F. Cipolletta, and L. Ennoggi, Implementing a new recovery scheme for primitive variables in the general relativistic magnetohydrodynamic code Spritz, Phys. Rev. D **105**, 103031 (2022), arXiv:2107.10620 [astro-ph.HE].

[1990] B. Giacomazzo, J. G. Baker, M. C. Miller, C. S. Reynolds, and J. R. van Meter, General Relativistic Simulations of Magnetized Plasmas around Merging Supermassive Black Holes, Astrophys. J. Lett. **752**, L15 (2012), arXiv:1203.6108 [astro-ph.HE]